Neuromethods 120

Springer Protocols

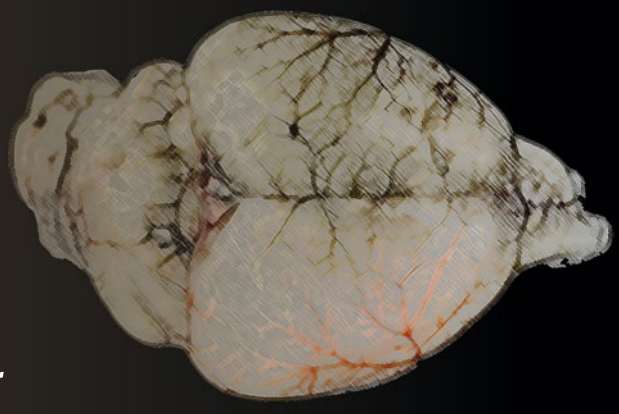

Ulrich Dirnagl *Editor*

Rodent Models of Stroke

Second Edition

Humana Press

NEUROMETHODS

Series Editor
Wolfgang Walz
University of Saskatchewan
Saskatoon, SK, Canada

For further volumes:
http://www.springer.com/series/7657

Rodent Models of Stroke

Second Edition

Edited by

Ulrich Dirnagl

Department of Experimental Neurology and Center for Stroke Research Berlin (CSB), Charité-Universitätsmedizin Berlin, Berlin, Germany; German Center for Neurodegenerative Diseases (DZNE) and German Center for Cardiovascular Diseases (DZHK), Berlin, Germany; Excellence Cluster NeuroCure, Berlin, Germany; Berlin Institute of Health, Berlin, Germany

Humana Press

Editor
Ulrich Dirnagl
Department of Experimental Neurology
and Center for Stroke Research Berlin (CSB)
Charité-Universitätsmedizin Berlin, Berlin, Germany

German Center for Neurodegenerative Diseases (DZNE)
and German Center for Cardiovascular Diseases (DZHK)
Berlin, Germany

Excellence Cluster NeuroCure, Berlin, Germany

Berlin Institute of Health, Berlin, Germany

Videos can also be accessed at http://link.springer.com/book/10.1007/978-1-4939-5620-3

ISSN 0893-2336 ISSN 1940-6045 (electronic)
Neuromethods
ISBN 978-1-4939-5618-0 ISBN 978-1-4939-5620-3 (eBook)
DOI 10.1007/978-1-4939-5620-3

Library of Congress Control Number: 2016951315

Printed on acid-free paper

This Humana Press imprint is published by Springer Nature
The registered company is Springer Science+Business Media LLC New York

Preface to the Series

Experimental life sciences have two basic foundations: concepts and tools. The *Neuromethods* series focuses on the tools and techniques unique to the investigation of the nervous system and excitable cells. It will not, however, shortchange the concept side of things as care has been taken to integrate these tools within the context of the concepts and questions under investigation. In this way, the series is unique in that it not only collects protocols but also includes theoretical background information and critiques which led to the methods and their development. Thus it gives the reader a better understanding of the origin of the techniques and their potential future development. The *Neuromethods* publishing program strikes a balance between recent and exciting developments like those concerning new animal models of disease, imaging, in vivo methods, and more established techniques, including immunocytochemistry and electrophysiological technologies. New trainees in neurosciences still need a sound footing in these older methods in order to apply a critical approach to their results.

Under the guidance of its founders, Alan Boulton and Glen Baker, the *Neuromethods* series has been a success since its first volume published through Humana Press in 1985. The series continues to flourish through many changes over the years. It is now published under the umbrella of Springer Protocols. While methods involving brain research have changed a lot since the series started, the publishing environment and technology have changed even more radically. *Neuromethods* has the distinct layout and style of the Springer Protocols program, designed specifically for readability and ease of reference in a laboratory setting.

The careful application of methods is potentially the most important step in the process of scientific inquiry. In the past, new methodologies led the way in developing new disciplines in the biological and medical sciences. For example, physiology emerged out of anatomy in the nineteenth century by harnessing new methods based on the newly discovered phenomenon of electricity. Nowadays, the relationships between disciplines and methods are more complex. Methods are now widely shared between disciplines and research areas. New developments in electronic publishing make it possible for scientists that encounter new methods to quickly find sources of information electronically. The design of individual volumes and chapters in this series takes this new access technology into account. Springer Protocols makes it possible to download single protocols separately. In addition, Springer makes its print-on-demand technology available globally. A print copy can therefore be acquired quickly and for a competitive price anywhere in the world.

Wolfgang Walz

Preface

Despite major advances in prevention, acute treatment, and rehabilitation, stroke remains a major burden on patients, relatives, and economies. The role and potential benefits of experimental models of stroke (i.e., focal cerebral ischemia) in rodents have been recently debated. Critics argue that numerous treatment strategies have been tested successfully in models only to be proven dismal failures when tested in controlled clinical trials.

When methods of systematic review and meta-analysis are applied, however, it turns out that experimental models actually did faithfully predict the negative outcomes of clinical trials. For example, thrombolysis with tissue plasminogen activator (t-PA), the only clinically effective pharmacological treatment of acute ischemic stroke, was first demonstrated and evaluated in an experimental model of stroke. Many other examples document the positive prediction of rodent stroke models even beyond the brain, such as changes in the immune system and susceptibility to infection after stroke. These were first described and can be faithfully modeled in rodents.

Beyond its role in investigating pathomechanisms of stroke and in preclinical testing for the efficacy of novel diagnostic and treatment strategies, rodent stroke is often used as a "model" for how the brain reacts to neurological injury (damage, protection, repair), with implications for many other neurological disorders such as brain and spinal cord injury, epilepsy, and even multiple sclerosis. Concepts such as "neuroprotection," "preconditioning," and "ischemic penumbra" are largely the result of experimental stroke research.

Nevertheless, the issue of the relevance of experimental stroke research, in particular in rodents, to human disease has to be taken seriously. A number of problems have been identified which are prevalent in this research field and impact on its predictiveness. These include low statistical power, deficiencies in experimental design, analysis, and reporting, as well as publication bias, just to name a few. In addition, the validity of experimental stroke research is affected when the effects of age, gender, and comorbidities are ignored in modeling of stroke.

The first edition of this volume was well received by the stroke research community. In this second edition, our international consortium of authors updated and expanded their comprehensive, critical, and very application-oriented approach to the toolbox of rodent models of stroke. From choosing the model and outcome measures, designing the experiment, and conducting and analyzing it to reporting it in a scientific publication, we are offering food for thought as well as practical advice. This book is the result of long-standing cooperation of many of the authors, not only scientific but also in teaching animal models of stroke and good scientific practice to students and researchers. It is also the result of an intense discussion of issues of validity and quality and its control. For more than 15 years, several of the authors have been organizing the international course "Methods in Cerebral Ischemia Research," and many are jointly organizing training and dissemination of practical knowledge in European Community-funded initiatives such as the European Stroke Network or Multi-PART (Multicentre Preclinical Animal Research Team), as well as in the Center for Stroke Research in Berlin. The structure and content of the book reflect both the authors' long-standing expertise in experimental and clinical stroke research and their roles in training the scientific community in the tools of the trade.

We hope that this updated second edition will help its readers understand the limitations and the opportunities of modeling stroke in rodents and enable them to conduct experiments which will not only improve our understanding of the pathophysiology of this devastating disorder but also serve as the basis for developing highly effective treatment.

Berlin, Germany ***Ulrich Dirnagl***

Contents

Preface to the Series . . . . . *v*
Preface . . . . . *vii*
Contributors . . . . . *xi*

1 From Bedside to Bench: How Clinical Reality Should Instruct Stroke Modeling 1
Dirk M. Hermann and Thorsten R. Doeppner

2 How to Avoid Bumping into the Translational Roadblock 7
Malcolm R. Macleod and Emily Sena

3 Modeling Focal Cerebral Ischemia in Rodents: Introduction and Overview . . . 19
Vincent Prinz and Matthias Endres

4 Focal Cerebral Ischemia in the Mouse and Rat by Intraluminal Suture 31
Ludmila Belayev, Matthias Endres, and Vincent Prinz

5 Focal Ischemia Models: Middle Cerebral Artery Occlusion Induced by Electrocoagulation, Occluding Devices, and Endothelin-1 45
I. Mhairi Macrae

6 Mouse Model of in situ Thromboembolic Stroke and Reperfusion 59
Orset Cyrille, Le Béhot Audrey, Bonnet Anne-Laure, Maysami Samaneh, and Vivien Denis

7 Photochemical Models of Focal Brain Ischemia 69
Anja Urbach and Otto W. Witte

8 Housing in an Enriched Environment: A Tool to Study Functional Recovery After Experimental Stroke 85
Karsten Ruscher and Tadeusz Wieloch

9 Modeling Risk Factors and Confounding Effects in Stroke 93
Barry McColl, David Howells, Nancy Rothwell, and Adam Denes

10 Effect of Anesthesia in Stroke Models 123
Richard J. Traystman

11 Noninvasive Brain Imaging in Small Animal Stroke Models: MRI, PET, and SPECT 147
Abraham Martín, Pedro Ramos-Cabrer, and Anna M. Planas

12 Noninvasive Optical Imaging in Rodent Models of Stroke 187
Markus Vaas and Jan Klohs

13 Behavioral Testing in Rodent Models of Stroke, Part I 199
René Bernard, Mustafa Balkaya, and André Rex

14 Behavioral Testing in Rodent Models of Stroke, Part II 225
Gerlinde A.S. Metz

15 Combining Classical Comprehensive with Ethological Based, High-Throughput Automated Behavioral Phenotyping for Rodent Models of Stroke 243
Anne-Christine Plank, Stephan von Hörsten, and Fabio Canneva

16 Histology and Infarct Volume Determination in Rodent Models of Stroke . . . 263
Clemens Sommer

17 Ethics of Modeling of Cerebral Ischemia in Small Animals. 279
Ute Lindauer

18 Quality Control and Standard Operating Procedures. 291
Ulrich Dirnagl

19 Statistics in Experimental Stroke Research: From Sample Size Calculation to Data Description and Significance Testing. 301
Ulrich Dirnagl

20 Complexities, Confounders, and Challenges in Experimental Stroke Research: A Checklist for Researchers and Reviewers 317
Ulrich Dirnagl

Index *333*

Contributors

Bonnet Anne-Laure • *INSERM UMRS-U919, Serine Proteases and Pathophysiology of the Neurovascular Unit, GIP Cyceron, Caen, France*

Le Béhot Audrey • *INSERM UMRS-U919, Serine Proteases and Pathophysiology of the Neurovascular Unit, GIP Cyceron, Caen, France*

Mustafa Balkaya • *Department of Physiology, Bahçeşehir University Istanbul, Istanbul, Turkey*

Ludmila Belayev, M.D. • *Department of Neurosurgery, Neurology and Neuroscience, LSUHSC Neuroscience Center, New Orleans, LA, USA*

René Bernard • *Department of Experimental Neurology, Charité-Universitätsmedizin Berlin, Charitéplatz, Berlin, Germany*

Fabio Canneva • *Preclinical-Experimental-Center, Experimental Therapy, Friedrich-Alexander-University Erlangen-Nürnberg, Erlangen, Germany*

Orset Cyrille • *INSERM UMRS-U919, Serine Proteases and Pathophysiology of the Neurovascular Unit, GIP Cyceron, Caen, France*

Adam Denes • *Faculty of Life Sciences, University of Manchester, Manchester, UK; Laboratory of Neuroimmunology, Institute of Experimental Medicine, Hungarian Academy of Sciences, Budapest, Hungary*

Vivien Denis • *INSERM UMRS-U919, Serine Proteases and Pathophysiology of the Neurovascular Unit, GIP Cyceron, Caen, France*

Ulrich Dirnagl • *Department of Experimental Neurology and Center for Stroke Research Berlin (CSB), Charité-Universitätsmedizin Berlin, Berlin, Germany; German Center for Neurodegenerative Diseases (DZNE) and German Center for Cardiovascular Diseases (DZHK), Berlin, Germany; Excellence Cluster NeuroCure, Berlin, Germany; Berlin Institute of Health, Berlin, Germany*

Thorsten R. Doeppner • *Department of Neurology, University of Duisburg-Essen, University Hospital Essen, Essen, Germany*

Matthias Endres • *Department of Neurology and Experimental Neurology, Center for Stroke Research Berlin, Charite Universitätsmedizin Berlin, Berlin, Germany*

Dirk M. Hermann • *Department of Neurology, University of Duisburg-Essen, University Hospital Essen, Essen, Germany*

David Howells • *School of Medicine, Medical Science Precinct, University of Tasmania, Hobart, TAS, Australia*

Jan Klohs • *Institute for Biomedical Engineering, University and ETH Zurich, Zurich, Switzerland*

Ute Lindauer • *Department of Neurosurgery, Translational Neurosurgery and Neurobiology, Universitätsklinikum Aachen, Aachen, Germany*

Malcolm R. Macleod • *Centre for Clinical Neurosciences, University of Edinburgh, Edinburgh, Scotland, UK; Collaborative Approach to Meta-Analysis and Review of Animal Data from Experimental Studies, Edinburgh, UK*

I. Mhairi Macrae • *Stroke and Brain Imaging, Institute of Neuroscience and Psychology, University of Glasgow, Glasgow, Scotland, UK*

Abraham Martín • *Molecular Imaging Unit, CIC biomaGUNE, San Sebastian, Spain*
Barry McColl • *The Roslin Institute & R(D)SVS, University of Edinburgh, Midlothian, UK*
Gerlinde A.S. Metz • *Department of Neuroscience, Canadian Centre for Behavioural Neuroscience, University of Lethbridge, Lethbridge, AB, Canada*
Anna M. Planas • *Department of Brain Ischemia and Neurodegeneration, Institute for Biomedical Research (IIBB), Consejo Superior de Investigaciones Científicas (CSIC), Barcelona, Spain; Institut de Investigaciones Biomédicas August Pi i Sunyer (IDIBAPS), Barcelona, Spain*
Anne-Christine Plank • *Preclinical-Experimental-Center, Experimental Therapy, Friedrich-Alexander-University Erlangen-Nürnberg, Erlangen, Germany*
Vincent Prinz • *Department of Neurology and Experimental Neurology, Center for Stroke Research Berlin, Charite Universitätsmedizin Berlin, Berlin, Germany; Department of Neurosurgery, Charite Universitätsmedizin Berlin, Berlin, Germany*
Pedro Ramos-Cabrer • *Molecular Imaging Unit, CIC biomaGUNE, San Sebastian, Spain; Ikerbasque, Basque Foundation for Science, Bilbao, Spain*
André Rex • *Department of Experimental Neurology and Center for Stroke Research Berlin (CSB), Charité-Universitätsmedizin Berlin, Charitéplatz, Berlin, Germany*
Nancy Rothwell • *Faculty of Life Sciences, University of Manchester, Manchester, UK*
Karsten Ruscher • *Laboratory for Experimental Brain Research, Wallenberg Neuroscience Center, Lund University, Lund, Sweden*
Maysami Samaneh • *Faculty of Life Sciences, The University of Manchester, Manchester, UK*
Emily Sena • *Centre for Clinical Neurosciences, University of Edinburgh, Edinburgh, Scotland, UK; Collaborative Approach to Meta-Analysis and Review of Animal Data from Experimental Studies, Edinburgh, UK*
Clemens Sommer • *Institute of Neuropathology, University Medical Center of the Johannes Gutenberg University Mainz, Mainz, Germany*
Richard J. Traystman • *Departments of Anesthesiology and Pharmacology, University of Colorado Denver, Aurora, CO, USA*
Anja Urbach • *Hans Berger Department of Neurology, University Hospital Jena, Jena, Germany*
Markus Vaas • *Institute for Biomedical Engineering, University and ETH Zurich, Zurich, Switzerland*
Stephan von Hörsten • *Preclinical-Experimental-Center, Experimental Therapy, Friedrich-Alexander-University Erlangen-Nürnberg, Erlangen, Germany*
Tadeusz Wieloch • *Laboratory for Experimental Brain Research, Wallenberg Neuroscience Center, Lund University, Lund, Sweden*
Otto W. Witte • *Hans Berger Department of Neurology, University Hospital Jena, Jena, Germany*

Chapter 1

From Bedside to Bench: How Clinical Reality Should Instruct Stroke Modeling

Dirk M. Hermann and Thorsten R. Doeppner

Abstract

Stroke is a complex and heterogeneous disease. Although animal models have provided valuable insight into its pathophysiology, the knowledge gained from animal experiments has not been fully transferred into clinical practice. Clinical trials testing for neuroprotective drugs have not been successful, and discussions questioning the usefulness of animal models in stroke research are still ongoing. In this chapter, we discuss conceptual strategies to overcome the gap between clinical practice and research.

Key words Focal cerebral ischemia, Animal model, Disease pathology, Risk factor

1 Introduction

Stroke is a sudden and life-changing event. Patients, on admission to hospital, often say that they feel like having been hit without warning out of the blue. Many considered themselves to be in good health prior to the event. The stroke physician knows that this is only rarely the case and that searching for the underlying cause of the disease and associated comorbidities is one of the main challenges of stroke therapy and secondary prevention. Research in animal models has made important contributions to stroke pathophysiology and the clinical management of stroke. However, the knowledge from clinical practice has not effectively been transferred into the modeling of the disease. Very young and healthy animals kept under standard laboratory conditions are used for animal experiments, even though three quarters of all strokes occur in people who are over 65 years old and commonly suffer from one or more chronic conditions. This discrepancy between clinical practice and stroke animal research has been blamed for the poor success in developing neuroprotective drugs from bench to bedside, and controversial discussions about the usefulness of stroke research in animal models have been ongoing. This chapter

Ulrich Dirnagl (ed.), *Rodent Models of Stroke*, Neuromethods, vol. 120,
DOI 10.1007/978-1-4939-5620-3_1,

emphasizes the need to improve the transfer from clinical practice to stroke animal research and presents conceptual strategies for overcoming the translation block.

2 Stroke in Clinical Practice

Stroke is a complex and heterogeneous disorder comprising different underlying pathologies. Patients reveal a broad variety in terms of etiology, clinical presentation, and risk factor profiles, so that for each patient an individual approach to therapy is required. Apart from rare single-gene disorders, stroke is considered a multifactorial disease. Genetic predisposition, life habits such as smoking and physical inactivity, and associated chronic diseases contribute to the risk of stroke. 85 % of all strokes are due to cerebral infarction, with the major part occurring in late middle and geriatric age. Many patients reveal one or more vascular risk factors—arterial hypertension, high cholesterol, diabetes, and obesity—which lead to vascular damage of small and large arteries. Hence, atherosclerosis of coronary and carotid arteries is highly prevalent among stroke patients, even in those with first-ever cerebrovascular events. With regard to therapy and secondary prevention, it is important for the patient to understand that although stroke is an acute event, it is the result of age-related damage to the cardiovascular system that has evolved over many decades. It is therefore neither surprising that patients suffer from recurrent events nor that the clinical presentation of stroke differs strongly between patients. Strokes vary in localization and size of the underlying brain lesion. They range from small lacunar infarcts of the subcortical white matter only a few millimeters in diameter up to large artery occlusions leading to malignant infarctions with secondary complications.

The clinical symptoms depend on the vascular territory affected by the occlusion. Motor dysfunction seems to be consistent with the site of the lesion, whereas in aphasia, the site of the brain lesion may differ between subjects due to a variable localization of the speech center. Additional neuropsychological symptoms such as apraxia, agnosia, and memory disturbance may complicate the recovery after stroke. Accordingly, it becomes evident that stroke is not a uniform entity and that understanding its heterogeneity is crucial.

3 Stroke Modeling in Animal Research

Stroke research has made significant progress in the past, and part of this is due to research in animal models. Clinicians and researchers have been provided with many valuable insights into the

underlying pathophysiological mechanisms involved in the disease, and new candidate targets of therapy have been identified. Despite this fact, for more than a decade, an intense debate about the limitations of animal models has been brought up time and time again because of the lack of concordance between clinical trials and animal studies. Many trials with promising neuroprotective compounds had been disappointing in humans, thus questioning the relevance of animal models for clinical benefit [1, 2]. Clinicians have always been skeptical about stroke animal experiments, claiming that animals are simply too different from the human species.

However, is this really the case? Fundamental biological processes such as cell survival and death have been strongly conserved throughout evolution. The molecular mechanisms underlying ischemic death are very similar in laboratory mice or rats and humans. In fact, the mechanisms of apoptosis, important in stroke injury, are even conserved in non-vertebrates such as the nematode *C. elegans* [3].

Stroke animal models have been established in many species, but among the most commonly used animals are small animals, in particular rodents. Small animals are easy to maintain, less costly, and less controversial from an ethical point of view than primate and higher mammals. Particularly mice are attractive for researchers for their genetic homogeneity and because their molecular biology is well understood. Furthermore, transgenic technologies can be applied easily in mice. Rodent stroke models have been found very useful in reconstructing crucial steps of neural death and cell repair.

For a correct interpretation of experimental outcome, however, differences in brain anatomy and physiology need to be taken into account. Rats and mice, for example, have very little white matter compared to humans, and their gray matter is not gyrated; neuroprotective and stroke studies thus always focus on implications for the gray matter [4]. Cerebral blood flow in mice is twice to three times higher than in human [5]. Some rodents have anomalies of the circle of Willis [6]. Collateral flow is poor in rodents, which results in severe ischemia when proximal occlusion models are used [5].

The experimental setup for animal models is homogeneous, controlling for the variables that may influence the experimental outcome to a maximal extent. Male animals are therefore usually used instead of females to avoid hormonal imbalance. Possible gender differences are widely disregarded. Inbred strains are used that fail to replicate the human genetic variety. Usually very young and healthy animals are used for the modeling of stroke. They are kept under standard laboratory conditions with little exercise [7] and no variation in diet. Some stroke studies have mimicked preexisting pathological conditions such as hyperlipidemia, diabetes, or hypertension. The knowledge about these conditions is still

relatively sparse. In the post-acute stroke phase, studies in hyperlipidemic or diabetic animals have provided evidence for attenuated or—in some studies—adverse restorative responses to therapy [8, 9], which underline that preexisting vascular disease should carefully be considered before studies in patients are initiated [10]. It is a general problem that the life span of a mouse or rat is short, too short to allow the natural development of the atherosclerosis encountered in humans of advanced age.

Thus, it becomes obvious that stroke is a disease entity characterized by heterogeneities on several levels, each of which influences disease processes. These include (1) the genetic constitution of patients, showing a higher variability than that of laboratory animals that are often taken from inbred strains, (2) the patients' life habits that are much less standardized than those of laboratory animals, (3) the risk factor profile. Patients are mostly of advanced age. Their vessels and peripheral organs have undergone multiple degenerative changes due to risk factors such as arterial hypertension, diabetes, and subclinical atherosclerosis. These conditions lead to a huge variability in disease processes. Heterogeneities in the manifestation of strokes affect (4) the localization and size of the lesion, (5) the severity of neurological deficits, and (6) the patient's ability to comply with the recommendations of his physician, to change life habits and take his medication regularly.

4 Linking Clinical Practice and Research in Stroke

Promising neuroprotective compounds have so far not been tested successfully in clinical trials, although they seemed to work in animal models. It is well established that there is a gap between clinical and animal experimental outcome in stroke, but how can this translation block be overcome?

Clinicians have criticized stroke animal research as being inaccessible to clinical practice because it does not replicate the clinical heterogeneity of the disease. While stroke models should be kept simple and easily reproducible, they should on the other hand be as close as possible to the clinical condition that they try to mimic. Although it is important to limit the variables in experimental planning, researchers need to focus more on the implications of age and important vascular risk factors in stroke modeling. Up to now, animal research has focused mainly on the underlying pathophysiology of cerebral ischemia and created ischemic models in healthy young animal brains. The neural apoptotic pathways evoked by a mature brain, however, are likely to be different from those evoked by a younger brain. It is thus questionable whether the basic scientific knowledge gained from animal experiments with very young and healthy animals can be simply transferred

into the clinical setting. Diet or exercise, for example, are two variables to consider when it comes to study design, as they have a big impact on the risk of stroke and can be easily applied in an experimental setting.

More communication between clinicians and scientists could only strengthen the effort to integrate scientific knowledge into clinical practice and avoid mistakes in study design. To be applicable to a wide variety of settings, animal research needs to be representative and generalizable. But how generalizable is data from animal research? Many animal studies consider just one species, commonly mice or rats, and findings from one species are not necessary applicable to other species.

A *stepwise upgrade* from rodents to primates, a kind of systematic proof of principle approach, would be a useful tool for verifying the findings from animal experiments. Currently, proof-of-concept strategies are only applied by pharmaceutical companies, but due to restricted financial resources, they are only used inconsistently. Unfortunately, this approach has found no access at all into investigator-driven research. The generalizability of data from stroke animal research would increase with such a conceptual strategy, particularly if the animal models mimicking thromboembolic strokes integrated clinical heterogeneity by using animals with preexisting vascular injury. In analogy to clinical trials, such proof-of-concept studies should also consider multicenter studies in animals [11], which should strongly increase the generalizability of the observations made.

Another major point to be considered is the time window of the disease. In animal models, the onset of ischemia is controlled, but clinical reality reflects a less homogeneous pattern. Many people who suffer a stroke are brought to hospital within hours of the clinical manifestation if the onset is very acute and help is immediately available. But if the symptoms of a stroke are not obvious or help is not available, admission to hospital is seriously delayed. It is therefore necessary to question whether the time windows that have been set in clinical practice are realistic. For example, the therapeutic window for the successful application of most neuroprotective agents has been shown to be very small, so that it is questionable whether these treatments can at all be successfully implemented in clinics. Drug research focusing on the post-stroke period could be more useful and applicable for a vast majority of stroke patients.

Stroke research in animal models has made useful contributions to understanding the disease, but clinical practice and animal research still seem to be too distant from each other. More effective effort to bring the two together will provide the steppingstone for overcoming the translation block.

References

1. Stroke Therapy Academic Industry Roundtable (1999) Recommendations for standards regarding preclinical neuroprotective and restorative drug development. Stroke 30:2752–2758
2. Fisher M, Feuerstein G, Howells DG, Hurn PD, Kent TA, Savitz SI, Lo EH (2009) Update of the Stroke Therapy Academic Industry Roundtable (STAIR) preclinical recommendations. Stroke 40:2244–2250
3. Danial NN, Korsmeyer SJ (2004) Cell death: critical control points. Cell 116:205–219
4. Hoyte L, Kaur J, Buchan AM (2004) Lost in translation: taking neuroprotection from animal models to clinical trials. Exp Neurol 188:200–204
5. Maeda K, Mies G, Olah L, Hossmann KA (2000) Quantitative measurement of local cerebral blood flow in the anesthetized mouse using intraperitoneal [14C]iodoantipyrine injection and final arterial heart blood sampling. J Cereb Blood Flow Metab 20:10–14
6. Dirnagl U, Iadecola C, Moskowitz MA (1999) Pathobiology of ischaemic stroke: an integrated view. Trends Neurosci 22:391–397
7. Gertz K, Priller J, Kronenberg G, Fink KB, Winter B, Schrock H, Ji S, Milosevic M, Harms C, Bohm M, Dirnagl U, Laufs U, Endres M (2006) Physical activity improves long-term stroke outcome via endothelial nitric oxide synthase-dependent augmentation of neovascularization and cerebral blood flow. Circ Res 99:1132–1140
8. Zechariah A, ElAli A, Hagemann N, Jin F, Doeppner TR, Helfrich I, Mies G, Hermann DM (2013) Hyperlipidemia attenuates vascular endothelial growth factor-induced angiogenesis, impairs cerebral blood flow, and disturbs stroke recovery via decreased pericyte coverage of brain endothelial cells. Arterioscler Thromb Vasc Biol 33:1561–1567
9. Chen J, Ye X, Yan T, Zhang C, Yang XP, Cui X, Cui Y, Zacharek A, Roberts C, Liu X, Dai X, Lu M, Chopp M (2011) Adverse effects of bone marrow stromal cell treatment of stroke in diabetic rats. Stroke 42:3551–3558
10. Hermann DM, Chopp M (2012) Promoting brain remodelling and plasticity for stroke recovery: therapeutic promise and potential pitfalls of clinical translation. Lancet Neurol 11:369–380
11. Dirnagl U, Fisher M (2012) International, multicenter randomized preclinical trials in translational stroke research: it's time to act. J Cereb Blood Flow Metab 32:933–935

Chapter 2

How to Avoid Bumping into the Translational Roadblock

Malcolm R. Macleod and Emily Sena

Abstract

Translating neuroprotective efficacy from animal studies to clinical trials in humans has been fraught with difficulty. This failure might be because animal studies were falsely positive or because clinical trials were falsely negative. Alternatively, animal studies as currently conducted may not model human stroke with sufficient fidelity to be a useful predictor of efficacy in clinical trials.

Here we focus on measures to improve the design, conduct, and reporting of animal studies to maximize both their internal and their external validity. These include, but are not limited to, randomization, allocation concealment, blinded assessment of outcome, sample size calculation, and measures to avoid publication bias. In addition, we give a brief introduction to systematic review and meta-analysis of data from animal experiments.

Key words Systematic review, Meta-analysis, Publication bias, Study quality, Validity, Experimental design, Randomization, Allocation concealment, Blinded assessment of outcome, Sample size calculation

1 Introduction

> …you will meet with several observations and experiments which, though communicated for true by candid authors or undistrusted eyewitnesses, or perhaps recommended by your own experience, may, upon further trial, disappoint your expectation, either not at all succeeding, or at least varying much from what you expected.—Robert Boyle (1693), Concerning the Unsuccessfulness of Experiments

Valid experiments are those which give appropriate descriptions of some biological truth in a system being studied. *Internal validity* relates to the extent to which the report of an individual experiment accurately describes what has happened in that model system. *External validity* relates to the extent to which the results from that model system can be generalized to predict what might happen, for instance, in another setting or in a group of patients with the disease being modeled in response to the drug being tested.

Ulrich Dirnagl (ed.), *Rodent Models of Stroke*, Neuromethods, vol. 120,
DOI 10.1007/978-1-4939-5620-3_2,

Stroke is one condition where, despite substantial efforts in the neuroscience community, translation of efficacy to humans has proved exceptionally difficult [1] The modeling of stroke in rodents usually involves measuring some outcome—be it a change in gene expression, an increase in protein phosphorylation, a volume of cerebral infarction, or a post-stroke behavior—and it may also involve determining a change in that outcome caused by an experimental intervention intended to test a mechanistic hypothesis. For our purposes here, we will concentrate on experiments testing the efficacy of candidate stroke drugs, but the same considerations apply to all hypothesis testing experiments modeling stroke. Exploratory research might also benefit from the same rigorous approach, but remember that every time you want to use an inferential statistical test, as opposed to descriptive statistics alone, you are by definition testing a hypothesis and not exploring!

1.1 The Validity of Individual Experiments

Following treatment, infarct volume and neurobehavioral score may improve, or worsen, or be unchanged. We hope that results from our experiments will reflect "biological truth," but of course this is not always the case. Measurement error and biological variability mean that our sample of animals can never describe completely what the outcome would be across all animals. These are random errors, and while they reduce the precision of the estimate of biological effect, they are as likely to underestimate effects as they are to overestimate effects. The likely scale of this random error can be estimated in preliminary experiments, and we can then predict how closely the results of an experiment of given size reflect the population response. This allows us to estimate how large an experiment should be to have a reasonable (specified) probability of detecting a treatment effect of a given size.

There are also, however, sources of nonrandom error (bias), which cause the estimate of effect consistently to be understated or, more usually in this context, overstated. These sources of bias include selection bias, performance bias, ascertainment bias, and attrition bias.

1.2 Selection Bias

The only difference between experimental groups should be the different treatments they receive. If there are consistent patterns in the way animals are allocated to groups, this may lead to additional, unwanted differences which might be responsible for any differences observed in outcome [2, 3]. For instance, if there is a standard allocation sequence, this may confound interpretation because the first animal from the cage is likely to be less anxious than later animals. Furthermore, while it is expected that the effectiveness of any intervention may be modulated by known factors (drug dose, time to treatment, comorbidities), effectiveness may also be altered by unknown or unidentified factors. The resulting selection biases can only be avoided if treatment group allocation is truly an explicitly random process, with each animal having an equal chance of entering any of the experimental groups.

1.3 Performance Bias

Knowledge of treatment group allocation might alter the way in which ischemia is induced or how the animal is managed in the recovery phase, including decisions about whether and when animals should be euthanized. These differences are probably due to subconscious and inadvertent changes in the behavior or practice of investigators and have been shown to be a potentially powerful source of bias [2, 3]. They can be avoided if the person conducting the experiment is unaware of treatment group allocation.

For example, more than half a century ago, Rosenthal had his student compare the performance of two cohorts of rats in the Skinner box (where outcome is recorded electronically); he explained that the first cohort had been bred over many generations to perform well in cognitive testing, while the second had been selectively bred for poor performance. Not only did the students confirm better initial performance in the maze-bright animals and enhanced learning, but they also found the maze-bright animals to be nicer to work with, and a number of students were bitten by maze-dull animals. In fact, his experiment had been on the students and not the rats, which were selected at random from the same cages in the same animal houses on the first day of the experiment. The only difference between the cohorts was in the minds of those handling them during the experiment, which must have been manifest in different experimenter behavior which in turn influenced animal behavior during automated cognitive testing.

1.4 Ascertainment Bias

Knowledge of treatment group may also confound the measurement of outcome [2, 3] It is only human nature that investigators wish their experiments to "work" and that they should desire that the intervention being tested should be found to have definite effects (negative or positive) rather than being neutral. This is partly because of the investment of time and energy in mounting the experiments, partly because the currency of science is publication and neutral studies are much less likely to be published, partly because the continuing funding of a project may depend on "positive" results, and partly because labs which are able reliably to report "positive" findings may be more likely to attract commercial funding.

1.5 Attrition Bias

Rodent stroke experiments only rarely report those animals which are excluded from the final analysis. Animals might be excluded for a number of reasons including a judgment that cerebral blood flow was not sufficiently reduced, that the induced neurobehavioral deficit was not sufficiently severe, or that the animal may die or be euthanized prior to the assessment of the outcome which is being reported. In some cases, the death of the most severely affected animals may cause a "healthy survivor" effect, so that if outcome is only measured in survivors, there may appear to be a treatment effect.

1.6 The Validity of Research Summaries

The decision to take a compound with promising animal data forward to clinical trial is usually based on a summary of the available animal data. The process of producing such research summaries is itself subject to sources of bias which may present an over-optimistic view of the prospects for success. These biases include publication bias, selective outcome reporting bias, false-positive bias, and selective citation bias.

1.7 Publication Bias

Where experiments are performed but remain unpublished, they are not usually available for inclusion in research summaries. If these unpublished experiments differ substantially in their outcomes from published work, conclusions drawn from published experiments may not reflect adequately the efficacy of the intervention being summarized. Statistical analysis of data derived from systematic reviews of stroke studies curated by the Collaborative Approach to Meta-Analysis and Review of Animal Data in Experimental Studies (CAMARADES) suggests that at around 20% of experiments remain unpublished and that this results—even following rigorous systematic review—in an overstatement of efficacy of 30% [4].

Publication bias is also important when studies have insufficient statistical power. For any given "true" underlying effect, experimental estimates of this effect will vary, some higher and some lower. Those estimating higher efficacy are more likely to achieve significance in statistical testing, and—in the presence of publication bias—these are more likely to be published. Where statistical power is low (and historically stroke experiments have been powered at 40% or lower), then even if there is a true effect, only 60% of studies will be published, and an analysis based on the 60% will give a higher estimate of efficacy than if all studies had been available for analysis. The lower the statistical power, the more pronounced the overstatement of efficacy.

1.8 Selective Outcome Reporting Bias

Where a number of different outcomes are measured but only some are published, conclusions drawn from the published literature will again mislead. For instance, an investigator may conduct five different neurobehavioral tests but only report those that reach the fashionable significance level of 5%. Again, it is possible to use statistical approaches to explore whether this is likely and this suggests that between 20 and 40% of outcomes measured in focal ischemia experiments are not reported in the resulting publication [5].

1.9 False-Positive (Low-Prior Probability) Bias

Where most studies are underpowered (as in the case for most reported rodent stroke experiments), the value of positive findings is reduced. The positive predictive value of a study in a given field—setting aside for the moment the issues of internal validity outlined above—is determined not just by the type I error-α but also by the type II error-β and the true proportion of positive

studies [6]. Where roughly 20% of all studies are truly positive, where the power is roughly 40%, and where the type I error is 5% (as in the case with rodent models of ischemia), the predictive value of positive studies is only 67%. That is, only two out of three statistically "positive" studies are truly positive.

Power 40%, $p<0.05$	Test positive	Test negative	Total
Truly positive	8%	12%	20%
Truly negative	4%	76%	80%
Sub total	12%: positive predictive value 67%	88%: negative predictive value 86%	100%

1.10 Selective Citation Bias

Stroke patients are not rodents and any assumptions of the translation of efficacy from rodents to man requires a leap of faith. However, it is important to systematically explore the limits to efficacy in animals and to make an informed judgment as to whether these are likely to affect efficacy adversely in man. Selective citation of individual studies supporting efficacy at low doses or late time points or in hypertensive animals are not substitute for a systematic summary of all experiments reporting efficacy at low doses or late time points or in hypertensive animals. Clinical trials generally require the recruitment of large numbers of patients, and industry usually seeks evidence for efficacy in as wide a potential market as possible. Because of these complimentary pressures, clinical trials have often recruited patients at extended time windows or with substantial comorbidities (typical of stroke patients) or where drug concentration at the site of their action is a fraction of that obtained in animal models. It is little surprise that so many of these trials in stroke have been neutral.

2 Materials

The implementation of Good Laboratory Practice in the context of middle cerebral artery occlusion requires no specific materials other than foresight, planning, and a computer with internet access. The UK National Centre for the Replacement, Refinement and Reduction of Animals in Research (NC3Rs) have recently launched a useful free online tool, Experimental Design Assistant (EDA), to guide researchers through the design of their experiments that use the minimum number of animals consistent with their scientific objectives, methods to reduce subjective bias, and appropriate statistical analysis (https://www.nc3rs.org.uk/experimental-design-assistant-eda). Resources are also available to support the design and conduct of multicenter animal studies (www.multi-part.org).

3 Methods

3.1 Before the Experiment

3.1.1 Systematic Review of Existing Data

It is probably unethical and it is certainly inefficient to unknowingly repeat work previously conducted by other groups unless explicitly for the purposes of replication, pilot studies, or as a positive control. You should therefore conduct a systematic review of existing published work to determine whether your hypothesis has been tested previously and what additional value your experiments can contribute. A simple approach to systematic review is given later.

3.1.2 Pilot Studies

Before conducting the planned experiments, it is important to show that you can reproducibly induce an infarct of the desired severity and behavioral deficit and to demonstrate that you can show a treatment effect where one is known beyond doubt to exist. Commonly, interventions such as hypothermia, MK801, or FK506 are used as this "positive control." This approach will also provide pilot data on the variance observed in the model in your own hands, important for sample size calculations (see below).

3.1.3 Protocol

Because of the multitude of opportunities for flexibility in study design and data analysis and the risk that analysis choices may in part be driven by emerging data, it is important for users of your research to be able to have confidence that your analysis was not in fact shaped by the data. You can achieve this by establishing a priori your experimental design, primary outcome measure, and statistical analysis plan. This can take the form of a study protocol or may be very brief indeed; the fundamental information required can be summarized in a PIPPHS statement—population (which animal, which lesion), intervention (what is the treatment), primary outcome measure, power (why the experiment is the size that it is), hypothesis, and statistical analysis plan. A dated version of the protocol can then be saved as a signed pdf, made available online (on an institutional website or using a third party platform such as Figshare), either open or closed, and made available at the time the work is submitted for review or published. Of course, things rarely go exactly as intended, but the discipline of having a public domain protocol means that you can explain what you changed and why, and the research user can judge whether this restricts the validity of your findings.

3.1.4 Sample Size Calculation

An assessment should be made of the size of the effect which the experiment should be able to detect (which may be the minimum biologically important effect). This is a matter of judgment; in some cases, a 10% difference in outcome might be considered biologically significant, while other experiments may set out to detect only much larger differences. For a simple two-group comparison, sample size calculations are reasonably straightforward and are enabled in most standard statistical packages. For more complex studies where statistical testing will use analysis of variance, specific

online tools are available (see [7] for an excellent online resource). Importantly, the estimate of variance used in these sample size calculations should be derived from your own pilot experiments rather than the lowest variance achieved in the best hands in your group. The sample size calculation can also make allowances for the proportion of animals which it is expected will be excluded from the final analysis.

3.1.5 Inclusion and Exclusion Criteria

Before the experiment starts, you should also establish clear and unambiguous rules about any inclusion criteria which will be applied, for instance, a prespecified decrease in perfusion detected with laser Doppler flowmetry or the development of neurologic impairment of a given severity. You should also establish rules about which animals will be excluded from the analysis (for instance, those which die spontaneously or are euthanized prior to completion of the experiment). Crucially, these rules should be applied without knowledge of treatment group allocation. Where the intervention being tested is delivered after the induction of ischemia, it is best if randomization (see below) occurs after the application of the inclusion criteria and is restricted to the pool of included animals.

3.2 During the Experiment

3.2.1 Randomization

Animals should be allocated to an experimental group by randomization. Experience from clinical trials suggests that manual methods of random allocation (coin toss, allocation in sealed envelopes) are open to subversion by enthusiastic researchers and so computerized methods are preferred. Random number tables or computerized random number generators (for instance, the MS Excel command RAND ()) allow a treatment allocation sequence to be generated, but it is important that the investigator have no prior knowledge of the allocation sequence (see blinding below). Alternatively, web-based randomization schedules are available at http://www.graphpad.com/quickcalcs/randomize1.cfm or http://www.randomization.com/. When using these, it is probably best to specify a blocked randomization design with block size set at least twice the number of experimental groups (so a 4-group experiment would have a block size of at least 8) .

3.2.2 Allocation Concealment

As far as is possible, the investigator responsible for the induction, maintenance, and reversal of ischemia and for decisions regarding the care of (including the early killing of) experimental animals should be unaware of the experimental group to which an animal belongs. For instance, you could have a colleague prepare and administer a drug or intervention or they could relabel or aliquot a drug which you have prepared. If this is done, it is better if the labeling is in the form of a reference number unique to each animal rather than simply relabel to A, B, C, etc. That is, it is better if the investigator does not know which animals belong to the same group, as they are likely to try to "guess" which group is which.

This is much more difficult if group allocation is not known. Similarly, the assessment of outcome should be carried out by someone who is not aware of treatment group allocation.

3.3 After the Experiment

3.3.1 Was Your Study Big Enough?

If large numbers of animals were excluded from the study or if the intervention was less effective than you had thought, it might be that your data will show the suggestion of an effect which is not statistically significant. Properly conducted pilot studies and sample size calculations based on reasonable estimates of efficacy will reduce this risk but will not remove it completely. If this becomes apparent after data have been analyzed, there is little that can be done except to repeat the experiment with adequate group sizes. However, before the data are analyzed, it is reasonable to add further animals to make up for exclusions as long as this can be done in a randomized fashion and with allocation concealment.

It is also possible to ask a colleague (usually a statistician) to examine unblinded data (send them outcome by animal reference number and have your colleague send them treatment grouping, although not necessarily the treatment associated with each grouping) to carry out a preliminary analysis. The purpose of this would be to ask them to make recommendations as to whether (1) there are significant differences between groups; (2) there may be a difference, and given the estimated effect size and variance, a further *x* animals per group would be required to give power of for example 80%; or (3) the differences between groups are such that the number of animals required makes further experiments futile [8]. Such an approach may also be used to conduct planned interim analyses, but if multiple such analyses are planned, the statistical methodology should take account of this.

3.3.2 Reporting Your Study

Your manuscript should describe how your work meets the principles outlined above, and specifically it should include details of the number of animals excluded and the reason for their exclusion. It should be set out according to the principles outlined in the international consensus statement on Good Laboratory Practice in the modeling of focal cerebral ischemia [9] and the ARRIVE guidelines [10].

Most academic institutions, funding organizations, and regulatory bodies require a commitment to publication and to data sharing, and you should make every effort to have your work published. Indeed, this is a component of the draft amendment to EU directive 86/609 on the approximation of laws, regulations, and administrative provisions of the member states regarding the protection of animals used for experimental and other scientific purposes. Work should be published within 3 years of being completed, and if this is not possible, then details should be posted on institutional websites. Outline details of unpublished work can also be submitted to CAMARADES at www.camarades.info, where they will be made available to those wishing to conduct systematic reviews.

3.4 Increasing the Validity of Research Summaries

3.4.1 Systematic Identification of Relevant Information

Narrative reviews are based on a selection of the available literature, often with the intention of supporting a particular point of view. Neutral studies are often published in journals of low impact, in languages other than English, and in conference abstracts rather than full publications. As such they may not be identified in superficial PubMed searches. If you really are trying to identify all relevant experiments in the public domain which might have been conducted using your compound, you should search the literature systematically. The availability of online datasets and conference abstracts has made this a simpler, faster process. A detailed description of the methodological approach is beyond the scope of this chapter, but see Vesterinen et al. [11] and Sena et al. [12].

3.4.2 Where to Search

PubMed (www.pubmed.com), ISI Web of Science (http://apps.isiknowledge.com), and EMBASE (www.embase.com). Access to PubMed is free, and most institutions purchase access to ISI WoS and EMBASE. Search filters are available for both PubMed and EMBASE to limit publications to those describing animal experiments (http://www.ncbi.nlm.nih.gov/pubmed/20551243 and http://www.ncbi.nlm.nih.gov/pubmed/23836850). For ISI WoS, ensure that you have checked to search conference proceedings as well as the Science Citation Index.

3.4.3 How to Search

Firstly, you should define the characteristics of publications which you wish to include—for instance, "studies reporting the efficacy of *compound* in animal models of focal cerebral ischemia, where the outcome is expressed as a change in infarct size or neurobehavioral score." Your search strategy should be designed to create two sets—firstly a set of all publications relating to your compound (using all known variations in the compound name) and secondly a set of publications relating to animal modeling of focal cerebral ischemia (we use {(stroke) OR (ischemia) OR (cerebrovascular) OR (middle cerebral artery) OR (MCA) OR (ACA) OR (anterior cerebral artery) OR (MCAO)}). Publications common to these sets are then identified and downloaded to your preferred reference management software.

3.4.4 Selecting Studies for Inclusion

The next step is to determine which publications meet your inclusion criteria and to exclude the rest. This process can be time-consuming, can be tedious, and is subject to error. These errors can be minimized if the task is carried out independently by two investigators, with disagreements resolved by discussion. The full text of remaining articles should then be retrieved.

3.5 Special Considerations in Creating a Research Synthesis

Qualitative summarizing of identified publications is straightforward. It may also be possible to carry out a quantitative summary (using meta-analysis), perhaps stratified for various characteristics of interest.

3.6 The Range of Circumstances Under Which Efficacy Has Been Tested

Efficacy at early time points and in healthy young animals may not be seen at the later (clinically more relevant) time points or in animals with (clinically relevant) comorbidities. Establishing efficacy under these circumstances is a crucial prelude to clinical trials. Similarly, it is important to demonstrate efficacy at concentrations obtained in human brain (if this is known). As a first step, simply tabulating the details of included studies can offer substantial insights:

1. **Study quality**: Given the known impact of the sources of bias described above, it is reasonable to establish the extent to which identified publications may be susceptible to bias. Key issues are randomization, allocation concealment, blinded assessment of outcome, and statement of a sample size calculation.
2. **Estimates of efficacy under various circumstances**: If there are sufficient data, it may be possible to explore the impact of, for instance, dose, time, or comorbidity, using normalized mean difference meta-analysis. A detailed understanding of statistics is not required, as online tools are available. The CAMARADES group have developed online tools which allow investigators to enter the details of publications and reported outcomes, which produce summary information or the range and quality of evidence, and which will perform normalized mean difference meta-analysis. Investigators wishing to use these tools should register at www.camarades.info. In large datasets, it is possible to explore the possible presence of publication bias using funnel plotting, Egger regression, or "trim and fill."

4 Future Developments

A key consideration, raised in Chap. 1, is the extent to which evidence from animal models of stroke can reliably be used as a premise for clinical trials. That is, can we improve their external validity? For many animal experiments, it appears that it is challenging even for findings in one lab to be replicated in a second [13] (Academy of Medical Sciences Report). One solution, which can also be brought to bear on the problems of internal validity described above, is for studies to be conducted across multiple laboratories, in multicenter animal studies, exploiting both known and unknown differences in laboratory practices. A clinical trialist might very reasonably have greater confidence in findings from animal research if this was seen in a much more diverse set of circumstances. This approach has already been used in stroke research [14], and the MultiPART consortium have established mechanisms—including a central project management, randomization, and outcome assessment platform—to assist such studies (www.multi-part.org).

5 Notes

Excellent is the enemy of good, and very few investigators adhere to all the considerations described above. We all try to do the best we can, and as we seek continually to improve the quality of our animal experiments, we should also be candid in where we have fallen short of these standards and how this might introduce bias to our conclusions. The stroke community has been at the forefront of dealing with such issues, which are widespread in in vivo research [15, 16].

References

1. O'Collins VE, Macleod MR, Donnan GA, Horky LL, van der Worp BH, Howells DW (2006) 1,026 experimental treatments in acute stroke. Ann Neurol 59(3):467–477
2. Macleod MR, van der Worp HB, Sena ES, Howells DW, Dirnagl U, Donnan GA (2008) Evidence for the efficacy of NXY-059 in experimental focal cerebral ischaemia is confounded by study quality. Stroke 39(10):2824–2829
3. van der Worp HB, Sena ES, Donnan GA, Howells DW, Macleod MR (2007) Hypothermia in animal models of acute ischaemic stroke: a systematic review and meta-analysis. Brain 130(Pt 12):3063–3074
4. Sena ES, van der Worp HB, Bath PM, Howells DW, Macleod MR (2010) Publication bias in reports of animal stroke studies leads to major overstatement of efficacy. PLoS Biol 8(3), e1000344
5. Tsilidis KK, Panagiotou OA, Sena ES, Aretouli E, Evangelou E, Howells DW, Al-Shahi SR, Macleod MR, Ioannidis JP (2013) Evaluation of excess significance bias in animal studies of neurological diseases. PLoS Biol 11(7), e1001609
6. Ioannidis JP (2005) Why most published research findings are false. PLoS Med 2(8), e124
7. Lenth RV, Java applets for power and sample size. Retrieved 31st March 2009, from http://www.stat.uiowa.edu/~rlenth/Power
8. Sena ES, Jeffreys AL, Cox SF, Sastra SA, Churilov L, Rewell S, Batchelor PE, Vander Worp HB, Macleod MR, Howells DW (2013) The benefit of hypothermia in experimental ischemic stroke is not affected by pethidine. Int J Stroke 8:180–185
9. Macleod MR, Fisher M, O'Collins V, Sena ES, Dirnagl U, Bath PM, Buchan A, van der Worp HB, Traystman RJ, Minematsu K, Donnan GA, Howells DW (2009) Reprint: good laboratory practice: preventing introduction of bias at the bench. Int J Stroke 4(1):3–5
10. Kilkenny C, Browne WJ, Cuthill IC, Emerson M, Altman DG (2010) Improving bioscience research reporting: the ARRIVE guidelines for reporting animal research. PLoS Biol 8(6), e1000412
11. Vesterinen HM, Sena ES, Egan KJ, Hirst TC, Churolov L, Currie GL, Antonic A, Howells DW, Macleod MR (2013) Meta-analysis of data from animal studies: a practical guide. J Neurosci Methods 221C:92–102. doi:10.1016/j.jneumeth.2013.09.010.:92-102
12. Sena ES, Currie GL, McCann SK, Macleod MR, Howells DW (2014) Systematic reviews and meta-analysis of preclinical studies: why perform them and how to appraise them critically. J Cereb Blood Flow Metab 34(5):737–742
13. Prinz F, Schlange T, Asadullah K (2011) Believe it or not: how much can we rely on published data on potential drug targets? Nat Rev Drug Discov 10(9):712
14. Llovera G, Hofmann K, Roth S, Salas-Perdomo A, Ferrer-Ferrer M, Perego C, Zanier ER, Mamrak U, Rex A, Party H, Agin V, Fauchon C, Orset C, Haelewyn B, De Simoni MG, Dirnagl U, Grittner U, Planas AM, Plesnila N, Vivien D, Liesz A (2015) Results of a preclinical randomized controlled multicenter trial (pRCT): Anti-CD49d treatment for acute brain ischemia. Sci Transl Med 7(299):299ra121
15. Macleod MR, Lawson McLean A, Kyriakopoulou A, Serghiou S, de Wilde A, Sherratt N, Hirst T, Hemblade R, Bahor Z, Nunes-Fonseca C, Potluru A, Thomson A, Baginskaite J, Egan K, Vesterinen H, Currie GL, Churilov L, Howells DW, Sena ES (2015) Correction: Risk of bias in reports of in vivo research: a focus for improvement. PLoS Biol 13(11):e1002301
16. Howells DW, Macleod MR (2013) Evidence-based translational medicine. Stroke 44(5):1466–1471

Chapter 3

Modeling Focal Cerebral Ischemia in Rodents: Introduction and Overview

Vincent Prinz and Matthias Endres

Abstract

The chapter provides an introduction and overview on the most widely used rodent models of focal cerebral ischemia, pointing out major characteristics of the respective model and basic differences between models. The specific models will be discussed in detail throughout the following chapters.

Key words Rodent models of stroke, Cerebral ischemia, Overview, Introduction, Advantages, Disadvantages

1 Introduction

Cardio- and cerebrovascular diseases are among the principal causes of mortality worldwide, with stroke following second after coronary heart disease [1]. However, mortality data conceal the true burden of stroke, as stroke is the number one cause of long-term disability in adulthood and exerts a tremendous socioeconomic impact [1, 2]. In the USA the direct and indirect costs have been estimated to consume about $62.7 billion per year (American Heart Association, 2007) [3]. In Asia stroke is even more frequent than myocardial infarction. Similarly, epidemiological evidence has demonstrated that cerebrovascular events are becoming more frequent than coronary vascular events (45 % vs. 42 %, respectively) in Europe as well. The relative incidence of cerebrovascular events compared with coronary events was 1.19 (95 % CI, 1.06–1.33) overall [4]. Because of the increasing life expectancy and elderly population, not only in industrialized but also in developing countries, the incidence of stroke is predicted to rise dramatically within the next few decades [1, 5]. Ischemic stroke accounts for 80 % of all strokes, while the incidence of primary hemorrhagic stroke is relatively low. Ischemic stroke probably is already and will continue to be the most challenging disease worldwide, underscoring the importance of further research in this field.

Ulrich Dirnagl (ed.), *Rodent Models of Stroke*, Neuromethods, vol. 120,
DOI 10.1007/978-1-4939-5620-3_3,

2 Cerebral Metabolism

Cerebral metabolism depends exclusively on oxygen and glucose, putting the brain into a unique and highly perilous situation compared to other organs. The brain consumes up to 75 l of molecular oxygen and 120 g of glucose daily. Although the brain accounts for only 2% of the total body weight, cerebral metabolism demands 20% of the total oxygen consumption and 20% of the total body perfusion. Even a short period of brain ischemia may result in irreversible structural damage. Variable "ischemia thresholds," which are region- and cell-type specific, determine whether a cell will survive the ischemic insult or die (see Table 1). "Ischemic preconditioning" might play a role in this context, as well [6].

3 Global vs. Focal Ischemia

There are two modes of cerebral ischemia, each with its own distinct mechanisms: global and focal ischemia (see also Table 2). *Global ischemia* develops after transient circulatory arrest with resuscitation or after near drowning. Within seconds, absolute cerebral blood flow is reduced from 8 to 0 ml/g/min. Loss of consciousness follows within 10 s, and EEG activity ceases after 30–40 s. Only a few minutes of global cerebral ischemia can cause irreversible cellular damage that becomes histologically apparent over days. Histologically, transient global ischemia results in delayed neuronal death, sparing glial cells (sometimes even associated with astrogliosis). As a rule of thumb, under normothermic conditions, 10 min of global ischemia is lethal in humans.

Focal ischemia (ischemic stroke) occurs after transient or permanent blood flow reduction in the territory of a cerebral artery and its branches. Typically, flow reduction is caused by the embolic or thrombotic occlusion of a cerebral artery (most frequently the middle cerebral artery, MCA) [7]. In contrast to

Table 1
Viability thresholds during cerebral ischemia

The following perfusion thresholds (ml/g/min) will result in	
Loss of protein synthesis	0.55 ml/g/min
Anaerobic glycolysis	0.35 ml/g/min
Synaptic release of transmitters (e.g., glutamate)	0.20 ml/g/min
Failure of energy metabolism	0.20 ml/g/min
Anoxic depolarization	0.15 ml/g/min

Table 2
Overview of animal models of cerebral ischemia and possible correlates to humans

Animal models of cerebral ischemia	Possible correlate to humans	Histological findings
Global ischemia		
A. Permanent (circulatory arrest)	Circulatory arrest, drowning, hanging	Brain swelling, cell death
B. Transient (four-vessel occlusion, transient circulatory arrest)	Circulatory arrest with resuscitation, near drowning	Delayed neuronal death, astrogliosis
Focal ischemia		
A. Permanent (e.g., MCAO)	Hemispheral stroke (thrombotic or embolic without recanalization or thrombolytic therapy) ("reperfusion injury")	Pannecrosis, inflammation
B. Transient (e.g., MCAO/reperfusion)	Stroke with spontaneous recanalization or thrombolytic therapy ("reperfusion injury")	Pannecrosis, inflammation
C. Mild (e.g., brief MCAO/reperfusion)	Transient ischemic attack?	Delayed neuronal death, astrogliosis

global ischemia, focal ischemia is characterized by the formation of a so-called ischemic penumbra. The penumbra is defined as the ischemic border zone which is functionally impaired and yet retains its structural integrity. While absolute blood flow in the ischemic core is reduced to levels <1 ml/g/min, regional blood flow in the penumbra remains at 2–4 ml/g/min. The extent of ischemia decreases with distance to the ischemic core. If reperfusion is established early, the expansion of the infarct core into the penumbra may be prevented. The "penumbra" is also referred to as "tissue at risk" [8]. The typical histological picture following focal cerebral ischemia is a pannecrosis including all cell types (neurons, astrocytes, oligodendrocytes, endothelial cells).

4 Animal Models of Focal Cerebral Ischemia

In the last decades, there has been an enormous increase in the pathophysiological understanding of brain ischemia [9, 10]. Experimental models of cerebral ischemia substantially contributed to elucidating the complex pathophysiological cascades triggered by ischemia. Periinfarct depolarization, excitotoxicity, inflammation, and apoptosis have been identified as the most relevant mediators of cell death following cerebral ischemia [9]. Moreover, important

concepts and treatments have been developed and validated using animal models of cerebral ischemia (e.g., "penumbra"/perfusion/diffusion mismatch, thrombolysis) [1, 8, 11].

Especially the combination of experimental stroke models and noninvasive imaging techniques (such as magnetic resonance imaging (MRI), positron emission tomography (PET), microcomputed tomography (CT), and optical imaging) enables the researcher to investigate hyperacute pathophysiological changes precipitated by the ischemic insult (see Chaps. 11 and 12). In addition to the spatiotemporal profile of the evolving lesion, changes resembling neuronal plasticity can be studied in a longitudinal manner and correlated to functional outcome, as well as histological findings.

Within the last years, further methodological advances have been made using the combination of cerebral ischemia models and in vivo microscopy via cranial windows. These new techniques allow investigators to analyze the neurovascular unit at the cellular and molecular level, with great analytic power and most particular in the living brain. Moreover in vivo microscopy imaging microcirculatory dynamics has revealed novel aspects of cerebral microvasculature function and angioarchitecture with significant pathophysiological relevance [12–15].

4.1 Animal Selection

Although stroke has been studied in different species (e.g., dogs, rabbits, monkeys), rodents are the most widely used. Besides practical advantages including relatively low costs for transportation, storage, and feeding, mice are especially useful because of the availability of unique strains that can be genetically engineered to over- or under-express selected target genes, allowing the researcher to investigate molecular mechanisms of stroke. In contrast to some rodents (e.g., gerbils), mice and rats form a complete circle of Willis, as do humans. However, certainly one disadvantage is that while the human brain is gyrencephalic, the morphology of the rodent brain is lissencephalic.

4.2 Model Selection

Human stroke is a highly variable disease, depending on the severity, duration, and localization of ischemia, as well as on comorbidities, age, and gender.

A number of different models of focal cerebral ischemia have been developed to mimic different conditions of human stroke (see Table 2). The translation of experimental findings from bench to bedside can only be successful, if the experimental model reflects essential criteria of the clinical situation (see Chap. 1). Basic research may demand different criteria than preclinical research evaluating neuroprotective strategies.

Certainly there is not one ideal model that mimics all criteria of human stroke. In the following sections, we want to give an overview of the basic characteristics of the different models and outline major advantages and disadvantages of the respective

technique, always keeping the clinical situation in mind (also see Table 3). A number of different models will be discussed in detail throughout the following chapters.

Experimental focal ischemia is most commonly studied using models of permanent or transient occlusion of an MCA as this is highly relevant to the clinical situation (vide supra). Basically, models of focal cerebral ischemia can be categorized into two groups: models requiring craniectomy and models retaining skull integrity. Within the two groups, the models can be divided into models leading to permanent and models leading to transient ischemia (see Fig. 1). Proximal and distal MCA occlusions also have to be distinguished.

Table 3
Overview: the table displays major advantages and disadvantages of commonly used rodent models of focal cerebral ischemia

Model	Advantage	Disadvantage
Thromboembolic	Close to human stroke, noninvasive, suitable for studying – Thrombolytic agents – Effects of thrombolysis and combined strategies – Reperfusion injury	High variability in lesion size, spontaneous recanalization
In situ thromboembolic	Close to human stroke, reproducible cortical lesions, suitable for studying – Thrombolytic agents – Effects of thrombolysis and combined strategies – Reperfusion injury	Requires craniectomy
Non-clot microsphere	Multifocal lesion	Heterogenous infarcts, high variability in lesion size, only permanent occlusion
Intraluminal monofilament	Reproducible lesions, transient and permanent ischemia, reperfusion injury, fast intervention, in-bore applicability, noninvasive, long-term studies after mild ischemia	High mortality rates using severe ischemia
Direct surgical	Controls the exact site of occlusion, reproducible lesions, high long-term survival rates	Requires craniectomy
Photothrombotic	Well-defined infarcted area, no craniectomy required	Basic differences in early lesion development
Endothelin-1	Application to different regions of the brain	Limited control of intensity and duration of ischemia

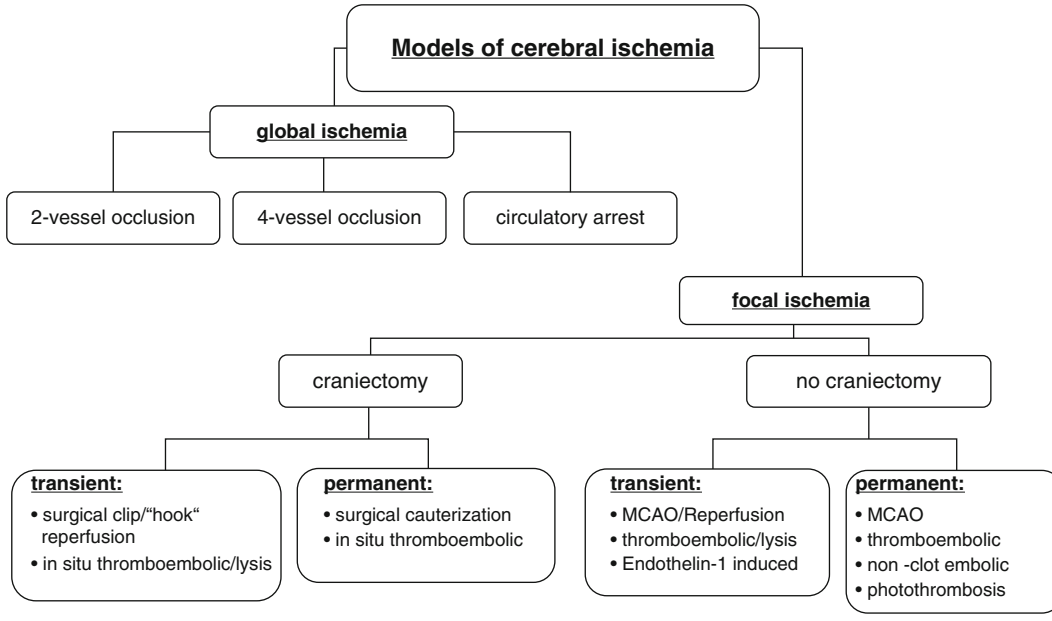

Fig. 1 Overview models of cerebral ischemia

4.2.1 Craniectomy vs. Non-craniectomy

In general, models requiring craniectomy (and incision of the dura) are considered more invasive and induce a number of confounding factors that vary highly from the clinical situation: (1) skull trauma, (2) changes in regional brain temperature, (3) intracranial pressure, and (4) blood–brain barrier (BBB) function are primarily affected.

Models which do not require craniectomy most often use an endovascular approach, typically accessing the cerebrovasculature via the common carotid artery (CCA) or the external carotid artery (ECA) (see Chap. 4). The surgeon needs to be very cautious to avoid injury of the vagal nerve, which runs right next to the common carotid artery. Although this technique is relatively noninvasive, advancing a filament intraluminally causes damage to the vascular endothelium.

The so-called *photothrombotic* model (see Chap. 7) produces a cortical infarction, while skull integrity is preserved. The systemic injection of a photodynamic dye (rose bengal) combined with focal irradiation of the cortex at a specific wavelength results in massive microvascular coagulation of the illuminated area [16]. The relevance of this model for stroke research, however, is debatable, given the emergence of basic differences in early lesion development.

Endothelin-1, a potent vasoconstrictor, can be used to induce ischemia (see Chap. 5) by direct application of endothelin-1 on the exposed MCA or cortex, requiring craniectomy. In addition endothelin-1 can be injected stereotactically next to a cerebral artery [17, 18]. Stereotactic injection is certainly less invasive and allows induction of ischemia in any desired region of the brain. However,

since the vasoconstrictive effect of endothelin-1 is dose dependent, the control over ischemic intensity and duration is limited. In addition some findings have suggested neurorestorative effects of endothelin-1 [19, 20].

4.2.2 Permanent vs. Transient Ischemia

Models resulting in permanent ischemia mimic clinical stroke without reperfusion, whereas transient models reflect human stroke with therapy-induced or spontaneous reperfusion, which account for the majority of all stroke cases. In some ways, the reperfused brain imitates restoration of blood flow in humans after spontaneous lysis of a thromboembolic clot. During reperfusion, NO generation and free radical production are particularly pronounced and contribute to "reperfusion injury" [21, 22]. Following longer periods of ischemia, reperfusion is incomplete as a result of microvascular occlusion; this has been termed the "no-reflow phenomenon" [23]. Since free radicals and NO promote apoptotic cell death, models of transient ischemia have become very useful for studying programmed cell death in vivo, which may particularly apply for models of "mild ischemia" [24, 25]. However, reperfusion after clot lysis is certainly more complex than an on-and-off phenomenon modeled by placement and retraction of a clip, suture, or intravascular filament. While opening a vascular clip or withdrawal of an intraluminal filament causes instant reperfusion, induced thrombolysis or spontaneous reperfusion restores blood flow more slowly.

In general, the infarct size directly depends on the duration of ischemia and the location of the occlusion. Sixty to ninety minutes of proximal intraluminal MCAO (vide infra) will cause a pannecrosis, involving the lateral striatum (caudoputamen) and the frontoparietal cortex. In this case, ischemia is severe and is thus associated with high mortality rates, making statistical evaluation of lesion size rather difficult [26]. In addition, lesions that include the hypothalamus may result in hyperthermia, which further affects evolution of the ischemic lesion (see also Chap. 19). In contrast, ischemia times below 60 min will lead to subcortical infarction, with selective neuronal death and long survival times [27, 28]. Ischemic lesions following distal MCAO are in general smaller and associated with high long-term survival rates.

4.2.3 Models of Clot Embolism

Most human strokes are of thromboembolic origin; thromboembolic animal models may therefore mimic human stroke more closely than other stroke models. In addition, thromboembolic models allow investigation of potential neurotoxic effects of rtPA, as has been suggested by experimental studies [29, 30]. However in human stroke, only about 5 % of all stroke patients will be eligible for rtPA treatment.

Models of clot embolism (see Chap. 6) are highly dependent on clot preparation and clot placement [31]. Besides the size and placement, the composition of the clot, either fibrin poor (red) or

fibrin rich (white), largely determines the speed of spontaneous reperfusion or rtPA-induced lysis. While surgical or intraluminal MCA occlusion allows highly reproducible infarction of the MCA territory, embolic models, injecting autologous blood clots into extracranial arteries to occlude more distal intracranial arteries, show high variability in lesion size and location.

The model of in situ thromboembolic stroke uses microinjection of murine thrombin to trigger in situ clot formation. This model shows reproducible cortical lesion sizes which can be reduced with rtPA treatment [32]. However, in contrast to other embolic models, the model requires craniectomy.

Besides the use of autologous clots, many compounds have been applied to induce ischemia by injection of artificial embolic material into the CCA or ICA. These models show a rather heterogenous and multifocal lesion development which progresses slower in comparison to other models [33].

4.2.4 Proximal vs. Distal Occlusion of the MCA

Occlusion of the MCA at its origin, *proximal MCAO*, disrupts blood flow to the vascular territory of the MCA comprising the lenticulostriate arteries which supply the basal ganglia (see Chap. 4). Since the lenticulostriate arteries are end arteries, the basal ganglia are exposed to severe ischemia. In contrast the cortex shows a gradual reduction in blood flow, which decreases from the periphery to the center of the vascular MCA territory, as cortical MCA branches have collaterals with contiguous vascular territories [34]. Proximal MCA occlusion can be induced by an intraluminal suture [35] (so-called filament model) and causes injury to cortex and deeper brain structures (basal ganglia) (please see Fig. 3.2).

Distal MCA occlusion (e.g., the so-called "Brint" model [36]) is usually produced by transcranial placement of a vascular clip on a distal MCA branch or by electrocauterization (see Chap. 5). Occlusion of the distal MCA typically spares the striatum and involves primarily the neocortex. The more distal the MCA occlusion is, the smaller the infarcted tissue will be. Pannecrosis develops in the territory supplied by the respective artery with glial and endothelial cell death (see Chap. 15).

Cerebral ischemia following proximal middle cerebral artery (MCA) occlusion may induce delayed neuronal cell death in non-ischemic brain regions remote from the primary lesion with histopathological changes occurring as late as days to weeks after the initial ischemic event [11, 37]. This phenomenon, also termed "exofocal postischemic neuronal death (EPND)," has been associated with impaired neurological function and the development of vascular Parkinson's disease [38–40]. Due to its delayed occurrence and prolonged development, EPND is discussed as a promising new target for neuroprotective treatments. Thus novel therapeutic approaches for the prevention of EPND following stroke may contribute to improved stroke outcomes [28].

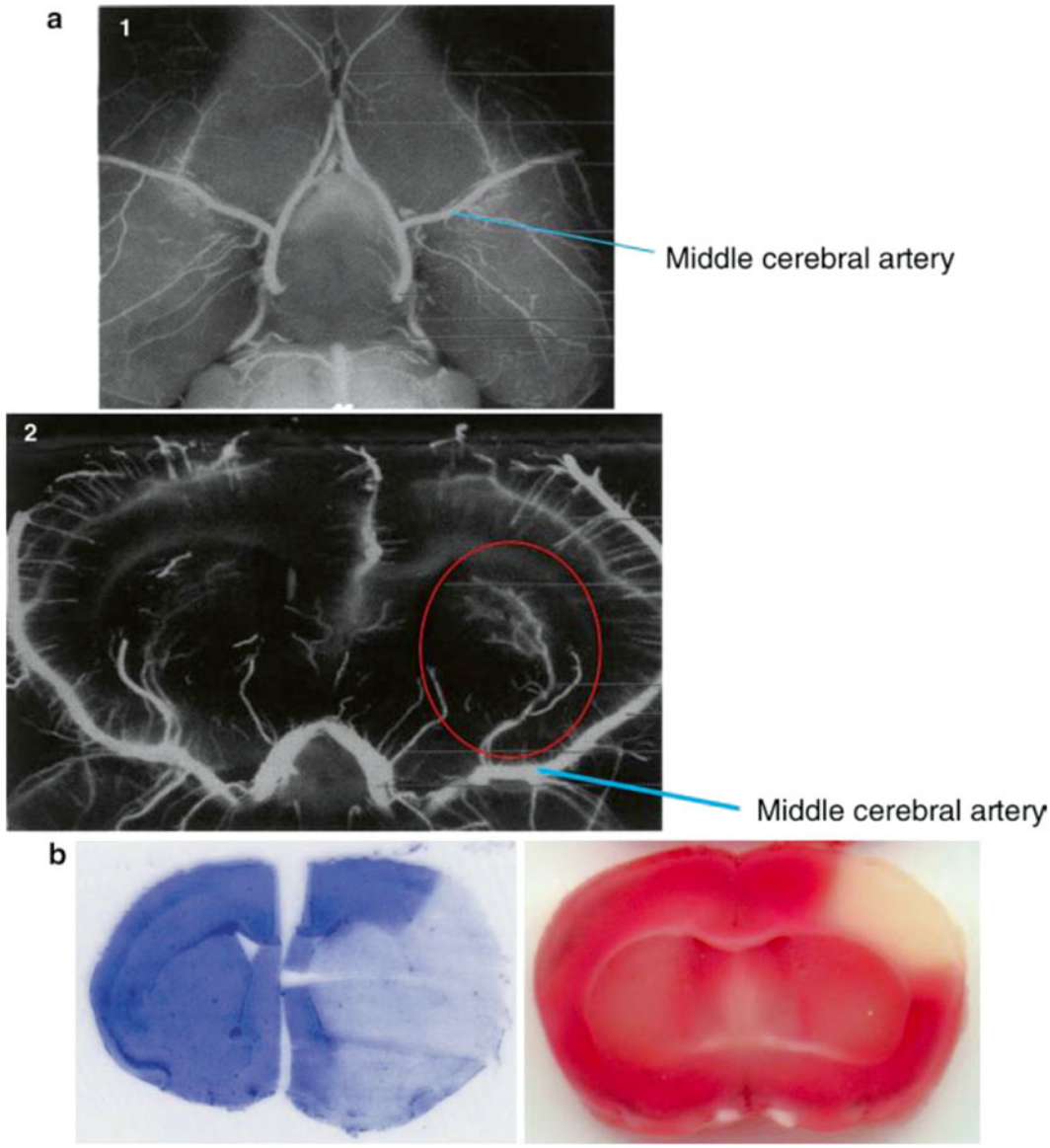

Fig. 2 (**a**) Fluorescein microangiography of the cerebral vasculature: 1: showing the Circle of Willis, 2: axial section at the level of the striatum, the lenticulostriate arteries (circled) are supplied by the MCA. (**b**) Proximal vs. distal MCAO, upper picture: Hematoxylin staining, following 60 min. MCAO and 23 h of reperfusion, lower picture: TTC staining, following permanent distal MCAO and 23 h of reperfusion. The pale areas represent the lesioned tissue. (This picture was kindly provided by Dr T. Malm, A.I. Virtanen-Institute for Molecular Sciences, University of Kuopio)

References

1. Donnan GA, Fisher M, Macleod M, Davis SM (2008) Stroke. Lancet 371(9624):1612–1623
2. Meairs S, Wahlgren N, Dirnagl U, Lindvall O, Rothwell P, Baron J-C et al (2006) Stroke research priorities for the next decade—a representative view of the European scientific community. Cerebrovasc Dis 22:75–82
3. Rosamond W, Flegal K, Friday G, Furie K, Go A, Greenlund K et al (2007) Heart disease and stroke statistics—2007 update: a report from the American Heart Association Statistics Committee and Stroke Statistics Subcommittee. Circulation 115(5):e69–e171
4. Rothwell PM, Coull AJ, Silver LE, Fairhead JF, Giles MF, Lovelock CE et al (2005) Population-based study of event-rate, incidence, case fatality, and mortality for all acute vascular events in all arterial territories (Oxford Vascular Study). Lancet 366(9499):1773–1783
5. Johnston SC, Mendis S, Mathers CD (2009) Global variation in stroke burden and mortality: estimates from monitoring, surveillance, and modelling. Lancet Neurol 8(4):345–354
6. Sommer C (2009) Neuronal plasticity after ischemic preconditioning and TIA-like preconditioning ischemic periods. Acta Neuropathol 117(5):511–523
7. Bogousslavsky J, Van Melle G, Regli F (1988) The Lausanne Stroke Registry: analysis of 1,000 consecutive patients with first stroke. Stroke 19(9):1083–1092
8. Ebinger M, De Silva DA, Christensen S, Parsons MW, Markus R, Donnan GA et al (2009) Imaging the penumbra - strategies to detect tissue at risk after ischemic stroke. J Clin Neurosci 16(2):178–187
9. Dirnagl U, Iadecola C, Moskowitz MA (1999) Pathobiology of ischaemic stroke: an integrated view. Trends Neurosci 22(9):391–397
10. Moskowitz MA, Lo EH, Iadecola C (2010) The science of stroke: mechanisms in search of treatments. Neuron 67(2):181–198
11. Dirnagl U, Endres M (2014) Found in translation: preclinical stroke research predicts human pathophysiology, clinical phenotypes, and therapeutic outcomes. Stroke 45:1510
12. Iadecola C, Dirnagl U (2013) The microcirculation—fantastic voyage: introduction. Stroke 44(6 Suppl 1):S83
13. Shih AY, Mateo C, Drew PJ, Tsai PS, Kleinfeld D (2012) A polished and reinforced thinned-skull window for long-term imaging of the mouse brain. J Vis Exp 61:3742
14. Shih AY, Driscoll JD, Drew PJ, Nishimura N, Schaffer CB, Kleinfeld D (2012) Two-photon microscopy as a tool to study blood flow and neurovascular coupling in the rodent brain. J Cereb Blood Flow Metab 32(7):1277–1309
15. Blinder P, Tsai PS, Kaufhold JP, Knutsen PM, Suhl H, Kleinfeld D (2013) The cortical angiome: an interconnected vascular network with noncolumnar patterns of blood flow. Nat Neurosci 16(7):889–897
16. Watson BD, Dietrich WD, Busto R, Wachtel MS, Ginsberg MD (1985) Induction of reproducible brain infarction by photochemically initiated thrombosis. Ann Neurol 17(5):497–504
17. Sharkey J, Ritchie IM, Kelly PA (1993) Perivascular microapplication of endothelin-1: a new model of focal cerebral ischaemia in the rat. J Cereb Blood Flow Metab 13(5):865–871
18. Sharkey J, Butcher SP (1995) Characterisation of an experimental model of stroke produced by intracerebral microinjection of endothelin-1 adjacent to the rat middle cerebral artery. J Neurosci Methods 60(1–2):125–131
19. Nakagomi S, Kiryu-Seo S, Kiyama H (2000) Endothelin-converting enzymes and endothelin receptor B messenger RNAs are expressed in different neural cell species and these messenger RNAs are coordinately induced in neurons and astrocytes respectively following nerve injury. Neuroscience 101(2):441–449
20. Koyama Y, Baba A, Matsuda T (2005) Endothelins stimulate the expression of neurotrophin-3 in rat brain and rat cultured astrocytes. Neuroscience 136(2):425–433
21. Warner DS, Sheng H, Batinić-Haberle I (2004) Oxidants, antioxidants and the ischemic brain. J Exp Biol 207(Pt 18):3221–3231
22. Hallenbeck JM, Dutka AJ (1990) Background review and current concepts of reperfusion injury. Arch Neurol 47(11):1245–1254
23. del Zoppo GJ, Mabuchi T (2003) Cerebral microvessel responses to focal ischemia. J Cereb Blood Flow Metab 23(8):879–894
24. Endres M, Namura S, Shimizu-Sasamata M, Waeber C, Zhang L, Gómez-Isla T et al (1998) Attenuation of delayed neuronal death after mild focal ischemia in mice by inhibition of the caspase family. J Cereb Blood Flow Metab 18(3):238–247
25. Bonfoco E, Krainc D, Ankarcrona M, Nicotera P, Lipton SA (1995) Apoptosis and necrosis: two distinct events induced, respectively, by mild and intense insults with N-methyl-D-aspartate or nitric oxide/superoxide in cortical cell cultures. Proc Natl Acad Sci U S A 92(16):7162–7166
26. Meisel C, Prass K, Braun J, Victorov I, Wolf T, Megow D et al (2004) Preventive antibacterial

treatment improves the general medical and neurological outcome in a mouse model of stroke. Stroke 35(1):2–6

27. Winter B, Bert B, Fink H, Dirnagl U, Endres M (2004) Dysexecutive syndrome after mild cerebral ischemia? Mice learn normally but have deficits in strategy switching. Stroke 35(1):191–195
28. Baron J-C, Yamauchi H, Fujioka M, Endres M (2014) Selective neuronal loss in ischemic stroke and cerebrovascular disease. J Cereb Blood Flow Metab 34(1):2–18
29. Nicole O, Docagne F, Ali C, Margaill I, Carmeliet P, MacKenzie ET et al (2001) The proteolytic activity of tissue-plasminogen activator enhances NMDA receptor-mediated signaling. Nat Med 7(1):59–64
30. Benchenane K, Castel H, Boulouard M, Bluthé R, Fernandez-Monreal M, Roussel BD et al (2007) Anti-NR1 N-terminal-domain vaccination unmasks the crucial action of tPA on NMDA-receptor-mediated toxicity and spatial memory. J Cell Sci 120(Pt 4):578–585
31. Dinapoli VA, Rosen CL, Nagamine T, Crocco T (2006) Selective MCA occlusion: a precise embolic stroke model. J Neurosci Methods 154(1–2):233–238
32. Orset C, Macrez R, Young AR, Panthou D, Angles-Cano E, Maubert E et al (2007) Mouse model of in situ thromboembolic stroke and reperfusion. Stroke 38(10):2771–2778
33. Mayzel-Oreg O, Omae T, Kazemi M, Li F, Fisher M, Cohen Y et al (2004) Microsphere-induced embolic stroke: an MRI study. Magn Reson Med 51(6):1232–1238
34. Hossmann K-A (2008) Cerebral ischemia: models, methods and outcomes. Neuropharmacology 55(3):257–270
35. Longa EZ, Weinstein PR, Carlson S, Cummins R (1989) Reversible middle cerebral artery occlusion without craniectomy in rats. Stroke 20(1):84–91
36. Tamura A, Graham DI, McCulloch J, Teasdale GM (1981) Focal cerebral ischaemia in the rat: 1. Description of technique and early neuropathological consequences following middle cerebral artery occlusion. J Cereb Blood Flow Metab 1(1):53–60
37. Zhao F, Kuroiwa T, Miyasaka N, Nagaoka T, Nakane M, Tamura A et al (2001) Characteristic changes in T(2)-value, apparent diffusion coefficient, and ultrastructure of substantia nigra evolving exofocal postischemic neuronal death in rats. Brain Res 895(1–2):238–244
38. Rodriguez-Grande B, Blackabey V, Gittens B, Pinteaux E, Denes A (2013) Loss of substance P and inflammation precede delayed neurodegeneration in the substantia nigra after cerebral ischemia. Brain Behav Immun 29:51–61
39. Kronenberg G, Balkaya M, Prinz V, Gertz K, Ji S, Kirste I et al (2012) Exofocal dopaminergic degeneration as antidepressant target in mouse model of poststroke depression. Biol Psychiatry 72(4):273–281
40. Zhang J, Zhang Y, Xing S, Liang Z, Zeng J (2012) Secondary neurodegeneration in remote regions after focal cerebral infarction: a new target for stroke management? Stroke 43(6):1700–1705

Chapter 4

Focal Cerebral Ischemia in the Mouse and Rat by Intraluminal Suture

Ludmila Belayev, Matthias Endres, and Vincent Prinz

Abstract

Filamentous occlusion of the middle cerebral artery (MCA) is probably the most frequently used model in experimental stroke research. It results in reproducible lesions in the cortex and striatum and can be used to induce both permanent and transient MCA occlusion (MCAo). It allows for the study of both acute stroke treatment as well as interventions that target stroke recovery. This chapter gives a practical "hands-on" approach for performing this model in mice and rats.

Key words Brain ischemia, Middle cerebral artery occlusion, Poly-L-lysine, Silicon, Filament model

1 Introduction

Proximal occlusion of the middle cerebral artery (MCA) via the intraluminal suture technique (so-called "filament" or "suture" model) is the most commonly used model in experimental stroke research and was initially developed in rats by Koizumi and co-workers in 1986 [1].

Subsequently, Longa et al. reported a variation of this method and stated that their technique reliably produced regional infarcts [2]. The Koizumi group used a silicone-coated 4-0 nylon surgical thread (diameter, 0.25–0.30 mm), while the Longa group used a 4-0 uncoated nylon thread with a tip that was blunted by heating near a flame. Both groups showed that reperfusion occurred when the threads were removed. As discussed by Laing et al., the method of Longa et al. has relatively low reproducibility, with a success rate in achieving infarction of only 56%, compared with 93% in the model of Koizumi et al. [3] Unsuccessful outcomes consisted of animals without neurological deficits and animals in which subarachnoid hemorrhage was caused by rupture of the intracranial ICA.

Since then, several modifications of the initial model have been developed [2, 4]. In addition, the model has been transferred to

Ulrich Dirnagl (ed.), *Rodent Models of Stroke*, Neuromethods, vol. 120,
DOI 10.1007/978-1-4939-5620-3_4, © Springer Science+Business Media New York 2016

mice [5]. Modifications of the model consist predominantly in the use of different filaments and filament coating, e.g., with silicone or poly-L-lysine, to reduce the incidence of subarachnoid hemorrhage (SAH) or premature reperfusion [6].

The procedure consists of inserting a nylon filament into the internal carotid artery (ICA) and then advancing it intracranially to block MCA blood flow (Fig. 1). The suture can be introduced either retrogradely through the external carotid artery (ECA) or directly into the common carotid artery (CCA). The suture is typically advanced in a distance of 20–22 mm from the carotid bifurcation in rats or 10–12 mm in mice, effectively occluding collateral circulation from the anterior communicating arteries. After different durations of the MCAO, the filament can be carefully removed to produce reperfusion. Permanent occlusion can be achieved by leaving the suture in place and then tying it at the stump of the external carotid artery.

This reperfusion model may imitate the restoration of blood flow after spontaneous lysis or therapeutically induced lysis in human stroke. During reperfusion, nitric oxide (NO) generation and free radical production are particularly pronounced and may contribute to "reperfusion injury" [7, 8]. Since free radicals and NO further apoptotic cell death [9], models of transient ischemia have become very useful for studying programmed cell death in vivo, which may particularly apply for models of "mild ischemia" [10]. However, clot lysis is certainly more complex than an on-off

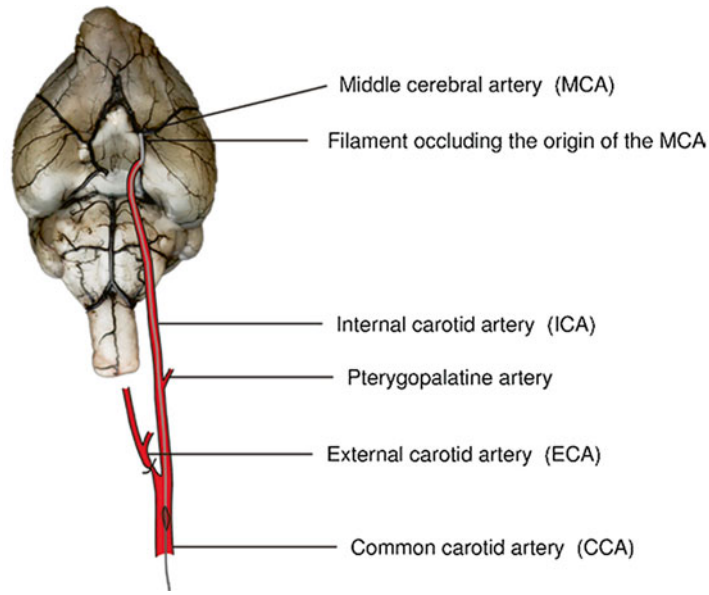

Fig. 1 Filamentous occlusion of the MCAO. The illustration was kindly provided by Dr. Nils Hecht, Department of Neurosurgery, Charité, Universitätsmedizin, Berlin

phenomenon as modeled by placement and retraction of an intravascular filament. While the retraction of an intravascular filament causes instant reperfusion, thrombolysis-induced or spontaneous reperfusion restores blood flow more slowly [11].

The intraluminal MCAo model provides the advantage of reproducible transient or permanent ischemia of the MCA territory in a relatively noninvasive manner. Nevertheless, advancing a filament intraluminally might cause direct damage to the vascular endothelium.

The reproducibility of lesion size is affected by a number of specific factors, such as the diameter of the suture, insertion length of the suture, as well as the coating of the thread [4, 12, 13]. Silicone-coated filaments have been shown to consistently produce larger and more reproducible lesions compared to uncoated sutures. The use of a nylon suture coated with poly-L-lysine (to increase adhesion to the vascular wall) leads to almost 100% incidence of ischemic damage [6]. The use of uncoated sutures causes a higher incidence of subarachnoid hemorrhage [12]. We strongly recommend using coated filaments. Modification of the model allows intraluminal MCAo to be carried out within a magnetic resonance imaging device ("in-bore MCAo model"), thus permitting very early and continuous observation of hyperacute pathophysiological changes [14, 15].

In contrast to *distal occlusion* of the MCA (Chap. 5), *proximal MCAo* interrupts blood flow to the vascular territory of the MCA, comprising the lenticulo-striate arteries that supply the basal ganglia. Since the lenticulo-striate arteries are end arteries, the basal ganglia are exposed to severe ischemia. Contrariwise, the cortex shows a gradual reduction in blood flow which decreases from the periphery to the center of the vascular MCA territory, as cortical MCA branches form collaterals with contiguous vascular territories [11]. Thus, in proximal MCAo, striatal infarction constitutes the ischemic core, with rapidly occurring pannecrosis, whereas the cortical lesion reflects "penumbra-like" characteristics, with progressive neuronal cell death [16, 17]. If recirculation is established early, the expansion of the infarct core from the striatum to the cortex may be prevented.

Variable durations of ischemia and reperfusion have been reported in mouse models of transient MCAo, with ischemic times ranging from 10 min to 3 h and reperfusion times ranging from 3 to 48 h [18, 19]. Most researchers agree that at least a 2-h period of MCAo is necessary to produce a reliable infarct [19, 20]. Different ischemia duration with a filament coated with poly-L-lysine was compared followed by 24 h of reperfusion [6]. Mice with 30-min MCAo developed significantly smaller infarcts compared to 180-min MCAo animals (Fig. 2). By contrast, animals subjected to 60-min, 120-min, or 180-min insults showed very similar infarct volumes, and there were no significant differences between groups (Fig. 2). However, in this case, ischemia is severe and associated with massive brain swelling, pronounced neurological deficits, and high mortality [21].

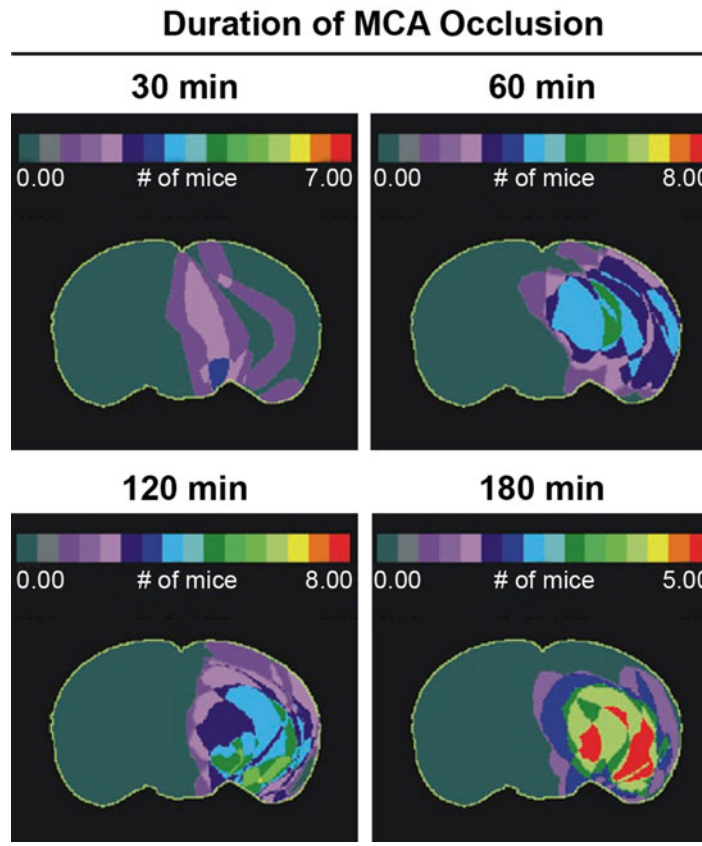

Fig. 2 Computer-generated maps depicting the frequency of histological infarction in mice with 30-, 60-, 120-, and 180-min MCAO followed by 24-h recirculation (bregma level −1.94 mm). In mice with 30-min MCAO, the infarctive lesion tended to be inconsistent and involved chiefly portions of the striatum and lateral septum. Increasing durations of MCAo led to more consistent involvement of frontoparietal somatosensory cortex, dorsolateral and central portions of striatum, ventral thalamus, hippocampus, and rostral midbrain

In addition, larger lesions that include the hypothalamus may result in thermal dysregulation, which further affects the evolution of the ischemic lesion [22]. Hypothalamic injury has been described in rats and mice. Interestingly, while in rats, it has been associated with a hyperthermic response [23]; mice tend to respond with hypothermia as they lose temperature in the postoperative period due to reduced activity and their large surface area/volume [22] (see Chap. 19). Therefore, temperature monitoring and control in the intra- and perioperative period is very important to reducing variability of lesion size.

In the following sections, the MCAo model for mice and rats will be described step by step.

2 MCAO in Mice Using a Silicon-Coated Monofilament

Filamentous occlusion of the MCA is the most commonly used stroke model in mice.

As in rats, it provides the advantages of highly reproducible transient or permanent ischemia, thus obviating the need for craniectomy. Moreover, the filament model is easy to perform and relatively noninvasive, thus limiting operation time. A skilled surgeon can induce MCAO within less than 10 min.

2.1 Materials and Supplies Using Silicon-Coated Monofilament

1. Filament USP 4/0 or 6/0 Suprama (for example)
2. 8.0 nylon monofilament for coating with Xantopren M and Activator NF Optosil (e.g., Xantopren M Mucosa Heraeus Kulzer (Germany) or Activator NF Optosil Xantropren (Germany))
3. Adhesive glue (e.g., Cyanoacrylate Weicon) or surgical needle and thread for suture
4. Equipment for use with volatile anesthetics
5. Dissecting microscope (max. ×40)
6. Temperature feedback-controlled heating plate
7. Forceps (tip 0.05 mm × 0.02 mm)
8. Scissors
9. Microvascular clip
10. Vascular scissors
11. Heated recovery cage

2.2 Preparation of the Filament

Silicone coating of the filament is easy to describe but very difficult to do. It takes a lot of practice to find the ideal proportion of activator (hardener) with silicone and the optimal shape. To minimize endothelial damage and vascular rupture with subsequent SAH, it is very important that the tip of the filament be evenly coated with silicone.

2.3 Filamentous MCAo in Mice: Surgical Procedure Step by Step

1. Anesthetize mice for induction with 1.5% (vol/vol) isoflurane and maintain them in 1.0% isoflurane in 69% nitrous oxide (N_2O) and 30% oxygen (O_2) administered via a facemask. Mice must be placed in supine position. Core temperature is controlled and kept constant at 36.5 ± 0.5 °C using a temperature control feedback unit [22].
2. Make a midline neck incision and dissect the soft tissues, exposing the trachea to the surgeon.
3. Carefully dissect the CCA from the surrounding tissue and nerves (CAVE: avoid harming the vagal nerve) and make a knot using a 6.0/7.0 suture.
4. Expose the ECA and make a second knot (6.0/7.0 suture).

5. Isolate the ICA and prepare a third knot with a 6.0 filament.
6. After obtaining a good view of the course of the ICA and the pterygopalatine artery (PA), clip both arteries using a microvascular clip. As an anatomical landmark, the glossopharyngeal nerve typically crosses right above the origin of the pterygopalatine artery.
7. Cut a small hole in the CCA before it bifurcates into the ECA and the ICA. Insert an 11-mm monofilament made of 8.0 nylon coated with silicon hardener mixture into the ICA until it stops at the microvascular clip.
8. Open the microvascular clip and gently advance the filament upward through the ICA to occlude the origin of the MCA. (CAVE: The surgeon needs to be cautious not to push the filament into the PA)
9. Close the third knot on the ICA to fix the filament in position.
10. After a defined duration of occlusion, reopen the third knot, withdraw the filament (if reperfusion is intended), and close the knot again.
11. Adapt the soft tissues and skin and fix the skin with adhesive or a surgical suture.

For pain relief in the peri-/postoperative period, topical lidocaine ointment, for example, can be applied. Body temperature of 36.5 ± 0.5 °C should be maintained after reperfusion (for at least 2 h) using a heated recovery cage.

For a video clip demonstrating filamentous MCAo in mice go to the following link:
http://www.jove.com/video/2423/modeling-stroke-mice-middle-cerebral-artery-occlusion-with-filament [24]

3 MCAo in Rats Using a Poly-L-Lysine-Coated Suture

3.1 Materials and Supplies

The following materials and instruments are recommended for the MCAo experiment in rats (see Fig. 3):

1. Intubation tubing (e.g., 2.1-mm O.D.×45 mm B&D, catalogue number 381467, Insyte catheter tubing, Becton Dickinson Infusion Therapy Systems Inc., Sandy, UT)
2. Polyethylene tubing for catetherization of femoral vessels (PE-50, e.g., catalogue number 427411, Fisher Scientific)
3. Microvascular clip (catalogue number 18055-04, Fine Science Tools, Inc, Foster City, CA)
4. GAS anesthesia instruments (Stoelting): Open isoflurane system (50251), isoflurane scavenger (50206), and induction chamber (50216)

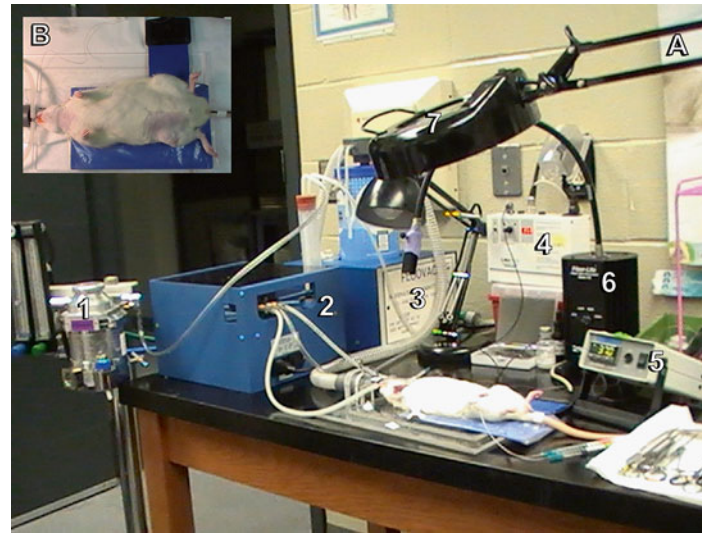

Fig. 3 A surgical setup for performing the rat MCAO procedure. The set includes (**a**): (*1*) Open isoflurane system; (*2*) Respirator; (*3*) Isoflurane scavenger; (*4*) Rectal temperature controller with a probe and heating pad; (*5*) Cranial temperature controller with a probe; (*6*) Fiber optic illuminator; (*7*) Fluorescent magnifier lamp. (**b**) (*Inset*): Position of rat on the surgical table

5. Cranial temperature controller (Omega Engineering): monogram benchtop controller CSC32T (unit set for type T only) and temperature probe: HYP-30-1/2 in. (30-gauge)
6. Rectal temperature controller (CMA/microdialysis AB): CMA/150 temperature controller (8315000), heating pad (8315001), temperature probe (8315002) and insulation pad (8315003)
7. Fiber optic illuminator (Model 190, KSE-Texas, Inc, Lewisville, TX)
8. Fluorecent magnifier lamp
9. Digi-Med blood pressure analyzer (Model 400, Micro-Med Inc, Tustin, CA)
10. Blood gas system (Model ABL 5, Radiometer America, Inc)
11. Glucose and L-lactate analyzer (Model 2300 STAT PLUS, Yellow Springs Instrument Co, Inc, Yellow Springs, OH)

3.2 Preparation of Poly-L-Lysine Coated Suture

A 4-cm length of 3-0 monofilament nylon suture (Harvard Apparatus, South Natick, MA, catalogue number 51-7847) is recommended in MCAo protocol. Blunt the tip of the suture before use by heating it near a flame. One hour before surgery (every day), a 25-mm distal segment of the suture must be coated with poly-L-lysine solution (0.1% (w/v), in deionized water, Sigma,

catalog number P 8920) (exposition ≈ 10 s) and dried in a 60 °C oven for 1 h. The solution of poly-L-lysine from Sigma is now ready for use (do not dilute). Shake the bottle of poly-L-lysine well before using. Prepared sutures must be stored at room temperature (18–26 °C) on a Petri dish for 2–3 h. The suture must be used within a 2–3-h time frame, maximum.

3.3 Filamentous MCAo in Rats, Surgical Procedure Step by Step (Please Also See Fig. 4)

1. Adult male Sprague Dawley rats weighing 280–320 g must be fasted overnight but allowed free access to water.
2. Anesthetize a rat with isoflurane (3% for induction and 1% for maintenance of anesthesia during surgical procedure) in a mixture of 69% nitrous oxide and 30% oxygen delivered by face mask. Shave the hairs over the neck and the right groin area.
3. Insert temperature probes into the rectum and the left temporalis muscle and use separate warming lamps to maintain rectal and temporalis muscle temperature at 36.0–37.5 °C.

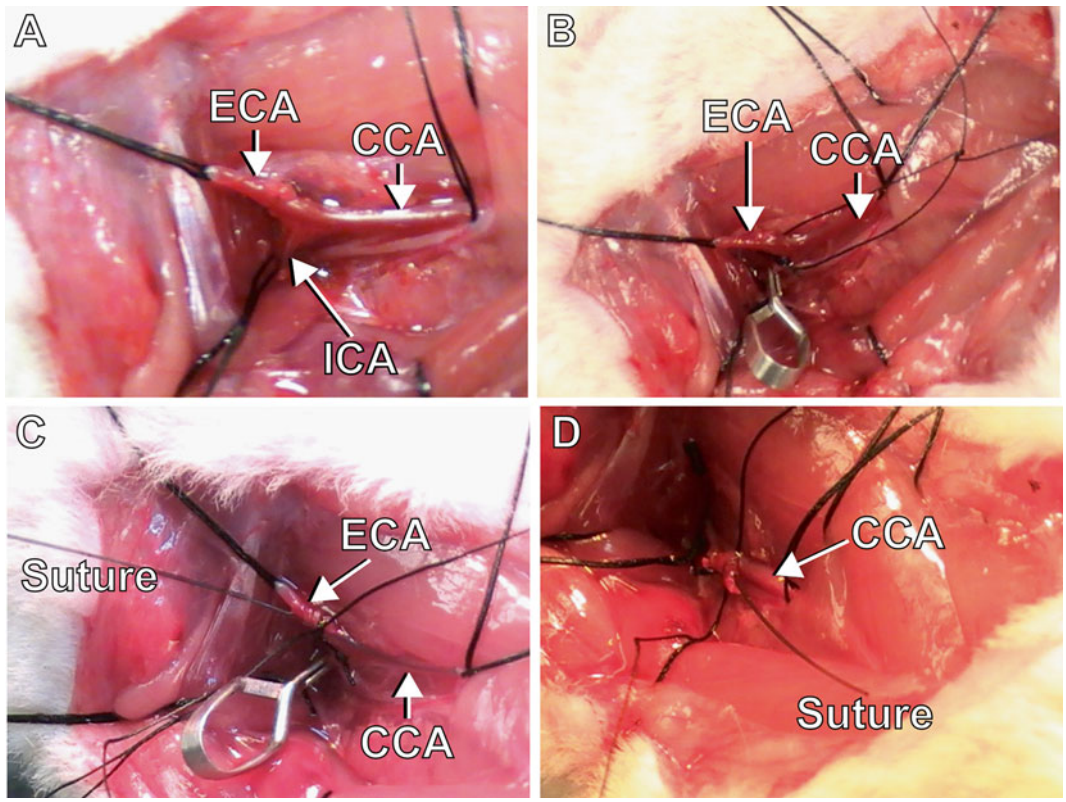

Fig. 4 Surgical procedures: *Panel A*: dissection of the CCA, ECA, and ICA from the surrounding tissue and nerves; *Panel B*: microvascular clip was placed on the ICA; *Panel C*: a small incision was made in the ECA between the two ligatures and suture was introduced and advanced into the CCA bifurcation. *Panel D*: microvascular clip was removed and suture was advanced into ICA and MCA. *Abbreviations*: *CCA* common carotid artery, *ECA* external carotid artery, *ICA* internal carotid artery, *MCA* middle cerebral artery

4. Administer atropine (0.15 mg/kg i.p.) to diminish tracheal secretions
5. Insert PE 50 catheters into the right femoral artery and vein for continuous blood pressure monitoring and periodic blood sampling for arterial gases, pH, and plasma glucose.
6. Immobilize the rat with pancuronium bromide (0.75 mg/kg i.v., and 0.35 mg/kg i.v. every half hour), intubate and mechanically ventilate with a rodent respirator.
7. Make a midline neck incision.
8. Carefully dissect the common carotid artery (CCA) from the surrounding tissue and nerves and block the CCA with a ligature.
9. Ligate and cut the occipital artery.
10. Expose the internal carotid artery (ICA) and ligate the pterygopalatine artery.
11. After exposing the external carotid artery (ECA), place two ligatures under the ECA to create an ECA stump (distal end of ECA must be permanently closed and the proximal end must be temporary blocked with ligature).
12. Clip the ICA and CCA using microvascular clips.
13. Make a small incision in the ECA between the two ligatures and introduce and advance the suture into the CCA bifurcation. Fix the suture in position by tying up a silk filament over the ICA and cut the distal part of the ECA.
14. A 3-0 monofilament nylon suture must be passed via the CCA bifurcation into the ICA till it stops at the microvascular clip.
15. Remove the microvascular clip and gently advance the filament from the ICA across to the origin of the MCA. The correct suture position can be confirmed by feeling a certain resistance during filament forwarding or by advancing the suture a defined distance according to the animal's body weight (270–300 g—18–20 mm; 310–330 g—20–22 mm; 340 g and up–23—25 mm) from the CCA bifurcation.
16. Close the neck incision. Allow animals to awaken from anesthesia and, at 60 min of MCAo, test them on a standardized neurobehavioral battery to confirm the presence of a high-grade neurological deficit. Rats that do not demonstrate an initial left upper extremity paresis must be excluded from further study [4].
17. After different durations of MCAo, rats must be re-anesthetized, temperature probes reinserted, and the intraluminal suture withdrawn to restore ICA-MCA blood flow.
18. Close incisions and return rats to the cages, providing them with free access to food and water.

4 General Issues

4.1 Monitoring Regional CBF via Laser Doppler Flow

Monitoring regional CBF (rCBF) via laser Doppler flow (LDF) is a useful technique for verifying filamentous occlusion of the MCA and reperfusion after removal of the thread. A drop in rCBF to levels of less than 20% of baseline value at filament insertion is considered a successful induction of ischemia.

However, positioning, fixing, and maintaining a flexible fiber optic probe in the skull of an animal for the pre-ischemic, ischemic, and post-ischemic period induces a number of additional difficulties, such as prolonged surgery time (resulting in longer exposure to anesthesia), changes in cranial temperature, and an additional wound, increasing the risk of infection.

Moreover, it is important to realize that LDF measurements can only provide very limited information. LDF can measure quantitative changes (in percentages) in blood flow within a tissue sample volume of approximately 1 mm^3. It does not give information on the spatial extent of blood flow reduction (see also Chap. 19). In addition, the existence of an initial neurological deficit characterized by high-grade sensorimotor dysfunction is a reliable predictor for successful occlusion of the MCA, resulting in histopathological ischemic brain damage [4, 19].

4.2 Strain Differences

In mice, cerebral ischemia shows a close correlation of ischemia time and increase in infarcted tissue. However, there are distinct inter-strain differences in susceptibility to cerebral ischemia [25]. Several studies applying filamentous MCAO have shown that C57Bl6 mice develop significantly larger infarcts than 129SV mice [5, 26]. Variability of the intracranial vasculature at the circle of Willis is another factor influencing the degree of ischemia in the MCA suture-occlusion model in rodents [27]. Typically, in C57Bl6 mice, the posterior communicating artery is poorly developed [28], which impedes collateral blood flow to the territory distal to the occluded MCA and results in larger lesion sizes [29]. In addition, it has been shown that in C57Bl6 mice the MCA supplies a larger vascular territory than it does in 129SV mice [29]. However, intrinsic factors other than hemodynamic variability may also contribute to inter-strain differences in ischemic vulnerability. At present, these mechanisms are poorly understood [26].

There are major differences in the outcome of focal cerebral ischemia between rat strains as well. A systematic review of literature reveals that in all publications using transient MCAo in rats, 41% of rats used were Sprague Dawley, 34% were Wistar, 2% were Long-Evans rats, and 2% were other inbred strains [30]. Our preference is given to Sprague Dawley rats, which develop more reproducible brain infarcts compared to Wistar and Long-Evans rats.

To avoid misinterpreting neuroprotective effects, the treatment and control groups should always be the same strain and supplied by the same vendor. Phenotyping of the cerebral vasculature via latex/carbon black perfusion might be necessary in genetically engineered animals [31]. In addition, experiments on neuroprotection or mechanisms of neuronal cell death should be replicated in different strains and different models of cerebral ischemia before results are accepted as facts (see Chap. 19).

4.3 ECA vs. ICA in Mice

To enter the vasculature, two approaches have been described. The filament can either be inserted at the trunk of the CCA, right below the bifurcation, or at the trunk of the ECA. Using the latter approach, after retraction of the filament, the circle of Willis will be supplied by three vessels, while using the approach via the CCA, the respective CCA is permanently closed. In this case, the circle of Willis will be supplied by only two vessels after retraction of the filament. Nevertheless, blood supply by two vessels sufficiently reverses ischemia, as cerebral blood flow rises to levels of around 80 % of baseline levels after retraction of the filament. Tying only one CCA does not result in cerebral ischemia, as collateral blood flow is well developed. In addition, it has to be taken into consideration that, especially in mice, the approach via the CCA is easier to perform, requires less manipulation of the vessels (making this approach less invasive), and shortens operation time as well as exposure to anesthesia.

4.4 Evaluation of Model Success

We predict that the existence of an initial neurological deficit characterized by high-grade sensorimotor dysfunction will result successful occlusion of the MCA and thus lead to histopathological ischemic brain damage [4, 19]. For behavioral and histological outcome evaluation, please see Chaps. 13–15.

5 Conclusion

Filamentous occlusion of the MCA is a very attractive model for studying focal cerebral ischemia. It offers advantages such as noninvasiveness, control of ischemia time, reproducibility of lesion size, and ease of performance. It is probably the most frequently used model in experimental stroke research and has been characterized extensively. Although this chapter gives a “hands-on” approach for performing the filament model, training in a specialized laboratory with a skilled and experienced MCAo surgeon is necessary for learning this model.

References

1. Koizumi J, Yoshida Y, Nakazawa T et al (1986) Experimental studies of ischemic brain edema. A new experimental model of cerebral embolism in rats in which recirculation can be introduced in the ischemic area. Jpn J Stroke 8:1–8
2. Longa E, Weinstein P, Carlson S et al (1989) Reversible middle cerebral artery occlusion without craniectomy in rats. Stroke 20:84–91
3. Laing R, Jakubowski J, Laing R (1993) Middle cerebral artery occlusion without craniectomy in rats. Which method works best? Stroke 24:297–298
4. Belayev L, Alonso O, Busto R et al (1996) Middle cerebral artery occlusion in the rat by intraluminal suture. Neurological and pathological evaluation of an improved model. Stroke 27:1616–1623
5. Hara H, Huang P, Panahian N et al (1996) Reduced brain edema and infarction volume in mice lacking the neuronal isoform of nitric oxide synthase after transient MCA occlusion. J Cereb Blood Flow Metab 16:605–611
6. Belayev L, Busto R, Zhao W et al (1999) Middle cerebral artery occlusion in the mouse by intraluminal suture coated with poly-L-lysine: neurological and histological validation. Brain Res 833:181–190
7. Warner D, Sheng H, Batinić-Haberle I (2004) Oxidants, antioxidants and the ischemic brain. J Exp Biol 207:3221–3231
8. Hallenbeck J, Dutka A (1990) Background review and current concepts of reperfusion injury. Arch Neurol 47:1245–1254
9. Endres M, Namura S, Shimizu-Sasamata M et al (1998) Attenuation of delayed neuronal death after mild focal ischemia in mice by inhibition of the caspase family. J Cereb Blood Flow Metab 18:238–247
10. Bonfoco E, Krainc D, Ankarcrona M et al (1995) Apoptosis and necrosis: two distinct events induced, respectively, by mild and intense insults with N-methyl-D-aspartate or nitric oxide/superoxide in cortical cell cultures. Proc Natl Acad Sci U S A 92:7162–7166
11. Hossmann K (2008) Cerebral ischemia: models, methods and outcomes. Neuropharmacology 55:257–270
12. Shah Z, Namiranian K, Klaus J et al (2006) Use of an optimized transient occlusion of the middle cerebral artery protocol for the mouse stroke model. J Stroke Cerebrovasc Dis 15:133–138
13. Hata R, Mies G, Wiessner C et al (1998) A reproducible model of middle cerebral artery occlusion in mice: hemodynamic, biochemical, and magnetic resonance imaging. J Cereb Blood Flow Metab 18:367–375
14. Li F, Han S, Tatlisumak T et al (1998) A new method to improve in-bore middle cerebral artery occlusion in rats: demonstration with diffusion- and perfusion-weighted imaging. Stroke 28:1715–1720
15. Kohno K, Back T, Hoehn-Berlage M et al (1995) A modified rat model of middle cerebral artery thread occlusion under electrophysiological control for magnetic resonance investigations. Magn Reson Imaging 13:65–71
16. Mies G, Ishimaru S, Xie Y et al (1991) Ischemic thresholds of cerebral protein synthesis and energy state following middle cerebral artery occlusion in rat. J Cereb Blood Flow Metab 11:753–761
17. Hossmann K (2009) Pathophysiological basis of translational stroke research. Folia Neuropathol 47:213–227
18. Winter B, Bert B, Fink H et al (2004) Dysexecutive syndrome after mild cerebral ischemia? Mice learn normally but have deficits in strategy switching. Stroke 35:191–195
19. Clark W, Lessov N, Dixon M et al (1997) Monofilament intraluminal middle cerebral artery occlusion in the mouse. Neurol Res 19:641–648
20. Li Y, Chopp M, Jiang N et al (1995) In situ detection of DNA fragmentation after focal cerebral ischemia in mice. Brain Res Mol Brain Res 28:164–168
21. Meisel C, Prass K, Braun J et al (2004) Preventive antibacterial treatment improves the general medical and neurological outcome in a mouse model of stroke. Stroke 35:2–6
22. Barber P, Hoyte L, Colbourne F et al (2004) Temperature-regulated model of focal ischemia in the mouse: a study with histopathological and behavioral outcomes. Stroke 35:1720–1725
23. Li F, Omae T, Fisher M (1999) Spontaneous hyperthermia and its mechanism in the intraluminal suture middle cerebral artery occlusion model of rats. Stroke 30:2464–2471
24. Engel O, Kolodziej S, Dirnagl U et al (2011) Modeling stroke in mice – middle cerebral artery occlusion with the filament model. J Vis Exp. doi:10.3791/2423
25. Barone F, Knudsen D, Nelson A et al (1993) Mouse strain differences in susceptibility to cerebral ischemia are related to cerebral vascular anatomy. J Cereb Blood Flow Metab 13:683–692
26. Majid A, He Y, Gidday J et al (2000) Differences in vulnerability to permanent focal

cerebral ischemia among 3 common mouse strains. Stroke 31:2707–2714

27. Kitagawa K, Matsumoto M, Yang G et al (1998) Cerebral ischemia after bilateral carotid artery occlusion and intraluminal suture occlusion in mice: evaluation of the patency of the posterior communicating artery. J Cereb Blood Flow Metab 18:570–579
28. Beckmann N (2000) High resolution magnetic resonance angiography non-invasively reveals mouse strain differences in the cerebrovascular anatomy in vivo. Magn Reson Med 44:252–258
29. McColl BW, Carswell HV, McCulloch J et al (2004) Extension of cerebral hypoperfusion and ischaemic pathology beyond MCA territory after intraluminal filament occlusion in C57Bl/6J mice. Brain Res 997:15–23
30. Dittmar M, Vatankhah B, Fehm N et al (2006) Fischer-344 rats are unsuitable for the MCAO filament model due to their cerebrovascular anatomy. J Neurosci Methods 156:50–54
31. Maeda K, Hata R, Hossmann K (1998) Differences in the cerebrovascular anatomy of C57black/6 and SV129 mice. Neuroreport 9:1317–1319

Chapter 5

Focal Ischemia Models: Middle Cerebral Artery Occlusion Induced by Electrocoagulation, Occluding Devices, and Endothelin-1

I. Mhairi Macrae

Abstract

This chapter covers established rodent models of middle cerebral artery occlusion (MCAO) where ischemia is induced by electrocoagulation of the artery, occluding devices applied to the artery, or application of the peptide endothelin-1 to the artery to induce vasospasm. Electrocoagulation induces a permanent occlusion of the artery, but the other models can be modified to induce permanent or transient MCAO.

All of the models involve some degree of cranial surgery, so the importance of aseptic technique is highlighted as is the importance of monitoring and maintaining the animals' physiology under anesthesia. Mortality rates are generally low in models which require a craniectomy. Since these models are used for both short- and long-term survival studies, some details of postoperative care are also included.

Key words Electrocoagulation, Diathermy, Endothelin-1, Compression, Microaneurysm clips, Tamura model, Brint model, Middle cerebral artery occlusion

1 Introduction

Models of MCA occlusion (MCAO) were first developed in primates in the 1930s [1] and later refined and scaled down for use in rodents in the 1970s and early 1980s [2, 3]. The subtemporal approach with MCAO by electrocoagulation, published by Akira Tamura and colleagues in Glasgow [3], has emerged as the standard method for permanent proximal MCAO in rats and has been cited over 1200 times since its publication in 1981. Its success is based on reproducible ischemia, infarction, and low mortality. Cerebral blood flow (CBF) is reduced to below 25 mls 100 g^{-1} min^{-1} within MCA territory, ischemic damage is evident within the cortex and dorsolateral striatum by 4 h post-occlusion, and infarct size (corrected for brain swelling) is maximal by 24 h. Subsequent variations in the model include:

Ulrich Dirnagl (ed.), *Rodent Models of Stroke*, Neuromethods, vol. 120,
DOI 10.1007/978-1-4939-5620-3_5,

1. Restricting infarction to the cortex by sparing the lenticulostriate branches and applying electrocoagulation more distally [4]. This variation is also less technically demanding.
2. Tandem occlusion of the MCA and ipsilateral common carotid artery (ICCA) to improve reproducibility of infarction [5, 6].
3. Replacing electrocoagulation with occluding devices such as microaneurysm clips, hooks, ligature snares, or compression devices [7–10], which in addition provide the opportunity to induce transient ischemia of defined duration followed by reperfusion.
4. Replacing electrocoagulation with application of the peptide endothelin-1 to induce vasospasm [11–13].

The size and reproducibility of infarction induced by the original Tamura model have also been investigated in aged versus adult rats and in different strains, including those with recognized stroke risk factors such as the spontaneously hypertensive rat, spontaneously hypertensive stroke-prone rat, and the streptozotocin-induced diabetic rat [14]. This chapter provides an overview of these models and the basic equipment and consumables needed to set them up.

2 Equipment and Materials

2.1 Laboratory Equipment

1. A good operating microscope is essential when setting up rodent stroke models which require surgical exposure of the MCA (*see* **Note 1**).
2. Equipment is required for sterilizing surgical instruments (e.g., autoclave). In some labs I have seen commercial equipment designed for sterilizing dental tools or hairdressers' scissors used. When operating on a number of animals in a single session, tips of instruments can be sterilized with bench top glass bead sterilizers (instrument tips should be cleaned and then inserted into the heated beads (>200 °C) for ~15 s, allowing time to cool before contacting tissues).
3. Sterile medical surgical drapes (e.g., Vet Tech Solutions Ltd, UK). Sterile instruments and consumables are placed on sterile drapes to maintain sterility during surgical procedures.
4. Homeothermic heating blanket (e.g., Harvard) or thick cork board (e.g., Pyramid Innovation Ltd, UK) and heating lamp to maintain body temperature under anesthesia. Extra vigilance is required when using heating lamps. Monitor body temperature continuously to avoid the possibility of overheating the animal.
5. Rectal temperature recording system (e.g., Physitemp). Fine needle probes for insertion into temporalis muscle are also available to gauge brain temperature during surgery.

6. Transparent anesthesia induction chamber for use with gaseous anesthetics. Chambers with scavenging function are recommended to protect the investigator from anesthetic gases.
7. Rodent Ventilator (e.g., Ugo Basile, Harvard).
8. Cool light source (e.g., swan neck flexible light source) to provide illumination without heat.
9. Fur shaver (e.g., Wahl Sterling 2 Plus Trimmer).
10. Dental drill, handpiece, and dental burrs (e.g., Fine Science Tools Worldwide and Wright Cottrell, UK). Make sure the handpiece is slim enough to use within the restricted space between the animal and operating microscope (e.g., NSK FX65M handpiece used with Komet Round Diamond Burs (K801104016P5), both available from Wright Cottrell, UK.)
11. Bipolar diathermy unit with finest-tipped diathermy forceps available (e.g., Aesculap, part of Downs Surgical, Eschmann)
12. Blood pressure transducer connected to a monitoring system (e.g., Biopac) for continuous readout of blood pressure and heart rate (particularly important for prolonged stroke experiments conducted under general anesthesia).
13. A blood gas analyzer and plasma glucose analyzer allow the investigator to record and maintain physiology within normal limits while the animal is under anesthesia.
14. A stereotaxic frame is required for intraparenchymal injection of endothelin-1. Gaseous anesthesia can be delivered to rats and mice via mask adaptors (e.g., from Harvard Apparatus) which fit onto the stereotaxic frame. Anesthesia is delivered locally at the nostrils and then, via an exit tube, is routed back to a closed circuit for recycling or connection to a scavenging system.
15. A micromanipulator is needed for the Brint [6], Kaplan [8], and Morancho [10] models where an 80 μm diameter stainless steel wire is inserted under the MCA to raise it off the surface of the cortex [6, 8] or a blunted 30G needle is used to directly compress the artery [10].

2.2 Surgical Tools and Consumables

1. Disinfectants for operating table (e.g., Distel/Trigene wipes or equivalent cleaning agent for medical surfaces), surgical instruments (e.g., Medistel and Reprochem), and skin (e.g., chlorhexidine- or iodine-based soap such as Hibitane, Betadine®, or Topionic).
2. Clean (or disposable) lab coat (or surgical greens), face mask, cap, and gloves.
3. Scalpel, with size 22A blade (e.g., Maersk Medical, Sheffield, UK).
4. Watchmaker's forceps, curved and straight (e.g., Downs Surgical, Sheffield, UK).

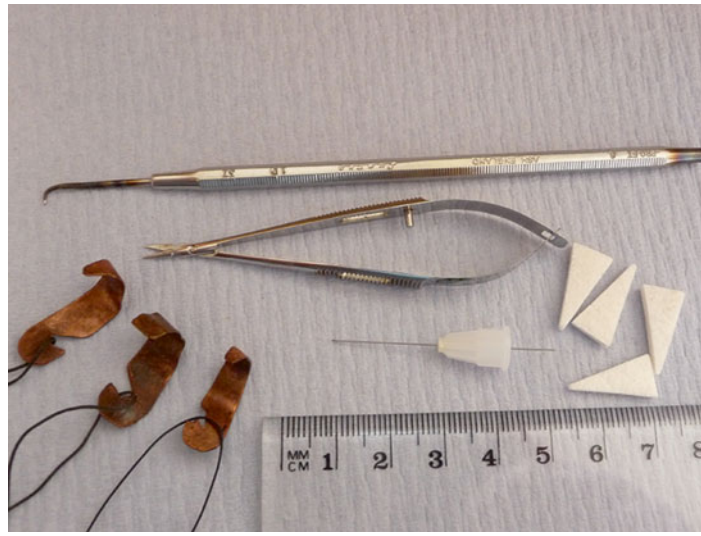

Fig. 1 Surgical tools used for MCAO: dural hook, spring-loaded microscissors, handmade copper retractors, 30-gauge dental needle, and *arrowhead* swabs

5. Dural hook and dental needles, 30 gauge (e.g., Terumo, Tokyo, Japan, see Fig. 1).
6. Surgical retractors for retracting skin and muscle when exposing the MCA (*see* **Note 2** and Fig. 1).
7. Surgical scissors for cutting sutures and Vannas Spring-loaded microscissors (e.g., Downs Surgical, UK) for cutting through MCA at the end of electrocoagulation to ensure complete occlusion (see Fig. 1).
8. Rat (or neonatal) laryngoscope and a stethoscope are very useful aids for carrying out oral intubation in rats.
9. Intubation tube for artificial respiration (for standard adult rat, Quick-cath 16G or Anicath 16G/45mm IV cannula, Millpledge).
10. For clip-induced MCA occlusion, the smallest available microaneurysm clips with lowest closing pressure and microaneurysm clip applicator (e.g., Codman AVM micro-clips with 10 g closing pressure).
11. Hamilton syringe for administration of small (μl) volumes of endothelin-1.
12. Local anesthetics (e.g., lidocaine, bupivacaine, and ropivacaine) and analgesics (e.g., buprenorphine, paracetamol, meloxicam, carprofen, ketoprofen, and butorphanol) to limit pain and suffering and maximize animal welfare post-stroke.
13. Atropine sulfate to control bronchial secretions under anesthesia.
14. Sterile saline for irrigating surgical sites, cooling drill tip during craniectomy, post-surgery subcutaneous injections to prevent dehydration, and heparinized saline for flushing vascular cannulae.

15. Bone wax to stem bleeding from bone during drilling.
16. Eye drops and ointment to prevent dry eye (e.g., Viscotears liquid eye gel, Novartis, and Lacri-lube, Allergan).
17. Cotton buds, gauze pads, and triangular arrowhead swabs (John Weiss & Son cat. no. 0111002, *see* **Note 3** and Fig. 1) to remove blood and excess fluid from craniectomy site.
18. Absorbable sutures (e.g., USS/DG sutures, Tyco Healthcare) for closing wounds after surgery.
19. Adhesive tape (e.g., masking tape, *see* **Note 4**).

3 Methods

3.1 Set-Up and Sterilization of Surgical Instruments

Surgery to induce cerebral ischemia should be carried out in as sterile an environment as possible. The operating room and operating table should be cleaned and disinfected. All equipment, surgical instruments, suture swabs, sterile saline, heparinized saline (10 units/ml), and other consumables required for surgery should be set up in advance on sterile surgical drapes. Surgical instruments should be autoclaved or sterilized by some other means, prior to the start of surgery.

3.2 Anesthesia, Intubation, and Animal Preparation for Surgery

Gaseous anesthesia is more controllable, enabling the investigator to alter depth of anesthesia quickly, for example, isoflurane administered in medical air (or N_2O/O_2, 70:30) or other suitable anesthetic (gaseous or injectable) (*see* **Note 5**). When using gaseous anesthesia, an adequate scavenging system is essential to protect the investigator from exposure to anesthetic gases. Anesthesia is first induced in a transparent induction chamber (usually with ~4–5% isoflurane in 70:30 N_2O/O_2), and once the animal is unconscious, it is transferred to a face mask delivering ~1.5–2% isoflurane or intubated for artificial respiration. Fur should be shaved from all incision sites and the skin cleaned with antiseptic prior to the start of surgery. This is best done away from the operating table to avoid any loose hairs getting into surgical sites. For adequate surgical anesthesia, the animal should be unresponsive to toe pinch, and the corner of a sterile saline-soaked swab should induce no blink reflex when applied to the eye. For animals anesthetized on a face mask, watch the animal's respiratory movements to ensure anesthesia is not too deep. Rat paws should stay a healthy pink color. Body temperature should be continuously monitored (e.g., with rectal probe) and maintained at 37 °C. Without a blink reflex, there is the potential for the eye to become dry and damaged during surgery. This can be avoided by closing the eye and securing it with a thin strip of adhesive tape or a temporary stitch. Alternatively, Viscotears or Lacri-lube ointment can be applied to the eye to prevent drying during surgery.

Surgical intubation is recommended for terminal experiments where the animal is anesthetized throughout the experiment and nonsurgical (oral) intubation for recovery experiments. An intubation tube size of 16 gauge is recommended for rats of 250–350 g. A specialized rat (or neonatal) laryngoscope and a stethoscope can aid oral intubation in the rat.

As a rough guide, ventilator settings for the rat are a tidal volume of 3–4 mls and a respiration rate from 45 (surgical tracheostomy) to 60 (nonsurgical, oral intubation) breaths per minute. Investigators should optimize artificial ventilation by adjusting settings to achieve stable blood pressure and blood gases within the normal range. With prolonged periods of anesthesia, a mucus plug can build up at the end of the intubation tube, compromising ventilation. A length of fine polythene tubing attached to a 5 or 10 ml syringe can be used to aspirate and withdraw any mucus buildup at the tube tip and/or atropine administered to reduce bronchial secretions (*see* **Note 6**). At the end of the surgical procedure, allow animals to regain spontaneous respiration before removing the intubation tube. Oral intubation is more challenging in mice but is possible. If your first attempt to intubate in either rats or mice is unsuccessful, you can try a second time, but stop after a failed second attempt so as not to cause any traumatic injury to the airway. If oral intubation is not possible, delivery of gaseous anesthesia via a face mask in a freely breathing animal can be considered as an alternative for recovery experiments (*see* **Note 7**).

3.3 Induction of Focal Ischemia: (i) Models That Involve a Craniectomy and Exposure of the Middle Cerebral Artery

Once stable anesthesia has been achieved, the animal is placed in the lateral position (on its side) and can be secured to the cork board or homeothermic blanket with masking tape. Always occlude the MCA on the same side of the brain for each study as there is some evidence that infarct size may vary in different hemispheres [15]. The fur between the left eye and ear should have been shaved and disposed of and the area swabbed with antiseptic prior to positioning the animal. Local/regional analgesia is recommended to control pain following surgery. Inject the local anesthetic into the subcutaneous space ("line block") below the planned incision line prior to surgery. Ropivacaine is a good choice of local anesthetic. It has a similar duration of action as bupivacaine but a wider safety margin (if there is inadvertent intravenous inoculation). It is purchased as Naropin (0.2% solution) and should be administered at the same dose as bupivacaine (1–2 mg/kg) with a maximum dose of 4 mg/kg.

A skin incision is made midway between the eye and the ear with a scalpel; the temporalis muscle is divided, separated, and retracted using retractors (see Fig. 1); and any tissue attached to the bone is scraped away. At this point a fine brain temperature probe (e.g., type IT-21 tissue-implantable thermocouple microprobe, Physitemp Instruments, Clifton, NJ, USA) can be inserted into the temporalis muscle to give a continuous assessment of brain temperature. The MCA is easier to locate in mouse as it can be

seen through the thinner skull. In the rat, the bone can be thinned using a saline-cooled dental drill (*see* **Note 8**) to aid exact location of the MCA. A circular craniectomy to expose the MCA is then made. In the original descriptions of proximal MCAO in the rat, the zygoma was removed to improve access to the proximal MCA. This should be avoided if possible as it will affect the animal's ability to eat on recovery. Once complete, the circle of thinned bone can be carefully teased off using watchmaker's forceps, a dural hook, or a dental needle (see Fig. 1). The dura is then carefully pierced and torn using a sterile 30-gauge dental needle (with the tip bent with pliers to form a hook) to reveal the middle cerebral artery. For a diagram of the craniectomy site and exposed MCA, see Figure 3 in ref [3]. Useful landmarks are the white myelinated fibers of the olfactory tract, which run rostro-caudally along the bottom of the craniectomy (if not visible, gently push the brain away from the ventral aspect of the craniectomy site with a blunt probe to see more ventrally), and the inferior cerebral vein which runs parallel to the olfactory tract, crossing the MCA more dorsally (see Fig. 2a). Although the craniectomy site represents a potential risk for infection, with good aseptic technique, stroke models which require a craniectomy are associated with very low

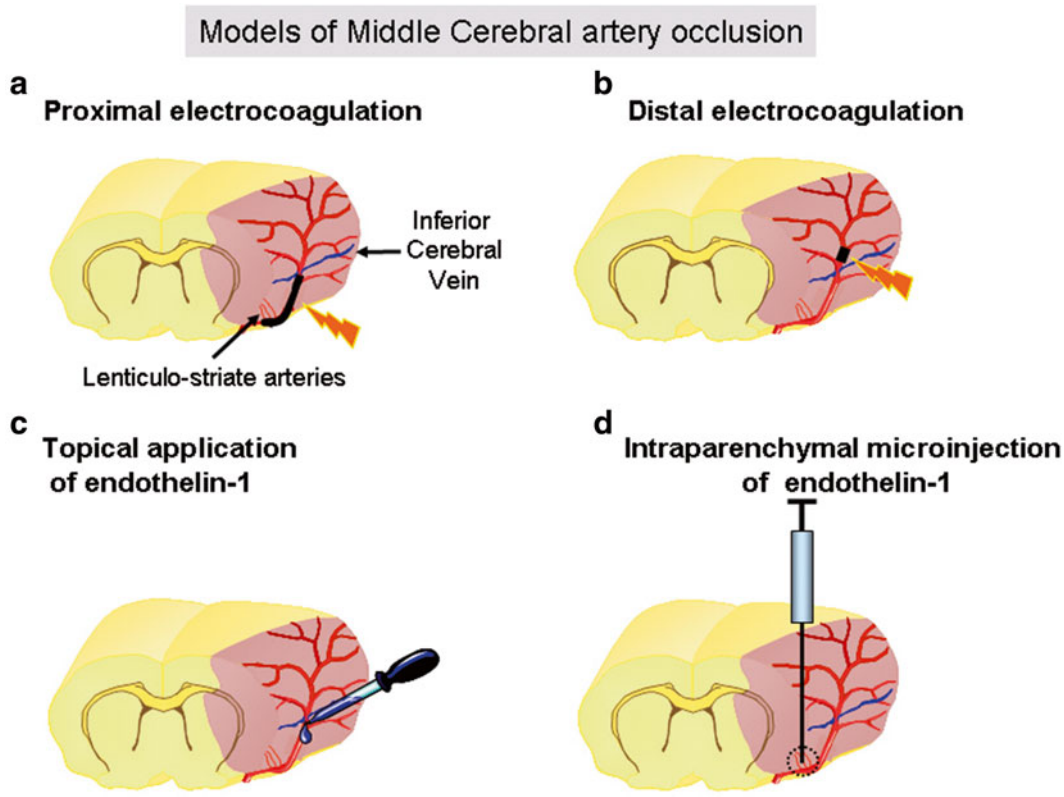

Fig. 2 Illustrations of MCAO models

or no mortality as the craniectomy provides space for the brain to swell and prevents increases in intracranial pressure in the brain. Edema and brain swelling correlate with infarct size and increase over the first 24–48 h post-stroke. In closed skull models (e.g., intraluminal filament model), significant brain swelling can occur within this period, leading to increased intracranial pressure and significant mortality.

The middle cerebral artery can be occluded by a number of different approaches. This chapter describes MCAO induced by electrocoagulation (diathermy occlusion); mechanical devices such as hooks, clips, and needles; and the vasoconstrictor endothelin-1 (ET-1). Methodology papers (including video clips of surgery) are available for a number of these models in the *Journal of Visualized Experiments* (JoVE) [16–20].

3.4 Electrocoagulation of MCA

The MCA is permanently occluded with this approach, and the size and location of ischemic damage can be controlled by altering the length and proximal/distal portion of the artery that is electrocoagulated. A short (e.g., 2 mm) occlusion of MCA, distal to the inferior cerebral vein, will induce ischemia confined to the cortex (Fig. 2b), while a longer and more proximal occlusion incorporating the lenticulostriate branches will induce cortical and subcortical ischemia (Fig. 2a). Sufficient current should be applied at the tips of the diathermy forceps to ensure there is no prospect of any remaining blood flow through the artery while minimizing damage to the underlying brain surface (*see* **Note 9**). When electrocoagulation is complete, the occluded part of the artery should be cut with spring-loaded microscissors to confirm complete occlusion. Sham-operated control animals undergo the same procedure up to and including removal of the dura. This model has been established in rats [3], mice [21], cats [22], and miniature pigs [23].

3.5 Electrocoagulation of MCA Combined with Ipsilateral Common Carotid Artery Occlusion

Modifications to the MCA electrocoagulation model have been developed to simplify the occlusion procedure, increase throughput, and improve reproducibility in infarct size. The severity of the ischemic insult can be increased by inducing hypotension, occluding the carotid arteries, and using strains with poor collateral supply such as the spontaneously hypertensive (SHR) and spontaneously hypertensive stroke-prone (SHRSP) rat. Brint and colleagues [6] combined a single-point distal MCAO with permanent ipsilateral common carotid artery occlusion (ICCAO) which produced a very reproducible cortical infarct in spontaneously hypertensive rats. Following ICCAO and exposure of the MCA, a fine (80 μm) stainless steel wire hook, inserted under the MCA just distal to the inferior cerebral vein, is elevated using a micromanipulator to raise the artery away from the underlying cerebral cortex. The artery in contact with the hook is then cauterized and severed by heating the wire with an electrocautery device, thus causing minimal damage to the underlying tissue.

3.6 Mechanical Occlusion of the MCA with Microaneurysm Clips, Ligatures, Hooks, and Direct Compression

The permanent MCAO/tandem ICCAO model in SHR rats [6] was further developed to produce a model of transient focal ischemia confined to the cortex [8]. A Silastic loop was used to reversibly occlude the ICCA, and the hook elevated the MCA sufficiently off the cortical surface to stem flow. This was checked by a continuous laser Doppler flowmetry readout from the cortical surface to allow readjustment of hook height, using the micromanipulator, during the period of ischemia. After the designated period of ischemia, recirculation was achieved by releasing the Silastic loop around the ICCA and lowering the MCA off the hook. The exposed brain and artery were bathed in warmed saline prior to and during ischemia to prevent desiccation.

Microaneurysm clips and ligatures have also been used successfully to permanently or transiently occlude the MCA [9, 24, 25] and are often accompanied by tandem ICCAO to improve reproducibility of infarction. Microaneurysm clips are too small to apply by hand and have to be loaded into a special applicator for attachment to the MCA. Some difficulties can be encountered when using these devices to induce transient MCAO, as removing microaneurysm clips after a period of ischemia (without inducing any damage) can be more challenging than applying the device (*see* **Note 10**). Mechanical compression of the M1 parietal branch of the MCA can also be used to induce distal MCAO in mice [10]. A laser Doppler probe, placed on the surface of the M1 parietal branch bifurcation, provides a flow readout, and compression of the blood vessel is applied until a reduction in CBF of ≥80 % is achieved.

The one issue with these techniques is the increased variability in ischemia and infarct size when only a single point on the MCA is occluded. Reproducibility can be improved by occluding more than 1 point along the MCA, combining MCAO with hypotension or ICCAO, and/or using strains with poor collateral supply. However, when considering models for testing neuroprotective compounds, it is worth considering that steps taken to improve reproducibility in infarct size might also result in less penumbral (potentially salvageable) tissue being available for rescue.

3.7 Topical Application of Endothelin-1 to MCA

Application of the peptide endothelin-1 (ET-1) to blood vessels induces a potent and prolonged vasoconstriction [26] capable of blocking flow and inducing downstream ischemia [11]. Following removal of the dura, exposure of the MCA, and puncture of the arachnoid membrane on either side of the blood vessel (to improve peptide access), topical application of ET-1 (25 μl of 10^{-7}–10^{-4} M) constricts the artery sufficiently to block blood flow (Fig. 2c). The higher the concentration of ET-1 applied, the more severe and prolonged the ischemia and the larger the infarct, which has both a cortical and subcortical component, similar to proximal MCAO. As the effect of the peptide wears off, the MCA diameter returns to normal and blood flow is gradually reestablished [12]. Therefore,

with this approach, ET-1 induces a transient MCAO (*see* **Note 11**). This model was developed in the rat but should work in mouse and has been set up in marmosets [27].

3.8 Induction of Focal Ischemia: (ii) Intraparenchymal Injection of Endothelin-1

A more prolonged focal ischemia can be induced by injecting ET-1 directly into brain tissue. Using a stereotaxic frame, ET-1 can be targeted to any neuroanatomical site within the brain, inducing discrete localized ischemic lesions in gray [10] or white matter [28, 29]. Sharkey and colleagues [13] used this approach to target the proximal MCA by injecting ET-1 (120 pmol in 3 μl) stereotaxically into the piriform cortex (Fig. 2d). This approach was technically less challenging than surgical exposure of the MCA and induced a reproducible and prolonged ischemia in MCA territory. [^{14}C]iodoantipyrine autoradiography revealed reductions in CBF of ~85 % in MCA territory 3 h after ET-1 injection (personal communication J Sharkey). This is in comparison to topical ET-1 application to the exposed MCA (Fig. 2c) where there was evidence of partial reperfusion within 60 min of ET-1 application [12].

3.9 Post-operative Care

Animals regaining consciousness following MCAO surgery should be carefully monitored and their recovery recorded. In terms of behavioral changes, up to 100% of animals exhibit circling and transient mild hemiparesis affecting the contralateral limbs, although these symptoms are less apparent in distal compared with proximal MCAO models. Lethargy, altered consciousness, hunching, and piloerection may be exhibited for up to 24 h postoperatively in up to 100% of animals. Post-op pain relief should be administered. Follow local guidelines and consult your local vet for advice on type, dose, and frequency of administration. Recommended analgesics include: buprenorphine, paracetamol, meloxicam, carprofen, ketoprofen, and butorphanol. Care should be taken in selecting an analgesia regime as certain analgesics may affect outcome measures such as performance in behavioral tests, inflammatory processes, and lesion volume.

Subcutaneous fluids should be administered acutely (5 mls/kg sterile saline for rat and 10 mls/kg for mouse, split between two sites) following surgery to prevent dehydration and animals kept in a warm environment (e.g., 28 °C) until fully conscious. Continue administering subcutaneous fluids until the animal is drinking normally, and provide animals with softened rodent chow and/or baby food, Complan, etc. to encourage feeding and limit weight loss. Introducing any new forms of diet prior to stroke surgery improves the animal's willingness to eat this diet after stroke.

Animals should first be housed individually to allow recovery from stroke and wound healing. Thereafter, group housing is recommended. Fresh bedding allows the investigator to check that the animal is urinating and defecating normally. Body weight should be recorded daily and any wounds checked for potential

infection or removal of stitches. Weight loss of >20 % is beyond the accepted severity limit, and euthanasia should be considered, particularly if movement, inquisitiveness, and grooming are absent. If failure to drink persists beyond 48 h or failure to eat persists beyond 72 h, the animal should be euthanized.

The intracranial temporal approach can affect the jaw alignment in rats. With prolonged survival periods, animals may need to be continually supplied with softened diet. Teeth overgrowth can become a problem, and teeth may require filing or clipping at regular intervals throughout the survival period if the animals do not eat dry diet or use chew blocks. Teeth clipping should be done under brief anesthesia if required. Chromodacryorrhea with unilateral loss of blink reflex and dry eye (up to 100 %) are often associated with intracranial MCAO and can be prevented and controlled by taping or suturing the ipsilateral eye shut during surgery. Eye ointment (e.g., chloromycetin, Orbenin) and/or drops (e.g., Viscotears, Lacri-lube) can be applied to the eye to limit this adverse effect.

4 Notes

1. When purchasing an operating microscope, discuss with the company the optimal working distance you require between the animal and the microscope to have adequate access for surgery. We have found that an angled binocular tube with 10 or 12.5× eyepieces provides the surgeon with a more comfortable seated position when operating for prolonged periods. Also consider a second, monocular eyepiece which can be fitted to some operating microscopes to allow trainees to observe the surgery.
2. Specialized retractors for rodent brain surgery can be purchased commercially (e.g., Small Animal Retractor System, Harvard Apparatus) or home made. In our lab we cut them to size from thick copper sheet, file them to shape (see Fig. 1), and keep them in place by connecting to surgical silk or rubber bands which are secured to a cork board with poster board pins.
3. Arrowhead swabs are incredibly useful tiny sponges which absorb blood and CSF from the craniectomy site to improve visualization of the MCA.
4. Masking tape is extremely useful for securing the anesthetized animal to the cork board or heated operating table. It is also useful for taping equipment cables to the table to avoid accidental movement of anything around the animal which might result in an intubation line or blood vessel cannula being inadvertently dislodged.
5. Isoflurane is a safer and less toxic alternative to halothane, which is gradually being phased out. N_2O/O_2 (70:30) is use-

ful as N_2O provides analgesia during surgery but must be used with a scavenging system.

6. Aspiration to clear mucous plugs from intubation cannula. Mark off the required length of fine polythene tubing needed to just clear the end of the intubation cannula, and connect it to a hypodermic needle attached to a 5 or 10 ml syringe. Quickly disconnect the intubation cannula from the ventilator, push the fine tubing down to just clear the end, aspirate, withdraw the fine tubing, and quickly reconnect the intubation cannula to the ventilator. Additionally, if you have problems with bronchial secretions and mucus plugs, consider a subcutaneous injection of atropine sulfate (0.05 ml of a 600 μg/ml solution).
7. When animals are artificially ventilated, the expired gases can be removed by connecting the ventilator exit pipe to the scavenging system. In freely breathing animals, double-tube systems with integrated face masks are available where anesthesia is delivered down an inner tune and removed by negative pressure via the surrounding outer tube.
8. Uncontrolled bleeding from muscle can be stopped using electrocoagulation forceps; bleeding from the bone can be stemmed by applying bone wax. Drilling the bone generates heat which can damage underlying tissue and disrupt the blood-brain barrier, thus producing surgery-induced artifacts. The bone and drill burr can be kept cool by spraying a steady stream of sterile saline (e.g., from a syringe with a hypodermic needle attached) onto the bone during drilling. Applying circular, lateral not downward pressure, when making the craniectomy, will avoid the possibility of the drill burr breaking through the bone and damaging the underlying cortex.
9. Flushing the MCA with saline and dipping forceps in saline before application help to prevent them from sticking to the artery during electrocoagulation. Start proximally and work distally, first with short zaps of electrocoagulation and, once the artery is constricted, with longer bursts of electrocoagulation. If the lenticulostriate branches of the MCA are to be occluded, they should be occluded first. Electrocoagulation induces heat; regularly replacing the saline that collects within the craniectomy site will ensure that the temperature does not rise above 38 °C. Keep the tips of the electrocoagulation forceps scrupulously clean at all times during surgery to avoid sticking. Polishing the tips after use will also help to minimize forceps sticking to the artery. We use Duraglit Metal Polish Wadding. Check with the manufacturer of the electrocautery equipment for their recommended product.
10. When clips or ligatures are applied to the proximal MCA (e.g., at the level of the lenticulostriate branches) for 1–2 h, ensuing

tissue swelling can hinder visualization and access to the device, making it very difficult to remove without damaging the artery.

11. Reproducibility of the ET-1 technique relies on consistency in the potency of the endothelin-1. The lyophilized peptide should be made up to the required concentration, aliquoted out into single-use vials, and frozen at –80 °C. A fresh aliquot should be thawed for each experiment and not refrozen.

Acknowledgments

The author wishes to thank Drs Hilary Carswell, Hideaki Imai, Chris McCabe, John Sharkey and Mrs. Lindsay Gallagher for help and advice in preparing this chapter.

References

1. Peterson JN, Evans JP (1937) The anatomical end results of cerebral artery occlusion: an experimental and clinical correlation. Trans Am Neurol Assoc 63:83–88
2. Robinson RG, Shoemaker WJ, Schlump M, Valk T, Bloom FE (1975) Effect of experimental cerebral infarction in rat brain on catecholamines and behaviour. Nature 255:332–334
3. Tamura A, Graham DI, McCulloch J, Teasdale GM (1981) Focal cerebral ischemia in the rat: 1. Description of technique and early neuropathological consequences following middle cerebral artery occlusion. J Cereb Blood Flow Metab 1:53–60
4. Shigeno T, McCulloch J, Graham DI, Mendelow AD, Teasdale GM (1985) Pure cortical ischemia versus striatal ischemia. Surg Neurol 24:47–51
5. Chen S, Hsu CY, Hogan EL, Maricq H, Balentine JD (1986) A model of focal ischemic stroke in the rat: reproducible extensive cortical infarction. Stroke 17:738–743
6. Brint S, Jacewicz M, Kiessling M, Tanabe J, Pulsinelli W (1988) Focal brain ischemia in the rat: methods for reproducible neocortical infarction using tandem occlusion of the distal middle cerebral and ipsilateral common carotid arteries. J Cereb Blood Flow Metab 8: 474–485
7. Dietrich WD, Nakayama H, Watson BD, Kanemitsu H (1989) Morphological consequences of early reperfusion following thrombotic or mechanical occlusion of the rat middle cerebral artery. Acta Neuropath 78:605–614
8. Kaplan B, Brint S, Tanabe J, Jacewicz M, Wang X-J, Pulsinelli W (1991) Temporal thresholds for neocortical infarction in rats subjected to reversible focal cerebral ischemia. Stroke 22:1032–1039
9. Shigeno T, Teasdale GM, McCulloch J, Graham DI (1985) Recirculation model following MCA occlusion in rats. Cerebral blood flow, cerebrovascular permeability and brain edema. J Neurosurg 63:272–277
10. Morancho A, García-Bonilla L, Barceló V, Giralt D, Campos-Martorell M, Garcia S, Montaner J, Rosell A (2012) A new method for focal transient cerebral ischaemia by distal compression of the middle cerebral artery. Neuropathol Appl Neurobiol 38:617–627
11. Fuxe K, Kurosawa N, Cintra A, Hallstrom A, Goiny M, Rosen L, Agnati LF, Ungerstedt U (1992) Involvement of local ischemia in endothelin-1 induced lesions of the neostriatum of the anaesthetized rat. Exp Brain Res 88: 131–139
12. Macrae IM, Robinson MJ, Graham DI, Reid JL, McCulloch J (1993) Endothelin induced reductions in cerebral blood flow: dose-dependency, time course and neuropathological consequences. J Cereb Blood Flow Metab 13:276–284
13. Sharkey J, Ritchie IM, Kelly PAT (1993) Perivascular microapplication of endothelin-1: a new model of focal cerebral ischemia in the rat. J Cereb Blood Flow Metab 13:865–871
14. Duverger D, Mackenzie ET (1988) The quantification of cerebral infarction following focal

ischemia in the rat: influence of strain arterial pressure blood glucose concentration and age. J Cereb Blood Flow Metab 8:449–461

15. Robinson RG, Coyle JT (1980) The differential effect of right versus left hemispheric cerebral infarction on catecholamines and behaviour in the rat. Brain Res 188:63–78
16. Wayman C, Duricki DA, Roy L, Haenzi B, Tsai S-Y, Kartje G, Beech J, Cash D, Moon L (2015) Performing permanent distal middle cerebral with common carotid artery occlusion in aged rats to study cortical ischemia with sustained disability. J Vis Exp. doi:10.3791/53106
17. Llovera G, Roth S, Plesnila N, Veltkamp R, Liesz A (2014) Modeling stroke in mice: permanent coagulation of the distal middle cerebral artery. J Vis Exp (89):e51729. doi:10.3791/51729
18. Colak G, Filiano AJ, Johnson GV (2011) The application of permanent middle cerebral artery ligation in the mouse. J Vis Exp (53):e3039. doi:10.3791/3039
19. Ansari S, Azari H, Caldwell KJ, Regenhardt RW, Hedna VS, Waters MF et al (2013) Endothelin-1 induced middle cerebral artery occlusion model for ischemic stroke with laser doppler flowmetry guidance in rat. J Vis Exp (72):e50014. doi:10.3791/50014
20. Regenhardt RW, Ansari S, Azari H, Caldwell KJ, Mecca AP (2013) Utilizing a cranial window to visualize the middle cerebral artery during endothelin-1 induced middle cerebral artery occlusion. J Vis Exp (72):e50015. doi:10.3791/50015
21. Backhauss C, Karkoutly C, Welsch M, Krieglstein J (1992) A mouse model of focal cerebral ischemia for screening neuroprotective drug effects. J Pharmacol Toxicol Methods 27:27–32
22. Bullock R, Graham DI, Chen MH, Lowe D, McCulloch J (1990) Focal cerebral ischemia in the cat: pre-treatment with a competitive NMDA receptor antagonist, D-CPP-ene. J Cereb Blood Flow Metab 10:668–674
23. Imai H, Konno K, Nakamura M, Shimizu T, Kubota C, Seki K, Honda F, Tomisawa S, Tanaka Y, Hata H, Saito N (2006) A new model of focal cerebral ischemia in the miniature pig. J Neurosurg 104:123–132
24. Buchan AM, Xue D, Slivka A (1992) A new model of temporary focal neocortical ischemia in the rat. Stroke 23:273–279
25. van Bruggen N, Thibodeaux H, Palmer JT, Lee WP, Fu L, Cairns B, Tumas D, Gerlai R, Williams SP, van Lookeren Campagne M, Ferrara N (1999) VEGF antagonism reduces edema formation and tissue damage after ischemia/reperfusion injury in the mouse brain. J Clin Invest 104:1613–1620
26. Robinson MJ, McCulloch J (1990) Contractile responses to endothelin in feline cortical vessels in situ. J Cereb Blood Flow Metab 10: 285–289
27. Virley D, Hadingham SJ, Roberts JC, Farnfield B, Elliott H, Whelan G, Golder J, David C, Parsons AA, Hunter AJ (2004) A new primate model of focal stroke: endothelin-1-induced middle cerebral artery occlusion and reperfusion in the common marmoset. J Cereb Blood Flow Metab 24:24–41
28. Frost SB, Barbay S, Mumert ML, Stowe AM, Nudo RJ (2006) An animal model of capsular infarct: endothelin-1 injections in the rat. Behav Brain Res 169:206–211
29. Lecrux C, McCabe C, Weir CJ, Gallagher L, Mullin J, Touzani O, Muir KW, Lees KR, Macrae IM (2008) Effects of magnesium treatment in a model of internal capsule lesion in spontaneously hypertensive rats. Stroke 39: 448–454

Chapter 6

Mouse Model of In Situ Thromboembolic Stroke and Reperfusion

Orset Cyrille, Le Béhot Audrey, Bonnet Anne-Laure, Maysami Samaneh, and Vivien Denis

Abstract

To mimic ischemic stroke in mice, thrombin is directly injected in the middle cerebral artery to prompt clot formation. This reproducible stroke model can be used to investigate fibrinolytic interventions and novel strategies to improve stroke therapy or prevention.

All therapeutic strategies validated in animal stroke models have failed in clinical settings, except tissue-type plasminogen activator (tPA)-induced thrombolysis. To better mimic the human stroke pathology and to test new therapeutic strategies, we describe here a mouse stroke model based on in situ clot formation.

The injection of thrombin in the middle cerebral artery results in the conversion of fibrinogen into fibrin, leading to clot formation and subsequent reproducible ischemic brain damages. In this model, tPA administration during the therapeutic window is beneficial, whereas late administration is deleterious.

The craniotomy performed during the surgery may reduce the additional deleterious consequences of raised intracranial pressure normally associated with cerebral ischemia and thus limit the final infarct volume due to the occlusion. This model of in situ clot formation and reperfusion is a relevant translational stroke model, close to the human stroke pathology. It should be an appropriate model to test new thrombolytics and/or neuroprotective strategies prior to clinical trials.

Key words Ischemic stroke, Thrombin, Mouse, Tissue plasminogen activator, Thrombolysis

1 Introduction

Ischemic stroke is due to the occlusion of a cerebral vessel, mainly the middle cerebral artery (MCA), either by a local thrombosis or by a peripheral embolus. To induce in vivo permanent or transient occlusion of the MCA, extravascular and endovascular approaches have been used, among others electrocoagulation [1], intraluminal thread

Electronic supplementary material The online version of this chapter (doi:10.1007/978-1-4939-5620-3_6) contains supplementary material, which is available to authorized users.

Ulrich Dirnagl (ed.), *Rodent Models of Stroke*, Neuromethods, vol. 120,
DOI 10.1007/978-1-4939-5620-3_6, © Springer Science+Business Media New York 2016

[2], injection of an autologous or a foreign thrombus [3, 4], microemboli [5], and induction of an in situ clot formation using rose bengal [6]. However, none of the widely neuroprotective agents tested in these models turned out to be efficient in the clinic for the acute treatment of stroke [7], because human pathophysiology was not closely recreated. Indeed, in human, stroke is rarely confined to one anatomical brain region and mainly occurs in patients with cardiovascular risk factors such as hypertension, dyslipidemia, or diabetes. These diseases can lead to a diffuse arteriopathy, which worsens the damages caused by an acute ischemia. Moreover, neurological deficits and subsequent clinical outcome can depend on the location of the ischemic lesion rather than on the infarct volume itself.

To mimic the human pathological conditions leading to stroke, we developed a mouse model of focal cerebral ischemia [8] in which thrombin is injected into the lumen of the MCA. The conversion of fibrinogen into fibrin by thrombin leads to in situ clot formation, obstructing the blood supply to the MCA territory. The infarcts are highly reproducible and no mortality is associated with this surgical intervention. In addition, the use of the only approved and available acute stroke treatment allows us to observe results rather similar as those observed in clinical studies. This MCA occlusion method offers the possibility to induce thrombolysis following the appropriate treatment [9]. This is a real advantage compared to other methods in which a pharmacologically induced reperfusion is not possible and potential mortality or complications are inevitable.

We believe that this stroke animal model is appropriate to induce focal brain ischemia and to further investigate the use of potent thrombolytic and/or neuroprotective therapies.

2 Protocol (Table 1)

2.1 Pipette Preparation

1. The glass micropipettes must be made from hematologic sampling pipette (non-heparinized, Assistent 555/5, Germany) using a pipette puller (PC-10 Narishige).
2. Insert the pipette in the pipette puller (heating level is determined to make two pipettes with the longest tip as possible).
3. Using a scalpel, cut the tip of the pipette (~20 μm external diameter) in order to make it sharp without dentation or edges to prevent inappropriate bleeding. This can be achieved using a scalpel or alternatively by polishing the tips using the second step in puller device. One microliter graduations are made if necessary (15 mm length = 1 μL).
4. Mount the pipette on the micromanipulator of the stereotaxic device, and connect it to a 10 ml syringe using the tubing.
5. Plunge the tip in the thrombin sample (1 UI/μL, Kordia), and apply a negative pressure by pulling the syringe to fill the pipette with thrombin.

Table 1
Table equipment reagents

	Company	Catalogue number	Comments
Name of the reagent			
Alpha-thrombin murine	Stago BNL	MIIA	Powder solved in PBS
tPA (Actilyse®)	Boehringer Ingelheim		Powder solved in saline
Name of the equipment			
Hematologic pipette	Assistant	555/5	Non-heparinized
Pipette puller	Narishige	PC-10	
Stereotaxic device	Stoelting	Rat frame	
Temperature control unit	Letica Scientific Instruments	HB 101/2	
LDF	Oxford Optronix	OxyLab LDF	Optic fiber probe
Mouse tail vein catheterization short term	Strategic Applications, Inc.	MTV-01	

6. Inject 1 μL at 1 UI of thrombin in Swiss mice. This is enough to promote clot formation. Adapt the doses if you are using other mouse strains (i.e., inject 1 μL at 1.5 UI in C57BL6 mice, to provide optimal occlusion and clot formation).
7. Disconnect the syringe from the tubing, when the pipette is filled with thrombin.
8. Store the pipette and its content at 4 °C (max 12 h) until used.

2.2 Surgical Procedures

1. Perform all procedures under aseptic conditions and according to institutional license and animal welfare at the European Union.
2. Anesthetize the mice (male Swiss, 35–40 g, Janvier, France) with isoflurane (5% for induction in a box and 2% during maintenance), using a face mask with a gas mixture of O_2:N_2O, 1:2.
3. Allow mice to breathe spontaneously during the procedure, but animals could also be mechanically ventilated to better control arterial blood gas.
4. Position the mice on a rat stereotaxic device (rat frame, Stoelting, UK).
5. Use a homeothermic blanket system with a retro-controlled heating pad and a rectal probe (temperature control unit, Letica Scientific Instruments) to maintain the body temperature at 37 °C during all surgical procedures.

2.3 Tail Vein Catheterization

1. Turn the tail slightly and gently, and fix it using adhesive tape, in order to present a vein on the dorsal plane.
2. Make a small incision on the tail skin (0.5 cm long) using a sterile scalpel blade.
3. Dissect the vein and isolate it from conjunctive tissues with sterile micro-scissors.
4. Incise the vein with micro-scissors to allow the insertion of a catheter filled with non-heparinized saline (30G, Strategic Applications, Inc., USA).
5. Inject a small volume of (20–50 μL) non-heparinized saline to verify the patency of the catheter.
6. Fix the catheter on the tail with hypoallergenic adhesive tape, and connect it to a syringe filled with saline (non-heparinized).

2.4 Clot Emplacement

1. Position the stereotaxic device perpendicularly to the manipulator.
2. Make an incision of the skin (2 cm) between the right eye and the right ear.
3. Position micro-clips (micro-bulldog clamp) on the skin at the side of the incision (corner of the eye and corner of the ear) to allow a better access to the surgical field and protect eyes with ophthalmic ointment.
4. Dissociate the temporalis muscle from the edge of the skull, using micro-scissors, and cut it transversely into two sections.
5. Place sutures (6/0) in both extremities to reflect the muscle in order to visualize the parietal part of the skull.
6. Incline the stereotaxic device for a better approach.
7. Hydrate the bone with warm sterile saline (non-heparinized) to enhance the observation of the middle cerebral artery (MCA) through the parietal part of the skull.
8. Perform a small craniotomy (0.8–1 mm Ø) using a saline-cooled dental drill. The bifurcation of the MCA is located through the translucent skull. In this region, the vessel wall is more resistant in structure and allows easier insertion of the glass pipette. Moreover, another advantage would be the fact that the blood flow disturbances in this region will promote faster and more stable clot formation.
9. Remove the residual bone using a needle (25G) and excise the dura using a (the same) needle.
10. Position the Doppler probe (fiber optic, Oxford Optronix) on the distal part of the MCA to monitor the cerebral blood flow (CBF) in the artery. Place a small quantity of paraffin oil around the probe to enhance the signal.

11. Mount the pipette containing the thrombin on the micromanipulator, and connect it to a syringe filled with air (the pipette tip should be sharpened prior to use, thus reducing the problems during its introduction into the lumen of the MCA) (fewer hemorrhagic complications and less damage to the arterial wall).
12. Position the pipette near the artery before the insertion.
13. Inject thrombin using the syringe filled with air, after inserting the tip of the pipette into the MCA lumen (below bifurcation). Perform the thrombin injection using a multiple step injection approach. If required, refill the syringe with air (gently disconnecting and reconnecting the syringe to the pipette tubing). Do not attempt to inject the thrombin all at once!
14. Perform the injection in no less than 3 min.
15. Remove the pipette 10 min after the injection of thrombin to allow the stabilization of the clot.
16. Hydrate the wound throughout the experiment, using non-heparinized sterile saline, and monitor the CBF continuously by the Doppler system.
17. Place a piece of hemostatic compress on the craniotomy to protect the brain, before suturing. Reposition the temporalis muscle, suture (6/0) the wound, and finally remove the tail catheter.

2.5 Reperfusion

1. *Early reperfusion*: Inject tPA (Actilyse®, 10 mg/kg, Boehringer Ingelheim) intravenously (200 μL, 10% bolus, 90% infusion over 40 min) 20 min after the thrombin injection, using an infusion pump (WPI) connected to the tail catheter. Other concentrations of tPA or neuroprotective drugs may also be administered according to the desired protocol.
2. *Late reperfusion:* Inject tPA 4 h after MCAO. Reanesthetize the mouse for tail vein catheterization (see Sect. 3), and inject tPA under anesthesia, as described above (see Sect. 2.5.1).
3. Sacrifice the mice 24 hours later by decapitation under isoflurane (5%) delivered in medical air. Remove rapidly the brains, immerse them into prechilled isopentane, and store at −80 °C until used.

3 Representative Results

The thrombin injection induces a rapid and stable thrombus formation in the MCA leading to a dramatic decrease of the CBF to a residual and stable level of about 20% of the baseline (Fig. 1). Moreover, the early intravenous administration of tPA (10 mg/kg, 20 min after occlusion) recovers the reduction in CBF (Fig. 1) and hence salvages the brain tissue.

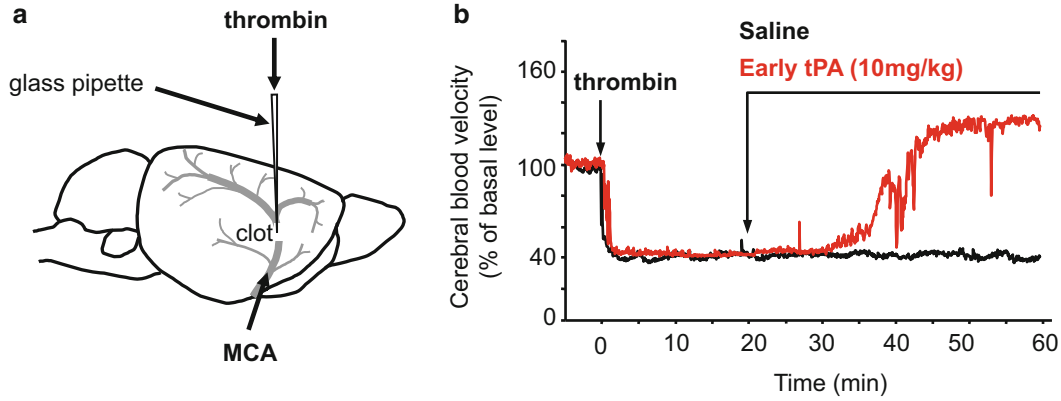

Fig. 1 Thrombin injection induces a rapid and stable thrombus formation. (**a**) Induction of stroke. Thrombus formation in the middle cerebral artery (MCA) of anesthetized mice is triggered by direct intra-arterial injection of thrombin (1 μL, 1 UI). (**b**) Representative laser Doppler profile. Thrombin injection (*black line*) induces a significant drop in the cerebral blood flow. Injection of Actilyse® (10 mg/kg) (*red line*), however, can completely rescue the blood flow when administered intravenously 20 min after occlusion

The analysis of the MCA patency using magnetic resonance angiography score shows a tPA-induced arterial recanalization either in early (20 min after MCAO) or in late administration (4 h after MCAO). Furthermore, this method usually leads to spontaneous reperfusion in all animals 24 h post-onset (Fig. 2). These observations are confirmed by perfusion-weighted imaging, where the deficit of the brain perfusion 20 min after MCAO is completely restored 24 h after the onset of occlusion with or without thrombolysis (Fig. 3).

As shown by histological and magnetic resonance imaging (MRI) analyses 24 h after the onset of ischemic stroke, this method of occlusion leads to an infarct restricted to the cortical part of the ipsilateral hemisphere (Fig. 4). As in the clinic, fibrinolytic treatment within the therapeutic window is beneficial with a reduction of the infarct size (from 24.29 ± 1 mm^3 to 17.9 ± 1.8 mm^3). However, it is noteworthy that the delayed administration of tPA has a deleterious effect and increases the lesion volume from 24.29 ± 1 mm^3 to 32.7 ± 1.4 mm^3 (Fig. 5).

4 Discussion

We described here a mouse model of in situ thromboembolic stroke induced by a local injection of thrombin, which results in reproducible ischemic brain damages and shows a significant improvement following tPA-induced reperfusion.

Using this model, an observer can closely monitor the formation of the clot as well as induced or spontaneous reperfusion. For optimal achievement, clot must be introduced exactly in the same position each and every time, and animals that demonstrate

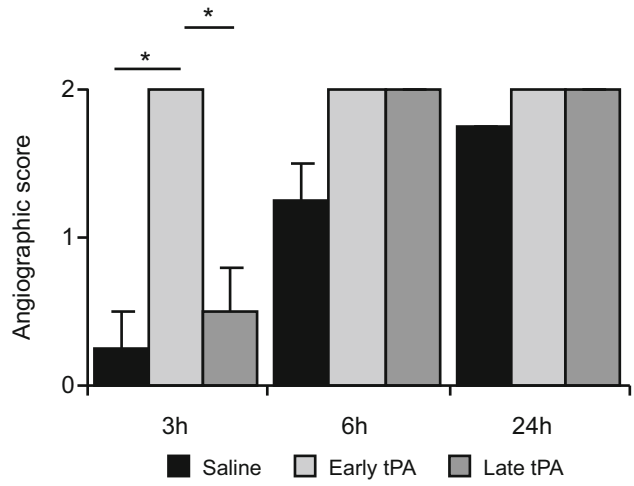

Fig. 2 The magnetic resonance angiography score shows a tPA-induced arterial recanalization. Twenty minutes (early) or 4 h (late) after MCAO, mice received an intravenous infusion of tPA (10 mg/kg). (**a**) Mean angiography score of longitudinally studied mice after MCAO ($n=4$ per group) showing spontaneous and tPA-induced reperfusion. (**b**) Representative MRI DR2* maps of mice immediately (20 min) or 24 h after MCAO. *Black arrows* indicate areas of perfusion defect. (**c**) Quantitative assessment of perfusion index ($n=4$ per group) ($*=p<0.05$, *ns* nonsignificant)

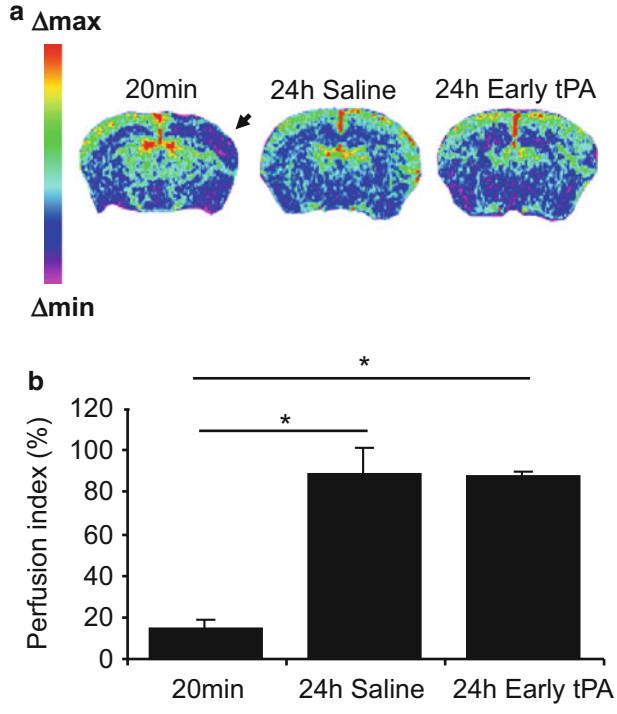

Fig. 3 The perfusion-weighted imaging shows a deficit of the brain perfusion 20 min after MCAO which is restored 24 h post-onset. (**a**) Representative MRI DR2* maps of mice immediately (20 min) or 24 h after MCAO. Twenty minutes (early) after MCAO, mice received an intravenous infusion of tPA (10 mg/kg). *Black arrows* indicate areas of perfusion defect. (**b**) Quantitative assessment of perfusion index ($n=4$ per group) ($*=p<0.05$, *ns* nonsignificant)

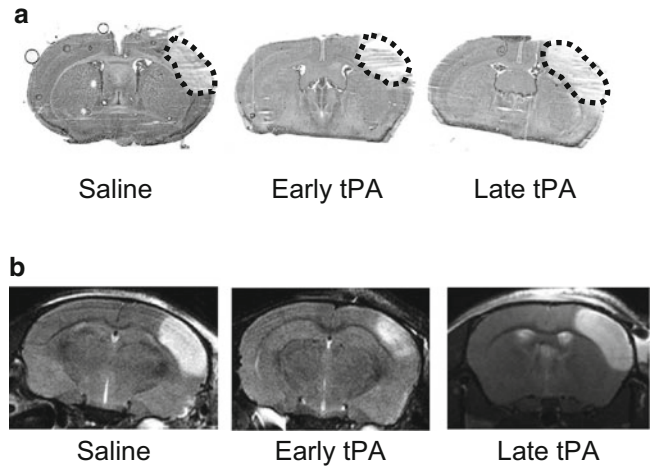

Fig. 4 Thrombin injection leads to a cortical brain lesion reduced by early tPA administration. Twenty minutes (early) or 4 h (late) after MCAO, mice received an intravenous infusion of tPA (10 mg/kg). (**a**) Representative images of thionin-stained brain sections, 24 h post-MCAO. *Dotted lines* represent the ischemic lesions. (**b**) Representative T2-weighted images of saline, early and late tPA 24 h post-MCAO

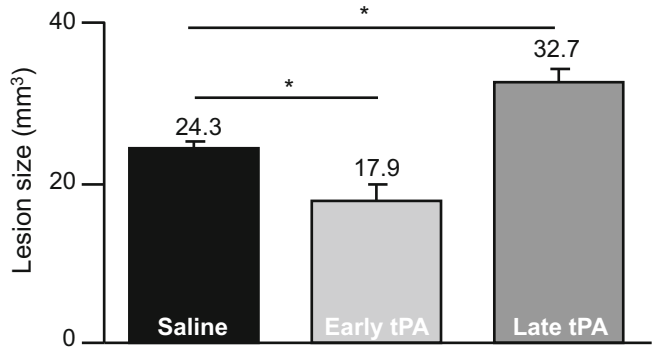

Fig. 5 Early tPA administration is beneficial, whereas late tPA administration is deleterious. Twenty minutes (early) or 4 h (late) after MCAO, mice received an intravenous infusion of tPA (10 mg/kg). Mean of lesion sizes 24 h after MCAO ($n = 10$ per group) ($* = p < 0.05$, *ns* nonsignificant)

early-onset spontaneous reperfusion can be excluded before unblinding the study and prior to the statistical analysis. The reproducibility and the cortical location of the infarcts could explain the absence of mortality rate. Moreover, this MCAO method offers the possibility to induce thrombolysis following the appropriate treatment. This is a real advantage compared to other methods including filament model or electrocoagulation in which a pharmacologically induced reperfusion is not possible and, respectively, potential mortality or complications are inevitable.

This technique, presented on Swiss mice here, could also be adapted to other mouse strains. The surgical procedure would be similar in all strains, but the thrombin concentration should be adapted to avoid undesirable early reperfusion, leading to the absence of lesion or inconsistency in infarct volume 24 h post-onset. It is also possible to adapt the concentration to produce more [10] or less stable thrombus depending on the objective of the study.

Several key points remain however to be highlighted. The cranium is not sealed after the surgical intervention. This is the major limitation of the in situ thromboembolic stroke model, as it reduces the consequences of secondary edema induced by ischemia which are normally observed in stroke patients. In addition, the intracranial pressure does not dramatically increase in this model which would also explain the high survival rate after the surgery. The specificity of the cortical lesion leads to subtle behavioral disturbances, and consequently evaluation of the motor function impairment is not obvious. Thus, after a few days after the induction of stroke, we cannot differentiate occluded and sham-operated animals, and complex cognitive tests are needed to show neurobehavioral dysfunctions.

We believe that this animal model of thromboembolic stroke would be appropriate to induce focal brain ischemia and allow the use of potent thrombolytic and/or neuroprotective therapies. Furthermore, the temporal evolution of the lesion and the time to treatment can be accurately determined through the use of histological methods and/or MRI techniques.

Acknowledgments

This work was supported by the "Institut National de la Santé Et de la Recherche Médicale" (INSERM), the French Ministry of Research and Technology, and the Eurostroke-Arise Program (FP7/2007-2013-201024).

Disclosures

All authors report no disclosure.

References

1. Tamura A, Graham DI, McCulloch J, Teasdale GM (1981) Focal cerebral ischaemia in the rat: 1. Description of technique and early neuropathological consequences following middle cerebral artery occlusion. J Cereb Blood Flow Metab 1:53–60
2. Longa EZ, Weinstein PR, Carlson S, Cummins R (1989) Reversible middle cerebral artery occlusion without craniectomy in rats. Stroke 20:84–91
3. Kudo M, Aoyama A, Ichimori S, Fukunaga N (1982) An animal model of cerebral infarction. Homologous blood clot emboli in rats. Stroke 13:505–508
4. Zhang ZG et al (2005) A model of mini-embolic stroke offers measurements of the neurovascular unit response in the living mouse. Stroke 36:2701–2704

5. Atochin DN et al (2004) Mouse model of microembolic stroke and reperfusion. Stroke 35:2177–2182
6. Nagai N et al (2002) Tissue-type plasminogen activator has paradoxical roles in focal cerebral ischemic injury by thrombotic middle cerebral artery occlusion with mild or severe photochemical damage in mice. J Cereb Blood Flow Metab 22:648–651
7. Young AR, Ali C, Durete A, Vivien D (2007) Neuroprotection and stroke: time for a compromise. J Neurochem 103:1302–1309
8. Orset C, Macrez R et al (2007) Mouse model of in situ thromboembolic stroke and reperfusion. Stroke 38:2771–2778
9. Macrez R, Obiang P et al (2011) Antibodies preventing the interaction of tissue-type plasminogen activator with N-methyl-D-aspartate receptors reduce stroke damages and extend the therapeutic window of thrombolysis. Stroke 42:2315–2322
10. García-Yébenes I, Sobrado M et al (2011) A mouse model of hemorrhagic transformation by delayed tissue plasminogen activator administration after in situ thromboembolic stroke. Stroke 42:196–203

Chapter 7

Photochemical Models of Focal Brain Ischemia

Anja Urbach and Otto W. Witte

Abstract

The photochemical stroke model has a number of advantages: size and location can be exactly determined, the skull does not have to be opened, the model works in rats and mice, and technical variations allow for the induction of subcortical stroke, stroke in newborn animals, or stroke with a penumbra. With photochemical reactions, thrombotic occlusions of large arteries as well as of small penetrating brain arteries may also be produced. However, the model does differ in some aspects from stroke in humans. We herein describe techniques for inducing these stroke models and discuss their potential limitations.

Key words Photochemical stroke model, Photochemical reactions, Stroke

1 Photochemical Models of Brain Ischemia

The photochemical stroke was introduced in 1985 by Watson et al. [1] as a simple model by which cortical infarcts can be induced in rats. To achieve the ischemic lesion, a photosensitive dye is injected systemically into the circulation and photoactivated by external illumination through the intact skull. The main incentive of Watson et al. was the production of more realistic models of stroke. They argued that mechanical stroke models such as the ligature or filament model do not sufficiently mimic the situation in humans: these models circumvent the active thrombosis process, the white matter lesion is not sufficiently modeled, and the fibrin-rich thrombi used in embolic stroke models cannot be resolved by recombinant tissue plasminogen activator (rt-PA).

In the following years, more sophisticated models were developed to more closely resemble the human pathology or to study certain aspects of ischemic stroke: the "ring" model was invented to mimic processes in the ischemic penumbra [2]. Later on, optical fibers were stereotactically implanted to selectively induce small infarcts in subcortical brain regions. Others developed techniques

Ulrich Dirnagl (ed.), *Rodent Models of Stroke*, Neuromethods, vol. 120,
DOI 10.1007/978-1-4939-5620-3_7,

that allow focal thrombosis of selected brain arteries or arterioles [3–5]. Some of these new models show features of an ischemic penumbra and even attenuation of ischemia with tPA [6].

2 Principles of Photochemical Stroke

The principles of photochemical lesions were extensively studied by Watson and colleagues [7–14]. They introduced rose bengal as photosensitizing drug ($\lambda_{max} = 560$ nm), which proved to be more effective than the previously tested fluorescein. Following irradiation with green light (filtered xenon arc lamp or laser), singlet oxygen and superoxide are produced via dye triplet energy transfer. The liberation of free radicals into the lumen of the vessel leads to NO inactivation and lipid peroxidation of cell membranes. This induces damage to the vessel endothelium, vasoconstriction, platelet activation, and formation of a white platelet-rich thrombus, culminating in vascular occlusion. As a consequence, this model produces a distal-territory ischemia.

As demonstrated in electron microscopic studies, high platelet content of the thrombi is a striking characteristic of different photothrombotic models. The main trigger for thrombus formation appears to be the endothelial injury, rather than direct activation of platelets by free oxygen radicals [1, 15]. Recently, the contribution of platelet activation to rose bengal-induced photothrombotic lesions was fundamentally questioned [16]. The authors used different approaches (platelet depletion or functional inhibition; inhibition of the clotting cascade) to prevent thrombus formation, and none of these treatments significantly affected the lesion size as estimated from MRI and histology. Similarly, rose bengal-induced thrombosis of mesenteric arterioles did not respond to antiplatelet therapy [17].

In addition to clot formation, photooxidative damage of endothelial cells leads to a breakdown of the blood–brain barrier associated with significant early vasogenic edema formation [11, 18, 19]. It has been suggested that the edema-induced secondary vascular compression could critically account for lesion development during PT [16].

As a main consequence of this discussion, the model should probably not be used for evaluation of antithrombotic pharmaceuticals. Furthermore, one has to realize that the commonly used denominator “photothrombosis” does not always correctly reflect the main mechanisms of photochemical lesion induction. It is nevertheless suggested to retain this well-established acronym.

3 Focal Cortical Photochemical Stroke in Rats

For the induction of photothrombotic infarcts, rats are usually anesthetized with volatile anesthetics (halothane or isoflurane) in a mixture of nitrous oxide and oxygen. Body temperature should be kept constant throughout the surgery at 36.5 °C. A catheter is inserted into the femoral vein for rose bengal injection and either a laser emitting light with wavelengths between 510 and 550 nm or a fiber-optic bundle mounted onto a cold light source is placed on the exposed skull to induce the photoreaction (see Fig. 1). Care has to be taken that the light source does not contain an internal filter which absorbs light in the required spectrum as is often the case. An interference filter (e.g., 560 nm) with a 10-nm bandwidth is advisable. The size of the required lesion can be adjusted by choosing the appropriate apertures of the cold light guide. Usually apertures of 1–4 mm are used.

In the original experiments by Watson and colleagues [1, 12], first rose bengal was injected intravenously (approx. 10 mg/kg), and brain illumination was started 2 min thereafter. Since the dye is most effective in the first minutes following injection, the sequence has been changed in most studies: the light source is switched on first and immediately thereafter the intravenous injection commences. The light is left on for 5–20 min. Most probably, the main effect is obtained within the first few minutes after injection and illumination for 5 min is sufficient to obtain a maximal effect. Sham animals are treated in the same way; they also receive rose bengal but the light source is not switched on.

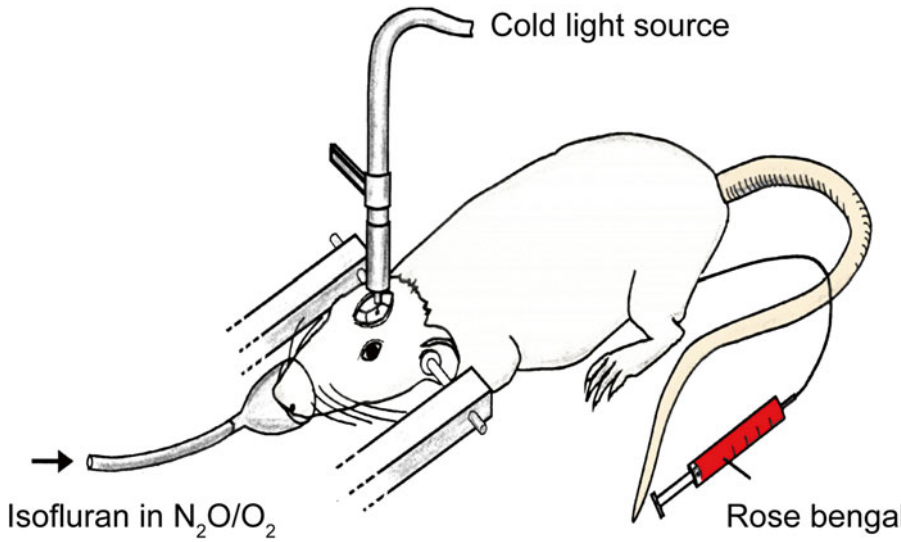

Fig. 1 Schematic drawing of setup for induction of focal photochemical lesion in the rat brain. The brain is illuminated through the intact skull of the anesthetized rat. The photosensitive dye is injected into the femoral brain

One of the main advantages of the technique is the very good reproducibility of the lesion location and lesion size (see Fig. 2) [20–31]. Common sources of unwanted variability are (a) aging of the light source which affects light intensity, (b) inappropriate placement of the optic fiber onto the skull, (c) insufficient injection of rose bengal, and (d) nonstandardized time between illumination and rose bengal injection if the dye is injected first. Photoactivation has to be performed promptly because rose bengal clears after intravenous injection with a τ of less than 3 min [5, 32]. With a placement of lesions in various positions of the brain, one has to furthermore consider that the bone is thicker in frontal areas than above the parietal cortex and that bone thickness increases with age. In certain experimental conditions, one therefore has to thin the skull over the selected brain area before placing the optic fiber. Finally, the technique might lead to off-target photoactivation. This can be avoided by protecting the animals from intense light during the first minutes after dye injection and, if necessary, a reduction of the intravenous rose bengal concentration. We previously showed that at least in a typical laboratory environment with normal external light (daylight plus ceiling lamp), the dye does not cause damage to the retina in mice (see description below [33]).

4 Materials and Equipment

1. Surgical microscope.
2. Equipment for use with isoflurane anesthesia.
3. Temperature control system with feedback-controlled heating pad and rectal thermal probe.
4. Stereotactic frame.

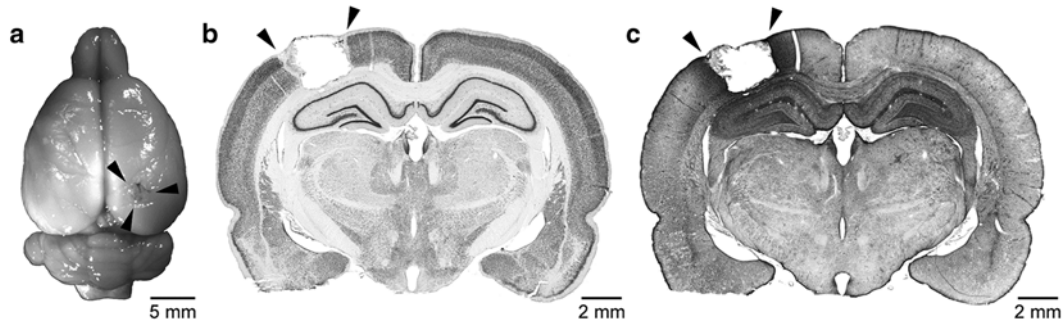

Fig. 2 Morphology of photochemically induced focal cortical infarcts. (**a**) Macroscopic view on the brain of an adult rat that received a photothrombotic lesion 2 days before. Using an aperture with a diameter of 1.5 mm resulted in well-defined infarcts with a diameter of approx. 2 mm (*arrowheads*). (**b**) Coronal section through a 7-day-old cortical infarct immunostained against the neuronal marker NeuN. Infarction affected all cortical layers, while the subcortical white matter was mostly intact. (**c**) GFAP immunostaining of a section adjacent to that depicted in (**b**) illustrates the glial scar around the cortical lesion

5. Cold light source (Schott KL1500; heat filter, Schott KG 1.45 × 45, $d = 4.2$; power rating, 300 W; beam light intensity of approximately 15 W/cm^2, color temperature 3200 K).
6. Apertures of appropriate size fitting to the optic fiber.
7. No. 23 scalpel (e.g., Figure 23 from Bayha, Tuttlingen, Germany).
8. Scissors.
9. Hemostats (e.g., cat. no. 13002-10, Fine Science Tools, Heidelberg, Germany).
10. Curved/splinter forceps (e.g., cat. no. BD311R, Aesculap, Melsungen, Germany).
11. Eye scissors (e.g., cat. no. OC498R, Aesculap).
12. Dural hook, type Adson (e.g., CareFusion, Rolle, Switzerland).
13. 23G needles with 1-ml syringes (1× for NaCl and 1× for rose bengal). The tips of the needles should be blunted with sandpaper to prevent damaging the catheter in which they have to be inserted.
14. Single-lumen tube with inner diameter of 0.58 mm and outer diameter of 0.96 mm (cat. no. 270117254, NeoLab, Heidelberg, Germany).
15. Single-lumen tube with inner diameter of 0.28 mm and outer diameter of 0.61 mm (cat. no. 270117250, Welabo, Düsseldorf, Germany).
16. Needle holder (e.g., cat. no. BM360, Aesculap).
17. Suture material (Mersilk suture 4-0, cat. no. EH6712H, Ethicon, Belgium).
18. Rose bengal (cat. no. R3877, Sigma-Aldrich, St. Louis, MO, USA); prepare a 10 mg/ml solution in saline; filtrate through a 0.2 μm sterile filter and draw it into a 1 ml syringe connected to a 23G needle; remove air; cover the solutions with aluminum foil to protect rose bengal from light.

4.1 Preparation of the Catheters

1. Cut 20 cm of the 0.58-mm/0.96-mm tube and 3 cm of the 0.28-mm/0.61-mm tube.
2. Gently expand the lumen of the thicker tube with the help of a splinter forceps to facilitate insertion of the thin tube.
3. Push the thinner tube approx. 2 mm into the thicker tube; fix the junction with nail polish.
4. Cut the thinner part of the catheter to 2.5 cm.
5. Prefill one of the catheters with 0.9% NaCl and the second with rose bengal.

4.2 Placement of the Femoral Vein Catheter

1. Anesthetize the rat with isoflurane (3 min at 3.5% for induction, use an induction box, and ~2.5% for maintenance during surgery via a face mask) in a mixture of 2:1 volumes of N_2O/O_2 (e.g., 40:20 l/h).

2. Place the rat in a supine position on a feedback-controlled heating pad, fix the legs using adhesive tape, and insert rectal probe to maintain body temperature constant at 36.5 °C.
3. Shave the left inguinal area and disinfect and make a 4-cm-long skin incision along the natural angle of the hind leg.
4. Remove connecting tissue with two curved forceps to expose the femoral bundle, and blunt dissect the femoral vein (at a length of ~1–1.5 cm) from the artery and nerve.
5. Place two pieces of suture under the vein. Pull one of them as far as possible toward the leg, secure the vein with two knots, fix the ends of the suture with a hemostat, and put it aside (to the right). Move the second suture toward proximal; make a very loose knot to form a loop. Fix the end of the suture with a second hemostat and lay it to the left side. The vein should now be slightly stretched.
6. Using a pair of eye scissors, make a small incision into the distal half of the exposed vein.
7. Open the incision with the help of a dural hook to insert the saline-filled catheter; advance it for 2.5 cm. Avoid perforation of the vein; the catheter should always move easily without resistance.
8. Confirm intraluminal placement of the catheter by shortly aspirating blood, and then flush it with sterile saline.
9. Secure the catheter with the proximal suture (one knot).

4.3 Photothrombotic Induction

1. Place the animal in ventral position in a stereotactic frame; maintain temperature as described above.
2. Shave the scalp, disinfect and incise the skin along the midline (approx. 1.5 cm), and remove periosteum to expose bregma and lambda.
3. Place the optic fiber equipped with an appropriately sized aperture above the region of interest. You can temporary turn on the light to facilitate correct placement. Ensure that the entire extent of the optic fiber has close contact with the calvaria to avoid light scattering.
4. Again shortly aspirate some blood and flush catheter with saline.
5. Remove the saline syringe from the catheter and replace it by the rose bengal syringe.
6. Switch on the cold light source and immediately inject rose bengal at a dose of 13 mg/kg body weight. Keep care that there gets no blood or fluid between the skull and the optic fiber.
7. After 20 min switch off the light and suture the head wound.
8. Remove the catheter and ligate the femoral vein with a second knot.

9. Suture the wound. Remove the animal from the stereotactic frame, cease the supply of anesthetics, and apply pure oxygen until the animal is awake.
10. Place the animal in a warm environment for 30 min (e.g., infrared lamp or heating pad below the cage) before returning it to the home cage.

5 Focal Cortical Photochemical Stroke in Mice

In mice, the procedure for induction of the photochemical lesion is essentially similar to that in rats. The application route of rose bengal may be either intraperitoneally [34–36] or intravenously [33, 37–39]. With intraperitoneal injection, rose bengal is usually applied at higher concentrations (100–150 mg/kg), and the light is turned on 5 min thereafter. We also tested this procedure extensively, and it usually worked well. However, the lesion size was much more variable than with intravenous injection of the dye, and therefore we prefer the intravenous applications route also in mice. For this purpose, either the jugular vein may be used [39] or the tail vein [33, 37, 38]. For the exposure of the jugular vein, a surgical microscope and a custom-modified catheter (e.g., PE20 170 mm, PE10 65 mm, silastic 0.025 in OD, 37 mm) may be used [39]. Application of the dye via the tail vein is much simpler: after the optic fiber is placed on the skull, the tail is dipped either into a beaker containing warm water (37 °C) or wrapped in a swab dampened with warm water (45 °C) to induce a vasodilatation. Using a 30G needle, we inject 100 μl of a 10-mg/ml rose bengal solution (approx. 40–50 mg/kg) into one of the lateral veins and switch on the light immediately thereafter.

6 The Ring Model of Photochemical Stroke

Characteristically, the photochemical model of cortical stroke has a comparatively sharp boundary. T cells infiltrate the edge of the lesion, followed by microglial/macrophage activation and both local and distant cytokine production [40–42]. The lesion develops immediately as consequence of a microvascular insult. There is no significant ischemic penumbra or region of local collateral flow and reperfusion, as typically seen in the "Tamura" and three-vessel occlusion models [43]. Oxidative damage occurs within the infarct core, rather than progressively extending to peri-infarct areas as in other models. Thus, in the classical photothrombotic model, there is no extensive tissue at risk to analyze processes in the ischemic penumbra and potential benefits of therapeutic interventions. To produce a more extended, yet well circumscribed penumbra, Wester and colleagues introduced a photothrombotic ring model [2, 44]. For this purpose, the output of a 514.5 nm laser beam was

focused with a plano-convex glass lens (focal length = 3 cm) into a 400 µm-diameter optical fiber (ST400E-FV with SL sleeves, Mitsubishi Cable America, Inc., New York, USA) at an input angle of 291° to the fiber axis, resulting in a ring beam output. In rats, the outside diameter of the ring beam was set at 5.0 mm, and the laser beam thickness on the skull was at 0.35 mm, whereas in mice the outside diameter was set at 3.0 mm, and the laser beam thickness was at 0.21 mm to fit the anatomy of an adult mouse [44, 45]. The exposed skull was irradiated by the laser ring beam with concurrent intravenous infusion of the photosensitizing dye erythrosin B (17 mg/kg in saline; Sigma, #330000). The described method results in a circular region of ischemic damage surrounding a circumscribed area of hypoperfusion with typical characteristics of an ischemic penumbra.

7 Photochemical Stroke in the Developing Brain

The photochemical model can also be applied to induce reproducible, permanent focal ischemic lesions in neonates. Working with animals younger than 10 days of age requires some special considerations:

1. They react differently to anesthetics than adult animals. It is recommended to use volatile anesthetics or hypothermia. In our hands, isoflurane worked well at ages between of P8 and P11. The dosage needed may be higher than in adults and needs to be continuously monitored and readjusted according to the respiratory rate and muscle tone of the animal.
2. Mothers tend to over-groom pups after surgery; therefore the wound has to be closed very neatly.
3. To prevent mothers rejecting pups, it is helpful to rub them with nesting material to cover smells from the surgery.

In the study of Maxwell and Dyk [46], photothrombotic lesions were successfully induced in mouse pups as young as P7. Animals were anesthetized with isoflurane (4% for induction, 2.5% for maintenance). Rose bengal was injected intraperitoneally at a concentration of 50 mg/kg. Fifteen minutes later the brain was irradiated with a 532-nm laser (20 mW B&WTek, Del., USA). The mortality rate of pups with photothrombotic infarcts was below 5% and comparable to that of control animals.

8 Photochemical Stroke in Subcortical Brain Regions and the Hippocampus

With appropriate devices, the photochemical model can also be used to produce subcortical stroke. Such experiments were recently reported for the caudoputamen [6], the internal capsule [47], and

the hippocampus [36]. In the study of Kuroiwa and coworkers, a thin polymethyl methacrylate optic fiber was stereotactically implanted to deliver cold light to the caudoputamen. These fibers are suitable for cold lighting because they transmit very little infrared light. Histological examination early after light exposure with rose bengal showed an almost spherical infarct around the tip of the fiber optic, surrounded by an area of selective neuronal death and ischemic edema. The lesion size was adjustable by changing the light intensity and illumination time. The model showed clear evidence of an ischemic penumbra: (1) 90 min after light exposure, an ischemic center of markedly reduced blood flow (to 15%) and a surrounding oligemic zone were observed on MRI scans; (2) the size of the infarct significantly increased within the next day, which could be attenuated by early tPA treatment.

Alternatively, an optic fiber connected to a laser source (532 nm) can be used for photostimulation and stereotactically guided to the target region with the help of a guidance cannula [36, 47].

9 Focal Thrombosis of the Middle Cerebral Artery or Small Surface and Penetrating Arterioles

As was already described by Watson and coworkers [48, 49], photosensitive dyes can also be used to occlude single vessels. Lasers are applied for photoactivation to specifically target arteries (e.g., the MCA) or arterioles before penetrating the cortex. Recent studies showed that photothrombic occlusion of localized MCA branches is sufficiently accurate to inactivate targeted regions of the somatosensory representation while leaving neighboring regions intact [5]. Furthermore, it could be demonstrated that surface arterioles form redundant interconnected networks and therefore can tolerate a local damage [4], whereas the territories of penetrating arterioles only partially overlap and have high specificity to cortical columns ($r = 350$ µm) [3].

To occlude the MCA, the distal MCA territory has to be surgically exposed [48]. A vertical skin incision is made between the lateral canthus of the eye and the ear, the skin is retracted with silk sutures, and the underlying temporal muscle is incised and retracted ventrally. A small craniectomy (approx. 3 mm) is drilled into the frontal-squamosal bone ventral to the coronal suture and above the zygomatic arch. A green laser beam (e.g., 514.5-nm argon or argon-pumped dye laser or 532-nm MicroGreen or Laserglow LCS-0532 lasers) is then placed onto the MCA. After intravenous injection of rose bengal or erythrosin B, the MCA is irradiated. The onset of thrombosis starts with a vasoconstriction, followed by the formation of a mural, continuously embolizing platelet-only thrombus occluding the MCA [49]. High-intensity pulsed lasers based on Q switching (532-nm Nd:YAG) or superradiance (337-nm nitrogen or nitrogen-pumped dye lasers) are not recommended.

Although they may be set at an average intensity equivalent to continuous-wave lasers, they cannot occlude arteries or arterioles since their 3- to 5-ns pulse widths are too short to sustain synergistic accumulation of platelet aggregation leading to occlusion. This technique results in robust cortical infarction which closely resembles the most common type and location of human stroke. Its size can be varied depending on the site of photostimulation (proximal occlusion results in larger infarcts affecting also the basal ganglia; distal MCA occlusion targets only a small cortical region).

Targeting of individual surface arterioles has been described in detail by Murphy and colleagues [5, 50]. To photoactivate rose bengal, they used a 532-nm diode-pumped laser beam (Beta Electronics MGM-20, Columbus, OH; 0.7–1.4 mW power measured at the objective back aperture) coupled to the microscope's epifluorescent light path and focused into a spot through a 40×, 0.8 NA water immersion lens. To reduce redundant paths of surface blood flow, they suggested to target an arteriole at multiple points by rotating every 1–2 min between two or three targeted sites. This ensures that clots are initiated at each site by a relatively high concentration of dye since it clears rapidly (see Fig. 3).

Kleinfeld and coworkers adapted a two-photon laser-scanning setup to simultaneously examine clot formation, hemodynamics, and neuronal activity after focal photothrombotic occlusion of single cortical arterioles [3, 4, 51]. For photoactivation of rose bengal, a 532-nm laser beam (0.1–5 mW; TIM-622, Transverse Industries, Taiwan) was focused coplanar with the near-infrared beam through a 0.8-NA, 40× water immersion objective, forming a 5-μm spot in the center of the same plane as the imaging beam (lumen of the target vessel). This method allows very precise occlusion of surface or penetrating arterioles up to a depth of 50 μm from the pial surface. It is very useful to model human micro-strokes which are often centered around penetrating arteries and arterioles with obstructed lumens (see Fig. 4) [51].

10 Characteristics, Advantages, and Disadvantages of Photochemical Stroke Models

Photochemical stroke models were developed in rodents to mimic certain characteristics of human stroke pathology. They have a number of advantages:

1. They allow a precise induction of circumscribed infarcts in any desired cortical or subcortical site.
2. The focal nature of the infarct facilitates the distinction between events in the lesion and remote brain areas.
3. The size of the lesion is very reproducible and can be easily controlled by adjusting the intensity and duration of light or the concentration of the photosensitive dye.

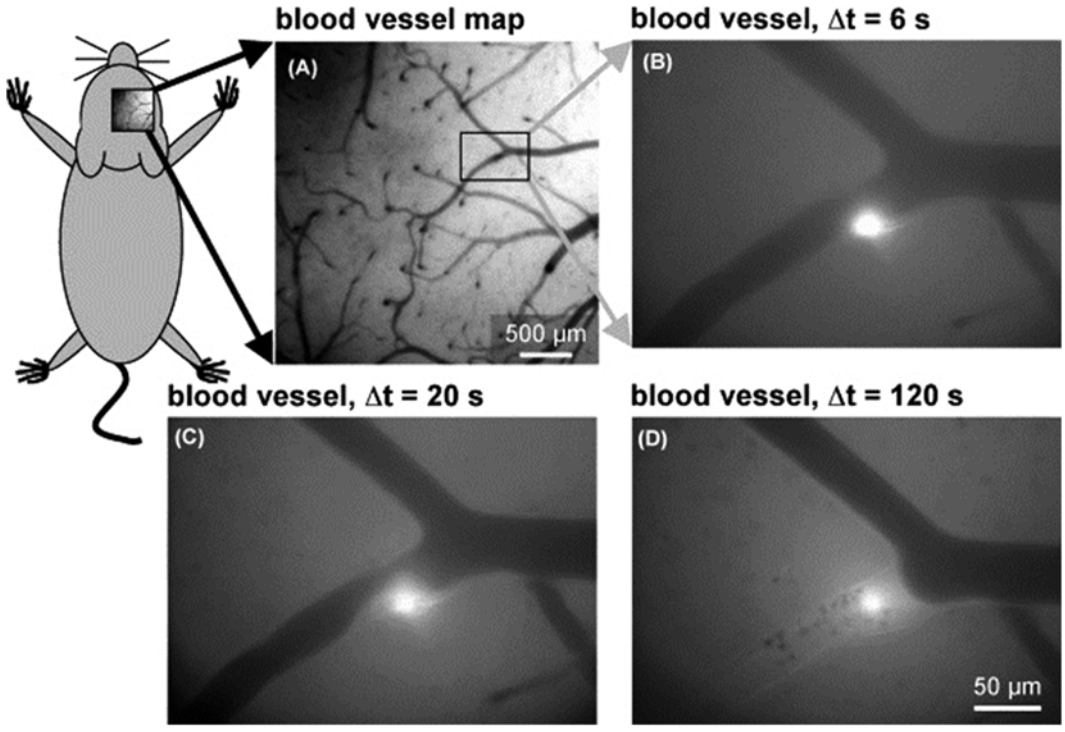

Fig. 3 Targeting individual brain arterioles for photoactivation of rose bengal. (**a**) Schematic showing experimental subject (C57Bl/6 mouse) and brain vasculature with regions for photoactivation indicated by *arrows*. (**b**) Photoactivation spot visualized by rose bengal fluorescence following excitation with 532-nm laser light in the arteriole segment shown in (**a**). The arterioles are visualized as dark structures applying dim illumination with blue background light (cutoff wavelength 480 nm). Scaling in the original 12-bit image was nonlinear to visualize both the very dim background structure as well as the laser spot, which showed several orders of magnitude higher intensity. (**c** and **d**) Subsequent images of the specimen shown in (**b**) during further fluorescent activation by laser light. The blood flow in the arteriole at the left bottom of the image was blocked within 2 min of photoactivation with green laser light. From Ref. [50], with permission

4. The classical photothrombosis and the "ring" model are furthermore minimally invasive and have a very low mortality rate.
5. The model is accompanied by a vessel thrombosis; the properties of the clot are similar to that of a thrombus in human stroke as they are responsive to rt-PA; thus it can be used to study the action of rt-PA in man.

As any model of experimental stroke, the photothrombosis has several limitations and differs in some respects from stroke in humans:

1. In the classical model, the photothrombosis is triggered in a large number of microvessels within the illuminated area, and both arteries and veins may be occluded. This primarily end-arterial nature of occlusion is different from human stroke, which is typically caused by occlusion of a single brain artery. There is no significant ischemic penumbra or region of local

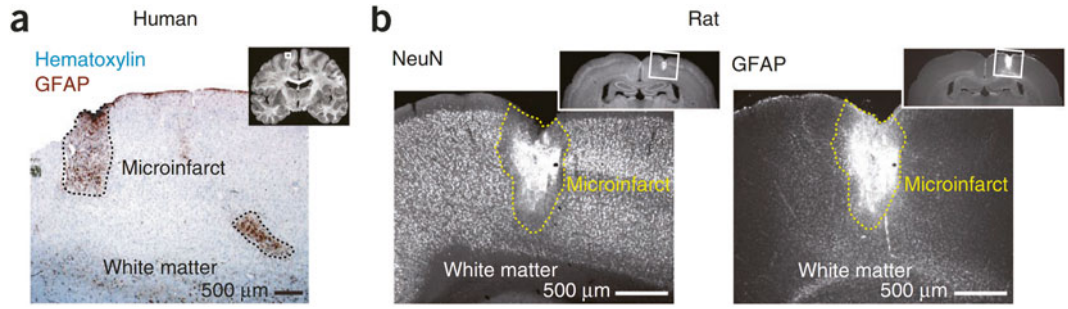

Fig. 4 Similarity between human and rat cortical microinfarcts. (**a**) Histology of microinfarcts detected in the cortex of an elderly human. The infarcted area is dense with reactive astrocytes that stained with glial fibrillary acidic protein (GFAP, *brown*). The tissue was counterstained with hematoxylin (*blue*). (**b**) Microinfarct as seen 7 days after occlusion of a single penetrating arteriole in rat cortex. Neuronal viability was assessed with antibody to NeuN and astrogliosis was assessed with antibody to GFAP. Copyright © 2013 by Macmillan Publishers Ltd: Nature Neuroscience [51]; reprinted by permission

collateral flow and reperfusion, rendering the lesion resistant to flow enhancement strategies. To overcome these issues, the photochemical ring model has been developed in which a circular region of ischemic damage surrounds a circumscribed area of reduced blood flow with typical characteristics of an ischemic penumbra. However, this penumbral area is located within the evolving vasogenic edema, and it is unclear if this accurately models the human penumbra [43].

2. Photothrombosis is associated with a pronounced disruption of endothelial integrity [11, 18, 19]. Especially in the classical and ring models, the ischemic damage evolves rapidly and is associated with simultaneous development of cytotoxic and vasogenic edema, whereas in humans infarction prevails edema by several hours. In this respect, photochemical lesions more closely resemble traumatic brain injury [43]. As recently reported, the edema might be the major cause of cerebral infarction following photothrombosis [16].
3. The photothrombotic model is inadequate for the study of antithrombotic agents since it occurs also after blocking of platelets or inhibition of intrinsic coagulation pathways [16].

The more recently developed models overcome many of these issues. Photothrombotic occlusion of single brain vessels more closely replicates human stroke. Focal thrombosis of the MCA results in circumscribed infarcts that can be adjusted in size by the positioning of the light beam. These lesions are surrounded by a region of reduced blood flow, resembling a typical penumbra. Photothrombosis of smaller arterioles allows studying the dependency of occlusion-related vasodynamics on different vessel types. Photothrombotic occlusion of small penetrating arterioles, for example, mimics processes during human micro-strokes.

References

1. Watson BD, Dietrich WD, Busto R, Wachtel MS, Ginsberg MD (1985) Induction of reproducible brain infarction by photochemically initiated thrombosis. Ann Neurol 17(5):497–504. doi:10.1002/ana.410170513
2. Wester P, Watson BD, Prado R, Dietrich WD (1995) A photothrombotic 'ring' model of rat stroke-in-evolution displaying putative penumbral inversion. Stroke 26(3):444–450
3. Nishimura N, Schaffer CB, Friedman B, Lyden PD, Kleinfeld D (2007) Penetrating arterioles are a bottleneck in the perfusion of neocortex. Proc Natl Acad Sci U S A 104(1):365–370. doi:10.1073/pnas.0609551104
4. Schaffer CB, Friedman B, Nishimura N, Schroeder LF, Tsai PS, Ebner FF, Lyden PD, Kleinfeld D (2006) Two-photon imaging of cortical surface microvessels reveals a robust redistribution in blood flow after vascular occlusion. PLoS Biol 4(2), e22. doi:10.1371/journal.pbio.0040022
5. Zhang S, Murphy TH (2007) Imaging the impact of cortical microcirculation on synaptic structure and sensory-evoked hemodynamic responses in vivo. PLoS Biol 5(5), e119. doi:10.1371/journal.pbio.0050119
6. Kuroiwa T, Xi G, Hua Y, Nagaraja TN, Fenstermacher JD, Keep RF (2009) Development of a rat model of photothrombotic ischemia and infarction within the caudoputamen. Stroke 40(1):248–253. doi:10.1161/STROKEAHA.108.527853
7. Lozano JD, Abulafia DP, Danton GH, Watson BD, Dietrich WD (2007) Characterization of a thromboembolic photochemical model of repeated stroke in mice. J Neurosci Methods 162(1–2):244–254. doi:10.1016/j.jneumeth.2007.01.018
8. Tseng SC, Feenstra RP, Watson BD (1994) Characterization of photodynamic actions of Rose Bengal on cultured cells. Invest Ophthalmol Vis Sci 35(8):3295–3307
9. Watson BD, Dietrich WD (1990) Animal models in stroke. Stroke 21(9):1376–1377
10. Nakayama H, Dietrich WD, Watson BD, Busto R, Ginsberg MD (1988) Photothrombotic occlusion of rat middle cerebral artery: histopathological and hemodynamic sequelae of acute recanalization. J Cereb Blood Flow Metab 8(3):357–366
11. Dietrich WD, Busto R, Watson BD, Scheinberg P, Ginsberg MD (1987) Photochemically induced cerebral infarction. II. Edema and blood-brain barrier disruption. Acta Neuropathol 72(4):326–334
12. Dietrich WD, Watson BD, Busto R, Ginsberg MD, Bethea JR (1987) Photochemically induced cerebral infarction. I. Early microvascular alterations. Acta Neuropathol 72(4):315–325
13. Dietrich WD, Ginsberg MD, Busto R, Watson BD (1986) Photochemically induced cortical infarction in the rat. 2. Acute and subacute alterations in local glucose utilization. J Cereb Blood Flow Metab 6(2):195–202
14. Dietrich WD, Ginsberg MD, Busto R, Watson BD (1986) Photochemically induced cortical infarction in the rat. 1. Time course of hemodynamic consequences. J Cereb Blood Flow Metab 6(2):184–194
15. Inamo J, Belougne E, Doutremepuich C (1996) Importance of photo activation of Rose Bengal for platelet activation in experimental models of photochemically induced thrombosis. Thromb Res 83(3):229–235
16. Kleinschnitz C, Braeuninger S, Pham M, Austinat M, Nolte I, Renne T, Nieswandt B, Bendszus M, Stoll G (2008) Blocking of platelets or intrinsic coagulation pathway-driven thrombosis does not prevent cerebral infarctions induced by photothrombosis. Stroke 39(4):1262–1268. doi:10.1161/STROKEAHA.107.496448
17. Jourdan A, Aguejouf O, Imbault P, Doutremepuich F, Inamo J, Doutremepuich C (1995) Experimental thrombosis model induced by free radicals. Application to aspirin and other different substances. Thromb Res 79(1):109–123
18. Stoll G, Kleinschnitz C, Meuth SG, Braeuninger S, Ip CW, Wessig C, Nolte I, Bendszus M (2009) Transient widespread blood-brain barrier alterations after cerebral photothrombosis as revealed by gadofluorine M-enhanced magnetic resonance imaging. J Cereb Blood Flow Metab 29(2):331–341. doi:10.1038/jcbfm.2008.129
19. Piao MS, Lee JK, Park CS, Ryu HS, Kim SH, Kim HS (2009) Early activation of matrix metalloproteinase-9 is associated with blood-brain barrier disruption after photothrombotic cerebral ischemia in rats. Acta Neurochir (Wien). doi:10.1007/s00701-009-0431-1
20. Keiner S, Witte OW, Redecker C (2009) Immunocytochemical detection of newly generated neurons in the perilesional area of cortical infarcts after intraventricular application of brain-derived neurotrophic factor. J Neuropathol Exp Neurol 68(1):83–93. doi:10.1097/NEN.0b013e31819308e9

21. Nowicka D, Rogozinska K, Aleksy M, Witte OW, Skangiel-Kramska J (2008) Spatiotemporal dynamics of astroglial and microglial responses after photothrombotic stroke in the rat brain. Acta Neurobiol Exp (Wars) 68(2):155–168
22. Keiner S, Wurm F, Kunze A, Witte OW, Redecker C (2008) Rehabilitative therapies differentially alter proliferation and survival of glial cell populations in the perilesional zone of cortical infarcts. Glia 56(5):516–527. doi:10.1002/glia.20632
23. Jablonka JA, Witte OW, Kossut M (2007) Photothrombotic infarct impairs experience-dependent plasticity in neighboring cortex. Neuroreport 18(2):165–169. doi:10.1097/WNR.0b013e328010feff
24. Shanina EV, Schallert T, Witte OW, Redecker C (2006) Behavioral recovery from unilateral photothrombotic infarcts of the forelimb sensorimotor cortex in rats: role of the contralateral cortex. Neuroscience 139(4):1495–1506. doi:10.1016/j.neuroscience.2006.01.016
25. Reinecke S, Dinse HR, Reinke H, Witte OW (2003) Induction of bilateral plasticity in sensory cortical maps by small unilateral cortical infarcts in rats. Eur J Neurosci 17(3):623–627
26. Redecker C, Wang W, Fritschy JM, Witte OW (2002) Widespread and long-lasting alterations in GABA(A)-receptor subtypes after focal cortical infarcts in rats: mediation by NMDA-dependent processes. J Cereb Blood Flow Metab 22(12):1463–1475. doi:10.1097/00004647-200212000-00007
27. Keyvani K, Witte OW, Paulus W (2002) Gene expression profiling in perilesional and contralateral areas after ischemia in rat brain. J Cereb Blood Flow Metab 22(2):153–160. doi:10.1097/00004647-200202000-00003
28. Schiene K, Bruehl C, Zilles K, Qu M, Hagemann G, Kraemer M, Witte OW (1996) Neuronal hyperexcitability and reduction of GABAA-receptor expression in the surround of cerebral photothrombosis. J Cereb Blood Flow Metab 16(5):906–914. doi:10.1097/00004647-199609000-00014
29. Buchkremer-Ratzmann I, August M, Hagemann G, Witte OW (1996) Electrophysiological transcortical diaschisis after cortical photothrombosis in rat brain. Stroke 27(6):1105–1109, discussion 1109-1111
30. Ding S, Wang T, Cui W, Haydon PG (2009) Photothrombosis ischemia stimulates a sustained astrocytic Ca2+ signaling in vivo. Glia 57(7):767–776. doi:10.1002/glia.20804
31. Karhunen H, Bezvenyuk Z, Nissinen J, Sivenius J, Jolkkonen J, Pitkanen A (2007) Epileptogenesis after cortical photothrombotic brain lesion in rats. Neuroscience 148(1):314–324. doi:10.1016/j.neuroscience.2007.05.047
32. Klaassen CD (1976) Pharmacokinetics of Rose Bengal in the rat, rabbit, dog and guinea pig. Toxicol Appl Pharmacol 38(1):85–100
33. Greifzu F, Schmidt S, Schmidt KF, Kreikemeier K, Witte OW, Lowel S (2011) Global impairment and therapeutic restoration of visual plasticity mechanisms after a localized cortical stroke. Proc Natl Acad Sci U S A 108(37):15450–15455. doi:10.1073/pnas.1016458108
34. Labat-gest V, Tomasi S (2013) Photothrombotic ischemia: a minimally invasive and reproducible photochemical cortical lesion model for mouse stroke studies. J Vis Exp (76). doi:10.3791/50370
35. Brown CE, Aminoltejari K, Erb H, Winship IR, Murphy TH (2009) In vivo voltage-sensitive dye imaging in adult mice reveals that somatosensory maps lost to stroke are replaced over weeks by new structural and functional circuits with prolonged modes of activation within both the peri-infarct zone and distant sites. J Neurosci 29(6):1719–1734. doi:10.1523/JNEUROSCI.4249-08.2009
36. Barth AM, Mody I (2011) Changes in hippocampal neuronal activity during and after unilateral selective hippocampal ischemia in vivo. J Neurosci 31(3):851–860. doi:10.1523/JNEUROSCI.5080-10.2011
37. Cha JH, Wee HJ, Seo JH, Ahn BJ, Park JH, Yang JM, Lee SW, Kim EH, Lee OH, Heo JH, Lee HJ, Gelman IH, Arai K, Lo EH, Kim KW (2014) AKAP12 mediates barrier functions of fibrotic scars during CNS repair. PLoS One 9(4), e94695. doi:10.1371/journal.pone.0094695
38. Cybulska-Klosowicz A, Liguz-Lecznar M, Nowicka D, Ziemka-Nalecz M, Kossut M, Skangiel-Kramska J (2011) Matrix metalloproteinase inhibition counteracts impairment of cortical experience-dependent plasticity after photothrombotic stroke. Eur J Neurosci 33(12):2238–2246. doi:10.1111/j.1460-9568.2011.07713.x
39. Kim GW, Sugawara T, Chan PH (2000) Involvement of oxidative stress and caspase-3 in cortical infarction after photothrombotic ischemia in mice. J Cereb Blood Flow Metab 20(12):1690–1701. doi:10.1097/00004647-200012000-00008
40. Jander S, Kraemer M, Schroeter M, Witte OW, Stoll G (1995) Lymphocytic infiltration and expression of intercellular adhesion molecule-1 in photochemically induced ischemia of the rat cortex. J Cereb Blood Flow Metab 15(1):42–51. doi:10.1038/jcbfm.1995.5
41. Schroeter M, Jander S, Witte OW, Stoll G (1999) Heterogeneity of the microglial

response in photochemically induced focal ischemia of the rat cerebral cortex. Neuroscience 89(4):1367–1377

42. Schroeter M, Kury P, Jander S (2003) Inflammatory gene expression in focal cortical brain ischemia: differences between rats and mice. Brain Res Mol Brain Res 117(1):1–7
43. Carmichael ST (2005) Rodent models of focal stroke: size, mechanism, and purpose. NeuroRx 2(3):396–409
44. Gu W, Jiang W, Wester P (1999) A photothrombotic ring stroke model in rats with sustained hypoperfusion followed by late spontaneous reperfusion in the region at risk. Exp Brain Res 125(2):163–170
45. Jiang W, Gu W, Hossmann KA, Mies G, Wester P (2006) Establishing a photothrombotic 'ring' stroke model in adult mice with late spontaneous reperfusion: quantitative measurements of cerebral blood flow and cerebral protein synthesis. J Cereb Blood Flow Metab 26(7):927–936. doi:10.1038/sj.jcbfm.9600245
46. Maxwell KA, Dyck RH (2005) Induction of reproducible focal ischemic lesions in neonatal mice by photothrombosis. Dev Neurosci 27(2-4):121–126. doi:10.1159/000085983
47. Kim HS, Kim D, Kim RG, Kim JM, Chung E, Neto PR, Lee MC, Kim HI (2014) A rat model of photothrombotic capsular infarct with a marked motor deficit: a behavioral, histologic, and microPET study. J Cereb Blood Flow Metab 34(4):683–689. doi:10.1038/jcbfm.2014.2
48. Dietrich WD, Prado R, Watson BD, Nakayama H (1988) Middle cerebral artery thrombosis: acute blood-brain barrier consequences. J Neuropathol Exp Neurol 47(4):443–451
49. Futrell N, Watson BD, Dietrich WD, Prado R, Millikan C, Ginsberg MD (1988) A new model of embolic stroke produced by photochemical injury to the carotid artery in the rat. Ann Neurol 23(3):251–257. doi:10.1002/ana.410230307
50. Sigler A, Goroshkov A, Murphy TH (2008) Hardware and methodology for targeting single brain arterioles for photothrombotic stroke on an upright microscope. J Neurosci Methods 170(1):35–44. doi:10.1016/j.jneumeth.2007.12.015
51. Shih AY, Blinder P, Tsai PS, Friedman B, Stanley G, Lyden PD, Kleinfeld D (2013) The smallest stroke: occlusion of one penetrating vessel leads to infarction and a cognitive deficit. Nat Neurosci 16(1):55–63. doi:10.1038/nn.3278

Chapter 8

Housing in an Enriched Environment: A Tool to Study Functional Recovery After Experimental Stroke

Karsten Ruscher and Tadeusz Wieloch

Abstract

Physical therapy and social interactions between the stroke patient and health-care professionals or relatives facilitate the process of recovery and promote improvement of lost neurological function after stroke. These observations can be mimicked in an experimental setting by multimodal stimulation provided in the concept of enriched environment. The enriched environment is a housing condition for rodents combining social interactions and sensorimotor stimulation that improves lost neurological function without affecting the extent of brain damage after experimental stroke. This chapter deals with the concept of enriched housing and about performing studies using enriched environment as tool to investigate mechanisms of recovery after brain injury.

Key words Functional recovery, Enriched environment, Plasticity, Remodeling, Cell genesis, Glial scar, Behavior, Rotating pole test, Rehabilitation

1 Introduction

In the USA, approximately 1.1 million adults that suffer a stoke continue living with a functional deficit [1]. Though approximately 50–70 % of the stroke victims recover sufficient neurological function to continue an independent life, up to 30 % will be afflicted by a permanent disability. Today, stroke therapy that aims at enhancing lost neurological function involves various modes of exercise, and at present no approved drugs that enhance particular aspects of recovery are available. Though stroke also affects speech and cognition and may cause pain, dysphagia, neglect, and depression, the motor deficits after stroke are commonly assessed or measured in clinical rehabilitative research and trials. Hence, physical exercise such as constraint-induced movement therapy, forcing the use of the paralyzed arm [2], or body-weight-supported gait training [3] has proven efficient, though this therapy is cumbersome, personnel intense, and thus costly. Also, the patients must be highly

Ulrich Dirnagl (ed.), *Rodent Models of Stroke*, Neuromethods, vol. 120,
DOI 10.1007/978-1-4939-5620-3_8,

motivated to be subjected to the quite harsh physical therapy. Positive tactile, visual and auditory stimulation, and social interactions appear to promote the outcome of physical therapy.

To find measures that speed the recovery process and enhance the extent of recovery is the aim of current clinical and preclinical rehabilitative research. However, the underlying mechanisms of recovery are complex and involve parallel processes of restoration and compensation that occur spontaneously and that may be enhanced by rehabilitation therapy. Several mechanisms have been identified, including resolution of edema, glial scar formation, and recovery of synaptic transmission or activation of alternative or silent neuronal pathways [4]. Prominent in this context is brain plasticity or cortical remodeling or reorganization, an experienced driven process that stimulates axonal growth and synaptogenesis. To study motor recovery processes, both rodent and primate models of stroke have been used. These models involve training sessions using particular limb movement protocols [5, 6] and/or housing rodents in an enriched milieu—an enriched environment [7, 8]. Interestingly, first proof-of-concept clinical trials implementing EE in stroke rehabilitation have been performed to evaluate benefits and risks for stroke patients [9].

An enriched environment from a rodent perspective stimulates their exploratory, sensorimotor, and social behavior. It is a paradigm of multiple sensori-stimulation originally developed to study learning processes [10]. The initial idea about the concept of enriched environment was introduced by Donald R. Hebb in 1947 [11]. Based on these findings, in the late 1950s Rosenzweig and colleagues initiated studies to investigate effects of enriched environment on the brain [12].

Interestingly, placing rodents in enriched environment provides a multimodal stimulation to the brain and among other effects stimulates memory and learning, neuronal plasticity processes, and cell genesis. This experimental paradigm was applied in models of experimental stroke using rats [7] and mice [8]. Housing injured animals in an enriched environment leads to neuroanatomical changes similar to those induced in uninjured animals, such as increasing the number of dendritic branches and dendritic spines and cell genesis, but in addition enriched housing enhanced the motor and cognitive performance of the animals. The complexity and robustness of the multimodal stimulation provided by the enriched housing is evident in the complex differential gene expression in stroke-damaged brains of animals in enriched housing conditions [13, 14]. Moreover, enriched environment profoundly affects cellular and molecular processes in the poststroke brain to improve recovery of lost neurological function [15, 16]. This chapter provides a protocol on how to establish a standardized enriched environment and discusses advantages and limitations of such an approach.

2 Which Model of Experimental Stroke Should Be Used

The variable location and size of the lesion in clinical stroke, age, and comorbidity of patients, as well as individual variations in anatomical and functional neuronal connections, affect functional outcome after stroke. In the experimental setting, some of these variables can be taken into consideration by choosing an appropriate stroke model and animal strain.

The recovery enhancing effect of enriched housing has been reported using several experimental stroke models and several common rodent strains have been used in these studies. In a model of endothelin-1-induced MCAO using Sprague Dawley rats, recovery of function was accomplished by specific limb training and housing in an enriched environment [6]. In spontaneous hypertensive rats of the SHR and SHR-SP strains, the penumbra region after permanent occlusion of the MCAO is small providing a large infarct that is dependent on the occlusion site (proximal or distal) of the MCA. In these rats strain recovery of function is also enhanced following housing in the enriched environment [17]. Recently we have used the Wistar strain with a 90–120 min using the filament model MCAO, where the enrichment effect is robust. Also, the photothrombotic model can be used [16, 18, 19].

3 Preparation of Enriched Environment Cages

In general, the enriched cages have to be constructed in way that the environment does not represent a potential danger to the injured animals. Moreover, the cage has to stimulate as many of the rat senses as possible, their exploratory behavior, their olfaction, their need of social interaction, and their motor functions. Also, it has to be large enough to house 5–8 animals, a prerequisite to develop proper social interactions. Animals should be able to move freely and should also have places to back away from the group. A proper cage should not be smaller than $600 \times 600 \times 1200$ mm for rat and $600 \times 600 \times 500$ mm for mouse studies. Oversized cages might result in an artificial unwilling isolation. To challenge the exploratory function, platforms, grids, pipes, and ropes must be included in the milieu and be removable so that the cage can be rebuilt twice a week. The “toys” should be of a material that can withstand frequent washing. A sufficient amount of free accessible food and water for 5 to 8 animals must be available at the bottom of the cages (Fig. 1).

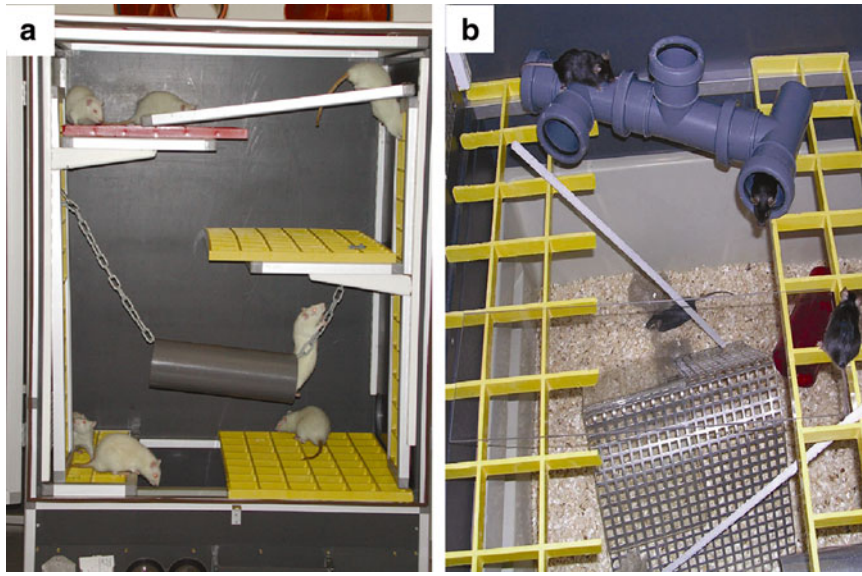

Fig. 1 Multilevel enriched environment cages for rats (**a**) and mice (**b**). Note that the cages are equipped with horizontal and vertical grids in various colors and sizes, as well as chains and ropes to allow animals to reach all cage levels. Pipes serve as artificial tunnels potentially providing a kind of security for injured animals

4 Exclusion Criteria

Inclusion and exclusion criteria are commonly used in clinical studies to reduce heterogeneities in a study population. For example, often stroke deficits affecting motor function of upper extremities are included in the studies. For example, in the CI therapy trial [2], some remaining movement ability of the limbs was a prerequisite for inclusion. Exclusion criteria must also be considered in experimental studies of recovery of function. Each experimental procedure should be prespecified before an animal enters a study. However using standardized surgery procedures, there is a variability in infarct size and in the loss of sensorimotor function after experimental stroke, possibly due to some variability in vessel anatomy. Therefore, to obtain a homogenous population of animals with approximately similar degree of motor deficit, function is assessed *prior* to exposure to the enriched environment, using a behavioral test (assessing loss of sensorimotor function). A simple test is the rotating pole test or a composite neuroscore providing a sensorimotor score after acute brain injury [20, 21]. The test is performed at 48 h after injury, a time point when the growth of the infarct has essentially subsided. Animals traverse a rotating wooden pole at 0, 3, and 10 rpm, and only those animals which are not able to traverse a pole (test score 0–2) are included into subsequent studies and assigned randomly into groups housed either in standard or enriched environment cages. Animals that traverse the

pole are used as cage mates in the enriched environment. Similarly, a significant deficit in the neuroscore should be obtained. Also those animals that display signs of complications such as wound infections, hyper- or hypothermia, seizures, bleedings, and abnormal cachexia have to be excluded by ethical considerations (Box 1).

Box 1: Exclusion Criteria for Recovery Studies After MCAO

Insufficient neurological deficit at 48 h after MCAO assessed at least by one reliable behavioral test

Signs of complications such as wound infections, hyper- or hypothermia, seizures, bleedings, and abnormal cachexia

5 Handling of Animals

It is important to keep in mind that every handling of an animal should be regarded as a potential enrichment of its environment and therefore might be a confounder in the studies. Hence, the pretraining episodes for the behavioral and performance tests are strong sensori-stimulants that have to be taken into account and controlled for in the design of the experiment.

The combination of a social and sensorimotor stimulation integrated in the enriched environment appears to be superior to isolated motor training [7] emphasizing the importance of the social component of an enriched environment. Hence, at least five rodents should be housed together for an optimal enriched environment. Often, sufficient numbers of injured animals cannot be accomplished in the beginning of a study. Therefore, animals excluded from the study and healthy animals may serve as mates until they are exchanged by injured animals during the course of the study.

At day 2 after injury, animals normally show low spontaneous motor activity and have a tendency to stay immobile. To overcome initial poststroke inactivity, animals are placed on the top level of an enriched environment cage. This promotes active movement to reach food and water located in the bottom of the cage. At this stage of recovery, once an injured animal has reached the bottom it should be placed back to the upper levels. All procedures in changing the environment must be done in a reproducible manner and follow a distinct protocol.

Placing 5–8 injured animals together is a social challenge. Rats adapt fast to the new environment and can be housed in the enriched environment during the entire course of the study. In contrast, mice show a pronounced tendency to become territorial,

and they form a strong social structure that may be detrimental for animals at a lower level of the hierarchy [8]. In fact the mortality due to aggressive behavior could exceed 50%. Based on our experience, a stay in the enriched environment for 3 h is sufficient to robustly improve functional recovery after experimental stroke and after transient MCAO. In between the "enrichment sessions," mice are returned into standard home cages. Regular check of the status of the animals during the first 3 days is essential since impaired animals are prone to secondary injuries. After photothrombosis in mice, however, the tendency to create new hierarchies has not been observed and mice could be kept in enriched environment cages permanently until the study endpoint [19].

6 Duration in an Enriched Environment

The duration an animal should spend in an enriched environment depends on the scientific question. However, previous studies have shown that early and forced physical activities during the first 24 h after stroke are harmful to the recovery process after experimental stroke [22]. Approximately at 48 h after experimental stroke, the acute degenerative processes have declined, the infarction has subsided, and housing animals in the enriched environment from 2 days after injury onwards does not expand infarct size [17]. We have experienced that a minimum stay in the enriched environment for 3 days is required to achieve a significant improvement of sensorimotor function, while the start of the enriched rehabilitation can be delayed for up to 15 days with preserved effect [23]. In order to preserve the functional recovery, enriched housing for at least 4 weeks is required. Housing for 2 weeks significantly improves outcome, but the beneficial effect is lost after additional 2 weeks in a standard cage.

7 Problems Encountered During Housing in an Enriched Environment

The brain ischemia and the subsequent tissue infarction in combination with the surgical procedures are a massive stress on the animal that does not only affect the neurological function. Often food and water intake is reduced, and poststroke animals develop a general weakness, which can be overcome by placing animals close to food and water in the enriched cages. In addition, injured animals are prone to infections due to poststroke immunodepression, which may become a significant problem if animals are housed in larger groups [24]. Hence, the cages and the enrichment toys have to be cleaned regularly. Laboratory rodents have no experience of the enriched cages and have an urge to explore the new environment. The exploration of the new environment occurs in a critical

period of recovery in which animals are limited to move due to the sensorimotor impairment and general weakness. Thus, there is a risk of secondary damages due to impairment while exploring the cage during the first days of recovery that has to be taken into consideration. As mentioned above, mice develop new social hierarchies when placed in an enriched environment. To avoid any fighting among animals, mice should be kept in the enriched environment cage for a period sufficient to increase voluntary motor activity and to initiate social interactions.

References

1. American Heart Association (2008) Heart and stroke statistical update. American Heart Association, Dallas
2. Wolf SL, Winstein CJ, Miller JP, Taub E, Uswatte G, Morris D, Giuliani C, Light KE, Nichols-Larsen D (2006) Effect of constraint-induced movement therapy on upper extremity function 3 to 9 months after stroke: the EXCITE randomized clinical trial. JAMA 296:2095–2104
3. Bogey R, Hornby GT (2007) Gait training strategies utilized in poststroke rehabilitation: are we really making a difference? Top Stroke Rehabil 14:1–8
4. Wieloch T, Nikolich K (2006) Mechanisms of neural plasticity following brain injury. Curr Opin Neurobiol 16:258–264
5. Plautz EJ, Barbay S, Frost SB, Friel KM, Dancause N, Zoubina EV, Stowe AM, Quaney BM, Nudo RJ (2003) Post-infarct cortical plasticity and behavioral recovery using concurrent cortical stimulation and rehabilitative training: a feasibility study in primates. Neurol Res 25:801–810
6. Biernaskie J, Chernenko G, Corbett D (2004) Efficacy of rehabilitative experience declines with time after focal ischemic brain injury. J Neurosci 24:1245–1254
7. Johansson BB, Ohlsson AL (1996) Environment, social interaction, and physical activity as determinants of functional outcome after cerebral infarction in the rat. Exp Neurol 139:322–327
8. Nygren J, Wieloch T (2005) Enriched environment enhances recovery of motor function after focal ischemia in mice, and downregulates the transcription factor NGFI-A. J Cereb Blood Flow Metab 25:1625–1633
9. White JH, Bartley E, Janssen H, Jordan LA, Spratt N (2015) Exploring stroke survivor experience of participation in an enriched environment: a qualitative study. Disabil Rehabil 37:593–600
10. Rosenzweig MR, Bennett EL (1996) Psychobiology of plasticity: effects of training and experience on brain and behavior. Behav Brain Res 78:57–65
11. Hebb DO (1947) The effects of early experience on problem solving at maturity. Am Psychol 2:306–307
12. Rosenzweig MR, Krech D, Bennett EL, Diamond MC (1962) Effects of environmental complexity and training on brain chemistry and anatomy: a replication and extension. J Comp Physiol Psychol 55:429–437
13. Keyvani K, Sachser N, Witte OW, Paulus W (2004) Gene expression profiling in the intact and injured brain following environmental enrichment. J Neuropathol Exp Neurol 63:598–609
14. Ruscher K, Shamloo M, Rickhag M, Ladunga I, Soriano L, Gisselsson L, Toresson H, Ruslim-Litrus L, Oksenberg D, Urfer R, Johansson BB, Nikolich K, Wieloch T (2011) The sigma-1 receptor enhances brain plasticity and functional recovery after experimental stroke. Brain 134:732–746
15. Ruscher K, Kuric E, Liu Y, Walter HL, Issazadeh-Navikas S, Englund E, Wieloch T (2013) Inhibition of CXCL12 signaling attenuates the postischemic immune response and improves functional recovery after stroke. J Cereb Blood Flow Metab 33:1225–1234
16. Madinier A, Quattromani MJ, Sjolund C, Ruscher K, Wieloch T (2014) Enriched housing enhances recovery of limb placement ability and reduces aggrecan-containing perineuronal nets in the rat somatosensory cortex after experimental stroke. PLoS One 9, e93121
17. Risedal A, Mattsson B, Dahlqvist P, Nordborg C, Olsson T, Johansson BB (2002) Environmental influences on functional outcome after a cortical infarct in the rat. Brain Res Bull 58:315–321
18. Keiner S, Wurm F, Kunze A, Witte OW, Redecker C (2008) Rehabilitative therapies

differentially alter proliferation and survival of glial cell populations in the perilesional zone of cortical infarcts. Glia 56:516–527

19. Quattromani MJ, Cordeau P, Ruscher K, Kriz J, Wieloch T (2014) Enriched housing down-regulates the Toll-like receptor 2 response in the mouse brain after experimental stroke. Neurobiol Dis 66:66–73
20. Mattiasson GJ, Philips MF, Tomasevic G, Johansson BB, Wieloch T, McIntosh TK (2000) The rotating pole test: evaluation of its effectiveness in assessing functional motor deficits following experimental head injury in the rat. J Neurosci Methods 95:75–82
21. Ruscher K, Kuric E, Wieloch T (2012) Levodopa treatment improves functional recovery after experimental stroke. Stroke 43:507–513
22. Risedal A, Zeng J, Johansson BB (1999) Early training may exacerbate brain damage after focal brain ischemia in the rat. J Cereb Blood Flow Metab 19:997–1003
23. Johansson BB (1996) Functional outcome in rats transferred to an enriched environment 15 days after focal brain ischemia. Stroke 27:324–326
24. Prass K, Meisel C, Hoflich C, Braun J, Halle E, Wolf T, Ruscher K, Victorov IV, Priller J, Dirnagl U, Volk HD, Meisel A (2003) Stroke-induced immunodeficiency promotes spontaneous bacterial infections and is mediated by sympathetic activation reversal by poststroke T helper cell type 1-like immunostimulation. J Exp Med 198:725–736

Chapter 9

Modeling Risk Factors and Confounding Effects in Stroke

Barry McColl, David Howells, Nancy Rothwell, and Adam Denes

Abstract

Most research to date has used experimental models in rodents which fail to mimic the underlying causes of stroke in patients or the primary confounding factors. Available data indicate that factors such as atherosclerosis, hypertension, obesity, diabetes, age, and inflammation have a major influence on outcome. These findings suggest that we need to rethink the preclinical data that are required before the selection of candidate interventions for clinical trials in stroke.

Key words Age, Atherosclerosis, Diabetes, Hypertension, Inflammation

1 Introduction

Animals have been used successfully to study the underlying mechanisms of diverse diseases and to successfully develop new treatments. In many cases the diseases in question are induced through a means which differs significantly from the clinical course and causes, e.g., implanted tumors in young and otherwise healthy animals, mechanical or pharmacological induction of hypertension and cardiac disease and pharmacological induction of diabetes. Some have used spontaneous mutations that result in the disease of interest (e.g., genetically obese animals), mutagenesis to cause a pathology (e.g., deafness), or specific genetic manipulation to induce disease (e.g., to cause mutations known to occur in Alzheimer's). All of these have been very helpful in the understanding of disease pathology and in the development and testing of new medicines.

The situation in experimental studies on stroke is quite different, because the animal models we have used have revealed much knowledge of underlying pathological mechanisms, but have (with the notable exception of tissue plasminogen activator, tPA) failed to deliver new medicines. Thus after many promising preclinical outcomes, we have numerous failed clinical trials in stroke. Many of these can be explained on the basis of inadequate preclinical

Ulrich Dirnagl (ed.), *Rodent Models of Stroke*, Neuromethods, vol. 120,
DOI 10.1007/978-1-4939-5620-3_9,

data, poor clinical trial design, or a mismatch between the preclinical findings and the clinical studies; some failures remain inexplicable. This has caused a serious reanalysis of our experimental approaches to stroke including the rigor of the experimental work and the relevance of commonly used methods [1–7].

To date, the vast majority of experimental studies on stroke have used young, male rodents, with no confounding comorbidities, no parallel treatments, and few detectable long-term consequences of stroke. Furthermore, few studies have used approaches to induce cerebral ischemia which mimic the clinical causes of stroke. Indeed most have employed mechanical occlusion of a major artery (the middle cerebral artery, MCA); very few have used thrombus or hemorrhage or indeed studied animals with spontaneous stroke. A further factor which may have influenced the apparent discrepancy between rodent studies and clinical trials may be that stroke has been considered as a neurological disorder—unsurprisingly given that the clinical outcomes are neurological. Yet stroke is profoundly influenced, and perhaps even caused, by systemic factors including atherosclerosis, impaired cardiac function, systemic inflammation, and infection.

It is clearly not feasible, or probably helpful, to fully mimic all the common clinical factors associated with stroke simultaneously in animals. To develop experimental models of aged, atherosclerotic animals, some of which have diabetes, many hypertension and obesity, some would be smokers, have a poor diet and others would have many other confounding factors and comorbidities, as well as exposure to a whole array of potential medicines would make animal studies as complex and expensive as clinical trials. It would also make interpretation of data near impossible. Animal research, in most countries, is further constrained by legislative and welfare considerations which quite rightly aim to limit suffering.

Thus, we focus here on the major confounding factors known to cause or exacerbate stroke, i.e., hypertension, diabetes, obesity, infection, inflammation, atherosclerosis, and age, and we attempt to review available methods, their robustness and limitations, and available data.

2 Hypertension

Hypertension is the single most important modifiable risk factor [6, 8–10], which increases stroke risk by 20–30% for a 10-mmHg increase in arterial blood pressure [9] and doubles lifetime risk in individuals with blood pressure above 120/80 mmHg [11]. Hypertension is evident in >50% of stroke patients [6, 8–10], and blood pressure reduction reduces stroke risk [12].

There are many animal paradigms of hypertension, but only a few have been used to study stroke. To date no stroke studies

appear to have been undertaken in hypertensive transgenic rats expressing an extra copy of the renin gene [13] or, in the New Zealand, Milan hypertensive or Lyon hypertensive rats [14–16]. Hypertension and stroke have been induced in cynomolgus monkeys by surgical coarctation and in animals fed with an atherogenic diet [17], but this would not seem to be a practical model for widespread use.

The most widely used hypertensive animals in stroke research are the spontaneous hypertensive rat (SHR) and the stroke-prone SHR (spSHR); the latter was derived by inbreeding of the offspring of SHRs that died of hemorrhagic stroke. Over 80% of the spSHR population develops stroke, which is characterized by multifocal microvascular and spongy-cystic parenchymal lesions [18]. Wistar–Kyoto rats were the parent strain for both [19].

In spSHRs, a high-salt diet precipitates renal injury, marked hypertension (>240 mmHg), and rapid onset of hemorrhagic stroke [20, 21], and ~70% of strokes are in the gray matter of the cortex [22]. While the number of anastomotic connections between anterior and middle cerebral artery territories in the cortex is similar to WKY rats, their luminal diameter is reduced [23–25], and their capacity for vasodilation is impaired [26–28].

SHRs become hypertensive within 2–4 months of birth and attain a stable systolic blood pressure (~200 mmHg) by 6 months. Salt sensitivity is not a major component of their phenotype [29]. The hypertension is accompanied by enlarged ventricles [30, 31], cerebral artery smooth muscle hypertrophy [32], increased macrophage activity [33], and reduced body and brain weight [30, 34, 35]. Losses after thread occlusion of the MCA are substantially lower [36] than reported for the Dahl salt-sensitive rat.

In both the SHR and spSHR, focal cerebral ischemia leads to greater infarct volumes and behavioral deficits than in normotensive controls and less variability [36–39]. The reduced variability is also evident when submaximal infarcts are induced (Howells, personal observation) indicating that this, and the greater propensity to damage, results from reduced cortical collateral flow [40] imposed because of reduced luminal diameter [23–25] and reduced capacity for vasodilation [26–28]. Reduced variability is not imposed by the absence of the posterior communicating arteries [41]; the mechanism is proposed for similar large infarcts and small variability in the gerbil [42].

We were unable to find evidence of studies of most neuroprotective agents in hypertensive or diabetic animals. For 502 therapies that have been the subject of systematic review and meta-analysis, only 10% of the publications identified included the modeling with high blood pressure or diabetes, and of the 58 tested in both normotensive and hypertensive animals, 12 were less effective in hypertensive animals, and 6 therapies were more effective [43]. For example, nicotinamide and FK506 were substantially

less effective in animals with diabetes or hypertension [44, 45]. NXY-059 was less effective in SHRs than healthy animals (17.6% versus 47.8%; $P<0.001$) [5], and tPA provided no benefit to infarct volume and worsened neurobehavioral score in hypertensive animals [46]. Hypothermia however was slightly more effective in SHR than in SD and Wistar rats [47].

Long-term control of hypertension with calcium or AT1 antagonists before middle cerebral artery occlusion (MCAo) appears to reduce infarction [48–51], while l-arginine has no effect when local CBF is unaltered [52] but reduces infarct volume when accompanied by increased cerebral blood flow [53]. MK-801, the archetypal neuroprotectant, has been reported to either have no effect [54] or to be less effective in hypertensive than in normotensive controls [55].

Renovascular hypertension can be induced by clipping one renal artery (keeping the kidneys in place, two kidneys, one clip) to produce mild but relatively unstable hypertension [56] that nevertheless exacerbates ischemic injury [57]. Clipping both renal arteries in Sprague–Dawley rats leads to stable hypertension with spontaneous stroke characterized by a mixture of small infarcts with thrombotic occlusion and hemorrhagic lesions caused by bleeding from the arteriolar wall in 62% of the animals within 40 weeks [58]. Development of spontaneous T2-weighted MRI lesions in these models is tightly dependent upon blood pressure. After partial occlusion of both renal arteries, consistent brain lesions were seen only when blood pressure exceeded 276 mmHg [59]. In agreement with these data is the observation that decompressive craniectomy reduces MCAo-induced mortality in renovascular hypertensive rats by ~85% [60].

The Dahl salt-sensitive rat rapidly develops marked hypertension (~200 mmHg) when fed a high-salt diet (8% NaCl), and this leads to blood–brain barrier disruption, stroke, and death [61, 62]. At lower salt concentrations (e.g., 1% NaCl), the same end is reached, but the animals survive at least until ~5 months of age [63]. Thread occlusion of the MCA after 5 weeks on a high-salt diet leads to excessive death or hemorrhage at the MCA/ICA bifurcation. When the MCA was occluded for 120 min, 80% of the animals died or suffered hemorrhage within 24 h; 90-min occlusion still left 40% of the animals with hemorrhage [64].

Like the spSHR and renovascular models, rats made hypertensive by treatment with mineralocorticoid receptor agonist deoxycorticosterone plus salt also suffer spontaneous strokes [65], but they are more readily protected against the effects of acute middle cerebral artery occlusion by antihypertensive treatment with agents such as captopril than by spSHRs [66]. Spontaneous stroke and worsening of the effects of MCAo in these animals may be mediated by stiffening and narrowing of the middle cerebral artery [67].

3 Diabetes/Hyperglycemia

Diabetes (types 1 and 2) or acute hyperglycemia is evident in 25% [68] and 40% [69] of stroke patients, respectively, and both are associated with poor outcome [70–73]. Diabetic control reduces stroke risk [74].

Diabetes can be induced by selectively poisoning pancreatic β cells with streptozotocin or alloxan, by selective breeding in the nonobese diabetic (NOD) mouse, the biobreeding (BB) rat, and occurs spontaneously in the Zucker diabetic fatty rat [75] and the Goto-Kakizaki rat [76]. Specific defects in the db gene on mouse chromosome 4 and the fa gene on rat chromosome 5 lead to leptin receptor defects [77, 78]. Isolated hyperglycemia can be induced by infusion of glucose or dextrose [75].

Hyperglycemia accelerates and extends infarct development after MCAo in rats [79], cats [80], dogs [81], and rabbits [82]. In cats [80], the three- to fourfold increase in infarct size due to hyperglycemia after permanent middle cerebral artery occlusion was associated with increased death due to edema upon reperfusion. In monkeys, infusing glucose prior to cardiac arrest causes seizures and muscle twitching due to mild edema and necrosis of the cortex and basal ganglia [83]. Some authors have reported that the effects of hyperglycemia on infarction are confined to the cerebral cortex [84], while others report that only very early and short-term hyperglycemia may be needed to cause injury [85, 86].

Blood–brain barrier damage and edema [87–90] together with faster and larger infarct development after transient and permanent ischemic lesions [88] are also features of diabetes induced by chemical poisoning of pancreatic β cells.

Where direct comparisons have been made between transient hyperglycemia and diabetes, the data are conflicting; some report similar degrees of exacerbation of postischemic injury [50] or that diabetes induces significantly more injury [91]. Interestingly, while acute hyperglycemia lessens the impact of tPA therapy [86, 92], it has no effect on endogenous tPA expression, while a similar but persistent elevation of blood glucose (~15 mmol/L) in streptozotocin-treated rats is reported to lead to a complete depletion of tPA protein and greater than sixfold loss of tPA mRNA expression [91].

In the biobreeding (BB) rat, the effects of hyperglycemia on ischemia are gender and region specific. Males and females exhibit similar degrees of cortical injury, but subcortical infarction is larger in males [93]. Similar observations have been made in the db/db mouse, where female diabetic mice became more hyperglycemic and acidotic than the males even though they were more resistant to ischemic damage [94].

The recently described Goto-Kakizaki rat which develops mild hyperglycemia at 6 weeks of age is unusual in producing smaller

infarcts after extended (3 h) MCAo (but high rates of subcortical hemorrhagic transformation) than nondiabetic controls [76]. While this has been interpreted as the result of diabetes-induced vascular remodeling [76], the infarcts look like the hypothalamic lesions produced when only hypothalamic-perforating arteries are occluded [42], suggesting that reduced effectiveness of thread occlusion might be a sensible alternative explanation. The observation that injury caused by compression-induced cortical ischemia is greater in Goto-Kakizaki rats than healthy Wistar controls [95] supports this hypothesis.

The impact of diabetes on efficacy of neuroprotection is not clear. Using insulin to control hyperglycemia has been reported to return neural injury to control levels and offer marked neuroprotection if blood glucose is reduced to below normal [96, 97]. Similar protective effects on infarction were reported when insulin was used together with tPA in normoglycemic animals to treat thromboembolic strokes. However, others report that tight glycemic control does not improve infarct size in male BB rats [93] and that, despite reduced infarct volumes, mortality was as high after insulin treatment alone (47%) as it was when combined with tPA (38%) [98].

4 Obesity

4.1 Association with Stroke Risk

Growing evidence suggests that obesity predisposes to cardiovascular disease including stroke [99–102]. This association may be mediated indirectly via the susceptibility of obese individuals to established stroke risk factors such as atherosclerosis, hypertension, hyperlipidemia, and insulin resistance/diabetes [103]. In addition, there are considerable data indicating an independent association between obesity and stroke. Some studies have reported a graded elevation in stroke risk for each unit increase in body mass index (BMI) greater than 25 [100, 102] although others have not observed such a close correlation [104, 105]. More recently, the validity of BMI as the optimal index for assessing the impact of obesity on cardiovascular disease has been questioned [106]. Abdominal adiposity as measured by waist-to-hip ratio may provide better estimates of the health risks associated with obesity [107, 108]. In support of this, a recent study demonstrated a significant and graded association between risk of stroke and transient ischemic attack and markers of abdominal obesity, including waist-to-hip ratio, that was independent of hypertension and diabetes [106]. Another important point to consider is that although the incidence of stroke is falling in elderly people in developed countries due to improved risk management, there is a shift toward an earlier age at stroke onset and that incidence of stroke is rising in young adults. Recent data indicate that increasing obesity in children and young

adults caused by sedentary lifestyles and unhealthy diets could translate into premature vascular disease, including stroke, through raised blood pressure and diabetes [109, 110].

4.2 Animal Models for the Study of Interactions Between Obesity and Stroke

A huge number of animal models of obesity have been reported although the extent of characterization for each of these varies widely [111]. In view of the predominance of rodent models in experimental stroke studies, obesity in mice and rats probably offers the greatest utility for experimental stroke researchers. Rodent models of obesity may arise through genetic mutation (spontaneous or targeted) or may be induced by some type of environmental stimulus, e.g., high-fat diet [111]. Genetic models may further be subdivided as monogenic and polygenic. Spontaneous mutants giving rise to monogenic rodent models of obesity are the most commonly used and have been characterized most extensively. Due to the diversity of models available, multiple factors deserve consideration when choosing an obese model to incorporate in experimental stroke studies. These include strain, method of induction, sex dependency, age of onset, severity, and associated phenotypes. The following sections summarize some of the benefits and limitations/constraints of the most commonly used rodent obese models that are likely to be most worthy of consideration for experimental stroke studies. Readers are referred to these excellent resources for detailed accounts of these and other obesity models [111–113].

4.2.1 *ob/ob* Mice

ob/ob mice carry a spontaneous mutation in the Lep gene encoding the leptin protein which is abundantly produced by adipocytes [114]. Mice homozygous for the Lep^{ob} mutation are deficient in leptin, which is an appetite-suppressing hormone. As a result, ob/ob mice (on Bl/6 background) are hyperphagic and are first recognizable as obese at 4 weeks of age when fed a normal diet. Adult ob/ob mice may become three times the weight of wild-type controls. They are glucose intolerant, insulin resistant, and hyperinsulinemic but are not hyperglycemic except during a short period in early adulthood (subsides by 12–16 weeks) [112, 113]. Our own studies [115] indicate a marked increase in hemorrhage on ob/ob mice exposed to MCAo.

4.2.2 *db/db* Mice

db/db mice carry a spontaneous mutation in the leptin receptor gene (Lepr); therefore there is a similar defect in the leptin axis as observed in ob/ob mice [116]. Although obese, male mice homozygous for the $Lepr^{db}$ mutation (on Bl/6J background) are most commonly used as a model of diabetes (or obesity with diabetes) [117]. These mice are also insulin resistant, hyperinsulinemic, and hyperlipidemic. Furthermore, and in contrast to ob/ob mice, they develop severe hyperglycemia and show symptoms consistent with overt diabetes [112].

4.2.3 Zucker (fa/fa) Rats

The "fatty" Zucker rat has been extensively used in studies of obesity. Similar to the db/db mouse, the Zucker rat has a spontaneous mutation in the leptin receptor (*fa* mutation) causing defective leptin signaling [118]. Homozygous (fa/fa) mutants develop obesity and become hyperlipidemic and moderately insulin resistant [118]. In contrast to db/db mice, however, Zucker rats do not develop overt diabetes [112, 118].

4.2.4 Corpulent (cp/cp) Rats

Corpulent rats carry the spontaneously arising corpulent (cp) mutation, which is another mutation affecting the leptin receptor rendering it dysfunctional. Rats homozygous for the mutation (*cp/cp*) develop obesity, insulin resistance, hyperinsulinemia, and hyperlipidemia but do not progress to type 2 diabetes [112]. The original hypertensive mutant strain (designated SHROB) was backcrossed to SHR, WKY, or LA strains, thus generating SHR/N-cp (hypertensive), WKY/N-cp (normotensive control for SHR/N-cp), and LA/N-cp (normotensive) models [112]. A further strain designated JCR:LA-cp was developed as an outbred colony from early LA/N-cp breeding stock. Significantly, male JCR:LA-cp rats homozygous for the cp mutation develop spontaneous vascular pathology that includes atherosclerotic lesions similar to those observed in humans and ischemic lesions in the heart [119]. Corpulent rats show neuroinflammatory changes (microglial activation, vascular inflammation) in the brain in the absence of any acute injury and display significantly larger BBB injury and worse neurological outcome after experimental stroke (see also below under the inflammation section) [120, 121].

4.2.5 Diet-Induced Obesity (DIO)

Several different types of dietary regimens have been used to induce obesity in rodents, including high-fat diets, high-energy diets (moderately high fat and high sugar), and palatable liquid diets. DIO has been characterized in both rats and mice, although there are strain-specific differences in susceptibility in both species. Sprague–Dawley and Long–Evans rats and C57Bl/6J mice are well established as susceptible strains, with males particularly predisposed [122, 123]. Hyperphagia, obesity, insulin resistance, hyperinsulinemia, glucose intolerance, and hyperlipidemia are common features on adjusted diets, although the relative severity of each of these will depend on the exact composition of diet and strain susceptibility [124, 125]. A commonly employed diet in male C57Bl/6J incorporates a 45% or 60% (by energy) fat component, with controls being fed 10% fat. Mice are typically maintained on diets for up to 20 weeks. Modified diets such as these are available commercially (e.g., from Research Diets Inc.).

General considerations when selecting obesity models for experimental stroke studies.

The animals described above illustrate some of the more commonly used rodent obesity models that may be applicable to

incorporate in experimental stroke studies. The optimal model for any study will depend on multiple factors including the experimental hypothesis under testing, confounding factors, purchase and maintenance costs of animals/diets, and stroke model used.

All the monogenic spontaneous mutant animals outlined above arise from deficiencies in the leptin/leptin receptor signaling axis. Leptin has a diverse array of actions in addition to its role in appetite regulation, including effects on the immune and cardiovascular systems [86, 126]. Accordingly, it could not be excluded that any effects on stroke responses in these models are because of leptin signaling insufficiency independent of obesity. To counter this, leptin replacement groups could be included although these are unlikely to fully restore the leptin axis to normal physiological conditions. This highlights a relative advantage of the diet-induced models. Furthermore, DIO is a more realistic model of the dietary component that is a key contributor to human obesity.

In humans, it is the vascular consequences which commonly accompany obesity and metabolic syndrome that are of most relevance to stroke, since these are likely to mediate the link between metabolic disturbances and stroke susceptibility. However, with the exception of the JCR:LA-*cp* strain, all obese models are resistant to the development of overt human-like vascular pathology [112]. For this reason, the JCR:LA-*cp* model perhaps most closely resembles the metabolic syndrome associated with obesity most likely to present in stroke patients, i.e., with downstream vascular abnormalities.

Hyperglycemia and diabetes are associated with poorer outcome in stroke patients (see above); therefore it may be desirable to induce obesity without also affecting glycemic status. This might enable the role of increased adiposity itself to be more easily delineated. This should be possible since some models (e.g., ob/ob mice after 12–16 weeks) are normoglycemic despite being markedly obese.

On a more practical note, it should be considered that obese animals, by definition, have large deposits of adipose tissue and that this has the potential to complicate the surgical induction of stroke (particularly filament models where access to the carotid vessels is a prerequisite). However, our own experience suggests that despite marginally extended surgery times, subcutaneous adiposity does not unduly affect success rates. This is also borne out by the recent studies that have emerged combining experimental obesity and stroke [127–130]. In contrast, we found that proximal MCAo was not feasible due to the size and expected high level of mortality of aged, corpulent rats; therefore a distal, transient model of MCAo (thread occlusion of the MCA after craniotomy) was chosen [121]. All such studies have found that the severity of brain damage and/or BBB injury is markedly increased in obese rodents compared to corresponding wild types (see below). This suggests

that the basal severity of the stroke model may need to be titrated (e.g., by adjusting occlusion duration) to avoid excessive mortality and morbidity in the obese experimental group. Experimental stroke is commonly induced in 10–12-week-old rodents. The rapid onset of obesity in the monogenic models enables similar aged animals to be used. In contrast, DIO involves long durations of feeding adjusted diet (perhaps up to 20 weeks); therefore the age at which stroke can be induced in these animals is likely to be significantly older. Thus, the age and also the cost of long-term dietary modification and animal housing are important to consider. A further consideration is the difficulty in determining the doses of any pharmacological intervention. Given the very different body weights, it is not possible to give interventions on a dose per unit body weight basis, and highly lipophilic substances may be preferentially taken up in to adipose tissue.

These are just some of the many important factors to consider when selecting an obesity model to incorporate in experimental stroke studies. With good experimental planning and design and with particular attention to potentially confounding variables, most models are likely to enable a better understanding of the impact of obesity on stroke.

5 Overview of Experimental Obesity–Cerebral Ischemia Studies

It is only in the last few years that studies investigating the impact of obesity on experimental stroke in rodents have emerged [127–132]. All studies have found significantly increased ischemic brain damage and/or larger BBB injury in the obese group (Table 1).

Table 1
The impact of obesity on infarct size after experimental stroke

Author	Model	% change in infarct	Reference no.
Nagai et al.	ob/ob 5 weeks 42% high-fat diet	30% ↑ 30% ↑	[127]
Terao et al.	ob/ob	75% ↑	[129]
Mayanagi et al.	ob/ob	43% ↑	[130]
Osmond et al.	Zucker (fa/fa)	170% ↑	[128]
McColl	ob/ob	120% ↑	[115]
Maysami et al.	DIO	40% ↑	[131]
Deng	DIO	30% ↑	[132]

6 Atherosclerosis

The significance of atherosclerosis in the context of stroke risk is highlighted by the estimation that thromboembolism of atherosclerotic origin is the principal etiological factor in approximately 50% of stroke patients [133]. These statistics suggest that incorporating atherosclerosis in at least some preclinical stroke models should be a priority and should help to more accurately recapitulate important features of clinical stroke.

7 Animal Models of Atherosclerosis

An extensive range of animal species has been used to study atherosclerosis, including large animals such as nonhuman primates, pigs, and rabbits and, more recently, mice. The majority of experimental stroke studies are performed in rodents; therefore murine models of atherosclerosis are likely to offer the greatest utility for experimental stroke researchers.

The mouse is naturally resistant to spontaneous atherosclerosis, which may in part be the result of the HDL-dominant and antiatherogenic lipid profile in mice compared to the atherogenic LDL-dominant profile in humans [134]. For this reason, feeding an atherogenic (commonly high-fat, high cholesterol) diet to genetically modified mice with enhanced susceptibility to atherosclerosis forms the basis of most currently used protocols of atherosclerosis. A variety of diets have been described, and the reader is referred to these excellent articles for more detailed information [134, 135].

7.1 C57Bl/6J

Most wild-type mice are resistant to atherosclerosis when fed a conventional rodent chow diet; therefore aggressive dietary manipulation is necessary to induce lesion formation. When fed a high-fat (30%), high-cholesterol (5%), and cholate-containing (2%) diet or the "Paigen" diet (15% fat, 1.5% cholesterol, 0.5% cholate) C57Bl/6J mice develop small aortic lesions resembling the fatty streaks in humans by 4–5 months of age [134, 135]. However, the lesions rarely progress beyond the early foam-cell/fatty-streak stage which represents the major limitation of these models.

7.2 ApoE−/− Mice

In order to induce advanced atherosclerosis in mice, it is necessary to use genetically modified, susceptible strains, most commonly in combination with dietary modification. The most frequently used and best characterized strains are the apolipoprotein E (apoE)−/− and low-density lipoprotein receptor (LDLR)−/− mice. ApoE is a glycoprotein synthesized in many tissues and at highest levels in the liver and brain. It is a structural component of lipoprotein

particles and acts as a ligand for receptors such as LDLR that mediate cellular internalization of apoE-containing particles [136]. ApoE−/− mice fed with a chow diet are hypercholesterolemic and significantly have human-like lipoprotein profiles (i.e., low HDL) [137, 138]. These mice develop lesions throughout the macrovasculature (but not in cerebral vessels) that progress to advanced plaques with a well-defined fibrous cap consisting of smooth muscle cells, extracellular matrix, and foam cells [134]. Feeding a Paigen diet or the more physiological "Western" diet (21% fat, 0.15% cholesterol, cholate free) accelerates the development of lesions at all stages [139]. When fed a Paigen diet for 8 weeks, apoE−/− mice develop inflammatory changes in the ventricles and the choroid plexus, characterized by lipid deposition, microglial activation, and recruitment of leukocytes [120]. Focal pathologies in the brain parenchyma and increased VCAM-1 expression on cerebral microvessels were also observed (see also in the inflammation section below) [120].

7.3 LDLR−/−

LDLR is the principal receptor mediating uptake of LDL via binding of its major ligand apoB [140]. LDLR−/− mice develop more modest lipid abnormalities relative to apoE−/− mice and therefore are much more resistant to atherosclerosis on a low-fat chow diet. However, when fed with the Paigen or Western diet, LDLR−/− can develop intermediate–advanced lesions affecting multiple parts of the vasculature after 2–3 months [135].

8 General Considerations When Choosing Models of Atherosclerosis for Experimental Stroke Studies

In view of the various models of atherosclerosis available, several factors are likely to be worthy of consideration when selecting a model to incorporate in experimental stroke studies. The similarity of the model to the human condition is of prime concern. In the context of atherosclerosis, the composition of the vascular lesions and the lipid profile are particularly important issues. As described above, the vascular pathology and lipid profiles observed in apoE−/− and LDLR−/− mice fed with modified diets most closely reflect the human disease. Another advantage of these models is that the progression to advanced lesions progresses fairly rapidly therefore reducing the duration of experiments and associated costs in maintenance. However, the use of genetically modified mice in combination with dietary modification also introduces potentially confounding [134] variables. For example, there is evidence that the diets themselves may be pro-inflammatory, and thus it may be difficult to distinguish between effects caused by atherosclerosis itself rather than diet alone. Analogous to this, genetic deficiency in apoE or LDLR may have important consequences independent of the induction of atherosclerosis. Notably, apoE has

a number of important activities in the CNS including homeostatic lipid transport [141]. In addition, apoE has several neuroprotective and neuroregenerative features [141]. For example, the extent of brain damage is significantly greater in apoE−/− mice (on regular chow diet) after a variety of acute brain injuries including focal and global cerebral ischemia [141]. Anti-inflammatory, antioxidant, and anti-excitotoxic properties have all been described for apoE in the brain [142]. Although LDLR is a major receptor for apoE in peripheral tissues, this is not the case in the brain, where receptors such as LDLR-like protein (LRP) and apoE receptor 2 (apoER2) are the predominant transducers of apoE signaling [143]. The use of LDLR−/− mice may therefore avoid some of the complications associated with apoE−/− mice since CNS apoE signaling pathways may be less severely compromised. Regardless, potential complications in interpreting results from studies combining genetic and/or dietary models of atherosclerosis with experimental stroke will require the inclusion of multiple strain and diet control groups. If these are adequate, then it should be possible to extract meaningful conclusions from such studies. Aside from these design issues, an important practical consideration relates to the potential disruption of atherosclerotic lesions if stroke is induced by filament advancement along the internal carotid artery. Although a full characterization of vascular pathology in the carotid and intracranial arteries is lacking, it is conceivable that filament advancement could dislodge atheromatous material, thus generating emboli-like particles which could complicate occlusion uniformity. It is also challenging to identify the exact mechanisms, which contribute to the outcome in complex comorbid animal models of atherosclerosis that commonly involve dyslipidemia, insulin resistance, obesity, and/or hypertension. Corpulent rats are obese, but also develop insulin resistance and atherosclerosis as they age, and similar considerations apply to most DIO models. It is also likely that different comorbidities interact and hence could shape infarct evolution and overall outcome via diverse actions. For example, synergistic effects of high blood cholesterol and hypertension have been reported on leukocyte and platelet recruitment in the cerebral microcirculation [144].

9 Aging

Since the incidence of stroke is higher in the elderly population compared to young people, it may be tempting to hypothesize that aging per se could facilitate stroke occurrence and/or impair outcome. It is, however, very difficult to separate the effect of age itself from many of its frequent peripheral or central comorbidities such as obesity, diabetes, hypertension, arteriosclerosis, or the presence of microhemorrhages and senile plaques in the brain. The use of aged animals (especially rodents) in experimental models of stroke

may not perfectly reflect the human situation due to life span, strain, and gender differences and many other confounding factors. Nevertheless, several data have indicated similar effects of aging regarding infarct size, maturation, and vascular and neuronal damage between patients and experimental animals.

It is known that in humans, cerebral blood vessels undergo profound changes with aging including the reduced capillary density and formation of thickened and fibrotic basement membranes. Endothelial cells exhibit a reduced number of mitochondria, and in pericytes (which regulate capillary constriction similarly to smooth muscle cells in larger vessels) degenerative processes are seen. In the aging human cortex, microhemorrhages become frequent, identified by their content of hem, red blood cells, collagen, and clotting factors and their spatial relationship to capillaries [145, 146]. Similarly, vascular density, arteriole–arteriole anastomoses, and basal blood flow decrease with age in rats [147], and structural changes are seen in basal lamina and endothelial cells [148]. In mice, aging markedly alters transcriptional responses in the brain after stroke affecting genes involved in inflammatory responses, oxidative stress, cell cycle activation and/or DNA repair, apoptosis, cytoskeleton reorganization, gliosis, synaptic plasticity, and/or neurotransmission [149].

Experimental stroke generally (although not uniformly) reveals many factors which are altered in aged rodents. In aged rats, increased mortality rate, but similar recovery and infarct volume were found [150]. Another study showed that aged rats suffer larger infarctions, reduced functional recovery, and increased BBB disruption that precede observable neuronal injury [151]. Aging has been shown to reduce hypoxia-induced microvascular growth in the rodent hippocampus [152]. Basal neurogenesis is impaired in the subgranular and subventricular zones of aged animals, although the magnitude of striatal neurogenesis after stroke is similar in young and old animals [153]. Spontaneous hypertensive rat (SHR) models revealed larger infarcts in aged (18–22 months old) animals after photothrombotic distal MCAo compared to adults [154], and ischemic neuronal damage in the hippocampus and striatum was produced by 20 min of transient global ischemia in aged but not in adult rats [155].

Infarct size was found to increase with aging in female mice, whereas male mice had decreased damage after MCAo, which correlated with blood–brain barrier permeability changes. Interestingly, edema formation was less profound in aging mice, independent of sex and extent of histologic damage [156].

These examples may indicate that depending on the ischemic model used, species, strain, or gender differences, the observable effect of aging can be largely different. This may require much more comprehensive studies in the future to understand the key elements of the process of aging on damage formation, inflammation, and recovery.

10 Inflammation and Infection: Risk Factors and Disease Consequences

To satisfactorily model inflammation and infection as risk factors in experimental stroke, it is important to understand the initiation, maintenance, and termination of both central and peripheral inflammatory changes, with special respect to their interactions in cerebral ischemia. These processes can occur simultaneously in stroke, but the root causes may have started decades before their *consequences* are observed in the clinical practice; hence this area of experimental research is fraught with confounding factors.

Inflammation is a highly complex and normally well-coordinated biological response of vascular tissues to harmful stimuli. Typically, in peripheral tissues, acute inflammation induced by pathogen invasion or tissue injury includes a sequence of events aimed at eliminating deleterious agents and helping wound-healing processes. Several elements of this reaction contain partially stimulus-specific components (e.g., the activation of certain toll-like receptors, which can recognize given pathogen-associated patterns), and also many common features, such as the dilation of local blood vessels and activation recruitment of leukocytes, release a wide range of active peptide and non-peptide mediators in inflamed tissues. While uncontrolled or prolonged inflammation can be highly detrimental in the periphery, its consequences may even be more serious in the brain, where anti-inflammatory and reparative processes would never result in complete recovery because of the very limited replacement of damaged neurons.

Many elements of cerebral ischemia-induced inflammatory changes in the brain are very similar to the general pattern of the peripheral inflammatory response. The early central inflammatory events include the production of reactive oxygen species (nitric oxide, superoxide) and expression of proteolytic enzymes (MMP-9, MMP-2), pro-inflammatory cytokines (IL-1β, TNF-α, IL-6), chemokines (CINC-1, KC, MCP-1, MIP-1α), and vascular adhesion molecules (ICAM-1, P-selectin, l-selectin). Activation of resident glial cells (astroglia, microglia) and early infiltration of granulocytes followed by monocytes, macrophages, and other hematogenous cells are observed within hours to weeks after experimental stroke [60, 123, 129, 157–160].

11 Inhibition of Inflammation Is Protective in Most Experimental Models of Stroke

Because central inflammatory processes in stroke are associated with the disruption of the BBB and the formation of the ischemic damage, it is not easy to decide whether these changes are consequences of the cerebral ischemic event itself or indeed contribute to damage formation. This may be one of the reasons why stroke has

long been considered as a neurological disorder and the potential effect of systemic factors was largely neglected. In line with this, several studies that showed neuroprotection after cerebral ischemia by inhibiting certain components of the inflammatory response failed to convincingly demonstrate whether this effect was centrally or peripherally mediated. In fact, inhibition or deletion of pro-inflammatory cytokines [161, 162], chemokines [163, 164], chemokine receptors [165, 166], treatment with tetracycline derivatives [167], etc., have all been shown to be protective in experimental rodent models of focal cerebral ischemia. One can also ask why such a robust inflammatory response is initiated in response to cerebral ischemia if it is harmful to the organism. Does postischemic inflammation involve similar mechanisms and/or effects in the periphery and in the brain? Although several reports showed that oxidative stress and recruitment of inflammatory cells are harmful mainly in stroke, superoxide-initiated inflammation and monocyte recruitment seem crucial for peripheral, flow- or ischemia-mediated vascular remodeling [168, 169]. May modest and well-controlled inflammation facilitate processes of repair? For example, inhibition of matrix metalloproteinases in several rat or mouse MCAo models reduced damage size, brain edema formation, and neuronal apoptosis [147, 170, 171], but facilitated cell death in intracerebral hemorrhage [172] or inhibited neuronal progenitor cell migration after photothrombotic ischemia in mouse [173]. These examples indicate that development of more appropriate animal models, tissue- and cell-specific deletion, and inhibition or overexpression of inflammatory mediators will be essential for a deeper understanding of underlying inflammatory mechanisms in stroke.

Inflammatory processes may differ between species and strains because of the differences in peripheral leukocyte populations, cerebral vasculature, size of the brain, kinetics of aging, etc.; therefore in the future, it may be advantageous to study cerebral ischemia more frequently in large mammals such as sheep [174] or swine [175]. However, the availability and cost of animals may limit the number of these kinds of experiments.

12 Systemic Inflammation and Infection: The Need for Appropriate Experimental Models

Inflammation is elicited as a defense mechanism against infectious agents but is not necessarily caused by infection. The co-occurrence of these factors and the large overlap between the expression of infection-induced and ischemia-induced mediators create many confounding effects in clinical practice and in experimental stroke research. Preexisting infection or systemic inflammation may induce and is very likely to affect cerebral ischemia, and relevant experimental models are crucial to understand the underlying mechanisms. In patients, acute and chronic infection can be a

trigger of stroke, and preceding infection worsens stroke outcome. Furthermore, poststroke infections affect clinical outcome [176]. Respiratory and urinary tract infections are the most common types of infection preceding stroke after adjustment for age and conventional vascular risk factors [177, 178].

To date, the effect of systemic inflammation and infection on experimental cerebral ischemia has been largely ignored in experimental research. Similarly, the effect of cerebral ischemia on the induction or modulation of peripheral inflammatory processes has also been overlooked. It is now established that cerebral ischemia itself induces a rapid, but often prolonged peripheral inflammatory response. The level of pro-inflammatory cytokines such as IL-6, IFNγ, and MCP-1 becomes elevated in the plasma within hours and may remain elevated for several days in stroke patients and for 1–3 days in animals with experimental stroke. This is accompanied by the induction of chemokines and chemokine receptors in peripheral organs: long-term elevation of acute-phase proteins and white blood cell count in the circulation [179, 180]. It is reasonable to ask how these processes are mediated and what the consequences of the activation of the peripheral inflammatory response on central inflammatory changes in stroke are.

It is crucial to reveal the mechanisms of peripheral inflammatory changes in ischemic damage formation and to understand how a preexisting inflammatory event can modulate all these processes in different experimental models. For example, depletion of neutrophils in the periphery showed that these cells are a major source of oxygen radicals during reperfusion after focal cerebral ischemia in the rat MCAo model [181]. Systemic inflammatory stimulus induced by intraperitoneal lipopolysaccharide (LPS) or IL-1β administration exacerbates brain damage via a neutrophil-dependent mechanism in a mouse MCAo [182] and alters the kinetics of cerebrovascular tight junction disruption through neutrophil-derived MMP-9 [183]. Therefore, studies using young, healthy animals with no additional inflammatory diseases may underestimate the impact that systemic factors have on patients with multiple comorbidities.

Recently established rodent models of systemic inflammation and infection show worse outcome after stroke, which is reversed by anti-inflammatory interventions. Blockade of IL-1 actions reversed brain inflammation associated with diet-induced atherosclerosis in apoE−/− mice [184]. Blockade of IL-1 receptor 1 (IL-1R1)-mediated signaling by IL-1 receptor antagonist (IL-1Ra) reduced infarct size, BBB injury, and inflammation in aged corpulent rats [121]. Chronic Th1-type polarization of the immune response induced by a nematode, *Trichuris muris*, leads to prolonged brain inflammation, increased platelet aggregation in cerebral microvessels, larger infarct size, and worse neurological outcome, which is reversed by blocking the pro-inflammatory chemokine CCL5 (RANTES). The same infection regimen was found

to increase infarct size synergistically with aging in mice [185]. RANTES was also found upregulated in the brain after stroke in mice with preceding influenza virus infection, which was associated with larger brain injury. Interestingly, tPA administration resulted in increased incidence of brain hemorrhage in influenza virus-infected animals [186]. Preceding pulmonary infection by a human, *Streptococcus pneumoniae* isolate resulted in larger brain injury after experimental stroke, which was reversed by the IL-1Ra and blockade of platelet glycoprotein Ibα [187]. Collagen-binding *Streptococcus* mutans also aggravate cerebral hemorrhage in mice after stroke [188]. These results indicate that inflammatory mechanisms associated with common stroke comorbidities are likely to be causal factors in outcome after stroke and anti-inflammatory interventions could be therapeutically advantageous, especially in patients with high systemic inflammatory burden.

Another aspect of the peripheral changes caused by cerebral ischemia is the induction of profound immunosuppression, both in patients and in experimental animals. These changes include splenic atrophy, reduced B- and T-cell counts and proliferation, and reduced pro-inflammatory protein expression by blood cells [180, 189, 190]. The underlying mechanisms may be similar to those leading to systemic immunodepression after brain trauma [191]. It is not surprising that stroke-associated pneumonia is an important independent contributor to poor outcome in patients [192, 193]. Experimental rodent models have been established to reveal the potential mechanisms and to find therapeutic targets. In a mouse model of focal cerebral ischemia, extensive apoptotic loss of lymphocytes and a shift from T-helper cell (Th)1 to Th2 cytokine production were observed, and animals developed spontaneous septicemia and pneumonia [194]. Preventive antibacterial treatment improved the general medical and neurological outcome [195]. It seems therefore that several parameters have to be taken into consideration for the experimental design to model the clinical situation because the interaction between ischemic and immune processes seems highly complex.

Due to the large overlap between inflammatory changes induced by ischemia and infection, in complex experimental models, it may be very difficult to interpret results and to dissect mechanisms. Several chemokines and pro-inflammatory cytokines, which become activated after stroke in the brain or in the periphery [179, 180], are expressed in response to viral [196] and systemic bacterial infections [197]. In addition, pathogen detecting sensors such as toll-like receptors (TLRs) and NOD-like receptors, activated by viral- [196] or microbial-derived molecules [198], not only recognize various self-ligands such as heat-shock proteins [199] or extracellular matrix components [171] but also function as endogenous damage sensors, becoming activated during neuroinflammation and stroke [200, 201], and play a role in the

production of cytokines such as IL-1β [196]. In line with this, mice lacking either functional TLR4 [202] or TLR2 [203] are less susceptible to transient focal cerebral ischemia and reperfusion damage. Unfortunately, only very few studies have been performed on gnotobiotic animals to date; continued research could give further insights to the potential effects of the endogenous flora. Nevertheless, recent data indicate that the gut microbiota controls the maturation and function of microglia in the CNS and influences blood–brain barrier permeability in mice [204, 205].

Timing can be another confounding factor in modeling the effects of inflammation or infection in experimental stroke research. As discussed above, acute or chronic (systemic) inflammation may worsen the outcome after stroke, but preconditioning with LPS or pre-activation of TLRs may be protective through mechanisms similar to ischemic tolerance. These events are most likely mediated through the hyporesponsiveness or reprogramming of TLR-mediated signaling [206, 207].

13 Inflammation is associated with most known comorbidities.

Interestingly, many comorbidities associated with stroke (such as diabetes, atherosclerosis or obesity) involve inflammation. For example, adipose tissue is now recognized as an abundant source of inflammatory mediators, and obesity is now considered a state of chronic inflammation with significantly elevated systemic levels of various cytokines, including tumor necrosis factor-α and interleukin-6. Inflammation is strongly implicated in the development and/or progression of insulin resistance/diabetes, hypertension, and vascular disease—key factors increasing stroke susceptibility—in obese individuals [208–210]. Markers indicative of an increased prothrombotic tendency (e.g., increased levels of von Willebrand factor, plasminogen activator inhibitor-1) are also evident in obese individuals [210, 211]. Inflammatory mediators such as TNF-α promote pro-coagulatory mechanisms and inhibit antithrombotic mediators [212], suggesting that increased inflammation in obesity could cause a shift from anti- to prothrombotic status, thus favoring the development of a "stroke-prone" state. Similarly, atherosclerosis is a chronic inflammatory disorder that primarily affects large- and medium-size arteries at sites of disturbed blood flow [213]. Atherosclerotic lesions consist of endothelial cells, vascular smooth cells, and various immune cells including T lymphocytes and monocytes and macrophages [214]. These cells, in concert with a diverse array of soluble inflammatory mediators, modified lipids, and proteases, drive the progression of plaques from a relatively benign to highly unstable state prone to rupture. Plaque instability and rupture trigger thrombosis and intravascular occlusion, leading to stroke. The contribution of inflammatory mediators to the

initiation or progression of these common comorbid conditions affecting stroke patients suggests that inflammation is a more important contributor to the incidence and consequences of stroke in clinical reality than it is in experiments undertaken to date. Recent data show that a preexisting inflammatory state resulting from acute (e.g., infection) or chronic (e.g., atherosclerosis) inflammatory conditions modifies the peripheral and central inflammatory processes prior to and after the onset of cerebral ischemia [182, 183] (see the following review articles for further details [215, 216]).

Beyond providing potential mechanisms for the interaction of systemic inflammation with stroke, the examples above also highlight some of the technical considerations and difficulties involved in experimental models. As peripheral inflammation may modify the expression of inflammatory mediators in the inflamed CNS, cerebral ischemia may increase or blunt infection-induced changes in the periphery. The examination of multiple organs, evaluation in various time points after ischemia, and systems biology approaches can therefore be of great importance for achieving a more complete understanding.

14 Conclusions

Our failure to adequately model the factors which cause a stroke and contribute to the outcome in experimental studies may have been a significant factor in the failure of potentially promising therapeutic interventions. It is clear from laboratory studies that factors such as obesity, diabetes, atherosclerosis, and age have a profound effect on ischemic brain injury in rodents. But their inclusion in experimental studies is not without problems. Many of the methods used to induce such conditions have confounding effects. We rarely study spontaneous stroke caused by the factors which are known to predispose humans to stroke, and few studies have assessed the effects of multiple interventions, for example, to mimic the cocktail of treatments applied to many patients. In spite of these difficulties, it seems clear that wider use of animal models with comorbidities is important for future research on stroke.

Acknowledgments

The authors are supported by the Medical Research Council and the Biotechnology and Biological Research Council of the European Union through the ARISE consortium, OTKA K109743 (AD), the Hungarian Brain Research Program KTIA_13_NAP-A-I/2 (AD), the Bolyai Janos Research Scholarship from the Hungarian Academy of Sciences (AD), and the Australian National Health and Medical Research Council.

References

1. Stair (1999) Recommendations for standards regarding preclinical neuroprotective and restorative drug development. Stroke 30(12):2752–2758
2. Del Zoppo GJ (1995) Why do all drugs work in animals but none in stroke patients? 1. Drugs promoting cerebral blood flow. J Intern Med 237(1):79–88
3. Gladstone DJ, Black SE, Hakim AM (2002) Toward wisdom from failure: lessons from neuroprotective stroke trials and new therapeutic directions. Stroke 33(8):2123–2136
4. Cheng YD, Al-Khoury L, Zivin JA (2004) Neuroprotection for ischemic stroke: two decades of success and failure. NeuroRx 1(1):36–45
5. Crossley NA, Sena E, Goehler J, Horn J, van der Worp B, Bath PM, Macleod M, Dirnagl U (2008) Empirical evidence of bias in the design of experimental stroke studies: a metaepidemiologic approach. Stroke 39(3):929–934
6. Fisher M (2008) Stroke and TIA: epidemiology, risk factors, and the need for early intervention. Am J Manag Care 14(6 Suppl 2):S204–S211
7. Dirnagl U, Fisher M (2012) International, multicenter randomized preclinical trials in translational stroke research: it's time to act. J Cereb Blood Flow Metab 32(6):933–935. doi:10.1038/jcbfm.2012.51
8. Hankey GJ (2006) Potential new risk factors for ischemic stroke: what is their potential? Stroke 37(8):2181–2188
9. Alberts MJ, Atkinson R (2004) Risk reduction strategies in ischaemic stroke: the role of antiplatelet therapy. Clin Drug Investig 24(5):245–254
10. Sacco RL, Adams R, Albers G, Alberts MJ, Benavente O, Furie K, Goldstein LB, Gorelick P, Halperin J, Harbaugh R, Johnston SC, Katzan I, Kelly-Hayes M, Kenton EJ, Marks M, Schwamm LH, Tomsick T (2006) Guidelines for prevention of stroke in patients with ischemic stroke or transient ischemic attack: a statement for healthcare professionals from the American Heart Association/American Stroke Association Council on Stroke: co-sponsored by the Council on Cardiovascular Radiology and Intervention: the American Academy of Neurology affirms the value of this guideline. Stroke 37(2):577–617
11. Kelly BM, Pangilinan PH Jr, Rodriguez GM (2007) The stroke rehabilitation paradigm. Phys Med Rehabil Clin N Am 18(4):631–650, v
12. Lawes CM, Bennett DA, Feigin VL, Rodgers A (2004) Blood pressure and stroke: an overview of published reviews. Stroke 35(4):1024
13. Wagner J, Klotz S, Haufe CC, Danser JA, Amann K, Ganten D, Ritz E (1997) Progression of renal failure after subtotal nephrectomy in transgenic rats carrying an additional renin gene [TGR(mREN2)27]. J Hypertens 15(4):441–449
14. Bianchi G, Ferrari P, Barber BR (1984) The Milan hypertensive strain. In: de Jong W (ed) Handbook of hypertension: experimental and genetic models of hypertension, vol 4. Elsevier Science Publishers, Amsterdam, pp 328–349
15. Phelan EL (1968) The New Zealand strain of rats with genetic hypertension. N Z Med J 67(429):334–344
16. Vincent M, Sacquet J, Sassard J (1984) The Lyon strains of hypertensive, normotensive and low-blood-pressure rats. In: de Jong W (ed) Handbook of hypertension: experimental and genetic models of hypertension. Elsevier Science Publishers, Amsterdam, pp 314–327
17. Prusty S, Kemper T, Moss MB, Hollander W (1988) Occurrence of stroke in a nonhuman primate model of cerebrovascular disease. Stroke 19(1):84–90
18. Fredriksson K, Kalimo H, Nordborg C, Johansson BB, Olsson Y (1988) Nerve cell injury in the brain of stroke-prone spontaneously hypertensive rats. Acta Neuropathol 76(3):227–237
19. Okamoto K, Aoki K (1963) Development of a strain of spontaneously hypertensive rats. Jpn Circ J 27:282–293
20. Shibota M, Nagaoka A, Shino A, Fujita T (1979) Renin-angiotensin system in stroke-prone spontaneously hypertensive rats. Am J Physiol 236(3):H409–H416
21. Hurn PD, Subramanian S, Parker SM, Afentoulis ME, Kaler LJ, Vandenbark AA, Offner H (2007) T- and B-cell-deficient mice with experimental stroke have reduced lesion size and inflammation. J Cereb Blood Flow Metab 27(11):1798–1805
22. Yamori Y, Horie R, Handa H, Sato M, Fukase M (1976) Pathogenetic similarity of strokes in stroke-prone spontaneously hypertensive rats and humans. Stroke 7(1):46–53
23. Jacewicz M (1992) The hypertensive rat and predisposition to cerebral infarction. Hypertension 19(1):47–48
24. Coyle P, Jokelainen PT (1982) Dorsal cerebral arterial collaterals of the rat. Anat Rec 203(3):397–404

25. Nabika T, Cui Z, Masuda J (2004) The stroke-prone spontaneously hypertensive rat: how good is it as a model for cerebrovascular diseases? Cell Mol Neurobiol 24(5):639–646
26. Coyle P, Heistad DD (1986) Blood flow through cerebral collateral vessels in hypertensive and normotensive rats. Hypertension 8(6 Pt 2):II67–II71
27. Baumbach GL, Heistad DD, Siems JE (1989) Effect of sympathetic nerves on composition and distensibility of cerebral arterioles in rats. J Physiol 416:123–140
28. Yang ST, Faraci FM, Heistad DD (1993) Effects of cilazapril on cerebral vasodilatation in hypertensive rats. Hypertension 22(2):150–155
29. Churchill PC, Churchill MC, Griffin KA, Picken M, Webb RC, Kurtz TW, Bidani AK (2002) Increased genetic susceptibility to renal damage in the stroke-prone spontaneously hypertensive rat. Kidney Int 61(5):1794–1800
30. Tajima A, Hans FJ, Livingstone D, Wei L, Finnegan W, DeMaro J, Fenstermacher J (1993) Smaller local brain volumes and cerebral atrophy in spontaneously hypertensive rats. Hypertension 21(1):105–111
31. Bendel P, Eilam R (1992) Quantitation of ventricular size in normal and spontaneously hypertensive rats by magnetic resonance imaging. Brain Res 574(1-2):224–228
32. Mangiarua EI, Lee RM (1992) Morphometric study of cerebral arteries from spontaneously hypertensive and stroke-prone spontaneously hypertensive rats. J Hypertens 10(10):1183–1190
33. Liu Y, Liu T, McCarron RM, Spatz M, Feuerstein G, Hallenbeck JM, Siren AL (1996) Evidence for activation of endothelium and monocytes in hypertensive rats. Am J Physiol 270(6 Pt 2):H2125–H2131
34. Fukushima M (1968) Histometric and histochemical studies of the hypothalamo-hypophyseal neurosecretory system of spontaneously hypertensive rats and rats with experimental hypertension. Jpn Circ J 32(4):485–516
35. Nelson DO, Boulant JA (1981) Altered CNS neuroanatomical organization of spontaneously hypertensive (SHR) rats. Brain Res 226(1-2):119–130
36. Spratt NJ, Fernandez J, Chen M, Rewell S, Cox S, van Raay L, Hogan L, Howells DW (2006) Modification of the method of thread manufacture improves stroke induction rate and reduces mortality after thread-occlusion of the middle cerebral artery in young or aged rats. J Neurosci Methods 155(2):285–290
37. Barone FC, Price WJ, White RF, Willette RN, Feuerstein GZ (1992) Genetic hypertension and increased susceptibility to cerebral ischemia. Neurosci Biobehav Rev 16(2):219–233
38. Ginsberg MD, Busto R (1989) Rodent models of cerebral ischemia. Stroke 20(12):1627–1642
39. Brint S, Jacewicz M, Kiessling M, Tanabe J, Pulsinelli W (1988) Focal brain ischemia in the rat: methods for reproducible neocortical infarction using tandem occlusion of the distal middle cerebral and ipsilateral common carotid arteries. J Cereb Blood Flow Metab 8(4):474–485
40. Gratton JA, Sauter A, Rudin M, Lees KR, McColl J, Reid JL, Dominiczak AF, Macrae IM (1998) Susceptibility to cerebral infarction in the stroke-prone spontaneously hypertensive rat is inherited as a dominant trait. Stroke 29(3):690–694
41. Ogata J, Fujishima M, Morotomi Y, Omae T (1976) Cerebral infarction following bilateral carotid artery ligation in normotensive and spontaneously hypertensive rats: a pathological study. Stroke 7(1):54–60
42. Baskaya MK, Dogan A, Dempsey RJ (1999) Application of endovascular suture occlusion of middle cerebral artery in gerbils to obtain consistent infarction. Neurol Res 21(6):574–578
43. O'Collins VE, Donnan GA, Macleod MR, Howells DW (2013) Hypertension and experimental stroke therapies. J Cereb Blood Flow Metab 33(8):1141–1147. doi:10.1038/jcbfm.2013.88
44. Macleod MR, O'Collins T, Howells DW, Donnan GA (2004) Pooling of animal experimental data reveals influence of study design and publication bias. Stroke 35(5):1203–1208
45. Macleod MR, O'Collins T, Horky LL, Howells DW, Donnan GA (2005) Systematic review and metaanalysis of the efficacy of FK506 in experimental stroke. J Cereb Blood Flow Metab 25(6):713–721
46. Sena ES, Briscoe CL, Howells DW, Donnan GA, Sandercock PA, Macleod MR (2010) Factors affecting the apparent efficacy and safety of tissue plasminogen activator in thrombotic occlusion models of stroke: systematic review and meta-analysis. J Cereb Blood Flow Metab 30(12):1905–1913. doi:10.1038/jcbfm.2010.116
47. Sena E, van der Worp HB, Howells D, Macleod M (2007) How can we improve the pre-clinical development of drugs for stroke? Trends Neurosci 30(9):433–439

48. Kawamura S, Li Y, Shirasawa M, Yasui N, Fukasawa H (1998) Effects of treatment with nilvadipine on cerebral ischemia in rats. Tohoku J Exp Med 185(4):239–246
49. Sauter A, Rudin M (1991) Prevention of stroke and brain damage with calcium antagonists in animals. Am J Hypertens 4(2 Pt 2):121S–127S
50. Alkayed NJ, Harukuni I, Kimes AS, London ED, Traystman RJ, Hurn PD (1998) Gender-linked brain injury in experimental stroke. Stroke 29(1):159–165, discussion 166
51. Yamakawa H, Jezova M, Ando H, Saavedra JM (2003) Normalization of endothelial and inducible nitric oxide synthase expression in brain microvessels of spontaneously hypertensive rats by angiotensin II AT1 receptor inhibition. J Cereb Blood Flow Metab 23(3):371–380
52. Prado R, Watson BD, Zhao W, Yao H, Busto R, Dietrich WD, Ginsberg MD (1996) L-arginine does not improve cortical perfusion or histopathological outcome in spontaneously hypertensive rats subjected to distal middle cerebral artery photothrombotic occlusion. J Cereb Blood Flow Metab 16(4):612–622
53. Morikawa E, Huang Z, Moskowitz MA (1992) L-arginine decreases infarct size caused by middle cerebral arterial occlusion in SHR. Am J Physiol 263(5 Pt 2):H1632–H1635
54. Roussel S, Pinard E, Seylaz J (1992) Effect of MK-801 on focal brain infarction in normotensive and hypertensive rats. Hypertension 19(1):40–46
55. Dirnagl U, Tanabe J, Pulsinelli W (1990) Pre- and post-treatment with MK-801 but not pretreatment alone reduces neocortical damage after focal cerebral ischemia in the rat. Brain Res 527(1):62–68
56. Amiri F, Garcia R (1997) Renal angiotensin II receptor regulation in two-kidney, one clip hypertensive rats: effect of ACE inhibition. Hypertension 30(3 Pt 1):337–344
57. Fujishima M, Onoyama K, Oniki H, Ogata J, Omae T (1978) Effects of acute hypertension on brain metabolism in normotensive, renovascular hypertensive and spontaneously hypertensive rats. Stroke 9(4):349–353
58. Zeng J, Zhang Y, Mo J, Su Z, Huang R (1998) Two-kidney, two clip renovascular hypertensive rats can be used as stroke-prone rats. Stroke 29(8):1708–1713, discussion 1713-1704
59. Del Bigio MR, Yan HJ, Kozlowski P, Sutherland GR, Peeling J (1999) Serial magnetic resonance imaging of rat brain after induction of renal hypertension. Stroke 30(11):2440–2447
60. Zhao BQ, Tejima E, Lo EH (2007) Neurovascular proteases in brain injury, hemorrhage and remodeling after stroke. Stroke 38(2 Suppl):748–752
61. Meneely GR, Ball CO (1958) Experimental epidemiology of chronic sodium chloride toxicity and the protective effect of potassium chloride. Am J Med 25(5):713–725
62. Payne GW, Smeda JS (2002) Cerebrovascular alterations in pressure and protein kinase C-mediated constriction in Dahl salt-sensitive rats. J Hypertens 20(7):1355–1363
63. Rapp JP, Dene H (1985) Development and characteristics of inbred strains of Dahl salt-sensitive and salt-resistant rats. Hypertension 7(3 Pt 1):340–349
64. Bright R, Steinberg GK, Mochly-Rosen D (2007) DeltaPKC mediates microcerebrovascular dysfunction in acute ischemia and in chronic hypertensive stress in vivo. Brain Res 1144:146–155
65. Sukamoto T, Shiono K, Watanabe TX, Sokabe H (1980) Effects of beta-adrenergic blocking drugs in hypertensive rats. J Pharmacobiodyn 3(1):1–10
66. Coyle P (1984) Outcomes to middle cerebral artery occlusion in hypertensive and normotensive rats. Hypertension 6(2 Pt 2):I69–I74
67. Dorrance AM, Rupp NC, Nogueira EF (2006) Mineralocorticoid receptor activation causes cerebral vessel remodeling and exacerbates the damage caused by cerebral ischemia. Hypertension 47(3):590–595
68. Kaarisalo MM, Raiha I, Sivenius J, Immonen-Raiha P, Lehtonen A, Sarti C, Mahonen M, Torppa J, Tuomilehto J, Salomaa V (2005) Diabetes worsens the outcome of acute ischemic stroke. Diabetes Res Clin Pract 69(3):293–298
69. Williams LS, Rotich J, Qi R, Fineberg N, Espay A, Bruno A, Fineberg SE, Tierney WR (2002) Effects of admission hyperglycemia on mortality and costs in acute ischemic stroke. Neurology 59(1):67–71
70. Sundquist K, Li X (2006) Type 1 diabetes as a risk factor for stroke in men and women aged 15-49: a nationwide study from Sweden. Diabet Med 23(11):1261–1267
71. Jeerakathil T, Johnson JA, Simpson SH, Majumdar SR (2007) Short-term risk for stroke is doubled in persons with newly treated type 2 diabetes compared with persons without diabetes: a population-based cohort study. Stroke 38(6):1739–1743
72. Poppe AY, Majumdar SR, Jeerakathil T, Ghali W, Buchan AM, Hill MD (2009) Admission hyperglycemia predicts a worse outcome in stroke patients treated with intravenous thrombolysis. Diabetes Care 32(4):617–622

73. Yong M, Kaste M (2008) Dynamic of hyperglycemia as a predictor of stroke outcome in the ECASS-II trial. Stroke 39(10):2749–2755
74. Boden-Albala B, Cammack S, Chong J, Wang C, Wright C, Rundek T, Elkind MS, Paik MC, Sacco RL (2008) Diabetes, fasting glucose levels, and risk of ischemic stroke and vascular events: findings from the Northern Manhattan Study (NOMAS). Diabetes Care 31(6):1132–1137
75. Rees DA, Alcolado JC (2005) Animal models of diabetes mellitus. Diabet Med 22(4):359–370
76. Ergul A, Elgebaly MM, Middlemore ML, Li W, Elewa H, Switzer JA, Hall C, Kozak A, Fagan SC (2007) Increased hemorrhagic transformation and altered infarct size and localization after experimental stroke in a rat model type 2 diabetes. BMC Neurol 7:33
77. Takaya K, Ogawa Y, Isse N, Okazaki T, Satoh N, Masuzaki H, Mori K, Tamura N, Hosoda K, Nakao K (1996) Molecular cloning of rat leptin receptor isoform complementary DNAs--identification of a missense mutation in Zucker fatty (fa/fa) rats. Biochem Biophys Res Commun 225(1):75–83
78. Chen H, Charlat O, Tartaglia LA, Woolf EA, Weng X, Ellis SJ, Lakey ND, Culpepper J, Moore KJ, Breitbart RE, Duyk GM, Tepper RI, Morgenstern JP (1996) Evidence that the diabetes gene encodes the leptin receptor: identification of a mutation in the leptin receptor gene in db/db mice. Cell 84(3):491–495
79. Lee JM, Zhai G, Liu Q, Gonzales ER, Yin K, Yan P, Hsu CY, Vo KD, Lin W (2007) Vascular permeability precedes spontaneous intracerebral hemorrhage in stroke-prone spontaneously hypertensive rats. Stroke 38(12):3289–3291
80. de Courten-Myers GM, Kleinholz M, Wagner KR, Myers RE (1989) Fatal strokes in hyperglycemic cats. Stroke 20(12):1707–1715
81. Palmon SC, Sieber FE, Brown PR, Koehler RC, Eleff SM, Traystman RJ (1995) Poor hemodynamic and metabolic recovery after global incomplete cerebral ischemia associated with short-term diabetes in dogs. J Cereb Blood Flow Metab 15(4):673–680
82. Kraft SA, Larson CP Jr, Shuer LM, Steinberg GK, Benson GV, Pearl RG (1990) Effect of hyperglycemia on neuronal changes in a rabbit model of focal cerebral ischemia. Stroke 21(3):447–450
83. Myers RE, Yamaguchi S (1977) Nervous system effects of cardiac arrest in monkeys. Preservation of vision. Arch Neurol 34(2):65–74
84. Martin A, Rojas S, Chamorro A, Falcon C, Bargallo N, Planas AM (2006) Why does acute hyperglycemia worsen the outcome of transient focal cerebral ischemia? Role of corticosteroids, inflammation, and protein O-glycosylation. Stroke 37(5):1288–1295
85. Ennis SR, Keep RF (2007) Effect of sustained-mild and transient-severe hyperglycemia on ischemia-induced blood-brain barrier opening. J Cereb Blood Flow Metab 27(9):1573–1582
86. Gualillo O, Gonzalez-Juanatey JR, Lago F (2007) The emerging role of adipokines as mediators of cardiovascular function: physiologic and clinical perspectives. Trends Cardiovasc Med 17(8):275–283
87. Wexler BC (1975) Chronic diabetes followed by chronic cerebral ischemia induced by bilateral carotid artery ligation in arteriosclerotic versus nonarteriosclerotic rats. Stroke 6(4):432–434
88. Huang NC, Wei J, Quast MJ (1996) A comparison of the early development of ischemic brain damage in normoglycemic and hyperglycemic rats using magnetic resonance imaging. Exp Brain Res 109(1):33–42
89. Kamada H, Yu F, Nito C, Chan PH (2007) Influence of hyperglycemia on oxidative stress and matrix metalloproteinase-9 activation after focal cerebral ischemia/reperfusion in rats: relation to blood-brain barrier dysfunction. Stroke 38(3):1044–1049
90. Panes J, Kurose I, Rodriguez-Vaca D, Anderson DC, Miyasaka M, Tso P, Granger DN (1996) Diabetes exacerbates inflammatory responses to ischemia-reperfusion. Circulation 93(1):161–167
91. Kittaka M, Wang L, Sun N, Schreiber SS, Seeds NW, Fisher M, Zlokovic BV (1996) Brain capillary tissue plasminogen activator in a diabetes stroke model. Stroke 27(4):712–719
92. Els T, Klisch J, Orszagh M, Hetzel A, Schulte-Monting J, Schumacher M, Lucking CH (2002) Hyperglycemia in patients with focal cerebral ischemia after intravenous thrombolysis: influence on clinical outcome and infarct size. Cerebrovasc Dis 13(2):89–94
93. Toung TK, Hurn PD, Traystman RJ, Sieber FE (2000) Estrogen decreases infarct size after temporary focal ischemia in a genetic model of type 1 diabetes mellitus. Stroke 31(11):2701–2706
94. Vannucci SJ, Willing LB, Goto S, Alkayed NJ, Brucklacher RM, Wood TL, Towfighi J, Hurn PD, Simpson IA (2001) Experimental stroke in the female diabetic, db/db, mouse. J Cereb Blood Flow Metab 21(1):52–60
95. Moreira T, Cebers G, Pickering C, Ostenson CG, Efendic S, Liljequist S (2007) Diabetic Goto-Kakizaki rats display pronounced hyperglycemia and longer-lasting cognitive impairments following ischemia induced by cortical

compression. Neuroscience 144(4):1169–1185
96. Hamilton MG, Tranmer BI, Auer RN (1995) Insulin reduction of cerebral infarction due to transient focal ischemia. J Neurosurg 82(2):262–268
97. Bomont L, MacKenzie ET (1995) Neuroprotection after focal cerebral ischaemia in hyperglycaemic and diabetic rats. Neurosci Lett 197(1):53–56
98. Meden P, Andersen M, Overgaard K, Rasmussen RS, Boysen G (2002) The effects of early insulin treatment combined with thrombolysis in rat embolic stroke. Neurol Res 24(4):399–404
99. Wilson PW, Bozeman SR, Burton TM, Hoaglin DC, Ben-Joseph R, Pashos CL (2008) Prediction of first events of coronary heart disease and stroke with consideration of adiposity. Circulation 118(2):124–130
100. Rexrode KM, Hennekens CH, Willett WC, Colditz GA, Stampfer MJ, Rich-Edwards JW, Speizer FE, Manson JE (1997) A prospective study of body mass index, weight change, and risk of stroke in women. JAMA 277(19):1539–1545
101. Hubert HB, Feinleib M, McNamara PM, Castelli WP (1983) Obesity as an independent risk factor for cardiovascular disease: a 26-year follow-up of participants in the Framingham Heart Study. Circulation 67(5):968–977
102. Kurth T, Gaziano JM, Berger K, Kase CS, Rexrode KM, Cook NR, Buring JE, Manson JE (2002) Body mass index and the risk of stroke in men. Arch Intern Med 162(22):2557–2562
103. Mathew B, Francis L, Kayalar A, Cone J (2008) Obesity: effects on cardiovascular disease and its diagnosis. J Am Board Fam Med 21(6):562–568
104. Khaw KT, Barrett-Connor E, Suarez L, Criqui MH (1984) Predictors of stroke-associated mortality in the elderly. Stroke 15(2):244–248
105. Lu M, Ye W, Adami HO, Weiderpass E (2006) Prospective study of body size and risk for stroke amongst women below age 60. J Intern Med 260(5):442–450
106. Winter Y, Rohrmann S, Linseisen J, Lanczik O, Ringleb PA, Hebebrand J, Back T (2008) Contribution of obesity and abdominal fat mass to risk of stroke and transient ischemic attacks. Stroke 39(12):3145–3151
107. Hu G, Tuomilehto J, Silventoinen K, Sarti C, Mannisto S, Jousilahti P (2007) Body mass index, waist circumference, and waist-hip ratio on the risk of total and type-specific stroke. Arch Intern Med 167(13):1420–1427
108. Suk SH, Sacco RL, Boden-Albala B, Cheun JF, Pittman JG, Elkind MS, Paik MC (2003) Abdominal obesity and risk of ischemic stroke: the Northern Manhattan Stroke Study. Stroke 34(7):1586–1592
109. Challenging age-old ideas about stroke (2012). Lancet Neurol 11(12):1013. doi:10.1016/S1474-4422(12)70274-0
110. Kissela BM, Khoury JC, Alwell K, Moomaw CJ, Woo D, Adeoye O, Flaherty ML, Khatri P, Ferioli S, De Los Rios La Rosa F, Broderick JP, Kleindorfer DO (2012) Age at stroke: temporal trends in stroke incidence in a large, biracial population. Neurology 79(17):1781–1787. doi:10.1212/WNL.0b013e318270401d
111. Speakman J, Hambly C, Mitchell S, Krol E (2007) Animal models of obesity. Obes Rev 8(Suppl 1):55–61
112. Russell JC, Proctor SD (2006) Small animal models of cardiovascular disease: tools for the study of the roles of metabolic syndrome, dyslipidemia, and atherosclerosis. Cardiovasc Pathol 15(6):318–330
113. Mayer J, Russell RE, Bates MW, Dickie MM (1953) Metabolic, nutritional and endocrine studies of the hereditary obesity-diabetes syndrome of mice and mechanism of its development. Metabolism 2(1):9–21
114. Zhang Y, Proenca R, Maffei M, Barone M, Leopold L, Friedman JM (1994) Positional cloning of the mouse obese gene and its human homologue. Nature 372(6505):425–432
115. McColl BW, Rose N, Robson FH, Rothwell NJ, Lawrence CB (2010) Increased brain microvascular MMP-9 and incidence of haemorrhagic transformation in obese mice after experimental stroke. J Cereb Blood Flow Metab 30(2):267–272. doi:10.1038/jcbfm.2009.217
116. Lee GH, Proenca R, Montez JM, Carroll KM, Darvishzadeh JG, Lee JI, Friedman JM (1996) Abnormal splicing of the leptin receptor in diabetic mice. Nature 379(6566):632–635
117. Herberg L, Coleman DL (1977) Laboratory animals exhibiting obesity and diabetes syndromes. Metabolism 26(1):59–99
118. Zucker LM, Antoniades HN (1972) Insulin and obesity in the Zucker genetically obese rat "fatty". Endocrinology 90(5):1320–1330
119. Richardson M, Schmidt AM, Graham SE, Achen B, DeReske M, Russell JC (1998) Vasculopathy and insulin resistance in the JCR:LA-cp rat. Atherosclerosis 138(1):135–146
120. Drake C, Boutin H, Jones MS, Denes A, McColl BW, Selvarajah JR, Hulme S, Georgiou RF, Hinz R, Gerhard A, Vail A, Prenant C, Julyan P, Maroy R, Brown G, Smigova A, Herholz K, Kassiou M, Crossman D, Francis S, Proctor SD, Russell JC, Hopkins

SJ, Tyrrell PJ, Rothwell NJ, Allan SM (2011) Brain inflammation is induced by co-morbidities and risk factors for stroke. Brain Behav Immun 25(6):1113–1122. doi:10.1016/j.bbi.2011.02.008
121. Pradillo JM, Denes A, Greenhalgh AD, Boutin H, Drake C, McColl BW, Barton E, Proctor SD, Russell JC, Rothwell NJ, Allan SM (2012) Delayed administration of interleukin-1 receptor antagonist reduces ischemic brain damage and inflammation in comorbid rats. J Cereb Blood Flow Metab 32(9):1810–1819. doi:10.1038/jcbfm.2012.101
122. Woods SC, Seeley RJ, Rushing PA, D'Alessio D, Tso P (2003) A controlled high-fat diet induces an obese syndrome in rats. J Nutr 133(4):1081–1087
123. Gallou-Kabani C, Vige A, Gross MS, Rabes JP, Boileau C, Larue-Achagiotis C, Tome D, Jais JP, Junien C (2007) C57BL/6J and A/J mice fed a high-fat diet delineate components of metabolic syndrome. Obesity (Silver Spring) 15(8):1996–2005
124. Winzell MS, Ahren B (2004) The high-fat diet-fed mouse: a model for studying mechanisms and treatment of impaired glucose tolerance and type 2 diabetes. Diabetes 53(Suppl 3):S215–S219
125. Surwit RS, Feinglos MN, Rodin J, Sutherland A, Petro AE, Opara EC, Kuhn CM, Rebuffe-Scrive M (1995) Differential effects of fat and sucrose on the development of obesity and diabetes in C57BL/6J and A/J mice. Metabolism 44(5):645–651
126. Lago F, Dieguez C, Gomez-Reino J, Gualillo O (2007) The emerging role of adipokines as mediators of inflammation and immune responses. Cytokine Growth Factor Rev 18(3-4):313–325
127. Nagai N, Van Hoef B, Lijnen HR (2007) Plasminogen activator inhibitor-1 contributes to the deleterious effect of obesity on the outcome of thrombotic ischemic stroke in mice. J Thromb Haemost 5(8):1726–1731
128. Osmond JM, Mintz JD, Dalton B, Stepp DW (2009) Obesity increases blood pressure, cerebral vascular remodeling, and severity of stroke in the Zucker rat. Hypertension 53(2):381–386
129. Terao S, Yilmaz G, Stokes KY, Ishikawa M, Kawase T, Granger DN (2008) Inflammatory and injury responses to ischemic stroke in obese mice. Stroke 39(3):943–950
130. Mayanagi K, Katakam PV, Gaspar T, Domoki F, Busija DW (2008) Acute treatment with rosuvastatin protects insulin resistant (C57BL/6J ob/ob) mice against transient cerebral ischemia. J Cereb Blood Flow Metab 28(12):1927–1935
131. Maysami S, Haley MJ, Gorenkova N, Krishnan S, McColl BW, Lawrence CB (2015) Prolonged diet-induced obesity in mice modifies the inflammatory response and leads to worse outcome after stroke. J Neuroinflammation 12:140. doi:10.1186/s12974-015-0359-8
132. Deng J, Zhang J, Feng C, Xiong L, Zuo Z (2014) Critical role of matrix metalloprotease-9 in chronic high fat diet-induced cerebral vascular remodelling and increase of ischaemic brain injury in micedagger. Cardiovasc Res 103(4):473–484. doi:10.1093/cvr/cvu154
133. Warlow C, Sudlow C, Dennis M, Wardlaw J, Sandercock P (2003) Stroke. Lancet 362(9391):1211–1224
134. Jawien J, Nastalek P, Korbut R (2004) Mouse models of experimental atherosclerosis. J Physiol Pharmacol 55(3):503–517
135. Getz GS, Reardon CA (2006) Diet and murine atherosclerosis. Arterioscler Thromb Vasc Biol 26(2):242–249
136. Mahley RW (1988) Apolipoprotein E: cholesterol transport protein with expanding role in cell biology. Science 240(4852):622–630
137. Zhang SH, Reddick RL, Piedrahita JA, Maeda N (1992) Spontaneous hypercholesterolemia and arterial lesions in mice lacking apolipoprotein E. Science 258(5081):468–471
138. Plump AS, Smith JD, Hayek T, Aalto-Setala K, Walsh A, Verstuyft JG, Rubin EM, Breslow JL (1992) Severe hypercholesterolemia and atherosclerosis in apolipoprotein E-deficient mice created by homologous recombination in ES cells. Cell 71(2):343–353
139. Nakashima Y, Plump AS, Raines EW, Breslow JL, Ross R (1994) ApoE-deficient mice develop lesions of all phases of atherosclerosis throughout the arterial tree. Arterioscler Thromb 14(1):133–140
140. Goldstein JL, Brown MS (2009) The LDL receptor. Arterioscler Thromb Vasc Biol 29(4):431–438
141. Horsburgh K, McCarron MO, White F, Nicoll JA (2000) The role of apolipoprotein E in Alzheimer's disease, acute brain injury and cerebrovascular disease: evidence of common mechanisms and utility of animal models. Neurobiol Aging 21(2):245–255
142. Laskowitz DT, Vitek MP (2007) Apolipoprotein E and neurological disease: therapeutic potential and pharmacogenomic interactions. Pharmacogenomics 8(8):959–969
143. Herz J (2001) Lipoprotein receptors: beacons to neurons? Trends Neurosci 24(4):193–195
144. Rodrigues SF, Almeida-Paula LD, Granger DN (2014) Synergistic effects of high blood

cholesterol and hypertension on leukocyte and platelet recruitment in the cerebral microcirculation. Hypertension 63(4):747–752. doi:10.1161/HYPERTENSIONAHA.113.02627
145. Farkas E, Luiten PG (2001) Cerebral microvascular pathology in aging and Alzheimer's disease. Prog Neurobiol 64(6):575–611
146. Cullen KM, Kocsi Z, Stone J (2006) Microvascular pathology in the aging human brain: evidence that senile plaques are sites of microhaemorrhages. Neurobiol Aging 27(12):1786–1796
147. Lynch CD, Cooney PT, Bennett SA, Thornton PL, Khan AS, Ingram RL, Sonntag WE (1999) Effects of moderate caloric restriction on cortical microvascular density and local cerebral blood flow in aged rats. Neurobiol Aging 20(2):191–200
148. Alba C, Vidal L, Diaz F, Villena A, de Vargas IP (2004) Ultrastructural and quantitative age-related changes in capillaries of the dorsal lateral geniculate nucleus. Brain Res Bull 64(2):145–153
149. Sieber MW, Guenther M, Jaenisch N, Albrecht-Eckardt D, Kohl M, Witte OW, Frahm C (2014) Age-specific transcriptional response to stroke. Neurobiol Aging 35(7):1744–1754. doi:10.1016/j.neurobiolaging.2014.01.012
150. Wang RY, Wang PS, Yang YR (2003) Effect of age in rats following middle cerebral artery occlusion. Gerontology 49(1):27–32
151. DiNapoli VA, Huber JD, Houser K, Li X, Rosen CL (2008) Early disruptions of the blood-brain barrier may contribute to exacerbated neuronal damage and prolonged functional recovery following stroke in aged rats. Neurobiol Aging 29(5):753–764
152. Ingraham JP, Forbes ME, Riddle DR, Sonntag WE (2008) Aging reduces hypoxia-induced microvascular growth in the rodent hippocampus. J Gerontol A Biol Sci Med Sci 63(1):12–20
153. Darsalia V, Heldmann U, Lindvall O, Kokaia Z (2005) Stroke-induced neurogenesis in aged brain. Stroke 36(8):1790–1795
154. Takaba H, Fukuda K, Yao H (2004) Substrain differences, gender, and age of spontaneously hypertensive rats critically determine infarct size produced by distal middle cerebral artery occlusion. Cell Mol Neurobiol 24(5):589–598
155. Yao H, Sadoshima S, Ooboshi H, Sato Y, Uchimura H, Fujishima M (1991) Age-related vulnerability to cerebral ischemia in spontaneously hypertensive rats. Stroke 22(11):1414–1418
156. Liu F, Yuan R, Benashski SE, McCullough LD (2009) Changes in experimental stroke outcome across the life span. J Cereb Blood Flow Metab 29(4):792–802
157. Murphy S, Gibson CL (2007) Nitric oxide, ischaemia and brain inflammation. Biochem Soc Trans 35(Pt 5):1133–1137
158. Feuerstein GZ, Liu T, Barone FC (1994) Cytokines, inflammation, and brain injury: role of tumor necrosis factor-alpha. Cerebrovasc Brain Metab Rev 6(4):341–360
159. Liu L, Wang Z, Wang X, Song L, Chen H, Bemeur C, Ste-Marie L, Montgomery J (2007) Comparison of two rat models of cerebral ischemia under hyperglycemic conditions. Microsurgery 27(4):258–262
160. Stoll G, Jander S, Schroeter M (1998) Inflammation and glial responses in ischemic brain lesions. Prog Neurobiol 56(2):149–171
161. Boutin H, LeFeuvre RA, Horai R, Asano M, Iwakura Y, Rothwell NJ (2001) Role of IL-1alpha and IL-1beta in ischemic brain damage. J Neurosci 21(15):5528–5534
162. Nawashiro H, Martin D, Hallenbeck JM (1997) Inhibition of tumor necrosis factor and amelioration of brain infarction in mice. J Cereb Blood Flow Metab 17(2):229–232
163. Hughes PM, Allegrini PR, Rudin M, Perry VH, Mir AK, Wiessner C (2002) Monocyte chemoattractant protein-1 deficiency is protective in a murine stroke model. J Cereb Blood Flow Metab 22(3):308–317
164. Soriano SG, Amaravadi LS, Wang YF, Zhou H, Yu GX, Tonra JR, Fairchild-Huntress V, Fang Q, Dunmore JH, Huszar D, Pan Y (2002) Mice deficient in fractalkine are less susceptible to cerebral ischemia-reperfusion injury. J Neuroimmunol 125(1-2):59–65
165. Villa P, Triulzi S, Cavalieri B, Di Bitondo R, Bertini R, Barbera S, Bigini P, Mennini T, Gelosa P, Tremoli E, Sironi L, Ghezzi P (2007) The interleukin-8 (IL-8/CXCL8) receptor inhibitor reparixin improves neurological deficits and reduces long-term inflammation in permanent and transient cerebral ischemia in rats. Mol Med 13(3-4):125–133
166. Denes A, Ferenczi S, Halasz J, Kornyei Z, Kovacs KJ (2008) Role of CX3CR1 (fractalkine receptor) in brain damage and inflammation induced by focal cerebral ischemia in mouse. J Cereb Blood Flow Metab 28(10):1707–1721
167. Yrjanheikki J, Tikka T, Keinanen R, Goldsteins G, Chan PH, Koistinaho J (1999) A tetracycline derivative, minocycline, reduces inflammation and protects against focal cerebral ischemia with a wide therapeutic window. Proc Natl Acad Sci U S A 96(23):13496–13500
168. Tang PC, Qin L, Zielonka J, Zhou J, Matte-Martone C, Bergaya S, van Rooijen N,

Shlomchik WD, Min W, Sessa WC, Pober JS, Tellides G (2008) MyD88-dependent, superoxide-initiated inflammation is necessary for flow-mediated inward remodeling of conduit arteries. J Exp Med 205(13):3159–3171
169. Stabile E, Kinnaird T, la Sala A, Hanson SK, Watkins C, Campia U, Shou M, Zbinden S, Fuchs S, Kornfeld H, Epstein SE, Burnett MS (2006) CD8+ T lymphocytes regulate the arteriogenic response to ischemia by infiltrating the site of collateral vessel development and recruiting CD4+ mononuclear cells through the expression of interleukin-16. Circulation 113(1):118–124
170. Romanic AM, White RF, Arleth AJ, Ohlstein EH, Barone FC (1998) Matrix metalloproteinase expression increases after cerebral focal ischemia in rats: inhibition of matrix metalloproteinase-9 reduces infarct size. Stroke 29(5):1020–1030
171. Copin JC, Goodyear MC, Gidday JM, Shah AR, Gascon E, Dayer A, Morel DM, Gasche Y (2005) Role of matrix metalloproteinases in apoptosis after transient focal cerebral ischemia in rats and mice. Eur J Neurosci 22(7):1597–1608
172. Grossetete M, Rosenberg GA (2008) Matrix metalloproteinase inhibition facilitates cell death in intracerebral hemorrhage in mouse. J Cereb Blood Flow Metab 28(4):752–763
173. Kang SS, Kook JH, Hwang S, Park SH, Nam SC, Kim JK (2008) Inhibition of matrix metalloproteinase-9 attenuated neural progenitor cell migration after photothrombotic ischemia. Brain Res 1228:20–26
174. Boltze J, Forschler A, Nitzsche B, Waldmin D, Hoffmann A, Boltze CM, Dreyer AY, Goldammer A, Reischauer A, Hartig W, Geiger KD, Barthel H, Emmrich F, Gille U (2008) Permanent middle cerebral artery occlusion in sheep: a novel large animal model of focal cerebral ischemia. J Cereb Blood Flow Metab 28(12):1951–1964
175. Imai H, Konno K, Nakamura M, Shimizu T, Kubota C, Seki K, Honda F, Tomizawa S, Tanaka Y, Hata H, Saito N (2006) A new model of focal cerebral ischemia in the miniature pig. J Neurosurg 104(2 Suppl):123–132
176. Emsley HC, Hopkins SJ (2008) Acute ischaemic stroke and infection: recent and emerging concepts. Lancet Neurol 7(4):341–353
177. Paganini-Hill A, Lozano E, Fischberg G, Perez Barreto M, Rajamani K, Ameriso SF, Heseltine PN, Fisher M (2003) Infection and risk of ischemic stroke: differences among stroke subtypes. Stroke 34(2):452–457
178. Smeeth L, Thomas SL, Hall AJ, Hubbard R, Farrington P, Vallance P (2004) Risk of myocardial infarction and stroke after acute infection or vaccination. N Engl J Med 351(25):2611–2618
179. Emsley HC, Smith CJ, Gavin CM, Georgiou RF, Vail A, Barberan EM, Hallenbeck JM, del Zoppo GJ, Rothwell NJ, Tyrrell PJ, Hopkins SJ (2003) An early and sustained peripheral inflammatory response in acute ischaemic stroke: relationships with infection and atherosclerosis. J Neuroimmunol 139(1-2):93–101
180. Offner H, Subramanian S, Parker SM, Afentoulis ME, Vandenbark AA, Hurn PD (2006) Experimental stroke induces massive, rapid activation of the peripheral immune system. J Cereb Blood Flow Metab 26(5):654–665
181. Matsuo Y, Kihara T, Ikeda M, Ninomiya M, Onodera H, Kogure K (1995) Role of neutrophils in radical production during ischemia and reperfusion of the rat brain: effect of neutrophil depletion on extracellular ascorbyl radical formation. J Cereb Blood Flow Metab 15(6):941–947
182. McColl BW, Rothwell NJ, Allan SM (2007) Systemic inflammatory stimulus potentiates the acute phase and CXC chemokine responses to experimental stroke and exacerbates brain damage via interleukin-1- and neutrophil-dependent mechanisms. J Neurosci 27(16):4403–4412
183. McColl BW, Rothwell NJ, Allan SM (2008) Systemic inflammation alters the kinetics of cerebrovascular tight junction disruption after experimental stroke in mice. J Neurosci 28(38):9451–9462
184. Denes A, Drake C, Stordy J, Chamberlain J, McColl BW, Gram H, Crossman D, Francis S, Allan SM, Rothwell NJ (2012) Interleukin-1 mediates neuroinflammatory changes associated with diet-induced atherosclerosis. J Am Heart Assoc 1(3), e002006. doi:10.1161/JAHA.112.002006
185. Dhungana H, Malm T, Denes A, Valonen P, Wojciechowski S, Magga J, Savchenko E, Humphreys N, Grencis R, Rothwell N, Koistinaho J (2013) Aging aggravates ischemic stroke-induced brain damage in mice with chronic peripheral infection. Aging Cell 12(5):842–850. doi:10.1111/acel.12106
186. Muhammad S, Haasbach E, Kotchourko M, Strigli A, Krenz A, Ridder DA, Vogel AB, Marti HH, Al-Abed Y, Planz O, Schwaninger M (2011) Influenza virus infection aggravates stroke outcome. Stroke 42(3):783–791. doi:10.1161/STROKEAHA.110.596783
187. Denes A, Pradillo JM, Drake C, Sharp A, Warn P, Murray KN, Rohit B, Dockrell DH, Chamberlain J, Casbolt H, Francis S,

Martinecz B, Nieswandt B, Rothwell NJ, Allan SM (2014) Streptococcus pneumoniae worsens cerebral ischemia via interleukin 1 and platelet glycoprotein Ibalpha. Ann Neurol 75(5):670–683. doi:10.1002/ana.24146
188. Nakano K, Hokamura K, Taniguchi N, Wada K, Kudo C, Nomura R, Kojima A, Naka S, Muranaka Y, Thura M, Nakajima A, Masuda K, Nakagawa I, Speziale P, Shimada N, Amano A, Kamisaki Y, Tanaka T, Umemura K, Ooshima T (2011) The collagen-binding protein of Streptococcus mutans is involved in haemorrhagic stroke. Nat Commun 2:485. doi:10.1038/ncomms1491
189. Emsley HC, Smith CJ, Gavin CM, Georgiou RF, Vail A, Barberan EM, Illingworth K, Scarth S, Wickramasinghe V, Hoadley ME, Rothwell NJ, Tyrrell PJ, Hopkins SJ (2007) Clinical outcome following acute ischaemic stroke relates to both activation and autoregulatory inhibition of cytokine production. BMC Neurol 7:5
190. Vogelgesang A, Grunwald U, Langner S, Jack R, Broker BM, Kessler C, Dressel A (2008) Analysis of lymphocyte subsets in patients with stroke and their influence on infection after stroke. Stroke 39(1):237–241
191. Woiciechowsky C, Schoning B, Lanksch WR, Volk HD, Docke WD (1999) Mechanisms of brain-mediated systemic anti-inflammatory syndrome causing immunodepression. J Mol Med 77(11):769–780
192. Hilker R, Poetter C, Findeisen N, Sobesky J, Jacobs A, Neveling M, Heiss WD (2003) Nosocomial pneumonia after acute stroke: implications for neurological intensive care medicine. Stroke 34(4):975–981
193. Katzan IL, Cebul RD, Husak SH, Dawson NV, Baker DW (2003) The effect of pneumonia on mortality among patients hospitalized for acute stroke. Neurology 60(4):620–625
194. Prass K, Meisel C, Hoflich C, Braun J, Halle E, Wolf T, Ruscher K, Victorov IV, Priller J, Dirnagl U, Volk HD, Meisel A (2003) Stroke-induced immunodeficiency promotes spontaneous bacterial infections and is mediated by sympathetic activation reversal by poststroke T helper cell type 1-like immunostimulation. J Exp Med 198(5):725–736
195. Meisel C, Prass K, Braun J, Victorov I, Wolf T, Megow D, Halle E, Volk HD, Dirnagl U, Meisel A (2004) Preventive antibacterial treatment improves the general medical and neurological outcome in a mouse model of stroke. Stroke 35(1):2–6
196. Takeuchi O, Akira S (2009) Innate immunity to virus infection. Immunol Rev 227(1):75–86
197. Sriskandan S, Altmann DM (2008) The immunology of sepsis. J Pathol 214(2):211–223
198. Delbridge LM, O'Riordan MX (2007) Innate recognition of intracellular bacteria. Curr Opin Immunol 19(1):10–16
199. Asea A (2008) Heat shock proteins and toll-like receptors. Handb Exp Pharmacol 183:111–127
200. Arumugam TV, Okun E, Tang SC, Thundyil J, Taylor SM, Woodruff TM (2008) Toll-like receptors in ischemia-reperfusion injury. Shock 32:4–16
201. Pineau I, Lacroix S (2009) Endogenous signals initiating inflammation in the injured nervous system. Glia 57(4):351–361
202. Kilic U, Kilic E, Matter CM, Bassetti CL, Hermann DM (2008) TLR-4 deficiency protects against focal cerebral ischemia and axotomy-induced neurodegeneration. Neurobiol Dis 31(1):33–40
203. Lehnardt S, Lehmann S, Kaul D, Tschimmel K, Hoffmann O, Cho S, Krueger C, Nitsch R, Meisel A, Weber JR (2007) Toll-like receptor 2 mediates CNS injury in focal cerebral ischemia. J Neuroimmunol 190(1-2):28–33
204. Braniste V, Al-Asmakh M, Kowal C, Anuar F, Abbaspour A, Toth M, Korecka A, Bakocevic N, Ng LG, Kundu P, Gulyas B, Halldin C, Hultenby K, Nilsson H, Hebert H, Volpe BT, Diamond B, Pettersson S (2014) The gut microbiota influences blood-brain barrier permeability in mice. Sci Transl Med 6(263):263ra158. doi:10.1126/scitranslmed.3009759
205. Erny D, Hrabe de Angelis AL, Jaitin D, Wieghofer P, Staszewski O, David E, Keren-Shaul H, Mahlakoiv T, Jakobshagen K, Buch T, Schwierzeck V, Utermohlen O, Chun E, Garrett WS, McCoy KD, Diefenbach A, Staeheli P, Stecher B, Amit I, Prinz M (2015) Host microbiota constantly control maturation and function of microglia in the CNS. Nat Neurosci 18(7):965–977. doi:10.1038/nn.4030
206. Marsh BJ, Williams-Karnesky RL, Stenzel-Poore MP (2009) Toll-like receptor signaling in endogenous neuroprotection and stroke. Neuroscience 158:1007–1020
207. Kariko K, Weissman D, Welsh FA (2004) Inhibition of toll-like receptor and cytokine signaling--a unifying theme in ischemic tolerance. J Cereb Blood Flow Metab 24(11):1288–1304
208. Malavazos AE, Corsi MM, Ermetici F, Coman C, Sardanelli F, Rossi A, Morricone L, Ambrosi B (2007) Proinflammatory cytokines and cardiac abnormalities in uncomplicated obesity: relationship with abdominal fat deposition. Nutr Metab Cardiovasc Dis 17(4):294–302
209. Bastard JP, Maachi M, Lagathu C, Kim MJ, Caron M, Vidal H, Capeau J, Feve B (2006) Recent advances in the relationship between

obesity, inflammation, and insulin resistance. Eur Cytokine Netw 17(1):4–12
210. Darvall KA, Sam RC, Silverman SH, Bradbury AW, Adam DJ (2007) Obesity and thrombosis. Eur J Vasc Endovasc Surg 33(2):223–233
211. De Pergola G, De Mitrio V, Giorgino F, Sciaraffia M, Minenna A, Di Bari L, Pannacciulli N, Giorgino R (1997) Increase in both pro-thrombotic and anti-thrombotic factors in obese premenopausal women: relationship with body fat distribution. Int J Obes Relat Metab Disord 21(7):527–535
212. De Pergola G, Pannacciulli N (2002) Coagulation and fibrinolysis abnormalities in obesity. J Endocrinol Invest 25(10): 899–904
213. Tedgui A, Mallat Z (2006) Cytokines in atherosclerosis: pathogenic and regulatory pathways. Physiol Rev 86(2):515–581
214. Weber C, Zernecke A, Libby P (2008) The multifaceted contributions of leukocyte subsets to atherosclerosis: lessons from mouse models. Nat Rev Immunol 8(10):802–815
215. Murray KN, Buggey HF, Denes A, Allan SM (2013) Systemic immune activation shapes stroke outcome. Mol Cell Neurosci 53:14–25. doi:10.1016/j.mcn.2012.09.004
216. Smith CJ, Lawrence CB, Rodriguez-Grande B, Kovacs KJ, Pradillo JM, Denes A (2013) The immune system in stroke: clinical challenges and their translation to experimental research. Journal of Neuroimmune Pharmacol 8(4):867–887. doi:10.1007/s11481-013-9469-1

Chapter 10

Effect of Anesthesia in Stroke Models

Richard J. Traystman

Abstract

Many investigators have examined or are examining the effects of focal and global cerebral ischemia on brain physiology, chemistry, genetics, molecular aspects, and function. Many animal and cellular models are utilized for these types of studies. However, anesthetics must be used for in vivo studies or at least in most animal models of cerebral ischemia. In many of these studies, there has been an intensive search for agents that are neuroprotective for cerebral ischemia. The use of anesthetics may complicate the issues relating to neuroprotection because many anesthetics themselves may possess neuroprotective or neurotoxic characteristics. This chapter addresses the more commonly used anesthetics for the study of cerebral ischemia. At the conclusion of the chapter, the issues related to why anesthetics have not been successfully used in humans as neuroprotective agents are discussed.

Key words Volatile and nonvolatile anesthetics, Focal and global cerebral ischemia, In vivo animal stroke models, Cerebral neuroprotection, Anesthetic neurotoxicity, Anesthetic mechanisms of action

1 Introduction

Focal (stroke) and global (cardiac arrest) cerebral ischemia are major causes of death and disability and have been extensively investigated over the past five decades. Despite much animal work concerning brain tissue injury and identifying the multiple mechanisms by which focal and global cerebral ischemia produce neuronal injury, little of this work has been translated to effective treatment modalities in humans with ischemic injury. One possible reason for this may be that several important mechanisms of injury have been identified, and these mechanisms may be overlapping, making the issue of mechanisms extremely complex. Also, some mechanisms of injury may be critical in certain species but not in others, so certain heavily studied mechanisms of injury in rodents, for example, may be relatively unimportant in humans. Different brain areas may also have different mechanisms further complicating the issue. Some mechanisms of injury from ischemia that have been heavily studied are production of oxygen free radicals, lipid peroxidation, release of

Ulrich Dirnagl (ed.), *Rodent Models of Stroke*, Neuromethods, vol. 120,
DOI 10.1007/978-1-4939-5620-3_10,

excitatory amino acids (glutamate and aspartate), involvement of ionic pumps for Ca^{2+} and Na^{+}, acidosis, alterations in brain blood flow and metabolism, hyperthermia, involvement of genes and gene products, and others. The notion of protecting neurons from injury (neuroprotection) is not an innovative concept and is not new. Many purported neuroprotective agents (such as anesthetics, free radical scavengers, excitatory amino acid antagonists, Ca^{2+} channel blockers), ionic pump modulators, antineutrophil and platelet factors, growth factors, hypothermia, and, more recently, manipulation of genes and gene products, and sex steroids have been investigated for years. Some of these have demonstrated varying degrees of success in certain species of animals, but none of these have been successful in humans, with the possible exception of hypothermia. The goal of this chapter is to discuss the most prominently used anesthetics in models of cerebral ischemia and their complicating role as neuroprotectants and/or neurotoxic agents. Finally, at the end of the chapter, we discuss the potential reasons why anesthetics and other pharmacologic agents have demonstrated little usefulness as neuroprotectants in humans following focal and global cerebral ischemia.

2 Anesthetic Neuroprotection

Clinical observations showing that patients under general anesthesia are more tolerant of cerebral ischemia than unanesthetized patients [1] led to the idea that anesthetics may have an impact on brain injury following hypoxia or cerebral ischemia. Anesthetics have many mechanisms of action that have been associated with neuroprotection. These include: inhibition of spontaneous depolarization [2], cerebral blood flow redistribution [3, 4], antioxidant potential [5, 6], NMDA receptor antagonism [7, 8], and GABA potentiation [9–13]. Anesthetic neuroprotection could be important, particularly in patients undergoing carotid endarterectomy, cardiac bypass, open-heart surgery, etc., and other procedures known to lead to cerebral ischemia. Should anesthetics be found to have neuroprotective attributes, it will be critical to know which anesthetic provides the greatest protection, when it should be administered, and whether that anesthetic could be used to improve overall outcome from focal and global cerebral ischemia.

Numerous manuscripts have appeared in the literature over the past five decades evaluating how different anesthetics affect neurological outcome from an ischemic or hypoxic insult in both in vitro and in vivo model systems. Many of these studies describe outcome related to neurologic examination or brain histopathology, whereas others evaluate cerebral hemodynamic or metabolic aspects of the brain following ischemia with different anesthetics. Unfortunately, most of these reports have compared different

anesthetics with other anesthetics already present in the animal model, making any interpretation of the effect of any one anesthetic difficult or impossible. Few studies have compared the efficacy of anesthetics with the unanesthetized state, and even fewer have evaluated the effects of anesthetics as neuroprotectants when administered following the onset of ischemia or reperfusion.

In considering the neuroprotective properties of anesthetics in cerebral ischemia, it must be remembered that each anesthetic has its own effect on the cerebral vasculature, brain metabolism, brain electrophysiology (evoked potentials), temperature, blood pressure, and other physiological parameters. In turn, each of these factors may have effects on neuroprotective cascades concerned with neuroprotective mechanisms. Thus, these aspects may confound the true effects of anesthetics on protection mechanisms with ischemia. For example, barbiturates decrease cerebral blood flow (CBF) , cerebral metabolism ($CMRO_2$), and somatosensory evoked potential (SEP) amplitude and increase SEP latency. However, halothane increases CBF but decreases $CMRO_2$ and SEP amplitude while increasing SEP latency. Fentanyl decreases CBF and $CMRO_2$, and ketamine increases CBF but has variable effects on $CMRO_2$. Thus, these basic physiological effects of different anesthetics could also alter their neuroprotective potential following focal or global cerebral ischemia.

The question of whether anesthetics actually protect the brain from cerebral ischemia is undetermined. Many studies in the literature evaluating many anesthetic agents have attempted to answer this question, but no clear "winner" has emerged. There are several appropriate mechanistic reasons why anesthetics should be effective as neuroprotectants, but evidence demonstrating anesthetic neuroprotection is extremely contradictory. Some investigators have shown positive neuroprotective effects of anesthetics in cerebral ischemia while others have not. Others have not been able to reproduce previously obtained positive data in the same or different animal or in vitro models. And still others have demonstrated that some anesthetics actually produce worse outcome after ischemic events and are neurotoxic, not neuroprotective. Investigators studying anesthetics as neuroprotective agents have utilized many animal species, including humans, and many different models, including middle cerebral artery occlusion, carotid ligation, cardiac arrest, neck tourniquet, air emboli, and carotid endarterectomy; however, the answer to the question of whether anesthetic neuroprotection exists remains elusive. Another additional aspect of anesthetic neuroprotection is that of anesthetic preconditioning [14–16]. Previous exposure of the brain to a variety of insults, chemical or pharmacological agents, can precondition or increase the brain's tolerance to future, more injurious events. Exposure of rodents to clinical concentrations of volatile anesthetic agents increases tolerance of the brain to subsequent

ischemic insults [17, 18], and this tolerance (preconditioning) has also been demonstrated in in vitro models [19]. Many potential mechanisms have been proposed to account for anesthetic preconditioning, and while many overlap with those proposed for anesthetic neuroprotection, it is likely that multiple mechanisms are involved and anesthetic preconditioning appears to occur almost immediately [18]. Thus, anesthetic preconditioning mechanisms are complex and likely overlap with the standard proposed mechanisms of anesthetic neuroprotection. These potential mechanisms may involve: Akt activation which can control the balance between survival and death signaling in the brain [15, 20–22]; nitric oxide (NO) [15, 18, 23]; opening of KATP channels, which alters oxygen radical production, reduces mitochondrial Ca^{2+} accumulation, and increases mitochondrial energy production [24–26]; adenosine Al receptor activation that could trigger KATP channel activation leading to the development of cerebral ischemic tolerance [27]; activation of p38 MARK [28]; inhibition of glutamate release [29, 30]; and others [14, 15].

The point of this brief discussion is to indicate that the potential mechanisms of anesthetic neuroprotection and anesthetic preconditioning may be quite similar and overlapping. This makes understanding of neuroprotection and preconditioning extremely complex, and for investigators utilizing cerebral ischemia animal models, which necessitate the use of one or more anesthetics, aspects of drug dose, timing of anesthetic administration, and preconditioning duration should be taken into consideration. All of these issues may alter the interpretation of data obtained. Nevertheless, there is great interest in anesthetic neuroprotection and preconditioning as it relates to clinical situations that can result in brain hypoxia or ischemia. Anesthetic neuroprotection and preconditioning of the brain may prevent or even delay neurological complications involving cerebral ischemia, thus expanding the therapeutic window for other prospective pharmacological neuroprotective agents.

3 Nonvolatile Anesthetics

3.1 Barbiturates

Barbiturates have been investigated as neuroprotective agents for almost five decades [31–33] mainly because they possess important characteristics of promising neuroprotective therapeutic agents such as reduction of cerebral metabolism [34], reduction of cerebral edema formation [35], reduction of intracranial pressure [36], and reduction of seizure activity [37]. Barbiturates also improve the ratio of cerebral oxygen supply to demand [38], improve the cell energy charge [39], improve cyclic AMP stores [40], and increased accumulation of free fatty acids [41], all important characteristics of pharmacological agents that might be of therapeutic

use. Thus, the simple strategic usefulness of barbiturates as neuroprotective agents is that only reduction in brain metabolism would allow the brain to withstand a period of impaired energy and oxygen supply as would occur in an ischemic event [42–45].

The work with barbiturates has had a checkered history in determining whether they are, or are not, neuroprotective. The early work [31–33] demonstrating possible neuroprotection was unfortunately flawed. Ischemic duration to produce neurological injury was longer in barbiturate-treated animals, and in other animals, they had been treated additionally with chloralose anesthesia. Other issues could also have biased the interpretation of the obtained data such as the investigators not having been blinded to the treatment groups and the control group having had significant surgical procedures and ischemia with light or minimal anesthesia. The resulting elevated catecholamine levels in this group could have altered the ability of the control animals to tolerate ischemia. There is also the matter of lack of control of temperature, blood pressure, glucose, and other physiological parameters in these animals. These points may have led to the conflicting data obtained [10, 46].

In 1978, exciting work in monkeys demonstrated that barbiturates ameliorated neurological damage after global cerebral ischemia [47]. Because of the positive nature of the monkey study, a clinical study was designed to determine the efficacy of barbiturates in patients following cardiac arrest [48]. This clinical trial resulted in a negative outcome although it stimulated additional studies to be undertaken in this area. Other investigators, using more sophisticated experimental designs, were unable to confirm the early positive results showing that barbiturates were effective neuroprotective agents following cerebral ischemia in dogs [46, 49] or cats [37]. More importantly, the same investigators that showed positive results in monkeys were unable to reproduce those results in the same monkey model [50]. Nevertheless, a subsequent randomized clinical trial was performed concerning thiopental loading in comatose survivors of cardiac arrest [51], and the authors concluded that “no support was found for the hypothesis that high-dose thiopental loading improves neurologic recovery after prolonged global brain ischemia.”

The neuroprotective effects of barbiturates in focal cerebral ischemia are less controversial than in global ischemia although the outcome is not absolutely clear. Many investigators have demonstrated barbiturate neuroprotection in permanent and transient focal cerebral ischemia [52–59], although this is not a universal finding [60]. There had been some controversy as to whether barbiturates were actually neuroprotective themselves or whether the resulting neuroprotection occurred because of the associated hypothermia [61]. This idea has mostly been put to rest by studies that rigorously controlled temperature and still demonstrated barbiturate neuroprotection, although the magnitude of the effect

was less than previously thought. Other possible mechanisms by which barbiturates produce protection are redistribution of cerebral blood flow [62], Na^+-channel and glutamate receptor blockade [63, 64], inhibition of Ca^{2+} influx [65], inhibition of free radical formation [66], and potentiation of GABAergic activity [67]. Thus, because there is so much conflicting data in the literature and because the clinical trials of neuroprotection with barbiturates are negative, over the past few years, interest in barbiturates as neuroprotective agents has subsided.

3.2 Propofol

Propofol (2,6-diisopropylphenol) has a very favorable pharmacokinetic profile, which makes it a popular short-acting anesthetic agent. It, like barbiturates, reduces cerebral blood flow and metabolism and relaxes the brain [59, 68]. Propofol exerts its sedative, hypnotic, and amnesic effects by interacting with a site on the GABAA receptor, potentiating currents elicited by GABA, increasing agonist efficacy, and opening the GABAA receptor Cl^- channel in the absence of GABA [69, 70]. Propofol also inhibits NMDA receptors [71] and has a structural analogy with the antioxidant vitamin E [72]. It also acts as an antioxidant, scavenges free radicals, and decreases lipid peroxidation [5, 73]. Although these important characteristics of propofol would make it an excellent candidate as a neuroprotectant, the neuroprotective qualities of propofol are very controversial [45, 59, 74–76]. Many investigators have demonstrated neuroprotective effects of propofol in focal cerebral ischemia [77–83] or in vitro [84]; others, however, have failed to demonstrate neuroprotection [75, 85, 86]. Finally, it has been demonstrated that propofol has neuroprotective effects (up to 3 days post-ischemia), but after 3 weeks this protection disappeared [87]. Thus, propofol may delay, but not prevent, cerebral infarction following focal ischemia. Thus, its neuroprotective effect is not sustained.

In addition, it has been well demonstrated that propofol may exert a significant neurotoxic effect [75, 88–90]. This effect was observed in a cell culture model in which propofol resulted in cell death in CA3 and dentate. The precise mechanism by which propofol induces neurotoxicity is not well understood; however, it has recently been demonstrated that microRNA-21 [91], p75 neurotrophin receptors [90], caspases [92], and STAT3 [91] may be involved. Rodent and primate models have also shown that propofol induces neuroapoptosis [90, 93]. There has been no major clinical study demonstrating that propofol may be a better neuroprotective agent than other anesthetics following cerebral ischemia. In one small clinical study [94] comparing propofol with isoflurane anesthesia during coronary artery bypass surgery, no difference in neuropsychological performance was observed after the intervention, and there was an increase in a surrogate marker for neuronal injury (S100B) in the propofol group. So, whether propofol acts to result in neuroprotection or neurotoxicity remains unclear.

3.3 Ketamine

Ketamine is an NMDA receptor antagonist and has anti-excitotoxic and antiapoptotic properties [95–99]. It also can stimulate the sympathetic nervous system and thereby preserve cerebral perfusion pressure [100] and reduce vasoactive drug requirements [101]. Ketamine has been shown to increase cerebral metabolic rate for O_2, cerebral blood flow, and intracranial pressure [102]. Ketamine is also known to suppress the inflammatory response to surgery systemically and in the central nervous system [103, 104]. These mechanistic characteristics of ketamine would indicate that ketamine has neuroprotective qualities. Indeed, a number of investigators have demonstrated ketamine to be neuroprotective in a variety of cerebral injury models [95, 96, 105–118]; however, others have demonstrated no beneficial effects [119, 120] or even toxic effects [97, 121–126], especially in young or developing animals. The potential neuroprotective effect of ketamine may occur via several mechanisms: inhibition of glutamate receptors [58], interfering with the inflammatory response to injury [127, 128], and blockade of the NMDA receptors [117].

While ketamine has certain features which would make it a good neuroprotective candidate, it also possesses certain features that would make it a good candidate to produce toxic effects or at least fail to produce neuroprotection. Ketamine can produce an increase in intracranial pressure [129] by dilating cerebral blood vessels through activation of the cholinergic vasodilator system [130]. Ketamine may also increase cerebral metabolism and thus increase cerebral blood flow [131, 132]. Of course, these physiological characteristics could not account for the neurotoxic effects of ketamine observed in cell culture models. Two other characteristics of ketamine are of interest: one is that ketamine appears to show neuroprotective effects only in very high doses [105, 107, 126, 133], and the other is that ketamine has distinct effects in different brain areas [126, 134, 135]. These two features of ketamine (dose and regional effects) may also account for the contradictory data obtained in the literature. Thus, there is substantial evidence in the literature, using many different models, to show that ketamine is neuroprotective and neurotoxic.

3.4 Midazolam

Midazolam is a benzodiazepine receptor agonist which increases gamma-aminobutyric acid (GABA) function by acting at the GABAA receptor. Midazolam decreases cerebral blood flow and cerebral oxygen consumption [136, 137], thereby making midazolam a prime candidate as a neuroprotective agent. In fact, several studies have shown midazolam to be neuroprotective when administered in high doses in cerebral ischemia models [60, 80, 82, 138], and neuroprotection has also been shown in in vitro models [139–142]. Thus, at least for higher midazolam doses, midazolam reduces infarct size, increases the number of surviving neurons in the lesion core, and improves neurologic outcome

following cerebral ischemia. At lower midazolam doses, neuroprotection may not occur. The neuroprotective effect of midazolam may result from prevention of lipid peroxidation and mitochondrial damage [82] or via its antiapoptotic effect [142]. Even though midazolam seems to be protective, its efficacy appears to be less than that of propofol [60].

However, a number of studies have demonstrated that midazolam produces neurotoxicity [143–147]. Possible mechanisms for the midazolam-induced neurotoxicity may be the release of intracellular Ca^{2+} [143], and that midazolam induces apoptosis via activation of the mitochondrial pathway which may involve caspase-dependent apoptosis [145]. Thus, it remains unclear whether midazolam provides neuroprotection or neurotoxicity.

3.5 Etomidate

Etomidate is an agonist at the GABA receptor (GABAA) producing hypnosis and CNS depression by enhancing the effects of the inhibitory neurotransmitter GABA. The binding of etomidate to the GABAA receptor increases chloride conduction producing hyperpolarization of postsynaptic cell membranes and making the postsynaptic neuron more resistant to excitation. Since GABAA receptors occur almost exclusively on postsynaptic nerve endings in the CNS, there are few peripheral effects. Thus, etomidate is an interesting anesthetic because it has no significant hemodynamic alteration when administered. Since etomidate can decrease cerebral metabolism, it was thought that it would be an outstanding neuroprotective anesthetic agent. Some studies have found that etomidate results in neuroprotection through a reduction in cerebral metabolism, inhibition of postischemic hyperemia, and attenuation of vascular mediated inflammation [148–153]. However, it has also been demonstrated that etomidate is not neuroprotective and in fact increases infarct volume following focal cerebral ischemia [58, 154]. The potential toxic effect of etomidate may be because of its ability to decrease the level of nitric oxide in ischemic brain tissue by either scavenging nitric oxide or by inhibiting nitric oxide synthase [154]. Thus, the use of etomidate for neuroprotection has fallen out of favor [155].

3.6 Lidocaine

Lidocaine is a widely used local anesthetic for topical anesthesia, local infiltration, nerve block, and spinal and epidural anesthesia [156]. Lidocaine is one of the most used local anesthetics in clinical treatment, and it exerts its primary effects of regional anesthesia and antiarrhythmic therapy by its action on voltage-gated Na^+ channels. Lidocaine readily crosses the blood–brain barrier and may result in neuroprotection by several possible mechanisms: decreasing the ischemic membrane ion shift [157], reducing cerebral metabolic rate [158, 159], reducing excitotoxic amino acid release [160], modulation of the ischemic inflammatory response, and maintaining or increasing cerebral blood flow [155, 161–163]. Neuroprotection

with lidocaine was first demonstrated to be effective in models of cerebral arterial gas embolism [161, 164, 165], and much of the in vivo neuroprotection of lidocaine was demonstrated as a treatment for decompression illness [161, 166]. Similar potential neuroprotection of lidocaine has also been observed in a variety of clinical trials involving cardiac surgery [167–169]. Despite these clinical studies showing a neuroprotective potential for lidocaine, in one of the largest randomized, double-blinded, placebo-controlled study of lidocaine neuroprotection, no neuroprotective effect of lidocaine was demonstrated following cardiac surgery [170]. In addition, in this study, diabetic subjects receiving lidocaine were more likely to suffer cognitive decline at 6 weeks post-surgery [170]. This study also demonstrated an association between higher total accumulated dose of lidocaine and increased neurocognitive deficit.

In yet another study [171], lidocaine failed to show neuroprotection following cardiac surgery. The effects of lidocaine neuroprotection in ischemic brain injury have been demonstrated in many studies [162, 167, 172–179]; however, a complicating feature of lidocaine as a neuroprotective agent is that low-dose lidocaine appears to be more effective than high doses in reducing ischemic brain injury whether administered prior to, during, or following the ischemia [175, 178]. Despite the considerable data showing lidocaine's neuroprotective effects, there are a number of studies that demonstrate that lidocaine shows no neuroprotection [180, 181] or is even neurotoxic [182–187]. Lidocaine can be applied topically as a local anesthetic, and while there are only few full studies concerning any neuroprotective or neurotoxic effects, almost all of these reports and case studies show neurotoxic effects [188–191]. Thus, whether lidocaine results in neuroprotection, has no effect, or is neurotoxic remains controversial, and conclusive data are lacking at this time.

4 Volatile (Inhalational) Anesthetics

4.1 *Isoflurane*

Isoflurane is one volatile anesthetic that has received much attention over the years, and there seems to be a general agreement that isoflurane and other inhalational agents are associated with cerebral neuroprotection, but even here, the data are not crystal clear. There are several potential mechanisms by which isoflurane could provide its neuroprotective effect: increasing cerebral blood flow [192, 193] and possibly attenuating post-injury hypoperfusion, decreasing glutamate release and decreasing excitotoxicity [194], blocking NMDA receptors [8], and decreasing NMDA-mediated calcium influx [8]. Also, the reaction of isoflurane on GABAA receptors may be protective [195]. Many investigators have shown that volatile anesthetics can reduce injury from cerebral ischemia [196–198], but there are conflicting reports. Early studies with isoflurane

demonstrated an increased survival time in mice with hypoxemia or ischemia in dogs [199]. The neuroprotection produced was similar to that offered by barbiturates [200, 201]. In humans, isoflurane is also neuroprotective in patients with carotid artery surgery [202].

However, isoflurane has not been shown to have such clear neuroprotective effects. In comparing the effects of thiopental and fentanyl–nitrous oxide with isoflurane in monkeys with focal cerebral ischemia, isoflurane showed worse outcome than that observed in the thiopental animals [200], and when isoflurane was compared with halothane in focal ischemia, there was no difference in outcome [203]. Isoflurane was also shown to have no protective effects in rats with focal cerebral ischemia [204]. There has been much discussion concerning the length of time any neuroprotection from isoflurane can last [14, 205–207], and it appears that if isoflurane does have a neuroprotective effect, it is not long lasting. Thus, volatile anesthetics may delay ischemic injury but not prevent, or perhaps even modify, long-term neuronal death. Therefore, the role of isoflurane as a true neuroprotectant must be questioned.

Finally, there have been many reports showing that isoflurane and other anesthetics have neurotoxic effects [208–210] that manifest apoptotic neurodegeneration [211–214]. Some anesthetics besides isoflurane that can produce neurotoxic effects are nitrous oxide and midazolam. It should be recalled that most anesthetics in use today work via two major mechanisms: GABAA receptors (benzodiazepines, barbiturates, propofol, isoflurane, etomidate, enflurane, and halothane) [215] and NMDA receptors (ketamine, nitrous oxide, and xenon) [216–218]. Drugs that work on either of these mechanisms can result in neuronal apoptosis [122, 219]. Thus, anesthetics are potential toxic substances.

4.2 Xenon

Xenon is a noble gas and exerts its anesthetic effects by antagonism of the NMDA subtype of the glutamate receptor [220]. Xenon has been shown to have neuroprotective characteristics in in vitro models of NMDA toxicity, and in oxygen–glucose deprivation, xenon attenuates the extent of injury [220–222]. In in vivo animal models, xenon also demonstrated neuroprotection following cerebral ischemia [223–227]. When xenon was administered in combination with hypothermia [227–229] or dexmedetomidine (α2 agonist) [230], it resulted in neuroprotection that was greater than each agent alone. Xenon also results in neuroprotection in neonates with hypoxia–ischemia [223, 229, 231], and xenon itself is known to produce hypothermia [232] which reduces excitotoxicity and interferes with oxygen radical formation. Major mechanisms that may be involved with xenon's neuroprotective effect are the reduction of ischemia-induced neurotransmitter release [233] and the antagonistic property of xenon against NMDA receptors [216, 225, 234, 235]. Finally, xenon, like other inhalational anesthetics, can precondition the brain against ischemic injury [14, 15, 236], although its mechanism of action for preconditioning is unclear.

5 Other Inhalational Anesthetics

5.1 Sevoflurane

Sevoflurane is thought to act as a positive allosteric modulator of the GABAA receptor. However, it also acts as an NMDA receptor antagonist, potentiates glycine receptor currents, and inhibits nACh and 5-HT_3 receptor currents. Sevoflurane has been shown to reduce ischemic cerebral injury when compared with the awake state [197]. Sevoflurane has also been shown to be involved in preconditioning, in both global [237, 238] and focal [239, 240] cerebral ischemias. One potential mechanism for sevoflurane preconditioning may involve opening of ATP-dependent potassium channels [237]. Other potential molecules such as free radicals [241], adenosine A1 receptors [242, 27], mitogen protein kinase, hypoxia-inducible factor-1α [243], antioxidant enzymes [244], and the Notch signaling pathway [245] have also been proposed to be involved in neuroprotection from anesthetic preconditioning. Sevoflurane, unlike isoflurane, does not induce apoptosis in cortical neurons [246], so the mechanisms involving sevoflurane neuroprotection need further evaluation. Whether sevoflurane would have neuroprotective and preconditioning effects in other types of brain injury, and by which mechanism, is not known.

5.2 Desflurane

Desflurane is usually used for the maintenance of general anesthesia. It reduces functional conductance by decreasing gap junction channel opening times and increasing gap junction channel closing times. It also activates calcium-dependent ATPase in the sarcoplasmic reticulum by increasing the fluidity of the lipid membrane. It also binds and antagonizes the GABA receptor, the large-conductance Ca^{2+}-activated potassium channel, and the glycine receptors and antagonizes the glutamate receptors. Desflurane has also been shown to be neuroprotective in newborn piglet models of deep hypothermic cardiac arrest [247], and low-flow cardiopulmonary bypass [248] confirmed both functionally and from histopathology. In focal cerebral ischemia, infarct reduction by desflurane was more pronounced than by halothane [249], which was attributed to a more pronounced decrease in sympathetic tone with desflurane. Desflurane has been shown to improve neurological outcome following global cerebral ischemia [250], and desflurane attenuates decrease in tissue oxygenation during focal stroke [251].

6 Summary

Like most potential drugs used for brain neuroprotection, anesthetics are similar in that they are complex agents. Some investigators have shown anesthetics to be neuroprotective, while others have shown no protection. Still others have shown some anesthetics to be neurotoxic. Precisely why the results differ widely and

why anesthetic neuroprotection appears often to be effective in in vitro cellular or in vivo animal models but does not appear to work well in humans are unclear, but there are several possible reasons. By far, the majority of studies with anesthetics have compared different anesthetics with one another when they have been administered as pretreatments in the setting of global or focal cerebral ischemia. In addition, the effects of anesthetics usually have been evaluated in animal models in which other anesthetics or analgesics were already present. Few studies have evaluated the efficacy of anesthetics with the unanesthetized state, and even fewer studies have evaluated the effects of anesthetics administered post-ischemia. In these types of studies, full physiological parameters, including brain temperature, arterial blood pressure, heart rate, blood gases (pH, $PaCO_2$, PaO_2), cerebral blood flow, and metabolism, should be monitored. This is and has been difficult because in many cases the animal model of choice is the mouse or rat. Nevertheless, unless these parameters are known, it is difficult or impossible to sort out anesthetic neuroprotection and its mechanisms of action.

The dose of anesthetic agent is also an important factor. Many investigators have used very different doses of anesthetic, and a particular dose effective in the mouse or rat may not be effective in humans. Thus, it is not correct to merely scale up the dose from the mouse and expect this same dose to be effective in humans. Some anesthetics may be effective as neuroprotectants at low doses and not at high doses, whereas others may be effective at high doses but not at low doses. Different species may also have different responses, or no response, to the same drug dose. Thus, knowledge of the true dose–response curve is important to determine the optimal neuroprotective dose. Another issue is to determine whether anesthetics can be administered pre-ischemia or post-ischemia for successful treatment and even at various times post-ischemia (window of opportunity). In animal models, the time of ischemia is precisely known, whereas in humans this is not the case except for certain surgical procedures such as cardiopulmonary bypass and carotid endarterectomy. As previously mentioned, in animal models, anesthetic drug administration is often given on a pretreatment basis (animals must be anesthetized for certain procedures) or given at reperfusion, with other anesthetics already present and with little attention given to administration at various times following reperfusion. There may be several anesthetics being given simultaneously; thus, the effects of combined anesthetics, each working via a different mechanism of action, must be considered. In addition, exactly how the combined anesthetics affect physiological and molecular parameters must also be considered. Much work needs to be done to elucidate these effects.

Another issue has to do with exactly when outcome measures (pathology, neurobehavior, neurologic examinations) are made.

Many neuroprotective agents appear effective when these outcome measures are made early after injury (24 h) but are ineffective when measured at later times (7 days or longer). One conclusion from these findings is that these potential anesthetic neuroprotectants merely delay injury until some later time. This, in itself, is not a bad thing since it protects the brain for a time until another better, more long-term neuroprotectant can be administered. One should also consider that genomics, species, and gender of each animal are not the same, and anesthetics may affect genes and gene products, species, and gender differently, thereby leading to inconsistent, variable, and confounding data. Finally, one extremely important issue has to do with the fact that anesthetics for neuroprotection most often are tested in young, normal, healthy animals and not in aged animals with diseases such as hypertension, diabetes, or cardiovascular disease. It is likely that anesthetics may act differently in either animals or humans with other comorbid diseases present, with different ages, with different genders, and in different physiologically or metabolically compromised situations. These issues have been greatly understudied concerning anesthetic neuroprotection.

7 Conclusions

Many anesthetic agents have been evaluated as potential neuroprotective agents in focal and global cerebral ischemia. This chapter has discussed several of the more common anesthetics used for studies of focal and global cerebral ischemia and whether they are neuroprotective, or not, or even neurotoxic. Unfortunately, the results concerning neuroprotection are unclear, with some investigators finding positive effects, some finding no effects, and still others finding neurotoxic effects. It is important to remember that like other potential neuroprotective drugs, anesthetics (many of them) have survived preclinical studies, some with great success, others not; but none have successfully progressed through a clinical trial in humans with clear positive results. Many anesthetics have shown neuroprotective potential, but none has emerged as a leading candidate despite much work in this area.

References

1. Wells BA, Keats AC, Cooley DA (1963) Increased tolerance to cerebral ischemia produced by general anesthesia during temporary carotid occlusion. Surgery 54:216–223
2. Patel P, Drummond JC, Cole DJ, Kelly PJ, Watson M (1998) Isoflurane and pentobarbital reduce the frequency of transient ischemic depolarization during focal ischemia in rats. Anesth Analg 86:773–780
3. Ochiai C, Asano T, Takakura K, Fukuda T, Horizoe H, Morimoto Y (1982) Mechanisms of cerebral protection by pentobarbital and nizofenone correlated with the course of local cerebral blood flow changes. Stroke 13:788–795
4. Warner DS, Hansen TD, Vust L, Todd MM (1989) The effects of isoflurane and pentobarbital on the distribution of cerebral blood flow during focal cerebral ischemia in the rat. J Neurosurg Anesthesiol 1:219–226

5. Wilson JX, Gelb AW (2002) Free radicals, antioxidants, and neurologic injury: possible relationships to cerebral protection by anesthetics. J Neurosurg Anesthesiol 14:66–79
6. Kahraman S, Demiryurek AT (1997) Propofol is a peroxynitrite scavenger. Anesth Analg 84:1127–1129
7. Harada H, Kelly PJ, Cole DJ, Drummond JC, Patel PM (1999) Isoflurane reduces N-methyl- D-aspartate toxicity in vivo in the rat cerebral cortex. Anesth Analg 89:1442–1447
8. Bickler PE, Buck LT, Hansen BM (1994) Effects of isoflurane and hypothermia on glutamate receptor-mediated calcium influx in brain slices. Anesthesiology 81:1461–1469
9. Jenkins A, Greenblatt EP, Faulkner HJ, Bertaccini E, Light A, Lin A, Andreasen A, Viner A, Trudell JR, Harrison NL (2001) Evidence for a common binding cavity for three general anesthetics within the GABAA receptor. J Neurosci 21:RC136
10. Harris BD, Moody EJ, Basile AS, Skolnick P (1994) Volatile anesthetics bidirectionally and stereospecifically modulate ligand binding to GABA receptors. Eur J Pharmacol 267:269–274
11. Gyulai FE, Mintun MA, Firestone LL (2001) Dose dependent enhancement of in vivo GABAA-benzodiazepine receptor binding by isoflurane. Anesthesiology 95:585–593
12. Sugimura M, Kitayama S, Morita K, Imai Y, Irifune M, Takavada T, Kawahara M, Dohi T (2002) Effects of GABAergic agents on anesthesia induced by halothane, isoflurane, and thiamylal in mice. Pharmacol Biochem Behav 72:111–116
13. Hirota K, Roth SH (1997) Sevoflurane modulates both GABAA and GABAB receptors in CA 1 or rat hippocampus. Br J Anaesth 78:60–65
14. Wang L, Traystman RJ, Murphy SJ (2008) Inhalational anesthetics as preconditioning agents in ischemic brain. Curr Opin Pharmacol 8:104–110
15. Kitano H, Kirsch JR, Hum PD, Murphy SJ (2007) Inhalational anesthetics as neuroprotectants or chemical preconditioning agents in ischemic brain. J Cereb Blood Flow Metab 27:1108–1128
16. McAuliffe JJ, Loepke AW, Miles L, Joseph B, Hughes E, Vorhees CV (2009) Desflurane, isoflurane and sevoflurane provide limited neuroprotection against neonatal hypoxia-ischemia in a delayed preconditioning paradigm. Anesthesiology 111:533–546
17. Bhardwaj A, Castro IA, Alkayed NJ, Hum PD, Kirsch JR (2001) Anesthetic choice of halothane versus propofol: impact on experimental perioperative stroke. Stroke 32:1920–1925
18. Kapinya KJ, Lowl D, Futterer C, Maurer M, Waschke KF, Isaev NK, Dirnagl U (2002) Tolerance against ischemic neuronal injury can be induced by volatile anesthetics and is inducible NO synthase dependent. Stroke 33:1889–1898
19. Zheng S, Zuo Z (2003) Isoflurane preconditioning reduces Purkinje cell death in an in vitro model of rat cerebellar ischemia. Neuroscience 118:99–106
20. Brunet A, Datta SR, Greenberg ME (2001) Transcription-dependent and independent control of neuronal survival by the P13k-AKt signaling pathway. Curr Opin Neurobiol 11:297–305
21. Garcia L, Burda J, Hrehorovska M, Burda R, Martin ME, Salinas M (2004) Ischaemic preconditioning in the rat brain: effect on the activity of several initiation factors, AKt and extracellular signal-regulated protein kinase phosphorylation, and GRP78 and GADD34 expression. J Neurochem 88:136–147
22. Nakajima T, Iwabuchi S, Miyazaki H, Okuma Y, Kuwabara M, Nomura Y, Kawahara K (2004) Preconditioning prevents ischemia-induced neuronal death through persistent AKt activation in the penumbra region of the rat brain. J Vet Med Sci 66:521–527
23. Huang PL (2004) Nitric oxide and cerebral ischemic preconditioning. Cell Calcium 36:232–239
24. Xiong L, Zheng Y, Wu M, Hou L, Zhu Z, Zhang X, Lu Z (2003) Preconditioning with isoflurane produces dose-dependent neuroprotection via activation of adenosine triphosphate-regulated potassium channels after focal cerebral ischemia in rats. Anesth Analg 96:233–237
25. Kehl F, Payne RS, Roever N, Schurr A (2004) Sevoflurane-induced preconditioning of rat brain in vitro and the role of K channels. Brain Res 1021:76–81
26. Wang ZP, Zhang ZH, Zeng YM, Jiang S, Wang SQ, Wang S (2006) Protective effect of sevoflurane preconditioning on oxygen-glucose deprivation injury in rat hippocampal slices: the role of mitochondrial K_{ATP} channels. Sheng Li Xue Bao 58:201–206
27. Liu Y, Xiong L, Chen S, Wang Q (2006) Isoflurane tolerance against focal cerebral ischemia is attenuated by adenosine A1 receptor antagonists. Can J Anaesth 53:194–201

28. Zheng S, Zuo Z (2004) Isoflurane preconditioning induces neuroprotection against ischemia via activation of P38 mitogen-activated protein kinases. Mol Pharmacol 65:1172–1180
29. Clarkson AN (2007) Anesthetic-mediated protection/preconditioning during cerebral ischemia. Life Sci 80:1157–1175
30. Perez-Pinzon MA (2007) Mechanisms of neuroprotection during ischemic preconditioning: lessons from anoxic tolerance. Comp Biochem Physiol A Mol Integr Physiol 147:291–299
31. Goldstein A Jr, Wells BA, Keats AS (1966) Increased tolerance to cerebral anoxia by pentobarbital. Arch Int Pharmacodyn Ther 161:138–143
32. Goldstein A Jr, Wells BA, Keats AS (1964) Effect of anesthesia on tolerance of dog brain to anoxia. Anesthesiology 25:98
33. Wright RL, Ames A III (1964) Measurement of maximal permissible cerebral ischemia and a study of its pharmacologic prolongation. J Neurosurg 22:567–574
34. Wechsler RL, Dripps RD, Kety SS (1951) Blood flow and oxygen consumption of the human brain during anesthesia produced by thiopental. Anesthesiology 12:308–314
35. Smith AL, Marque JJ (1976) Anesthetics and cerebral edema. Anesthesiology 45:64–72
36. Shapiro HM (1975) Intracranial hypertension: therapeutic and anesthetic considerations. Anesthesiology 43:445–471
37. Todd MM, Chadwick HS, Shapiro HM, Dunlop BJ, Marshall LF, Dueck R (1982) The neurologic effects of thiopental therapy following experimental cardiac arrest in cats. Anesthesiology 57:76–86
38. Kofke WA, Nemoto EM, Hossmann KA, Taylor F, Kessler PD, Stezoski SW (1979) Brain blood flow and metabolism after global ischemia and post-insult thiopental therapy in monkeys. Stroke 10:554–560
39. Nordstrom CH, Calderini G, Rehncrona S, Siesjo BK (1977) Effects of phenobarbital anesthesia on post-ischemic cerebral blood flow and oxygen consumption in the rat. Acta Neurol Scand Suppl 64:148–149
40. Nemoto EM (1979) Studies on the pathogenesis of ischemic brain damage and its amelioration by barbiturate therapy. In: Zuelch KJ, Kaufman W, Hossmann KA, Hossmann V (eds) Brain and heart infarct II. Springer, Berlin, pp 306–317
41. Nemoto EM, Shiu GK, Nemmer JP, Bleyaert AL (1983) Free fatty acid accumulation in the pathogenesis and therapy of ischemic-anoxic brain injury. Am J Emerg Med 1:175–179
42. Traystman RJ (2004) Anesthetic mediated neuroprotection: established fact or passing fancy? J Neurosurg Anesthesiol 16:308–312
43. Warner DS (2004) Anesthetics provide limited but real protection against acute brain injury. J Neurosurg Anesthesiol 16:303–307
44. Fukuda S, Warner DS (2007) Cerebral protection. Br J Anaesth 99:10–17
45. Head B, Patel P (2007) Anesthetics and brain protection. Curr Opin Anaesthesiol 20:395–399
46. Steen PA, Michenfelder JD (1979) No barbiturate protection in a dog model of complete cerebral ischemia. Ann Neurol 5:343–349
47. Bleyaert AL, Nemoto EM, Safar P, Stezoski SM, Mickell JJ, Moossy J, Rao GR (1978) Thiopental amelioration of brain damage after global ischemia in monkeys. Anesthesiology 49:390–398
48. Breivik H, Safar P, Sands P, Fabritius R, Linol B, Lust P, Mollies A, Orr M, Renck H, Snyder JV (1978) Clinical feasibility trials of barbiturate therapy after cardiac arrest. Crit Care Med 6:228–244
49. Snyder BD, Ramirez-Lassepas M, Sukhum P, Fryd D, Sung JH (1979) Failure of thiopental to modify global anoxic injury. Stroke 10:135–141
50. Gisvold SE, Safar P, Hendrickx HH, Rao G, Moossy J, Alexander H (1984) Thiopental treatment after global brain ischemia in pigtailed monkeys. Anesthesiology 60:88–96
51. Brain Resuscitation Clinical Trial I Study Group (1986) Randomized clinical study of thiopental loading in comatose survivors of cardiac arrest. N Engl J Med 314:397–403
52. Smith AL, Hoff JT, Nielsen SL, Larson CP (1974) Barbiturate protection in acute focal cerebral ischemia. Stroke 5:1–7
53. Hoff JT, Smith AL, Hankinson HL, Nielsen SL (1975) Barbiturate protection from cerebral infarction in primates. Stroke 6:28–33
54. Michenfelder JD, Milde JH, Sundt TM (1976) Cerebral protection by barbiturate anesthesia: use after middle cerebral artery occlusion in JAVA monkeys. Arch Neurol 33:345–350
55. Carkill G, Sivalingam S, Reitan JA, Gilroy BA, Helphrey MG (1978) Dose dependency of the post-insult protective effect of pentobarbital in the canine stroke model. Stroke 9:10–12
56. Selman WR, Spetzler RF, Roski RA, Roessmann V, Crumrine R, Macko R (1982) Barbiturate coma in focal cerebral ischemia:

relationship of protection to timing of therapy. J Neurosurg 56:685–690

57. Warner DS, Zhou JG, Ramani R, Todd MM (1991) Reversible focal ischemia in the rat: effects of halothane, isoflurane and methohexital anesthesia. J Cereb Blood Flow Metab 11:794–802
58. Drummond JC, Cole DJ, Patel PM, Reynolds LW (1995) Focal cerebral ischemia during anesthesia with etomidate, isoflurane or thiopental: a comparison of the extent of cerebral injury. Neurosurgery 37:742–748
59. Kawaguchi M, Fukuya H, Patel PM (2005) Neuroprotective effects of anesthetic agents. J Anesth 19:150–156
60. Chen L, Gong Q, Xiao C (2003) Effects of propofol, midazolam, and thiopental sodium on outcome and amino acids accumulation in focal cerebral ischemia-reperfusion in rats. Chin Med J 116:292–296
61. Drummond JC (1993) Do barbiturates really protect the brain? Anesthesiology 78:611–613
62. Nillson L, Siesjo BK (1975) The effect of phenobarbitone anaesthesia on blood flow and oxygen consumption in the rat brain. Acta Anaesthesiol Scand Suppl 57:18–24
63. Zhu H, Cottrell JE, Kass IS (1997) The effect of thiopental and propofol on NMDA- and AMPA-mediated glutamate excitotoxicity. Anesthesiology 87:944–951
64. Kimbro JR, Kelly PJ, Drummond JC, Cole DJ, Patel PM (2000) Isoflurane and pentobarbital reduce AMPA toxicity in vivo in the rat cerebral cortex. Anesth Analg 89:1442–1447
65. Zhan RZ, Fujiwara N, Endoh H, Yamakura T, Taga K, Fukuda S, Shimoji K (1998) Thiopental inhibits increases in Ca++ induced by membrane depolarization, NMDA receptor activation and ischemia in rat hippocampal and cortical slices. Anesthesiology 89:456–466
66. Smith DS, Rehncrona S, Westerberg E, Akesson B, Siesjo BK (1979) Lipid peroxidation in brain tissue in vitro: antioxidant effects of barbiturates. Acta Physiol Scand 105:527–529
67. Meldrum B (1982) Pharmacology of GABA. Clin Neuropharmacol 5:293–316
68. Pittman JE, Sheng H, Pearlstein R, Brinkhaus A, Dexter F, Warner DS (1997) Comparison of the effects of propofol and pentobarbital on neurologic outcome and cerebral infarct size after temporary focal ischemia in the rat. Anesthesiology 87:1130–1144
69. Concas A, Santoro G, Serra M, Sanna E, Biggio G (1991) Neurochemical action of the general anesthetic propofol on the chloride ion channel coupled with GABAA receptors. Brain Res 542:225–232
70. Orser BA, Wang LY, Pennefather PS, MacDonald JF (1994) Propofol modulates activation and desensitization of GABAA receptors in cultured murine hippocampal neurons. J Neurosci 14:7747–7760
71. Orser BA, Bertlik M, Wang LY, MacDonald JF (1995) Inhibition by propofol (2,6-diisopropylphenol) of the N-methyl-D-aspartate subtype of glutamate receptor in cultured hippocampal neurons. Br J Pharmacol 116:1761–1768
72. Boisset S, Steghens JP, Favetta P, Terreux R, Guitton J (2004) Relative antioxidant capacities of propofol and its main metabolites. Arch Toxicol 8:835–842
73. Sagara Y, Hendler S, Khoh-Reiter S, Gillenwater G, Carlo D, Schubert D, Chang J (1999) Propofol hemisuccinate protects neuronal cells from oxidative injury. J Neurochem 73:2524–2530
74. Adembri C, Venture L, Pellegrini-Giampietro DE (2007) Neuroprotective effects of propofol in acute cerebral injury. CNS Drug Rev 13:333–351
75. Feiner JR, Bickler PE, Estrada S, Donohoe PH, Fahlman CS, Schuyler JA (2005) Mild hypothermia, but not propofol, is neuroprotective in organotypic hippocampal cultures. Anesth Analg 100:215–225
76. Fan W, Zhu X, Wu L, Wu Z, Li D, Huang F, He H (2012) Propofol: an anesthetic possessing neuroprotective effects. Eur Rev Med Pharmacol Sci 19:1520–1529
77. Kochs E, Hoffman WE, Werner C, Thomas C, Albrecht RF, Schulte EJ (1992) The effects of propofol on brain electrical activity, neurologic outcome, and neuronal damage following incomplete ischemia in rats. Anesthesiology 6:245–252
78. Young Y, Menon DK, Tisavipat N, Matta BF, Jones JG (1997) Propofol neuroprotection in a rat model of ischemia reperfusion injury. Anesthesiology 4:320–326
79. Yano T, Nakayama R, Ushijima K (2000) Intracerebroventricular propofol is neuroprotective against transient global ischemia in rats: extracellular glutamate level is not a major determinant. Brain Res 883:69–76
80. Ito H, Watanabe Y, Isshiki A, Uchino H (1999) Neuroprotective properties of propofol and midazolam, but not pentobarbital on neuronal damage induced by forebrain ischemia based on the GABAA receptors. Acta Anaesthesiol Scand 43:153–162

81. Gelb AW, Bayona NA, Wilson JX, Cechetto DF (2002) Propofol anesthesia compared to awake reduces infarct size in rats. Anesthesiology 96:1183–1190
82. Harman F, Hasturk AE, Yaman M, Arca T, Kilinc K, Sargon MF, Kaptanoglu E (2012) Neuroprotective effects of propofol, thiopental, etomidate, and midazolam in fetal rat brain in ischemia-reperfusion model. Childs Nerv Syst 28:1055–1062
83. Adembri C, Venturi L, Tani A, Chiarugi A, Gramigny E, Cozzi A, Pancani T, De Gaudio RA, Pellegrino-Giampietro DE (2006) Neuroprotective effects of propofol in models of cerebral ischemia: inhibition of mitochondrial swelling as a possible mechanism. Anesthesiology 104:80–89
84. Zhang DX, Ding HZ, Jiang S, Zeng YM, Tang QF (2014) An in vitro study of the neuroprotective effect of propofol on hypoxic hippocampal slice. Brain Inj 28:1758–1765
85. Tsai YC, Huang SI, Lai YY, Chang CL, Cheng JT (1994) Propofol does not reduce infarct volume in rats undergoing permanent middle cerebral artery occlusion. Acta Anaesthesiol Sin 2:99–104
86. Zhan R, Qi S, Wu C, Fujihara H, Taga K, Shimoji K (2001) Intravenous anesthetics differentially reduce neurotransmission damage caused by oxygen-glucose deprivation in rat hippocampal slices in correlation with N-methyl-D-aspartate receptor inhibition. Crit Care Med 9:808–813
87. Bayona NA, Gelb AW, Jiang Z, Wilson JX, Urquhart BL, Cechetto DF (2004) Propofol neuroprotection in cerebral ischemia and its effects on low-molecular weight antioxidants and skilled motor tasks. Anesthesiology 100:1151–1159
88. Honegger P, Matthieu JM (1996) Selective toxicity of the general anesthetic propofol for GABAergic neurons in rat brain cell cultures. J Neurosci Res 45:631–636
89. Spahr-Schopher I, Vutskits L, Toni N, Buchs PA, Parisi L, Muller D (2000) Differential neurotoxic effects of propofol on dissociated cortical cells and organotypic hippocampal cultures. Anesthesiology 92:1408–1417
90. Pearn M, Hu Y, Patel HH, Drummond JC, Roth DM, Akassoglou K, Patel PM, Head BP (2012) Propofol neurotoxicity is mediated by p75 neurotrophin receptor activation. Anesthesiology 116:352–361
91. Twaroski D (2014) Down-regulation of microRNA-21 is involved in the propofol-induced neurotoxicity observed in human stem cell-derived neurons. Anesthesiology 121:786–800
92. Milanovic D, Popic J, Pesic V, Loncarevic-Vasiljkovic N, Kanazir S, Jevtovic-Todorovic V, Ruzdijic S (2010) Regional and temporal profiles of calpain and caspase-3 activities in postnatal rat brain following repeated propofol administration. Dev Neurosci 32:288–301
93. Creeley C, Dikranian K, Dissen G, Martin L, Olney J, Brambrink A (2013) A propofol induced apoptosis of neurones and oligodendrocytes in fetal and neonatal Rhesus macaque brain. Br J Anesth 110:129–138
94. Kanbak M, Saricaoglu F, Avci A, Ocal T, Koray Z, Aypar U (2004) Propofol offers no advantage over isoflurane anesthesia for cerebral protection during cardiopulmonary bypass: a preliminary study of S100 beta protein levels. Can J Anesth 1:712–717
95. Engelhard K, Weiner C, Eberspacher E, Bachl M, Blobner M, Hildt E, Hutzler P, Kochs E (2003) The effect of the alpha 2-agonist dexmedetomidine and the N-methyl-D-aspartate antagonists (+)-ketamine on the expression of apoptosis-regulating proteins after incomplete cerebral ischemia and reperfusion in rat. Anesth Analg 96:524–531
96. Himmelscher S, Pfenninger E, Georgieff M (1996) The effects of ketamine-isomers on neuronal injury and regeneration in rat hippocampal neurons. Anesth Analg 83:505–512
97. Young C, Jevtovic-Todorovic V, Qin YQ, Tenkova T, Wang H, Labruyere J, Olney JW (2005) Potential of ketamine and midazolam, individually or in combination, to induce apoptotic neurodegeneration in the infant mouse brain. Br J Pharmacol 146:189–197
98. Huang L, Liu Y, Jin W et al (2012) Ketamine potentiates hippocampal neurodegeneration and persistent learning and memory impairment through the PKC(gamma)-ERK signaling pathway in the developing brain. Brain Res 1476:1264–1271
99. Hudetz JA, Pagel PS (2010) Neuroprotection by ketamine: a review of the experimental and clinical evidence. J Cardiothorac Vasc Anesth 24:131–142
100. Kolenda H, Gremmrlt A, Raching S, Braun D, Markakis E (1996) Ketamine for analgosedative therapy in intensive care treatment of head-injured patients. Acta Neurochir (Wien) 138:1193–1199
101. Botero CA, Smith CE, Holbrook C, Chavez AM, Snow NJ, Hagen JF, Pinchak AC (2000) Total intravenous anesthesia with a propofol-ketamine combination during coronary artery surgery. J Cardiothorac Vasc Anesth 14:409–415

102. Takashita H, Okuda A, Sari A (1972) The effects of ketamine on cerebral circulation and metabolism in man. Anesthesiology 36:69–75
103. Laffey JC, Boglan JF, Cheng DC (2002) The systemic inflammatory response to cardiac surgery: implications for the anesthesiologist. Anesthesiology 97:215–252
104. Xu J, Wen Y, Cibelli M, Ma D, Maze M (2006) Postoperative cognitive dysfunction: a role for cytokine-mediated inflammation in the hippocampus. Anesthesiology 105:A1175
105. Church J, Zeman S, Lodge D (1988) The neuroprotective action of ketamine and MK-801 after transient cerebral ischemia in rats. Anesthesiology 69:702–709
106. Hoffman W, Pelligrino D, Werner C, Kochs E, Albrecht RF, SchulteamEsh J (1992) Ketamine decreases plasma catecholamines and improves outcome from incomplete cerebral ischemia in rats. Anesthesiology 76:755–762
107. Lees GJ (1995) Influence of ketamine on the neuronal death caused by NMDA in the rat hippocampus. Neuropharmacology 34:411–417
108. Chan P, Chu L (1998) Ketamine protects cultured astrocytes from glutamate induced swelling. Brain Res 487:380–383
109. Shibuta S, Varathan S, Mashimo T (2006) Ketamine and thiopental sodium: individual and combined neuroprotective effects on cortical cultures exposed to NMDA or nitric oxide. Br J Anaesth 97:517–524
110. Wang L, Jing W, Hang YN (2008) Glutamate-induced c-Jun expression in neuronal PC12 cells: the effect of ketamine and propofol. J Neurosurg Anesthesiol 20:124–130
111. Hudetz JA, Iqbal SD, Patterson KM, Burne AJ, Hudetz AG, Pagel PS, Warltier DC (2009) Ketamine attenuates post-operative cognitive dysfunction after cardiac surgery. Acta Anesth Scand. doi:10.1111/j.1399-6576
112. Himmelscher S, Durieux ME (2005) Revising a dogma: ketamine for patients with neurological injury? Anesth Analg 101:524–534
113. Anis NA, Berry SC, Burton NR, Lodge D (1983) The dissociative anesthetics ketamine and phencyclidine selectively reduce excitation of central mammalian neurons by N-methyl aspartate. Br J Pharmacol 79:565–575
114. Clifford DB, Zorumski CF, Olney JW (1989) Ketamine and MK-801 prevent degeneration of thalamic neurons induced by cortical seizures. Exp Neurol 105:272–279
115. Shapiro Y, Lam AM, Eng CC, Lashaprasit Y, Michel M (1994) Therapeutic time window and dose response of the beneficial effects of ketamine in experimental head injury. Stroke 25:1637–1643
116. Proescholdt M, Heimann A, Kempski O (2001) Neuroprotection of S(+) ketamine isomer in global forebrain ischemia. Brain Res 904:245–251
117. Himmelseher S, Pfenninger E, Kochs E, Auchter M (2000) S(+)-ketamine up-regulates neuronal regeneration associated proteins following glutamate injury in cultured rat hippocampal neurons. J Neurosurg Anesthesiol 12:84–94
118. Gonzales JM, Loeb AL, Reichard PS, Irvine S (1995) Ketamine inhibits glutamate-, N-methyl-D-aspartate-, and quisqualate-stimulated cGMP production in cultured cerebral neurons. Anesthesiology 82:205–213
119. Jensen ML, Auer RN (1988) Ketamine fails to protect against ischemic neuronal necrosis in the rat. Br J Anaesth 61:206–210
120. Ridenour TR, Warner DS, Todd MM, Baker MT (1991) Effects of ketamine on outcome from temporary middle cerebral artery occlusion in the spontaneously hypertensive rat. Brain Res 565:116–122
121. Church J, Zeman S (1991) Ketamine promotes hippocampal CA1 pyramidal neuron loss after a short-duration ischemic insult in rats. Neurosci Lett 123:65–68
122. Ikonomidou C, Bosch F, Miksa M, Bittigau P, Vockler J, Dikranian K, Tenkova TI, Stefovska V, Turski L, Olney JW (1999) Blockade of NMDA receptors and apoptotic neurodegeneration in the developing brain. Science 283:70–74
123. Pohl D, Bittigau P, Ishimura MJ, Stadthaus D, Hubner C, Olney JW, Turski L, Ikonomidou C (1999) N-methyl-D-aspartate antagonists and apoptotic cell death triggered by head trauma in developing rat brain. Proc Natl Acad Sci U S A 96:2508–2513
124. Slikkor W Jr, Zou X, Hotchkiss CE, Divine RL, Sadovova N, Twaddle NC, Doerge DR, Scallet AC, Patterson TA, Hanig JP, Paule MG, Wang C (2007) Ketamine-induced neuronal cell death in the perinatal rhesus monkey. Toxicol Sci 98:145–158
125. Wang C, Sadovova N, Hotchkiss CE, Fu X, Scallet AC, Patterson TA, Hanig J, Paule MG, Slikkor W Jr (2006) Blockade of N-methyl-D-aspartate receptors by ketamine produces loss of postnatal day 3 monkey frontal cortical neurons in culture. Toxicol Sci 91:192–201
126. Yan J, Jiang H (2014) Dual effects of ketamine: neurotoxicity versus neuroprotection

in anesthesia for the developing brain. J Neurosurg Anesthesiol 26:155–160

127. Kawasaki T, Ogata M, Kawasaki C, Ogata J, Inoue Y, Shigematsu A (1999) Ketamine suppresses proinflammatory cytokine production in human whole blood in vitro. Anesth Analg 89:665–669
128. Szekeley A, Heindl S, Zahler S, Conzen PF, Becker BF (1999) S(+)-ketamine, but not R(-)-ketamine, reduces post ischemic adherence of neutrophils in the coronary system of isolated guinea pig hearts. Anesth Analg 88:1017–1024
129. Pfenninger E, Reith A (1990) Ketamine and intracranial pressure. In: Domino EF (ed) Status of ketamine in anesthesiology. NPP Books, Ann Arbor, pp 109–117
130. Reicher D, Bhalla P, Rubinstein EH (1987) Cholinergic cerebral vasodilator effects of ketamine in rabbits. Stroke 18:445–447
131. Dawson B, Michenfelder RA, Theye RA (1971) Effect of ketamine on canine cerebral blood flow and metabolism: modification by prior administration of thiopental. Anesth Analg 50:443–447
132. Schwedler M, Miletich DJ, Albrecht RF (1982) Cerebral blood flow and metabolism following ketamine administration. Can Anesth Soc J 29:222–226
133. Hayashi H, Dikkes P, Soriano SG (2002) Repeated administration of ketamine may lead to neuronal degeneration in the developing rat brain. Pediatr Anaesth 12:770–774
134. Crosby G, Crane AM, Sokoloff L (1982) Local changes in cerebral glucose utilization during ketamine anesthesia. Anesthesiology 56:437–443
135. Nelson SR, Howard RB, Cross RS, Samson F (1980) Ketamine-induced changes in regional glucose utilization in the rat brain. Anesthesiology 52:330–334
136. Fleischer JE, Milde JH, Moyer TP, Michenfelder JD (1988) Cerebral effects of high-dose midazolam and subsequent reversal with RO 15-1788 in dogs. Anesthesiology 68:234–242
137. Obraclović DI, Savi MM, Andjelkovi DS, Ugresić ND, Bokojić DR (2003) The influence of midazolam and flumazenil on rat brain slices oxygen consumption. Pharmacol Res 47:127–131
138. Lei B, Popp S, Cottrell JE, Kass IS (2009) Effects of midazolam on brain injury after transient focal cerebral ischemia in rats. J Neurosurg Anesthesiol 21:131–139
139. Abramowicz AE, Kass IS, Chambers G, Cottrell JE (1991) Midazolam improves electrophysiologic recovery after anoxia and reduces the changes in ATP levels and calcium influx during anoxia in the rat hippocampal slice. Anesthesiology 74:1121–1128
140. Rekling JC (2003) Neuroprotective effects of anticonvulsants in rat hippocampal slice cultures exposed to oxygen/glucose deprivation. Neurosci Lett 335:167–170
141. Xue QS, Yu BW, Wang ZJ, Chen HZ (2004) Effects of ketamine, midazolam, thiopental, and propofol on brain ischemia injury in rat cerebral cortex slices. Acta Pharmacol Sin 25:115–120
142. Liu L, You Q, Tu Y, Li Q, Zheng L, Li X, Gu J, Wang G (2015) Midazolam inhibits the apoptosis of astrocytes induced by oxygen glucose deprivation via targeting JAK2-STAT3 signaling pathway. Cell Physiol Biochem 35:126–136
143. Yilmaz E, Hough KA, Gebhart GF, Williams BA, Gold MS (2014) Mechanisms underlying midazolam-induced peripheral nerve block and neurotoxicity. Reg Anesth Pain Med 39:525–533
144. Todorovic VJ, Hartman RE, Izumi Y, Benshoff ND, Dikranian K, Zorumski CF, Olney JW, Wozniak DF (2003) Early exposure to common anesthetic agents causes widespread neurodegeneration in the developing rat brain and persistent learning deficits. J Neurosci 23:876–882
145. Stevens MF, Werdehausen R, Gaza N, Hermanns H, Kremer D, Bauer I, Kury P, Hollmann MW, Braun S (2011) Midazolam activates the intrinsic pathway of apoptosis independent of benzodiazepine and death receptor signaling. Reg Anesth Pain Med 36:343–349
146. Erdine S, Yucel A, Ozyalcin S, Ozyuvaci E, Talu GK, Ahiskali B, Apak H, Savci N (1999) Neurotoxicity of midazolam in the rabbit. Pain 80:419–423
147. Svennson BA, Welin M, Gordh T Jr, Westman J (1995) Chronic subarachnoid midazolam (Dormicum) in the rat: morphologic evidence of spinal cord neurotoxicity. Reg Anesth 20:426–434
148. Frizell RT, Meyer YJ, Borchers DJ, Weprin BE, Allen EC, Pogue WR, Reisch JS, Cherrington AD, Batjer HH (1991) The effects of etomidate on cerebral metabolism and blood flow in a canine model for hypoperfusion. J Neurosurg 74:263–269
149. Guo J, White JA, Batjer HH (1995) Limited protective effects of etomidate during brainstem ischemia in dogs. J Neurosurg 82:278–283

150. Taylor GA, Trescher WH, Johnston MV, Traystman RJ (1995) A comparison of N-methyl-D-aspartic acid receptor blockade and nitric oxide synthesis inhibition on lesion size and cerebral hyperemia. Pediatr Res 38:644–651
151. Tulleken CAF, van Dieren A, Jonkman J, Kalanda Z (1982) Clinical and experimental experience with etomidate as a brain protective agent. J Cereb Blood Flow Metab 2(Suppl 1):S92–S97
152. Van Reempts J, Borgers M, Van Eyndhoven J, Hermans C (1982) Protective effects of etomidate in hypoxic-ischemic brain damage in the rat: a morphologic assessment. Exp Neurol 76:181–195
153. Yu Q, Zhou Q, Huang H, Wang Y, Tian S, Duan D (2010) Protective effect of etomidate on spinal cord ischemia-reperfusion injury induced by aortic occlusion in rabbits. Ann Vasc Surg 24:225–232
154. Drummond JC, McKay LD, Cole DJ, Patel PM (2005) The role of nitric oxide synthase inhibition in the adverse effects of etomidate in the setting of focal cerebral ischemia in rats. Anesth Analg 100:841–846
155. Bilotta F, Stazi E, Zlotnik A, Gruenbaum SE, Rosa G (2014) Neuroprotective effects of intravenous anesthetics: a new critical perspective. Curr Pharm Des 20(34):5469–5475
156. Lin J, Chu X, Maysami S, Li M, Si H, Cottrell J, Simon RP, Xiong Z (2011) Inhibition of acid sensing ion channel currents by lidocaine in cultured mouse cortical neurons. Anesth Analg 112:977–981
157. Fried E, Amorin P, Chambers G, Cottrell JE, Kass IS (1995) The importance of sodium for anoxic transmission damage in rat hippocampal slices: mechanisms of protection by lidocaine. J Physiol 489:557–565
158. Sakabe T, Maekawa T, Ishikawa T, Takashita H (1974) The effects of lidocaine on canine cerebral metabolism and circulation related to the electroencephalogram. Anesthesiology 40:433–441
159. Astrup J, Srensen PM, Srensen HR (1981) Inhibition of cerebral oxygen and glucose consumption in the dog by hypothermia, pentobarbital and lidocaine. Anesthesiology 55:263–268
160. Taylor CP, Burke SP, Weber ML (1995) Hippocampal slices: glutamate overflow and cellular damage from ischemia as reduced by sodium channel blockade. J Neurosci Methods 59:121–128
161. Mitchell SJ (2001) Lidocaine in the treatment of decompression illness: a review of the literature. Undersea Hyperb Med 28:165–174
162. Shokunbi MT, Gelb AW, Wu XM, Miller DJ (1990) Continuous lidocaine infusion and focal feline cerebral ischemia. Stroke 21:107–111
163. Dutka AJ, Mink R, McDermott J, Clark JB, Hallenbeck JM (1992) Effect of lidocaine on somatosensory evoked response and cerebral blood flow after canine cerebral air embolism. Stroke 23:1515–1521
164. Evans DE, Catron PW, McDermott JJ, Thomas LB, Korbine AL, Flynn ET (1989) Protective effect of lidocaine after experimental cerebral ischemia induced by air embolism. J Neurosurg 70:97–102
165. Evans DE, Korbine AL, LeGrys DC, Bradley ME (1984) Protective effect of lidocaine in acute cerebral ischemia induced by air embolism. J Neurosurg 60:257–263
166. Weenink RP, Hollmann MW, Zomervrucht A, van Ooij PJ, van Hulst RA (2014) A retrospective cohort study of lidocaine in divers with neurological decompression illness. Undersea Hyperb Med 41:119–126
167. Mitchell SI, Pellett O, Gorman DF (1999) Cerebral protection by lidocaine during cardiac operations. Ann Thorac Surg 67:1117–1124
168. Butterworth J, Hammon JW (2002) Lidocaine for neuroprotection: more evidence of efficacy. Anesth Analg 95:1131–1133
169. Wang D, Wu X, Li J, Xiao F, Meng M (2002) The effect of lidocaine on early postoperative cognitive dysfunction after coronary artery bypass surgery. Anesth Analg 95:1134–1141
170. Mathew JP, Mackensen GB, Phillips-Bute B, Grocott HP, Glower DD, Laskowitz DT, Blumenthal JA, Newman MF (2009) Randomized, double-blinded, placebo controlled study of neuroprotection with lidocaine in cardiac surgery. Stroke 40:880–887
171. Mitchell SJ, Merry AF, Frampton C, Davies E, Grieve D, Mills BP, Webster CS, Milsom FP, Wilcox TW, Gorman DF (2009) Cerebral protection by lidocaine during cardiac operations: a follow-up study. Ann Thorac Surg 87:820–825
172. Wang D, Wu X, Zhou Y, Shan G, Hu X, Li J, Liu Y, Qin X, Wang G, Xia Z (1998) Lidocaine improved the cerebral protection provided by retrograde cerebral perfusion: an experimental study. Chin Med J 111:885–890
173. Zhou Y, Wong D, Du M, Zhu J, Shan G, Ma D, Xie D, Ma Q, Hu X, Li J (1998) Lidocaine prolongs the safe duration of circulatory

arrest during deep hypothermia in dogs. Can J Anesth 45:692–698

174. Wang D, Wu X, Zhong Y, ZhouY SG, Hu X, Li J, Liu Y, Qin X, Xia Z (1999) Effect of lidocaine on improving cerebral protection provided by retrograde cerebral perfusion: a neuropathologic study. J Cardiothorac Vasc Anesth 13:176–189
175. Lei B, Cottrell JE, Kass IS (2001) Neuroprotective effect of low dose lidocaine in a rat model of transient focal cerebral ischemia. Anesthesiology 95:445–451
176. Rasool N, Faroqui M, Rubinstein EH (1990) Lidocaine accelerates neuroelectrical recovery after incomplete global ischemia in rabbits. Stroke 21:929–935
177. Sutherland G, Ong BY, Louw D, Sima AF (1989) Effect of lidocaine on forebrain ischemia in rats. Stroke 20:119–122
178. Lei B, Popp S, Capuano-Waters C, Cottrell JF, Kass IS (2004) Lidocaine attenuates apoptosis in the ischemic penumbra and reduces infarct size after transient focal cerebral ischemia in rats. Neuroscience 125:691–701
179. Popp SS, Lei B, Kelemen E, Fenton AA, Cottrell JE, Kass IS (2011) Intravenous antiarrhythmic doses of lidocaine increase the survival rate of CA1 neurons and improve cognitive outcome after transient global cerebral ischemia in rats. Anesthesiology 192:537–549
180. Warner DS, Godersky JC, Maj-Lis S (1988) Failure of pre-ischemic lidocaine administration to ameliorate global ischemic brain damage in the rat. Anesthesiology 68:73–78
181. Shokunbi MT, Gelb AW, Peerless SJ, Mervart M, Floyd P (1986) An evaluation of the effect of lidocaine in experimental focal cerebral ischemia. Stroke 17:962–965
182. Gold MS, Reichling DB, Hampl KF, Drasner K, Levine JD (1998) Lidocaine toxicity in primary afferent neurons from the rat. J Pharmacol Exp Ther 285:413–421
183. Haschke RH, Fink BR (1975) Lidocaine effects on brain mitochondrial metabolism in vitro. Anesthesiology 42:737–740
184. Blas-Valdiva V, Cano-Europa E, Hernandez-Garcia A, Ortiz-Butron R (2007) Hippocampus and amygdala neurotoxicity produced by systemic lidocaine in adult rats. Life Sci 81:P691–P694
185. Johnson ME, Uhl CB, Spittler KH, Wang H, Gores GJ (2004) Mitochondrial injury and caspase activation by the local anesthetic lidocaine. Anesthesiology 101:1184–1194
186. Johnson ME (2004) Neurotoxicity of lidocaine: implications for spinal anesthesia and neuroprotection. J Neurosurg Anesthesiol 16:80–83
187. Werdehausen R, Braun S, Essmann F, Schulze-Osthoff K, Walczak H, Lipfert P, Stevens MF (2007) Lidocaine induces apoptosis via the mitochondrial pathway independently of death receptor signaling. Anesthesiology 107:136–143
188. Brosh-Nissimov T, Ingbir M, Weintal I, Fried M, Porat R (2004) Central nervous system toxicity following topical skin application of lidocaine. Eur J Clin Pharmacol 60:683–684
189. Gomez Martin-Zarco JM, Lumbreras Fernandez de Cordoba J, Ortiz Garcia P (2003) Toxicity of topical administration of lidocaine. Acta Otorrinolaringol 54:657–660
190. Wu FL, Razzaghi A, Souney PF (1993) Seizure after lidocaine for bronchoscopy: case report and review of the use of lidocaine in airway anesthesia. Pharmacotherapy 13:72–78
191. Chiang YY, Tseng KF, Lih YW, Tsai TC, Liu CT, Leung HK (1996) Lidocaine-induced CNS toxicity-a case report. Acta Anaesthesiol Sin 34:243–246
192. Lenz C, Rebel A, VanAckern K, Kuschinsky W, Waschke KF (1998) Local cerebral blood flow, local cerebral glucose utilization and flow metabolism coupling during sevoflurane versus isoflurane anesthesia in rats. Anesthesiology 89:1480–1488
193. Hendrick KS, Kochanek PM, Melick JA, Scheding JK, Statler KD, Williams DS, Marion DW, Ho C (2001) Cerebral perfusion during anesthesia with fentanyl, isoflurane, or pentobarbital in normal rats studied by arterial spin-labeled MRI. Magn Reson Med 46:202–206
194. Patel PM, Drummond JC, Goskowicz R, Sano T, Cole DJ (1993) The volatile anesthetic isoflurane reduces ischemia induced release of glutamate in rats. J Cereb Blood Flow Metab S685
195. Bickler PE, Warner DS, Stratmann G, Schulyer JA (2003) Gamma-aminobutyric acid-A receptors contribute to isoflurane neuroprotection in organotypic hippocampal cultures. Anesth Analg 97:564–571
196. Baughman VL, Hoffman WE, Thomas C, Miletich DJ, Albrecht RF (1990) Comparison of methohexital and isoflurane on neurologic outcome and histopathology following incomplete ischemia in rats. Anesthesiology 72:85–94
197. Warner DS, McFarlane G, Todd MM, Ludwig P, McAllister AM (1993) Sevoflurane and halothane reduces focal ischemic brain damage in the rat: possible influence on thermoregulation. Anesthesiology 79:985–992
198. Warner DS, Ludwig PS, Pearlstein R, Brinkhous AD (1995) Halothane reduces

focal ischemic injury in the rat when brain temperature is controlled. Anesthesiology 82:1237–1245

199. Newberg LA, Michenfelder JD (1983) Cerebral protection by isoflurane during hypoxemia or ischemia. Anesthesiology 59:229–235
200. Nehls DG, Todd MM, Spetzler RF, Drummond JC, Thompson RA, Johnson PC (1987) A comparison of the cerebral protective effects of isoflurane and barbiturates during temporary focal ischemia in primates. Anesthesiology 66:453–464
201. Milde LN, Milde JH, Lanier WL, Michenfelder JD, Gallagher W, Koenig R, Kroening A, Phelps L, Wilson R (1988) Comparison of the effects of isoflurane and thiopental on neurologic outcome and neuropathology after temporary focal ischemia in primates. Anesthesiology 69:905–913
202. Michenfelder JD, Sundt TM, Fode N, Sharbrough FW (1987) Isoflurane when compared to enflurane and halothane decreases the frequency of cerebral ischemia during carotid endarterectomy. Anesthesiology 67:336–340
203. Gelb AW, Boisvert DP, Tang C, Lam AM, Marchak BE, Dowman R, Mielke BW (1989) Primate brain tolerance to temporary focal cerebral ischemia during isoflurane or sodium nitroprusside induced hypotension. Anesthesiology 70:678–683
204. Sarraf-Yazdi S, Sheng H, Miura Y, McFarlane C, Dexter F, Pearlstein R, Warner DS (1998) Relative neuroprotective effects of dizocilpine and isoflurane during focal cerebral ischemia in the rat. Anesth Analg 87:72–78
205. Kawaguchi M, Drummond JC, Cole DJ, Kelly PJ, Spurlock MP, Patel PM (2004) Effect of isoflurane on neuronal apoptosis in rats subjected to local cerebral ischemia. Anesth Analg 98:798–805
206. Kawaguchi M, Kimbro JR, Drummond JC, Cole DJ, Kelly PJ, Patel PM (2000) Isoflurane delays but does not prevent cerebral infarction in rats subjected to focal ischemia. Anesthesiology 92:1335–1342
207. Elsersy H, Sheng H, Lynch JR, Moldovan M, Pearlstein RD, Warner DS (2004) Effects of isoflurane versus fentanyl-nitrous oxide anesthesia on long-term outcome from severe forebrain ischemia in the rat. Anesthesiology 100:1160–1166
208. Jevtovic-Todorovic V, Hartman RE, Izumi Y, Benshoff ND, Dikranian K, Zorumski CF, Olney JW, Wozniak DF (2003) Early exposure to common anesthetic agents causes widespread neurodegeneration in the developing rat brain and persistent learning deficits. J Neurosci 23:876–882.
209. Wise-Faberowski L, Zhang H, Lng R, Pearlstein RD, Warner DS (2005) Isoflurane-induced neuronal degeneration: an evaluation in organotypic hippocampal slice cultures. Anesth Analg 101:651–657
210. Boscolo A, Ori C, Bennett J, Wiltgen B, Jevtovic-Todorovic V (2013) Mitochondrial protectant pramipexole prevents sex-specific long-term cognitive impairment from early anaesthesia exposure in rats. Br J Anaesth 110(Suppl 1):147–152
211. Li G, Xue Q, Luo Y, Hu X, Yu B (2015) S6 inhibition contributes to isoflurane neurotoxicity in the developing brain. Toxicol Lett 233:102–113
212. Loepke AW, Istaphanous GK, McAuliffe JJ 3rd, Miles L, Hughes EA, McCann JC, Harlow KE, Kurth CD, Williams MT, Vorhees CV, Danzer SC (2009) The effects of neonatal isoflurane exposure in mice on brain cell viability, adult behavior, learning, and memory. Anesth Analg 108:90–104
213. Head BP, Patel HH, Niesman IR, Drummond JC, Roth DM, Patel PM (2009) Inhibition of p75 neurotrophin receptor attenuates isoflurane-mediated neuronal apoptosis in the neonatal central nervous system. Anesthesiology 110:813–825
214. Schallner M, Ulbrich U, Engelstaedter H, Biermann J, Auwaerter V, Loop T, Goebel U (2014) Isoflurane but not sevoflurane or desflurane aggravates injury to neurons in vitro and in vivo via p75NRT-NF-kB activation. Anesth Analg 119:1429–1441
215. Franks NP, Lieb WR (1994) Molecular and cellular mechanism of general anesthesia. Nature 367:607–614
216. Franks NP, Dickinson R, de Souza SLM, Hall AC, Lieb WR (1998) How does xenon produce anesthesia? Nature 396:324
217. Jevtovic-Todorovic V, Todorovic SM, Mennerick S, Powell S, Dikranian K, Benshoff N, Zorumski CF, Olney JW (1998) Nitrous oxide (laughing gas) is an NMDA antagonist, neuroprotectant and neurotoxin. Nat Med 4:460–463
218. Mennerick S, Jeutovic-Todorovic V, Todorovic SM, Shen LG, Olney JW, Zorumski CF (1998) Effects of nitrous oxide on excitatory and inhibitory synaptic transmission in hippocampal cultures. J Neurosci 18:9716–9726
219. Ishimaru MJ, Ikonomidou C, Tenkove TI, Der TC, Dikranian K, Sesma MA, Olney JW (1999) Distinguishing excitotoxic from apoptotic neurodegeneration in the developing rat brain. J Comp Neurol 408:461–476

220. Sanders RD, Maze M (2005) Xenon: from stranger to guardian. Curr Opin Anesth 18:405–411
221. Wilhelm S, Ma D, Maze M, Franks NP (2002) Effects of xenon on in vitro and in vivo models of neuronal injury. Anesthesiology 96:1485–1491
222. Homi HM, Yokoo N, Ma D, Warner DS, Franks NP (2003) The neuroprotective effect of xenon administration during transient middle cerebral artery occlusion in mice. Anesthesiology 99:876–881
223. Dingley J, Tooley J, Porter H, Thoresen M (2006) Xenon provides short term neuroprotection in neonatal rat when administered after hypoxia-ischemia. Stroke 37:501–506
224. David HN, Haelewyn B, Rouillon C, Lecoq M, Chazalviel L, Apiou G, Risso JJ, Lemair M, Abraini JH (2008) Neuroprotective effects of xenon: a therapeutic window of opportunity in rats subjected to transient cerebral ischemia. FASEB J 22:1275–1286
225. Fries M, Nolte KW, Coburn M, Rex S, Timper A, Korrmann K, Stepmann K, Hausler M, Weis J, Rossaint P (2008) Xenon reduces neurohistopathological damage and improves the early neurological deficit after cardiac arrest in pigs. Crit Care Med 36:2420–2426
226. Esencan E, Yuksel S, Tosun YB, Robinot A, Solaroglu I, Zhang JH (2013) Xenon in medical area: emphasis on neuroprotection in hypoxia and anesthesia. Med Gas Res 3:4
227. Sheng SP, Lei B, James ML, Lascola CD, Venkatraman TN, Jung JY, Maze M, Franks NP, Pearlstein RD, Sheng H, Warner DS (2012) Xenon neuroprotection in experimental stroke. Anesthesiology 117:1262–1275
228. Ma D, Hossain M, Chow A, Arshad M, Battsen RM, Saunders RD, Mehmete H, Edwards AD, Franks NP, Maze M (2005) Xenon and hypothermia combine to provide neuroprotection from neonatal asphyxia. Ann Neurol 58:182–193
229. Hobbs C, Thoresen M, Tucker A, Aquilina K, Chakkarapani E, Dingley J (2008) Xenon and hypothermia combine additively, offering long-term functional and histopathologic neuroprotection after neonatal hypoxia/ischemia. Stroke 39:1307–1313
230. Rajakumaraswamy N, Ma D, Hossain M, Sanders RD, Franks NP, Maze M (2006) Neuroprotective interaction produced by xenon and dexmedetomidine on in vitro and in vivo neuronal injury models. Neurosci Lett 409:128–133
231. Thoresen M, Hobbs CE, Wood T, Chakkarapani E, Dingley J (2009) Cooling combined with immediate or delayed xenon inhalation provides equivalent long-term neuroprotection after neonatal hypoxia-ischemia. J Cereb Blood Flow Metab 29:707–714
232. Abraini JH, David HN, Lemaire M (2005) Potentially neuroprotective and therapeutic properties of nitrous oxide and xenon. Ann N Y Acad Sci 1053:289–300
233. Dinse A, Fohr KJ, Georgieff M, Beyer C, Bulling A, Weigt HU (2005) Xenon reduces glutamate-, AMPA-, and kainite-induced membrane currents in cortical neurones. Br J Anesth 94:479–485
234. Chakkarapani E, Thoresen M, Hobbs CE, Aquilina K, Liu X, Dingley J (2009) A closed-circuit neonatal xenon delivery system: a technical and practical neuroprotection feasibility study in newborn pigs. Anesth Analg 109: 451–460
235. Natale G, Cattano D, Abramo A, Forfori F, Fulceri F, Fornai F, Paperelli A, Giunta F (2006) Morphological evidence that xenon neuroprotects against N-methyl-DL-aspartic acid induced damage in the rat arcuate nucleus: a time-dependent study. Ann N Y Acad Sci 1074:650–658
236. Ma D, Hossain M, Pettet GK, Luo Y, Akimov S, Sanders RD, Franks NP, Maze M (2006) Xenon preconditioning reduces brain damage from neonatal asphyxia in rats. J Cereb Blood Flow Metab 26:199–208
237. Payne RS, Akca O, Roewer N, Schurr A, Kahl F (2005) Sevoflurane-induced preconditioning protects against cerebral ischemic neuronal damage in rats. Brain Res 1034: 147–152
238. Wang J, Lei B, Popp S, Ming F, Cottrell JE, Kass IS (2007) Sevoflurane immediate preconditioning alters hypoxic membrane potential changes in rat hippocampal slices and improves recovery of CA1 pyramidal cells after hypoxia and global cerebral ischemia. Neuroscience 145:1097–1107
239. Zuo Z (2012) A novel mechanism for sevoflurane preconditioning-induced neuroprotection. Anesthesiology 117:942–944
240. Chen Y, Nie H, Tian L, Tong L, Deng J, Zhang Y, Dong H, Xiong L (2015) Sevoflurane preconditioning-induced neuroprotection is associated with Akt activation via carboxy-terminal modulator protein inhibition. Br J Anaesth 114:327–335
241. Song H, Coo L, Qiu P, Xiong L, Wong R, Yan G (2006) Isoflurane produces delayed preconditioning against spinal cord ischemic injury via release of free radicals in rabbits. Anesthesiology 105:953–960

242. Liu Y, Xiong L, Chen S, Wang Q, (2006) Isoflurane tolerance against focal cerebral ischemia is attenuated by adenosine A1 receptor antagonists. Can J Anesth 53:194–201.
243. Li QF, Zhu YS, Jiang H (2008) Isoflurane preconditioning activates HIF-1alpha, iNOS, and Erk1/2 and protects against oxygen-glucose deprivation neuronal injury. Brain Res 1245:26–35
244. Yang Q, Dong H, Deng J, Wang Q, Ye R, Li X, Hu S, Dong H, Xiong L (2011) Sevoflurane preconditioning induces neuroprotection through reactive oxygen species-mediated up-regulation of antioxidant enzymes in rats. Anesth Analg 112:931–937
245. Yang Q, Yan W, Li X, Hou L, Dong H, Wang Q, Zhang X, Xiong L (2012) Activation of canonical Notch signaling pathway is involved in the ischemic tolerance induced by sevoflurane preconditioning in mice. Anesthesiology 117:996–1005
246. Wei H, Kang B, Wei W, Liang G, Ming QC, Li Y, Eckenhoff RG (2005) Isoflurane and sevoflurane affect cell survival and BCL-2/ BAX ratio differently. Brain Res 1037:139–147
247. Kurth CD, Priestley M, Watzman HM, McCann J, Golden J (2001) Desflurane confers neurologic protection for deep hypothermic circulatory arrest in newborn pigs. Anesthesiology 95:959–964
248. Loepke AW, Priestley M, Schultz SE, McHann J, Golden J, Kurth CD (2002) Desflurane improves neurologic outcome after low-flow cardiopulmonary bypass in newborn pigs. Anesthesiology 97:1521–1527
249. Haelewyn B, Yvon A, Hanouz TL, MacKenzie ET, Ducouret P, Gerard JL, Roussel S (2003) Desflurane affords greater protection than halothane against focal cerebral ischemia in the rat. Br J Anaesth 91:390–396
250. Engelhard K, Werner C, Reeker W, Lu H, Mollenberger O, Mielke L, Kochs E (1999) Desflurane and isoflurane improve neurological outcome after incomplete cerebral ischemia in rats. Br J Anaesth 83:415–421
251. Hoffman WE, Charbel FT, Edelman G, Ausman JL (1998) Thiopental and desflurane treatment for brain protection. Neurosurgery 43:1050–1053

Chapter 11

Noninvasive Brain Imaging in Small Animal Stroke Models: MRI, PET, and SPECT

Abraham Martín, Pedro Ramos-Cabrer, and Anna M. Planas

Abstract

Acute brain damage after stroke produces remarkable changes in the brain that can be visualized with a variety of neuroimaging techniques. Some of these techniques are used in patients for diagnostic purposes and are now available to image the rodent brain. However, noninvasive imaging of the brain of rodents is challenging because of the size of the animals and the fact that their handling normally requires sedation or deep anesthesia to avoid stress and movement during image acquisition. In this chapter we will discuss the purpose, advantages, and difficulties of applying magnetic resonance imaging (MRI) (part A), positron emission tomography (PET) (part B), and single-photon emission computed tomography (SPECT) (part C) to image the ischemic brain in rodents.

Key words Rodents, Stroke, MRI, DWI, ADC, PWI, DTI, fMRI, PET, SPECT

1 Magnetic Resonance Imaging

1.1 Introduction

MRI is a widely used technique to image stroke patients for diagnostic and therapeutic purposes [1]. With the accessibility of high magnetic field horizontal magnets, animal-dedicated MRI has emerged as a powerful tool to investigate the brain of living animals. MRI has great potential for studying animal models of brain ischemia as it can provide in vivo information on the magnitude of the alterations caused by brain lesions and on their progression with time [2]. Due to its noninvasive nature, animals can be followed up in longitudinal studies, and multiparametric studies can offer complementary information on different aspects of the brain lesion [3–6]. The aim of this text is to provide an overview of the MRI imaging techniques useful for studying the brain in animal models of stroke. Neuroimaging techniques have a complex theoretical and physical base, and for this reason the readers will be directed to specialized literature for detailed technological information on physical principles [7–9] and quantification [10].

Ulrich Dirnagl (ed.), *Rodent Models of Stroke*, Neuromethods, vol. 120,
DOI 10.1007/978-1-4939-5620-3_11, © Springer Science+Business Media New York 2016

2 Materials

2.1 Instrumentation

Conventional MRI is based on the effect that a magnetic field has on protons (hydrogen nuclei, mainly from water and fat molecules) as their magnetic moments either align themselves parallel or (in less proportion) antiparallel to the direction of the applied field. Image acquisition requires a process by which electromagnetic radiofrequency pulses are applied to excite protons (i.e., promote parallel to antiparallel transitions, up to a maximum where both populations are equaled), and after an evolution time, protons release the acquired energy in the form of radiofrequencies that can be detected in the receiver coil and transformed into an image. Magnetic field gradients are also applied prior, during, and after excitation to generate image contrast and for spatial encoding of the signal [8, 9].

The main requisites for MRI are instrumentation and a multidisciplinary team of specialized and well-trained personnel. Imaging rodents using clinical equipment, with magnetic fields usually ranging 1–3 Tesla (T), is feasible, and findings in the field of stroke research have been reported using these systems [11–13]. However, animal-dedicated MRI systems are preferred because they render better performance in terms of sensibility and spatial, temporal, and spectral resolution. Also, current legislation in some countries does not allow the mixed use of clinical equipment for animal experimentation. Most animal studies are now performed with horizontal magnets at high magnetic fields of 4.7, 7, 9.4, or 11.7 T. Horizontal magnets with very high magnetic fields are also available for animal research, and studies in ischemic rats have been reported at 21.1 T for diffusion-weighted imaging (DWI) [14] or T1 [15]. Nonetheless, images of interest in brain ischemia such as diffusion-weighted imaging (DWI) and T2-weighted (T2W) imaging (see below) offer sufficiently good quality at 4.7 and 7 T in adult rats and mice. Higher magnetic fields are useful to increase sensitivity, yielding better image quality, better spatial resolution, or reduced acquisition times, by improving the signal-to-noise ratio. These factors may be critical in certain MRI techniques such as diffusion tensor imaging (DTI) or functional MRI (fMRI), in which increasing the strength of the magnetic field dramatically improves the results. Ultrahigh magnetic fields are also advantageous in localized spectroscopy (because of the higher spectral resolution achieved at higher fields), angiography, or molecular imaging.

Signal transmission and reception are performed by using radiofrequency (RF) coils. Volume coils or resonators (e.g., birdcage, saddle, solenoids, or Helmholtz pair configurations) are a good choice for signal transmission or for combined signal transmission–reception, since these devices offer better RF homogeneity

over their volume. Instead, surface coils (single loops adapted to the object geometry) are much more sensitive than volume coils for signal detection in the proximity of the coil, though their range drops very fast with the distance to it, and are a good choice for signal reception. The combination of a volume resonator for signal transmission and a brain adapted surface coil for signal reception into it is probably the best selection to achieve optimal signal-to-noise for brain studies in small animals. With the development of electronics and computing solutions, the use of several surface coils working in parallel (n-elements arrayed coils) attached to multiple-channel receivers in the MRI systems or the use of cryo-coils, in which electronic noise is reduced by working at low temperatures, has allowed the achievement of impressive signal-to-noise ratios, covering larger sample volumes and achieving faster acquisition times in modern MR systems. Considering the importance of the coils to obtain good signals, some specialized laboratories like to build up their own homemade collections of coils. However, coils of a sufficient quality for imaging the head of mice and rats are now commercially available.

Gradient coils, inserted in the bore of MRI systems, are another critical aspect of the architecture of the equipment for successful imaging of the brain of rodents. Gradient coils are needed to induce image contrast and to spatially encode the signal, that is, to resolve the spatial position of the protons that generate the signal, within a specific space volume. The performance of the gradients on an MRI system, specially ramping times and strength, is a critical feature that will determine the acquisition times (faster with fast-switching gradients), contrast (minimum echo times), and spatial resolution. With 400–1000 mT/m XYZ gradients (such as those found in conventional preclinical MRI systems), spatial resolutions of 100 to 20 μm are readily accessible.

2.2 Anesthesia

General anesthesia or sedation is an issue of high concern for in vivo neuroimaging studies in animals (see ref. [16] for a review; see also Chap. 10). The comments below apply therefore not only to MRI but also to PET and SPECT studies. Generally, animals need to be anesthetized to prevent movement and to avoid stress during image acquisition (see Note 1). For stroke animal models, gaseous anesthetics (such as isoflurane or sevoflurane) are an adequate choice as they can keep the animals anesthetized for variable periods of time, recovery is rapid, and repeated anesthesia protocols with short recovery times are possible. Gaseous anesthetics can be delivered to the animals by carrier gases (usually air, oxygen, or oxygen/nitrous oxide mixtures at different proportions) while they are inside the magnet using a facial mask or after tracheotomy. Often the system delivering anesthesia into the magnet needs to be adjusted in order that animals maintain their blood gases within the physiological range. Continuous or repeated monitoring of

physiological parameters is necessary as animals need to be maintained under anesthesia throughout image acquisition. MR compatible monitoring devices for respiration and heart beating rates (among other parameters) are common accessories to preclinical neuroimaging scanners. Anesthesia is critical in functional MRI (fMRI) and metabolic PET studies as many anesthetics alter cerebral blood flow and metabolism (*see* Note 2). Furthermore, in pharmacological MRI, where a blood flow response is assessed after drug challenges, anesthetics can interfere with the drugs [17].

2.3 Physiological Parameter Monitoring

Blood $PaCO_2$, PaO_2, and pH can be assessed by taking blood samples and measuring them in a blood gas analyzer. However, the choice is often measuring $PaCO_2$ with transcutaneous systems for continuous monitoring [18]. It is very important to monitor $PaCO_2$ for the known effects of hypercapnia increasing cerebral blood volume (CBV) and cerebral blood flow (CBF) [19]. Endovascular probes and fiber-optic pulse oximetry sensors are also available in the market. Monitoring blood pressure and temperature while the animal is inside the magnet is also important. Temperature control is often carried out with a warming, circulating water system that is placed surrounding the animal in the holder or using hot air blowers. To avoid movement artifacts in MR images (especially critical in mice), it is essential to synchronize signal acquisition with respiration of the animals. For this reason, monitoring respiratory frequency is essential for the prospective gating of signal acquisition. Monitoring can be achieved with equipment adapted to be MRI compatible. It is also possible to perform retrospective gating, through self-gated image acquisition schemes that incorporate navigation modules to obtain physiological information from the MR signal itself, avoiding the need for external monitoring. Although heart beating is not critical for brain imaging, it can also be considered for triggering.

3 Methods

MRI is an optimal tool for translational studies. Theoretically, clinical and preclinical scanners are identical in their concept; thus MR techniques should be readily translatable between both fields. Nevertheless, some of the sequences used in clinical MRI are sometimes not readily available in animal-dedicated magnets, and often specific sequences must be developed. Fortunately, this is now changing as more and more animal-dedicated machines are being equipped with sequences compatible with those used in the clinical setting. Also, some manufacturers now supply machines that are theoretically fully compatible with clinical equipment. For further information on the MRI scans and sequences mentioned below, see Note 3.

3.1 What Is the Best MRI Technique to Study the Ischemic Brain Lesion?

Brain lesions after stroke have a very dynamic component that evolves with time. For this reason, the MRI tools for use in stroke research will depend on the stage of the lesion after the initiation of ischemia at the time of imaging, and full assessment will require the use of multimodal imaging (see ref. [2] for review). (For a comment on image acquisition before, during, and after induction of experimental ischemia, see Note 4.)

3.1.1 Acute Phase (<12 h)

The best MRI method for demonstrating the affected brain parenchyma in the first hours after ischemia onset is *diffusion-weighted imaging* (DWI), which assesses the diffusion movement of water molecules. Signal intensity alterations in DWI are thought to reflect cytotoxic edema. Therefore, DWI is very sensitive to ischemic conditions in the brain and it shows increased signal intensity (hyperintensity) only a few minutes after ischemia onset [20, 21]. At this very early stage, interruption of blood supply, causing arrest of cell metabolic activity and of the movement of fluids across the intracellular space, is thought to contribute to hyperintense signals in DWI, indicating areas of restricted diffusion [20–23]. Thus, DWI is the most sensitive technique for detecting brain lesion in the first 2–4 h after ischemia, whereas other MRI techniques, such as *T2-weighted* (T2W), are not sensitive enough at this early stage [4]. Acquisition of multiple images with different weight on water diffusion dynamics allows the absolute quantification of diffusion coefficients in the tissue, and therefore diffusion maps showing parametric images can be constructed. Since diffusion is an anisotropic property (depends on the spatial orientation), usually mean values (MD) or apparent diffusion coefficient (ADC) maps are provided [22–25].

Information on CBF is also extremely useful at this stage and can be obtained with p*erfusion-weighted imaging* (PWI) (see Note 3). Studies of PWI and DWI in stroke patients were conceived with the concept that the mismatch between these two images identifies the penumbra or "tissue at risk," where the reduction in blood supply is not yet reflected in DWI [26]. This is an important imaging concept that we will discuss in this chapter (see Sect. 2.3 below), as studies of PWI and DWI are also feasible in rodent models of ischemia [27, 28].

Finally, valuable information can be obtained by visualizing the occluded/reperfused arteries with *magnetic resonance angiography* (MRA) in humans and also in small animals [29] (see Note 3) (Fig. 1).

3.1.2 Subacute Phase (First Days)

After the first hours of evolution of the lesion, T2-weighted (T2W) imaging and proton density-weighted (PDW) imaging become also useful for detecting injury in the ischemic brain, as they show alteration (hyperintensity) in response to increased water content (PDW) and mobility (T2W) [30]. T2W is very sensitive to

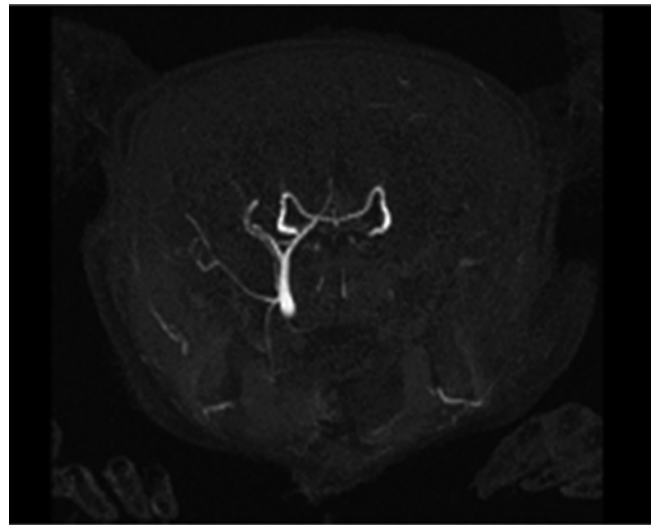

Fig. 1 MRA of the rat brain evidences the circulation in *white*. Lack of circulation is evidenced in the right-hand side of the image during MCAO

vasogenic edema [31], which is a hallmark in focal ischemia, and it is useful to image the lesion during the first days after stroke onset [32]. After the first day, T1-weighted (T1W) imaging can also show some hypointensity, but is much less sensitive to injury than T2W. FLAIR-T2W (fluid-attenuated inversion recovery T2W) is a variant of T2W on which signal from large amounts of free water (such as CSF in the ventricles) is suppressed and is the gold-standard imaging technique in the clinics, at this stage. DWI and ADC maps are still useful for imaging the lesion the first days after stroke, but the less technically demanding nature of T2W imaging favors the use of the latter at this stage (Fig. 2).

3.1.3 Chronic Phase

Plasticity events, including axonal sprouting, have been reported in rodent models of stroke [33]. Therefore, the area of interest in brain imaging in the chronic stages might be in the fiber tracts and also to get functional information of brain activation to study degeneration and regeneration processes. The advent of cell-based therapies for stroke has also promoted the use of cell tracking techniques to follow up such therapies by MR.

Diffusion tensor imaging (DTI) provides an interesting tool to investigate the brain after stroke (Fig. 3), to gather information on degeneration, demyelination, and regenerative processes (*see* **Note 3**). DTI provides measures of diffusion in multiple directions, and it is based on the fact that water does not diffuse homogeneously in all directions through brain parenchyma but rather has facilitated diffusion along nerve fiber tracts. DTI changes have been shown to take place at the time of histological remodeling and

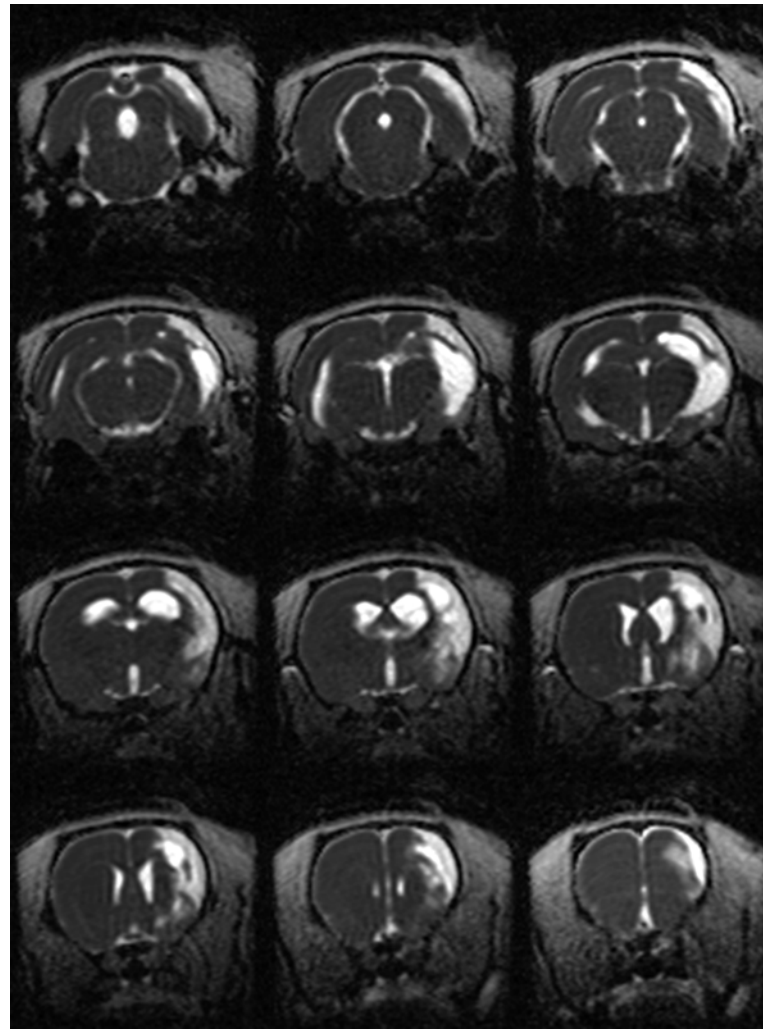

Fig. 2 ADC maps 24 h after 2-hour MCAO occlusion in the rat. *White zones* in the right-hand side of each image illustrate the lesion

recovery of function after middle cerebral artery occlusion (MCAO) in mice [34]. DTI alterations were reported in the white matter after ischemia [35, 36]. Also, structural changes were found in zones at the periphery of the infarcted core after transient MCAO in rats [37] and mice [34]. These zones are thought to be critically involved in functional recovery after stroke [37]. Microstructural alterations in brain tissue imaged with DTI correlate with functional deficits and can provide an assessment of functional recovery [38]. A variant of DTI named diffusion kurtosis imaging (DKI) based on non-Gaussian methods [39] and diffusion spectrum imaging (DSI), able to directly image multiple fiber orientations within a single voxel [40], can potentially provide

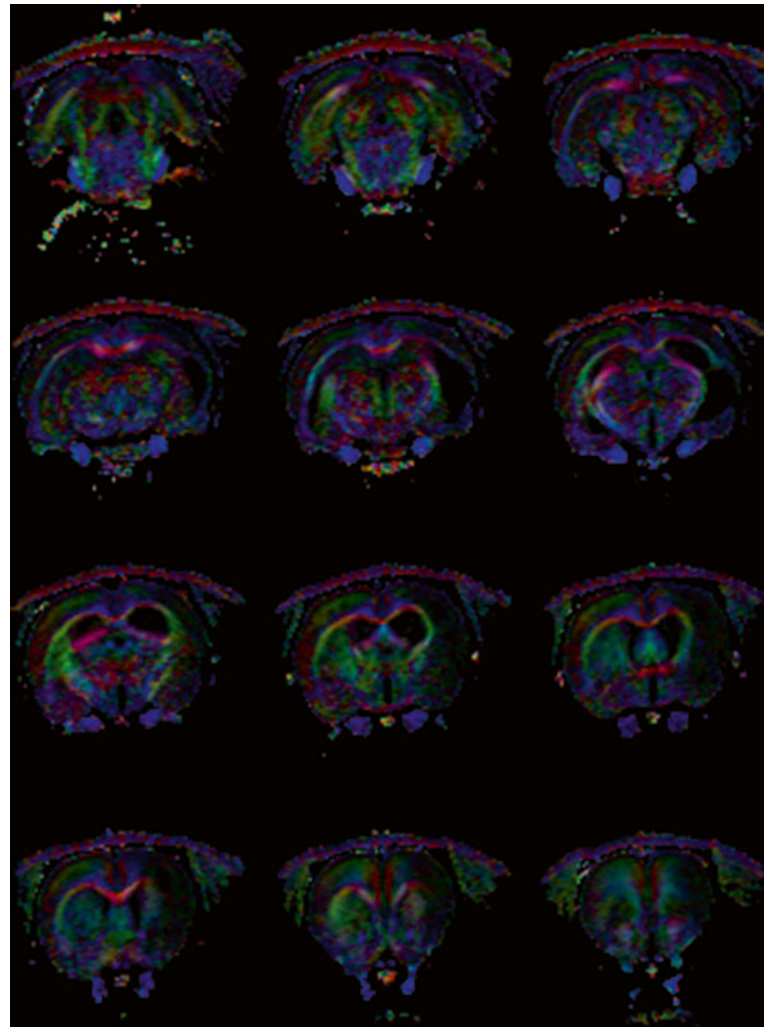

Fig. 3 DTI brain images obtained in the living rat showing loss of white matter fibers (*dark zones* on the right-hand side of each image) 7 days after transient MCAO

more valuable information on the gray matter microstructure than DTI, which is particularly sensitive to changes in the white matter. DKI has been used in studies in animal models of stroke concluding that DKI can be more sensitive than DTI in detecting microstructural changes throughout the brain in the chronic phases [41, 42]. Although scanning time is usually an issue that hampers the use of DKI methods, the advantages of a fast-mapping DKI experimental protocol to study ischemic animals have been recently tested [43]. Furthermore, combinations of several non-Gaussian diffusion models can provide new information on spatial properties of stroke lesions [44].

Functional MRI (fMRI) based on the blood-oxygen-level-dependent (BOLD) effect provides indirect information about neural activity. In its various variants, fMRI is based on the fact that neuronal activity is normally coupled to energy metabolism and to CBF. This technique is of interest in stroke research because it allows distinction between the specific loss of certain neurons and circuitries after brain ischemia. Altered hemodynamic fMRI responses have been reported during stroke recovery in animals [45]. fMRI may be useful to study degeneration and regeneration after therapeutic strategies. For example, fMRI revealed functional recovery in animals that received delayed albumin treatment after 90 min MCAO [46] and also spontaneous recovery of function [36]. Currently, a lot of attention has been set in the field of resting-state or low-frequency fluctuation functional MRI (rs-fMRI or lff-fMRI), a variant of fMRI techniques allowing the study of the reorganization of functional networks in the ischemic brain without requiring external stimulation or task performance [47, 48].

Manganese-enhanced MRI (*MEMRI*) has been used as a surrogate marker for calcium influx and can be used to monitor brain activity [49] in spite of the need to overcome important limitations, including poor BBB penetration and toxicity [50]. In spite of this, the improved contrast provided by this technique enables direct tracking of laminar-specific neurodegeneration [51] and has been used in stroke models to study neuroanatomical connectivity [47, 52], brain plasticity [53], or gliosis [54].

MRA

Finally, the study of angiogenesis can provide valuable information, particularly at chronic stages after induction of ischemia. Angiogenesis can be studied using MR by examining vessel morphology at high resolution with MRA [55] or contrast-enhanced T2/T2* mapping of the brain, which allows the estimation of vessel densities and mean vessel sizes in the tissues [56]. Furthermore, the blood vessels show hypointensity in PDW images and this feature can be exploited to examine the vasculature, particularly in view of new developments in segmentation analysis [57]. In addition, susceptibility-weighted imaging is another interesting technique to highlight vascular remodeling [8].

3.2 Diffusion–Perfusion Mismatch or the "MRI" Concept of Penumbra

Within the first hours after stroke onset, MRI often evidences tissue with altered DWI immersed in a larger zone of CBF disturbance [58]. The zone with altered DWI is taken as the irreversibly damaged zone (although this is not fully accurate, see below). The difference or "mismatch" between DWI and PWI is associated with tissue at risk that has abnormal perfusion but is above the limits of cell viability according to normal ADC [23, 26, 59, 60]. Then, in the following hours, infarction (DWI) will frequently grow to occupy the full region of PWI deficit, and thus the tissue

at risk will be lost unless active interventions are undertaken [23, 59, 61, 62]. The tissue at risk is assumed to correspond to the physiological definition of penumbra as a region where neurons cannot maintain electric activity, but have sufficient energy to maintain their membrane potential [63]. There are, indeed, several definitions of penumbra depending on the tools used to assess it [23, 64–66]. The MRI definition has clinical relevance as it is proposed as instrumental to select patients for clinical trials in acute stroke [67]. Nonetheless, the zone of DWI alteration is metabolically heterogeneous [68], and there is now evidence from PET [69–72] and MRI [73] studies that it may contain some viable tissue. Likewise, the zone of PWI might include zones with non-relevant reductions in CBF without dangerous consequences for the tissue (benign oligemia), as assessed with multimodal MRI [73] or the use of chemical exchange saturation transfer (CEST)-based contrast for pH maps of the brain by MRI [74].

The DWI/PWI mismatch is also observed in rats during ischemia [27]. Rat strain differences have been reported for the extent and evolution of mismatch tissue after ischemia [28]. Interestingly, a typical neuroprotective drug, the immunosuppressant FK506, protected the mismatch cortex only [75], and treatment with normobaric oxygen 30 min after induction of ischemia prevented expansion of the mismatch zone toward infarction [76]. Another condition known to exert protective action preserving the mismatch zone in rats is stimulation of the sphenopalatine ganglion [77]. Notably, the DWI/PWI mismatch has been studied less in animals than in humans, possibly because of the technical difficulties involved. Nevertheless, the animal studies can provide additional useful information, as scans can be repeated as many times as necessary in animals and a correlation can be established with the histological damage as evaluated postmortem. MRI animal work can also bring about new developments that may help to further understand the tissue at risk. For instance, new advances in the MRI definition of the penumbra have been recently reported in ischemic rats with the use of an oxygen challenge that induces changes in the oxyhemoglobin/deoxyhemoglobin ratios and a subsequent T2* signal change [78]. For further information, we refer to previous reviews on the identification of the penumbra with imaging modalities in experimental animal models and in stroke patients [79].

3.3 Reperfusion

Some of the strong MRI alterations occurring during ischemia may normalize with early reperfusion [5, 11, 80, 81]. However, despite initial normalization, MRI alterations can reappear later in some regions and infarction may develop [5, 11, 80, 81]. Furthermore, the extent of reperfusion can be variable, ranging from incomplete reperfusion to hyperperfusion [82], and this may affect tissue outcome [83]. The important role that MRI can play in detecting signs of reperfusion injury has been revised [84].

3.4 Do MRI Data Have Predictive Value?

Given the dynamic nature of the ischemic process, MRI data obtained at more than a single time point may provide valuable information for predicting outcome [32, 85]. Complex multispectral approaches have been developed to characterize the ischemic tissue and to estimate the ischemic penumbra [30]. Recent work showed that tissue fate can be predicted precisely in rats after stroke by using statistical algorithms combining multiple MRI modalities [86, 87]. Wu et al. [86] developed a voxel-based generalized linear model algorithm incorporating various input parameters (including rADC, rCBF, rCBV, and rMTT) that was a highly accurate predictor of infarction in the rat after embolic stroke. In this latter study, the predictor method was particularly precise in the absence of reperfusion, as prediction was better in controls than in rats treated with rt-PA [86]. Also, predictive algorithms have been developed for the early identification of potentially salvageable tissue [87, 88]. Overall, these techniques are powerful in predicting infarct volume, but they are computationally quite complex. Simplifications have been suggested, but they require MRI acquisitions during ischemia and after reperfusion [89]. Predictor methods may help to stratify the animals according to the extent of the injury induced by the surgical technique. Better identification of the lesion would add robustness to the evaluation of the effects of drug treatments or genetic conditions.

3.5 Alterations of Blood–Brain Barrier Permeability

Alterations in BBB permeability can be visualized with Gd-DTPA-enhanced T1-weighted imaging (by evaluating extravasation of i.v. injected contrast agent in vivo (Fig. 4). Disturbances of blood–brain barrier (BBB) after ischemia have been correlated with the hemodynamic and biophysical consequences of reperfusion [83]. Early changes in permeability following transient MCAO have been shown using other contrast agents such as manganese (Mn^{2+}) [90]. Using MRI techniques, early alteration of vascular barrier function was shown and was characterized quantitatively by measuring the transvascular water exchange rate in a mouse model of permanent focal ischemia [91]. Nonetheless, quantification of

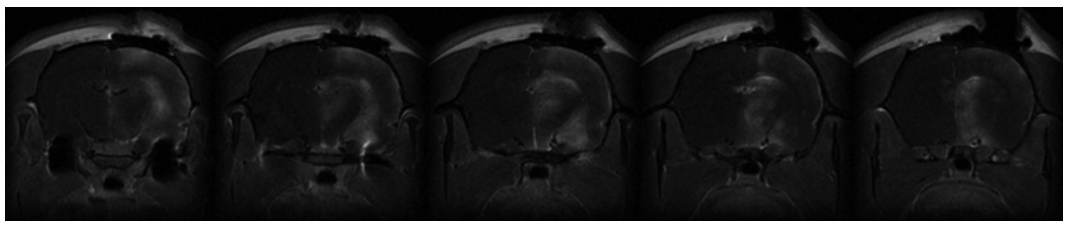

Fig. 4 MRI (T1W) showing BBB permeability alteration in the rat brain as revealed by contrast extravasation (*bright areas*) in the ipsilateral hemisphere shown on the right-hand side of each image) 24 h after transient MCAO. Contrast agent was Gd-DTPA-BMA Omniscan®, 0.5 mmol/ml, i.v

contrast agent concentration is influenced by several factors that have been discussed in detail elsewhere [92, 93]. The very active ongoing investigation in MRI contrast agents will likely in the near future provide an assortment of compounds that will allow a better understanding of the different stages of alterations of BBB permeability after stroke [94, 95].

3.6 Hemorrhagic Transformation

Hemorrhages or hemorrhagic transformation of infarction can be detected in research animals with T2*-weighted (T2*W) imaging [96] and susceptibility-weighted imaging (SWI), which is especially a useful technique for the detection of microbleedings following stroke [97].

3.7 Inflammation: Nanoparticles

Inflammation is a main imaging target in stroke research. Iron oxide-based contrast agents of different sizes, i.e., small (SPIO) or ultrasmall (USPIO) superparamagnetic iron oxides, can induce positive or negative contrast on T1W and T2W MRI, respectively (although T2 effect usually prevails and masks T1 effects). After injection into the circulation of a living organism, these particles are eagerly phagocytosed by monocytes, and it is assumed that under inflammatory conditions migration of monocytes into injured tissues should lead to accumulation of paramagnetic material in macrophages. These strategies have been explored in models of brain ischemia (see reviews refs [98, 99]). However, a number of controversies still surround their actual applicability to image inflammation after brain ischemia. It is not fully clear whether nanoparticle-charged macrophages or free nanoparticles reach the brain from blood when the BBB is damaged leading to nonspecific contrast enhancement. For further information the reader is referred to specialized studies on this subject [94, 100–106].

3.8 Advanced Contrast Agents

Imaging advances rely in part in the development of new contrast agents for molecular imaging. Several contrast agents that can label a specific biological process have developed with applicability in stroke research [107]. For instance, redox processes have been imaged after brain ischemia in rats using a nitroxide MRI contrast agent [108]. Many new adventures in MRI research are based on the synthesis of novel functionalized nanoparticles with paramagnetic properties. These nanoparticles are directed toward specific targets, and one main interest is the field of inflammation. Given the difficulties of getting nanoparticles into the brain, some studies in animal models of brain inflammation, including stroke, are using nanoparticles which target the inflamed endothelium to visualize vascular inflammation in the brain tissue [109]. Functionalizing strategies include using antibody-conjugated microparticles against vascular cell adhesion molecules [110–114] or using glyconanoparticles displaying the natural complex glycan ligand of selectins [109]. An interesting approach is the use of enzyme-activatable

MRI agents that only manifest paramagnetic properties after enzyme cleavage. An elegant example of this strategy has been reported noninvasively in living animals after stroke using a compound capable of tracking the oxidative activity of the proteolytic enzyme myeloperoxidase, which is derived from infiltrated neutrophils first and then from reactive microglia/macrophages in a later stage [115].

3.9 New Developments in MRI in Stroke Research

The development of contrast agents for MRI is a very active field of research that is already witnessing interesting developments with application in stroke research. Paramagnetic functionalized nanoparticles have been designed to contain therapeutic agents that can be directed to specific sites and thus combine therapeutic and diagnostic capabilities (theranostics). For instance, anti-72 kDa heat-shock protein vectorized stealth immunoliposomes containing paramagnetic probes have been used to encapsulate a therapeutic agent for the treatment of cerebral ischemia [116]. In the recent years, many stroke studies have used MRI for noninvasively tracking transplanted stem cells labeled with different sorts of paramagnetic agents [117–121] or with ^{19}F [122]. More challenging is the possibility that paramagnetic nanoparticles can be used for tracking neural progenitor cells after ischemia, with some studies claiming its feasibility using specific silica-coated nanoparticles [123] and others showing the opposite [124].

Also, MRI techniques have been developed to measure pH using the CEST effects from amide protons in mobile peptides and proteins [125]. Novel developments in this field have allowed quantitative tissue pH measurement during cerebral ischemia with MRI using corrected CEST [126] or amine and amide concentration-independent detection (AACID) [127].

Improving the detection of the penumbra is challenging and efforts are made using contrast agents. An MRI technique enabling the identification of the penumbra as a region of increased T2* signal change during a transient oxygen (100%) challenge [78] has been recently refined using oxygen-carrying perfluorocarbon (PFC) emulsion to enhance the sensitivity with lower levels of inspired oxygen [128]. Multinuclear H^1/Na^{23} MRI has been used to measure the changing sodium signal and ADC in the ischemic core and penumbra after rat MCAO, and reduced sodium-MRI signal has been suggested as a viability marker for penumbra detection [129]. Quantitative Na^{23} MRI has been combined with histochemical K^+ staining to study local Na^+ and K^+ imbalances within the ischemic tissue [130]. Moreover, K^+ images of the ischemic brain have also been obtained using K^{39} MRI, in spite that it provides a poor signal-to-noise ratio that can be improved using a cryogenic surface resonator [131].

Multiparametric quantitative MRI using the BOLD effect (see Note 3) seems to be a promising tool to map tissue oxygen

saturation with high spatial resolution, as recently shown in a rat stroke model highlighting the hypoxic zones [132]. Recent developments in fMRI include spin-lock (SL) fMRI, which is sensitive to energy metabolism alterations and responds to cortical spreading depression [133], with potential applicability to stroke research. Also, high-field (11.7 T) fMRI implemented with a line scanning method provides high temporal (50 ms) and spatial (50 μm) resolution [134] that might have applicability to study functional neural organization in chronic stages after stroke.

In the last few years, magnetic resonance elastography (MRE) has been applied to stroke research. MRE allows the noninvasive assessment of tissue elasticity [135]. Using this technique, brain tissue softening was correlated with reduced neuronal density after MCAO in mice [136]. Conversely, it has been suggested that neurogenesis increases brain stiffness assessed with MRE [137]. Further studies using MRE are needed to fully understand the potential usefulness of this technique in stroke research.

4 PET

4.1 Introduction

PET is a unique tool to image brain metabolism and function and it finds extensive application in neurosciences. PET images are generated after injection of a tracer molecule that is radioactively labeled with a positron emitter isotope with high energy but a very short half-life (from minutes to hours). The main advantages of this technology are the generation of tomographic images and the possibility of obtaining fully quantitative information on molecules in living organisms. Its main limitations for studies in small animals are low availability and relatively high cost and poor spatial resolution. PET has certainly had a strong impact on the current knowledge of metabolic and functional alterations in stroke, and it has contributed to cerebral blood flow studies and to defining the ischemic penumbra. Some of these achievements have been obtained in animals (nonhuman primates and cats) but fewer in rodents because of their size limitation. Animal-dedicated PET cameras are now available for imaging rodents and their spatial resolution has increased (generally within 1–2 mm). The spatial resolution of PET is therefore much lower than that of MRI, and often co-registration of PET images with 3D-MRI images from the same individual helps to localize the anatomy of the regions with affected signals. For these reasons, hybrid PET/MRI systems are being used in experimental and clinical setting for high-resolution and anatomical detail to better visualize and localize the functional data and allow the correction for attenuation of the PET data [138]. The limitation of the use and quantification of PET studies in small animals is addressed in Note 5.

4.2 Materials

4.2.1 Instrumentation

Positron emitter isotopes are generated in a cyclotron located in situ near the PET cameras. In order that the PET tracers can target specific molecules, the radioactive isotopes must also be incorporated to precursor compounds to finally generate the labeled molecule of interest. This requires the cooperation of a radiopharmaceutical department that can produce the labeled tracers fast. After in vivo tracer administration, positrons emitted by the isotope can only travel a very short distance (mm) before they encounter electrons. Annihilation occurs, emitting two photons in opposite directions, which can be detected simultaneously by the scanner ring of the PET camera. Tomographic images thus generated bear information from which fully quantitative data can be obtained. A typical PET isotope is ^{11}C, which can easily be incorporated to organic compounds. ^{11}C has a half-life of 20.3 min, which means that the radio-synthesis must occur very fast, before the radioactive decay is too advanced. This makes preclinical and validation studies with [^{11}C]-labeled compounds technically difficult. One of the preferred PET isotopes is ^{18}F, which with a half-life of 109.8 min allows more extensive preclinical ex vivo studies with the labeled molecule and thus facilitates images of a better quality.

4.2.2 Specific Activity

The injected radioactive molecules are tracers as the injected mass is very low while the radioactive content is high. Therefore, the specific activity (SA) of the injected molecules is normally very high, while the biological activity of the injected radioactive molecules is expected to be negligible.

4.2.3 Anesthesia

See Sect. 2.2 above, as well as Note 1 and Note 2. Anesthetized animals must also be monitored for physiological constants as described above for MRI (see Sect. 2.3).

5 Methods

5.1 Glucose Utilization

The study of glucose utilization by PET using [^{18}F]fluorodeoxyglucose ([^{18}F]FDG) is by far the most frequently used PET technique in humans as it has many different clinical applications, particularly to evaluate tumors and alterations in cerebral energy metabolism. The PET technique is based on Sokoloff's autoradiographic technique [139], which has been extensively used in animal models of brain ischemia (e.g., [140]). In vivo PET studies with [^{18}F]FDG are feasible in rodents and have been used in rats (e.g., ref. [141]) and mice (e.g., ref. [142]) to assess neurodegeneration under various experimental conditions. By using [^{18}F]FDG and taking into account the arterial input function, the full quantification of regional cerebral glucose utilization is feasible in rats [143, 144] and also in mice [145, 146]. PET imaging studies using [^{18}F]FDG have mainly demonstrated reductions in glucose consumption in

the ischemic regions. Nevertheless, depressed glucose metabolism at reperfusion was not always associated with later development of infarction [147]. In other studies, [^{18}F]FDG has appeared as a sensitive approach to distinguish between the recruited tissue and the recoverable tissue that can be salvaged with the presence of reperfusion after cerebral ischemia [14, 148, 149]. Overall, PET with [^{18}F]FDG can be considered as a valuable method for the prediction of tissue fate following preclinical models of stroke [150]. Furthermore, [^{18}F]FDG has been used as a valuable imaging modality to demonstrate functional recovery after transplantation of induced pluripotent stem cells [151] and bone marrow stromal cells [152] after cerebral ischemia in rats.

5.2 Oxygen Metabolism and CBF

PET studies in acute stroke patients have provided singular data on the metabolic status of the ischemic brain. Cerebral metabolic rate for oxygen ($CMRO_2$) and the oxygen extraction fraction (OEF), both relevant measures in acute stroke, can be obtained after inhalation of O-15-labeled oxygen gas ([^{15}O]O_2). OEF is taken as a marker of the ischemic penumbra. Indeed, increased oxygen consumption under conditions of moderate decreases in blood flow translates the metabolic demand of viable penumbral tissue with deficient blood supply. Interestingly, comparisons of regions with increased OEF and hyperintense DWI underscored that the DWI lesion may contain some viable tissue, as the DWI/PWI mismatch area overestimated the penumbra as defined by PET [69–72].

Unfortunately, studies of oxygen metabolism using inhaled gas in rodents are technically difficult as the radioactivity in the gas tubing reaching the anesthetized animal causes interference in the brain image [153]. To overcome this, a complex system was developed for administration into rats of an injectable preparation of [^{15}O]-O_2 that was obtained after gas circulation through an artificial lung [154]. This procedure allowed the in vivo study of oxygen metabolism and OEF in rat brain [153, 154]. The same technique was applied to study $CMRO_2$ and OEF in rat stroke models [155, 156]. Nonetheless, images obtained with [^{15}O]O_2 have a low spatial resolution due to the ^{15}O isotope's features (high energy, very short half-life), and the images barely reach useable quality. In spite of these limitations, these authors showed a compensatory increase in the oxygen extraction fraction (OEF) 1 h after MCAO in rats in the ipsilateral versus the contralateral hemisphere [156]. More recently, the feasibility of quantitative PET measurement of CBF, OEF, and $CMRO_2$ has been demonstrated using the steady-state inhalation method of [^{15}O]O_2 and [^{15}O]CO_2 gases in anesthetized rats [157].

PET with [^{15}O]H_2O is a robust and well-validated imaging technique to study cerebral perfusion in humans [158], but the availability of [^{15}O]H_2O is rare in routine clinical settings. Likewise, the same limitations of the ^{15}O isotope apply in terms of spatial

resolution in the small animal. Nevertheless, quantitative measures of CBF can be obtained in the rat brain in vivo with PET using [^{15}O]H_2O as the tracer [156, 159, 160]. PET with [^{15}O]H_2O has evidenced the ability to detect subacute hemodynamic changes after cerebral ischemia involving hyperperfusion that might be related to angiogenesis and functional recovery [161].

Several indirect strategies including measuring [^{18}F]FDG influx [162] can also be undertaken to assess CBF. These approaches are used in vivo in the ischemic rat and they can, in combination with other tracer studies [155, 162], provide valuable information on cerebral perfusion. Finally, PET imaging of cerebral perfusion has been also carried out by using [^{13}N]ammonia showing similar results than that obtained with [^{15}O]H_2O [163].

5.3 Neuronal Viability and Neurogenesis

The PET tracer [^{11}C]flumazenil has been proposed as a surrogate marker of neuronal fate after stroke [164–168]. Flumazenil (Ro 15–1788) binds the central-type benzodiazepine receptors that are principally located on neurons; as a result, the receptor density changes according to the neuronal density [169]. In humans and cats, reduced [^{11}C]flumazenil binding is associated with development of infarction. However, autoradiographic studies in rodents with [^{3}H]flumazenil showed that binding was not decreased in the striatum and cerebral cortex until several days after ischemia/reperfusion in rats [170] and mice [171]. Therefore, controversy exists over the results with radioactive flumazenil after ischemia in vivo by PET in cats and humans [164–168] versus in vitro autoradiographic studies in rodents [170, 171]. Using in vivo PET with [^{11}C]flumazenil in rats after transient MCAO, we found no alteration of tracer binding during the first 8 h postischemia [172]. While reduced [^{11}C]flumazenil is a precise marker of neuronal death [167], it is possible that lack of detectable changes does not necessarily imply lack of cell death since decreased [^{11}C]flumazenil binding might depend on the extent of cell death and kind of affected neurons. Further in vivo studies with [^{11}C]flumazenil in rodents are required using several degrees of ischemia and longitudinal studies in the same animals to better understand the sensibility of this technique to mark neuronal cell death.

A few years ago, a novel PET imaging technique using [^{18}F]-fluoro-3′-deoxy-3′-L-fluorothymidine ([^{18}F]FLT) was established to evaluate endogenous neural stem cell (NSC) mobilization after cerebral ischemia [173]. [^{18}F]FLT is a radiotracer used to image cell proliferation that visualizes neurogenic processes in vivo. These authors have demonstrated that [^{18}F]FLT can be used to monitor NCSs in adult rat induced by experimental stroke [173]. Therefore, PET with [^{18}F]FLT might be useful for monitoring the efficacy of treatments promoting neurogenesis in longitudinal studies following stroke.

5.4 Imaging Brain Inflammation

Imaging inflammation in the brain with noninvasive methods is a main goal in experimental and clinical research in various brain pathologies, including stroke [174]. The most extensively used PET tracer targeting inflammation is [^{11}C]PK11195. This compound is an antagonist of the peripheral benzodiazepine receptor (PBR) [175], also called translocator protein-18 (TSPO) [176]. Autoradiographic studies showed that binding of several TSPO ligands increased after experimental focal ischemia [177, 178]. [^{3}H]PK11195 binds to microglia/macrophages after ischemia [179, 180], but several studies also suggested some binding to reactive astroglia [181]. PET studies with [^{11}C]PK11195 have shown increased binding in the brain of stroke patients [182–185]. PET studies with [^{11}C]PK11195 in animal models of stroke (Fig. 5) show increased binding of this tracer in the infarcted region and the periphery at 4–7 days following transient MCAO in rats [186]. The latter study illustrated that this tracer is useful for imaging the cerebral inflammatory reaction after ischemia, but emphasized that the expression of TSPO was not homogeneous through the population of reactive microglia/macrophages. A recent study in a model of permanent ischemia in rats showed predominant [^{11}C]PK11195 binding in peripheral regions [162], thus suggesting that the regional pattern and features of microglia activation might be different after permanent and transient ischemia. Over the last decade, the aims to provide a better signal-to-noise ratio and reduce the high level of nonspecific binding have triggered a renewed effort to develop improved TSPO PET radiotracers [187]. Most of these tracers, such as [^{11}C]PBR28, [^{11}C]DAC, [^{18}F]FEAC, [^{18}F]FEDAC, [^{18}F]GE-80, and [^{18}F]DPA-714, have been used to monitor TSPO expression following rodent models of cerebral ischemia [188–194]. In addition, [^{18}F]DPA-714 has shown TSPO binding decrease in ischemic rats treated with minocycline, evidencing its usefulness to evaluate novel anti-inflammatory strategies in experimental cerebral ischemia [195]. Likewise, among the alternative PET radiotracers for TSPO, the labeling with fluorine-18 has extended its use from the bench to the bedside. For all these reasons, [^{18}F]DPA-714 has been considered as a promising radiotracer which is becoming widely used, particularly in experimental animal studies.

Therefore, the in vivo PET imaging of neuroinflammation has been almost exclusively limited to the study of TSPO. A very recent study has used PET imaging with 2[^{18}F]-fluoro-A85380, a selective radioligand for the nicotinic acetylcholine receptors (nAChRs) $\alpha_4\beta_2$, to evaluate $\alpha_4\beta_2$ binding after cerebral ischemia in rats [196]. These authors have demonstrated the increase of $\alpha_4\beta_2$ binding in microglia/macrophages and astrocytic cells that was consistent with the binding profile of [^{11}C]PK11195 following stroke. In addition, the treatment with the $\alpha_4\beta_2$ antagonist dihydro-β-erythroidine hydrobromide (DHβE) showed an increase of [^{11}C]

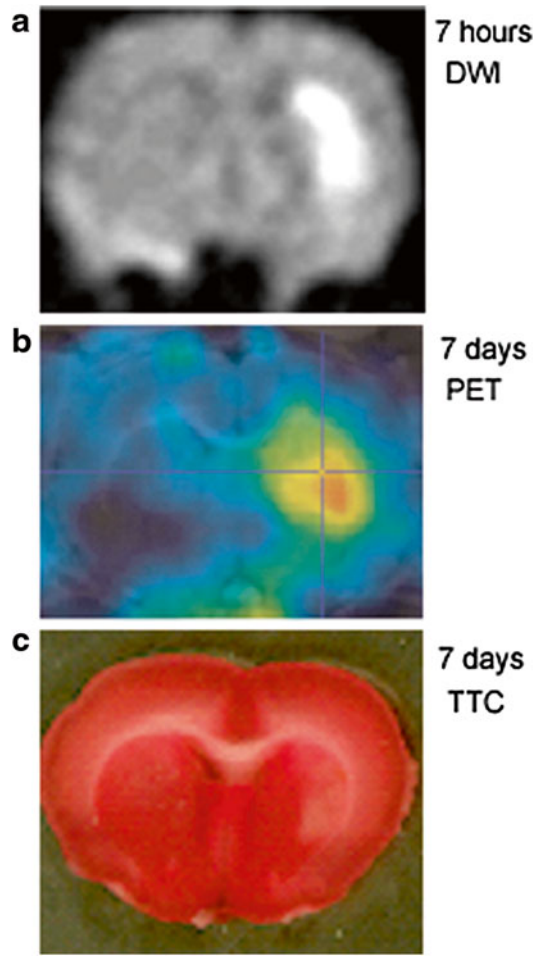

Fig. 5 Imaging inflammation in vivo in the rat 7 days after transient MCAO with PET using the TSPO ligand ^{11}C-PK11195. PET images were co-registered with a rat brain atlas. (**a**) MRI image obtained by DWI at 7 h after MCAO. *White area* shows the affected region (striatum). (**b**) ^{11}C-PK11195 PET image of the same rat at 7 days postischemia. Color code for higher binding is: *red*> *yellow*> *blue*. (**c**) Histological staining (TTC) of the postmortem tissue at day 7 of the above rat showing a small striatal infarction (*pale zone* in the striatum at the right-hand side of the image)

PK11195 binding at day 7 after reperfusion [196]. Altogether, these findings suggest the existence of novel and suitable PET imaging markers to evaluate neuroinflammation following stroke. Active research is currently ongoing to develop novel tracers for imaging neuroinflammation by PET.

5.5 New PET Developments Relevant to Stroke Research

Imaging hypoxia is one of the recent achievements in PET research that has had an impact in animal models of ischemia. This was achieved using a tracer named [^{18}F]fluoromisonidazole ([^{18}F]FMISO) that images hypoxia [197, 198]. The first study with [^{18}F]

FMISO in rats after 2 h MCAO was an autoradiographic study that suggested that this tracer was a marker of the ischemic penumbra [197]. Later, in vivo PET studies with [^{18}F]FMISO in rats subjected to permanent or transient MCAO again supported it as a marker of viable hypoxic tissue after stroke [198].

In vivo imaging of neurotransmitter receptors with [^{11}C]raclopride, [^{11}C]DASB, and [^{18}F]altanserin, ligands for dopamine D_2 receptors, serotonin transporter (SERT), and serotonin receptor 5-HT_{2A}, has evidenced changes in receptor expression. Binding alterations became apparent in both the ischemic and the contralateral brain regions suggesting receptor involvement in functional recovery after cerebral ischemia [199, 200].

Recently, PET imaging of cystine/glutamate antiporter (xc^- system) with (4S)-4-(3-[18F]fluoropropyl)-L-glutamate [^{18}F] FSPG has displayed increased xc^- system function at few hours after cerebral ischemia in rats, supporting the contribution of xc^- system to the glutamate release during stroke [201].

Likewise, PET findings have also been reported in the field of angiogenesis, as was published for the rat after transient MCA occlusion by using the tracer 64Cu-DOTA-VEGF121, that allows imaging VEGFR expression in vivo by PET [202].

The application of PET studies to stroke research in the future will rely on the development of newer tracers able to track the molecular processes involved in the physiopathology of brain ischemia. Developments, for instance, in the field of imaging activated matrix metalloproteinases [203–207], may have a future application for in vivo PET/SPECT imaging in animal models of stroke and likely in stroke patients.

6 SPECT

6.1 Introduction

Single-photon emission computed tomography (SPECT) is a nuclear imaging technique that together with PET has provided valuable knowledge on pathological brain function. SPECT images are generated after injection of single gamma-emitting radioisotopes with lower energy and higher half-life (from hours to days) than PET tracers. The main advantages of this technology are (1) the capability to perform longitudinal tracking of labeled cell-based therapies due to the long half-lives of the radiotracers, (2) the possibility to distinguish between two different radioisotopes when injected simultaneously owing to the emission at different energies by gamma-emitting radioisotopes, and (3) the fact that it does not require a cyclotron for the production of radiotracers increases the availability and decreases costs in relation to PET. The main disadvantages are the worst resolution and sensitivity with respect to PET. Despite this, new generation of microSPECT cameras have improved these limitations decreasing its differences with microPET

technology [208], and SPECT can be a useful tool in experimental animal research [209]. The use of SPECT imaging to evaluate preclinical stroke has been much more restricted than PET, despite its usefulness to evaluate cerebral perfusion and cell therapy in animal models of cerebral ischemia. SPECT imaging provides functional and anatomical information of pathologic events. High-resolution detail from computed tomography (CT) scanner is used to localize and correct the SPECT signal for attenuation. For this reason, hybrid SPECT/CT systems are becoming more common in hospital and imaging laboratories. The limitation of the use and quantification of SPECT studies in small animals is addressed in Note 6.

6.2 Materials

6.2.1 Instrumentation

The single-photon emitting radiotracers allow for long-distance transportation due to its long half-lives or can be obtained on site via generator systems. Likewise, radiotracers for SPECT can be easily prepared on site using commercial reagents and kits. Therefore, in contrast with PET, the infrastructure associated with cyclotron production is not required. After in vivo tracer administration, gamma photons are detected in gamma cameras that utilize lead or tungsten collimators to capture photons with correct trajectories. To obtain tomographic images of the subject, detectors with collimators rotate around the subject acquiring sufficient number of angular views. Despite methods for reconstruction being similar, principles of acquisition might be different depending on the use of different types of collimators (e.g., parallel hole, pinhole). Collimators are designed to eliminate all photons with a different trajectory to the detector surface. However, the design of a collimator can also limit the direction of the incoming photons resulting in a loss of sensitivity. Finally, the gamma-emitting isotopes for SPECT include ^{99m}Tc (half-life ($t_{1/2}$) = 6 h), ^{123}I ($t_{1/2}$ = 13.3 h), ^{111}In ($t_{1/2}$ = 2.8 days), and ^{67}Ga ($t_{1/2}$ = 2.8 days), among others.

6.2.2 Specific Activity

See Sect. 4.2.2.

6.2.3 Anesthesia

See Sect. 2.2 above, as well as Note 1 and Note 2. Anesthetized animals must also be monitored for physiological constants as described above for MRI (see Sect. 2.3).

7 Methods

7.1 Brain Perfusion

Imaging of brain perfusion with SPECT has been performed with [^{99m}Tc]hexamethylpropylene-amino-oxime ([^{99m}Tc]HMPAO). HMPAO is removed from blood during its first pass through the brain and decomposes rapidly into a hydrophilic secondary complex. The hydrophilic metabolite of [^{99m}Tc]HMPAO is trapped in the parenchyma in a manner dependent on the CBF rate [210].

SPECT images of [^{99m}Tc]HMPAO distribution have shown regional CBF before, during, and after cerebral ischemia in rats [110, 157]. In fact, [^{99m}Tc]HMPAO SPECT signal ratios have evidenced a good correlation with [^{15}O]H_2O PET during and after ischemia in rats [211]. In addition, [^{99m}Tc]HMPAO has also been used to predict the extent of infracted tissue in rodents following stroke [211].

7.2 Neuronal Activity and Viability

Neuronal integrity can be visualized with SPECT using [^{123}I]iomazenil that is a selective radioligand for the central type of benzodiazepine receptor (CBR), a selective receptor of neurons. [^{123}I] iomazenil uptake in the human brain decreases after stroke [212]. In animal models of cerebral ischemia, [^{123}I]iomazenil has been used to monitor preservation of neuronal integrity following bone marrow stromal cell-based therapy. These studies supported the usefulness of this radiotracer to evaluate functional recovery after cell therapy [213].

Tissue viability following stroke has been assessed by [^{99m}Tc] ethylcysteinate dimer ([^{99m}Tc]ECD), a small lipophilic molecule that crosses the blood–brain barrier and is hydrolyzed to [^{99m}Tc] ethylcysteinate monomer ([^{99m}Tc]ECM) in the brain. [^{99m}Tc]ECM is hydrophilic and does not permeate back to the blood stream. Cerebral infarction reduces the enzymatic activity that mediates the hydrophilic conversion of Accordingly, [^{99m}Tc]ECD [214]. [^{99m}Tc]ECD uptake decreases in the infarcted brain regions after cerebral ischemia in rats [214].

7.3 Cellular Apoptosis

[^{99m}Tc]hydrazine nicotinamide-labeled annexin V ([^{99m}Tc]-HYNIC-annexin V) has been used as a tool to evaluate cellular stress and apoptosis in humans [215] and in a model of global cerebral ischemia [216]. Likewise, SPECT imaging of annexin V in ischemic rats showed signal uptake in distant regions to the site of infarction suggesting its capability to define tissues at risk for cell death that may recover over time [217].

7.4 Neuro-inflammation

As previously described, imaging of brain inflammation following ischemia has been mainly concentrated in the use of TSPO PET radiotracers (see Sect. 5.4). Despite this, SPECT imaging of brain inflammation is also possible with the TSPO tracer [^{125}I]-CLINDE [165]. [^{125}I]-CLINDE is a valuable tool to explore increased density of TSPO after cerebral ischemia in rats by SPECT as a marker of brain inflammation [218].

7.5 Cell Tracking

Long half-lives of SPECT radiotracers allow for tracking of initial movement, localization, and engraftment efficiency of infused cells. The main strategy to track cells for SPECT imaging has been the labeling of human umbilical cord blood (HBUC) and bone marrow-derived mesenchymal stromal/stem (BMMSC) cells with

[^{111}In]oxine [219–222]. This strategy allows monitoring the in vivo biodistribution of the labeled cells. While intravenous administration of [^{111}In]oxine-labeled human umbilical tissue-derived cells (hUTC) has shown histological improvements after cerebral ischemia [221], other studies have not observed functional recovery or histological protection after [^{111}In]oxine-hUTC cell treatment [219, 220]. Likewise, intra-arterial infusion of [^{111}In]oxine-labeled BMMSCs has evidenced increased cell recruitment in the ischemic hemisphere compared to the nonischemic region [222]. Finally, other strategies, such as the reporter gene-probe system HSV1-tk–[^{131}I]-29-fluoro-29-deoxy-1-b-D-arabinofuranosyl-5-iodouracil ([^{131}I]-FIAU), can be useful to monitor stem cells in experimental cerebral ischemia in rats [223].

8 Notes

8.1 Note 1: MRI in Awake Rats

MRI can be performed in non-anesthetized rats after a training period habituating them to the holder and the magnet environment (e.g., [224–229, 230]) and using a chronically implanted surface coil [231]. The use of MRI in awake rodents has grown in the last years, particularly for the investigation of functional neuronal networks. This technology has allowed for comparisons between the responses of awake and anesthetized animals (e.g., [232, 233]). Furthermore, recent developments enabled combining fMRI and optogenetics in awake rats [234]. Likewise, PET studies have been performed in non-anesthetized rats (e.g., [175, 235–238]), and PET combined with optogenetic stimulation has been used for mapping brain metabolic connectivity in awake rats [239].

8.2 Note 2: Anesthetics and Brain Metabolism

In spite of efforts to image the brain in awake animals, most imaging works use anesthetics. It has been estimated that anesthesia-induced loss of consciousness reduces cerebral energy consumption by 45 % [240]. Anesthetics minimizing alteration of neuronal activity or blood flow are required in functional imaging studies (for review on anesthetics in imaging studies, see refs [16, 241, 242]). Although isoflurane anesthesia is widely used in many imaging works [243, 244], PET studies have shown that it depresses brain glucose metabolism [146] and it can induce several alterations in neuroreceptor binding, for instance, as reported using a tracer for the serotonin receptor 5HT-1A [245]. α-Chloralose and urethane are the most widely used anesthetics in functional MRI studies but are highly toxic and therefore not suitable for longitudinal studies. Several works (e.g., [18, 246–251]) highlighted the greater suitability of sedation with medetomidine hydrochloride, a non-opioid synthetic α2-adrenoreceptor agonist with sedative action that provides pain relief as well as muscle relaxation and does not seem to alter blood flow, compared with general anesthesia. The drug is

approved for veterinary use and is appropriate for imaging studies in rodents, particularly those involving evaluation of brain activity and CBF. Several studies in rodents have investigated the effects of different anesthetics or different levels of anesthesia on imaging data, such as the binding of various PET tracers (e.g., [252, 253]), brain blood oxygenation levels [254], and fMRI responses [255–259].

8.3 Note 3: MRI Images and Sequences

Some basic comments on the MRI scans and sequences most frequently used to study animal models of stroke are given below (for specialized reading, see refs [7, 8]). MR images are obtained by using the relaxation of the excited nuclei after application of a radiofrequency pulse. The relaxation following the time course of the longitudinal component of the net magnetization is called T1 (longitudinal relaxation time), whereas that of the transversal component corresponds to T2 or T2* (transversal relaxation time). T2* parameter includes all factors that influence the nuclei asynchrony, whereas T2 is exclusively based on influences due to the intrinsic composition and structure of the tissue. The T1 and T2 relaxation times are the major determinants of signal intensity and contrast. The fact that many parameters are involved in the generation of images has inspired the development of an extensive variety of MR sequences (acquisition schemes). Most common sequences can be grouped in two main classes: gradient-echo (GRE) and spin-echo (SE). These sequences have various parameters that can be tuned for contrast definition, such as repetition time (TR), flip angle (θ), echo time (TE), and time of inversion (TI). GRE sequences can be faster than the SE [8, 9]. This rich assortment of sequences allows for the generation of a variety of different images. Combinations of the imaging parameters (e.g., TR, θ, TE, TI, etc.) can power the image toward T1- or T2-weighted images. Also, proton density-weighted images can be obtained that have minimal T1 and T2 components, but the contrast depends on the density of protons in the tissue. Investigation is required to find out which scans best show up alterations that correspond with pathology and are useful for characterizing the brain lesion. The following is a list of basic images of interest in animal stroke research:

1. *T1-weighted* (*T1W*) *imaging*: This scan is generally made with GRE sequences and the correct choice of a short TR is very important. T1W provides a good contrast between white and gray matter, and it is very useful for obtaining high-resolution 3D reconstructions. White matter appears in pale gray in T1, whereas fluids, such as the cerebrospinal fluid (CSF), look dark. 3D T1-weighted imaging using a 3D-modified driven equilibrium Fourier transform (MDEFT)-based acquisition is suited to voxel-based morphometry analysis at 3 T in humans [260], and MDEFT protocols are also useful in animal studies of cerebrovascular diseases [261]. Several contrast agents used to assess

BBB integrity, such as the clinically used gadolinium-based contrasts, shorten the T1 relaxation time and give a positive signal in T1 (hyperintensity) (see Sect. 3.4 above).

2. *T2-weighted* (*T2W*) *imaging*: This image uses SE sequences. Here, the choice of TE is important to obtain images of good quality. In T2, the white matter is seen in dark gray, whereas CSF appears white. These images are very sensitive to brain pathology and show up ongoing or recent neuronal cell death and also evidence vasogenic edema. Paramagnetic gadolinium contrasts induce a signal decrease in T2-weighted images.
3. *T2*-weighted* (*T2*W*) *imaging* : T2*W has a T2 component, but it uses GRE sequences. Gradient-echo sequences are very sensitive to magnetic field inhomogeneities, such as those caused by deoxyhemoglobin, and thus are useful for detecting hemorrhage or hemorrhagic transformation of brain infarction [85]. Also T2*W is useful to evidence iron accumulation, as was shown in the thalamus of the rat secondary to infarction in the MCA region [262]. T2*W imaging can be used for fMRI (see below).
4. *Perfusion-weighted imaging* (*PWI*) is used mainly to assess and quantify CBF. Several PWI techniques have been developed and are in use in small animals. Contrast-based perfusion allows measurement of the curve of contrast flowing through a brain region or a voxel after an i.v. bolus injection of a gadolinium chelate, which causes a negative signal in T2 or T2* sequences [263]. The area under the curve can then be measured to generate maps of cerebral blood volume (CBV). Various functional maps can be generated from the raw data, such as the mean transit time (MTT) and the time to peak (TTP) that refer to the time course kinetics of contrast passage through a particular zone. These parameters allow the quantification of CBF. In addition, completely noninvasive contrast-free images of brain perfusion can be obtained with arterial spin labeling (ASL) techniques [264, 265]. ASL thus offers a great advantage over other PWI techniques and is being used successfully in rodents (e.g., [266, 267]). Several improvements in the technique can provide a rapid and quantitative in vivo assessment of tissue perfusion [268] and estimations of arterial oxygen saturation among other measurements [269]. Its limitations are generally a low signal-to-noise ratio and the complexity of kinetics for fully quantitative data. Nonetheless, imaging and quantification have been achieved and are being carried out in rodents after brain ischemia (e.g., [92, 270, 271]).
5. *Proton density-weighted* (*PDW*) *images*: these sequences can provide anatomic images [30] that are useful for the construction of an MRI brain atlas. Glial scars can become evident as hyperintensities in PDW images, which are also known to reveal

changes in water content [272]. Also, vascular regions show hypointensity in PDW images [56].

6. *Diffusion-weighted imaging* (*DWI*) assesses the diffusion movement of water molecules. Long scanning times due to the use of diffusion gradients usually requires the use of fast SE echo-planar imaging (EPI) sequences for SWI that allows for enough sensitivity to changes in the signal due to molecular motion at affordable scanning times. A diffusion map can be constructed, i.e., the apparent diffusion coefficient (ADC) map, showing parametric images, which allow for absolute quantification of diffusion data [22–25].
7. *Diffusion tensor imaging* (*DTI*) is one of the most suitable techniques for studying white matter and fiber tracts. DTI is based on the fact that tissue water diffusion is affected by the presence and orientation of barriers to translational motion (such as cell membranes and myelin fibers) [35]. This phenomenon is called diffusion anisotropy [273] and can be expressed as an index called fractional anisotropy (FA). Then, brain maps of diffusion directions in each voxel can be reconstructed and used for in vivo 3D tractography that is used not only in humans (e.g., [274]) but also in animal studies of brain connectivity (e.g., [275, 276]) including experimental models of cerebral ischemia (e.g., [36, 277]).
8. *Functional MRI* (*fMRI*). This technique is based on the blood-oxygen-level-dependent (BOLD) effect that depends on the magnetic properties of oxyhemoglobin and deoxyhemoglobin and on the hemodynamic response to brain activity. Increases in brain activity enhance the oxygen demand and trigger proportionally higher increases in CBF, leading to a rise in the fraction of blood oxyhemoglobin, which in turn enhances the T2* signal [278]. This technique is extensively used in humans to study brain activation under different tasks [279]. In animals, fMRI is suitable for studying somatosensory neuronal circuits after different stimuli, such as whisker stimulation [280], visual [281], and the most frequently used model of electrical forepaw stimulation [246, 282, 283]. Currently, stimuli-free functional imaging by detection of low-frequency fluctuations in resting animals (resting-state- or lff-fMRI) is a very active field of research to depict neuronal networks, remodeling, and brain plasticity, eliminating the (usually complex) task of external stimulation of the animals [47, 48].

   A variation of this functional MRI termed pharmacological fMRI (ph-fMRI) [284] may also give valuable information in stroke research [285]. This technique is based on the neural activation produced by drug-driven stimulation of brain activity. Selective drugs can be used to specifically activate certain neurotransmitter pathways.

9. *Magnetic resonance angiography* (*MRA*): MR angiograms in small animals can be obtained in a fully noninvasive manner using a contrast-free technique called time-of-flight MRA (TOF-MRA). This technique can be somewhat improved by reducing the acquisition time after intravenous (i.v.) administration of a low dose of a gadolinium-based contrast agent [286]. New developments allow for high-resolution structural and functional assessment of the cerebral microvasculature with modified MRA protocols [287].

8.4 Note 4: Time Point of Image Acquisition

It is often useful to perform a pre-scan of the animal before inducing ischemia using the sequence of choice and the same scanning protocol. This image can be co-registered with subsequent images obtained after induction of ischemia. It may also allow correction for individual differences and facilitate quantification of changes. Methods have nonetheless been developed for performing ischemia inside the magnet [288, 289]. While technically highly demanding, this procedure is feasible and is currently being used by a few laboratories. Alternatively, after a pre-scan, the animal is taken out of the magnet, ischemia is induced, and animals are brought back to scanning as many times as necessary during or after the arterial occlusion.

8.5 Note 5: Difficulties for Quantification PET Studies

PET studies in small animals are difficult because of the low spatial resolution of the technique and partial volume effects that are complex to correct. Limitations on the use of [^{18}F]-FDG and other tracers in noninvasive PET studies in mice are discussed in the literature [290]. Full quantification of a biological process (e.g., binding of a molecule to a receptor) is often achieved after complex modeling signals from PET images that may require information of the arterial input function. This means that the time-activity curves of the injected radioactive molecule have to be measured, which often requires not only measures of plasma radioactive concentration but also separation of possible metabolites using analytical techniques (e.g., high-performance liquid chromatography or others) to account for the biological metabolism of the injected radioactive compound. These processes are obviously limiting given the extremely short half-life of the PET isotopes. In small animals, withdrawing multiple blood samples is possible (e.g., ref. [291], but difficult. Also, rapid reduction of blood volume may affect the process under study, and the procedure may not be practical when animals need to be kept for longitudinal studies. Recently, an automated blood sampling device to withdraw small blood samples from mice has been reported and used in an [^{18}F]-FDG PET study [145]. Nevertheless, alternative methods have also been developed for accurate signal quantification to avoid invasive blood sampling. For instance, a method was developed to measure the arterial input function in regions of interest drawn

over the heart, which was imaged at the same time as the brain, and this was applied to noninvasive quantitative measurement of CBF with [^{15}O]-H_2O [145]. Another method obtained an input function from dynamic image data and 0 or 1 blood sample for small animal [^{18}F]-FDG PET studies [291]. Correction of partial volume effects produced accurate quantification of glucose metabolic rate in rats and mice [291]. Most [^{18}F]-FDG PET studies in rodents, however, are semiquantitative only and rely on defining regional changes in signal intensity in relation to a reference region). In animal models of MCAO, signal intensity values of the ipsilateral hemisphere are frequently referred to values in the homologous contralateral region to assess pathological signal alterations.

8.6 Note 6: Difficulties for Quantification SPECT Studies

SPECT quantification is compromised by several factors including photon attenuation, photon scatter, partial volume effect, and motion artifacts. These variables can alter the capacity of SPECT to quantify the concentration of radioactivity in a given volume of interest and in absolute units. The development of iterative image reconstruction techniques has improved SPECT image reconstruction [292]. In addition, the appearance of hybrid systems SPECT/CT has provided the correction for photon attenuation, increasing the accuracy of SPECT imaging in quantifying radioactivity concentrations in tissues.

Acknowledgment

Supported by National Projects (SAF2014-56279-R, SAF2014-53412-R, SAF2014-54070-JIN) and European Projects from FP7 (INMIND, HEALTH-F2-2011-278850). MRI images presented in this text were obtained at the Experimental MRI Unit of IDIBAPS (Barcelona, Spain), using a 7T-BioSpec Magnet (Bruker). PET images were obtained at the Institut d'Alta Tecnología (IAT), Parc de Recerca Biomèdica de Barcelona (PRBB) (Barcelona, Spain), using a Concorde-R4 (Siemens) animal-dedicated PET camera.

References

1. Davis S, Fisher M, Warach S (2003) Magnetic Resonance Imaging in Stroke. Cambridge University Press, Cambridge, England
2. Weber R, Ramos-Cabrer P, Hoehn M (2006) Present status of magnetic resonance imaging and spectroscopy in animal stroke models. J Cereb Blood Flow Metab 26:591–604
3. Shen Q, Meng X, Fisher M et al (2003) Pixel-by-pixel spatiotemporal progression of focal ischemia derived using quantitative perfusion and diffusion imaging. J Cereb Blood Flow Metab 23:1479–1488
4. Knight RA, Dereski MO, Helpern JA et al (1994) Magnetic resonance imaging assessment of evolving focal cerebral ischemia. Comparison with histopathology in rats. Stroke 25:1252–1261
5. Neumann-Haefelin T, Kastrup A, de Crespigny A et al (2000) Serial MRI after transient focal cerebral ischemia in rats:

dynamics of tissue injury, blood–brain barrier damage, and edema formation. Stroke 31:1965–1972
6. Jacobs MA, Zhang ZG, Knight RA et al (2001) A model for multiparametric MRI tissue characterization in experimental cerebral ischemia with histological validation in rat: part 1. Stroke 32:943–949
7. Mitchell DG, Cohen MS (2003) MRI Principles. Elsevier Science, Philadelphia, PA
8. Brown RW, Cheng YCN, Haacke EM et al (2014) Magnetic Resonance Imaging: Physical Principles and Sequence Design, 2nd edn. Wiley-Blackwell, New York, NY
9. Roberts TP, Mikulis D (2007) Neuro MR: principles. J Magn Reson Imaging 26:823–837
10. Tofts P (2003) Quantitative MRI of the Brain: Measuring Changes Caused by Disease. John Wiley & Sons Ltd, West Sussex, England
11. Rojas S, Martin A, Justicia C et al (2006) Modest MRI signal intensity changes precede delayed cortical necrosis after transient focal ischemia in the rat. Stroke 37:1525–1532
12. Chen F, Suzuki Y, Nagai N et al (2007) Rodent stroke induced by photochemical occlusion of proximal middle cerebral artery: evolution monitored with MR imaging and histopathology. Eur J Radiol 63:68–75
13. Yang YM, Feng X, Yao ZW et al (2008) Magnetic resonance angiography of carotid and cerebral arterial occlusion in rats using a clinical scanner. J Neurosci Methods 167:176–183
14. Leftin A, Rosenberg JT, Solomon E et al (2015) Ultrafast in vivo diffusion imaging of stroke at 21.1 T by spatiotemporal encoding. Magn Reson Med 73:1483–1489
15. Shemesh N, Rosenberg JT, Dumez JN et al (2014) Metabolic T1 dynamics and longitudinal relaxation enhancement in vivo at ultrahigh magnetic fields on ischemia. J Cereb Blood Flow Metab 34:1810–1817
16. Hanusch C, Hoeger S, Beck GC (2007) Anaesthesia of small rodents during magnetic resonance imaging. Methods 43:68–78
17. Gozzi A, Schwarz A, Crestan V et al (2008) Drug-anaesthetic interaction in phMRI: the case of the psychotomimetic agent phencyclidine. Magn Reson Imaging 26:999–1006
18. Ramos-Cabrer P, Weber R, Wiedermann D, Hoehn M (2005) Continuous noninvasive monitoring of transcutaneous blood gases for a stable and persistent BOLD contrast in fMRI studies in the rat. NMR Biomed 18:440–446
19. Lin W, Paczynski RP, Kuppusamy K et al (1997) Quantitative measurements of regional cerebral blood volume using MRI in rats: effects of arterial carbon dioxide tension and mannitol. Magn Reson Med 38:420–428
20. Moseley ME, Cohen Y, Mintorovitch J et al (1990) Early detection of regional cerebral ischemia in cats: comparison of diffusion- and T_2-weighted MRI and spectroscopy. Magn Reson Med 14:330–346
21. Kohno K, Hoehn-Berlage M, Mies G et al (1995) Relationship between diffusion-weighted MR images, cerebral blood flow, and energy state in experimental brain infarction. Magn Reson Imaging 13:73–80
22. Hoehn-Berlage M, Norris DG, Kohno K et al (1995) Evolution of regional changes in apparent diffusion coefficient during focal ischemia of rat brain: the relationship of quantitative diffusion NMR imaging to reduction in cerebral blood flow and metabolic disturbances. J Cereb Blood Flow Metab 15:1002–1011
23. Hossmann KA (2008) Cerebral ischemia: models, methods and outcomes. Neuropharmacology 55:257–270
24. Dijkhuizen RM, Knollema S, van der Worp HB et al (1998) Dynamics of cerebral tissue injury and perfusion after temporary hypoxia-ischemia in the rat: evidence for region-specific sensitivity and delayed damage. Stroke 29:695–704
25. Kazemi M, Silva MD, Li F et al (2004) Investigation of techniques to quantify in vivo lesion volume based on comparison of water apparent diffusion coefficient (ADC) maps with histology in focal cerebral ischemia of rats. Magn Reson Imaging 22:653–659
26. Røhl L, Ostergaard L, Simonsen CZ et al (2001) Viability thresholds of ischemic penumbra of hyperacute stroke defined by perfusion-weighted MRI and apparent diffusion coefficient. Stroke 32:1140–1146
27. Meng X, Fisher M, Shen Q et al (2004) Characterizing the diffusion/perfusion mismatch in experimental focal cerebral ischemia. Ann Neurol 55:207–212
28. Bardutzky J, Shen Q, Henninger N et al (2007) Characterizing tissue fate after transient cerebral ischemia of varying duration using quantitative diffusion and perfusion imaging. Stroke 38:1336–1344
29. Reese T, Bochelen D, Sauter A et al (1999) Magnetic resonance angiography of the rat cerebrovascular system without the use of contrast agents. NMR Biomed 12:189–196
30. Carano RAD, Li F, Irie K et al (2000) Multispectral analysis of the temporal evolution of cerebral ischemia in the rat brain. J Magn Reson Imaging 12:842–858
31. Dijkhuizen RM, Nicolay K (2003) Magnetic resonance imaging in experimental models of

brain disorders. J Cereb Blood Flow Metab 23:1383–1402
32. Jacobs MA, Knight RA, Soltanian-Zadeh H et al (2000) Unsupervised segmentation of multiparameter MRI in experimental cerebral ischemia with comparison to T2, diffusion, and ADC MRI parameters and histopathological validation. J Magn Reson Imaging 11:425–437
33. Carmichael ST (2003) Plasticity of cortical projections after stroke. Neuroscientist 9:64–75
34. Granziera C, D'Arceuil H, Zai L et al (2007) Long-term monitoring of post-stroke plasticity after transient cerebral ischemia in mice using in vivo and ex vivo diffusion tensor MRI. Open Neuroimag J 1:10–17
35. Sotak CH (2002) The role of diffusion tensor imaging in the evaluation of ischemic brain injury -a review. NMR Biomed 15:561–569
36. Po C, Kalthoff D, Kim YB et al (2012) White matter reorganization and functional response after focal cerebral ischemia in the rat. PLoS One 7, e45629. doi:10.1371/journal.pone.0045629
37. Van der Zijden JP, van der Toorn A, van der Marel K et al (2008) Longitudinal in vivo MRI of alterations in perilesional tissue after transient ischemic stroke in rats. Exp Neurol 212:207–212
38. Van Meer MPA, Otte WM, van der Marel K et al (2012) Extent of bilateral neuronal network reorganization and functional recovery in relation to stroke severity. J Neurosci 13:4495–4507
39. Jensen JH, Helpern JA, Ramani A et al (2005) Diffusional kurtosis imaging: the quantification of non-Gaussian water diffusion by means of magnetic resonance imaging. Magn Reson Med 53:1432–1440
40. Kim YB, Kalthoff D, Po C, Wiedermann D, Hoehn M (2012) Connectivity of thalamocortical pathway in rat brain: combined diffusion spectrum imaging and functional MRI at 11.7 T. NMR Biomed 25:943–952
41. Hui ES, Fieremans E, Jensen JH et al (2012) Stroke assessment with diffusional kurtosis imaging. Stroke 43:2968–2973
42. Umesh RS, Wieloch T, Beirup K et al (2014) Can diffusion kurtosis imaging improve the sensitivity and specificity of detecting microstructural alterations in brain tissue chronically after experimental stroke? Comparisons with diffusion tensor imaging and histology. Neuroimage 97:363–373
43. Sun PZ, Wang Y, Mandeville E et al (2014) Validation of fast diffusion kurtosis MRI for imaging acute ischemia in a rodent model of stroke. NMR Biomed 27:1413–1418
44. Grinberg F, Farrher E, Ciobanu L et al (2014) Non-Gaussian diffusion imaging for enhanced contrast of brain tissue affected by ischemic stroke. PLoS One 9, e89225. doi:10.1371/journal.pone.0089225
45. Kim YR, Huang IJ, Lee SR et al (2005) Measurements of BOLD/CBV ratio show altered fMRI hemodynamics during stroke recovery in rats. J Cereb Blood Flow Metab 25:820–829
46. Kim YR, van Meer MP, Mandeville JB et al (2007) fMRI of delayed albumin treatment during stroke recovery in rats: implication for fast neuronal habituation in recovering brains. J Cereb Blood Flow Metab 27:142–153
47. van Meer MP, van der Marel K, Otte WM et al (2010) Correspondence between altered functional and structural connectivity in the contralesional sensorimotor cortex after unilateral stroke in rats: a combined resting-state functional MRI and manganese-enhanced MRI study. J Cereb Blood Flow Metab 30:1707–1711
48. van Meer MP, van der Marel K, Wang K et al (2010) Recovery of sensorimotor function after experimental stroke correlates with restoration of resting-state interhemispheric functional connectivity. J Neurosci 17:3964–3972
49. Silva AC (2012) Using manganese-enhanced MRI to understand BOLD. Neuroimage 62:1009–1013
50. Eschenko O, Canals S, Simanova I et al (2010) Mapping of functional brain activity in freely behaving rats during voluntary running using manganese-enhanced MRI: implication for longitudinal studies. Neuroimage 49:2544–2555
51. Saar G, Cheng N, Belluscio L et al (2015) Laminar specific detection of APP induced neurodegeneration and recovery using MEMRI in an olfactory based Alzheimer's disease mouse model. Neuroimage 118:183–192
52. Soria G, Wiedermann D, Justicia C et al (2008) Reproducible imaging of rat corticothalamic pathway by longitudinal manganese-enhanced MRI (L-MEMRI). Neuroimage 41:668–674
53. van der Zijden JP, Bouts MJ, Wu O et al (2008) Manganese-enhanced MRI of brain plasticity in relation to functional recovery after experimental stroke. J Cereb Blood Flow Metab 28:832–840
54. Kawai Y, Aoki I, Umeda M et al (2010) In vivo visualization of reactive gliosis using manganese-enhanced magnetic resonance imaging. Neuroimage 49:3122–3131
55. Jacoby C, Böring YC, Beck A et al (2008) Dynamic changes in murine vessel geometry

assessed by high-resolution magnetic resonance angiography: a 9.4T study. J Magn Reson Imaging 28:637–645
56. Boehm-Sturm P, Farr TD, Adamczak J et al (2013) Vascular changes after stroke in the rat: a longitudinal study using optimized magnetic resonance imaging. Contrast Media Mol Imaging 8:383–392
57. Descoteaux M, Collins DL, Siddiqi K (2008) A geometric flow for segmenting vasculature in proton-density weighted MRI. Med Image Anal 12:497–513
58. Schlaug G, Benfield A, Baird AE et al (1999) The ischemic penumbra: operationally defined by diffusion and perfusion MRI. Neurology 53:1528–1537
59. Neumann-Haefelin T, Wittsack HJ, Wenesrski F et al (1999) Diffusion- and perfusion-weighted MRI: the DWI/PWI mismatch region in acute stroke. Stroke 30:1591–1597
60. Karonen JO, Vanninen RL, Liu Y et al (1999) Combined diffusion and perfusion MRI with correlation to single-photon emission CT in acute ischemic stroke. Ischemic penumbra predicts infarct growth. Stroke 30:1583–1590
61. Baird AE, Benfield A, Schlaug G et al (1997) Enlargement of human cerebral ischemic lesion volumes measured by diffusion weighted magnetic resonance imaging. Ann Neurol 41:581–589
62. Grandin CB, Duprez TP, Smith AM et al (2001) Usefulness of magnetic resonance-derived quantitative measurements of cerebral blood flow and volume in prediction of infarct growth in hyperacute stroke. Stroke 32:1147–1153
63. Astrup J, Siesjö BK, Symon L (1981) Thresholds in cerebral ischemia - the ischemic penumbra. Stroke 12:723–725
64. Hossmann KA (1994) Viability thresholds and the penumbra of focal ischemia. Ann Neurol 36:557–565
65. Hata R, Maeda K, Hermann D et al (2000) Evolution of brain infarction after transient focal cerebral ischemia in mice. J Cereb Blood Flow Metab 20:937–946
66. Ginsberg MD (2003) Adventures in the pathophysiology of brain ischemia: penumbra, gene expression, neuroprotection. Stroke 34:214–223
67. Donnan GA, Baron JC, Ma H et al (2009) Penumbral selection of patients for trials of acute stroke therapy. Lancet Neurol 8:261–269
68. Nicoli F, Lefur Y, Denis B et al (2003) Metabolic counterpart of decreased apparent diffusion coefficient during hyperacute ischemic stroke: a brain proton magnetic resonance spectroscopic imaging study. Stroke 34:e82–e87
69. Guadagno JV, Warburton EA, Aigbirhio FI et al (2004) Does the acute diffusion-weighted imaging lesion represent penumbra as well as core? A combined quantitative PET/MRI voxel-based study. J Cereb Blood Flow Metab 24:1249–1254
70. Guadagno JV, Warburton EA, Jones PS et al (2005) The diffusion-weighted lesion in acute stroke: heterogeneous patterns of flow/metabolism uncoupling as assessed by quantitative positron emission tomography. Cerebrovasc Dis 19:239–246
71. Sobesky J, Weber OZ, Lehnhardt FG et al (2005) Does the mismatch match the penumbra? Magnetic resonance imaging and positron emission tomography in early ischemic stroke. Stroke 36:80–85
72. Takasawa M, Jones PS, Guadagno JV et al (2008) How reliable is perfusion MR in acute stroke? Validation and determination of the penumbra threshold against quantitative PET. Stroke 39:870–877
73. Kidwell CS, Alger JR, Saver JL (2003) Beyond mismatch evolving paradigms in imaging the ischemic penumbra with multimodal magnetic resonance imaging. Stroke 34:2729–2735
74. Sun PZ, Zhou J, Sun W et al (2007) Detection of the ischemic penumbra using pH-weighted MRI. J Cereb Blood Flow Metab 27:1129–1136
75. Ebisu T, Mori Y, Katsuta K et al (2004) Neuroprotective effects of an immunosuppressant agent on diffusion/perfusion mismatch in transient focal ischemia. Magn Reson Med 51:1173–1180
76. Henninger N, Bouley J, Nelligan JM et al (2007) Normobaric hyperoxia delays perfusion/diffusion mismatch evolution, reduces infarct volume, and differentially affects neuronal cell death pathways after suture middle cerebral artery occlusion in rats. J Cereb Blood Flow Metab 27:1632–1642
77. Henninger N, Fisher M (2007) Stimulating circle of Willis nerve fibers preserves the diffusion-perfusion mismatch in experimental stroke. Stroke 38:2779–2786
78. Santosh C, Brennan D, McCabe C et al (2008) Potential use of oxygen as a metabolic biosensor in combination with T2*-weighted MRI to define the ischemic penumbra. J Cereb Blood Flow Metab 28:1742–1753
79. Fisher M, Bastan B (2012) Identifying and utilizing the ischemic penumbra. Neurology 79:S79–S85
80. Ringer TM, Neumann-Haefelin T, Sobel RA et al (2001) Reversal of early diffusion-

weighted magnetic resonance imaging abnormalities does not necessarily reflect tissue salvage in experimental cerebral ischemia. Stroke 32:2362–2369
81. Li F, Liu KF, Silva MD et al (2002) Acute postischemic renormalization of the apparent diffusion coefficient of water is not associated with reversal of astrocytic swelling and neuronal shrinkage in rats. Am J Neuroradiol 23:180–188
82. Kastrup A, Engelhorn T, Beaulieu C et al (1999) Dynamics of cerebral injury, perfusion, and blood–brain barrier changes after temporary and permanent middle cerebral artery occlusion in the rat. J Neurol Sci 166:91–99
83. Yang GY, Betz AL (1994) Reperfusion-induced injury to the blood–brain barrier after middle cerebral artery occlusion in rats. Stroke 25:1658–1664
84. Pan J, Constas AA, Bateman B et al (2007) Reperfusion injury following cerebral ischemia: pathophysiology, MR imaging, and potential therapies. Neuroradiology 49:93–102
85. Jiang Q, Chopp M, Zhang ZG et al (1997) The temporal evolution of MRI tissue signatures after transient middle cerebral artery occlusion in rat. J Neurol Sci 145:15–23
86. Wu O, Sumii T, Asahi M, Sasamata M et al (2007) Infarct prediction and treatment assessment with MRI-based algorithms in experimental stroke models. J Cereb Blood Flow Metab 27:196–204
87. Shen Q, Ren H, Fisher M et al (2005) Statistical prediction of tissue fate in acute ischemic brain injury. J Cereb Blood Flow Metab 25:1336–1345
88. Bouts MJ, Tiebosch IA, van der Toorn A et al (2013) Early identification of potentially salvageable tissue with MRI-based predictive algorithms after experimental ischemic stroke. J Cereb Blood Flow Metab 33:1075–1082
89. Tudela R, Soria G, Pérez-De-Puig I et al (2014) Infarct volume prediction using apparent diffusion coefficient maps during middle cerebral artery occlusion and soon after reperfusion in the rat. Brain Res 1583:169–178
90. Grillon E, Provent P, Montigon O et al (2008) Blood–brain barrier permeability to manganese and to Gd-DOTA in a rat model of transient cerebral ischaemia. NMR Biomed 21:427–436
91. Kim YR, Tejima E, Huang S et al (2008) In vivo quantification of transvascular water exchange during the acute phase of permanent stroke. Magn Reson Med 60:813–821
92. Tanaka Y, Nagaoka T, Nair G et al (2011) Arterial spin labeling and dynamic susceptibility contrast CBF MRI in postischemic hyperperfusion, hypercapnia, and after mannitol injection. J Cereb Blood Flow Metab 31:1403–1411
93. Armitage PA, Farrall AJ, Carpenter TK et al (2011) Use of dynamic contrast-enhanced MRI to measure subtle blood–brain barrier abnormalities. Magn Reson Imaging 29: 305–314
94. Weise G, Stoll G (2012) Magnetic resonance imaging of blood brain/nerve barrier dysfunction and leukocyte infiltration: closely related or discordant? Front Neurol 3:178. doi:10.3389/fneur.2012.00178
95. Liu DF, Qian C, An YL et al (2014) Magnetic resonance imaging of post-ischemic blood–brain barrier damage with PEGylated iron oxide nanoparticles. Nanoscale 6:15161–15167
96. Henning EC, Latour LL, Hallenbeck JM et al (2008) Reperfusion-associated hemorrhagic transformation in SHR rats: evidence of symptomatic parenchymal hematoma. Stroke 39:3405–3410
97. Jiang Y, Yin D, Xu D et al (2015) Investigating microbleeding in cerebral ischemia rats using susceptibility-weighted imaging. Magn Reson Imaging 33:102–109
98. Jander S, Schroeter M, Saleh A (2007) Imaging inflammation in acute brain ischemia. Stroke 38:642–645
99. Stoll G, Bendszus M (2009) Imaging of inflammation in the peripheral and central nervous system by magnetic resonance imaging. Neuroscience 158:1151–1160
100. Saleh A, Schroeter M, Ringelstein A et al (2007) Iron oxide particle-enhanced MRI suggests variability of brain inflammation at early stages after ischemic stroke. Stroke 38:2733–2737
101. Engberink RD, Blezer EL, Hoff EI et al (2008) MRI of monocyte infiltration in an animal model of neuroinflammation using SPIO-labeled monocytes or free USPIO. J Cereb Blood Flow Metab 28:841–851
102. Kim J, Kim DI, Lee SK et al (2008) Imaging of the inflammatory response in reperfusion injury after transient cerebral ischemia in rats: correlation of superparamagnetic iron oxide-enhanced magnetic resonance imaging with histopathology. Acta Radiol 49:580–588
103. Desestret V, Brisset JC, Moucharrafie S et al (2009) Early-stage investigations of ultrasmall superparamagnetic iron oxide-induced signal change after permanent middle cerebral artery occlusion in mice. Stroke 40:1834–1841
104. Henning EC, Ruetzler CA, Gaudinski MR et al (2009) Feridex preloading permits tracking of CNS-resident macrophages after transient middle cerebral artery occlusion. J Cereb Blood Flow Metab 29:1229–1239

105. Harms C, Datwyler AL, Wiekhorst F et al (2013) Certain types of iron oxide nanoparticles are not suited to passively target inflammatory cells that infiltrate the brain in response to stroke. J Cereb Blood Flow Metab 33:e1–e9
106. Walter HL, Walberer M, Rueger MA et al (2015) In vivo analysis of neuroinflammation in the late chronic phase after experimental stroke. Neuroscience 292:71–80
107. Heckl S (2007) Future contrast agents for molecular imaging in stroke. Curr Med Chem 14:1713–1728
108. Hyodo F, Chuang KH, Goloshevsky AG et al (2008) Brain redox imaging using blood–brain barrier-permeable nitroxide MRI contrast agent. J Cereb Blood Flow Metab 28:1165–1174
109. van Kasteren SI, Campbell SJ, Serres S et al (2009) Glyconanoparticles allow pre-symptomatic in vivo imaging of brain disease. Proc Natl Acad Sci U S A 106:18–23
110. McAteer MA, Sibson NR, von Zur Muhlen C et al (2007) In vivo magnetic resonance imaging of acute brain inflammation using microparticles of iron oxide. Nat Med 13:1253–1258
111. Fréchou M, Beray-Berthat V, Raynaud JS et al (2013) Detection of vascular cell adhesion molecule-1 expression with USPIO-enhanced molecular MRI in a mouse model of cerebral ischemia. Contrast Media Mol Imaging 8:157–164
112. Deddens LH, van Tilborg GA, van der Toorn A et al (2013) MRI of ICAM-1 upregulation after stroke: the importance of choosing the appropriate target-specific particulate contrast agent. Mol Imaging Biol 15:411–422
113. Deddens LH, van Tilborg GA, van der Toorn A et al (2013) PECAM-1-targeted micron-sized particles of iron oxide as MRI contrast agent for detection of vascular remodeling after cerebral ischemia. Contrast Media Mol Imaging 8:393–401
114. Bai YY, Gao X, Wang YC et al (2014) Image-guided pro-angiogenic therapy in diabetic stroke mouse models using a multi-modal nanoprobe. Theranostics 4:787–797
115. Breckwoldt MO, Chen JW, Stangenberg L et al (2008) Tracking the inflammatory response in stroke in vivo by sensing the enzyme myeloperoxidase. Proc Natl Acad Sci U S A 105:18584–18589
116. Agulla J, Brea D, Campos F et al (2013) In vivo theranostics at the peri-infarct region in cerebral ischemia. Theranostics 4:90–105
117. Adamczak J, Hoehn M (2012) In vivo imaging of cell transplants in experimental ischemia. Prog Brain Res 201:55–78
118. Tarulli E, Chaudhuri JD, Gretka V et al (2013) Effectiveness of micron-sized superparamagnetic iron oxide particles as markers for detection of migration of bone marrow-derived mesenchymal stromal cells in a stroke model. J Magn Reson Imaging 37:1409–1418
119. Tennstaedt A, Aswendt M, Adamczak J et al (2013) Noninvasive multimodal imaging of stem cell transplants in the brain using bioluminescence imaging and magnetic resonance imaging. Methods Mol Biol 1052:153–166
120. Wen X, Wang Y, Zhang F et al (2014) In vivo monitoring of neural stem cells after transplantation in acute cerebral infarction with dual-modal MR imaging and optical imaging. Biomaterials 35:4627–4635
121. Bai YY, Wang L, Peng XG et al (2015) Non-invasive monitoring of transplanted endothelial progenitor cells in diabetic ischemic stroke models. Biomaterials 40:43–50
122. Boehm-Sturm P, Aswendt M, Minassian A et al (2014) A multi-modality platform to image stem cell graft survival in the naïve and stroke-damaged mouse brain. Biomaterials 35:2218–2226
123. Zhang L, Wang Y, Tang Y et al (2013) High MRI performance fluorescent mesoporous silica-coated magnetic nanoparticles for tracking neural progenitor cells in an ischemic mouse model. Nanoscale 5:4506–4516
124. Granot D, Shapiro EM (2014) Accumulation of micron sized iron oxide particles in endothelin-1 induced focal cortical ischemia in rats is independent of cell migration. Magn Reson Med 71:1568–1574
125. Zhou J, Payen JF, Wilson DA et al (2003) Using the amide proton signals of intracellular proteins and peptides to detect pH effects in MRI. Nat Med 9:1085–1090
126. Zaiss M, Xu J, Goerke S et al (2014) Inverse Z-spectrum analysis for spillover-, MT-, and T1 -corrected steady-state pulsed CEST-MRI--application to pH-weighted MRI of acute stroke. NMR Biomed 27:240–252
127. McVicar N, Li AX, Gonçalves DF et al (2014) Quantitative tissue pH measurement during cerebral ischemia using amine and amide concentration-independent detection (AACID) with MRI. J Cereb Blood Flow Metab 34:690–698
128. Deuchar GA, Brennan D, Griffiths H et al (2013) Perfluorocarbons enhance a T2*-based MRI technique for identifying the penumbra in a rat model of acute ischemic stroke. J Cereb Blood Flow Metab 33:1422–1428
129. Wetterling F, Gallagher L, Mullin J et al (2015) Sodium-23 magnetic resonance imaging has potential for improving penumbra

detection but not for estimating stroke onset time. J Cereb Blood Flow Metab 35:103–110
130. Yushmanov VE, Kharlamov A, Yanovski B et al (2013) Correlated sodium and potassium imbalances within the ischemic core in experimental stroke: a 23Na MRI and histochemical imaging study. Brain Res 1527:199–208
131. Elabyad I, Kalayciyan R, Shanbhag NC et al (2014) First in vivo potassium-39 (^{39}K) MRI at 9.4 T using conventional copper radio frequency surface coil cooled to 77 K. IEEE Trans Biomed Eng 61:334–345
132. Christen T, Bouzat P, Pannetier N et al (2014) Tissue oxygen saturation mapping with magnetic resonance imaging. J Cereb Blood Flow Metab 34:1550–1557
133. Autio JA, Shatillo A, Giniatullin R et al (2014) Parenchymal spin-lock fMRI signals associated with cortical spreading depression. J Cereb Blood Flow Metab 34:768–775
134. Yu X, Qian C, Chen DY et al (2014) Deciphering laminar-specific neural inputs with line-scanning fMRI. Nat Methods 11:55–58
135. Muthupillai R, Ehman RL (1996) Magnetic resonance elastography. Nat Med 2:601–603
136. Freimann FB, Müller S, Streitberger KJ et al (2013) MR elastography in a murine stroke model reveals correlation of macroscopic viscoelastic properties of the brain with neuronal density. NMR Biomed 26:1534–1539
137. Klein C, Hain EG, Braun J et al (2014) Enhanced adult neurogenesis increases brain stiffness: in vivo magnetic resonance elastography in a mouse model of dopamine depletion. PLoS One 9, e92582. doi:10.1371/journal.pone.0092582
138. Werner P, Barthel H, Drzezga A et al (2015) Current status and future role of brain PET/MRI in clinical and research settings. Eur J Nucl Med Mol Imaging 42:512–526
139. Sokoloff L, Reivich M, Kennedy C et al (1977) The [^{14}C]deoxyglucose method for the measurement of local cerebral glucose utilization: theory, procedure and normal values in the conscious and anesthetized albino rat. J Neurochem 28:897–916
140. Belayev L, Zhao W, Busto R et al (1997) Transient middle cerebral artery occlusion by intraluminal suture: I. Three-dimensional autoradiographic image-analysis of local cerebral glucose metabolism-blood flow interrelationships during ischemia and early recirculation. J Cereb Blood Flow Metab 17:1266–1280
141. Brownell AL, Chen YI, Yu M et al (2004) 3-Nitropropionic acid-induced neurotoxicity--assessed by ultra high resolution positron emission tomography with comparison to magnetic resonance spectroscopy. J Neurochem 89:1206–1214
142. Wang X, Sarkar A, Cicchetti F et al (2005) Cerebral PET imaging and histological evidence of transglutaminase inhibitor cystamine induced neuroprotection in transgenic R6/2 mouse model of Huntington's disease. J Neurol Sci 231:57–66
143. Moore AH, Osteen CL, Chatziioannou AF et al (2000) Quantitative assessment of longitudinal metabolic changes in vivo after traumatic brain injury in the adult rat using FDG-microPET. J Cereb Blood Flow Metab 20:1492–1501
144. Shimoji K, Ravasi L, Schmidt K et al (2004) Measurement of cerebral glucose metabolic rates in the anesthetized rat by dynamic scanning with 18F-FDG, the ATLAS small animal PET scanner, and arterial blood sampling. J Nucl Med 45:665–672
145. Wu HM, Sui G, Lee CC et al (2007) In vivo quantitation of glucose metabolism in mice using small-animal PET and a microfluidic device. J Nucl Med 48:837–845
146. Toyama H, Ichise M, Liow JS et al (2004) Absolute quantification of regional cerebral glucose utilization in mice by 18F-FDG small animal PET scanning and 2-14C-DG autoradiography. J Nucl Med 45:1398–1405
147. Martin A, Rojas S, Pareto D et al (2009) Depressed glucose consumption at reperfusion following brain ischemia does not correlate with mitochondrial dysfunction and development of infarction: an in vivo Positron Emission Tomography study. Curr Neurovasc Res 6:82–88
148. Yuan H, Frank JE, Hong Y et al (2013) Spatiotemporal uptake characteristics of [18] F-2-fluoro-2-deoxy-D-glucose in a rat middle cerebral artery occlusion model. Stroke 44:2292–2299
149. Sobrado M, Delgado M, Fernandez-Valle E et al (2011) Longitudinal studies of ischemic penumbra by using 18F-FDG PET and MRI techniques in permanent and transient focal cerebral ischemia in rats. Neuroimage 57:45–54
150. Walberer M, Backes H, Rueger MA et al (2012) Potential of early [(18)F]-2-fluoro-2-deoxy-D-glucose positron emission tomography for identifying hypoperfusion and predicting fate of tissue in a rat embolic stroke model. Stroke 43:193–198
151. Wang J, Chao F, Han F et al (2013) PET demonstrates functional recovery after transplantation of induced pluripotent stem cells in a rat model of cerebral ischemic injury. J Nucl Med 54:785–792
152. Miyamoto M, Kuroda S, Zhao S et al (2013) Bone marrow stromal cell transplantation

enhances recovery of local glucose metabolism after cerebral infarction in rats: a serial 18F-FDG PET study. J Nucl Med 54:145–150
153. Magata Y, Temma T, Iida H et al (2003) Development of injectable O-15 oxygen and estimation of rat OEF. J Cereb Blood Flow Metab 23:671–676
154. Magata Y, Saji H, Choi SR et al (1995) Noninvasive measurement of cerebral blood flow and glucose metabolic rate in the rat with high-resolution animal positron emission tomography (PET): a novel in vivo approach for assessing drug action in the brains of small animals. Biol Pharm Bull 18:753–756
155. Temma T, Kuge Y, Sano K et al (2008) PET O-15 cerebral blood flow and metabolism after acute stroke in spontaneously hypertensive rats. Brain Res 1212:18–24
156. Temma T, Magata Y, Kuge Y et al (2006) Estimation of oxygen metabolism in a rat model of permanent ischemia using positron emission tomography with injectable ^{15}O-O_2. J Cereb Blood Flow Metab 26:1577–1583
157. Watabe T, Shimosegawa E, Watabe H et al (2013) Quantitative evaluation of cerebral blood flow and oxygen metabolism in normal anesthetized rats: 15O-labeled gas inhalation PET with MRI Fusion. J Nucl Med 54:283–290
158. Heiss WD (2000) Ischemic penumbra: evidence from functional imaging in man. J Cereb Blood Flow Metab 20:1276–1293
159. Yamamoto S, Teng W, Kakiuchi T et al (1999) Disturbance of cerebral blood flow autoregulation in hypertension is attributable to ischaemia following subarachnoid haemorrhage in rats: a PET study. Acta Neurochir (Wien) 141:1213–1219
160. Yee SH, Jerabek PA, Fox PT (2005) Noninvasive quantification of cerebral blood flow for rats by microPET imaging of ^{15}O labelled water: the application of a cardiac time-activity curve for the tracer arterial input function. Nucl Med Commun 26:903–911
161. Martin A, Mace E, Boisgard R et al (2012) Imaging of perfusion, angiogenesis, and tissue elasticity after stroke. J Cereb Blood Flow Metab 32:1496–1507
162. Schroeter M, Dennin MA, Walberer M et al (2009) Neuroinflammation extends brain tissue at risk to vital peri-infarct tissue: a double tracer [(11)C]PK11195- and [(18)F]FDG-PET study. J Cereb Blood Flow Metab 29:1216–1225
163. Martin A, San SE, Gomez-Vallejo V et al (2012) Positron emission tomography with [(13)N]ammonia evidences long-term cerebral hyperperfusion after 2h-transient focal ischemia. Neuroscience 213:47–53
164. Heiss WD, Graf R, Fujita T et al (1997) Early detection of irreversibly damaged ischemic tissue by flumazenil positron emission tomography in cats. Stroke 28:2045–2051
165. Heiss WD, Kracht L, Grond M et al (2000) [^{11}C]Flumazenil/H_2O positron emission tomography predicts irreversible ischemic cortical damage in stroke patients receiving acute thrombolytic therapy. Stroke 31:366–369
166. Heiss WD, Kracht LW, Thiel A et al (2001) Penumbral probability thresholds of cortical flumazenil binding and blood flow predicting tissue outcome in patients with cerebral ischaemia. Brain 124:20–29
167. Heiss WD, Sobesky J, Smekal U et al (2004) Probability of cortical infarction predicted by flumazenil binding and diffusion-weighted imaging signal intensity: a comparative positron emission tomography/magnetic resonance imaging study in early ischemic stroke. Stroke 35:1892–1898
168. Yamauchi H, Kudoh T, Kishibe Y et al (2005) Selective neuronal damage and borderzone infarction in carotid artery occlusive disease: a 11C-flumazenil PET study. J Nucl Med 46:1973–1979
169. Matsuda H, Tsuji S, Kuji I et al (1995) Dual-tracer autoradiography using 125I-iomazenil and 99Tcm-HMPAO in experimental brain ischaemia. Nucl Med Commun 16:581–590
170. Abe K, Kashiwagi Y, Tokumura M et al (2004) Discrepancy between cell injury and benzodiazepine receptor binding alter transient middle cerebral artery occlusion in rats. Synapse 53:234–239
171. Katchanov J, Waeber C, Gertz K et al (2003) Selective neuronal vulnerability following mild focal ischemia in the mouse. Brain Pathol 13:452–464
172. Rojas S, Martin A, Pareto D et al (2011) Positron emission tomography with 11C-flumazenil in the rat shows preservation of binding sites during the acute phase after 2 h-transient focal ischemia. Neuroscience 182:208–216
173. Rueger MA, Backes H, Walberer M et al (2010) Noninvasive imaging of endogenous neural stem cell mobilization in vivo using positron emission tomography. J Neurosci 30:6454–6460
174. Wunder A, Klohs J, Dirnagl U (2009) Noninvasive visualization of CNS inflammation with nuclear and optical imaging. Neuroscience 158:1161–1173
175. Benavides J, Quarteronet D, Imbault F et al (1983) Labelling of "peripheral-type" benzo-

diazepine binding sites in the rat brain by using 3H-PK11195, an isoquinoline carboxamide derivative: kinetic studies and autoradiographic localization. J Neurochem 41:1744–1750
176. Papadopoulos V, Baraldi M, Guilarte TR et al (2006) Translocator protein (18kDa): new nomenclature for the peripheral-type benzodiazepine receptor based on its structure and molecular function. Trends Pharmacol Sci 27:402–409
177. Myers R, Manjil LG, Cullen BM et al (1991) Macrophage and astrocyte populations in relation to 3HPK 11195 binding in rat cerebral cortex following a local ischaemic lesion. J Cereb Blood Flow Metab 11:314–322
178. Myers R, Manjil LG, Frackowiak RSJ et al (1991) 3HPK 11195 and the localisation of secondary thalamic lesions following focal ischaemia in rat motor cortex. Neurosci Lett 133:20–24
179. Stephenson DT, Schober DA, Smalstig EB et al (1995) Peripheral benzodiazepine receptors are colocalized with activated microglia following transient global forebrain ischemia in the rat. J Neurosci 15:5263–5274
180. Banati RB, Myers R, Kreutzberg GW (1997) PK ('peripheral benzodiazepine')--binding sites in the CNS indicate early and discrete brain lesions: microautoradiographic detection of [^{3}H]PK11195 binding to activated microglia. J Neurocytol 26:77–82
181. Moynagh PN, Schousboe A, Williams DC (1994) The peripheral-type benzodiazepine receptor is present in astrocytes but is not a primary site of action for convulsants/anticonvulsants. J Neurochem 62:673–679
182. Ramsay SC, Weiller C, Myers R et al (1992) Monitoring by PET of macrophage accumulation in brain after ischaemic stroke. Lancet 339:1054–1055
183. Gerhard A, Neumaier B, Elitok E et al (2000) In vivo imaging of activated microglia using [11C]PK11195 and positron emission tomography in patients after ischemic stroke. NeuroReport 11:2957–2960
184. Gerhard A, Schwarz J, Myers R et al (2005) Evolution of microglial activation in patients after ischemic stroke: a [^{11}C](R)-PK11195 PET study. NeuroImage 24:591–595
185. Pappata S, Levasseur M, Gunn RN et al (2000) Thalamic microglial activation in ischemic stroke detected in vivo by PET and [^{11}C]PK11195. Neurology 55:1052–1054
186. Rojas S, Martín A, Arranz MJ et al (2007) Imaging brain inflammation with [^{11}C]PK11195 by PET and induction of the peripheral-type benzodiazepine receptor after transient focal ischemia in rats. J Cereb Blood Flow Metab 27:1975–1986
187. Damont A, Roeda D, Dolle F (2013) The potential of carbon-11 and fluorine-18 chemistry: illustration through the development of positron emission tomography radioligands targeting the translocator protein 18 kDa. J Labelled Comp Radiopharm 56:96–104
188. Imaizumi M, Kim HJ, Zoghbi SS et al (2007) PET imaging with [^{11}C]PBR28 can localize and quantify upregulated peripheral benzodiazepine receptors associated with cerebral ischemia in rat. Neurosci Lett 411:200–205
189. Martin A, Boisgard R, Theze B et al (2010) Evaluation of the PBR/TSPO radioligand [(18)F]DPA-714 in a rat model of focal cerebral ischemia. J Cereb Blood Flow Metab 30:230–241
190. Yui J, Maeda J, Kumata K et al (2010) 18F-FEAC and ^{18}F-FEDAC: PET of the monkey brain and imaging of translocator protein (18 kDa) in the infarcted rat brain. J Nucl Med 51:1301–1309
191. Yui J, Hatori A, Kawamura K et al (2011) Visualization of early infarction in rat brain after ischemia using a translocator protein (18 kDa) PET ligand [^{11}C]DAC with ultra-high specific activity. Neuroimage 54:123–130
192. Boutin H, Prenant C, Maroy R et al (2013) [18F]DPA-714: direct comparison with [11C]PK11195 in a model of cerebral ischemia in rats. PLoS One 8, e56441. doi:10.1371/journal.pone.0056441
193. Boutin H, Murray K, Pradillo J et al (2015) ^{18}F-GE-180: a novel TSPO radiotracer compared to ^{11}C-R-PK11195 in a preclinical model of stroke. Eur J Nucl Med Mol Imaging 42:503–511
194. Toth M, Little P, Arnberg F et al (2015) Acute neuroinflammation in a clinically relevant focal cortical ischemic stroke model in rat: longitudinal positron emission tomography and immunofluorescent tracking. Brain Struct Funct. doi:10.1007/s00429-014-0970-y
195. Martin A, Boisgard R, Kassiou M et al (2011) Reduced PBR/TSPO expression after minocycline treatment in a rat model of focal cerebral ischemia: a PET study using [(18)F]DPA-714. Mol Imaging Biol 13:10–15
196. Martin A, Szczupak B, Gomez-Vallejo V et al (2015) In vivo PET Imaging of the alpha-4beta2 nicotinic acetylcholine receptor as a marker for brain inflammation after cerebral ischemia. J Neurosci 35:5998–6009
197. Saita K, Chen M, Spratt NJ et al (2004) Imaging the ischemic penumbra with 18F-fluoromisonidazole in a rat model of ischemic stroke. Stroke 35:975–980
198. Takasawa M, Beech JS, Fryer TD et al (2007) Imaging of brain hypoxia in permanent and temporary middle cerebral artery occlusion in

the rat using 18F-fluoromisonidazole and positron emission tomography: a pilot study. J Cereb Blood Flow Metab 27:679–689
199. Martin A, Gomez-Vallejo V, San SE et al (2013) In vivo imaging of dopaminergic neurotransmission after transient focal ischemia in rats. J Cereb Blood Flow Metab 33:244–252
200. Martin A, Szczupak B, Gomez-Vallejo V et al (2013) PET imaging of serotoninergic neurotransmission with [(11)C]DASB and [(18)F]altanserin after focal cerebral ischemia in rats. J Cereb Blood Flow Metab 33:1967–1975
201. Soria FN, Perez-Samartin A, Martin A et al (2014) Extrasynaptic glutamate release through cystine/glutamate antiporter contributes to ischemic damage. J Clin Invest 124:3645–3655
202. Cai W, Guzman R, Hsu AR et al (2009) Positron emission tomography imaging of poststroke angiogenesis. Stroke 40:270–277
203. Zheng QH, Fei X, Liu X et al (2004) Comparative studies of potential cancer biomarkers carbon-11 labeled MMP inhibitors (S)-2-(4′-[^{11}C]methoxybiphenyl-4-sulfonylamino)-3-methylbutyric acid and N-hydroxy-(R)-2-[[(4′-[^{11}C]methoxyphenyl) sulfonyl]benzylamino]-3-methylbutanamide. Nucl Med Biol 31:77–85
204. Zheng QH, Fei X, DeGrado TR et al (2003) Synthesis, biodistribution and micro-PET imaging of a potential cancer biomarker carbon-11 labeled MMP inhibitor (2R)-2-[[4-(6-fluorohex-1-ynyl)phenyl] sulfonylamino]-3-methylbutyric acid [^{11}C]methyl ester. Nucl Med Biol 30:753–760
205. Wagner S, Breyholz HJ, Höltke C et al (2009) A new 18F-labelled derivative of the MMP inhibitor CGS 27023A for PET: radiosynthesis and initial small-animal PET studies. Appl Radiat Isot 67:606–610
206. Wagner S, Breyholz HJ, Law MP et al (2007) Novel fluorinated derivatives of the broad-spectrum MMP inhibitors N-hydroxy-2(R)-[[(4-methoxyphenyl)sulfonyl](benzyl)- and (3-picolyl)-amino]-3-methyl-butanamide as potential tools for the molecular imaging of activated MMPs with PET. J Med Chem 50:5752–5764
207. Wagner S, Breyholz HJ, Faust A et al (2006) Molecular imaging of matrix metalloproteinases in vivo using small molecule inhibitors for SPECT and PET. Curr Med Chem 13:2819–2838
208. Beekman FJ, van der Have F, Vastenhouw B et al (2005) U-SPECT-I: a novel system for submillimeter-resolution tomography with radiolabeled molecules in mice. J Nucl Med 46:1194–1200
209. Franc BL, Acton PD, Mari C et al (2008) Small-animal SPECT and SPECT/CT: important tools for preclinical investigation. J Nucl Med 49:1651–1663
210. Bullock R, Patterson J, Park C (1991) Evaluation of ^{99}mTc-hexamethylpropyleneamine oxime cerebral blood flow mapping after acute focal ischemia in rats. Stroke 22:1284–1290
211. Ceulemans AG, Hernot S, Zgavc T et al (2011) Serial semiquantitative imaging of brain damage using micro-SPECT and micro-CT after endothelin-1-induced transient focal cerebral ischemia in rats. J Nucl Med 52:1987–1992
212. Hatazawa J, Satoh T, Shimosegawa E et al (1995) Evaluation of cerebral infarction with iodine 123-iomazenil SPECT. J Nucl Med 36:2154–2161
213. Saito H, Magota K, Zhao S et al (2013) ^{123}I-iomazenil single photon emission computed tomography visualizes recovery of neuronal integrity by bone marrow stromal cell therapy in rat infarct brain. Stroke 44:2869–2874
214. Inoue Y, Abe O, Kawakami T et al (2001) Metabolism of ^{99}mTc-ethylcysteinate dimer in infarcted brain tissue of rats. J Nucl Med 42:802–807
215. Blankenberg FG, Kalinyak J, Liu L et al (2006) ^{99}mTc-HYNIC-annexin V SPECT imaging of acute stroke and its response to neuroprotective therapy with anti-Fas ligand antibody. Eur J Nucl Med Mol Imaging 33:566–574
216. D'Arceuil H, Rhine W, de Crespigny A et al (2000) ^{99}mTc annexin V imaging of neonatal hypoxic brain injury. Stroke 31:2692–2700
217. Mari C, Karabiyikoglu M, Goris ML et al (2004) Detection of focal hypoxic-ischemic injury and neuronal stress in a rodent model of unilateral MCA occlusion/reperfusion using radiolabeled annexin V. Eur J Nucl Med Mol Imaging 31:733–739
218. Arlicot N, Petit E, Katsifis A et al (2010) Detection and quantification of remote microglial activation in rodent models of focal ischaemia using the TSPO radioligand CLINDE. Eur J Nucl Med Mol Imaging 37:2371–2380
219. Makinen S, Kekarainen T, Nystedt J et al (2006) Human umbilical cord blood cells do not improve sensorimotor or cognitive outcome following transient middle cerebral artery occlusion in rats. Brain Res 6:207–215
220. Lappalainen RS, Narkilahti S, Huhtala T et al (2008) The SPECT imaging shows the accumulation of neural progenitor cells into internal organs after systemic administration in

middle cerebral artery occlusion rats. Neurosci Lett 440:246–250
221. Arbab AS, Thiffault C, Navia B et al (2012) Tracking of In-111-labeled human umbilical tissue-derived cells (hUTC) in a rat model of cerebral ischemia using SPECT imaging. BMC Med Imaging 12:33. doi:10.1186/1471-2342-12-33
222. Mitkari B, Kerkela E, Nystedt J et al (2013) Intra-arterial infusion of human bone marrow-derived mesenchymal stem cells results in transient localization in the brain after cerebral ischemia in rats. Exp Neurol 239:158–162
223. Wu T, Lang J, Sun X et al (2013) Monitoring bone marrow stem cells with a reporter gene system in experimental middle cerebral artery occlusion rat models. J Nucl Med 54:984–989
224. Skoubis PD, Hradil V, Chin CL et al (2006) Mapping brain activity following administration of a nicotinic acetylcholine receptor agonist, ABT-594, using functional magnetic resonance imaging in awake rats. Neuroscience 137:583–591
225. Chin CL, Fox GB, Hradil VP et al (2006) Pharmacological MRI in awake rats reveals neural activity in area postrema and nucleus tractus solitarius: relevance as a potential biomarker for detecting drug-induced emesis. Neuroimage 33:1152–1160
226. Chin CL, Pauly JR, Surber BW et al (2008) Pharmacological MRI in awake rats predicts selective binding of α4β2 nicotinic receptors. Synapse 62:159–168
227. Luo F, Li Z, Treistman SN et al (2007) Confounding effects of volatile anesthesia on CBV assessment in rodent forebrain following ethanol challenge. J Magn Reson Imaging 26:557–563
228. Tsurugizawa T, Uematsu A, Uneyama H et al (2012) Functional brain mapping of conscious rats during reward anticipation. J Neurosci Methods 206:132–137
229. Reed MD, Pira AS, Febo M (2013) Behavioral effects of acclimatization to restraint protocol used for awake animal imaging. J Neurosci Methods 217:63–66
230. Momosaki S, Hatano K, Kawasumi Y et al (2004) Rat-PET study without anesthesia: anesthetics modify the dopamine D1 receptor binding in rat brain. Synapse 54:207–213
231. Martin CJ, Kennerley AJ, Berwick J et al (2013) Functional MRI in conscious rats using a chronically implanted surface coil. J Magn Reson Imaging 38:739–744
232. Liang Z, King J, Zhang N (2012) Intrinsic organization of the anesthetized brain. J Neurosci 32:10183–10191
233. Liang Z, Liu X, Zhang N (2015) Dynamic resting state functional connectivity in awake and anesthetized rodents. Neuroimage 104:89–99
234. Liang Z, Watson GD, Alloway KD et al (2015) Mapping the functional network of medial prefrontal cortex by combining optogenetics and fMRI in awake rats. Neuroimage 117:114–123
235. Mizuma H, Shukuri M, Hayashi T et al (2010) Establishment of in vivo brain imaging method in conscious mice. J Nucl Med 51:1068–1075
236. Kyme AZ, Zhou VW, Meikle SR et al (2011) Optimised motion tracking for positron emission tomography studies of brain function in awake rats. PLoS One 6, e21727. doi:10.1371/journal.pone.0021727
237. Ravasi L, Shimoji K, Soto-Montenegro ML et al (2011) Use of [^{18}F]fluorodeoxyglucose and the ATLAS small animal PET scanner to examine cerebral functional activation by whisker stimulation in unanesthetized rats. Nucl Med Commun 32:336–342
238. Rohleder C, Jung F, Mertgens H et al (2014) Neural correlates of sensorimotor gating: a metabolic positron emission tomography study in awake rats. Front Behav Neurosci 8:178. doi:10.3389/fnbeh.2014.00178
239. Thanos PK, Robison L, Nestler EJ et al (2013) Mapping brain metabolic connectivity in awake rats with μPET and optogenetic stimulation. J Neurosci 33:6343–6349
240. Shulman RG, Hyder F, Rothman DL (2009) Baseline brain energy supports the state of consciousness. Proc Natl Acad Sci U S A 106:11096–11101
241. Hildebrandt IJ, Su H, Weber WA (2008) Anesthesia and other considerations for in vivo imaging of small animals. ILAR J 49:17–26
242. Lukasik VM, Gillies RJ (2003) Animal anaesthesia for in vivo magnetic resonance. NMR Biomed 16:459–467
243. Kannurpatti SS, Biswal BB, Kim YR et al (2008) Spatio-temporal characteristics of low-frequency BOLD signal fluctuations in isoflurane-anesthetized rat brain. NeuroImage 40:1738–1747
244. Haensel JX, Spain A, Martin C (2015) A systematic review of physiological methods in rodent pharmacological MRI studies. Psychopharmacology (Berl) 232:489–499
245. Tokugawa J, Ravasi L, Nakayama T et al (2007) Distribution of the 5-HT(1A) receptor antagonist [(18)F]FPWAY in blood and brain of the rat with and without isoflurane anesthesia. Eur J Nucl Med Mol Imaging 34:259–266

246. Van Camp N, Verhoye M, De Zeeuw CI et al (2006) Light stimulus frequency dependence of activity in the rat visual system as studied with high-resolution BOLD fMRI. J Neurophysiol 95:3164–3170
247. Weber R, Ramos-Cabrer P, Wiedermann D et al (2006) A fully noninvasive and robust experimental protocol for longitudinal fMRI studies in the rat. NeuroImage 29: 1303–1310
248. Pawela CP, Biswal BB, Cho YR et al (2008) Resting-state functional connectivity of the rat brain. Magn Reson Med 59:1021–1029
249. Zhao F, Zhao T, Zhou L et al (2008) BOLD study of stimulation-induced neural activity and resting-state connectivity in medetomidine-sedated rat. NeuroImage 39:248–260
250. Kalthoff D, Po C, Wiedermann D et al (2013) Reliability and spatial specificity of rat brain sensorimotor functional connectivity networks are superior under sedation compared with general anesthesia. NMR Biomed 26:638–650
251. D'Souza DV, Jonckers E, Bruns A et al (2014) Preserved modular network organization in the sedated rat brain. PLoS One 9, e106156. doi:10.1371/journal.pone.0106156
252. Du C, Tully M, Volkow ND et al (2009) Differential effects of anesthetics on cocaine's pharmacokinetic and pharmacodynamic effects in brain. Eur J Neurosci 30:1565–1575
253. Casteels C, Bormans G, Van Laere K (2010) The effect of anaesthesia on [(18)F]MK-9470 binding to the type 1 cannabinoid receptor in the rat brain. Eur J Nucl Med Mol Imaging 37:1164–1173
254. Ciobanu L, Reynaud O, Uhrig L et al (2012) Effects of anesthetic agents on brain blood oxygenation level revealed with ultra-high field MRI. PLoS One 7, e32645. doi:10.1371/journal.pone.0032645
255. Wang K, van Meer MP, van der Marel K et al (2011) Temporal scaling properties and spatial synchronization of spontaneous blood oxygenation level-dependent (BOLD) signal fluctuations in rat sensorimotor network at different levels of isoflurane anesthesia. NMR Biomed 24:61–67
256. Liu X, Li R, Yang Z et al (2012) Differential effect of isoflurane, medetomidine, and urethane on BOLD responses to acute levo-tetrahydropalmatine in the rat. Magn Reson Med 68:552–559
257. Jonckers E, Delgado y Palacios R, Shah D et al (2014) Different anesthesia regimes modulate the functional connectivity outcome in mice. Magn Reson Med 72:1103–1112
258. Magnuson ME, Thompson GJ, Pan WJ et al (2014) Time-dependent effects of isoflurane and dexmedetomidine on functional connectivity, spectral characteristics, and spatial distribution of spontaneous BOLD fluctuations. NMR Biomed 27:291–303
259. Schroeter A, Schlegel F, Seuwen A et al (2014) Specificity of stimulus-evoked fMRI responses in the mouse: the influence of systemic physiological changes associated with innocuous stimulation under four different anesthetics. Neuroimage 94:372–384
260. Tardif CL, Collins DL, Pike GB (2009) Sensitivity of voxel-based morphometry analysis to choice of imaging protocol at 3 T. Neuroimage 44:827–838
261. Soria G, Tudela R, Márquez-Martín A et al (2013) The ins and outs of the BCCAo model for chronic hypoperfusion: a multimodal and longitudinal MRI approach. PLoS One 8, e74631. doi:10.1371/journal.pone.0074631
262. Justicia C, Ramos-Cabrer P, Hoehn M (2008) MRI detection of secondary damage after stroke: chronic iron accumulation in the thalamus of the rat brain. Stroke 39:1541–1547
263. Rosen BR, Belliveau JW, Vevea JM et al (1990) Perfusion imaging with NMR contrast agents. Magn Reson Med 14:249–265
264. Williams DS, Detre JA, Leigh JS et al (1992) Magnetic resonance imaging of perfusion using spin inversion of arterial water. Proc Natl Acad Sci U S A 89:212–216
265. Koretsky AP (2012) Early development of arterial spin labeling to measure regional brain blood flow by MRI. Neuroimage 62:602–607
266. Wells JA, Lythgoe MF, Choy M et al (2009) Characterizing the origin of the arterial spin labelling signal in MRI using a multiecho acquisition approach. J Cereb Blood Flow Metab 29:1836–1845
267. Duhamel G, Callot V, Tachrount M et al (2012) Pseudo-continuous arterial spin labeling at very high magnetic field (11.75 T) for high-resolution mouse brain perfusion imaging. Magn Reson Med 67:1225–1236
268. Gao Y, Goodnough CL, Erokwu BO et al (2014) Arterial spin labeling-fast imaging with steady-state free precession (ASL-FISP): a rapid and quantitative perfusion technique for high-field MRI. NMR Biomed 27:996–1004
269. Wells JA, Siow B, Lythgoe MF et al (2013) Measuring biexponential transverse relaxation of the ASL signal at 9.4 T to estimate arterial oxygen saturation and the time of exchange of labeled blood water into cortical brain tissue. J Cereb Blood Flow Metab 33:215–224
270. van Dorsten FA, Hata R, Maeda K et al (1999) Diffusion- and perfusion-weighted MR imaging of transient focal cerebral ischemia. NMR Biomed 12:525–534

271. Thomas DL (2005) Arterial spin labeling in small animals: methods and applications to experimental cerebral ischemia. J Magn Reson Imaging 22:741–744
272. Qiao M, Latta P, Meng S et al (2004) Development of acute edema following cerebral hypoxia-ischemia in neonatal compared with juvenile rats using magnetic resonance imaging. Pediatr Res 55:101–106
273. Moseley ME, Cohen Y, Kucharczyk J et al (1990) Diffusion-weighted MR imaging of anisotropic water diffusion in cat central nervous system. Radiology 176:439–445
274. Kamali A, Hasan KM, Adapa P et al (2014) Distinguishing and quantification of the human visual pathways using high-spatial-resolution diffusion tensor tractography. Magn Reson Imaging 32:796–803
275. Gutman DA, Keifer OP Jr, Magnuson ME et al (2012) A DTI tractography analysis of infralimbic and prelimbic connectivity in the mouse using high-throughput MRI. Neuroimage 63:800–811
276. Harsan LA, Dávid C, Reisert M et al (2013) Mapping remodeling of thalamocortical projections in the living reeler mouse brain by diffusion tractography. Proc Natl Acad Sci U S A 110:E1797–E1806
277. Ramos-Cejudo J, Gutiérrez-Fernández M, Otero-Ortega L et al (2015) Brain-derived neurotrophic factor administration mediated oligodendrocyte differentiation and myelin formation in subcortical ischemic stroke. Stroke 46:221–228
278. Norris DG (2006) Principles of magnetic resonance assessment of brain function. J Magn Reson Imaging 23:794–807
279. Bartsch AJ, Homola G, Biller A et al (2006) Diagnostic functional MRI: illustrated clinical applications and decision-making. J Magn Reson Imaging 23:921–932
280. Lu H, Soltysik DA, Ward BD et al (2005) Temporal evolution of the CBV-fMRI signal to rat whisker stimulation of variable duration and intensity: a linearity analysis. NeuroImage 26:432–440
281. Koyama M, Hasegawa I, Osada T et al (2004) Functional magnetic resonance imaging of macaque monkeys performing visually guided saccade tasks: comparison of cortical eye fields with humans. Neuron 41:795–807
282. Schwindt W, Burke M, Pillekamp F et al (2004) Functional magnetic resonance imaging and somatosensory evoked potentials in rats with a neonatally induced freeze lesion of the somatosensory cortex. J Cereb Blood Flow Metab 24:1409–1418
283. Gsell W, Burke M, Wiedermann D et al (2006) Differential effects of NMDA and AMPA glutamate receptors on functional magnetic resonance imaging signals and evoked neuronal activity during forepaw stimulation of the rat. J Neurosci 26:8409–8416
284. Steward CA, Marsden CA, Prior MJW et al (2005) Methodological considerations in rat brain BOLD contrast pharmacological MRI. Psychopharmacology 180:687–704
285. Hoff EI, Steinbusch HW, van Oostenbrugge RJ et al (2011) Alterations in the cholinergic system after frontal cortical infarction in rat brain: pharmacological magnetic resonance imaging of muscarinic receptor responsiveness and stereological analysis of cholinergic forebrain neurons. Neurobiol Dis 43: 625–634
286. Miraux S, Serres S, Thiaudière E et al (2004) Gadolinium-enhanced small-animal TOF magnetic resonance angiography. MAGMA 17:348–352
287. Huang CH, Chen CC, Siow TY et al (2013) High-resolution structural and functional assessments of cerebral microvasculature using 3D Gas ΔR2*-mMRA. PLoS One 8, e78186. doi:10.1371/journal.pone.0078186
288. Kohno K, Back T, Hoehn-Berlage M et al (1995) A modified rat model of middle cerebral artery thread occlusion under electrophysiological control for magnetic resonance investigations. Magn Reson Imaging 13:65–71
289. Gerriets T, Stolz E, Walberer M et al (2004) Middle cerebral artery occlusion during MR-imaging: investigation of the hyperacute phase of stroke using a new in-bore occlusion model in rats. Brain Res Brain Res Protoc 12:137–143
290. Kuntner C, Kesner AL, Bauer M et al (2009) Limitations of small animal PET imaging with [(18)F]FDDNP and FDG for quantitative studies in a transgenic mouse model of Alzheimer's disease. Mol Imaging Biol 11:236–240
291. Fang YH, Muzic RF Jr (2008) Spillover and partial-volume correction for image-derived input functions for small-animal ^{18}F-FDG PET studies. J Nucl Med 49:606–614
292. Vandeghinste B, Van Holen R, Vanhove C et al (2014) Use of a ray-based reconstruction algorithm to accurately quantify preclinical microSPECT images. Mol Imaging 13:1–13

Chapter 12

Noninvasive Optical Imaging in Rodent Models of Stroke

Markus Vaas and Jan Klohs

Abstract

With recent advances in optical imaging instrumentation and reconstruction algorithms, preclinical optical imaging has become almost a commodity in biomedical research. Given the availability of specific fluorescent probes and reporter gene technologies, which allow the noninvasive visualization of a variety of pathophysiological processes. The technology might also pose an attractive research tool for preclinical stroke research. This chapter gives a practical overview about near-infrared fluorescence (NIRF) imaging and bioluminescence imaging (BLI), the two most common noninvasive optical imaging techniques. Furthermore, we will provide examples about the application of these methods to rodent models of stroke and discusses practical aspects and limitations.

Key words Bioluminescence imaging, Cerebral ischemia, Fluorescent proteins, Near-infrared fluorescence imaging, Molecular imaging, Small animal imaging

1 Introduction

The development of new optical imaging devices over the past decade has facilitated the translation of optical imaging from microscopic scale to macroscopic level imaging. Novel probes and reporter gene assays have become available, which allow the visualization of a variety of pathophysiological processes in the intact animal. The technology is particularly suited for the use in rodent models of stroke: specific pathophysiological processes can be visualized in vivo, while all regulatory processes are preserved in the live animal and without impeding animal physiology and welfare. Moreover, the noninvasiveness of the methods allows combining them with other readouts, for example, behavior (see Chap. 13) or magnetic resonance imaging (see Chap. 11) in the same animal, thus reducing the overall number of animals needed for preclinical studies. In addition, it allows repetitive imaging to establish the dynamics of a process over the disease course, thus improving statistical power, and to monitor the response to therapeutic intervention. In this chapter, we briefly describe the application of

Ulrich Dirnagl (ed.), *Rodent Models of Stroke*, Neuromethods, vol. 120,
DOI 10.1007/978-1-4939-5620-3_12,

near-infrared fluorescence (NIRF) imaging and bioluminescence imaging (BLI), the two most common noninvasive optical imaging methods, to rodent models of stroke. Furthermore, we discuss practical aspects and limitations of these techniques.

2 Near-Infrared Fluorescence (NIRF) Imaging

2.1 NIRF Instrumentation and Techniques

Near-infrared (NIR) fluorescence makes use of the fact that major absorbers in the tissue like water and hemoglobin have their lowest absorption coefficient in the NIR range (700–900 nm), thus allowing NIR photons to penetrate deep into tissue. In addition, structural components in animal tissue have low autofluorescence emission in the NIR range compared to the visible and mid-infrared spectrum [1]. This gives the unique opportunity of NIR light to detect fluorochrome distribution in biological tissue using sophisticated hardware and reconstruction algorithms.

A number of NIRF imaging devices with different setups and modes of data acquisition have been developed and are commercially available. The standard NIRF imaging instrumentation consists of an excitation light source, e.g., a laser diode, and fiber optics to direct the excitation light to the animal under study (Fig. 1). The emitted fluorescence is captured using a charge-coupled device (CCD) camera fitted with adequate emission filters and a lens to adjust the focal plane. By choosing different combinations of excitation sources and emission filters, multichannel imaging in the same animal can be achieved [2].

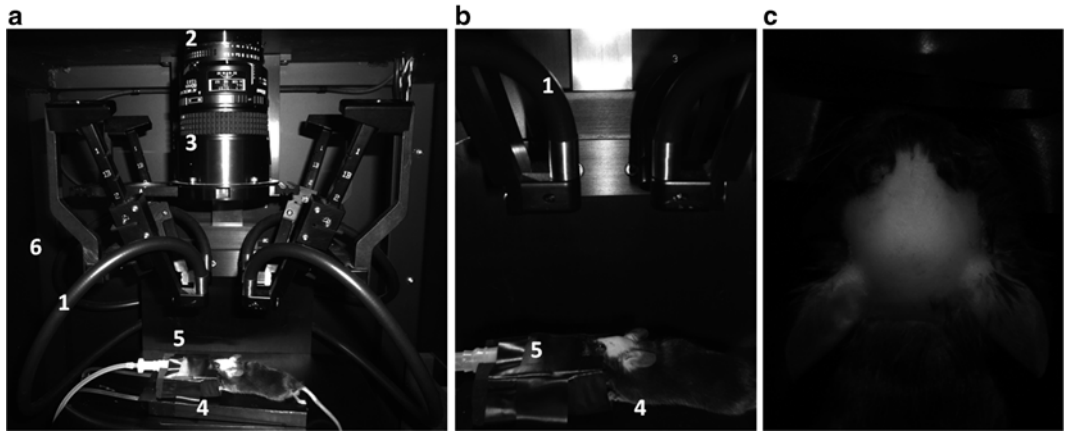

Fig. 1 A standard planar NIRF imaging system (**a**, **b**, Maestro 500 multispectral imaging system, Cambridge Research & Instruments Inc, Woburn, USA). The system consists of fiber optics (*1*) which direct the excitation light to the animal under study. The emitted fluorescence is captured using a charge-coupled device camera (*2*) fitted with adequate emission filters and a lens to adjust the focal plane (*3*). The mouse is placed onto a heated support to maintain body temperature (*4*). Volatile anesthesia is provided in an air/oxygen mixture via a nose cone (*5*). The whole set-up is placed in a lighttight container (*6*). A white light image of a C57Bl6 mouse head taken with a charge-coupled device camera (**c**). The head has been depilated

The most common method for NIRF imaging is to illuminate the object with a plane wave referred to as planar NIRF imaging. Planar NIRF imaging can be applied both in reflectance and transillumination mode. In fluorescence reflectance imaging (FRI), the excitation light source and the detector are on the same side of the object. The excitation photons propagate a few millimeters below the surface of the object. Scattered excitation and emission photons travel back to the surface. In transillumination fluorescence imaging (TFI), the excitation light source and the detector are on opposite sides. The advantage of TFI is that the entire volume of the object is sampled upon the passage of the excitation light. Furthermore, reflection of excitation photons and autofluorescence of the skin is reduced in TFI compared to FRI [3].

Planar NIRF imaging methods have the advantage that they require relatively inexpensive instrumentation (systems are commercially available or can be self-built), are easy to operate, and facilitate high-throughput imaging of animals. However, planar NIRF imaging methods have some limitations: tissue scattering limits spatial resolution to about 2–3 mm. The obtained images are two-dimensional and surface-weighted. Moreover, the detected fluorescence emission depends linearly on the fluorochrome concentration and nonlinearly on the depth of the fluorescent object and the optical properties of the surrounding tissue. As a consequence, planar NIRF images do not allow for absolute quantification of the detected fluorescence. Hence, in most studies, the fluorescence emission is expressed in terms of contrast, i.e., as a ratio of the fluorescence intensity measured over the disease-affected region to the intensity measured over a non-affected region, termed target-to-background ratio (TBR [4]).

Quantitative analysis of fluorescence emission can be achieved using fluorescence molecular tomography (FMT). In contrast to FRI and TFI, FMT uses a point laser source instead of planar ones. By scanning the laser point on the surface, coupled excitation and emission images are sequentially recorded. Based on the diffuse light propagation model, reconstruction leads to an improved image resolution of the order of 1 mm in all three dimensions as compared to planar NIRF techniques [5, 6]. The combination of FMT with other imaging modalities like magnetic resonance imaging and computed tomography can be used to allocate imaging signals on low-resolution NIRF imaging data to a specific anatomical location [7, 8]. In addition, the use of anatomical information as prior knowledge can improve the reconstruction accuracy of FMT data.

2.2 NIRF Imaging Probes and Reporter Genes

A large number of fluorochromes emitting in the NIR including cyanine dyes, lanthanide chelates, squaraines, tetrapyrrole-based probes, quantum dots, and others are available [9]. The fluorochromes can be used for the generation of NIRF probes by conjugation to ligands such as antibodies, antibody fragments,

oligonucleotides, peptides, and enzyme substrates or by labeling cell populations. Probe generation might be simple: for example, the labeling of cysteine residues with N-hydroxysuccinimide esterification of NIR dyes or might involve complex chemistry. Cells can be labeled by using membrane-bound NIR dyes or fluorochromes, e.g., nanoparticles, which are internalized by the cells. Alternatively cells can be transfected to express an NIR fluorescent protein as a reporter gene assay [10]. The advantage is that transfected cells do not lose signal intensity after cell division as compared to cells, where fluorochromes are membrane bound or internalized.

2.3 Bioluminescence Approaches

In BLI the light detected using a CCD camera is produced within the organism by an enzymatic reaction. BLI assays are reporter gene assays, in which the oxygenase gene is inserted into the genome of cells under the control of a promoter of a gene of interest. The enzymes are expressed whenever the promoter is active. The strength of the promoter is important. When the promoter is too weak, luciferase is not produced in sufficient amounts. The luciferase should emit photons at wavelength >600 nm as light below this wavelength will be absorbed. The most frequently used reporter is firefly luciferase which produces light with a spectral peak of 590 nm at 37 °C [11]. Light is emitted when the substrate d-luciferin is administered and both oxygen and adenosine triphosphate are present at sufficient concentration. BLI uses the same instrumentation as NIRF imaging, but does not require a light source for illumination. BLI is like NIRF imaging also affected by scattering of emitted photons which limits the spatial resolution to 1–2 mm. BLI approaches can be used for studying gene expression, protein-protein interactions, enzymatic activities in whole organism, and to monitor cell trafficking of transfected cells.

2.4 General Protocol for Optical Imaging in Rodent Stroke Models

This is a general protocol planar NIRF imaging of mice and rats. FMT might require a different hardware handling.

1. Administration of fluorescent probe, inject or implant labeled or transfected cells.

   Probes are generally administered by intravenous (i.v.) injection into the tail vein. The time lag between administration of the probe/cells and the imaging depends on the research question but also on the mechanism of contrast generation, e.g., a probe might require time for activation or time is needed for washout of unbound probe, etc. BLI requires also the i.v. or intraperitoneal (i.p.) administration of d*-luciferin before imaging.*

2. Anesthetize animals.

   The use of injectable anesthetics is in principle feasible, but isoflurane is most widely used for ease of control. Anesthesia is induced

in an induction box using 3% isoflurane in a mixture of oxygen and air. Anesthesia is maintained using 1.5% isoflurane.

3. The head of animals is depilated in strains that have fur.

   First the fur is trimmed using an electrical trimmer and then an epilation cream is applied. Care has to be taken to avoid eye contact with the cream or skin irritations through the shaving procedure.

4. Animals are placed on a heated support on stage within the lighttight box of the imaging system.

   Real-time brightfield imaging might be used during positioning of the animal. The height of the stage is adjusted that the head fits the field of view of the camera. Body temperature is kept at 37 °C. For NIRF imaging, a sample of an NIR dye can be placed next to the animal serving as an internal reference and to check for system performance. Positioning of animals and adjustments of the system (i.e., stage height, binning, and aperture setting) should be kept the same for a set of animals to obtain comparable quantitative data.

5. White light and fluorescence emission images or BL images are acquired using the instrument software.

   For NIRF imaging, appropriate excitation and emission filters are selected. The exposure time is chosen, depending on the software, automatically or at a value, that the camera is saturated to around 90% to capture as many photons as possible and obtain high quality images.

6. After in vivo imaging, animals are allowed to recover from anesthesia or are sacrificed for harvesting organs.

   The firefly luciferase signal remains strong for 45 min post mortem so the tissue origin of the measured signal can be verified by ex vivo imaging. Ex vivo NIRF imaging can be used to assess biodistribution of the injected probe or cells in organs or tissue sections.

7. Images are normalized to the acquisition times, and region-of-interest analysis is performed.

   For NIRF imaging, an automated baseline correction is performed to remove readout noise, and images are corrected for illumination inhomogeneities. Analysis can be performed using commercial or open-source software such as ImageJ (http://rsbweb.nih.gov/ij/).

3 Noninvasive Optical Imaging in Small Animal Models of Stroke

Cerebral ischemia initiates a plethora of pathophysiological processes which are potential targets for the visualization with optical imaging. Here we present some examples of the application of optical imaging to rodent models of stroke.

3.1 Examples of NIRF Imaging of Stroke Pathophysiology

3.1.1 NIRF Imaging of Hemodynamic Dysfunction and Vascular Thrombosis

NIRF imaging can be used to noninvasively assess hemodynamic parameters in the rodent brain and can hence be employed to assess the perfusion status in experimental stroke. Ku et al. have shown that planar NIRF imaging can be performed dynamically during the intravenous bolus administration of indocyanine green [12]. Hemodynamic parameters are computed from the dynamics of the passage of the bolus of dye through the brain. Using this technique, persisting perfusion deficits were revealed in the ischemic territory of the mouse brain after middle cerebral artery occlusion (MCAO) [12] and photothrombotic stroke [13]. However, the low spatial resolution and lack of three-dimensional information of planar NIRF imaging limits considerably the information about the spatial extent of hemodynamic dysfunction that can be obtained with this method. Different approaches might aim to directly visualize molecular mediators underlying the perfusion deficit. For example, Zhang et al. have used an FXIIIa-targeted NIRF probe to visualize secondary thrombosis after inducing a thromboembolic stroke in mice with planar NIRF imaging [14]. The coagulation factor FXIIIa and fibrinogen are the key proteins involved in intravascular fibrin formation. NIRF imaging revealed a time-dependent increase in fluorescence over the ischemic hemisphere. Such approaches might be useful to monitor the effects of recanalization therapies in stroke models in vivo.

3.1.2 NIRF Imaging of Inflammation and Tissue Remodeling

Ischemic stroke initiates complex and dynamic inflammatory processes that occur hours to weeks after the onset of ischemia. Inflammation has been implicated in secondary lesion growth but also to partake in repair and recovery of the tissue. A study by Klohs et al. demonstrated that stroke-induced inflammation after MCAO in mice can be visualized after injection of a fluorescently labeled monoclonal antibody against the CD40-receptor [15]. NIRF imaging showed high TBR in the brain of MCAO mice injected with the CD40 receptor antibody compared to controls. Histological workup revealed that the fluorescence detected within the ischemic lesion with NIRF imaging was attributed to the presence of blood-derived with $Iba1^+$ mononuclear phagocyte that have taken up the labeled antibody. The use of whole-labeled antibodies however requires long washout times of unbound probes, and approaches using antibody fragments might be more suitable to achieve contrast more rapidly.

Several studies have employed NIRF imaging to visualize matrix metalloproteinase (MMP) activity in stroke models. MMPs, in particular MMP-2 and MMP-9, are upregulated after cerebral ischemia and have been implicated in blood-brain barrier (BBB) damage and hemorrhagic transformation as well as in tissue regeneration and repair [16, 17]. Klohs et al. have shown that MMP activity after MCAO can be visualized with planar NIRF imaging using a MMP-activatable probe (Fig. 2 [18]). The effects of therapeutic interventions on MMP activity using this approach has been investigated in several studies. The administration of recombinant tissue plasminogen activator increases MMP activity in the ischemic brain as detected with NIRF imaging [19, 20]. The coadministration of a reactive oxygen species scavenger or the intravenous administration of bone marrow stromal cells can ameliorate this effect. In contrast, hypothermia, which is neuroprotective after ischemia, leads to a reduction of MMP activity [21].

Bai et al. have used a $\alpha_v\beta_3$-targeted nanoprobe to investigate angiogenesis after MCAO in mice with NIRF imaging [22]. They showed that most angiogenesis took place after 10 days after MCAO and that signal increase was not related to unspecific accumulation due to BBB impairment. In contrast, fluorescently labeled bovine serum albumin has been used to visualize BBB impairment after MCAO [23, 24]. The approach can be useful to noninvasively assess the status of the BBB after experimental stroke, which might be relevant for treatment studies. The breakdown of the BBB leads to secondary damage and cell death. Bahmani et al. demonstrated that cell death can be detected in mice after MCAO with NIRF imaging using labeled annexin A5 as probe [25].

3.1.3 NIRF Imaging the Fate of Cell Transplants

Attempts are made to use cell-based therapies in stroke. Due to its sensitivity, NIRF imaging is ideally suited to track the fate of labeled cells in rodent models of stroke. Examples have demonstrated that marrow stromal cells can be labeled with quantum dots [26, 27]. Cells were transplanted into the ipsilateral striatum of rats after permanent MCAO, and engraftment of cells into the ischemic territory for up to 8 weeks was monitored. Cell tracking approaches might also be useful to study the role of specific immune cell populations.

3.2 Examples of BLI of Stroke Pathophysiology

3.2.1 BLI of Inflammation and Tissue Remodeling

Cordeau et al. generated transgenic mice that carry the luciferase gene under the transcriptional control of the GFAP promoter [28]. After MCAO BLI signal in mice peaked at 24 and 72 h and showed a decline at days 5 and 7 days, indicating astrogliosis at these subacute time points. Similarly, Lalancette-Hebert et al. generated a transgenic mouse model that carried the luciferase under the transcriptional control of the murine toll-like receptor 2 promoter to assess microglia activation [29]. Increased BLI signal was detected with noninvasive BLI up to 3 months after MCAO in mice. Using this reporter mouse and BLI, it was further shown

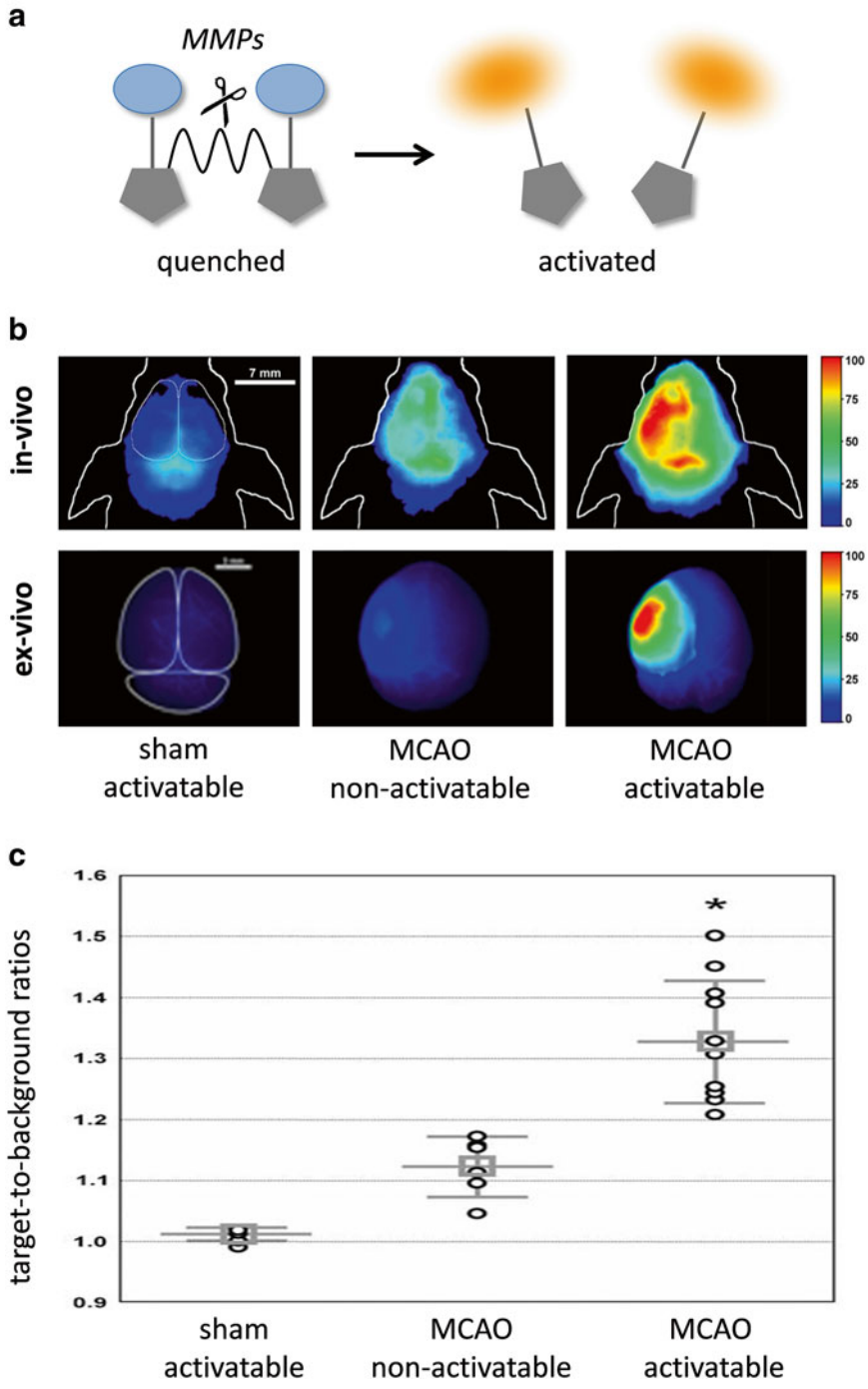

Fig. 2 The use of an MMP-activatable NIRF probe for visualizing MMP activity after MCAO in mice. Two NIR fluorochromes are coupled to each other in close proximity that fluorescence is dark quenched (**a**). The linker of the molecule is a substrate for the proteolytic activity of MMPs. Upon cleavage of the binder, the fluorochromes become liberate and emit photons (**b**). NIRF imaging in MCAO mice 24 h after MCAO (and 24 h after injection of the MMP-activatable probe) reveals high fluorescence intensities over the ischemic hemisphere (**b**). Target-to-background ratios are significantly higher in MCAO-injected mice with the MMP-activatable probe compared to controls (**c**). Figure adapted from [18]

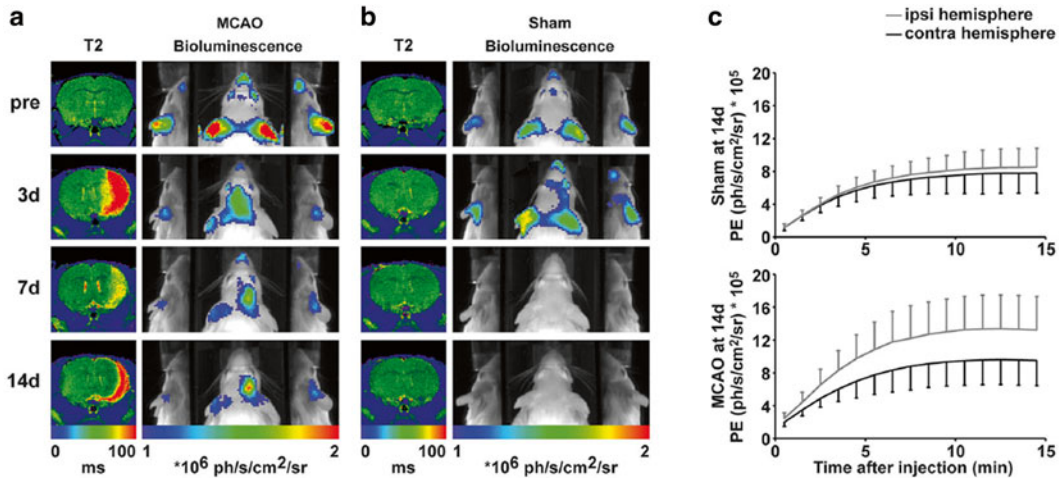

Fig. 3 A transgenic mouse strain expressing firefly luciferase under the control of the VEGFR2 promoter was used to assess vascular remodeling after experimental stroke. Longitudinal magnetic resonance imaging and BLI data sets of mice after MCAO (**a**) or sham surgery (**b**). BLI are shown as a horizontal planar projection of photon emission onto a mouse white light image. BLI signal intensity starts to increase 3 days post-MCAO, and photon emission is clearly increased over the ischemic hemisphere compared to the contralateral hemisphere at 7 and 14 days post-MCAO. BLI kinetics of the ischemic and the intact hemisphere at 14 days post sham surgery (**c**, *upper graph*) and MCAO surgery (**c**, *lower graph*). Figure adapted from [19]

that diet and the environment can modulate toll-like receptor 2 expression/microglia activation [30, 31]. Adamczak et al. investigated a transgenic mouse line which expresses firefly luciferase under the control of the vascular endothelial growth factor receptor 2 promotor after MCAO [32]. Increase BLI signals were detected at 3 days after MCAO with peak values at 7 days, indicative of vascular remodeling at this time point (Fig. 3).

3.2.2 BLI of Cell Trafficking

BLI can be used to monitor the trafficking of transplanted cells. Kim et al. transfected neural progenitor cells to express firefly luciferase [33]. They used noninvasive BLI to track the fate of the neural progenitor cells after injection into the brain of nude mice following permanent MCAO. Similarly, Pendharkar et al. transduced mouse neural stem cells with a firefly luciferase reporter gene [34]. BLI was used to track transplanted cells up to 2 weeks after transplantation, and ex vivo BLI was used to determine single organ biodistribution.

4 Critical Parameters of Optical Imaging in Rodent Models of Stroke

4.1 Critical Parameters for NIRF Imaging

Several critical parameters will determine the suitability of NIRF imaging assays for experimental stroke studies. For the generation of bright fluorescent probes, fluorochromes with both a high

extinction coefficient and quantum yield should be chosen. However, the metabolic stability and toxicity of the fluorochrome (e.g. quantum dots) should be considered. After labeling of compounds, it should be tested that the labeling procedure has not led to an alteration of ligand properties (binding affinity, solubility, etc.). Cells labeled or transfected need to be tested for their viability and proper function. High amounts of dye, for example, internalized in cells or bound to the cell membrane, might compromise cell function and lead to cell death and can also lead to a quenching of the dye with a decrease in fluorescence intensity.

Successful NIRF imaging also critically depends on the pharmacokinetics and biodistribution of the injected probe. Blood-tissue barriers like the BBB might prevent delivery of probes to targets in the brain parenchyma. But conversely, impairment of BBB integrity after stroke can lead to an unspecific extravasation of injected probe for intravascular targets.

Moreover, optical properties of the tissue govern the ability to perform NIRF imaging in the rodent brain. Absorption and scattering of photons in the tissue (which can both change under pathological conditions) make quantification of fluorescence emission challenging. In addition, tissue autofluorescence might increase as a result of tissue remodeling after stroke. While FMT systems, where quantification can be achieved, are commercially available, most researchers use planar NIRF imaging systems that do not allow for absolute quantification. For planar NIRF imaging, positioning of animals and adjustments of the imaging system should be set reproducibly and checked (e.g. use of reference standards) to obtain comparable quantitative data sets.

4.2 Critical Parameter for BLI

It is assumed that the luciferase activity is linearly correlated to the transcriptional activity of the reporter gene. However, many factors can affect the luciferase reactions and hence be potential confounders in BLI experiments. For example, the luciferase expression can be affected by the degree of tissue oxygenation and body temperature (which can both be severely affected by the stroke pathology) as well as by use of anesthetics [35]. Moreover, the BLI signal depends on the d-luciferin substrate availability [36]. When transfected cells are used, it is important that membranes are permeable for the substrate. Moreover, the location of cells is important as delivery of d-luciferin might differ at different sites. Differences in the distribution exist also if the substrate is administered i.p. or i.v. [37]. Moreover, clearance depends on the heart rate, temperature of the animals, and hence depth of anesthesia. Therefore, physiological parameters need to be carefully controlled in BLI studies.

References

1. Billinton N, Knight AW (2001) Seeing the wood through the trees: a review of techniques for distinguishing green fluorescent protein from endogenous autofluorescence. Anal Biochem 291:175–197
2. Kobayashi H, Koyama Y, Barrett T, Hama Y, Regino CA, Shin IS, Jang BS, Le N, Paik CH, Choyke PL, Urano Y (2007) Multimodal nanoprobes for radionuclide and five-color near-infrared optical lymphatic imaging. ASC Nano 1:258–264
3. Ntziachristos V, Turner G, Dunham J, Windsor S, Soubret A, Ripoll J, Shih HA (2005) Planar fluorescence imaging using normalized data. J Biomed Opt 10:64007
4. Klohs J, Steinbrink J, Nierhaus T, Bourayou R, Lindauer U, Bahmani P, Dirnagl U, Wunder A (2006) Non-invasive near-infrared imaging of fluorochromes within the brain of live mice: an in-vivo phantom study. Mol Imaging 5:180–187
5. Ntziachristos V, Tung CH, Bremer C, Weissleder R (2002) Fluorescence molecular tomography resolves protease activity in vivo. Nat Med 8:757–760
6. Bourayou R, Boeth H, Benav H, Betz T, Lindauer U, Nierhaus T, Klohs J, Wunder A, Dirnagl U, Steinbrink J (2008) Fluorescence tomography technique for non-invasive imaging of the mouse brain. J Biomed Opt 13:041311
7. Hyde D, de Kleine R, MacLaurin SA, Miller E, Brooks DH, Krucker T, Ntziachristos V (2009) Hybrid FMT-CT imaging of amyloid-beta plaques in a murine Alzheimer's disease model. Neuroimage 44:1304–1311
8. Stuker F, Baltes C, Dikaiou K, Vats D, Carrara L, Charbon E, Ripoll J, Rudin M (2011) Hybrid small animal imaging system combining magnetic resonance imaging with fluorescence tomography using single photon avalanche diode detectors. IEEE Trans Med Imaging 30:1265–1273
9. Klohs J, Wunder A, Licha K (2008) Near-infrared fluorescent probes for imaging vascular pathophysiology. Basic Res Cardiol 103:144–151
10. Filonov GS, Piatkevich KD, Ting LM, Zhang J, Kim K, Verkhusha VV (2011) Bright and stable near-infrared fluorescent protein for in vivo imaging. Nat Biotechnol 29:757–761
11. Zhao H, Doyle TC, Coquoz O, Kalish F, Rice BW, Contag CH (2005) Emission spectra of bioluminescent reporters and interactions with mammalian tissue determine the sensitivity of detection in vivo. J Biomed Opt 10:41210
12. Ku T, Choi C (2012) Noninvasive optical measurement of cerebral blood flow in mice using molecular dynamics analysis of indocyanine green. PLoS One 7, e48383
13. Kang HM, Sohn I, Park C (2015) Use of indocyanine green for optical analysis of cortical infarcts in photothrombotic ischemic brains. J Neurosci Methods 248:46–50.
14. Zhang Y, Fan S, Yao Y, Ding J, Wang Y, Zhao Z, Liao L, Li P, Zang F, Teng GJ (2012) In vivo near-infrared imaging of fibrin deposition in thromboembolic stroke in mice. PLoS One 7:e30262
15. Klohs J, Gräfe M, Graf K, Steinbrink J, Dietrich T, Stibenz D, Bahmani P, Kronenberg G, Harms C, Endres M, Lindauer U, Greger K, Stelzer EHK, Dirnagl U, Wunder A (2008) In-vivo imaging of the inflammatory receptor CD40 after cerebral ischemia using a fluorescent antibody. Stroke 39:2845–2852
16. Wang X, Tsuji K, Lee SR, Ning M, Furie KL, Buchan AM, Lo EH (2004) Mechanisms of hemorrhagic transformation after tissue plasminogen activator reperfusion therapy for ischemic stroke. Stroke 35:2726–2730
17. Zhao BQ, Wang S, Kim HY, Storrie H, Rosen BR, Mooney DJ, Wang X, Lo EH (2006) Role of matrix metalloproteinases in delayed cortical responses after stroke. Nat Med 12:441–445
18. Klohs J, Baeva N, Steinbrink J, Bourayou R, Boettcher C, Royl G, Megow D, Dirnagl U, Priller J, Wunder A (2009) In vivo near-infrared fluorescence imaging of matrix metalloproteinase activity after cerebral ischemia. J Cereb Blood Flow Metab 29:1284–1292
19. Takamiya M, Miyamoto Y, Yamashita T, Deguchi K, Ohta Y, Abe K (2012) Strong neuroprotection with a novel platinum nanoparticle against ischemic stroke- and tissue plasminogen activator-related brain damages in mice. Neuroscience 221:47–55
20. Tian F, Yamashita T, Deguchi K, Omote Y, Kawai H, Ohta Y, Abe K (2013) In vivo optical imaging correlates with improvement of cerebral ischemia treated by intravenous bone marrow stromal cells (BMSCs) and edaravone. Neurol Res 35:1051–1058
21. Barber PA, Rushforth D, Agrawal S, Tuor UI (2012) Infrared optical imaging of matrix metalloproteinases (MMPs) up regulation following ischemia reperfusion is ameliorated by hypothermia. BMC Neurosci 13:76
22. Bai YY, Gao X, Wang YC, Peng XG, Chang D, Zheng S, Li C, Ju S (2014) Image-guided proangiogenic therapy in diabetic stroke mouse models using a multi-modal nanoprobe. Theranostics 4:787–797

23. Abulrob A, Brunette E, Slinn J, Baumann E, Stanimirovic D (2008) Dynamic analysis of the blood-brain barrier disruption in experimental stroke using time domain in vivo fluorescence imaging. Mol Imaging 7:248–262
24. Klohs J, Steinbrink J, Bourayou R, Mueller S, Cordell R, Licha K, Schirner M, Dirnagl U, Lindauer U, Wunder A (2009) Near-infrared fluorescence imaging with fluorescently labeled albumin: a novel for non-invasive optical imaging of blood-brain barrier impairment after focal cerebral ischemia. J Neurosci Methods 180:126–132
25. Bahmani P, Schellenberger E, Klohs J, Steinbrink J, Cordell R, Zille M, Müller J, Harhausen D, Hofstra L, Reutelingsperger C, Farr TD, Dirnagl U, Wunder A (2011) Visualization of cell death in mice with focal cerebral ischemia using fluorescent annexin A5, propidium iodide, and TUNEL staining. J Cereb Blood Flow Metab 31:1311–1320
26. Sugiyama T, Kuroda S, Osanai T, Shichinohe H, Kuge Y, Ito M, Kawabori M, Iwasaki Y (2011) Near-infrared fluorescence labeling allows noninvasive tracking of bone marrow stromal cells transplanted into rat infarct brain. Neurosurgery 68:1036–1047
27. Kawabori M, Kuroda S, Ito M, Shichinohe H, Houkin K, Kuge Y, Tamaki N (2013) Timing and cell dose determine therapeutic effects of bone marrow stromal cell transplantation in rat model of cerebral infarct. Neuropathology 33:140–148
28. Cordeau P, Lalancette-Hebert M, Wenig YC, Kriz J (2008) Live imaging of neuroinflammation reveals sex and estrogen effects on astrocyte response to ischemic injury. Stroke 39:935–942
29. Lalancette-Hébert M, Phaneuf D, Soucy G, Weng YC, Kriz J (2009) Live imaging of Toll-like receptor 2 response in cerebral ischemia reveals a role of olfactory bulb microglia as modulators of inflammation. Brain 132:940–954
30. Lalancette-Hébert M, Julien C, Cordeau P, Bohacek I, Weng YC, Calon F, Kriz J (2011) Accumulation of dietary docosahexaenoic acid in the brain attenuates acute immune response and development of postischemic neuronal damage. Stroke 42:2903–2909
31. Quattromani MJ, Cordeau P, Ruscher K, Kriz J, Wieloch T (2014) Enriched housing downregulates the Toll-like receptor 2 response in the mouse brain after experimental stroke. Neurobiol Dis 66:66–73
32. Adamczak JM, Schneider G, Nelles M, Que I, Suidgeest E, van der Weerd L, Löwik C, Hoehn M (2014) In vivo bioluminescence imaging of vascular remodeling after stroke. Front Cell Neurosci 8:274
33. Kim DE, Schellingerhout D, Ishii K, Shah K, Weissleder R (2004) Imaging of stem cell recruitment to ischemic infarcts in a murine model. Stroke 35:952–957
34. Pendharkar AV, Chua JY, Andres RH, Wang N, Gaeta X, Wang H, De A, Choi R, Chen S, Rutt BK, Gambhir SS, Guzman R (2010) Biodistribution of neural stem cells after intravascular therapy for hypoxic-ischemia. Stroke 41:2064–2070
35. Keyaerts M, Remory I, Caveliers V, Breckpot K, Bos TJ, Poelaert J, Bossuyt A, Lahoutte T (2012) Inhibition of firefly luciferase by general anesthetics: effect on in vitro and in vivo bioluminescence imaging. PLoS One 7:e30061
36. Badr CE (2014) Bioluminescence imaging: basics and practical limitations. Methods Mol Biol 1098:1–18
37. Berger F, Paulmurugan R, Bhaumik S, Gambhir SS (2008) Uptake kinetics and biodistribution of 14C-D-luciferin--a radiolabeled substrate for the firefly luciferase catalyzed bioluminescence reaction: impact on bioluminescence based reporter gene imaging. Eur J Nucl Med Mol Imaging 35:2275–2285

Chapter 13

Behavioral Testing in Rodent Models of Stroke, Part I

René Bernard, Mustafa Balkaya, and André Rex

Abstract

For the past decades, experimental intervention showed therapeutic promise in animal models of stroke has largely failed to produce beneficial effects in human stroke patients. The difficulty in translating preclinical findings represents a major challenge in cerebrovascular research. The reasons for this translational road block might be explained by a number of factors, including poor quality control in various stages of the research process, insufficient experimental power, the validity of experimental stroke model, and the different choices of end point or outcome measures. In this chapter, we present, next to general introduction to behavioral research in rodents, some widely used and reliable behavioral tests by which various sensory, motoric, cognitive, and psychological impairments in rodent stroke models can be assessed. Each test is described in detail and important protocol keypoints for successful testing in rodent stroke models are included.

Key words Focal ischemia, Behavior, RotaRod, Neuroscore, Pole test, Wire hanging, Corner test, Gait, Passive avoidance, Plus maze, Hole board, Sucrose consumption, Open field

1 Introduction

The inability to move therapeutic advances from preclinical to clinical setting, also called translational roadblock, has led to a number of suggestions on how the conduct of stroke research needs to change [1]. One proposal includes the call for long-term studies with complex end points that include a number of functional tests. This marks a sharp turn from decades of stroke research in which histological assessment was the only end point, using lesion size determination to predict the potential therapeutic effectiveness of an agent in in vivo stroke models. Lesion sizes are evaluated post-stroke after varying survival times that range from hours to weeks, and any significant reduction of the lesion size in the treatment group is considered as the evidence of the beneficial effect of the respective substance or intervention. But also a reexamination of stroke models and techniques is required, especially a matching appropriateness of rodent stroke model and behavioral tests.

Ulrich Dirnagl (ed.), *Rodent Models of Stroke*, Neuromethods, vol. 120,
DOI 10.1007/978-1-4939-5620-3_13,

According to popular dictionaries, behavior is defined as (a) anything that an organism does involving action and response to stimulation or (b) a response of an individual, group, or species to its environment. The dichotomy to the two definitions explains the dilemma of behavioral research. While behavior is an individual trait, inferences are made for a large, sometimes, diverse population, sometimes even an entire species. However, most preclinical studies are dramatically underpowered, which can lead to wrong conclusions that infiltrate the scientific literature. But low power is not the only problem in behavioral research. Study design and conduction problems need to be addressed early on.

Behavioral tests have to be designed so that possible responses to well-defined stimuli are clearly defined and quantifiable. For interlaboratory comparison, behavioral tests also need to be described unambiguously and ideally video recorded which does not only show the execution of the test but illustrate the differentiation or scale. In the light of translation, behavioral tests also need to assess congruent deficiencies as they exist in human behavior.

Rodent stroke models, whether permanent or transient, induce sensory, motor, and memory impairments. Consequently, many functional tests focus on motor/sensory behavior. Behavioral testing is also highly relevant to post-stroke emotional and cognitive disturbances. A variety of emotional disturbances including depression, mania, bipolar disorder (very rarely), anxiety disorders, and apathy are observed in stroke patients [5]. These disturbances not only affect the overall well-being of the patient but also confound the recovery process, so modeling post-stroke emotional disturbances and emotional testing draws considerable attention. Cognitive deficits that decrease the quality of life of stroke survivors are also frequently observed after stroke [6, 7]. Stroke researchers who aim at exploring post-stroke cognitive deficits in animal models must inevitably use behavioral tools at some point of their research (Table 1).

Since the emergence of comparative psychology, rats have widely been used in behavior research as well as in any experiment using an animal model. The pioneering works in the field used dogs and cats; however, rats with their ease of handling, good performance in complex tasks, and relatively short breeding cycles immediately became popular and remained the most “popular” species, especially during the first half of the twentieth century. Only with the emergence of new molecular techniques that enable genetic manipulations have mice in the last decade begun to replace rats in many research fields. As a natural outcome of this historical timeline, almost all the behavioral tests that we have at our disposal were initially developed for rats. The increase in the use of mice led scientists to modify tests developed essentially for rats and adapt them in mice models. While this approach was successful in a number of cases, some tests that were successfully used in rats failed to

Table 1
Ten general advices for the planning and execution of behavioral experiments with rodents

Hints for setup and conduction of rodent behavioral experiments
1. *Blinding and randomization*
Especially manually rated scores are subject of bias. Blinding and randomization ensures the validity of behavioral tests. Otherwise an excessive number of presumably false-positive results may lead to wrong conclusions [2, 3]
2. *Repetition*
Repetition is always desired in the experimental setup because it monitors the course of the stroke recovery at different temporal stages. Tests that involve self-motivation or rely on explorative behavior need to be carefully spaced with limited repetition
3. *Habituation and training*
Rodents are sensitive to external stress. Always give animals sufficient time to acclimate to a new environment or test setup. Test compliance generally improves with several training sessions on separate days.
4. *Consistency*
Behavioral tests need to be performed in the same environment, at the same time of day by the same laboratory personnel. Any sudden change in those elements can dramatically distort test results and thus increase variability. For tests that require experimenter rating, if possible video record all test and use the same "blinded" rater
5. *Standardization of experimental operation*
Next to a written protocol, have detailed instructions or a video demonstrating the test with a sham animal and a rodent after ischemia. For scale rates tests, make video recording of animals that represent each point on the scale. Not only for teaching others but as general reference for all users
6. *Dynamic range*
Can the test be performed by sham-operated and ischemic animals? What is the group variability? How big and stable is the test effect size over time? Is variance small enough to reliably detect a treatment effect?
7. *Test validity*
Each newly introduced test in a laboratory setting needs to be validated first. This should also involve positive and negative control groups
8. *Test compliance*
Most behavioral tests require training and baseline assessments. Predetermining thresholds for in- and exclusion parameters for baseline recordings can help in identifying animals that are incompatible with the test
9. *Rodent-experimenter interactions*
Time after arrival from vendor until first training can be used for frequent handling. Rodents use olfaction as a main sense, therefore avoiding strong odors. Note that the gender of the experimenter might also influence test results [4]

(continued)

Table 1
(continued)

Hints for setup and conduction of rodent behavioral experiments
10. *Test battery*
To increase experimental output and efficiency, studies are often designed with multiple behavioral tests, sometimes on the same day. Researchers must note that these tests can influence each other and one should test whether the interaction is beneficial or not. Animals should be allowed to rest in their familiar home cages in between tests. A battery of long-lasting tests is not advised for it can be stressful and negatively influence test results. For multiple test setups, balance out self-motivated and enforced tests

produce satisfactory results in mice. As the usage of mice in behavioral research grows exponentially, scientists today have a variety of behavioral tests for almost any parameter which work reliably in mice. However, current literature on post-stroke behavioral testing in mice is surprisingly limited. Only a handful of papers focus on establishing batteries of tests for different focal ischemia models and time points. As the importance of testing at later time points is being acknowledged, the main difficulty in the field emerges as the lack of sensory motor tests that are able to evaluate deficits with high sensitivity at late time points post-stroke. The low number of reports, differences in the ischemia models, and time of testing and strain differences make it impossible to create a full-scale listing of behavioral tests suitable for each and every time point and focal ischemia model. Nevertheless, there are tests that have been used by various labs and proved successful in post-stroke testing in mice.

In this chapter, we introduce a selection of tests that have been used successfully by various laboratories. We aimed at presenting a battery of tests which can easily be set up with minimum need for sophisticated equipment or high budgets. Since many of these tests were reviewed in detail in the previous chapter, some tests that can be used both in rats and mice were left out to avoid repetition. To alert the readers that post-stroke behavioral testing is not only about sensorimotor function, we have added several tests for memory, anxiety, despair-like behavior, and anhedonia ("depression"). In many cases, the reliability of a behavioral testing relies mainly on the personal experience of the experimenter, which can only be gained by trial and error, yet sometimes a few tips may be a lifesaver. To make choosing a test easier and to point out possible pitfalls, we provide tips and notes of caution regarding the experiments.

2 Motor and Sensory Testing

Sensory and motor are the most striking deficits that stroke survivors suffer from. Similar deficits are observed in varying severity depending on the model and duration of focal ischemia in mice and can be

evaluated by using behavior tasks which test the beneficial or detrimental effects of interventions and substances. It is not possible to cover all sensory motor tests in the scope of this chapter. We have chosen six tests that have been used by various studies and groups in mice models of stroke. Tests that are covered in Chap. 14, such as the sticky-dot test and cylinder test, have also been applied to mice models of ischemia with success.

2.1 Composite Behavioral Score

Stroke in humans and in rodent stroke models is characterized by common functional deficiencies. This includes among others loss of limb function, immune depression, sickness behavior, sensorimotor deficiencies, learning, and memory impairments. Various standardized subtests are necessary to assess the severity of stroke impairments. These tests are helpful to monitor the progression and recovery and assess effectiveness of therapies in rats and mice (Fig. 1). Composite scores, which usually do not require any extra equipment, assess general, motor, and sensory properties and therefore serve as measure respective functional brain areas and fiber tracts. Damaged brain volume correlates well with the sum of functional subscores. A well-known standard to assess the neurological status in rodent MCAO is the Bederson score and modifications of it [8]. It consists of a summary 0–3 grading scale, judging forelimb flexion, forelimb gripping, and circling behavior. While the test is rather simple, its grade correlates with the anatomical site and extension of the infarct (cortex and striatum). However, the Bederson score has drawbacks: The test works well as an acute assessment and therefore for the test of neuroprotective therapies applied as pretreatment or near the onset of MCAO. The test often fails to distinguish sham and stroked rodents after 5 days already. Therefore, more extensive neurobehavioral assessments were developed. One of them is the modified neurological severity (mNSS) score which contains, like the Bederson, tests for

Composite Behavioral Score	
Material	- 45° platform (e.g. cage grid) - Type IV cage (38cmx59 cm) - camera above cage (optional)
Procedure	- Judgment of general (5) and focal-specific (8) deficits by descriptive severity scores
Measurement	- Severity scale (0 to4) of deficits; often only summary score of all deficits is reported

Fig. 1 Photograph of various motor and sensory tests assessing severity of focal deficits. On the right side is a brief overview over general composite behavioral test

forelimb flexion and circling behavior but also more advanced proprioceptive, balancing, and reflex tests. Consequently the possible maximal score is 18 for rats and 14 for mice [9, 10]. The mNSS score has the advantage to assess multiple impairments and permits long time monitoring after stroke.

Another composite test aimed to determine stroke deficits in rodents is the De Simoni behavioral score [11–13]. In addition to other tests, it takes account the physical appearance of the rodent (hair, ears, eyes), certain sensory responses, seizure activity, basic gait, and limb and body symmetry assessments (Table 2). While the De Simoni score is most comprehensive and detailed, it is affected by the same problem as all behavioral scoring tests: It requires a trained investigator, blinded to experimental conditions. Even trained scorers often differ in their assessment and understanding of certain score states. The more subscores a composite test contains, the higher the degree in which two or more test scorers can differ among another. Therefore, either the person who scores remains the same for one study or a video reference exists displaying all tests and score possibilities. Another approach to reduce scorer bias is the use automated open field testing of post-stroke rodents as general behavioral assessment [14].

2.2 Rotarod

The rotarod is one of the most widely used tests for evaluating motor coordination and balance in rats and mice. The rotarod setup [15] consists of a cylinder with a diameter of 3 cm for mice and 6 cm for rats (Fig. 2), which rotates either at a constant speed or in an accelerating fashion (4–40 rpm in 300 s), the latter program is wildly preferred in stroke research. In order to stay on the rod, rodents must continuously walk forward and keep gait coordination between forelimbs and hind limbs. Rodents are trained to stay on the rotating rod as long as they can, and the total time before falling is a measure for motor coordination and balance as well as ataxia [16].

Training is not required but can reduce group variability and decreases the frequency of defecation and urination which can cause an animal to prematurely fall off. If training is desired, three trails separated by 15 min intervals recommended. To achieve significant improvement, 4 trails per day for 5 days starting one week before stroke induction are suggested [17], but other training routines also exist [18, 19]. Especially in long-term repetitive post-stroke testing, preoperative training is crucial to differentiate between actual recovery and motor learning. During the training trials, animals must immediately be placed back on the rod if they fall before the test is finished and must only be returned to their home cage from the rod to increase motivation to stay on the rod. At the preoperative baseline recording, it is important to exclude animals that cannot achieve a self-determined minimum time to fall. Preoperative testing is also recommended when using transgenic animals to avoid false-positive results due to baseline differences to wild-type animals.

Table 2

Detailed description of all parts and subscores of the modified De Simoni behavioral test

Modified De Simoni behavioral score	
General deficits	
Hair (Mouse observed on open bench top (OS). Observation with no interference)	0—hair neat and clean 1—lack of grooming, piloerection, and dirt on the fur around nose and eye 2—lack of grooming, piloerection, and dirty coat, extending beyond just the nose and eyes
Ears (Mouse on OS. Observation at the beginning with no interference and then stimulation by snapping fingers)	0—normal. Ears are stretched laterally and behind. They react by straightening up following noise 1—stretched laterally but not behind (one or both). They react to noise 2—same as 1. They do not react to noise
Eyes (Mouse on OS. Observation with no interference or stimulation)	0—open and clear (no discharge) 1—open and characterized by milky white or dark mucus 3—closed
Posture (Place the mouse on the palm of your hand and rock gently to observe stability)	0—the mouse stands in the upright position on four limbs with the back parallel to the palm. During the rocking movement, it uses its limbs to stabilize itself 1—the mouse stands humpbacked. During the rocking movement, it lowers its body instead of using its limbs to gain stability 2—the head or part of the trunk lies on the palm 3—the mouse reclines to one side but may be able to turn to an upright position with some difficulty
Spontaneous activity (Mouse on OS. Observation with no interference or stimulation for 1 min)	0—the mouse is alert and explores actively 1—the mouse seems alert, but it is calm and quiet and it starts and stops exploring repeatedly and slowly 2—the mouse is listless, moves sluggishly but does not explore 3—the mouse is lethargic or stuporous and barely moves during the 60 s
Focal deficits	
Body symmetry (Mouse on OS. Observation of undisturbed resting behavior and description of the virtual nose-tail line)	0—normal. a. Body: normal posture, trunk elevated from the bench, with fore and hind limbs leaning beneath the body. b. Tail: straight 1—slight asymmetry. a. Body: leans on one side with fore- and hind limbs leaning beneath the body. b. Tail: slightly bent 2—moderate asymmetry. a. Body: leans on one side with fore- and hind limbs stretched out. b. Tail: slightly bent
Gait (Mouse on OS. Observation of undisturbed movements)	0—normal. Gait is flexible, symmetric and quick 1—stiff, inflexible. The mouse walks humpbacked, slower than normal mice 2—limping with asymmetric movements 3—more severe limping, drifting, falling with obvious deficiency in gait 4—does not walk spontaneously

(continued)

Table 2
(continued)

Modified De Simoni behavioral score	
Climbing (Mouse is placed in the center of a gripping surface at an angle of 45° to OS)	0—normal. The mouse climbs quickly 1—climbs with difficulty, limb weakness present 2—holds onto slope, does not slip or climb 3—slides down slope, unsuccessful effort to prevent fall
Circling behavior (Mouse on OS. Observation of the mouse walking undisturbed on the OS)	0—circling behavior absent. The mouse turns equally to left or right 1—predominantly one-sided turns. Optional: record to which side the mouse turns 2—circles to one side, although not constantly 3—circles constantly to one side. This one is now highlighted in yellow
Forelimb symmetry (Mouse suspended by the tail. Movements and position of forelimbs are observed)	0—normal. Both forelimbs are extended toward the bench and move actively 1—light asymmetry. Contralateral forelimb does not extend entirely 2—marked asymmetry. Contralateral forelimb bends toward the trunk. The body slightly bends on the side ipsilateral to the stroke 3—prominent asymmetry. Contralateral forelimb adheres to the trunk 4—slight asymmetry, no body/limb movement
Compulsory circling (Forelimbs on bench, hind limbs suspended by the tail. This position reveals the presence of the contralateral limb palsy. In this handstand position, limb weakness is displayed by a circling behavior when the animal attempts forward motion)	0—absent. Normal extension of both forelimbs 1—both forelimbs extended but begins to circle predominantly to one side 2—circles only to one side and may show slower motion than healthier mice 3—pivots to one side sluggishly and does not rotate in a full circle
Whisker response (Mouse is placed on the bench. Using a pen, touch the whiskers and the tip of the ears gently from behind, first on the lesioned side and then on the contralateral side)	0—normal symmetrical response. The mouse turns the head toward the stimulated side and withdraws from the stimulus 1—light asymmetry. The mouse withdraws slowly when stimulated on the paretic side. Normal response on the side ipsilateral to the stroke 2—prominent asymmetry. No response when stimulated on the paretic side. Normal response on the side ipsilateral to the stroke 3—absent response on the paretic side, slow response when stimulated on the side ipsilateral to the stroke 4—absent response bilaterally
Gripping test of the forepaws (Mouse is held by the tail on the wire bar cage lid, so that the forepaws touch the grid)	0—mouse grasps the grid firmly with forepaws and tries to place the hind paws also onto the grid by pulling the hind paws under the body 1—mouse accesses the grid, but has less power. A slight pull breaks the grip of the forepaws [hard to assess on video] 2—mouse cannot grip with the impaired forepaw 3—mouse cannot grip the grid

RotaRod	
Material	- RotaRod apparatus - paper towels and isopropanol
Procedure	- habituation at 4 rpm, training recommended, baseline recording - testing: speed ramp from 4 to 40 rpm - testing can occur at any time, short or long-term
Measurement	- time to fall; or time when a rodent makes a passive rotation - speed at falling time

Fig. 2 Photograph of a 5-lane mouse RotaRod. On the right side is a brief overview over the test

In the actual testing phase, animals in their cage should acclimate for at least 15 min to the test room. Animals are then placed on the rotating rod (4 rpm constant) and when all rodents are in their lanes, acceleration protocol is started [19–21]. Latency to fall or if mouse is clinging to the rod, latency to full passive rotation is recorded. The trials are repeated 3–5 times for each mouse and the average is taken as the final score. If inter-trail variance is very large, alternatively the longest time of all trials can be taken as final score. Inter-trial recovery time for each rodent should be 15–20 min which is spend in the home cage. For data analysis, commonly postoperative values are compared as percent of preoperative data [18, 19, 21].

RotaRod can be also used to assess motor learning behavior by comparing first trial with subsequent trials, especially when the first trial is introduced after the stroke induction. Latency to fall should increase with time. Another procedural variation is the testing of long-term motor memory by introducing the test, then stopping trails for a period of time, and reintroducing the test at a later point [22].

Basically most commercially available RotaRod apparatuses are very similar and will deliver comparable results. However, one important difference, is the height of rotor drum over the floor. Most models have falling height smaller than 20 cm which motivates many mice to jump off the RotaRod. Even the constant return to the rotating drum sometimes does not induce the desired training effect. Some manufacturers, such as San Diego Instruments or TSE, offer RotaRod apparatuses which take advantage of the natural fear of height in rodents with drum heights of 45 cm for mice and 120 cm for rats which can improve the cooperation of the rodents and training results.

2.3 (Vertical) Pole Test

The pole test was originally developed as a measure of bradykinesia in mouse models of Parkinson's disease [23]. This motor coordination test requires minimal equipment, in which a mouse is placed

head upward near the top of a vertical positioned pole that is situated in a cage with bedding. The mouse then turns around and descends the pole with its head first until it reaches the cage with a four paws. A 50 cm wooden or metal pole of 8–10 mm diameter is used for this purpose. If the surface of the pole is too smooth, such as mice sliding rather than actively traveling down, adhesive tape can be used to cover the pole surface area (Fig. 3). The "time to turn around" and the "time to reach the floor" are measured. If a mouse is unable to fully turn head-down, the total time to come down is also assigned to "time to turn around." The cutoff time and therefore maximal time can be set to either 60 or 120 s.

The pole test has been successfully introduced to animal models of focal ischemia (mostly MCAO) and distinguishes sham- and MCAO-operated mice at early and relatively late time points [18, 24, 25] with elevated "time to turn around" and "time to reach the floor" times in ischemic animals. In a 60 min transient MCAO model, the neuroprotective effects of rosuvastatin were successfully demonstrated using the pole test as functional measure [24].

Mice in training are initially placed downward on the pole, in later sessions head upward. Mice are trained (min. 2 days) and tested on 3–5 trials per day with minimum resting intervals of 5 min in their home cage. Animals that do not turn, however, can be encouraged to turn by a gentle. The actual testing can be scored real time by an experienced person using a stopwatch, but a video recording with subsequent analysis is preferable. In a successful run, animal must not pause or stop once it starts moving. If the mouse pauses, the trial is not supposed to be included in the final results.

Pol Test	
Material	- 50 cm pole; 10 mm diameter - large cage with bedding - adhesive tape to cover pole surface (optional) - stopwatch - video camera (optional)
Procedure	- 1 day training, pre-testing (optional), post-operative testing at any time
Measurement	- Time to turn around downwards - Time to reach the ground

Fig. 3 Photograph of a mouse performing the pole test. On the right side is a brief overview over the test

In the conventional pole test used for assessing bradykinesia, the best score out of five trials is taken as the final value for that individual animal. This method was also used in post-stroke testing. Alternatively, the average of five trials can also be used as the final score. We believe the letter method might be a better indicator of post-stroke deficits, especially for milder ischemic paradigms and later time points.

2.4 Wire Hanging

Wire hanging is a motor strength test where the animal has to hold onto a wire with all four paws to avoid a fall. In an adapted version of this test, the animal suspends its body only with its forepaws on a single wire, while hind limbs are gently covered with a sticky tape. The wire located approximately 40 cm above the ground is stretched between two posts which are 50–60 cm apart. A soft pillow or thick layer of bedding is placed between the posts to avoid injury from falling (Fig. 4) [26, 27]. This test evaluates an animal's grasping ability, requiring grip strength as well as strength endurance. Focal brain ischemia, e.g., MCAO, causes impairment in the contralateral forepaw muscle strength, which affects the wire hanging performance.

Compared to the conventional 4-paw hanging wire tests, the animals only using forepaws are more distressed and uncomfortable, partly also because weight that is supported by one paw is now doubled. That makes mice more likely to let go of the wire and try to escape; thus pre-training is required to increase the animals' motivation to hold on as long as they physically can. Training can be achieved by several rounds of habituation and trials. Animals should be allowed to grasp the wire and then are gently released to suspend their own weight. If an animal in training drops before the designated time, it should be immediately returned and forced to grasp the wire. Animals should only be brought back to home cage by taking them from the wire when the trial time is over. If the animals are returned to home cage after a fall from the pillow, they may

Wire Hanging	
Material	- 2 mm wire - 2 posts of approxiamtely. 60 cm height - a soft pillow or blanket - adhesive tape - stopwatch
Procedure	- 1-2 days of training, pre-testing (optional), postoperative testing at any time
Measurement	- time to drop from the wire

Fig. 4 Photograph of hanging wire setup. The function of the plate-shaped dividers on each side is to prevent the rodent to escape the test setup. On the right side is a brief overview over the test

learn to let go of the wire as an escape strategy. In the actual experimental phase, tests are repeated three times with 5 min rest between trials. For the final score, values from three trails are averaged [28]. The maximum test duration is strictly strain dependent.

There are striking differences among strains in their wire hanging performance and behavior. 129/SV mice are easily trained in this task and naïve animals can hold onto the wire up to 300 s. Using 129/SV strain sham vs. animals subjected to only 30 min, MCAO can easily be differentiated even after 3 weeks post operation [24, 26, 29]. On the other hand, C57/BL6 mice can rarely hold on to the wire for more than 60 s, tend to let go, and try to escape more often, which complicates the training procedure. Surprisingly, more severe MCAO paradigms, ranging from 45 to 90 min occlusion, failed to show difference in wire hanging between sham vs. MCAO animals at days 13–19 in C57/BL6 mice [27]. Another 30 min MCAO study using C57/BL6 mice successfully demonstrated neuroprotective drug effects on stroke outcome inkling the wire hanging test for up to 8 days [30]. These findings indicate that strain differences should be taken into consideration when deciding whether to use the wire hanging test and the timing of the test.

2.5 Corner Test

The corner test assesses sensory and motor deficits following both cortical and striatal injury in mice and rat models [31, 32]. It was later adapted in a mouse model of focal ischemia to test long-term functional impairments as late as 90 days after the operation [33]. The test apparatus consists of two cardboards, each with a dimension of $30 \times 20 \times 1$ cm, attached to each other from the edges with an angle of 30°. Along the joint of the two boards, a small opening of a few millimeters is left to encourage the mice to enter all the way to the corner. Mice are introduced into the apparatus by placing them between two boards halfway to the corner. As the animal reaches deep into the corner, facial whiskers touch the boards from both sides and get stimulated. The mice then rear up on their hind limbs and turn back to face the open end of the two boards (Fig. 5) [18, 33, 34]. Naïve mice as a group do not show a side preference, but animals subjected to ischemia turn toward the non-impaired side [33, 35]. However, individual naïve mice might display left or right preference. This individual laterality in pretests can be used to designate the (contralateral) brain hemisphere which should be targeted for ischemic insult.

There is no need for training in the corner test, but testing before ischemia operations can be done to compare pre- vs. post-stroke values as well as to identify a baseline. Usually affixed number of 10 or 15 turns are evaluated in one trial and the percentage of right turns is calculated. Video recording for this test is optional. Important to note is that turning movements without prior rearing are not scored. The only potential problem during the corner

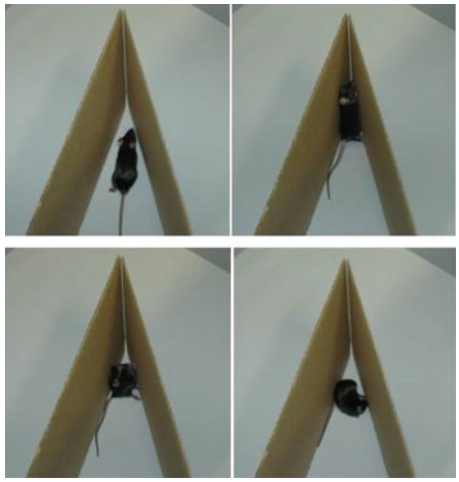

Corner Test	
Material	- Type IV cage (38cmx59 cm) - 2 or 4 boards forming a 30° angle with a slight (1-2 mm) opening - camera above cage (optional) - adhesive tape for board stabilization
Procedure	- pre-testing (for individual side preference); post-operative testing short and long term possible
Measurement	- number of turns and direction after rodent touches board with both paws

Fig. 5 Photograph of a mouse performing the corner test. On the right side is a brief overview over the test

test—especially after severe ischemic manipulations—is that animals can be too sick to perform or show lack of motivation at early time points. The main strength of the corner test lies in its ability to demonstrate functional deficits as late as 90 days after ischemia [33]. Several other studies also confirmed successful observation at earlier time points [18, 34]. It has also been reported that the corner test can demonstrate functional improvements due to therapeutic treatments [30, 35].

2.6 Unforced Locomotion Gait Analysis

More than 50% of stroke survivors suffer from at least partial motor disabilities. The most common impairment is hemiplegia which negatively impacts gait performance. While most stroke patients partially regain gait independence, many do not achieve the ability to independently perform all daily activity. The gait-underlying neurophysiology is complex and relies on a dynamic interaction between central pattern generators in the spinal cord; feedback loops involving motor cortex, cerebellum, and brain stem; and constant peripheral sensory information. Especially the latter is important for the neural control of musculoskeletal system and the adjustments to changes in the environment. While most ischemic strokes result from blockage of the middle cerebral artery (MCA), the motor cortex in human is mainly supplied by the anterior cerebral artery. Therefore, damage of the motor cortex is less likely the major cause for stroke-induced gait impairments. In agreement, the MCA-supplied posterolateral putamen is suggested to be associated with temporal gait asymmetry in post-stroke patients [36]. Several rodent stroke models have been used to investigate post-stroke—gait impairments, many of them performed in rats, but there are recent studies in mice. Gait is best investigated in an environment where rodents can move freely.

Commercially available systems, like Noldus CatWalk™, TSE MotoRater, or Cleversys Runway, permit automated recording and analysis of unforced locomotion along a unidirectional straight pathway (Fig. 6). Little training is required and repeated measurements at various time point permit short and long-term analyses of gait after stroke. The advantage of such a system is the integration of spatial and temporal information of each paw recorded and a multitude of relationships can be assessed. This advantage has its drawbacks because each individual run can generate up to 233 parameters. Many of them correlate with speed, but the relationship can be linear, logarithmic, inverse, or independent [37, 38]. Since walking speed in acute and chronic stroke patients as well as rodent stroke models can be reduced, controlling for speed as cofactor is indispensable [37, 39]. Though problematic, running velocity is an important gait parameter indicative of the rodent and human post-stroke phenotype. Other parameters that are known to be altered in the MCAO model include stand duration, swing speed, stride length, step and duty cycle, base of support, as well as certain phase dispersions. Run data can be analyzed in two different manners: (1) using runs only with predefined run criteria for minimal and maximal run duration and speed variation and (2) using data segmentation to set speed and variation criteria for a certain minimum number of consecutive steps within a run. While the first analysis takes into account the entire run, the second type uses a certain portion within the run. The latter one has the advantage that previously non-complaint runs can still be used for

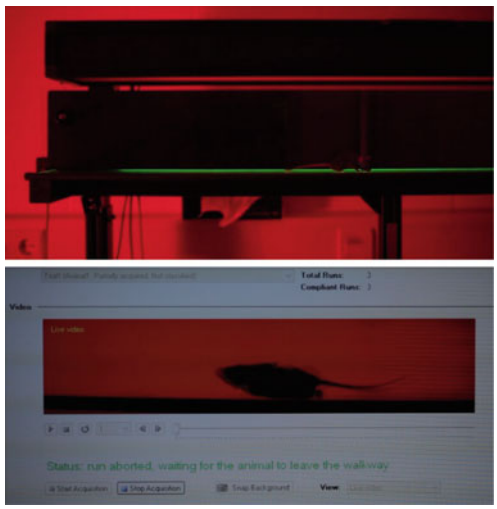

Gait Analysis	
Material	- automated rodent gait recording and analysis system, e.g. Noldus CatWalk XT System, TSE MotoRator or Cleversys Runway
Procedure	- weight-adjusted sensitivity calibration - 3 times training; base line record - post-operative testing from day 2 or3 on - frequent cleaning between runs using glass cleaner and lint-free wipes
Measurement	- video footprint recording of each rodent's time and speed variation for passage of a 40-60 cm corridor - after automatic footprint assignment 233 individual parameters/ run are calculated

Fig. 6 Photograph of CatWalk apparatus and screen capture of gait video analysis. On the right side is a brief overview over the test

analysis and that data variability within each run can be reduced. Consider to separate the data segmentation in low, medium, and high running speed intervals to compare gait parameters between groups in similar speed ranges [39, 40].

Training to motivate rodents for uninterrupted walkway passage can be achieved by placing a goal at the end of the platform, ideally the open cage containing littermates. This helps also the otherwise anxious rodents to move quickly toward a goal of familiar odor and vocalization. It is also advised to let the rodent explore the end of the platform near the home cage before entering the walkway for the first time.

3 Learning and Memory

Cognitive impairment is very common after stroke in patients and therefore also a point of interest in stroke research in animals. There are numerous tests, ranging from conditioning task to spatial memory tasks, that can be used to determine different types and aspects of memory. However, the assessment of cognitive abilities in experimental stroke research may be problematic because transient ischemia is mostly accompanied by sensorimotor impairments that may evolve as confounding factors in cognitive testing. Up to date, only very few of these tests have been used in stroke research in mice. Here, we discuss one version of the passive avoidance task and the hole board test. The Morris Water maze is another memory test which has been used in stroke research and is described in the following chapter. Although there are distinct differences in performance in the water maze task [41], there are only few differences between mice and rat water maze procedures. Readers interested in memory tests in more detail may refer to Chap. 14.

3.1 Passive Avoidance

The one trial fear-motivated passive avoidance task is a simple memory test and has been commonly used in learning and memory research. There are different modifications of this paradigm. Here, we will only discuss the passive avoidance task that requires the transition of the test animal from one chamber to the other, also called “step-through” passive avoidance. In this task, animals learn to avoid the location in which an aversive experience took place.

Step-through passive avoidance is a two-day task. The animals are trained in a step-through inhibitory avoidance apparatus involving a large brightly illuminated start partition and a smaller not illuminated partition with a shocking grid on the floor. Both parts of the test apparatus are connected by a sliding door (Fig. 7).

Usually, on day 1 (training), an animal is placed into the start partition with the sliding door closed. After a short habituation period, the sliding door opens [18, 34, 42, 43] and the animal is allowed to enter the non-aversive dark partition. Generally, the

Passive Avoidance	
Material	- illuminated start box (16 × 16 × 20 cm) with a 3 × 3 cm sliding door to a dark goal box (11 × 9 × 7 cm) with a grid floor - programmable stimulator - stop watch
Procedure	Day 1:-place mouse in the start box. - close sliding door when the animal enters the dark box - apply foot-shock -remove animal Day 2:-Same procedure, except for receiving the foot-shock
Measurement	Day 1 entering latency (max. 60 sec) Day 2 Entering latency (max. 300 sec)

Fig. 7 Photograph of a passive avoidance apparatus. On the right side is a brief overview over the test

latency to enter the dark compartment is recorded to compare it with the retention test results. Animals with step-through latencies longer than 60 s are commonly rejected from further experimentation. After the animal enters the dark compartment with all four paws, the sliding door is closed and the animal receives an unavoidable foot shock (0.2 mA) for 1 s. The shock intensity must be sufficient to induce a vocalization and a rapid escape reaction from the animal that can be heard by the experimenter. If the animal does not display these reactions, the intensity may be too low or there may be a problem with the setup that prevents the proper shock administration. Various shock intensities and durations have been used in different studies, ranging from 1 to 5 s and 0.1 to 0.8 mA. After the cessation of the shock, animals are typically left 10 more seconds in the dark chamber to enable the formation of an association between the shock and the compartment.

24–96 h later, the animals are placed again in the brightly lit compartment and the time until reentering the dark compartment, this time without a foot shock, is determined. Testing is terminated either when the mouse reenters the dark compartment or after 180–600 s without entry. To avoid any olfactory cues, the compartments should be cleaned between two animals.

To date, only few studies used passive avoidance tasks to measure learning and memory performance after focal ischemia models in mice [18, 27, 34, 44]. There are considerable differences in the models used in terms of the duration of ischemia and timing of the testing, so therefore more studies are required to fully portray the effects of focal ischemic manipulations on passive avoidance performance in mice.

3.2 Hole Board Test

The hole board test is essentially a test for the assessment of exploratory behavior in mice [45] and rats [46]. Repeated testing is also seen as a non-conditioned test of habituation learning, which does not require motivational stimulation [46]. The test arena represents an open field with usually 16 holes in the floor (Fig. 8). The animals are placed on the floor and will explore the new surroundings by dipping their heads into the holes. The number of head dips into the holes (nose pokes) is regarded as a measure of exploration. Repeated exposure of the animals to the hole board results in habituation determined by a reduced number of nose pokes. It could be shown that the hole board is suitable for the detection of hypo- and hypermnestic effects.

Usually, on the first day, a single animal is placed in the center of the dimly lit hole board and left there for 5–10 min. The number of the nose pokes is counted. 24 h later, the animals are placed again in the test arena for 5–10 min and the number of nose pokes on the second day is determined. A reduction of nose pokes during the second exposure indicates habituation and therefore intact memory processes, whereas impairment of learning and memory will be shown by no changes in the number of nose pokes on the second exposure.

Until now, there are only unpublished results using the hole board after focal transient ischemia models in mice [18, 27, 34, 44]. Since the hole board relies on naturally occurring behavior without punishment, it could be favorably used for the assessment of different facets of learning and memory. Therefore, more studies are required to fully portray the effects of focal ischemic manipulations on the behavior in the hole board in mice.

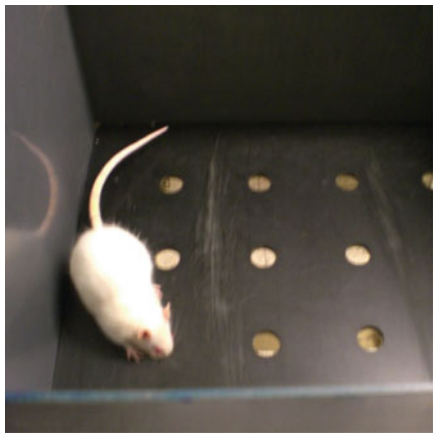

Holeboard	
Material	- Perspex open field (50 × 50 × 40 cm) with 9-16 holes, 2.5 cm ø – infrared light beams under the floor - stop watch
Procedure	day 1 + day 2: -place mouse in the open field (5-10 min) - optional video tracking
Measurement	-number of nose pokes, -number of rearings - optional locomotor activity

Fig. 8 Photograph of a rat in a hole board apparatus. On the right side is a brief overview over the test

4 Anxiety

Approximately 20–25 % of stroke patients suffer from long-lasting post-stroke anxiety disorders or posttraumatic stress disorder. Therefore, it is of interest in translational research whether or not a stroke treatment would affect anxiety-like behavior in animals.

There are a number of tests that are used to asses anxiety-like behavior in rodent models, such as dark-light box, Vogel conflict test, Geller-Seifter conflict test, elevated plus maze, and open field. Here, we introduce two tests, namely, the elevated plus maze and open field, as reliable options for mice.

4.1 Elevated Plus Maze

The elevated plus maze is a popular, ethologically based test of anxiety-related behavior, using the natural aversion of rodents to open spaces. The principle of this test was developed by Montgomery (1955) [47]. He observed that rats avoided the "open" part without protecting the walls of an elevated Y-shaped maze. Untreated animals stayed most of the time in the less-aversive "closed" arms (surrounded by walls). Later, a plus-form test apparatus (X-maze) with two opposite open and closed arms [48] was developed. With the X-maze both "anxiolytic" and "anxiogenic," effects can be detected in rats and mice. A prolonged stay in the open arms and an increased percentage of all visits in the open arms are considered as "anxiolytic-like" behavior [49].

An important advantage of the X-maze is the possibility to assess locomotor activity, number of entries into and time spent in the open and closed arm, by video tracking systems. In a refinement approach to the X-maze analysis, "ethological" measures like closed arm returns and stretch-attend postures as risk assessment behavior were validated [50]. With video recording software, the total distance covered by an animal can be calculated and used along with total arm entries to assess hyperactivity or sedation.

The X-maze consists of two closed arms and two open arms (for the use with mice even the open arms should have small ledgers approx. 2–3 mm high to prevent unintended downfalls). The arms extend from a central platform and the X-maze is elevated 50–75 cm from the floor according to different protocols (Fig. 9). Preferably, the X-maze is placed in a soundproof chamber with neutral environment and a dim light. For testing, animals are placed on the central platform facing one of the closed arms. In a 5 min session, the animal is allowed to explore the X-maze freely, and scoring is done by an observer and/or a video tracking software. After each session, the apparatus is carefully cleaned to avoid introducing bias in the next animal.

A few studies used X-maze to measure the potential anxiogenic effects of focal ischemia in rats [51] and mice. It has been reported that 30 min of transient focal ischemia is sufficient to induce

Elevated Plus Maze	
Material	- Perspex plus maze with two open arms and two enclosed arms (5× 30 cm, 45cm high [mice] or 10 x 50 cm, 55cm high [rats]) with video tracking - stop watch
Procedure	-place the animal in the centre of the X-maze (5 min)
Measurement	-number and percentage of entries into the open and closed arms -time spent in the open and closed arms -number of rearings, closed arm returns and stretch-attend postures

Fig. 9 Photograph of an elevated plus maze apparatus. On the right side is a brief overview over the test

anxiety-like behavior in 129SV mice when tested at 9 weeks after the operation [52]. In another study, neither 60 min nor 90 min of transient focal ischemia induced an anxious phenotype, when tested at 13 days post operation [27]. Apparently, more studies are needed to understand the nature and the time window of post-ischemic anxiety in mice.

4.2 Open Field Test

Open field exploration tests can be used to evaluate both emotionally influenced locomotion and spontaneous, unidirected locomotor activity in mice and rats. Open field setups of different sizes ranging from 40 × 40 cm to 1 × 1 m or larger and different shapes such as circular, square, or rectangular are in use. Rodents are placed inside an open arena surrounded by insurmountable walls, and rodents are allowed to explore the field freely for a predetermined time period ranging from 5 min to several hours, though 10 min is generally sufficient to detect gross changes in locomotor activity. The floor of the open field can be divided into small squares through drawn lines or photoelectric barriers, and resulting line or beam crossed by the rodents can be assessed manually or automatically. Today, automated video-assisted open field systems can not only analyze two-dimensional activity but also vertical locomotion patterns like grooming or rearing in addition to total distance traveled and time spent in quadrants (Fig. 10).

Rodent behavior in the open field is influenced by various factors such as lighting. Bright lights are an aversive stimulus in rodents and reduce exploration, while low lighting conditions are generally associated with reduced anxiety and increased exploratory behavior [53]. The relatively large territory is unfamiliar to them and thus a potential threat. Therefore, rodents prefer to stay near the walls and avoid the open center. To assess anxiety-like

Open Field	
Material	- Perspex open field (50 × 50 × 40 cm[mice] or 100 x 100 x 40 cm [rats]) with video tracking or other means to measure locomotor activity - stop watch
Procedure	-place the animal in the open field (5-10 min)
Measurement	-determine distance travelled - number of rearings - optional time spent in the center (measurement of anxiety)

Fig. 10 Photograph of an open field setup. On the right side is a brief overview over the test

behavior in the open field, the time spent in the "wall zone," "transition zone," and "center zone" and the number of zone visits can be distinguished. An increase in time spent in the "wall zone," compared to control animals, indicates an increased anxiety-like behavior [54]. There is considerable habituation especially in smaller automated open field system, which results in a decrease in movement activity.

The rodent behavior in the open field after stroke is biphasic. In the acute phase after focal ischemia, overall activity is reduced. Severity of this hypoactivity is dependent on the duration of ischemia and rodent strain. After a few days, mice can transition into a hyperactive state which is characterized by high locomotor activity with body rotating tendencies and possible motor deficits [52].

5 Depression-Like Behavior

Post-stroke depression is the most frequent psychological sequel following stroke and is associated with increased mortality and poor recovery. Similar to post-stroke anxiety disorders, its etiology is still unclear [55]. The Porsolt forced swim test, tail suspension, sucrose consumption/preference, and learned helplessness tests are well-established tests used to assess depression-like behavior in mice. Potentially, all of these can be used to evaluate depression-like behavior after stroke. However, we only discuss sucrose consumption/preference test in this chapter because there is a dearth of reports using other tests in mice models of stroke.

5.1 Sucrose Consumption/ Preference

Anhedonia is the loss of interest in pleasurable activities and rewarding stimuli and is specified as one of the core symptoms of depression. Tests of sucrose consumption/preference can be used

for anhedonia evaluations in rodents. Animals tend to consume substantial amounts of sweet substances or solutions since it constitutes a natural reward. When introduced to sucrose solutions, rodents consume higher amounts compared to their normal daily liquid intake and show a significantly higher preference to sucrose solutions over water given simultaneously. There are signs of reward system dysfunction in depressed individuals, as well as in animal models of depression [56]. In line with this finding, consumption of sucrose solutions or pellets is reduced in animals subjected to depression models [56–59].

Sucrose consumption/preference paradigms are far from being standardized, and there is a great variability in terms of preferred sucrose concentration, training duration, schedules, and testing duration among laboratories. A simple way to perform sucrose consumption tests is to offer animals a single bottle filled with a sucrose solution and measure the amount consumed in ml. Generally, solutions of 1–3% sucrose are used. For optimum results, animals are introduced to the sucrose solution in a course of several days before the actual test. In order to increase the motivation to consume the test solution, some studies apply a water restriction to the animals before testing. In the actual testing, both the amount of sucrose solution and water consumed must be recorded to see if the intervention has had any effect on the amount of water consumed.

An alternative way is to introduce two bottles to animals, one containing the sucrose solution and the other regular tap water (Fig. 11). To rule out the effect of bottle location on the outcome, the sucrose and water bottles must be switched during the test, ensuring that each bottle stays in both locations for the same amount of time. With this method, the animals' sucrose preference

Sucrose Preference	
Material	- 2 ball point rodent drinking tubes - 2% sucrose solution and water - measuring cylinder
Procedure	Habituation to 2 drinking bottles for 3-4 days Test: Sucrose or Water bottles are present for 4 days, switch every days in orientation
Measurement	Sucrose preference is calculated as ratio sucrose/tap water intake volume

Fig. 11 Photograph of a cage with sucrose preference setup. On the right side is a brief overview over the test

over water can be evaluated in percentages. It has been proposed that this method may not be suitable for testing ischemic animals at early time points after operation because of the fact that ischemic animals have cognitive deficits that may prevent them from making the necessary association between the location of the bottle and its contents [57]. To our knowledge, two studies employed sucrose consumption testing after models of focal ischemia. Both reported a significant decrease in sucrose consumption in MCAO-operated animals [25, 57].

Sucrose consumption/preference tests require minimum materials and at first glance seem very easy to perform. However, it may prove difficult to obtain a stable baseline and decide on the optimum schedule and sucrose concentration. Every laboratory must establish its own optimum parameters, depending on the strain and ischemia procedure.

6 Conclusion

Behavioral testing of therapeutic interventions is the ultimate preclinical experimental step before clinical testing. Therefore, the appropriate design and proper execution of those experiments are key prerequisites for the decision making on whether a drug or therapy should enter the clinical testing phase. The tests that have been described here along with several others covered in the next chapter represent a good compilation for researchers who consider using behavioral outcome measures in their stroke research. A variety of mouse and rat models for brain ischemia combined with multitude of transgenic modifications present an enormous toolbox for exploring novel strategies for neuroprotection or neurorehabilitation approaches. Such studies need to include successfully conducted behavioral experiments as one important step to improve or prevent stroke disabilities in humans.

References

1. Endres M, Engelhardt B, Koistinaho J, Lindvall O, Meairs S, Mohr JP, Planas A, Rothwell N, Schwaninger M, Schwab ME, Vivien D, Wieloch T, Dirnagl U (2008) Improving outcome after stroke: overcoming the translational roadblock. Cerebrovasc Dis 25(3):268–278. doi:10.1159/000118039
2. Bebarta V, Luyten D, Heard K (2003) Emergency medicine animal research: does use of randomization and blinding affect the results? Acad Emerg Med 10(6):684–687
3. Ioannidis JP, Haidich AB, Pappa M, Pantazis N, Kokori SI, Tektonidou MG, Contopoulos-Ioannidis DG, Lau J (2001) Comparison of evidence of treatment effects in randomized and nonrandomized studies. JAMA 286(7):821–830
4. Sorge RE, Martin LJ, Isbester KA, Sotocinal SG, Rosen S, Tuttle AH, Wieskopf JS, Acland EL, Dokova A, Kadoura B, Leger P, Mapplebeck JC, McPhail M, Delaney A, Wigerblad G, Schumann AP, Quinn T, Frasnelli J, Svensson CI, Sternberg WF, Mogil JS (2014) Olfactory exposure to males, including men, causes stress and related analgesia in rodents. Nat Methods 11(6):629–632. doi:10.1038/nmeth.2935
5. Robinson RG (1997) Neuropsychiatric consequences of stroke. Annu Rev Med 48:217–229. doi:10.1146/annurev.med.48.1.217

6. Elwan O, Hashem S, Helmy AA, el Tamawy M, Abdel Naseer M, Elwan F, Madkour O, Abdel Kader A, el Tatawy S (1994) Cognitive deficits in ischemic strokes: psychometric, electrophysiological and cranial tomographic assessment. J Neurol Sci 125(2):168–174
7. Tatemichi TK, Desmond DW, Stern Y, Paik M, Sano M, Bagiella E (1994) Cognitive impairment after stroke: frequency, patterns, and relationship to functional abilities. J Neurol Neurosurg Psychiatry 57(2):202–207
8. Bederson JB, Pitts LH, Tsuji M, Nishimura MC, Davis RL, Bartkowski H (1986) Rat middle cerebral artery occlusion: evaluation of the model and development of a neurologic examination. Stroke 17(3):472–476
9. Chen J, Zhang C, Jiang H, Li Y, Zhang L, Robin A, Katakowski M, Lu M, Chopp M (2005) Atorvastatin induction of VEGF and BDNF promotes brain plasticity after stroke in mice. J Cereb Blood Flow Metab 25(2):281–290. doi:10.1038/sj.jcbfm.9600034
10. Li Y, Chen J, Wang L, Lu M, Chopp M (2001) Treatment of stroke in rat with intracarotid administration of marrow stromal cells. Neurology 56(12):1666–1672
11. Clark WM, Lessov NS, Dixon MP, Eckenstein F (1997) Monofilament intraluminal middle cerebral artery occlusion in the mouse. Neurol Res 19(6):641–648
12. De Simoni MG, Storini C, Barba M, Catapano L, Arabia AM, Rossi E, Bergamaschini L (2003) Neuroprotection by complement (C1) inhibitor in mouse transient brain ischemia. J Cereb Blood Flow Metab 23(2):232–239
13. Orsini F, Villa P, Parrella S, Zangari R, Zanier ER, Gesuete R, Stravalaci M, Fumagalli S, Ottria R, Reina JJ, Paladini A, Micotti E, Ribeiro-Viana R, Rojo J, Pavlov VI, Stahl GL, Bernardi A, Gobbi M, De Simoni MG (2012) Targeting mannose-binding lectin confers long-lasting protection with a surprisingly wide therapeutic window in cerebral ischemia. Circulation 126(12):1484–1494. doi:10.1161/CIRCULATIONAHA.112.103051
14. Desland FA, Afzal A, Warraich Z, Mocco J (2014) Manual versus automated rodent behavioral assessment: comparing efficacy and ease of bederson and garcia neurological deficit scores to an open field video-tracking system. J Cent Nerv Syst Dis 6:7–14. doi:10.4137/JCNSD.S13194
15. Jones BJ, Roberts DJ (1968) A rotarod suitable for quantitative measurements of motor incoordination in naive mice. Naunyn Schmiedebergs Arch Exp Pathol Pharmakol 259(2):211
16. Barlow C, Hirotsune S, Paylor R, Liyanage M, Eckhaus M, Collins F, Shiloh Y, Crawley JN, Ried T, Tagle D, Wynshaw-Boris A (1996) Atm-deficient mice: a paradigm of ataxia telangiectasia. Cell 86(1):159–171. pii:S0092-8674(00)80086-0
17. Homanics GE, Quinlan JJ, Firestone LL (1999) Pharmacologic and behavioral responses of inbred C57BL/6J and strain 129/SvJ mouse lines. Pharmacol Biochem Behav 63(1):21–26. pii:S0091-3057(98)00232-9
18. Bouet V, Freret T, Toutain J, Divoux D, Boulouard M, Schumann-Bard P (2007) Sensorimotor and cognitive deficits after transient middle cerebral artery occlusion in the mouse. Exp Neurol 203(2):555–567. pii:S0014-4886(06)00544-9 doi:10.1016/j.expneurol.2006.09.006
19. Li Y, Chopp M, Chen J, Wang L, Gautam SC, Xu YX, Zhang Z (2000) Intrastriatal transplantation of bone marrow nonhematopoietic cells improves functional recovery after stroke in adult mice. J Cereb Blood Flow Metab 20(9):1311–1319. doi:10.1097/00004647-200009000-00006
20. Gibson CL, Bath PM, Murphy SP (2005) G-CSF reduces infarct volume and improves functional outcome after transient focal cerebral ischemia in mice. J Cereb Blood Flow Metab 25(4):431–439. pii:9600033 doi:10.1038/sj.jcbfm.9600033
21. Gibson CL, Murphy SP (2004) Progesterone enhances functional recovery after middle cerebral artery occlusion in male mice. J Cereb Blood Flow Metab 24(7):805–813. pii:00004647-200407000-00011 doi:10.1097/01.WCB.0000125365.83980.00
22. Rustay NR, Wahlsten D, Crabbe JC (2003) Influence of task parameters on rotarod performance and sensitivity to ethanol in mice. Behav Brain Res 141(2):237–249
23. Ogawa N, Hirose Y, Ohara S, Ono T, Watanabe Y (1985) A simple quantitative bradykinesia test in MPTP-treated mice. Res Commun Chem Pathol Pharmacol 50(3):435–441
24. Prinz V, Laufs U, Gertz K, Kronenberg G, Balkaya M, Leithner C, Lindauer U, Endres M (2008) Intravenous rosuvastatin for acute stroke treatment: an animal study. Stroke 39(2):433–438. pii:STROKEAHA.107.492470 doi:10.1161/STROKEAHA.107.492470
25. Royl G, Balkaya M, Lehmann S, Lehnardt S, Stohlmann K, Lindauer U, Endres M, Dirnagl U, Meisel A (2009) Effects of the PDE5-inhibitor vardenafil in a mouse stroke model. Brain Res 1265:148–157. pii:S0006-8993(09)00220-0 doi:10.1016/j.brainres.2009.01.061 [doi]

26. Gertz K, Priller J, Kronenberg G, Fink KB, Winter B, Schrock H, Ji S, Milosevic M, Harms C, Bohm M, Dirnagl U, Laufs U, Endres M (2006) Physical activity improves long-term stroke outcome via endothelial nitric oxide synthase-dependent augmentation of neovascularization and cerebral blood flow. Circ Res 99(10):1132–1140. pii:01.RES.0000250175.14861.77 doi:10.1161/01.RES.0000250175.14861.77
27. Hattori K, Lee H, Hurn PD, Crain BJ, Traystman RJ, DeVries AC (2000) Cognitive deficits after focal cerebral ischemia in mice. Stroke 31(8):1939–1944
28. Cho S, Park EM, Febbraio M, Anrather J, Park L, Racchumi G, Silverstein RL, Iadecola C (2005) The class B scavenger receptor CD36 mediates free radical production and tissue injury in cerebral ischemia. J Neurosci 25(10):2504–2512. doi:10.1523/JNEUROSCI.0035-05.2005
29. Ji S, Kronenberg G, Balkaya M, Farber K, Gertz K, Kettenmann H, Endres M (2009) Acute neuroprotection by pioglitazone after mild brain ischemia without effect on long-term outcome. Exp Neurol 216(2):321–328. pii:S0014-4886(08)00473-1 doi:10.1016/j.expneurol.2008.12.007
30. Abe T, Kunz A, Shimamura M, Zhou P, Anrather J, Iadecola C (2009) The neuroprotective effect of prostaglandin E2 EP1 receptor inhibition has a wide therapeutic window, is sustained in time and is not sexually dimorphic. J Cereb Blood Flow Metab 29 (1):66–72. pii:jcbfm200888 doi:10.1038/jcbfm.2008.88
31. Schallert T, Upchurch M, Lobaugh N, Farrar SB, Spirduso WW, Gilliam P, Vaughn D, Wilcox RE (1982) Tactile extinction: distinguishing between sensorimotor and motor asymmetries in rats with unilateral nigrostriatal damage. Pharmacol Biochem Behav 16(3):455–462
32. Schallert T, Upchurch M, Wilcox RE, Vaughn DM (1983) Posture-independent sensorimotor analysis of inter-hemispheric receptor asymmetries in neostriatum. Pharmacol Biochem Behav 18(5):753–759
33. Zhang L, Schallert T, Zhang ZG, Jiang Q, Arniego P, Li Q, Lu M, Chopp M (2002) A test for detecting long-term sensorimotor dysfunction in the mouse after focal cerebral ischemia. J Neurosci Methods 117(2):207–214. pii:S0165027002001140
34. Li X, Blizzard KK, Zeng Z, DeVries AC, Hurn PD, McCullough LD (2004) Chronic behavioral testing after focal ischemia in the mouse: functional recovery and the effects of gender. Exp Neurol 187(1):94–104. doi:10.1016/j.expneurol.2004.01 pii:004S0014488604000135
35. Hao J, Mdzinarishvili A, Abbruscato TJ, Klein J, Geldenhuys WJ, Van der Schyf CJ, Bickel U (2008) Neuroprotection in mice by NGP1-01 after transient focal brain ischemia. Brain Res 1196:113–120. pii:S0006-8993(07)02871-5 doi:10.1016/j.brainres.2007.11.075
36. Alexander LD, Black SE, Patterson KK, Gao F, Danells CJ, McIlroy WE (2009) Association between gait asymmetry and brain lesion location in stroke patients. Stroke 40(2):537–544. doi:10.1161/STROKEAHA.108.527374
37. Batka RJ, Brown TJ, McMillan KP, Meadows RM, Jones KJ, Haulcomb MM (2014) The need for speed in rodent locomotion analyses. Anat Rec (Hoboken) 297(10):1839–1864. doi:10.1002/ar.22955
38. Balkaya M, Krober J, Gertz K, Peruzzaro S, Endres M (2013) Characterization of long-term functional outcome in a murine model of mild brain ischemia. J Neurosci Methods 213(2):179–187. doi:10.1016/j.jneumeth.2012.12.021
39. Neckel ND, Dai H, Bregman BS (2013) Quantifying changes following spinal cord injury with velocity dependent locomotor measures. J Neurosci Methods 214(1):27–36. doi:10.1016/j.jneumeth.2013.01.008
40. Neckel ND (2015) Methods to quantify the velocity dependence of common gait measurements from automated rodent gait analysis devices. J Neurosci Methods 253:244–253. doi:10.1016/j.jneumeth.2015.06.017
41. Whishaw IQ, Tomie J (1996) Of mice and mazes: similarities between mice and rats on dry land but not water mazes. Physiol Behav 60(5):1191–1197
42. Kawamata T, Akiguchi I, Yagi H, Irino M, Sugiyama H, Akiyama H, Shimada A, Takemura M, Ueno M, Kitabayashi T, Ohnishi K, Seriu N, Higuchi K, Hosokawa M, Takeda T (1997) Neuropathological studies on strains of senescence-accelerated mice (SAM) with age-related deficits in learning and memory. Exp Gerontol 32(1–2):161–169
43. Sarter M, Hagan J, Dudchenko P (1992) Behavioral screening for cognition enhancers: from indiscriminate to valid testing: Part II. Psychopharmacology (Berl) 107(4):461–473
44. Freret T, Bouet V, Leconte C, Roussel S, Chazalviel L, Divoux D, Schumann-Bard P, Boulouard M (2009) Behavioral deficits after distal focal cerebral ischemia in mice: Usefulness of adhesive removal test. Behav Neurosci 123(1):224–230. pii:2009-00623-016 doi:10.1037/a0014157
45. Fassino S, Torre E (1980) Short-term memory. An experimental model. Boll Soc Ital Biol Sper 56(6):601–605

46. Voits M, Fink H, Gerhardt P, Huston JP (1995) Application of 'nose-poke habituation' validation with post-trial diazepam- and cholecystokinin-induced hypo- and hypermnesia. J Neurosci Methods 57(1):101–105. pii:0165027094001435
47. Montgomery KC (1955) The relation between fear induced by novel stimulation and exploratory behavior. J Comp Physiol Psychol 48(4):254–260
48. Handley SL, Mithani S (1984) Effects of alpha-adrenoceptor agonists and antagonists in a maze-exploration model of 'fear'-motivated behaviour. Naunyn Schmiedebergs Arch Pharmacol 327(1):1–5
49. Pellow S, Chopin P, File SE, Briley M (1985) Validation of open:closed arm entries in an elevated plus-maze as a measure of anxiety in the rat. J Neurosci Methods 14(3):149–167. pii:0165-0270(85)90031-7
50. Rodgers RJ, Cole JC (1993) Influence of social isolation, gender, strain, and prior novelty on plus-maze behaviour in mice. Physiol Behav 54(4):729–736. pii:0031-9384(93)90084-S
51. Sarkaki A, Farbood Y, Badavi M, Khalaj L, Khodagholi F, Ashabi G (2015) Metformin improves anxiety-like behaviors through AMPK-dependent regulation of autophagy following transient forebrain ischemia. Metab Brain Dis. doi:10.1007/s11011-015-9677-x
52. Winter B, Juckel G, Viktorov I, Katchanov J, Gietz A, Sohr R, Balkaya M, Hortnagl H, Endres M (2005) Anxious and hyperactive phenotype following brief ischemic episodes in mice. Biol Psychiatry 57(10):1166–1175. pii:S0006-3223(05)00175-7 doi:10.1016/j.biopsych.2005.02.010
53. Crawley JN (1985) Exploratory behavior models of anxiety in mice. Neurosci Biobehav Rev 9(1):37–44
54. Kilic E, Kilic U, Bacigaluppi M, Guo Z, Abdallah NB, Wolfer DP, Reiter RJ, Hermann DM, Bassetti CL (2008) Delayed melatonin administration promotes neuronal survival, neurogenesis and motor recovery, and attenuates hyperactivity and anxiety after mild focal cerebral ischemia in mice. J Pineal Res 45(2):142–148. pii:JPI568 doi:10.1111/j.1600-079X.2008.00568.x
55. Whyte EM, Mulsant BH (2002) Post stroke depression: epidemiology, pathophysiology, and biological treatment. Biol Psychiatry 52(3):253–264. pii:S0006322302014245
56. Monleon S, D'Aquila P, Parra A, Simon VM, Brain PF, Willner P (1995) Attenuation of sucrose consumption in mice by chronic mild stress and its restoration by imipramine. Psychopharmacology (Berl) 117(4):453–457
57. Craft TK, DeVries AC (2006) Role of IL-1 in poststroke depressive-like behavior in mice. Biol Psychiatry 60(8):812–818. pii:S0006-3223(06)00376-3 doi:10.1016/j.biopsych.2006.03.011
58. Willner P, Moreau JL, Nielsen CK, Papp M, Sluzewska A (1996) Decreased hedonic responsiveness following chronic mild stress is not secondary to loss of body weight. Physiol Behav 60(1):129–134. pii:0031938495022562
59. Wu C, Zhang J, Chen Y (2015) Study on the behavioral changes of a post-stroke depression rat model. Exp Ther Med 10(1):159–163. doi:10.3892/etm.2015.2450

Chapter 14

Behavioral Testing in Rodent Models of Stroke, Part II

Gerlinde A.S. Metz

Abstract

The critical test of a therapeutic intervention is whether it affects clinically relevant outcomes. Therefore, a vital part of preclinical stroke research includes the use of reliable tests of functional outcome. This chapter presents select behavioral tests commonly used for evaluating somatosensory, locomotor, and skilled and cognitive functions in rodent models of stroke. The methods described emphasize the value of careful quantitative and qualitative assessment of acute and long-term behavioral deficits. Some of the protocols presented allow us to determine whether a preclinical treatment restores the original function or simply enhances performance by improving the learning of alternative strategies. Recommendations are given to assist the reader in the choice of individual tests to develop a test battery for the assessment of chronic deficits and functional improvements in rodent models of experimental stroke.

Key words Neurological test battery, Rat, Mouse, Somatosensory, Motor, Locomotion, Skilled movement, Learning and memory

1 Introduction

Behavioral tests are essential components of preclinical research in rodent models of focal ischemic or hemorrhagic stroke. A comprehensive behavioral assessment may require a rather extensive battery of tests with each test describing specific aspects of behavior. There is no static test battery that could be recommended for animal models of stroke. Rather, existing test batteries are constantly being modified to address the demands of particular experiments. At a minimum, a useful test battery comprises tests that are sensitive to the type and severity of deficits predicted after the injury. It is important to choose tests that avoid a ceiling or floor effect, i.e., the inability to distinguish between lesion and control animals due to limited sensitivity of a test. Rather, it is preferred to choose a test strategy with maximum sensitivity in regard to individual differences. Furthermore, each test of a test battery should provide graded outcome in response to a therapeutic intervention chronically after injury and should not be influenced by repeated testing.

Ulrich Dirnagl (ed.), *Rodent Models of Stroke*, Neuromethods, vol. 120,
DOI 10.1007/978-1-4939-5620-3_14,

To expedite research, a suitable test should produce a number of different measurements, such as a combination of observational descriptions along with end point measures.

There are some practical considerations that determine the choice of test. Some tests may require habituation to the test apparatus or pretraining prior to testing, which will then allow for longitudinal testing once habituation or training is completed. Learned compensatory behaviors may develop through repeated testing and lead to false conclusions about the efficacy of an intervention. Another important consideration is the type of evaluation strategy. Compared to complex scoring systems, simple scores may be easier to use, yet the outcome may not display small differences between graded levels of injury and subtle therapeutic effects. Therefore, it is usually a worthy investment of time to use a complex scoring procedure that provides an array of outcome measures. Sometimes, an ideal evaluation strategy may not be the commercially available automated version but the one that requires thorough observation of the animals' behavior by an experimenter, thus allowing for unambiguous interpretation of any functional deficits. Furthermore, measuring quantitative (end point) along with qualitative (descriptive) data will help dissociate mechanisms of improvement through brain repair versus behavioral compensation.

The following chapter will not attempt to provide an all-inclusive review of the numerous behavioral tests available. It will rather introduce select core tests that can be used to create a reliable test battery for the assessment of typical sensory, motor, and cognitive deficits in rodent models of stroke. Although some of the tests may have been used mainly in rats, the training and test protocols described can be adapted for use in other rodents. Further details can be found in the cited method papers and in Chap. 13.

2 Neurological Tests for Models of Stroke

2.1 Somatosensory Functions

A number of somatosensory tests such as feeding and food manipulation can be performed by observation of animals in their home cage. In addition, stroke models often use more formal tests that require removing the animal from its home cage. Some of these tests are outlined below.

2.1.1 Sensorimotor Asymmetry (Sticky Dot Removal) Test

In stroke patients, simultaneous extinction is a reliable predictor of chronic residual deficits [1]. The sticky dot test can be used to determine cutaneous sensitivity and sensorimotor integration in rats and mice [2, 3]. This test is commonly used to assess sensorimotor impairments after unilateral lesions involving the sensorimotor cortex, the corticospinal tract, and the striatum.

Sticky Dot Test	
Material	- 1.2 cm Ø round adhesive labels - Familiar home cage, no bedding - Stop watch - Video camera, VCR (optional)
Procedure	- Place label on distal-radial aspect of each forelimb at the same time, place in home cage - Pre-testing; post-operative testing at any time
Measurement	- Latency to contact left versus right forelimb

Fig. 1 Photograph of a rat contacting the sticky dot adhering to the distal aspect of the forelimb. The table summarizes the test procedure

A round adhesive-backed label, 1.2 cm in diameter, is attached to the relatively hairless distal-radial aspect of each wrist of the rat (Fig. 1) [4]. When returned to its home cage, a normal rat will orient toward the stimuli and rapidly remove each of the labels using its teeth. The time and order in which it contacts and removes each label is recorded over four trials. After unilateral lesion, an animal first contacts and removes the label attached to the good forelimb and later orients toward the label on the bad forelimb. It may require more time to remove the dot from the bad forelimb. The order of contact and removal reflects whether the animal shows a bias for one forelimb. Asymmetry in sensory function is determined by the percentage of trials for which the label on the good paw is contacted prior to the one on the bad paw. A bias in animals with a unilateral deficit will be reflected by removal of the stimulus from the unaffected limb first in at least 70% of the trials. The latency to remove the patch also represents a secondary measure of motor function. Impairments in the mouth and forelimb movement lead to difficulty in removing the sticky label. The latency to remove the label from the bad forelimb is usually longer in duration than the latency to contact the label. A follow-up test can determine the magnitude of the asymmetry by progressively increasing the size of the label on the bad forelimb while at the same time decreasing the size on the good forelimb [5]. If the stimulus on the bad limb becomes more salient than the stimulus on the good limb, the animal starts contacting and removing the stimulus from the bad limb first.

2.1.2 Limb Use Asymmetry (Cylinder) Test

Stroke patients might present with asymmetry in upper limb use. In rat [4] and mouse [6] models, forelimb use can be measured when exploring a vertical surface of an enclosure. Chronic asymmetry in forelimb use can be observed after unilateral damage to the sensorimotor cortex, corticospinal tract, and striatum [4].

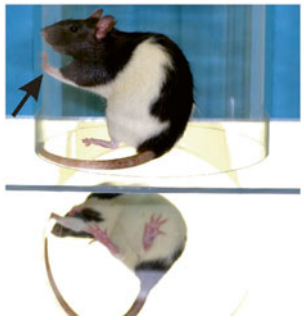

Cylinder Task	
Material	- Clear Plexiglas cylinder 20 cm Ø - Mirror (behind or underneath cylinder) - Video camera, VCR
Procedure	- Pre-testing; post-operative testing at any time
Measurement	- Use of left versus right forelimb

Fig. 2 Photograph illustrating the cylinder task to test limb use asymmetry. A mirror has been placed underneath the cylinder to view the animal's limb use from any direction. The table summarizes the test procedure

Further discrete motor disturbances and compensatory adjustments might be detected by descriptive analysis of the exploratory movements [7].

In the cylinder test to determine forelimb asymmetry, rats are placed in a clear Plexiglas cylinder 20 cm in diameter and 30 cm high (Fig. 2) [4]. The cylinder is placed on a table surface with a mirror positioned at an angle behind the cylinder for observation of limb use from any direction. Alternatively, the cylinder can also be placed on a transparent surface with a mirror or a video camera placed underneath. Forelimb use is video recorded and scored by an observer blind to the experimental conditions. A normal rat will scan the cylinder surface by vertical exploration using both forelimbs equally often for support against the wall. A unilateral lesion may bias the animal to prefer one limb, usually the less affected one.

When watching the video recordings in slow motion, three main categories of forelimb use can be scored: limb use during lifting, limb use during exploration of the cylinder wall, and limb use during landing. Limb use is scored as independent use of the left or right forelimb or as simultaneous use of both forelimbs. Behavior is expressed as percent use of left forelimb, percent use of right forelimb, and percent simultaneous limb use, relative to the total number of all limbs used [4]. In animals with a unilateral lesion, a single score can be obtained by subtracting the percent use of the bad forelimb from the percent use of the good forelimb. The higher score indicates greater asymmetry. This method has high inter-rater reliability even among inexperienced raters.

2.2 Locomotion

Motor instability and postural compensation are prominent functional deficits among patients afflicted by stroke. Most cortical and subcortical stroke models in rodents will affect at least one measure of locomotion, such as walking, turning, and swimming. The deficits, however, may be subtle and may require analysis of videotapes in slow motion or even frame by frame. This also applies to the following two tests.

Ledged/Tapered	Beam
Material	- Tapered beam with ledge on each side - Home cage as goal - Mirror placed behind beam - Video camera, VCR with frame-by-frame option
Procedure	- Pre-training to consistent walking - Post-operative testing at any time - Video recording of each trial
Measurement	- Limb placement on ledge by video analysis

Fig. 3 Illustration of the ledged/tapered beam to measure locomotion and limb placement. The *arrow points* to a foot fault of the left hind limb. The table summarizes the test procedure

2.2.1 Ledged/Tapered Beam Walking Test

The ledged/tapered beam walking test for rats involves the quantification of foot faults when traversing a specially constructed beam [8]. This test takes into consideration that lesion animals will, over time, adopt alternate, compensatory movement strategies to overcome some of their deficits. By adding ledges to this tapered beam, animals are offered a support that reduces the need for adopting compensatory strategies and thus reveals their true deficits. The ledged/tapered beam has been used after middle cerebral artery occlusion or focal sensorimotor cortex lesions [9, 10]. Depending on the extent of damage to the sensorimotor cortex or striatum, a rat will display chronic changes in limb placement.

The length of the ledged/tapered beam is typically 165 cm long with a tapered width that drops from 6 cm to 1.5 cm. To facilitate scoring, the length of the beam is divided into three 45 cm bins of varying difficulty along the tapered section (Fig. 3). The beginning and the end of the beam are untapered (15 cm width), which serves as a comfortable starting point and goal area for the animals. The goal area might also contain a refuge (dark box or home cage) to motivate the animal to cross the beam. Only foot faults made on the tapered section of the beam are scored. Along each side of the beam are 2 cm wide ledges located 2 cm below the upper surface of the beam. The ledges allow the animal to place an impaired fore- or hind limb off the beam so that it does not fall. A normal rat readily learns to walk down the beam on the upper surface, rarely using the ledges. An animal with a bad limb will use the ledge for weight-bearing steps on the side of the ledge corresponding to the deficit. The bad limbs will be placed on the ledge on the wider section of the beam more often than the good limbs, and as the beam tapers, animals will increasingly rely on using the ledges for foot placements. A mirror placed behind the beam will help to visualize the placements of all four limbs.

Animals are pretrained for 5 days, with 5 trials on each day. On postoperative test days, five trials per test session are recorded. Each trial is videotaped, and tapes are analyzed in slow motion to

count foot faults for each limb. Steps onto the ledge are scored as a full slip, and a half slip is recorded if the limb touches the side of the beam. For each limb, foot fault counts over five trials are averaged, and the total number of steps for each of the three bins of varying difficulty is counted. After a unilateral lesion, the number of contralateral and ipsilateral limb faults in each bin is divided by the number of total steps per bin. A percentage of asymmetry for each of the three bins can be calculated by subtracting the percentage of ipsilateral faults per step from that of contralateral faults per step. A higher percentage indicates greater impairments in the contralateral limb [8].

2.2.2 *Forelimb Inhibition (Swimming) Test*

Consequences of experimental motor system damage in rats often include loss of motor inhibition in the affected forelimb while swimming. The forelimb inhibition test was developed to display and quantify forelimb use during swimming [11, 12]. Healthy rats, when swimming in a straight line, use the hind limbs for propulsion, while the forelimbs are held immobile underneath the chin or are tilted for steering [13]. Although the ability to swim is rarely abolished by experimental manipulations, the performance of swimming movements changes after lesions to sensorimotor cortex, posterior hypothalamus, or cerebellum [14]. Rats with these lesions tend to use the bad forelimb for stroking movements, while holding the good forelimb motionless as do normal rats. This behavioral change persists even after long intervals after lesion.

To perform this test, a rat is trained prior to surgery to swim from one end of a rectangular, transparent water tank, about 120 cm long, to the other end of the tank to reach a visible escape platform made of wire mesh (Fig. 4) [12]. The water in the tank is kept at a temperature of 18–20 °C, and the level of the water reaches a height of about 30 cm to prevent the rat from touching the bottom. It is important to train the rat to swim in a straight line toward the escape platform because rats will usually paddle with their forelimbs when turning. After surgery, a trained rat will continue to swim straight to the escape platform when released

Forelimb Inhibition Task	
Material	- Rectangular glass tank (120 cm long) with water at 18-20°C and 30 cm high - Video camera, VCR
Procedure	- Pre-training, post-operative testing at any time (video recorded)
Measurement	- Number of forelimb strokes pre- vs. post-operative

Fig. 4 Photograph of a normal rat swimming. Note that both forelimbs are held immobile in front of the upper body, while only the hind limbs are used for propulsion. The table summarizes the test procedure

from the opposite end, but will typically display some stroking with the bad forelimb as opposed to holding it still. On test days, the rat is given five trials, and performance is video recorded from a side view. The tapes are analyzed in slow motion in order to count the number of forelimb strokes per limb. Forelimb inhibition scores are calculated by subtracting the number of strokes made with the good forelimb from the number of strokes made with the bad forelimb divided by the number of trials. This scoring method indicates the degree of asymmetry without being affected by individual differences in limb use between rats. Trials in which the rat does not swim directly to the platform need to be excluded from scoring.

The number of forelimb strokes may vary depending on the location and extent of the lesion. If the effect of unilateral lesions is being assessed, the intact side serves as a control for the lesion side. Bilateral lesions might impair both sides, so that data from control animals or pre-lesion test sessions will be necessary for comparison.

2.3 Skilled Movements

A common consequence of human stroke is loss of distal hand and arm movement. In rodent models of stroke, these functions can be assessed in a number of formal tasks for skilled movement. Skilled movements are voluntary movements requiring irregular motor patterns. They are characterized by a complex sequence of movement components, which can be observed in rodents eating specialty food items, such as sunflower seeds or pasta, or when navigating across difficult territory. Formal tests of skilled movement allow objective and reproducible evaluation of limb function and have the advantage of producing a wealth of information, such as that derived from end point and descriptive analyses [15]. Ultimately, a refined description can be obtained by using a movement notation system or kinematic analysis to record the movement of body parts in space.

2.3.1 Tray Reaching Task

The tray reaching task is a simple version of a forelimb reaching-for-food task applicable to rats and mice. It can be used as a method of motor skill training or to evaluate limb preference and reaching performance in stroke models involving lesions to the sensorimotor cortex [16] and corticospinal tract [17]. Compared to single pellet reaching tasks, the design of tray reaching tasks is more permissive for the development of task-specific compensatory movement strategies [18].

A typical tray reaching apparatus consists of three Plexiglas walls and a front wall made of thin vertical metal bars, spaced 9 mm, to allow the animal to extend the forelimb through the full width of the front wall [19]. Mounted on the outside and extending to the entire width of the front wall is a 5-cm-deep tray. The tray can be filled with small food pieces, such as chicken feed or food pellets, so that animals can reach through the bars and retrieve

Tray Reaching Task	
Material	- Reaching box with bars (0.9 cm apart) in front wall - Chicken feed or small food pellets - Video camera, VCR with frame-by-frame option
Procedure	- Food restriction to 95% of body weight - Pre-training to reach - Post-operative testing at any time - Video recordings at any time
Measurement	- Reaching success by video analysis

Fig. 5 Photograph of a right-handed rat reaching for chicken feed in the tray reaching task. The grid floor allows measuring the amount of food dropped. The table summarizes the test procedure

food from any angle and position in the box (Fig. 5). The box is mounted on a grid floor, so that lost and dropped food items fall through and can be counted or weighed. To perform this task, animals reach through the bars, grasp food items, and withdraw the paw to consume the food.

Training requires moderate food deprivation induced by restricting access to food the night prior to the first training session. If necessary, the restricted feeding regimen can be continued throughout the experiment by providing an adequate amount of food in the animal's home cage to maintain the animal's body weight. Training can be completed in a few sessions, each lasting about 30 min, as there is no need to replace food items or handle the animals while in the apparatus. It is also possible to train animals overnight while they live in the test apparatus, with water provided ad libitum. After completed training, test sessions can be as brief as 5 min, and performance can be video recorded for analysis.

There are two main methods for analysis of limb use asymmetry and reaching performance in tray reaching tasks. First, animals can be allowed to use either forelimb, and the preference of one limb over the other can be evaluated. Thus, when unilateral lesions are assessed, the ratio of the use of the good limb versus the bad limb reveals the degree of limb use asymmetry. Second, to measure success rates of one limb exclusively, the use of the other limb can be prevented with a small bracelet made from adhesive fabric tape wrapped around the distal aspect of the limb [20]. Success rates are determined by counting the reaching movements that obtain food and bring the food to the mouth for consumption. Performance is then described as hit percent, i.e., the number of successful reaches divided by the number of total reaches multiplied by hundred. In addition, the amount of food dropped and collected underneath the grid floor can be quantified.

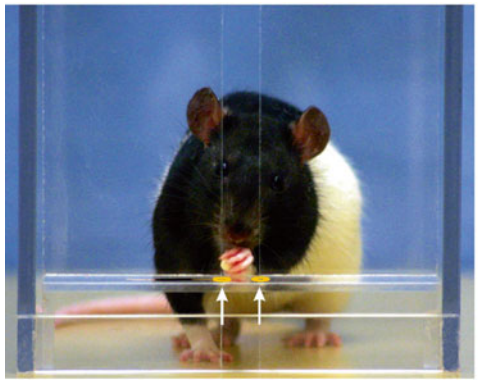

Pellet Reaching Task	
Material	- Clear Plexiglas box with 1.3 cm wide slit in front wall - 45 mg food pellets - Video camera, VCR with frame-by-frame option
Procedure	- Food restriction to 95% of body weight - Pre-training to asymptotic reaching success - Post-operative testing almost daily - Video recordings at any time
Measurement	- Reaching success, pellets eaten, attempts per pellet by observation - Descriptive analysis from video tapes

Fig. 6 Photograph of a left-handed rat reaching for a food pellet through a slit. *Arrows highlight* the two indentations to hold a single food pellet. The table summarizes the test procedure

2.3.2 Single Pellet Reaching Task

The single pellet reaching task is one of the most sensitive tests for motor control and postural adjustments in rats [20] and mice [21]. The task is designed in a way that allows for measuring successful reaching, while at the same time performance is being filmed and scored frame by frame [22]. Performance in this task can be differentially affected by even discrete damage to the sensorimotor cortex, corticospinal tract, basal ganglia, dorsal columns, and red nucleus. In addition, physiological conditions such as stress, strain, sex, and aging affect reaching success, movement performance, and postural adjustments [23].

The apparatus for the single pellet reaching task consists of a Plexiglas box with a slit in the front wall. Attached to the outside of the front wall is a shelf to hold single small food pellets (Fig. 6). Two indentations to hold the pellet are aligned with the slit. Pellets are placed in the indentation opposite to the preferred paw to reinforce use of this paw throughout the experiment. Animals are pretrained to extend their preferred forelimb through the opening to grasp and retrieve small food pellets from the shelf. Within 2 weeks, performance of the animals can be shaped to optimize their reaching success. Because most animals show a preference to use either left or right forelimb for reaching, unilateral lesions are usually placed on the side contralateral to the preferred limb. Rats with unilateral lesion might tend to use the good limb for pellet retrieval. A bracelet made of fabric tape can be wrapped around the good forelimb to obstruct its movement, thus reinforcing use of the bad (previously preferred) limb. Through practice rats with brain damage might considerably improve their reaching success through the adoption of compensatory movement strategies. Descriptive analysis of reaching movements from video recordings is then of particular importance, as it will reveal the permanent deficits [24].

Video recordings from a frontal view allow scoring of individual components of reaching movements for descriptive analysis. Several systems have been devised to describe reaching movements. The most commonly used systems are based on movement notations by Eskhol and Wachmann [25, 26].

Qualitative analysis of performance has revealed that the rat's skilled reaching movements consist of a distinctive sequence of components [22]. Consequently, even subtle brain damage may permanently compromise reaching movement performance while sparing coordinated movements of swimming and locomotion. Notably, comparisons have shown that the essential components of skilled reaching movements are similar between humans and rodents, emphasizing the translational value of skilled reaching studies for preclinical research [27].

2.3.3 Ladder Rung Walking Task

When navigating across difficult territory, rats use skilled hind limb movements to modify their gait pattern and prevent placement mistakes. The ladder rung walking task is a simple and sensitive test to simultaneously assess skilled fore- and hind limb movements [28]. It resembles a horizontal ladder with metal rungs that can be individually adjusted. A regular pattern of rungs allows animals to anticipate rung location and learn a specific sequence of patterns across repeated test sessions [29]. An irregular pattern prevents animals from learning the rung sequences. Thus, rung patterns can be changed from session to session to modify the level of challenge. Furthermore, modifications such as placing the ladder at an inclined plane [30] or dislodging rungs [31] can provide additional task-specific challenges. Skilled walking as measured by the ladder rung walking task is affected by damage to the sensorimotor cortex, corticospinal tract, basal ganglia, and cerebellum [28]. The rung walking task also detects changes in error rates in response to physiological variables, such as stress [32], and has been widely used to demonstrate therapeutic effectiveness of pharmacological and rehabilitation treatments. The ladder rung walking task in mice [33] also effectively distinguishes different genetic manipulations [34].

Animals can easily be trained in a single session to cross the horizontal ladder to reach their home cage or another refuge (Fig. 7). On postoperative test days, at least three trials per test session are recorded. Each trial is videotaped from a ventrolateral perspective to view all four limbs. The tapes are analyzed in slow motion to count limb placement errors for each limb. Analysis of end point measures includes the number of placement errors, such as total misses and foot slips. For each limb, error counts from three trials are averaged, and the number of contralateral and ipsilateral limb faults is divided by the number of total steps. Furthermore, descriptive analysis includes digit flexion and the type of error made [28].

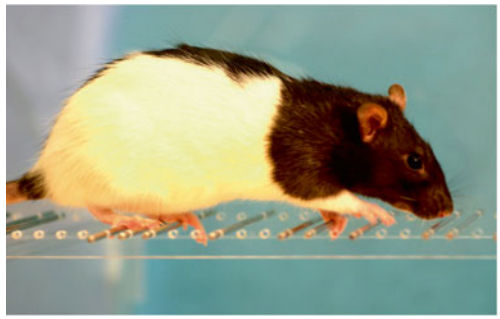

Ladder Rung Walking Task	
Material	- Elevated horizontal ladder with Plexiglas walls, 1 m long with adjustable rungs at distances 1-5 cm - Home cage as goal - Video camera, VCR with frame-by-frame option
Procedure	- Pre-training to consistent walking - Post-operative testing at any time - Video recordings of each trial
Measurement	- Errors, limb placement score, digit flexion by video analysis

Fig. 7 Photograph of a rat crossing the *horizontal* ladder rung walking task. Note the irregular spacing of the rungs. The table summarizes the test procedure

A unilateral lesion affecting skilled walking impairs contralateral limb placement. As a result, animals will engage in compensatory adjustments that may result in errors in the ipsilateral limbs. It is thus important to collect data from preoperative test sessions or intact controls for comparison.

2.4 Learning and Memory

Stroke in human patients is frequently associated with loss of cognitive functions. The study of neuronal damage and therapeutic interventions in animal models of stroke may require examination of cognitive function. Common cognitive assessments include tests of spatial memory using dry-land or water mazes. Water mazes are not only flexible tests for animal studies, but their methodology is also directly applicable to human spatial behavior [35]. In addition, novel object recognition tasks provide a sensitive measurement of working memory, attention, and even anxiety. The advantages of the two presented tasks are that they require no external reinforcement, such as food rewards or punishment, and they can be completed in a reliable and time-efficient manner to produce robust assessment of cognition after brain damage and recovery in experimental stroke. Both of the tasks require some training and habituation.

2.4.1 Water Maze Task

Water mazes using a swimming pool are most popular for measuring procedural and working memory in laboratory rodents [36]. Rats are good swimmers, and so they can be trained to locate a hidden platform within a pool filled with water by using visual cues around the pool as a guide. Although the water maze generally also applies to mice, caution has to be taken with regard to the test protocols [37]. Different protocols have shown that acquisition, retention, and reversal of navigational strategies in the water maze involve a number of brain regions and neurochemical systems, each affecting specific parameters of performance in the water maze. Since 1982, when two studies showed that the water maze

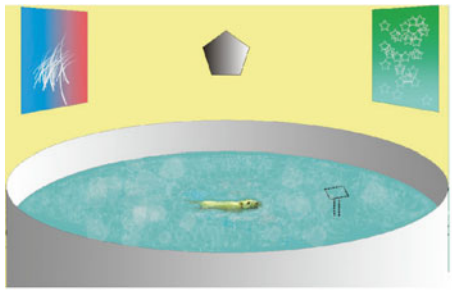

Water Maze Task (Rat)	
Material	- Round 2 m Ø swimming pool filled with 30 cm high 21-23°C water - Skim milk powder - Video camera or computerized system
Procedure	- Pre-training to find platform - Post-operative testing at any time - Video recording at any time
Measurement	- Escape latency, swim distance, time in each quadrant

Fig. 8 Illustration of the water maze task with the hidden platform. The walls of the test room are covered with distinctive visual cues. The table summarizes the main test procedure for rats

is sensitive to hippocampal damage [38, 39], spatial learning has been related to function of hippocampal regions CA1 and CA3 and hippocampal connectivity such as the fimbria fornix (e.g., [40]). Other brain structures influencing water maze performance include the prefrontal cortex, striatum, cerebellum, and various neurochemical and neuromodulator systems [41]. Various test protocols for spatial navigation in the water maze task have been developed, such as protocols for trial-dependent, latent, and discrimination learning. The following will focus on a basic procedure that applies to most versions of the water task.

A training or test session begins by placing an animal into a round swimming pool, about 2 m in diameter, which contains a hidden platform (Fig. 8). The hidden platform is submerged about one centimeter underneath the water surface, and the water is made opaque by adding skim milk powder or nontoxic tempera paint. The water level is about 30 cm high and kept at a temperature of 21–23 °C. Distal visual cues, such as posters and differently shaped objects, are placed around the pool in plain sight of the animal. The goal is for the animal to use the spatial cues to localize the platform and use it to escape from the water. With the platform in the same position, the time to locate it decreases in subsequent trials as the animal learns to swim directly to the invisible platform relative to the distal cues surrounding the pool. In a water maze, animals rely on using the visual cues surrounding the swimming pool, as water contains no local cues such as scent trails. The animal's performance is measured as the time it takes to find the platform (escape latency), the distance traveled (swim distance), and the accuracy in targeting the platform over consecutive trials (time spent in each quadrant of the water tank). For more convenient data analysis, a number of commercial automated systems have been developed.

The procedural simplicity of the water task is opposed to the complex underlying processes that determine its performance, such as navigation strategy, place learning and memory, and the performance of visually guided behavior [39, 42]. Various protocols exist

to assess spatial learning in cued and un-cued conditions. Once an animal has learned the procedure of searching for the hidden platform, it can be tested for spatial learning ability using a *matching-to-place* challenge. Each day the platform is moved to a new location, for a total of 5–7 days. Each day, the animal starts twice from the same location. It first receives a sample swim in which it has to locate the platform at its new location, and then it receives a matching swim, in which it demonstrates that it has learned the new location on the sample trial. Typically, animals have long latencies on the first trial, because they search for the platform at its old location, and a shorter latency in the second trial, because they now learned the new location. Distance swum is used as the primary measure. If animals are not able to learn to search for the hidden platform, a protocol to test *cue learning* can be used. Animals are then presented with a visible platform that is raised slightly above water level. A cue trial procedure is used to demonstrate that an animal is physically able to see, swim, and escape.

2.4.2 Novel Object Recognition Task

Since its introduction in 1988, the novel object recognition task has become a benchmark test to study working memory, attention, anxiety, and preference for novelty in rodents [43]. This test is based on the spontaneous tendency of rodents to approach and investigate novel objects or environments. Thus, if a rat or mouse had encountered a particular object before, it will prefer to explore a novel object rather than the familiar one. The learning and memory of familiarity with an object is disrupted by hippocampal and cortical lesions, in particular the perirhinal cortex and medial temporal lobe [44]. Discrimination is also affected by damage to parahippocampal regions of the temporal lobe in tests focusing on visual object recognition memory. Aside from CNS lesions, this task is also frequently used to assess cognitive abilities in transgenic mice [45] and pharmacological studies.

The standard version of the novel object recognition test consists of a habituation period and a familiarization period followed by a test period (Fig. 9). During the initial habituation period, an

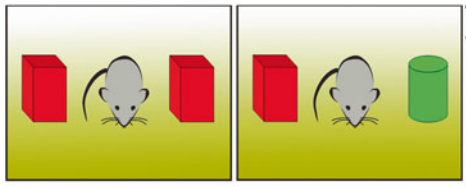

Novel Object Recognition Task	
Material	- Open field arena 65 x 65 x 45 cm
	- Video camera or computerized system
Procedure	- Habituation period
	- Familiarization period
	- Discrimination test
	- Video recording at any time
Measurement	- Index of discrimination/preference

Fig. 9 Illustration of the novel object recognition task showing the familiarization period with two similar objects and the test period that requires recognition and discrimination of a familiar versus a novel object. The table summarizes the main test procedure

animal is allowed to explore an empty open-field arena. During the familiarization period, the animal is allowed to explore the familiar open-field arena in the presence of two identical objects placed at an equal distance. During the test period, the animal is exposed to the open-field arena that now contains one of the familiar objects and a novel object to assess recognition memory. The two objects are generally consistent in height and volume, but are different in shape and appearance. The amount of time spent to explore each of the objects is recorded. The choice to explore the novel object reflects the use of learning and recognition memory. The results can be converted to an index of discrimination or preference, depending on the aim of the study.

By varying the interval between familiarization and test periods, i.e., the length of time that animals must retain memory of sample objects presented to them in prior sessions, either short-term, intermediate-term, or long-term memory, can be investigated [45]. For example, if an animal is presented with the sample object repeatedly over a period of a few days, it can still discriminate the sample from a novel object several weeks later [44]. Thus, object recognition is influenced by the time animals are allowed to spend with the sample object, and the interval between the familiarization period and the test session when the familiar and the novel object will be encountered. This range of modifiable variables assists in maximizing the sensitivity to detect brain lesions and potential therapeutic effects in animal models of stroke [43].

3 Conclusion

The battery of tests presented in this chapter can be used to describe the most prominent behavioral characteristics of a rodent with experimental focal ischemic or hemorrhagic injury. The described tests can be regarded as a starting point for more thorough follow-up tests of specific deficits. They are not the only ones, however, that should be considered useful for assessing functional outcome in stroke models. When designing a test battery, it is important to choose tests that are sensitive to the specific type and location of injury, to detect chronic deficits and allow repeated testing in longitudinal studies. Long-term repeated observations are important because eventual residual deficits may be subtle and not obvious in the acute stages after injury. Furthermore, it is the interpretation of the nature of the deficit and functional recovery that is critical for a meaningful translation to the clinic. For example, animals develop strategies to solve a task by using compensatory strategies. In order to unambiguously determine the true clinical potential of an intervention, the behavioral analysis technique needs to dissociate between compensation and genuine restoration. Lastly, an in-depth behavioral analysis allows conclusions

about the functional state of the brain. Anatomical, physiological, biochemical, and molecular processes are important to understand the brain's function and individual differences, and all of these will be reflected by behavior as the ultimate outcome.

Acknowledgments

The author acknowledges support by grants from the Canadian Institutes of Health Research, the Natural Sciences and Engineering Research Council of Canada, and the Alberta Heritage Foundation for Medical Research.

References

1. Rose L, Bakal DA, Fung TS, Farn P, Weaver LE (1994) Tactile extinction and functional status after stroke. Stroke 25:1973–1976
2. Schallert T, Whishaw IQ (1984) Bilateral cutaneous stimulation of the somatosensory system in hemidecorticate rats. Behav Neurosci 98:518–540
3. Hines DJ, Haydon PG (2013) Inhibition of a SNARE-sensitive pathway in astrocytes attenuates damage following stroke. J Neurosci 33:4234–4240
4. Schallert T, Fleming SM, Leasure JL, Tillerson JL, Bland ST (2000) CNS plasticity and assessment of forelimb sensorimotor outcome in unilateral rat models of stroke, cortical ablation, parkinsonism and spinal cord injury. Neuropharmacology 39:777–787
5. Schallert T, Upchurch M, Lobaugh N, Farrar SB, Spirduso WW, Gilliam P, Vaughn D, Wilcox RE (1982) Tactile extinction: distinguishing between sensorimotor and motor asymmetries in rats with unilateral nigrostriatal damage. Pharmacol Biochem Behav 16:455–462
6. Kadam SD, Mulholland JD, Smith DR, Johnston MV, Comi AM (2009) Chronic brain injury and behavioral impairments in a mouse model of term neonatal strokes. Behav Brain Res 197:77–83
7. Gharbawie OA, Whishaw PA, Whishaw IQ (2004) The topography of three-dimensional exploration: a new quantification of vertical and horizontal exploration, postural support, and exploratory bouts in the cylinder test. Behav Brain Res 151:125–135
8. Schallert T, Woodlee MT, Fleming SM (2002) Disentangling multiple types of recovery from brain injury. In: Krieglstein J, Klumpp S (eds) Pharmacology of cerebral ischemia. Medpharm Scientific, Stuttgart
9. van Groen T, Puurunen K, Maki HM, Sivenius J, Jolkkonen J (2005) Transformation of diffuse beta-amyloid precursor protein and beta-amyloid deposits to plaques in the thalamus after transient occlusion of the middle cerebral artery in rats. Stroke 36:1551–1556
10. Zhao CS, Puurunen K, Schallert T, Sivenius J, Jolkkonen J (2005) Effect of cholinergic medication, before and after focal photothrombotic ischemic cortical injury, on histological and functional outcome in aged and young adult rats. Behav Brain Res 156:85–94
11. Kolb B, Tomie JA (1988) Recovery from early cortical damage in rats. IV. Effects of hemidecortication at 1, 5 or 10 days of age on cerebral anatomy and behavior. Behav Brain Res 28:259–274
12. Stoltz S, Humm JL, Schallert T (1999) Cortical injury impairs contralateral forelimb immobility during swimming: a simple test for loss of inhibitory motor control. Behav Brain Res 106:127–132
13. Schapiro S, Salas M, Vukovich K (1970) Hormonal effects on ontogeny of swimming ability in the rat: assessment of central nervous system development. Science 168:147–150
14. Kolb B, Whishaw IQ (1983) Dissociation of the contributions of the prefrontal, motor, and parietal cortex to the control of movement in the rat: an experimental review. Can J Psychol 37:211–232
15. Whishaw IQ (2004) Prehension. In: Whishaw IQ, Kolb B (eds) The behavior of the laboratory rat. Oxford University Press, pp 162–170
16. Kolb B, Cote S, Ribeiro-da-Silva A, Cuello AC (1997) Nerve growth factor treatment pre-

vents dendritic atrophy and promotes recovery of function after cortical injury. Neuroscience 76:1139–1151

17. Whishaw IQ, Metz GA (2002) Absence of impairments or recovery mediated by the uncrossed pyramidal tract in the rat versus enduring deficits produced by the crossed pyramidal tract. Behav Brain Res 134:323–336
18. Kirkland SW, Smith LK, Metz GA (2012) Task-specific compensation and recovery following focal motor cortex lesion in stressed rats. J Integr Neurosci 11:33–59
19. Whishaw IQ, O'Connor WT, Dunnett SB (1986) The contributions of motor cortex, nigrostriatal dopamine and caudate-putamen to skilled forelimb use in the rat. Brain 109(Pt 5):805–843
20. Whishaw IQ, Miklyaeva EI (1996) A rat's reach should exceed its grasp: analysis of independent limb and digit use in the laboratory rat. In: Ossenkopp KP, Kavaliers M (eds) Measuring movement and locomotion: from invertebrates to humans. RG Landes, Austin, pp 135–169
21. Farr TD, Whishaw IQ (2002) Quantitative and qualitative impairments in skilled reaching in the mouse (Mus musculus) after a focal motor cortex stroke. Stroke 33:1869–1875
22. Metz GA, Whishaw IQ (2000) Skilled reaching an action pattern: stability in rat (Rattus norvegicus) grasping movements as a function of changing food pellet size. Behav Brain Res 116:111–122
23. Merrett DL, Kirkland SW, Metz GA (2010) Synergistic effects of age and stress in a rodent model of stroke. Behav Brain Res 214:55–59
24. Metz GA, Antonow-Schlorke I, Witte OW (2005) Motor improvements after focal cortical ischemia in adult rats are mediated by compensatory mechanisms. Behav Brain Res 162:71–82
25. Eskhol N, Wachmann A (1958) Movement notation. Weidenfeld and Nicolson, London
26. Whishaw IQ, Pellis SM, Gorny BP, Pellis VC (1991) The impairments in reaching and the movements of compensation in rats with motor cortex lesions: an endpoint, videorecording, and movement notation analysis. Behav Brain Res 42:77–91
27. Whishaw IQ, Pellis SM, Gorny BP (1992) Skilled reaching in rats and humans: evidence for parallel development or homology. Behav Brain Res 47:59–70
28. Metz GA, Whishaw IQ (2002) Cortical and subcortical lesions impair skilled walking in the ladder rung walking test: a new task to evaluate fore- and hindlimb stepping, placing, and coordination. J Neurosci Methods 115:169–179
29. Wallace DG, Winter SS, Metz GA (2012) Serial pattern learning during skilled walking. J Integr Neurosci 11:17–32
30. Antonow-Schlorke I, Ehrhardt J, Knieling M (2013) Modification of the ladder rung walking task-new options for analysis of skilled movements. Stroke Res Treat 2013:418627
31. Lopatin D, Caputo N, Damphousse C, Pandey S, Cohen J (2015) Rats anticipate damaged rungs on the elevated ladder: applications for rodent models of Parkinson's disease. J Integr Neurosci 14:97–120
32. Metz GA, Schwab ME, Welzl H (2001) The effects of acute and chronic stress on motor and sensory performance in male Lewis rats. Physiol Behav 72:29–35
33. Farr TD, Liu L, Colwell KL, Whishaw IQ, Metz GA (2006) Bilateral alteration in stepping pattern after unilateral motor cortex injury: a new test strategy for analysis of skilled limb movements in neurological mouse models. J Neurosci Methods 153:104–113
34. Hunsaker MR, von Leden RE, Ta BT, Goodrich-Hunsaker NJ, Arque G, Kim K, Willemsen R, Berman RF (2011) Motor deficits on a ladder rung task in male and female adolescent and adult CGG knock-in mice. Behav Brain Res 222:117–121
35. Hamilton DA, Driscoll I, Sutherland RJ (2002) Human place learning in a virtual Morris water task: some important constraints on the flexibility of place navigation. Behav Brain Res 129:159–170
36. Morris R (1981) Spatial localization does not require the presence of local cues. Learn Motiv 12:239–260
37. Whishaw IQ (1995) A comparison of rats and mice in a swimming pool place task and matching to place task: some surprising differences. Physiol Behav 58:687–693
38. Morris RG, Garrud P, Rawlins JN, O'Keefe J (1982) Place navigation impaired in rats with hippocampal lesions. Nature 297:681–683
39. Sutherland RJ, Whishaw IQ, Regehr JC (1982) Cholinergic receptor blockade impairs spatial localization by use of distal cues in the rat. J Comp Physiol Psychol 96:563–573
40. Whishaw IQ, Cassel JC, Jarrad LE (1995) Rats with fimbria-fornix lesions display a place response in a swimming pool: a dissociation between getting there and knowing where. J Neurosci 15:5779–5788
41. McNamara RK, Skelton RW (1993) The neuropharmacological and neurochemical basis of

place learning in the Morris water maze. Brain Res Brain Res Rev 18:33–49

42. Cain DP, Saucier D (1996) The neuroscience of spatial navigation: focus on behavior yields advances. Rev Neurosci 7:215–231
43. Ennaceur A, Delacour J (1988) A new one-trial test for neurobiological studies of memory in rats. 1. Behavioral data. Behav Brain Res 31:47–59
44. Mumby DG, Piterkin P, Lecluse V, Lehmann H (2007) Perirhinal cortex damage and anterograde object-recognition in rats after long retention intervals. Behav Brain Res 185:82–87
45. Taglialatela G, Hogan D, Zhang WR, Dineley KT (2009) Intermediate- and long-term recognition memory deficits in Tg2576 mice are reversed with acute calcineurin inhibition. Behav Brain Res 200:95–99

Chapter 15

Combining Classical Comprehensive with Ethological Based, High-Throughput Automated Behavioral Phenotyping for Rodent Models of Stroke

Anne-Christine Plank, Stephan von Hörsten, and Fabio Canneva

Abstract

Comprehensive behavioral phenotyping of rodents is a process of specifying neurobehavioral characteristics during their ontogeny. In medical translational research, it is a crucial step to define a disease model's value for predictive experimental preclinical therapy and to detect relevant behavioral outcomes of such therapeutic intervention as endpoints. Over the past 20–30 years, rather standardized approaches evolved using combinations of classical assays spanning all different behavioral domains, as described in the preceding chapters. Specific guidelines for the appropriate conduction of such classical phenotyping work have been proposed and will be outlined in this chapter. However, more recently, due to the consideration of certain limitations of classical approaches (non-ethological based, stress-confounded, non-repeatable under the same test construct), intra-home-cage automated phenotyping technologies have been developed, partly validated, and are now available to be integrated into comprehensive phenotyping approaches at a larger scale. A technical description of different automated systems as well as information on application fields and data mining will be given in this chapter. Besides, the capabilities of such technologies regarding their integration into comprehensive screens of rodent models of stroke will be discussed.

Key words Rats/mice, Classical comprehensive behavioral phenotyping, Automated home-cage technology, Ethological, High-throughput, Standardization, Sensitivity, Reduction, Refinement

1 Introduction

1.1 Guidelines for a Systematic and Comprehensive Classical Behavioral Phenotyping Approach

The investigation of highly predictive animal models is an essential component of medical research in the field of neurodegenerative diseases. They provide an opportunity for deeper insight into the complex pathological processes involved and for the development and improvement of therapeutic strategies, which are urgently needed. However, any translational approach requires the establishment of dedicated neurobehavioral screening systems in order to provide reliable readouts and fill the gap between bench and bedside. The importance of a rational strategy in the design, composition, and evaluation of behavioral test

Ulrich Dirnagl (ed.), *Rodent Models of Stroke*, Neuromethods, vol. 120,
DOI 10.1007/978-1-4939-5620-3_15,

batteries is emphasized in Chap. 14 and represents to a large extent the "state of the art" in classical phenotyping nowadays. At least ten major guidelines for a comprehensive classical phenotyping approach were derived from general considerations, examples in the literature, and our own experience [1]:

1. Every firm conclusion based on certain differences in a specific behavioral performance must be substantiated by the proof that the experimental animal is not only healthy but also is equipped with the corresponding sensory and motoric abilities.
2. A systematic screening for physiological abnormalities (e.g., glucose utilization, stress hormones, etc.) must be combined with every basic phenotyping work, even if the goal is primarily a behavioral one.
3. The screening of general health, neurological status, basic physiological parameters, as well as behavioral assessment must be conducted repeatedly, since several changes may become overt at later stages of age or of disease progression in mice and rats.
4. A behavioral phenotyping approach must be comprehensive and should not only be hypothesis driven, but instead should be composed of a complete test battery in order to detect behavioral differences even in domains that are out of the scope of the hypothesis.
5. At least two different tasks that test similar behavioral abilities but vary in their presuming nonresponse-relevant requirements should be incorporated, since these requirements may differ in regard to perception, motor abilities, motivation, or stress.
6. Testing procedures should be ethologically based, i.e., the right tasks for the right species must be designed.
7. Rearing conditions (number of pups per litter, etc.) must be standardized and maternal behavior screened. Thus, handling, especially postnatal manipulation, as well as environmental enrichment must be standardized/controlled. In the same line, (test) biographies of the animals must be considered as potentially interfering with the expression of a particular phenotype or its onset.
8. Social behavior and social housing as well as its implications (social rank, aggression, isolation stress, etc.) must be considered, wherever applicable.
9. Apart from validation of a particular test, positive and negative controls as well as controls across different strains of rats/mice should be included, if possible, in order to improve comparability with other laboratories and to validate the specific task applied.
10. Standardized protocols (SOPs) should be used or developed in order to increase validity and reliability.

1.2 Reasons for the Application of High-Throughput Automated Screening Systems in a Home-Cage Environment

A carefully designed battery of classical tests in compliance with these guidelines is a valuable tool for investigations in preclinical stroke research. However, defining the appropriate configuration of such a battery is not straightforward due to the range and complexity of potential deficits occurring in rodent models of stroke. Besides, many tests are time consuming and therefore do not allow for high-throughput screening. The experimenter's physical presence, including animal handling immediately before testing, is required in most cases, and the observational time window is usually rather limited, which bears the risk of obtaining stress-confounded results. Moreover, some readouts are sensitive to variable testing conditions (day phase, light intensity, etc.); hence, interlaboratory comparability might not be warranted. Finally, certain paradigms are not repeatable under the same test construct as prior behavioral testing influences the animal's performance. For instance, this has been demonstrated in the Morris water maze or elevated plus maze performance of naïve mice compared to mice with prior behavioral testing experience [2, 3].

These limitations of classical phenotyping approaches in throughput, sensitivity, reliability, and reproducibility across laboratories can be overcome by the integration of automated phenotyping techniques into comprehensive behavioral screens. Such systems monitor the animals within home-cage-like environments and are equipped with dedicated devices and multiple sensors, which continuously detect behavioral, physiological, and metabolic parameters, such as cognitive performance, activity, feeding, drinking, respiratory gas concentrations, temperature, etc. In addition, these fully automated units simultaneously record large data sets from several animals, allowing for a standardized, high-throughput approach. In an undisturbed, "handling-free home-cage-like" measuring environment, artifacts induced by the experimenter and novelty-induced stress can be circumvented, which enhances screening sensitivity and reliability. Furthermore, continuous data collection over a longer period of time in a familiar environment provides more information per test animal than classical readouts, maximizing the likelihood of detecting less obvious differences between experimental groups.

2 Automated Phenotyping: Systems and Applications

Over the past years, major developments in the field of automated phenotyping for rodents have been achieved. In Europe, a few companies have developed dedicated technologies meeting different scientific demands. The following paragraphs describe a selection of the systems available (based on the authors' experience), along with examples of how they can be applied.

2.1 IntelliCage

Designed for long-term, high-throughput, intra-home-cage investigations of cognitive abilities in laboratory rodents, the IntelliCage (NewBehavior, Zurich, Switzerland) was the first social housing system where animals could perform a variety of freely programmable behavioral tasks (Fig. 1). A single IntelliCage contains four identical operant conditioning corners, each equipped with a combination of actors for shaping the animals' behavior according to individualized reinforcement and conditioning protocols. Key feature of the system is the application of subcutaneously injected RFID-transponders, allowing for animal recognition within a social group of up to 16 mice or 8 rats. An RFID antenna recognizes each individual, and two motorized doors block or allow access of the animal to water bottles on both sides of each operant corner (positive reinforcement). Multicolor LEDs above these doors constitute the conditional stimuli used for operant experiments, while an air-puff valve can be automatically operated to deliver a negative reinforcement, discouraging access to the corner (Fig. 1). Simple

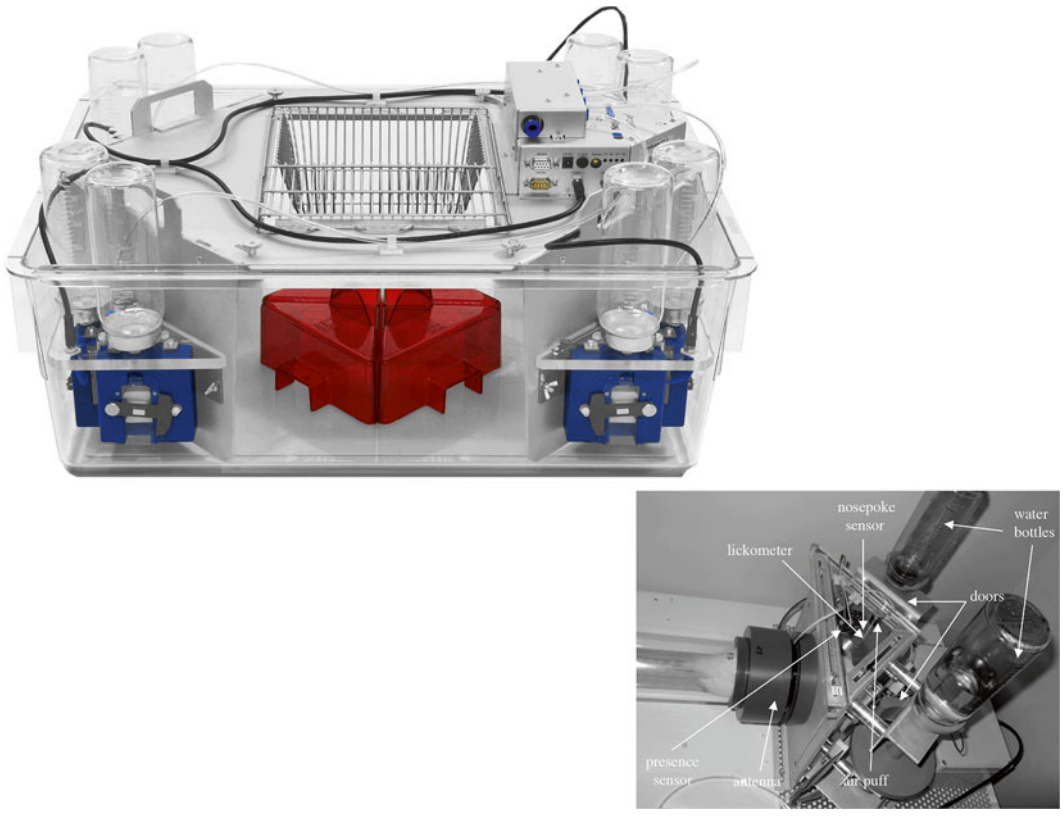

Fig. 1 *IntelliCage*. General setup of the IntelliCage (New Behavior AG, Zürich, Switzerland). In this system, up to 16 mice or 8 rats can be screened in a social environment. In each corner, an operant conditioning element is connected containing water bottles as conditioning reward. Detailed view of the operant corner indicating the position of the nose-poke sensor, doors, lickometer, and air-puff generator. The antenna detects the transponder chip of the animal, while a thermic sensor registers the actual presence of the animal

to complex experiments can be designed with the help of a flexible software interface, automatically run and controlled for each individual animal in the IntelliCage.

Social setting and customized planning of the experimental paradigms are the greatest advantages of the IntelliCage system, allowing for the acquisition of high-quality ethological data within a high-throughput setup. It provides an opportunity to detect completely novel qualities of behaviors as the animals are kept in social groups, remaining totally undisturbed though being monitored for social and cognitive performance. However, space required for the setup and handling of the system are presently considered problematic. Monitoring social groups—in a way—represents a double-edged sword as on the one hand ethological-based behaviors flourish in the group, most likely providing higher sensitivity in detecting pathological behaviors, and on the other hand the requirement of group housing limits throughput (groups have to be established and have to remain stable; furthermore, drug screening appears to be more difficult). Finally, competitive behaviors are detectable in certain circumstances (unpublished observation), with dominant animals controlling access to specific areas of the arena, including the operant corners, and thus impairing the experimental design.

Developed owing to the scientific interest of Hans-Peter Lipp in investigating social behavior in rodents under minimally disturbing conditions, the IntelliCage was successfully used to analyze the cognitive behavior of wild-caught mice [4], proving its usefulness in analyzing rodents' behavior under conditions where response to handling or novel environments must be minimized. More recent work has used the IntelliCage system for the high-throughput analysis of cognitive rigidity in mouse models of autism [5]. Also, results obtained in this system were shown to quite accurately screen for and predict deficits observed with more laborious tests, for instance, when comparing strains, lesions, or mutations in mice [6] or evaluating the impact of environmental or cognitive enrichment [7].

2.2 PhenoMaster

The PhenoMaster (TSE Systems, Germany) represents a multipurpose and modular system that allows monitoring single-housed mice and rats in a standard Makrolon cage (home-cage-like environment) (Fig. 2). TSE Systems introduced the home-cage principle a decade ago [1] in an effort to maintain experimental animals in a familiar, ideally stress-free environment. Such conditions are not only consistent with increased awareness and respect for animal welfare but also enhance accuracy and reproducibility of the results. The system is equipped for the continuous and synchronized monitoring of behavioral, physiological, and metabolic parameters in a computer-assisted and fully automated fashion.

Spontaneous activity is constantly monitored by infrared light beam frames (ActiMot), which store precise records of the animal's

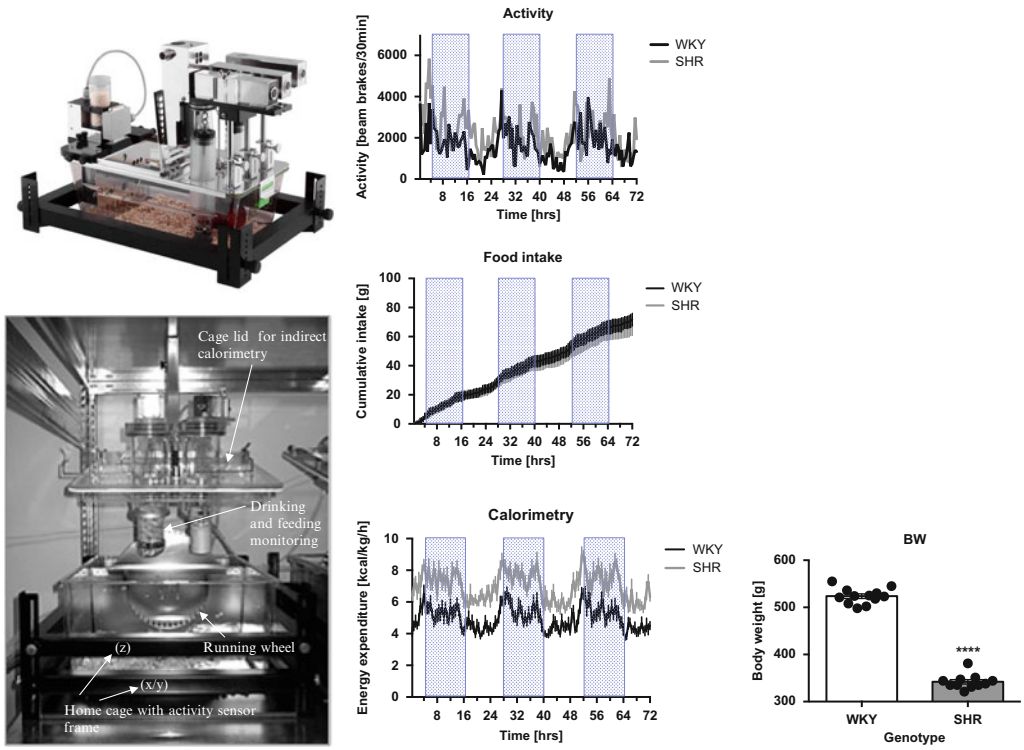

Fig. 2 *PhenoMaster System.* Setup of the PhenoMaster home-cage. The cage lid containing dedicated sensors and features for measuring indirect calorimetry can be mounted onto the rack roof, which makes it more comfortable to work with the system (i.e., clean the cages). The home-cage is surrounded by a light beam-based activity frame, which detects the animal's activity in all three dimensions (*xyz*). In this modular concept, different components or modules can be integrated, such as running wheels or operant conditioning walls. The sample graphs show a selection of parameters measured in spontaneous hypertensive rats (SHR) as compared to wt Wistar controls (WKY) during a 3-day (72 h) experimental protocol. Although displaying "normal" circadian activity and food consumption, SHR rats are characterized by increased metabolism (energy expenditure) and correspondingly reduced body weight

exploration pattern in the *x*, *y*, and *z* plane with high spatial and temporal resolution. Built-in algorithms can filter raw data sets in order to ethologically describe the animal's movements and explorative activity in defined regions of the cage during the selected observational window. Specialized in-cage voluntary running wheels allow the experimenter to generate running profiles and evaluate motor skills, as well as to restrict running in time and/or distance (workload control).

High-precision weighing stations, in combination with leak- and spill-proof containers, permit the accurate analysis of feeding and drinking behavior. Modular access control units restrict feeding and/or drinking by time, duration, or amount according to customized schedules, which can be conditioned to activity performance (running wheel) or other behaviors. A suspended, sit-in enclosure connected to a weighing station enriches the environment while reporting the body weight as the animal visits (Fig. 2).

Furthermore, respiratory gases of each cage are continuously analyzed by indirect calorimetry (PULL or PUSH mode): samples collected from each cage are dehydrated first and subsequently measured by O_2 and CO_2 sensors. A number of variables are automatically calculated, including O_2 consumption, CO_2 production, respiratory exchange ratio (RER), and energy expenditure.

The PhenoMaster system allows a thorough analysis of spontaneous behavioral patterns and circadian rhythmicity under highly controlled and undisturbed conditions. In the classical setup, animals require to be single-housed, which is definitely an important factor experimenters must keep in mind for the evaluation of the results gathered. Due to social deprivation experienced by the tested animals, experiments are typically performed over 48–72 h, after which subjects are returned to the original social groups. Nonetheless, animals can be monitored several times during their experimental life, thus offering the possibility to generate longitudinal datasets representative of the biographical history of each subject (Fig. 2).

This approach was recently used for the comprehensive phenotyping of an established rat model of Huntington's disease [8]. Age-matched cohorts of wild-type (wt) and transgenic (tg) rats were monthly tested in the PhenoMaster, as well as in classical behavioral paradigms descriptive of the most salient traits associated with disease progression in this animal model. The results gathered revealed previously undetected aspects of the phenotype of tgHD rats, including alterations of circadian activity, metabolism, and locomotion. Moreover, a positive correlation was found between spontaneous rearing in the home-cage and individual performance in the accelerod (RotaRod) test. Data mining and classical statistical approaches were supplemented by multivariate statistics (MVA) in this study. In particular, principal component analysis (PCA) and partial least squares discriminant analysis (PLS-DA) were applied, in order to take advantage of the intraindividual longitudinal multidimensional quality of the data acquired under the standardized conditions provided by the system. Segregation by genotype was observed in juvenile tg rats that differed from adult animals, detecting "temperature" (juvenile) and "rearing" (adult) as phenotypic key features of the tgHD model.

2.2.1 Automated Operant Conditioning

Since the invention of the Skinner boxes in the early 1930s, operant conditioning has been an extremely valuable tool for the analysis of cognitive behavior in rodents, allowing for the dissection of motivational, emotional, and purely cognitive aspects of learning and memory performance. A few years ago, fully automated Operant Walls (OW) have been developed as plug-in modules that can be integrated into the home-cage living space of the PhenoMaster (Fig. 3). The system uses classical elements of operant learning tasks such as stimulus elements (light/sound), response devices (levers/nose-poke holes), and reinforcement elements (pellet/water dispenser). Behavioral paradigms are programmed by the experimenter

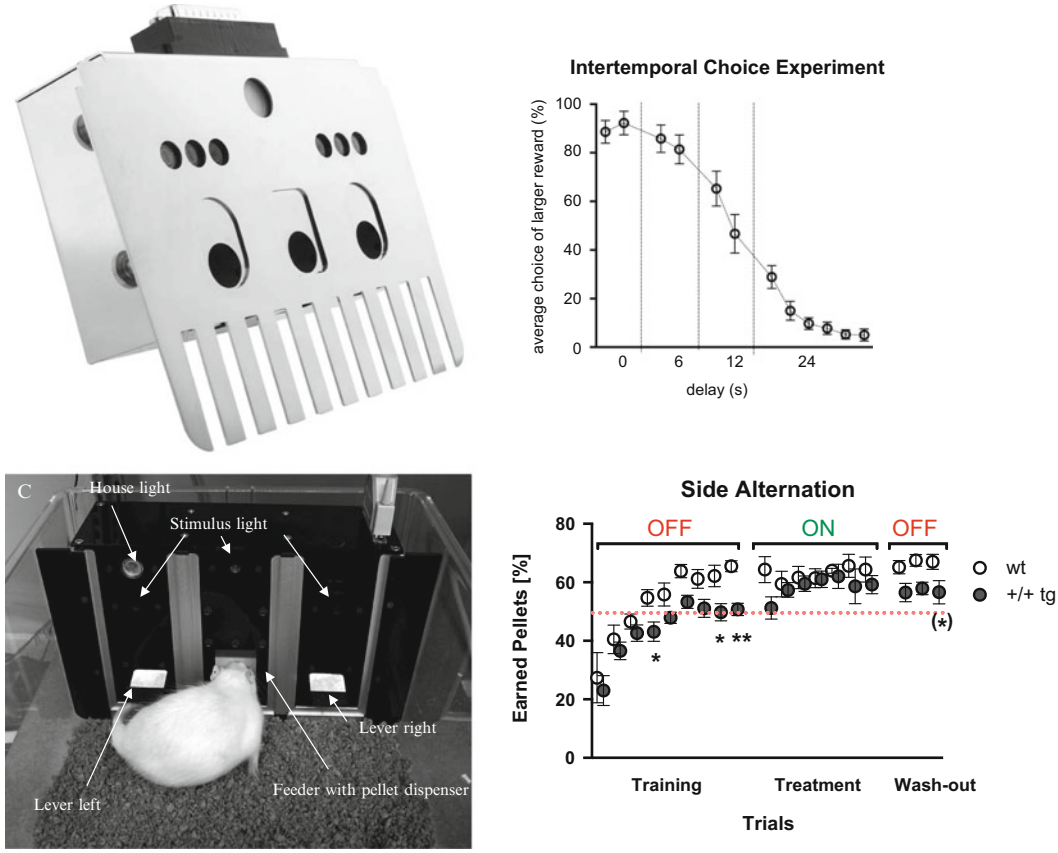

Fig. 3 *Operant Walls.* Operant conditioning unit for mice (*upper picture*) and rats (*lower picture*) equipped with two nose-poke holes/retractable levers positioned on either side of a central food crib, a food pellet dispenser, and different stimulus lights. Graphs show sample results from an intertemporal choice procedure (*upper*) and a side alternation paradigm (*lower*). In the first experiment, choice of a larger, delayed, over a smaller, immediate, reward decreases as the waiting time between a lever-press (e.g., right lever) and the delivery of the pellet increases. In the second experiment, rats learned to alternately press one of the two levers in order to obtain a reward: performance of tg rats (transgenic model for Alzheimer's-like pathology) in comparison to wt littermates was measured during the training phases, under treatment with an acetyl-cholinesterase inhibitor, and again off-drug, in order to dissect treatment from learning effects

via the dedicated software (IntelliMaze, NewBehavior), which provides full experimental flexibility. Based on the automated nature of the system, the animals can perform the scheduled tasks freely within defined time frames, allowing adaptability of the testing sessions to the circadian rhythmicity of the experimental animals (i.e., rodents are typically more active during the dark phase, but inversion of light/dark cycle is not a feasible option in most animal facilities). Once integrated in the PhenoMaster, various possibilities are available for the coordinated access/withdrawal of other modules (food/water, running wheel), thus permitting the design of more elaborate behavioral tasks.

Due to the high level of flexibility regarding programming and redefining experimental tasks, the OW technology is adaptable to various fields of research, as well as to specific experimental conditions. For instance, a minimal amount of "free" rewards can be delivered throughout an experimental paradigm, in order to maintain sufficient motivation in all experimental animals irrespective of the individual cognitive performance. Moreover, while active in parallel, each OW runs the scheduled paradigm independently, thus allowing each animal to proceed through complex, multistep protocols at their own speed. As a result, animals typically adapt to using the OW much quicker than reported for the standard Skinner boxes, for the benefit of both the animals and the experimenters.

OW systems for rats have been established in our lab for a few years as part of a development collaboration with TSE Systems [8]. The operant conditioning units used in our studies consist of two retractable levers positioned on either side of a central food crib, covered with a clear Perspex panel hinged at the top, so that the animal could push it open to retrieve the food pellets delivered upon completion of a successful trial. The walls are equipped with five different light sources, including a house light at the top left corner, three signaling lights positioned above the food crib (white) and each lever (red and green, respectively), and finally a yellow light inserted inside the food compartment, classically used to indicate the presence of a food pellet (Fig. 3). With such setup, we were recently able to develop and validate a number of cognitive/emotional tasks relevant to our specific interests in the field of neurodegeneration (unpublished data). Testing sessions are typically preceded by one/two nights of habituation/adaptation to the OW, during which animals initially have access to automatically delivered ("free") rewards and then are progressively trained to operate the response devices (levers/nose-poke holes) in order to obtain similar rewards. By the end of the second, if not the first, training sessions (performed during the dark phase), reliable responses are usually achieved in most experimental animals (although strain/genetic differences may be expected). Once conditioned, behavioral adaptability is tested within dedicated experimental paradigms. Spontaneous alternation can be measured, as the natural trend of rodents is to explore available options alternatively, thus allowing food rewards to be obtained only if response elements are visited in turn (Fig. 3). Additionally, associative conditioning can be trained by signaling to the animals which of the available response devices should be operated (typically with a lighting stimulus). For emotional investigation, impulsivity tasks are easily designed, in which the animals must operate one of the response elements only after a defined waiting time to obtain a reward (restraining from behavior), yet has the freedom to choose the opposite response element in change for an immediate but smaller reward, similar to the procedure described in the rather

famous "Stanford marshmallow experiment" conducted by Walter Mischel in 1972 [9] (Fig. 3). Operant walls were recently used to assess timing and decision-making in mice [10], demonstrating the sensitivity of an intra-home-cage system to analyze complex psychological processes in rodents.

2.2.2 Telemetric Biopotentials

Radiotelemetric (wireless) measurement of biopotentials has been used in basic and applied research for a few years, allowing for the investigation of physiological, as well as emotional, alterations in animal models of disease. Implantable devices controlled by an antenna system are in charge of transmitting information to and from a computerized system, regulating parameters' measurement and data storage.

The recently developed Stellar Telemetry System (TSE Systems) represents a new generation of such implantable devices (Fig. 4). Its surgically implanted transmitters are able to record activity, blood pressure, tidal volume, electrocardiogram (ECG), electroencephalogram (EEG), electromyography (EMG), electrooculography (EOG), heart rate, and core body temperature in a hermetically sealed and surgically sterile system. Once activated by one central receiver, data can be collected by each individual implant independently and transferred when connection to the antenna is resumed. One main feature of Stellar, in contrast to other systems, is the use of "radio wave telemetry" permitting

Fig. 4 *Telemetric biopotentials—Stellar Telemetry System.* The system consists of implantable transmitters which are able to record a variety of parameters (activity, blood pressure, tidal volume, electrocardiogram (ECG), electroencephalogram (EEG), electromyography (EMG), electrooculography (EOG), heart rate, and core body temperature) and a central receiver regulating parameters' measurement and data storage

longer distances (up to 5 m) between emitter and receiver; hence, the experimental animals can be placed in virtually all classical assays while biopotentials are still recorded. This in turn allows full flexibility of experimental settings, such as group housing and social interaction studies, while each animal is individually observed.

Due to these features, the Stellar Telemetry device is ideal for the integration into a home-cage environment (such as the PhenoMaster setup), paving the way for the combined analysis of behavioral, metabolic, and physiological data in freely moving rodents.

While the system is fairly new on the market, studies in monkeys have recently reported on the effectiveness of their application in freely moving and behaving animals [11, 12].

2.3 PhenoWorld

The PhenoWorld (TSE Systems, Germany) is a combinatorial approach that integrates the functionalities from the abovementioned automated phenotyping systems into one multidimensional setup (Fig. 5). Spontaneous behavioral, cognitive, metabolic, and physiological parameters as measured in TSE PhenoMaster and IntelliCage systems are implemented into multiple home/satellite cages or mazes, which are strategically interconnected. One master software operates all modules, synchronizes, and integrates all incoming data, allowing fully automated experimentation with no/minimal human interference. In the PhenoWorld, animals live in social groups and are therefore capable of developing and displaying species-specific ethological behaviors—a prerequisite for

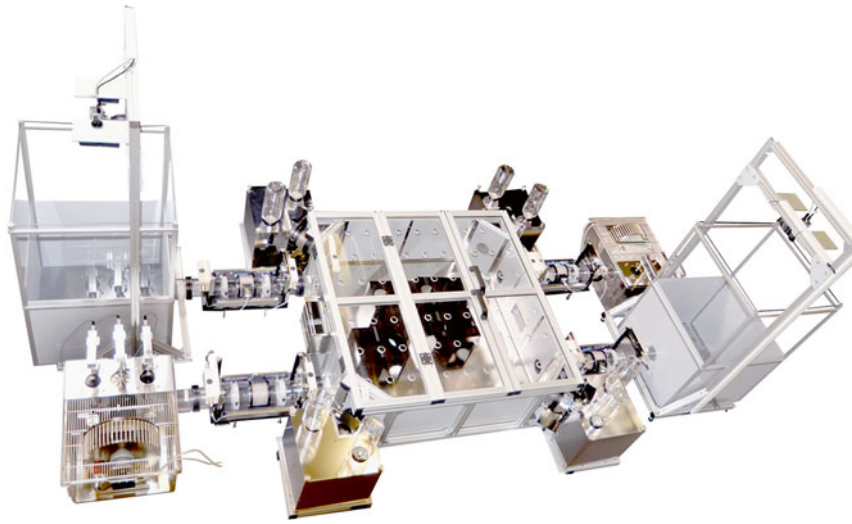

Fig. 5 *PhenoWorld.* General setup of the system. Spontaneous behavior, cognition, metabolic and physiological parameters as measured in TSE PhenoMaster and IntelliCage systems are implemented into multiple home/satellite cages or mazes, which are strategically interconnected

animal welfare and high translational value of experimental data. Every animal is tagged with an RFID transponder and is recognized at strategic places for individualized data acquisition. The animals shuttle between compartments and levels through a number of different gating structures (tunnels, doors, stairways), which can be equipped with ID-recognition devices (RFID antennas), restricting access to compartments in an individualized fashion. A number of technological implementations allow live video feeds for fine tracking of animals' movements, activity, and behavioral display. Acquisition of physiological (Stellar Telemetry) and neurological (EEG measurement, NeuroLogger, NewBehavior) parameters can also be included, as part of the experimental setup.

The integrated technology of the PhenoWorld gives life to an ethologically complex paradigm that can be adapted to specific experimental requirements and better mimics real-life naturally enriched conditions under standardized laboratory settings. The setup promises to monitor spontaneous and conditioned behaviors in freely moving rodents in an undisturbed, and therefore experimenter-free, setting. Consequently, data gathered are expected to be more sensitive and reliable in discriminating behavioral features of interest for investigating mechanisms of complex human diseases—such as stroke.

The PhenoWorld represents a rather newly developed technology, which is why it is only partially established and explored in broad-range research. A very interesting publication from Castelhano-Carlos et al. [13] reports on the application and validation of the system in rats. This study demonstrates that animals living in the PhenoWorld displayed similar but more striking behavioral differences (despair, resting patterns and social behavior) when exposed to unpredictable chronic mild stress, a validated model for depression in rodents [14], as compared to rats living in standard conditions. Moreover, several home-cage behaviors in the PhenoWorld, such as willingness to feed and exercise in running wheels, proved to be sensitive indicators of depressive-like behavior.

2.4 PhenoTyper

Based on the use of video-tracking leading technology (EthoVision XT, Noldus, Netherlands), the PhenoTyper (Noldus, Netherlands) is an observational cage for rats and mice equipped with an infrared-sensitive camera, infrared LED lights, white and yellow light sources, and loudspeakers (Fig. 6). Video-tracking of single or socially housed animals is possible throughout light and dark phases, owing to the infrared technology, and fully automated control of the experimental setting within a designed protocol is exerted by the application of a dedicated software package (e.g., EthoVision XT). The PhenoTyper has a rather simple basic structure, which can also be used for short-term observational experiments (e.g., open field). Setup extensions (i.e., drinking bottles, feeder, shelter) transform the environment into a home-cage, allowing for prolonged experiments to investigate the circadian rhythmicity or rare

behavioral events (e.g., seizures). Additionally, a wide variety of supplementary hardware can be connected to the PhenoTyper, such as a food dispenser, a feeding monitor, an activity wheel, or operant conditioning devices, thus expanding the range of possible investigations under identical experimental conditions.

The most interesting feature offered by the PhenoTyper system is the integration with the EthoVision tracking package. A "Multiple Body Points" module allows tracking the nose-point and tail-base in addition to the center point of experimental animals, leading to a very accurate detection of their position and movements. For instance, in certain tests, the proximity of the animal's nose to a certain object (novel object recognition) and the direction the animal's head is pointed toward are very informative aspects from which relevant behavioral parameters can be inferred (Fig. 6). Up to 100 arenas can be tracked simultaneously, while

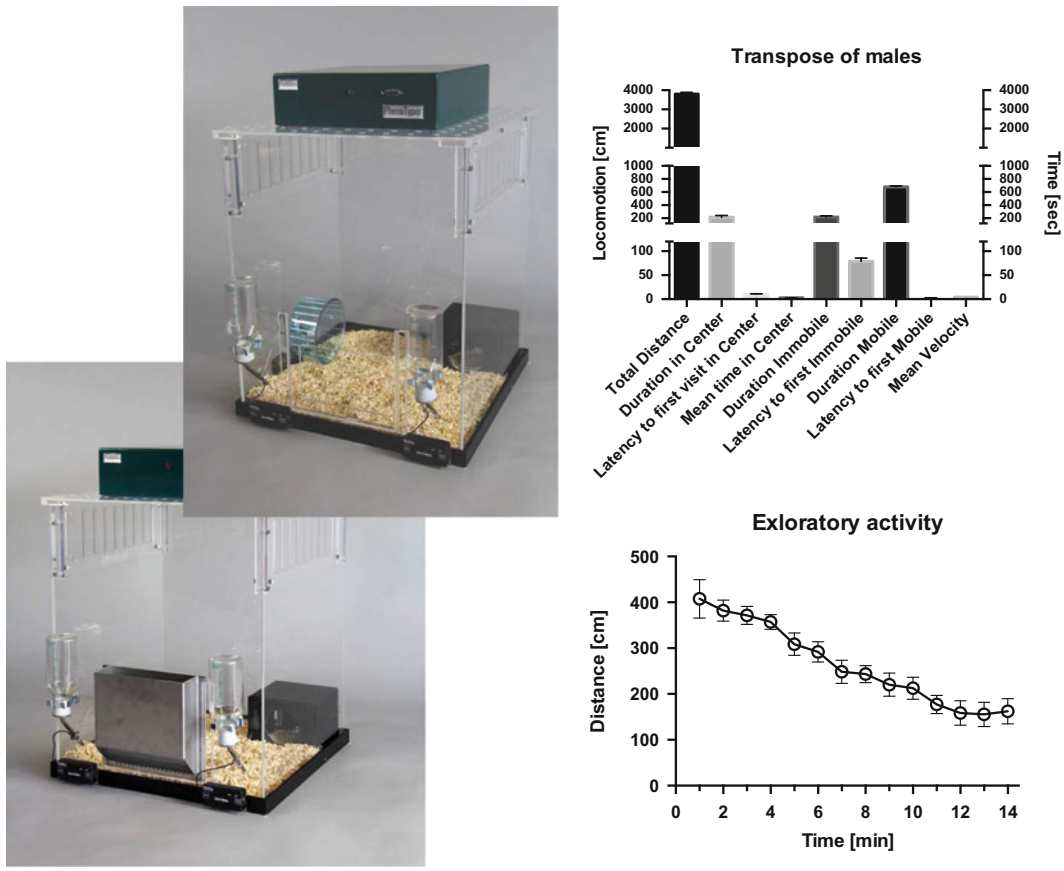

Fig. 6 *PhenoTyper.* The PhenoTyper (Noldus, Netherlands) is equipped with an infrared-sensitive camera, infrared LED lights, *white* and *yellow light* sources, and loudspeakers. It can either be used for short-term observational experiments (e.g., open field) or transformed into a home-cage by setup extensions (i.e., drinking bottles, feeder, shelter), allowing for prolonged experiments to investigate the circadian rhythmicity or rare behavioral events. On the right, sample graphs show how activity profiles can be analyzed by the EthoVision software to calculate a number of parameters relevant for the study

applying start and stop conditions for each of them individually. A "social interaction" module allows tracking multiple animals per arena and calculating a number of social parameters, such as proximity of one subject to another, social exploration, etc. Because of the setup construction, the PhenoTyper constitutes a one-piece, all-inclusive system that does not comprise the use of standard Makrolon cages. Cleaning of the environment between or during experiments poses therefore a certain restraint to the throughput of the investigations.

A long list of publications attests the use of the PhenoTyper in the experimental pipeline associated with the analysis of rodents' behavior [15–17]. An especially interesting example is described in a recent paper [18] where anxiety was assessed in mice by evaluating their response to a light stimulus (aversive) during the dark phase of their circadian cycle. This test is based on the ethological preference of mice to be nocturnal in association with their feeding behavior. It measures the effect of a spotlight—shone right outside of the mouse shelter in the direction of the feeding compartment—on the inhibition of overall activity and feeding behavior. Advantageous over the most commonly used light/dark box transition test, the spotlight paradigm permits to monitor animals' behavior in a familiar, home-cage-like environment, can be repeated over time, and therefore allows detecting changes of the animals' display during an experimental manipulation.

2.5 Multi-conditioning System

Although not based on the concept of home-cage-like testing, a multi-conditioning system (e.g., TSE Systems, Germany) is a very interesting solution for high-throughput automated measures of rodents' behaviors, under highly standardized and experimentally flexible conditions (Fig. 7). The system is typically equipped with high-resolution infrared light beam frames for fast (100 Hz) movement detection in the three dimensions, white/red house lighting sources, noise and sine sound generators, an ultrasonic loud speaker, and species-specific electric shock grids. The equipment is usually located in sound attenuating and ventilated cabinets and is operated by a dedicated software package. Arenas of various sizes, designs, and materials can be used with or without the shocking grids for the execution of up to nine different behavioral paradigms (trace/delay fear conditioning (Fig. 7), active/passive avoidance, place preference, learned helplessness, latent inhibition, light-dark test, open field). The modular nature of the hardware and software components allows to integrate new/different experimental designs to validate procedures.

While the system incorporates several classical paradigms used for cognitive and emotional assessment of rodents, it offers the advantage of a standardized and automated setup. The computerized interface promises highest quality and refinement of the

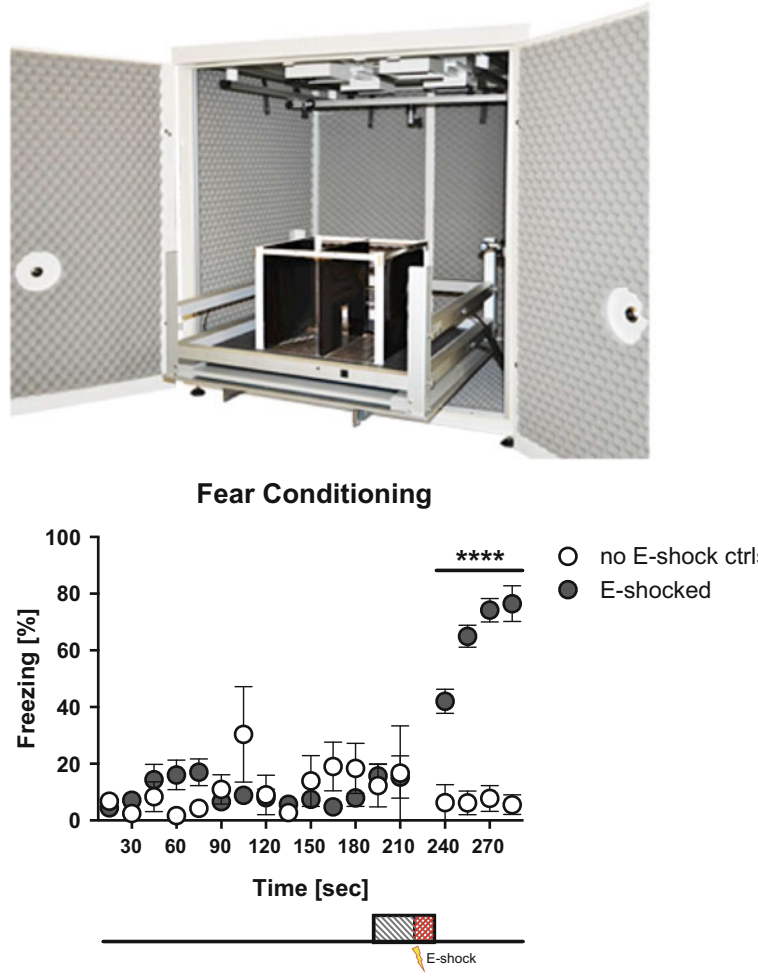

Fig. 7 *Multi-conditioning system.* The system is equipped with infrared light beam frames for movement detection in the three dimensions, *white*/*red* house lighting sources, noise and sine sound generators, an ultrasonic loud speaker, and species-specific electric shock grids. The equipment is usually located in sound attenuating and ventilated cabinets. Arenas of various sizes, designs, and materials can be used with or without the shocking grids for the execution of up to nine different behavioral paradigms. The graph shows the typical course of a fear-conditioning experiment, with shocked animals developing a fear response (freezing) after receiving the unconditioned stimulus (foot shock)

behavioral parameters measured, thus significantly reducing the impact of the experimenter on the data generated and analyzed. Initial validation of the experimental settings is still advisable with this system, in order to adapt the scoring thresholds to the expected behaviors displayed by the animals tested.

3 Considerations on the Incorporation of Automated Phenotyping into Stroke Assays

Common features of all automated behavioral phenotyping systems described above are increased reproducibility, sensitivity, reliability, and throughput compared to most classical behavioral tests. Accordingly, their integration into comprehensive behavioral phenotyping assays of preclinical stroke research provides advantages on several levels.

Firstly, automated screening can be integrated at different stages of an experimental design. If pilot studies are planned to be conducted beforehand (as in the case of surgical manipulations), highest reliability of the results obtained from a limited number of animals is required. Therefore, the implementation of these technologies would certainly be beneficial due to their high level of sensitivity and standardized, unbiased data acquisition. A careful postoperative observation of the animal's health status and recovery is also essential, as it is emphasized in other chapters. Automated techniques such as the PhenoMaster are suitable for a continuous and sensitive monitoring of basic physiological and metabolic parameters, e.g., food and water intake, activity, body weight, and indirect calorimetry, including core body temperature. Applying such a multidimensional experimental approach might also provide further insight into more complex systemic post-ischemic processes, for instance, stroke-induced cachexia or hypothermia. Additionally, the PhenoTyper could be appropriate for postoperative monitoring as it allows for constant video-tracking and recording of the animal's behavior in a stress-free, undisturbed home-cage-like environment. Such video-based observation might be particularly helpful during the first dark phase post-stroke, in outlying stereotypical behaviors indicative of distress and/or sickness, in which rodents often conceal when the experimenter is present. Finally, most automated testing procedures can be repeated on the same animal within longitudinal behavioral screens, which is crucial in order to get a thorough picture of recovery progression in therapeutic intervention studies.

Secondly, especially at later time points after inducing the infarct lesion, major advantage can be taken of the high level of sensitivity provided by automated behavioral testing systems. Even subtle differences between experimental and control groups in physiological and metabolic parameters can be revealed, as well as disturbances in motoric, emotional, and cognitive display, which might not become evident in classical behavioral procedures. For instance, automated cognitive testing paradigms can be adapted in terms of complexity and endpoint definition. In addition, they are performed in an undisturbed home-cage environment, thus avoiding potential sources of bias and stress introduced by the

experimenter's presence. These features consequently allow for more refined cognitive testing compared to classical readouts. Regarding motoric dysfunction, on the one hand subtle deficits that are not sufficiently measurable by standard tests can be detected by means of video-tracking or longitudinal activity profiles. On the other hand, automated techniques can be used to collect meaningful data from animals that are unable to perform classical tests such as the RotaRod due to the severity of their phenotype. Furthermore, setups such as the multi-conditioning system also provide flexibility and high sensitivity for emotional assessment via several paradigms (trace/delay fear conditioning, active/passive avoidance, place preference, learned helplessness, latent inhibition, light/dark test, open field).

Thirdly, automated data collection provides several advantages over manual or experimenter-assisted systems. The experimenter obtains unbiased, quantitative, as well as qualitative information on multiple parameters in high temporal resolution, and systems such as the PhenoMaster generate hypothesis-independent raw data. Appropriate analysis of these large data sets by complex statistics can provide a meaningful insight into pathological and recovery processes. Additionally, it might allow differentiating between improved performance based on restoration of the original function and behavioral compensation learned in the course of repeated testing, a critical aspect which is outlined in Chap. 14. Moreover, throughput of behavioral screens is increased owing to automated data collection from several animals in parallel.

Lastly, comprehensive data acquisition clearly translates into a refined use of laboratory animals for research, which is an important ethical principle, as highlighted in the "3Rs" (reduction, refinement, replacement, addressed in Chap. 16). By implementing the "refinement" of the experimental investigation, as obtained by automated phenotyping techniques owing to their high level of standardization and sensitivity, "reduction" of the number of experimental animals recruited in a study is also achieved, due to the improved quality of data gathered and diminished need of extended and/or replicated data sets (more data from each animal=less animals in the study).

4 Conclusion

It appears that "classical behavioral phenotyping" of rodents—when following certain guidelines as outlined in this chapter—represents today's standard; nonetheless, it requires considerable resources and still does not provide highest reliability, sensitivity, and cross-lab comparability. However, reliable and highly sensitive readouts are essential in preclinical stroke research to detect even subtle improvements in performance and to differentiate if this

improvement is either based on restoration of the original function or merely on behavioral compensatory strategies. Additionally, the simple fact that many classical assays may not be applicable to stroke models due to their motor dysfunction also challenges the further development of behavioral phenotyping approaches in the field. The integration of automated intra-home-cage approaches into comprehensive behavioral screening of stroke models has the potential to overcome some of those limitations and to unravel novel aspects of post-stroke phenotype that classical observational studies cannot document.

References

1. Urbach YK, Bode FJ, Nguyen HP, Riess O, von Horsten S (2010) Neurobehavioral tests in rat models of degenerative brain diseases. Methods Mol Biol 597:333–356. doi:10.1007/978-1-60327-389-3_24
2. McIlwain KL, Merriweather MY, Yuva-Paylor LA, Paylor R (2001) The use of behavioral test batteries: effects of training history. Physiol Behav 73(5):705–717. pii:S0031-9384(01)00528-5
3. Voikar V, Vasar E, Rauvala H (2004) Behavioral alterations induced by repeated testing in C57BL/6J and 129S2/Sv mice: implications for phenotyping screens. Genes Brain Behav 3(1):27–38. pii:044
4. Galsworthy MJ, Amrein I, Kuptsov PA, Poletaeva II, Zinn P, Rau A, Vyssotski A, Lipp HP (2005) A comparison of wild-caught wood mice and bank voles in the intellicage: assessing exploration, daily activity patterns and place learning paradigms. Behav Brain Res 157(2):211–217. doi:10.1016/j.bbr.2004.06.021
5. Puscian A, Leski S, Gorkiewicz T, Meyza K, Lipp HP, Knapska E (2014) A novel automated behavioral test battery assessing cognitive rigidity in two genetic mouse models of autism. Front Behav Neurosci 8:140. doi:10.3389/fnbeh.2014.00140
6. Vannoni E, Voikar V, Colacicco G, Sanchez MA, Lipp HP, Wolfer DP (2014) Spontaneous behavior in the social homecage discriminates strains, lesions and mutations in mice. J Neurosci Methods 234:26–37. doi:10.1016/j.jneumeth.2014.04.026
7. Codita A, Mohammed AH, Willuweit A, Reichelt A, Alleva E, Branchi I, Cirulli F, Colacicco G, Voikar V, Wolfer DP, Buschmann FJ, Lipp HP, Vannoni E, Krackow S (2012) Effects of spatial and cognitive enrichment on activity pattern and learning performance in three strains of mice in the IntelliMaze. Behav Genet 42(3):449–460. doi:10.1007/s10519-011-9512-z
8. Urbach YK, Raber KA, Canneva F, Plank AC, Andreasson T, Ponten H, Kullingsjo J, Nguyen HP, Riess O, von Horsten S (2014) Automated phenotyping and advanced data mining exemplified in rats transgenic for Huntington's disease. J Neurosci Methods 234:38–53. doi:10.1016/j.jneumeth.2014.06.017
9. Mischel W, Ebbesen EB, Zeiss AR (1972) Cognitive and attentional mechanisms in delay of gratification. J Pers Soc Psychol 21(2):204–218
10. Tucci V, Kleefstra T, Hardy A, Heise I, Maggi S, Willemsen MH, Hilton H, Esapa C, Simon M, Buenavista MT, McGuffin LJ, Vizor L, Dodero L, Tsaftaris S, Romero R, Nillesen WN, Vissers LE, Kempers MJ, Vulto-van Silfhout AT, Iqbal Z, Orlando M, Maccione A, Lassi G, Farisello P, Contestabile A, Tinarelli F, Nieus T, Raimondi A, Greco B, Cantatore D, Gasparini L, Berdondini L, Bifone A, Gozzi A, Wells S, Nolan PM (2014) Dominant beta-catenin mutations cause intellectual disability with recognizable syndromic features. J Clin Invest 124(4):1468–1482. doi:10.1172/JCI70372
11. Rhoads MBA, Huggins D, Collet J, Osborn J (2014) Spontaneous essential hypertension in the non-human primate Chlorocebus aethiops sabaeus, the African green monkey. FASEB J 28(Supplement 1136.16)
12. Collet JHM, Beierschmitt A, Descanio J, Knot H, Osborn J (2014) Circadian measurement of blood pressure and core body temperature in conscious, freely moving vervet monkeys. FASEB J 28(Supplement LB857)
13. Castelhano-Carlos M, Costa PS, Russig H, Sousa N (2014) PhenoWorld: a new paradigm to screen rodent behavior. Transl Psychiatry 4, e399. doi:10.1038/tp.2014.40

14. Willner P (2005) Chronic mild stress (CMS) revisited: consistency and behavioural-neurobiological concordance in the effects of CMS. Neuropsychobiology 52(2):90–110. doi:10.1159/000087097
15. Loos M, Koopmans B, Aarts E, Maroteaux G, van der Sluis S, Neuro BMPC, Verhage M, Smit AB (2015) Within-strain variation in behavior differs consistently between common inbred strains of mice. Mamm Genome. doi:10.1007/s00335-015-9578-7
16. Morse SJ, Butler AA, Davis RL, Soller IJ, Lubin FD (2015) Environmental enrichment reverses histone methylation changes in the aged hippocampus and restores age-related memory deficits. Biology 4(2):298–313. doi:10.3390/biology4020298
17. Remmelink E, Loos M, Koopmans B, Aarts E, van der Sluis S, Smit AB, Verhage M, Neuro BMPC (2015) A 1-night operant learning task without food-restriction differentiates among mouse strains in an automated home-cage environment. Behav Brain Res 283:53–60. doi:10.1016/j.bbr.2015.01.020
18. Aarts E, Maroteaux G, Loos M, Koopmans B, Kovacevic J, Smit AB, Verhage M, Sluis SV, Neuro BMP (2015) The light spot test: measuring anxiety in mice in an automated home-cage environment. Behav Brain Res. doi:10.1016/j.bbr.2015.06.011

Chapter 16

Histology and Infarct Volume Determination in Rodent Models of Stroke

Clemens Sommer

Abstract

While there are many and in part very different staining protocols for determining and calculating infarct volumes after experimental stroke in rodents, this plethora can ultimately be reduced to a few basic methods such as histological staining, contrast-enhanced staining, immunohistochemistry, and enzyme histochemistry. In this chapter, each of these will be briefly introduced with an exemplary protocol. Since each method requires specific tissue pretreatment and consequently determines the possibility of performing additional investigations, all options should carefully be considered before starting with the experiments. Although each of the methods has its advantages and disadvantages and there is no "best" solution, the preparation of serial cryostat sections clearly offers the most options. Other frequently used and practicable methods of brain tissue preparation—fixation, storage, and slicing—are nevertheless also discussed. Finally, the basics of infarct volume calculation are presented. Attached are the most important protocols and their potential pitfalls.

Key words Contrast-enhanced staining, Conventional staining, Edema correction, Enzyme histochemistry, Histology, Immunohistochemistry, Infarct, Microtubule-associated protein 2 (MAP2), NeuN, Paraformaldehyde, Penumbra, Shrinkage, Silver staining, Stroke, 2,3,5-Triphenyltetrazolium hydrochloride (TTC)

1 Introduction

One of the first and most important steps when planning and designing a stroke experiment is deciding how to treat the brain tissue of the experimental animals. The wrong decision will cause problems later on, so this step calls for timely and careful consideration. The researcher's decision, in turn, depends on having a clear idea of which endpoints will be analyzed. This seemingly trivial aspect is frequently ignored in practice. While determination of the infarct volume is certainly one important issue in experimental stroke research, it is nevertheless only one parameter among several. Analyses of gene expression, protein expression, protein synthesis, pH, glucose, lactate, ATP content, regional blood flow, and

Ulrich Dirnagl (ed.), *Rodent Models of Stroke*, Neuromethods, vol. 120,
DOI 10.1007/978-1-4939-5620-3_16,

receptor binding densities are just a few examples of potential complementary investigations which might call for a specific way of tissue pretreatment. Taking all this into consideration, the first step should be to define the endpoints to be analyzed.

The next step is to check whether it is possible to do all experiments using the same brain tissue or whether different groups are needed for the various investigations. When performing morphological analyses, one has to decide whether or not the brain will be perfused. If perfusion is necessary, two possibilities arise: perfusion with saline to simply wash out brain vessels or perfusion, e.g., with paraformaldehyde (PFA), for additional fixation of the brain tissue. Perfusion should be performed under standardized conditions concerning perfusion pressure and perfusion time. This is especially important when a thorough analysis of vessels is planned. The next decisions concern the tissue workup steps. Tissue can be used natively or it can be frozen or otherwise specifically prepared, e.g., for cryostat sections, for free-floating vibratome sections, or for paraffin embedding. While infarct volume calculation is in principle possible with all of these workup methods, plans to perform additional experiments may influence the decision. For example, if complementary immunohistochemical investigations are planned, the choice may be narrowed down to native cryostat material or PFA-fixed tissue, because only they would allow work with certain specific antibodies. If brilliant morphology is of major importance, paraffin-embedded material will provide the best results. For infarct volume determination, one can choose among different staining methods. All procedures have their advantages and disadvantages, so the researcher should know and carefully consider all potential options. Although there is no ideal solution, most options are left open by the use of serial cryostat sections allowing multimodal imaging [1].

In the context of infarct volume determination, several terms and definitions are briefly outlined to avoid possible misunderstandings. Infarct is defined as pannecrosis after focal ischemia and has to be distinguished from selective neuronal loss occurring in the penumbra, in brain areas remote from the ischemic territory, or in chronic arterial obstructive disease [2]. Depending on the ischemia model used, the size of the infarct may vary significantly, i.e., from large pannecrosis as seen after middle cerebral artery occlusion to small lesions after photothrombotic ischemia. The ischemic penumbra surrounding the lethally damaged infarct core—originally defined as peri-infarct tissue with reduced blood flow, impaired neuronal functionality, but preserved structural integrity [3, 4]—can perhaps be saved from irreversible damage. It is therefore the current focus of most neuroprotective therapies. This therapeutic potential is evidenced by the fact that early after stroke onset, the penumbra can account for up to 50% of the volume which finally evolves into infarction. However, the exact identification of “the” (one) ischemic penumbra on brain slices is,

strictly speaking, impossible. Over the past decades, it has become clear that the penumbra is a highly dynamic structure which can be characterized in vivo by various imaging techniques and in vitro by a multitude of factors, each of which defines one aspect of this so-called tissue at risk. The other way around, after focal ischemia, "multiple" molecular and cellular penumbras are present which may differ with regard to their spatial and temporal expansion [5, 6]. New concepts speculate that the penumbra comprises the transition zone between ischemic injury and repair [7]. Therefore, when using the term penumbra for a peri-infarct area on a tissue slice, an exact, context-related definition of the penumbra has to be given. Alternatively, one could tone down statements concerning the penumbra and refer to it as peri-infarct area or tissue adjacent to the infarct core.

There exists a plethora of techniques to identify various pathological features after cell death in stroke [8]. The following paragraphs will provide examples of four principal methods of determining the infarct volume after focal cerebral ischemia in rodents: routine histology staining, contrast-enhanced staining, immunohistochemistry, and enzyme histochemistry. It bears repeating that there is no "perfect" solution. All procedures have their pros and cons, so one should know precisely and consider precisely all potential options. The possibilities for tissue storage and fixation will be provided in the following, and finally, the essential features of infarct volume determination will be covered. Protocols including the material necessary for the staining methods are attached.

2 How to Get Slices for Staining and Infarct Volume Determination: Fixation, Storage, and Slicing of Brain Tissue

Before any staining procedure and infarct volume calculations can be performed, the brains have to be removed, potentially fixed, sliced, and/or stored. As already mentioned, these initial steps largely will determine the range of possible staining methods and further investigations and therefore merit careful consideration well in advance of any procedures.

2.1 Fixation

Different fixation methods significantly alter the absolute infarct volume and the degree of edema. In cryostat sections from unfixed material, the infarct will expand by up to 22% [9] because it contains more water than the surrounding tissue; paraffin embedding, on the other hand, may cause shrinkage of the tissue by up to 36% [10] because of the organic solvents used to dehydrate it [11]. The whole situation is further complicated by the fact that different brain structures are differently affected by shrinkage [10]. Finally, the hemispheric volume also depends on the fixation procedure, as demonstrated by a 7% increase after immersion compared to

perfusion fixation [11]. These artifacts become a serious issue when stating absolute infarct volumes; relative infarct volumes, which are also corrected for edema (c.f. Sect. 4), are a favorable possibility for overcoming these problems. If fixation of the brain is necessary, transcardial perfusion will lead to better morphological results than immersion fixation which, nevertheless, may suffice for mere infarct volume determination by H&E staining. A further advantage of perfusion fixation is the washout of vessels from blood cells to avoid interference with immunohistochemistry. One of the most applicable fixation solutions is 4% PFA (c.f. Sect. 5) which also provides good results for many immunohistochemical investigations. In order not to spoil the options for additional experiments, the use of unbuffered formalin should be avoided. Postfixation of perfused brains for 24 h and immersion fixation of unfixed tissue for approximately 48 h are usually sufficient. As already mentioned, perfusion should be performed under standardized conditions concerning perfusion pressure (by the use of a perfusion pump or, alternatively, bottles with the fixative placed between 100 and 150 cm above the operating table) and perfusion time. This is especially important when histologic analysis of vessels (walls, diameter, etc.) is planned. If electron microscopy is intended, material should be fixed primarily in 3% glutaraldehyde.

2.2 Storage

Unfixed frozen brains are usually stored in a freezer between –70 and –80 °C. For storage of fixed brains or brain slices, there are several possibilities: PFA-fixed, paraffin-embedded (or glutaraldehyde-fixed and plastic-embedded) material can be stored for decades (an advantage not to be underestimated). Apart from that, PFA-fixed brains may be stored as a whole for several weeks in phosphate-buffered saline (PBS) with 0.5% sodium azide at 4 °C or cryoprotected in 30% sucrose and then stored at –20 °C. However, fixed brains may also be sliced on a vibratome (e.g., 50 µm thick) and slices then stored again in PBS with 0.5% sodium azide or cryoprotected in 30% sucrose and stored at –20 °C. Concerning freezing techniques of native unfixed tissue for optimal preservation of morphology, it seems that every lab has its own secret recipe. The only method definitely unsuitable is direct freezing in liquid nitrogen since it usually leads to fragmentation of the brain (Fig. 1) and cryostat artifacts in the slices. Snap-freezing on dry ice, with or without an aluminum foil between the brain and ice, is frequently carried out, but the resulting cold effect is unevenly distributed. We achieve a gentle freezing by cooling the brain immediately after removal in –20 °C isopentane for 10 min; we then either process (cryostat) the tissue right away or store it at –70 °C. If any kind of immunohistochemistry is intended, frozen cryostat sections should be thawed and air-dried. Fixation can be performed in 4% PFA for 5 min at 4 °C. Alternatively, fixation for 10 min in acetone at –20 °C is possible (depending on the respective antibodies).

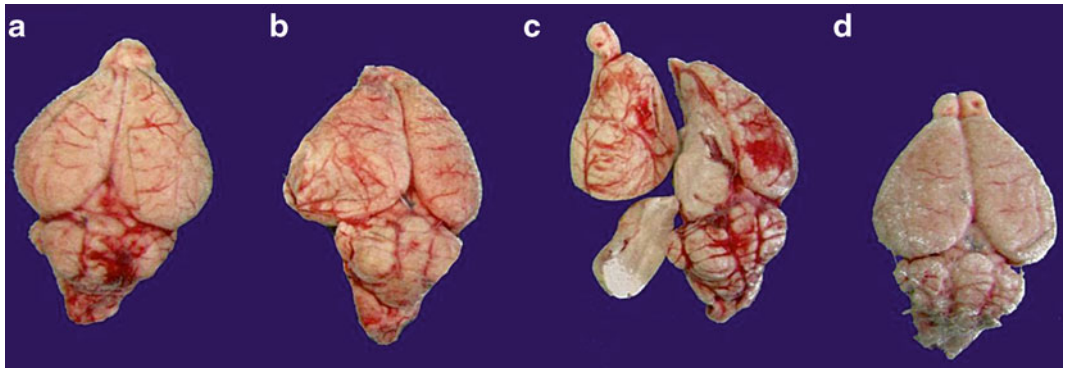

Fig. 1 Freezing methods of brain tissue. Snap-freezing on dry ice, with (**a**) or without (**b**) an aluminum foil between the brain and ice, is frequently carried out and provides acceptable results. Definitely unsuitable is direct freezing in liquid nitrogen since it usually leads to breach of the brain (**c**). In our hands, gentle freezing with optimal preservation of morphology is achieved by immediate cooling of the brain in −20 °C isopentane for 10 min before processing or storage at −70 °C (**d**)

2.3 Slicing

For the detection of infarct volumes, sometimes a minimum of eight slices is recommended [12, 13], but reliable results can also be achieved by analysis at five levels [14, 15]. One possibility is to slice the entire brain (fixed or unfixed) with a "brain slicer," i.e., matrices with variable distances which are commercially available (Fig. 2). If slices are intended to be used for paraffin embedding, thickness should amount to 2 mm, since thinner slices are difficult to handle and often fragment (Fig. 2). Cutting the brains on the vibratome or cryostat allows preparation of serial sections (most favorable) or sections at defined intervals, which makes calculation of the total infarct volume possible. For exact overall orientation, purchase of a brain atlas is highly recommendable (e.g., the atlases by Paxinos and Watson).

3 Staining Methods for Infarct Volume Determination

See also Sect. 5.

3.1 Hematoxylin Eosin (H&E) Staining

Hematoxylin eosin (H&E) staining, which is routinely used in diagnostic pathology, is also a valuable tool for detecting ischemic brain lesions and is sometimes considered as the "gold standard." H&E staining will in fact be sufficient in most cases. It can be performed on cryostat sections, on free-floating vibratome sections, as well as on paraffin-embedded ones. This staining further allows assessment of potential morphological alterations in the brain tissue outside the infarct core. H&E also allows for detection of selective neuronal loss, e.g., in penumbral regions. While the normal brain tissue stains eosinophilic red, the infarcted region appears pale. A clear and reliable distinction between infarct and adjacent

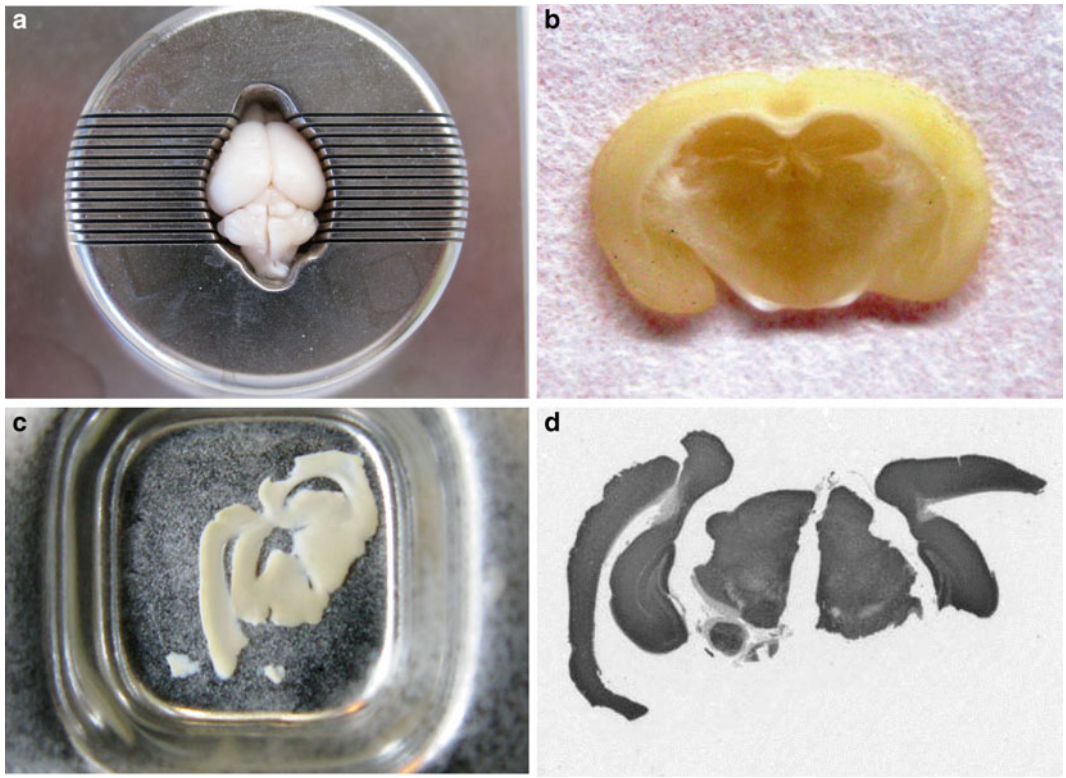

Fig. 2 Slicing the brain including pitfalls. There exist commercially available "brain slicers" for mouse and rat brains. Here, a model for mouse brains is shown (Rodent Brain Matrix, Adult Mouse, 30 g, coronal, Item no. RBM—2000 C; ASI Instruments, USA), which perfectly fits the shape of the brain (**a**). The matrix allows preparation of 1 mm thick slices which can easily be made (**b**). However, after treatment for paraffin embedding, slices are frequently distorted (**c**, gross morphology; **d**, histological slice stained for MAP2). Therefore, 2 mm thick sections are recommended

tissue is possible after 24 h [1]. For the sake of thoroughness, it should be mentioned that other "routine" stainings such as cresyl violet/thionine allow detection of infarcted brain tissue with results comparable to those rendered by H&E.

3.2 Silver Staining

The great advantage of the silver staining method over H&E staining is the markedly enhanced contrast between infarct and normal tissue, which allows computer-assisted analysis of infarct volumetry. A sharp demarcation of ischemic and normal tissue is also evident in the white matter, normally posing a major problem when using microtubule-associated protein 2 (MAP2) immunohistochemistry (c.f. Sect. 3.3.1) or TTC staining (c.f. Sect. 3.4). A further advantage of this method is its early detection of infarcted brain tissue including the penumbra, as shown by parallel determination of local cerebral blood flow with autoradiography starting 2 h after ischemia [16]. Although slightly more complicated than H&E staining, silver staining can also be performed rapidly and

rather easily, and it has therefore become a standard method for infarct volume determination. However, silver staining only works with cryostat sections.

3.3 Immunohistochemical Methods

3.3.1 Microtubule-Associated Protein 2 (MAP2) Immunohistochemistry

A convenient alternative to the aforementioned staining methods is the detection of microtubule-associated protein (MAP2) for infarct volumetry by immunohistochemistry. This can be performed on cryostat sections, vibratome sections, and paraffin-embedded material. Furthermore, MAP2 is also a well-established marker protein for the early detection of brain injury, after both permanent and transient ischemia [17, 18]. Reduced MAP2 immunostaining has been reported as early as 1 h subsequent to the onset of permanent middle cerebral artery occlusion in the rat [17]. Reduction of MAP2 immunoreactivity in the necrotic infarct core and, thus, its reliable detection are possible as from 24 h after ischemia. A good correlation between silver staining, MAP2 immunohistochemistry, and T2-weighted MRI has also been reported [19]. Since MAP2 is present mainly in dendrites, where it may be involved in stabilization and maintenance of synaptic circuits in the mature brain [20], detecting a distinct delineation of brain damage in the white matter is problematic (Fig. 3).

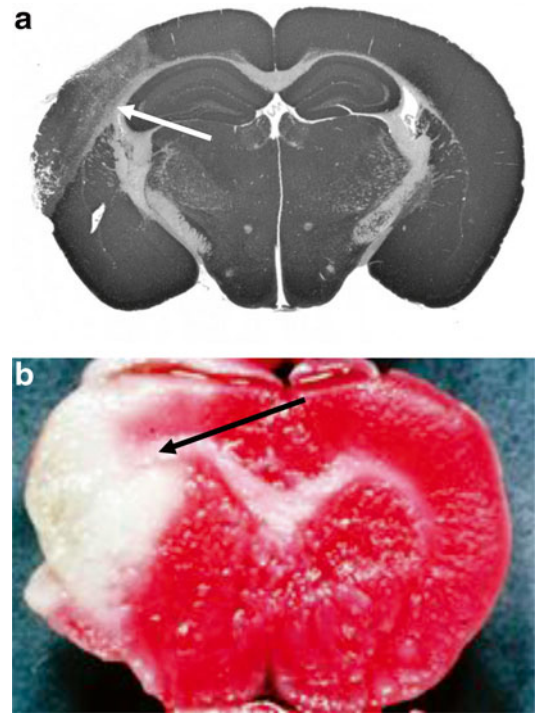

Fig. 3 Problems of MAP2 and TTC staining. The border between infarct and the normal tissue is clearly evident in the *gray matter* both after staining with MAP2 immunohistochemistry (**a**) or TTC (**b**). However, involvement of the *white matter* can hardly be distinguished from the uncolored infarct (*arrows*)

3.3.2 NeuN Immunohistochemistry

NeuN immunohistochemistry for the analysis of ischemic brain damage is a frequently used alternative to MAP2 immunohistochemistry [21]. Fortunately, it can also be performed on cryostat sections, vibratome sections, and paraffin-embedded material. NeuN is a DNA-binding neuron-specific protein which is detectable predominantly in the nuclei and perikarya of neuronal cells [22]. NeuN staining decreases early after ischemic injury and allows a reliable delineation of the infarct from about 6 h after ischemia [23]. Some authors report a reduction of NeuN immunoreactivity as early as 1 h after severe transient focal ischemia in rats [24]. On the other hand, NeuN is also a perfect marker to check for neuronal loss in the long run after the ischemic event [21]. Thus, NeuN does not only allow assessment of the total infarct but also the detection of selective neuronal loss [21]. The only caveat with NeuN immunohistochemistry is the notion that early postischemic loss of staining intensity may be caused by a change in antigenicity not inevitably indicating cell death but possibly a transient cell damage [25]. Finally, there are promising but still evolving approaches using NeuN immunohistochemistry for automated and quantitative selective neuronal loss after ischemic injury [26].

3.4 2,3,5-Triphenyltetrazolium Hydrochloride (TTC) Staining

Tetrazolium salts such as 2,3,5-triphenyltetrazolium hydrochloride (TTC) can be used as histochemical indicators of mitochondrial oxidative enzymes. By accepting electrons, TTC is reduced to a red-colored, lipid-soluble formazan, indicating that functioning mitochondria are present. Vice versa, if mitochondria are damaged, TTC cannot be reduced to the colored formazan. Based on these properties, TTC staining has become a convenient marker for detecting infarcts in tissue slices, which remain unstained in contrast to the viable tissue staining deep red (Fig. 3). The use of TTC staining for infarct volumetry in rodent stroke models dates back to the 1980s [27]. This method is rather easy to apply and the results are immediately available, revealing a high contrast between normal and infarcted tissue (Fig. 3) and thus allowing for automated analysis of scanned images [28]. Furthermore, although not ideal, slices can in principle be used for additional histological and immunohistochemical investigations [18]. However, if indeed additional sections are prepared, the argument given most frequently for using this method, i.e., its quickness, loses its relevance. Last but not least, delayed TTC staining still provides reliable results 8 h after the death of the experimental animal (kept at room temperature!) [29]. The main limitations of TTC staining have also been known for a long time [30]. Since, strictly speaking, TTC staining only labels mitochondria, tissues with a low density of mitochondria such as white matter do not stain, which makes demarcation of the infarct impossible (Fig. 3). Another limiting factor with TTC is the narrow time window. Although in cases of severe ischemia TTC staining has repeatedly been reported to delineate infarcts as early as 2–3 h

after reperfusion [18, 30], reliable detection of infarcts after milder ischemia requires about 24 h [18]. On the other hand, since infiltrating inflammatory cells harbor intact mitochondria, TTC should not be used for time points beyond 24 h after ischemia [30].

4 Infarct Volume Calculation

After brain tissue has been stained, successfully by any method, infarct volume can be determined. Slices or slides must first be photographed or scanned. As already stated, a minimum of 5–8 levels is recommended to accurately assess the infarct volume [12–15]. There is a whole range of software available (e.g., NIH software available free of charge on the Internet or commercially available versions) which might even allow automatic infarct volume determination. Otherwise, one has to manually mark regions of interest, i.e., infarct, ipsilateral, and contralateral hemispheres, on the monitor to calculate their areas. Infarct volumes can then be calculated as the sum of the sectional infarct areas multiplied by the interval thickness. In general, infarct volume can be determined directly or indirectly. Furthermore, infarct volume can be expressed as an absolute value or relatively, as a fraction of the ipsilateral or contralateral hemispheres. Since both freezing and paraffin embedding cause either artifactual extension or shrinkage of the tissue, expression as relative value is more favorable. In addition, relative values allow better comparability between different studies. Depending on the model used, severe edema may develop during the early phase following ischemia, and this distorts infarct volume calculations. Edema correction is then necessary and can easily be performed according to the method provided by Swanson and colleagues [13]: $\text{Area}_{\text{corrected}} = \text{Area}_{\text{Infarct}} \times (1 - (\text{Area}_{\text{ipsilateral hemisphere}} - \text{Area}_{\text{contralateral hemisphere}}) / \text{Area}_{\text{contralateral hemisphere}}))$. While originally only the gray matter (cortex and basal ganglia) in each hemisphere was measured but not the white matter [13], current protocols include the white matter [31]. Edema correction is necessary within 3 days after ischemia [11]. However, at the peak of stroke-induced edema, brain swelling involves both infarct and the surrounding tissue and sometimes also the contralateral hemisphere; thus, this correction method may still be confounded by edema. Furthermore, as a rule of thumb, the smaller the infarct is, the higher the variations [11]. Another issue arises in chronic stroke studies with survival times of about 1 week or more. The necrotic tissue will then be removed by microglia/macrophages resulting in a growing pseudocystic brain defect and an enlargement of the ventricular system ("hydrocephalus e vacuo"). Measurement of tissue loss calculating the difference between the volume of the remaining normal hemisphere and the remaining volume of the injured hemisphere will then be more accurate than simply measuring the infarct volume. The average

volume of a hemisphere can easily be calculated using the following formula: (area of the complete coronal section of the hemisphere—area of ventricle—area of damage) × interval between sections × number of sections [32].

5 Protocols

For the following protocols, no companies or catalogue numbers are given, since change in this field is so rapid. All materials are standard materials which can be purchased everywhere if not explicitly stated otherwise. *Pitfalls are indicated by an exclamation mark.*

5.1 Buffered 4% Paraformaldehyde (PFA) Solution

This 4% buffered PFA solution is absolutely essential and should be used whenever formalin/paraformaldehyde fixation is required.

5.1.1 Materials

$NaH_2PO_4 \times H_2O$, Na_2HPO_4, PFA, 1N NaOH

1. First, prepare a Sorensen's phosphate buffer (2 L) with:
   (a) Solution A = 0.2 M $NaH_2PO_4 \times H_2O$ = 27.6 g/L
   (b) Solution B = 0.2 M Na_2HPO_4 = 28.4 g/L
   (c) OR $Na_2HPO_4 \times 2\ H_2O$ = 35.6 g/L
2. Mix 230 mL of solution A with 770 mL of solution B plus 1000 mL distilled water and you will get your Sorensen's phosphate buffer (pH should be 7.3–7.4).
3. To prepare the 4% PFA solution, add 80 g PFA to about 1500 mL Sorensen's phosphate buffer and dissolve the mixture on a stirring hot plate by slowly heating to nearly 70 °C. Just before 70 °C is reached, add about 5 mL 1N NaOH.
4. Let the solution cool down to room temperature and fill it up with phosphate buffer to a total of 2000 mL.
5. Adjust pH to 7.4.
6. This 4% PFA solution will stay stable for at least 2 weeks at 4–8 °C; before use, check pH again.
   (a) The critical point is to slowly heat the PFA and not to pass the 70 °C mark; otherwise, the procedure has to be repeated (with fresh PFA).

5.2 H&E Staining

Staining procedure and staining times vary, depending on the tissue pretreatment, the thickness of the section, and, last but not least, the normal differences from lab to lab. The following protocols are therefore just guidelines which have to be optimized by each user.

5.2.1 Materials

Eosin, hematoxylin, alcohol, xylol, mounting medium

5.2.2 Cryostat Sections (Unfixed Tissue)

1. Cut 10–20 μm thick sections on a cryostat.
2. Collect sections on glass slides (to avoid floating off, slides should be precoated with poly-l-lysine or 3-aminopropyl-triethoxysilane (TESPA); alternatively, commercially available SuperFrost® slides are recommendable).
   (a) Warm slides before mounting the frozen tissue slices (thawing of the slices on the warmed slides will increase adherence to the coating).
   (b) Slices may curl if they are thawing too quickly. Adjust temperature in the cryostat chamber and temperature of the blades.
3. Dry sections for 10 min.
4. Stain 1 min in hematoxylin.
5. 10 min running water ("blueing").
6. Stain 15 s in eosin.
7. Dehydrate by 96% ethanol, 2 × 100% ethanol and 3 × xylol.
8. Cover slides with mounting medium.

5.2.3 Vibratome Sections (PFA Fixed)

1. Cut 50 μm thick vibratome sections on a vibratome; due to the relative thickness, further treatment is best done "free floating," e.g., in cell culture well plates.
2. 3 × 5 min PBS.
3. Stain 2 min in hematoxylin.
4. 5 × 5 min running water ("blueing").
5. Stain 30 s in eosin.
6. Dehydrate with 70% ethanol, 96% ethanol, 2 × 100% ethanol, and 3 × xylol.
7. Mount slices on slides and cover with mounting medium.

5.2.4 Paraffin-Embedded Material

1. Cut 3–5 μm thick paraffin sections on a microtome (after precooling the paraffin block).
2. Dewax with 3 × xylol, 2 × 100% ethanol, 96% ethanol, distilled water.
3. Stain 2 min in hematoxylin.
4. 5 min running water ("blueing").
5. 96% ethanol.
6. Stain 2 min in eosin.
7. Dehydrate by 96% ethanol, 2 × 100% ethanol, and 3 × xylol.
8. Cover slides with mounting medium.

5.3 Silver Staining (According to Vogel et al. [16])

5.3.1 Materials

Lithium carbonate, 10% silver nitrate solution, 25% (28%) ammonia solution, 37% formaldehyde solution, hydroquinone, acetone, trisodium citrate dihydrate

5.3.2 Silver Impregnation Solution (90 mL)

1. Add 10 mL saturated lithium carbonate solution (about 0.6 g in 50 mL H_2O) to 5 mL of a 10% silver nitrate solution.
2. A precipitate will form which will be dissolved with continuous stirring by adding a 25% (28% does also work) ammonia solution (about 500 µL) drop by drop until the solution gets—slowly—clear (don't get impatient at this point, since too much ammonia solution spoils the staining).
3. Add 75 mL distilled water and store in the dark until use.
   (a) Prepare all solutions daily.

5.3.3 Developer Solution (105 mL)

1. Mix 20 mL of a 37% formaldehyde solution with 70 mL of distilled water.
2. Add 0.3 g hydroquinone and 15 mL acetone by gentle agitation.
3. Add and dissolve 1.1 g trisodium citrate dihydrate.
4. Expose the solution to room air until it gets copper colored (after about 30–60 min).
   (a) Prepare all solutions daily.
   (b) Clean glassware carefully (65% nitric acid/distilled water).

5.3.4 Staining Procedure

1. Use 20 µm thick unfixed cryostat sections on poly-l-lysine precoated slides (or SuperFrost®).
2. Submerge slides for 2 min in the silver impregnation solution with continuous and vigorous shaking.
3. Wash six times for 1 min in distilled water with shaking.
4. Transfer slides for 3 min to the, again, vigorously shaken developer solution.
5. Wash three times for 1 min in distilled water with shaking.
6. Slides are now air-dried and covered.

5.4 Immunohistochemistry

Depending on the pretreatment of the brain tissue, the protocols for immunohistochemistry have to be substantially modified. Furthermore, there are many different detection systems. Therefore, when doing immunohistochemistry, look for suitable protocols and/or follow the suggestions given by the manufacturer of the primary antibody.

(a) Using mouse models of stroke, remember that your primary antibody must not be a mouse antibody.

5.5 2,3,5-Tripheny-ltetrazolium Hydrochloride (TTC) Staining

Performing TTC staining after 24 h, as given below, is the most frequently used protocol and will provide reliable results both after transient and permanent focal ischemia [18, 33].

1. Prepare coronal brain sections, ideally using a brain slicer (various matrices for rats and mice are commercially available).
   (a) For easy handling, sections should normally not be thinner than 2 mm (Fig. 3).
2. Immerse slices in 2% TTC, e.g., in a cell culture dish, (TTC is light sensitive: mask solution with aluminum foil) in 0.9% phosphate-buffered saline (PBS) at 37 °C for 15–30 min.
3. Remove TTC solution and wash three times with PBS.
4. Transfer slices to a fixation solution, normally 4% PFA for 24 h, to potentially perform additional histological/immunohistochemical investigations (fixation in 3% glutaraldehyde is also possible if further electron microscopy is intended; keep dark until the slices have been digitized).
   (b) Photograph or scan slices for infarct volumetry within the next [3–7] days [34], since the staining fades and the contrast gets lost; keep slices dark (fixation before further manipulating prevents distortion of the slices; photographs can be made immediately after TTC staining).
5. Slices may then be stored in 30% sucrose at –20 °C until further analysis.
   (a) There are some modified protocols to optimize the staining procedure. Two major steps can be varied to improve the results:
   (b) The contrast of TTC staining may be enhanced by perfusing the brains with TTC solution or at least with a flush of saline before staining; this may improve unsatisfying results, in particular when using a permanent ischemia model [30].
   (c) The second parameter which may be modified is the concentration of the TTC solution. Joshi and colleagues [35] describe improved delineation of the infarct by use of a 0.05% TTC solution for 2 mm thick slices.

References

1. Hossmann K-A (2008) Cerebral ischemia: models, methods and outcomes. Neuropharmacoloy 55:257–270
2. Baron J-C, Yamauchi H, Fujioka M et al (2014) Selective neuronal loss in ischemic stroke and cerebrovascular disease. J Cereb Blood Flow Metab 34:2–18
3. Astrup J, Symon L, Branston NM et al (1977) Cortical evoked potential and extracellular K^+ and H^+ at critical levels of brain ischemia. Stroke 8:51–57
4. Astrup J, Siesjö BK, Symon L (1981) Thresholds in cerebral ischemia – the ischemic penumbra. Stroke 12:723–725
5. Sharp FR, Lu A, Tang Y et al (2000) Multiple molecular penumbras after focal cerebral ischemia. J Cereb Blood Flow Metab 20:1011–1032
6. del Zoppo GJ, Sharp FR, Heiss W-D et al (2011) Heterogeneity in the penumbra. J Cereb Blood Flow Metab 31:1836–1851
7. Lo EH (2008) A new penumbra: transitioning from injury into repair after stroke. Nat Med 14:497–500
8. Zille M, Farr TD, Przesdzing I et al (2012) Visualizing cell death in experimental focal cerebral ischemia: promises, problems, and perspectives. J Cereb Blood Flow Metab 32:213–231
9. Brint S, Jacewicz M, Kiessling M et al (1988) Focal brain ischemia in the rat: methods for reproducible neocortical infarction using tandem occlusion of the distal middle cerebral and ipsilateral common carotid arteries. J Cereb Blood Flow Metab 8:474–485
10. Diemer NH (1982) Quantitative morphological studies of neuropathological changes. Part 1. Crit Rev Toxicol 10:215–263
11. Overgaard K, Meden P (2000) Influence of different fixation procedures on the quantification of infarction and oedema in a rat model of stroke. Neuropathol Appl Neurobiol 26:243–250
12. Osborne KA, Shigeno T, Balarsky AM et al (1987) Quantitative assessment of early brain damage in a rat model of focal cerebral ischemia. J Neurol Neurosurg Psychiatry 50:402–410
13. Swanson RA, Morton MT, Tsao-Wu G et al (1990) A semiautomated method for measuring brain infarct volume. J Cereb Blood Flow Metab 10:290–293
14. Schäbitz W-R, Kollmar R, Schwaninger M et al (2003) Neuroprotective effect of granulocyte-colony stimulating factor after focal cerebral ischemia. Stroke 34:745–751
15. Endres M, Ahmadi M, Kruman I et al (2005) Folate deficiency increases postischemic brain injury. Stroke 36:321–325
16. Vogel J, Möbius C, Kuschinsky W (1999) Early delineation of ischemic tissue in rat brain cryosections by high-contrast staining. Stroke 30:1134–1141
17. Dawson DA, Hallenbeck JM (1996) Acute focal ischemia-induced alterations in MAP2 immunostaining: description of temporal changes and utilization as a marker for volumetric assessment of acute brain injury. J Cereb Blood Flow Metab 16:170–174
18. Popp A, Jaenisch N, Witte OW et al (2009) Identification of ischemic regions in a rat model of stroke. PLoS ONE 4:e4764. doi:10.1371
19. Kloss CUA, Thomassen N, Fesl G et al (2002) Tissue-saving infarct volumetry using histochemistry validated by MRI in rat focal ischemia. Neurol Res 24:713–718
20. Tucker RP (1990) The role of microtubule-associated proteins in brain morphogenesis: a review. Brain Res Rev 15:101–120
21. Ejaz S, Williamson DJ, Ahmed T et al (2013) Characterizing infarction and selective neuronal loss following temporary focal cerebral ischemia in the rat: a multi-modality imaging study. Neurobiol Dis 51:120–132
22. Wolf HK, Buslei R, Schmidt-Kastner R et al (1996) NeuN: a useful neuronal marker for diagnostic histopathology. J Histochem Cytochem 44:1167–1171
23. Liu F, Schafer DP, McCullough LD (2009) TTC, Fluoro-Jade B and NeuN staining confirm evolving phases of infarction by middle cerebral artery occlusion. J Neurosci Methods 179:1–8
24. Lee DR, Helps SC, Gibbins IL et al (2003) Losses of NG2 and NeuN immunoreactivity but not astrocytic markers during early reperfusion following severe focal cerebral ischemia. Brain Res 989:221–230
25. Unal-Cevik I, Kilinç M, Gürsoy-Ozdemir Y et al (2004) Loss of NeuN immunoreactivity after cerebral ischemia does not indicate neuronal cell loss: a cautionary note. Brain Res 1015:169–174
26. Emmrich JV, Ejaz S, Neher JJ et al (2015) Regional distribution of selective neuronal loss and microglial activation across the MCA territory after transient focal ischemia: quantitative versus semiquantitative systematic immunohistochemical assessment. J Cereb Blood Flow Metab 35:20–27
27. Bederson JB, Pitts LH, Germano SM et al (1986) Evaluation of 2,3,5-triphenyltetrazolium

chloride as a stain for detection and quantification of experimental cerebral infarction in rats. Stroke 17:1304–1308

28. Goldlust EJ, Pacynski RP, He YY et al (1996) Automated measurement of infarct size with scanned images of triphenyltetrazolium chloride-stained rat brains. Stroke 27:1657–1662
29. Li F, Irie K, Anwer MS et al (1997) Delayed triphenyltetrazolium chloride staining remains useful for evaluating cerebral infarct volume in a rat stroke model. J Cereb Blood Flow Metab 17:1132–1135
30. Liszczak TM, Hedley-Whyte ET, Adams JF et al (1984) Limitations of tetrazolium salts in delineating infarcted brain. Acta Neuropathol 65:150–157
31. Liesz A, Suri-Payer E, Veltkamp C et al (2009) Regulatory T cells are key cerebroprotective immunomodulators in acute experimental stroke. Nat Med 15:192–199
32. Clark DL, Penner M, Orellana-Jordan IM et al (2008) Comparison of 12, 24 and 48 h of systemic hypothermia on outcome after permanent focal ischemia in rat. Exp Neurol 212:386–392
33. Hatfield RH, Mendelow AD, Perry RH et al (1991) Triphenyltetrazolium chloride (TTC) as a marker for ischaemic changes in rat brain following permanent middle cerebral artery occlusion. Neuropathol Appl Neurobiol 17:61–67
34. Isayama K, Pitts LH, Nishimura MC (1991) Evaluation of 2,3,5-triphenyltetrazolium chloride staining to delineate rat brain infarcts. Stroke 22:1394–1398
35. Joshi CN, Jain SK, Murthy PSR (2004) An optimized triphenyltetrazolium chloride method for identification of cerebral infarcts. Brain Res Brain Res Protoc 13:11–17

Chapter 17

Ethics of Modeling of Cerebral Ischemia in Small Animals

Ute Lindauer

Abstract

Animal models of cerebral ischemia have deepened our insight into the pathophysiology of ischemic brain damage. Success rates in translation to the bedside, however, are low. This fact entails unmet hopes for patients and ineffective deployment of money and time. It also highlights the important ethical issue of the quality of animal experiments in stroke research. Attention to this issue should start with the planning phase. This chapter will help researchers to design studies at a high ethical level and thus provide important arguments for obtaining permission from regulatory authorities.

Key words Animal experiments, ARRIVE, STAIR, Ethical consideration, 3Rs, Refinement, Reduction, Replacement, Burden, Pain, Euthanasia, Permission from authorities

1 Introduction

Important advances in human and animal medicine have been made by using animals in research. Animal models have provided us with deeper insight into the pathophysiology of ischemic brain damage, but so far, their contribution to clinical practice in stroke therapy has been limited. To date, only one therapy for acute ischemic stroke, tPA initiated within 3 h of stroke onset, has been approved [1]. However, there are many arguments explaining the failure to translate therapeutic benefit in animal stroke models into successful clinical trials. Very recently, an interesting debate on the usefulness of animal models of neurodegenerative diseases has been published in *Nature* (news feature [2] with comments [3, 4]) suggesting a more differentiated use of the term "animal model of disease X." Potential problems with animal studies for acute stroke therapies are discussed by Fisher and Tatlisumak [5], and detailed information can be found in this handbook in Chaps. 17–19. Poor success rates in the translation to bedside cause ineffective employment of money and time and, in the end, leave the patients alone with their unmet hopes of ameliorating their symptoms. In addition, unsuccessful translation from bench to bedside also raises an

Ulrich Dirnagl (ed.), *Rodent Models of Stroke*, Neuromethods, vol. 120,
DOI 10.1007/978-1-4939-5620-3_17,

important ethical issue when animals are used for stroke research (*see* **Note 1**). Consequently, close attention should already be given in the planning phase to the quality of animal experiments.

The approval of applications for permission to conduct animal research is based on national and international animal research laws and regulations. Those with broad validity for readers are listed in the following:

International regulation: Good laboratory practice (GLP). Compliance with GLP regulations is a critical requirement for certain types of research and testing involving laboratory animals. The principles of GLP deal mainly with responsibility, quality assurance, test facilities, and documentation.

USA: The Public Health Service issued the "Guide for the Care and Use of Laboratory Animals," which is the primary reference in the USA for animal care and use programs.

European Union: Directive 2010/63/EU of the European Parliament and of the Council of 22 September 2010 on the protection of animals used for scientific purposes.

National and institutional regulations may differ in many details; but some important aspects seem to be held in common. This chapter helps design studies on animal experiments in stroke research at a high ethical level and thus provides important arguments for obtaining permission from regulatory authorities.

2 General Standards as Prerequisite for Considering the Ethical Viewpoint

In order to reduce, refine, or replace animal experiments whenever possible; avoid or minimize discomfort, stress, and pain for the animal; and thus reduce suffering and burden within the experiment, the following principles should be observed [6–8].

2.1 Decision on the Model

Which model: cell culture/brain slice/in vivo. Important information on the pathophysiology of damage in stroke is revealed with cell culture or brain slice systems, but the actual interaction of different cell types within the brain, the vasculature, and the immune system is an essential aspect of the disease and can only be investigated in the living animal. The possibility of replacing animal experiments in stroke research is therefore very limited. As soon as the decision on the in vivo model is made, it has to be considered whether the specific question can be answered in acute (animals investigated under final anesthesia) or chronic experiments and whether the study aims mainly at advancing knowledge of pathophysiological aspects or at investigating new therapeutic concepts. Because new animal models may have been developed, a thorough literature search should always be conducted to determine what

models might be suitable, which models are the most relevant to the specific question, and which alternatives are available. An alternative is any procedure that reduces the number of animals used, refines techniques (to minimize pain and distress and/or to better model the disease), or replaces animals altogether (reduction, refinement, replacement: the so-called 3Rs defined in 1959 by Russell and Burch [9]).

2.2 Decision on the Animals

Only animals that are lawfully acquired are used for experiments. The selection of the appropriate species, strain, gender, age, quality, etc., has to be considered thoroughly. So far, in most experimental stroke studies in young adult, healthy male animals have been used. This may be appropriate if the main interest is in getting knowledge on specific pathophysiological aspects of the cause and progression of disease. However, in support of the very recent NIH initiative to balance the sex of cells and animals in preclinical research, it has been recommended to raise the awareness of sex as an important biological variable and to allow exceptions only in conditions dealing with specific questions [10]. In addition, when testing therapeutic options, it is highly recommended to perform studies on older animals of both sexes with a possible comorbidity (hypertension, diabetes), which would better resemble the patients' situation.

Decision on a specific model or species should not be based on availability, familiarity, or cost. The easily available, familiar, or inexpensive species may not necessarily provide the best conditions needed for the proposed project. Overall health status of the animals must be assessed because it can influence their response to the planned procedure.

On the basis of the expected standard deviation of the data of outcome measures, prior statistical testing for sample size provides important information on the number of animals needed to detect a certain (biologically relevant) difference between groups. Reducing the number of animals in a certain study is highly recommended; however, it has to be taken care that not too few animals are used. The lowering of the number of animals shall not lead to underpowered studies with the consequence of unreliable results and wasted animals [11].

2.3 Study Design

The allocation of the animals to the different study groups should be performed by randomization. The study should be conducted by an experimenter blinded to the treatment groups whenever possible. The question of what control groups are appropriate (vehicle, sham operation, naïve; do you need positive controls?) has to be considered in advance, because they will have to be included in the randomization process. No historical controls should be used. Standardization of the time of day planned for the procedure may be important in minimizing experimental variability in species with well-defined circadian rhythms (see also Chaps. 17 and 19).

2.4 Defining Handling Procedures and Animal Training

To avoid or minimize animal discomfort and stress during the experiments, the main handling procedures necessary before, during, and after surgery should be trained beforehand. Most experimental animals are accustomed to basic handling procedures due to regular cage changes. It has to be decided whether the animals have to be kept alone or in groups during the experiment. In principle, social species like rats or mice should not be kept alone; otherwise, good arguments have to be given and the animals should be trained to the new housing situation in advance. Stroke-operated mice can easily be kept in groups if all were operated at the same time; however they should not be grouped with healthy or unoperated animals.

2.5 Decision on Sedation, Analgesia, and Anesthesia

The use of appropriate sedation, analgesia, or anesthesia and of alternatives to painful or distressful procedures should be thoroughly considered. Surgical or other painful procedures must not be performed on unanesthetized animals. The use of paralytic agents in the absence of anesthetics during painful procedures is prohibited. Potential effects of anesthetic agents on study parameters have to be anticipated and minimized by choice of the best agent and its optimal dosage. To choose the appropriate agent for stroke studies, possible neuroprotective and cerebrovascular effects have to be considered; see also Chap. 10.

Analgesic agents should be given to prevent pain whenever it is likely to occur. In stroke research, pain from operation procedures and skin wounds should be primarily addressed because acute cerebral ischemia itself induces no pain, as is known from patients. In small animals such as rats and mice, suffering and pain cannot easily be ascertained. Most common unspecific signs are decreased activity, unusual body posture, unusually aggressive behavior, and an ungroomed appearance. In addition, the recently developed "rat grimace scale" can be used to quantify pain by thoroughly assessing facial expressions in rats and other rodents [12]. When individual animals show obvious signs of suffering, in most cases they are already experiencing severe pain. Analgesic agents should therefore not be given only to those animals displaying obvious signs but to any animal likely to be suffering.

To prevent pain from operation procedures and skin wounds unavoidable during stroke induction, local analgesia is strongly recommended during and after operation. For example, bupivacaine, a long-acting analog of lidocaine, in a dose of 0.1–0.3 mL, can be applied locally before closing the wound.

For systemic analgesia during procedures which may induce moderate to severe pain in small rodents, systemic application of buprenorphine is recommended. However, it also acts as a neuroprotectant, possibly interacting with pathophysiological aspects of stroke and thus with outcome parameters of the study.

Not only during the surgery but also within the first hours during the recovery phase after general anesthesia, body temperature has to be measured and kept within physiological range. Hypothermia—as well as hyperthermia—has to be prevented by placing the animals in a temperature-regulated recovery chamber for 2–3 h after surgery.

2.6 Support for Survival During the First Critical Days After Stroke

In studies with long-term survival after stroke, an effective protocol for supported feeding, diet supplementation, and antibiotics in the acute phase is strongly recommended. A high incidence of suffering and high death rates due to weight loss and infection [13] occur in the acute phase after stroke in mice at day 2–3, predominantly in stroke models of >30 min ischemia duration. Supported feeding and antibiotics prevent weight loss and infection. Gel food or soft food should be given to the animals in the first days after operation, possibly complemented by s.c. bolus application of glucose-enriched saline (maximal injection volume per injection side: 0.2–0.3 mL, up to 5–6 injection sides, total injection volume 1–2 mL per day).

2.7 Decision on Outcome Parameters and End Points

Establishing sound experimental end points in relation to the research subject is of fundamental importance for study success and for its possible translation into the clinical situation. The outcome parameters (infarct/lesion volume, outcome scores, tests on sensory performance and/or motor performance, behavior, etc.) must be determined as well as the time points for assessing them (see Chap. 15). Determination of the early lesion volume may be an appropriate parameter if the involvement of a specific molecular pathway is being investigated. However, it has been shown that conclusions drawn from (early) determination of infarct or lesion volumes often dissociate from results obtained by investigation of behavioral parameters assessed at later time points. Thus, if the study aims at the investigation of new therapeutic options rather than pure knowledge on pathophysiological aspects, it may be more appropriate to perform behavioral tests at advanced time points after stroke which are sensitive enough to detect residual deficits [14, 15] (see Chaps. 13 and 14).

A good supplement within an experimental stroke protocol in small animals may also be the repetitive application of modern noninvasive imaging techniques such as diffusion/perfusion magnetic resonance imaging (MRI) [16] or molecular imaging modalities [17] to evaluate the temporal and spatial evolution of ischemic brain injury. These techniques can then be adapted to evaluate the same characteristics in stroke patients and better direct them to specific therapeutic options.

2.8 Cancelation of Experiments: Criteria for Euthanasia of Severely Suffering Animals

Even under best conditions it cannot be totally avoided that individual animals suffer severely during the experiment. Regular inspection of the animals under investigation by an experienced person (the experimenter) is mandatory (time interval depends on

the model; at least 1–2*x*/day is recommended during the first days after stroke induction). For situations in which an individual animal shows unusual and/or conspicuous behavior, an intelligible catalogue of measures should be available to the housing personnel to ensure that the experimenter is quickly informed and/or that the personnel intervene correctly (in worst case with euthanasia). From this catalogue, a score sheet may be developed to ease documentation and decision making. The catalogue and score sheet should be prepared in advance and attached to the application for permission from the authorities. A suggestion for a catalogue of measures adapted to the situation of experimental ischemia models in mice and rats is provided in Table 1 (see Table 1).

2.9 Euthanasia Techniques

Euthanasia techniques should result in rapid unconsciousness followed by cardiac or respiratory arrest and ultimate loss of brain function (*see* **Note 2**). In addition, the technique should minimize any stress and anxiety experienced by the animal prior to unconsciousness [6]. While deciding on the right procedure, the recommendations of the institution where the experiments are performed should be followed. In many institutions, efforts are being undertaken to prohibit CO_2 or CO inhalation as a means of euthanasia because shortage of oxygen causes severe stress for the still conscious animal. For the EU, within the Directive 2010/63/EU of the European Parliament and of the Council, the methods of killing animals are clearly described and exceptions are only allowed if thoroughly justified.

2.10 Provision of Professional Housing and Husbandry

Appropriate animal housing and husbandry, approved by the authorities and directed and performed by qualified personnel, has to be made available. Early in the planning process, the person responsible for housing and maintenance of animals at the institution where the experiments are to be performed should be consulted to determine if sufficient facilities and space are available to accommodate the project. Acclimatization time of at least 1 week should be provided for the animals to become accustomed to the new housing conditions during the experiment. The appropriate enrichment of the animals' environment within the cage should be selected to provide them maximal comfort without influencing stroke pathophysiology or outcome and without increasing variation in the data [18] (see also Chap. 8).

2.11 Qualifications of the Experimenter

Experimentation on living animals may only be conducted by or under the close supervision of qualified and experienced persons. Regulations in most European countries stipulate that this person previously attended a certified course on experimentation on living animals. The course content must comply with the recommendations of the Federation of European Laboratory Animal Science Associations (FELASA recommendations) for the education and

Table 1

General instructions for care personnel for clinical examination of research animals in cerebral ischemia experiments

Symptom	Instruction
Please pay attention to the following symptoms and follow the instructions	
1. Daily control of the animal within the cage	
Isolation	**a**
Scrubby fur	**a**
Blown-up belly	**a**
Intensified/reduced or shallow breathing, hyper-/hypoventilation	**a**
Diarrhea	**b**
Gasping	**b**
Brief convulsion **Epileptic seizures >5 minutes, status epilepticus**	**b** **c**
Obvious signs of **pain** (posture, mimic, behavior)	**b–c**
Paleness (eyes, ears, skin)	**b**
Blood at the eyes, mouth, anus, etc.	**b**
Reeling and apathia	**b**
Inability to stand or move, loss of postural reflexes due to infarct development (Bederson score 3)	**c**
2. During change of cages	
Injury or change in the skin	**a**
Teeth anomalies	**a**
Animal avoids moving	**a**
Apathia	**a**
Signs of pain when being touched	**a/b**
Swelling, neoplasia	**a/b**
Tense belly	**a/b**
Signs of exsiccosis (**skin fold test**: fold does not resolve)	**b**
3. During weighing	
Acute reduction >10% of body weight	**a/b**
Acute reduction 20% of body weight	**b/c**

Instructions

a Only one symptom: further observation of the animal in combination with other symptoms of (a): call the principal investigator/the veterinarian

b **Call the principal investigator/veterinarian**; in combination with reeling, obvious pain, paleness, blood: **euthanasia**

c **Call the principal investigator/veterinarian**: **immediate euthanasia**

(These instructions comply with recommendations of the "Arbeitskreis Berliner Tierschutzbeauftragter" for advance euthanasia of severely suffering research animals. Forschungseinrichtung für Experimentelle Medizin, Krahmerstraße 6, D-12207 Berlin, Germany, 1997; modified for the specific demands of stroke research in rodents)

training of persons carrying out animal experiments (Category B) [19]. Experience in experimentation on living animals in general and in a specific experimental model reduces invasiveness during operation, significantly decreases anesthesia and operation time, and thus minimizes pain and suffering for the animal under investigation.

The animal model chosen should be discussed with an experienced individual (identified, for instance, through publications or Internet inquiry) if the investigator is not personally familiar with the model. Site visits at the laboratory of an experienced investigator may be very helpful to successfully establish a new animal model. Discussions with someone familiar with the model can provide very helpful information and advice that cannot be found in any publication.

3 Ethical Considerations

The principal ethical decision is based on the weight of the burden for animals against the benefit for humans. In the following two paragraphs, suggestions are provided to correctly estimate the burden for rats and mice in common ischemia models, on the one hand, and the benefit for humans/society, on the other.

3.1 Burden for Animals

On the side of the animals, an integrated assessment of all periods of stress, pain, and discomfort due to handling, operation, substance administration, and/or behavioral testing should be performed, resulting in a classification of the overall amount of suffering throughout the experiment (no burden to mild burden to moderate burden to severe burden) in relation to its duration (*see* **Note 3**).

Table 2 presents an exemplary assessment of burden in a typical stroke study in mice.

3.2 Expected Benefit for Humans

On the side of the humans, expected advantages have to be listed. Important arguments may be:

- More knowledge of pathways of lesion volume progression which generate or enrich ideas for new strategies for therapy especially at later time windows.
- Testing of new diagnostics or new concepts or new substance classes for therapy aiming at the decrease of suffering or at the decrease of death rates in humans.
- By developing new therapeutics, the rate and severity of stroke-induced lifelong disability can be reduced.
- The ethical consideration may be introduced by epidemiological data on numbers of newly diseased patients per year and their outcomes (rate of disability, death) to put emphasis on the side of burden for human individuals and the society.

Table 2

Assessment of burden in an exemplary study

Procedure[a]	Remark	Burden
MCAO by filament model in isoflurane anesthesia and local application of bupivacaine to the operation site; occlusion time 60 min	As known from patients, stroke itself does not induce pain; pain is only induced by the operation wound, which is postoperatively reduced by local application of analgesics. During the first days, food and water intake is restricted and activity is reduced due to the invasiveness of the operation. The animals very easily cope with the sensory and motor impairments induced by MCAO (see also Bederson score)	Day 0–3: mild to moderate >3 days: no burden
Bederson score once daily at day 0–5	The animals are used to the necessary handling during testing; on an average a score of 1–2 is achieved, indicating only mild impairment which does not prevent the animals from normal behavior (eating and drinking, grooming, locomotion, and social interaction)	Mild burden
Body temperature control, injections: s.c. glucose and saline and i.p. antibiotics (every 12 h) until day 3	Insertion of the temperature probe: mild burden; s.c. and i.p. injections twice a day for 3 days performed by the experienced experimenter induce only a very brief pain at the injection site (*see* **Note 4** for longer injection periods)	Mild burden
DW/T2-MRI in isoflurane anesthesia at 3, 6, and 24 h and 3, 7, and 21 days after ischemia	The imaging procedure is performed under anesthesia; therefore, the animals only very mildly suffer from the repeated handling and administration of isoflurane anesthesia	Mild burden on selected days
Functional outcome measured 14–21 days after ischemia by three tests (sucrose consumption test, wire grip test, pole test)	The three tests only induce mild stress to the animals, which are used to the necessary handling	Mild burden
Testing of the anti-inflammatory substance X against saline as vehicle (starting 6 h after reperfusion, i.p. injection once a day for 3 days)	i.p. injections once a day for only a few days performed by the experienced experimenter induce only a very brief pain at the injection site. It must be guaranteed that the test substances do not induce local irritation and have no side effects	Mild burden
Day 21: sacrifice of the animals in deep anesthesia, removal of the brain for further analysis	Performed in deep anesthesia	No burden
Overall assessment: mild throughout the study period of 3 weeks with a slightly higher—but at the most—moderate suffering during the acute phase after MCAO		

[a]All procedures performed by an experienced experimenter

3.3 Ethical Decision

For most stroke studies using rats or mice and designed according to the exemplary study described in Table 2, the weight of burden for the animals against the benefit for the individual human and for society results in the decision that the planned study is ethically justified.

4 Recommendations by the Stroke Therapy Academic Industry Roundtable (STAIR)

In addition to the above-described general standards that should be followed, further recommendations were compiled by the stroke therapy academic industry roundtable, referred to as "STAIR recommendations," first documented in 1999 [20] and further updated in 2009 [21]. Besides recommendations to improve the quality and validity of preclinical studies, the chance for translational success for neuroprotective strategies should further be enhanced by showing efficacy in two or more laboratories and replication in a second species.

5 Quality of Reporting Animal Research: The ARRIVE Guidelines

The failure of success in translating the results of preclinical research into the clinical situation has many reasons. The lack of transparency in reporting animal research in biomedical journals has been identified as one possible factor. Without detailed report on how the experiments have been performed and how the data have been analyzed, a peer review process is almost impossible, and further experiments build on the reported results are highly speculative. The report should therefore provide reliable and valid information for other investigators to judge the biological relevance of the study, to design further studies based on the results, and also to make it possible to repeat the experiments. For standardization of the reporting, guidelines have been developed by an international consortium. These guidelines are referred to as "ARRIVE—Animals in Research: Reporting In Vivo Experiments" and have been published in 2010 [22] and since then implemented in the "Author Guidelines" of many biomedical journals. Working in line with ARRIVE will, at its best, not only improve the reporting of animal experiments already performed but, if considered in advance in the planning phase of the experiments, improve the design and by this the reliability, validity, and relevance of the study.

6 Notes

1. Avoidance or minimization of discomfort, distress, and pain is not only an issue of ethics but also an issue of reasonable results.
2. It is absolutely necessary to verify death after euthanasia and before disposal of the animal. An animal in deep narcosis may eventually recover! Death should be confirmed by examining the animal for cessation of vital signs. Professional judgment taking into consideration the animal species and method of euthanasia should be exercised to determine the most appropriate means of confirming death.
3. Assessment of burden: As an example, 10 days of five interventions, each inducing mild suffering if assessed alone, will result in a summed amount of moderate suffering, because the interventions cannot be judged in isolation.
4. Repeated systemic injections necessary: If the experimental protocol demands longer periods of systemic injections, the implantation of infusion pumps (e.g., Alzet® osmotic pumps from Charles River Labs) is strongly recommended.

References

1. Kaste M (2005) Use of animal models has not contributed to development of acute stroke therapies: pro. Stroke 36:2323–2324
2. Schnabel J (2008) News feature: standard model. Nature 454:682–685
3. Suckling K (2008) Opinion: animal research: too much faith in models clouds judgement. Nature 455:460
4. Green S (2008) Opinion: animal research: raise standards to protect patients. Nature 455:460
5. Fisher M, Tatlisumak T (2005) Use of animal models has not contributed to development of acute stroke therapies: con. Stroke 36:2324–2325
6. Wright KC (1997) Working with laboratory animals: general principles and practical considerations. J Vasc Interv Radiol 8:363–373
7. American Physiological Society (2002) Guiding principles for research involving animals and human beings. Am J Physiol Regul Integr Comp Physiol 283:R281–R283
8. Festing MFW (2003) Principles: the need for better experimental design. Trends Pharmacol Sci 24:341–345
9. Russell WMS, Burch RL (1959) The principles of humane experimental technique. Methuen, London
10. Sandberg K, Umans JG, Georgetown Consensus Conference Work Group (2015) Recommendations concerning the new U.S. National Institutes of Health initiative to balance the sex of cells and animals in preclinical research. FASEB J 29:1646–1652
11. Cressey D (2015) News in focus: UK funders demand strong statistics for animal studies. Nature 520:271–272
12. Sotocinal SG, Sorge RE, Zaloum A, Tuttle AH, Martin LJ, Wieskopf JS, Mapplebeck JC, Wei P, Zhan S, Zhang S, McDougall JJ, King OD, Mogil JS (2011) The rat grimace scale: a partially automated method for quantifying pain in the laboratory rat via facial expressions. Mol Pain 7:55
13. Meisel C, Prass K, Braun J, Victorov I, Wolf T, Megow D, Halle E, Volk HD, Dirnagl U, Meisel A (2004) Preventive antibacterial treatment improves the general medical and neurological outcome in a mouse model of stroke. Stroke 35:2–6
14. Corbett D, Nurse S (1998) The problem of assessing effective neuroprotection in experimental cerebral ischemia. Prog Neurobiol 54:531–548
15. Cenci MA, Whishaw IQ, Schallert T (2002) Animal models of neurological deficits: how relevant is the rat? Nat Rev Neurosci 3:574–579
16. Meng X, Fisher M, Shen Q, Sotak CH, Duong TQ (2004) Characterizing the diffusion/perfusion mismatch in a rat stroke model of focal cerebral ischemia. Ann Neurol 55:207–212

17. Klohs J, Gräfe M, Graf K, Steinbrink J, Dietrich T, Stibenz D, Bahmani P, Kronenberg G, Harms C, Endres M, Lindauer U, Greger K, Stelzer EHK, Dirnagl U, Wunder A (2008) In vivo imaging of the inflammatory receptor CD40 after cerebral ischemia using a fluorescent antibody. Stroke 39:2845–2852
18. Würbel H, Garner JP (2007) Refinement of rodent research through environmental enrichment and systematic randomization. NC3Rs #9:1–9
19. Nevalainen TC, Dontas I, Forslid A, Howard BR, Klusa V, Käsermann HP, Melloni E, Nebendahl K, Stafleu FR, Vergara P, Verstegen J (2000) FELASA recommendations for the education and training of persons carrying out animal experiments (Category B). FELASA working group on education of persons carrying out animal experiments. Lab Anim 34:229–235
20. Stroke Therapy Academic Industry Roundtable STAIR (1999) Recommendations for standards regarding preclinical neuroprotective and restorative drug development. Stroke 30:2752–2758
21. Fisher M1, Feuerstein G, Howells DW, Hurn PD, Kent TA, Savitz SI, Lo EH, STAIR Group (2009) Update of the stroke therapy academic industry roundtable preclinical recommendations. Stroke 40:2244–2250
22. Kilkenny C, Browne WJ, Cuthill IC, Emerson M, Altman DG (2010) Improving bioscience research reporting: the ARRIVE guidelines for reporting animal research. PLoS Biol 8:e1000412

Chapter 18

Quality Control and Standard Operating Procedures

Ulrich Dirnagl

Abstract

Recently, systematic reviews have found quantitative evidence that low study quality may have introduced a bias into preclinical stroke research. Monitoring, auditing, and standard operating procedures (SOPs) are already key elements of quality control in randomized clinical trials and will hopefully be widely adopted by preclinical stroke research in the near future. Increasingly, funding bodies and review boards overseeing animal experiments are taking a proactive stance and demand auditable quality control measures in preclinical research. Every good quality control system is based on its SOPs. This chapter introduces the concept of quality control by using SOPs and provides practical advice on how to write them for experimental stroke research. Write down what you do; do what is written down!

Key words Accreditation, Auditing, Certification, Good clinical practice, Good laboratory practice, Monitoring, Quality control, Standard operating procedures

1 Introduction

Thus far, the translation of promising results from preclinical stroke research into effective clinical therapy has not met with success [1]. A straightforward explanation for the almost 100% attrition rate for the preclinical to clinical transition in stroke could be that rodent models of stroke are simply not predictive for humans. In a recent article, however, we have collected evidence that this is actually not the case: Preclinical stroke research predicts human pathophysiology, clinical phenotypes, and therapeutic outcomes [2]. Among the numerous alternative reasons for this high failure rate, quality problems in some of the basic research or preclinical studies have to be considered. False-positive results, inflated effect sizes, and marginal reproducibility may have overestimated or even affected the potential of novel stroke therapeutics [3]. Systematic reviews have found quantitative evidence that low study quality may have introduced a bias into preclinical stroke research [3–6] (see Chap. 2). As opposed to many other causes of the "translational roadblock," study quality is fully under the control of the researcher and thus a prime target for improvement.

Ulrich Dirnagl (ed.), *Rodent Models of Stroke*, Neuromethods, vol. 120,
DOI 10.1007/978-1-4939-5620-3_18,

Increasingly, funding bodies and review boards overseeing animal experiments are taking a proactive stance and demand auditable measures of quality control in preclinical research [7–9]. The Stroke Treatment Academic Industry Roundtable (STAIR) recently updated its recommendations for the evaluation of preclinical data on neuroprotective drugs [10] to include good laboratory practice (GLP) issues [11].

Monitoring, auditing, and standard operating procedures (SOPs) are key elements of quality control in randomized clinical trials (RCTs). It has been proposed that experimental stroke research adapt some of the tools used in clinical stroke research. In particular, stroke laboratories should set up and publish their SOPs (e.g., on their institutional websites) and guarantee that their studies adhere to these standards [12, 13]. This is all the more important, as a certain portion of their experiments, evaluations, etc. are not performed by professionals but rather by students in training who are unaware of these issues.

Write down what you do; do what is written down! It is the aim of this chapter to introduce the concept of using SOPs to improve quality control in experimental stroke research and to provide practical advice on how to write them.

2 The Concepts

Every good quality control system is based on its standard operating procedures (SOPs). SOPs are defined by the International Conference on Harmonisation (ICH) as "detailed, written instructions to achieve uniformity of the performance of a specific function." They are necessary for a preclinical research organization—be it a pharmaceutical company, a contract research organization, academic laboratory, internal review board, funding organization, or any other party involved in preclinical research—striving to achieve maximum transparency, reproducibility, robustness, and efficiency in its preclinical research operations.

Good clinical practice (GCP) is an international ethical and scientific quality standard for designing, conducting, recording, and reporting trials that involve the participation of human subjects. Compliance with this standard provides public assurance that the rights, safety, and well-being of trial subjects are protected in accordance with the principles of the Declaration of Helsinki and that the clinical trial data are credible. Important instruments of GCP are SOPs and auditing.

Good laboratory practice (GLP) embodies a set of principles that provides a framework within which laboratory studies are planned, performed, monitored, recorded, reported, and archived. It is essentially a general attitude that becomes an attitude toward work. It is about the way in which research is planned and

conducted, the results are recorded and reported, and the fruits of research are disseminated, applied, and exploited. GLP allows ready verification of the quality and integrity of research data, provides a transparent basis for investigating allegations of bad practice or fraud, and leads to better research.

A *standard operating procedure (SOP)* is a set of instructions with the force of a directive covering those features of operations that lend themselves to a definite or standardized procedure without loss of effectiveness.

Auditing is the process by which an external certification body (external audit) or internal staff trained for this process (internal audit) regularly reviews, assesses, and verifies that the GCP/GLP is working as it is supposed to. Audits can and should point out where practices can be improved to correct or prevent problems identified. Auditing requires the audited laboratory to (1) describe the laboratory process, to (2) produce a reference to procedure manuals, and to (3) exhibit evidence in documented records. SOPs are the backbone of this process.

Certification and accreditation: Certification ensures, through certification standards, that a laboratory provides the minimum essential knowledge and skills needed to achieve predefined outcomes. Certified laboratories must successfully analyze testing samples annually, use approved methods, and successfully pass periodic on-site audits. Organizational certification, e.g., by a professional society, is usually referred to as accreditation. Certification and accreditation bodies can issue standards for quality management conforming to the International Organization for Standardization (ISO) family of standards ISO 9000. The ISO 9000 is a set of procedures that cover all key processes in the field: monitoring processes to ensure they are effective; keeping adequate records; checking output for defects with appropriate and corrective action where necessary; regularly reviewing individual processes and the quality system itself for effectiveness; and facilitating continual improvement.

3 Writing SOPs

The primary purpose of an SOP in experimental stroke research is to guide and standardize working procedures in order to ensure data reliability and integrity. It is crucial that researchers, students, and technicians read and follow the SOPs. If this is not the case, SOPs will not only fail to achieve their goal; they will also engender a false sense of security. Failures are often due to technical shortcomings in the SOPs themselves. SOPs should be written by the user, as they must convey a clear instruction. The user must not only understand the instruction but also be prepared to carry it out.

3.1 An SOP Should Have

1. A descriptive title
2. A clear and concise header block to ensure a procedure communicates the purpose and scope
3. The date on which the SOP became operative
4. Clear delineation of responsibilities and identification of who does what
5. Key term definitions to avoid confusion
6. Measures of effectiveness to quantify outcomes
7. References to related documents to improve usability
8. Listing of applicable laws or regulations which require user compliance
9. Detailed list of revisions to track edit history
10. Forms to ensure proper control and record keeping
11. The signature of the person responsible for writing the SOP
12. The signature of the person responsible for authorizing the SOP

3.2 When Writing an SOP, You Should Focus On

1. *Context*. Actions must properly describe the activity to be performed.
2. *Consistency*. All references and terms are used the same way every time, and the procedure must ensure consistent results.
3. *Completeness*. There must be no gaps in information, logic, or design.
4. *Control*. The document and its described actions demonstrate feedback and controlling.
5. *Correctness*. The document must be grammatically correct without spelling errors.
6. *Clarity*. Documents must be easy to read and understandable.

After being authorized, the SOP needs to be distributed and archived. Most importantly, all staff members involved need adequate training on the SOPs!

SOPs need to be regularly reviewed and updated to ensure that they encourage efficient working practices that comply with the ever-increasing requirements, improvements, and modifications in models and experimental procedures. When mistakes are found in an SOP, or when procedures have changed, SOPs need to be updated.

4 Limitations of SOPs

SOPs are a powerful tool for controlling research activities, assuring data reliability, and improving the reproducibility and robustness of preclinical findings, but like any tool, they are subject to limitations.

4.1 SOPs

1. Cannot and should not replace training and opportunities for dialogue
2. Cannot deal with exceptional circumstances
3. May restrict the exercise of professional judgment
4. May curb an inquisitive and probing spirit and thus the scientific process in general

The last point is one of the most frequent objections to the use of SOPs in basic and preclinical research. However, it should be noted that SOPs are usually not meant to guide the search for new models or procedures. Rather, they ensure that established procedures can be faithfully repeated and their results reproduced internally as well as by other laboratories (externally).

5 Sample SOP for Middle Cerebral Artery Occlusion (MCAO), as Used in the Department of Experimental Neurology, Center for Stroke Research Berlin

Title	Middle cerebral artery occlusion (MCAO) in the mouse (intraluminal suture)
Date	Version 4: 04.08.2015
Version history	Version 1: 28.07.2009 Version 2: 17.8.2010 Version 3: 12.7.2011
Names of authors	Ulrich Dirnagl, Odilo Engel, Karen Gertz, Tracy Farr, André Rex
Purpose	Experimental induction of focal cerebral ischemia after occlusion of the middle cerebral artery in mice
Scope and applicability	Applies to a procedure in a standard lab equipped and certified for in vivo experimentation in mice (including anesthesia with volatile anesthetics). Experimental procedures require approval by the relevant committees
Introduction	Experimental focal ischemia is most commonly studied after permanent or transient occlusion of the middle cerebral artery (MCA) in rodents. Proximal MCA occlusion can be induced by an intraluminal suture (the so-called filament model) and causes injury to cortex and deeper brain structures (striatum). Distal MCA occlusion (the so-called "Brint" or "Tamura" models) is usually produced by placing a vascular clip on a pial vessel or by cautery. Distal occlusion typically spares the striatum and primarily involves the neocortex. Pannecrosis develops in the territory supplied by the respective artery with glial and endothelial cell death. If recirculation is established early (2 h or less), the outcome is better (transient MCA occlusion). In some ways, the reperfused brain imitates restoration of blood flow after spontaneous lysis of a thromboembolic clot in humans, even though reperfusion after clot lysis is certainly more complex than an on-off phenomenon as modeled by placement and retraction of an intravascular filament This SOP describes a mouse model of transient proximal MCAO (30–60 min occlusion time)

(continued)

(continued)

Title	Middle cerebral artery occlusion (MCAO) in the mouse (intraluminal suture)
References	Carmichael, S.T. (2005) Rodent models of focal stroke: size, mechanism, and purpose *NeuroRx.* **2(3)**, 396-409. Review Dirnagl, U. (2006) Bench to bedside: The quest for quality in experimental stroke research *J Cereb Blood Flow Metab* **26,** 1465-78 Dirnagl, U., Iadecola, C., Moskowitz, M.A. (1999) Pathobiology of ischaemic stroke: an integrated view *Trends Neurosci.* 22(9), 391-7 Engel O, Kolodziej S, Dirnagl U, Prinz V (2011) Modeling Stroke in Mice - Middle Cerebral Artery Occlusion with the Filament Model. J Vis Exp:e2423 Shah, Z.A., Namiranian, K., Klaus, J., Kibler, K., Dore, S. (2006) Use of an optimized transient occlusion of the middle cerebral artery protocol for the mouse stroke model *J Stroke Cerebrovasc Dis.* **15,** 133-8
Materials Instrumentation	• Ready coated filaments, e.g., Doccol® • Or 8.0 nylon monofilament for coating • Filament USP 4/0 or 6/0 Suprama • Surgical needle and thread for suture • Dissecting microscope (max. × 40) • Temperature feedback-controlled heating plate • Surgical instruments • Forceps (Dumont Medical #5 straight tip 0.05 mm × 0.02 mm) • Surgical scissors (skin cut) • Forceps for skin handling and suture (e.g., standard anatomical) • Vascular spring scissors (Vannas) • Two hemostats (Hartmann) • Microvascular clamp (e.g., S&G B1-V) and applying forceps • Needle holder (Olsen-Hegar or others) • Anesthesia system for isoflurane and nitrous oxide • Heated recovery cage
Cautions	Maintain a body temperature of 36.5 +/- 0.5 °C during occlusion and after reperfusion (for 2 h) Ensure proper pain relief in the perioperative and postoperative period, e.g., by repeated topical application of a long-acting local anesthetic, like bupivacaine ointment serving as an absorption depot For specific details, see maximizing animal welfare in experimental rodent stroke SOP Surgical procedures should be carried out under clean conditions (sterile surgical instruments and materials, clean gown, gloves, etc.). See aseptic technique and anesthesia SOP and Appendix below
Personnel qualifications	In general, surgeons need: • General supervision and instruction • The appropriate certification • Official registration/approval by appropriate authorities
Names of SOP Reviewers	Ulrich Dirnagl (ulrich.dirnagl@charite.de) André Rex (andre.rex@charite.de) Berlin, 20.08.2015

(continued)

(continued)

Title	Middle cerebral artery occlusion (MCAO) in the mouse (intraluminal suture)
Protocol	**General: Please follow maximizing animal welfare in experimental rodent stroke SOP and aseptic technique and anesthesia SOP** 1. Mice are anesthetized with 1.5% isoflurane and maintained in 1.0% isoflurane with 2/3 N_2O and 1/3 O_2. For additional analgesic treatment, follow the maximizing animal welfare in experimental rodent stroke SOP 2. Use any noninvasive physiological monitoring available locally (e.g., laser Doppler) 3. Maintain body temperature at 36–37.5 °C 4. Shave the fur and disinfect the skin of the ventral neck and place the mouse in supine position **MCAO Surgery:** 5. The left MCA will be occluded. Right MCA occlusion is also permitted. Left or right must be defined in advance and reported with your data. Reasons to change sides could be planned behavioral experiments to determine functional outcome more robustly, like paw preference or the handedness of the surgeon 6. A midline neck incision is made and the soft tissues are pulled apart 7. The common carotid artery (CCA) is carefully dissected free from the surrounding nerves (without harming the vagus nerve), and a ligature is made using 6.0/7.0 suture thread 8. Then the left external carotid artery (LECA) is separated, and a loose thread (6.0/7.0) is looped around it above the occipital artery bifurcation and secured externally with a pair of hemostats 9. Next, the left internal carotid artery (LICA) is isolated and a knot is prepared with 6.0 suture thread 10. After obtaining a good view of the left internal carotid artery (LICA) and the left pterygopalatine artery (LPA), the LICA is clipped 11. A small hole is cut in the LCCA before it bifurcates to the LECA and the LICA 12. A Doccol® filament or a local alternative such as a monofilament made of 8.0 nylon coated with silicon hardener mixture is then introduced into the artery. Doccol® filaments should be disinfected with 70% ethanol or sterilized with ethylene oxide 13. The clipped arteries are opened while the filament is inserted about 9 mm into the LICA to occlude LMCA 14. The third knot on the LICA is closed to fix the filament in position and the thread around the LECA is removed 15. Ischemia is confirmed by laser Doppler flowmetry, by MRI, or by withdrawing GA and checking for neurological deficit according to local protocols, like circling behavior during occlusion time and twisting of the mice when held by the tail 16. The mice are allowed to recover in the heated recovery cage at thermoneutral temperature (30–31 °C) for the duration of the MCA occlusion 17. After X min/hours of occlusion, the mice are re-anesthetized, and the third knot is opened and the filament withdrawn (if reperfusion is intended) 18. The common carotid artery is then permanently ligated 19. Release the ligature on the ECA 20. The remaining sutures are cut and the skin is adapted with a surgical suture 21. Rehydration and pain relief. Refer to the maximizing animal welfare in experimental rodent stroke SOP and follow one of the recommended protocols **Sham procedure:** For sham operations, the filament is inserted to occlude the MCA and withdrawn immediately to allow instant reperfusion (12). The subsequent operation is identical to the animals undergoing cerebral ischemia (13–21) A video is available which demonstrates the above described procedure (see references)

6 Appendix to SOP

1. Entry qualification experiment for mouse MCAO surgeons
2. Randomized selection of animals from cage and concealment of treatment allocation
   2a. Pharmacological study
   2b. Genetically manipulated animals
3. Temperature control
4. Outcome assessment
5. Physiological parameters
6. Quasi-sterile surgery

1. Entry qualification experiment for mouse MCAO surgeons

New surgeons need to demonstrate in a series of experiments that they perform the MCAO operation within 15 min. Reproducibility is verified by induction of a certain infarct volume within a standard deviation of 40%. Mortality must not exceed 10% within 24 h.

2. Randomized selection of animals from cage and concealment of treatment allocation

2a. Pharmacological study:

Animals in cage are marked with bar/dot code at the beginning of the procedure. Computer program (random number generator) selects an animal and assigns it to the concealed treatment arm ("A," "B," etc.).

Stock solution or pharmaceutical ready for application is prepared by assistant and randomly assigned code ("A," "B," etc.).

2b. Genetically manipulated animals:

Animals in both cages (e.g., knockout/wild type) are marked with bar/dot code at the beginning of the procedure. Computer program (random number generator) selects an animal and assigns it to the concealed experimental arm ("A," "B," etc.), blinded intervention whenever possible.

3. Temperature control

The body temperature of mice during surgery is maintained at 36.5 °C ± 0.5 °C using a temperature-controlled heating plate. Maintain a body temperature of 36.5 +/- 0.5 °C also after reperfusion (for 2 h) using a heated recovery box set at thermoneutral temperature (30–31 °C).

4. Outcome assessment

Infarct volume should be evaluated blinded. Functional outcome (*more than Bederson Score!*) should be assessed as well. Mortality and exclusion of animals have to be reported, including specific causes for exclusion.

For exclusion, follow the inclusion exclusion criteria SOP.

Main criteria:

no stroke, indicated by absence of functional deficit like circling behavior during occlusion time, insufficient Doppler flow reduction or missing functional deficit or missing infarct in MRI at 24 h after MCAo

Problems during induction of MCAo (excessive bleeding, prolonged operation time ≥15 min, thread placement).

CAVE:

Especially in genetically manipulated animals, be aware of vascular alterations, which might directly affect stroke outcome.

5. Physiological parameters

MABP, HR, blood gases, and CBF should be measured in selected animals.

6. Quasi-sterile surgery

Prior to surgery, the surgeon has to scrub his hands. It is advisable to wear clean gown and non-sterile gloves at all times the animal is being handled. The surgeon has to wear a clean gown, cap, and mask during surgery. Surgical gloves ought to be worn. If gloves cannot be used, a surgical hand scrub from tips to elbows must precede every operation.

The necessary components of aseptic techniques in rodents include also sterile instruments and separate surgical and animal prep areas. The use of glass bead sterilizer for re-sterilization of instruments during repetitive procedures is recommended.

- All instruments used must be sterilized prior to each group of surgeries.
- Instruments must be kept on sterile nonporous drapes during use.
- Separate instruments should be used for skin and tissue handling.
- Instruments must be cleaned of blood and debris by brushing or wiping with sterile water or saline and sterile gauze sponges between surgeries (best cleaned with distilled water).
- If contamination has occurred, instruments must be placed in 70% ethanol or a glass bead sterilizer for the appropriate period of time for the method used to be effective (or the instrument pack replaced by a new sterile instrument pack) between animals.
- If 70% ethanol is used, instruments must be rinsed with sterile water or saline before being used on the next animal.
- Surgical gloves and blades should be changed after contamination.

- Following surgery, all instruments must be thoroughly cleaned and rinsed.

7. Postoperative care:

Please see maximizing animal welfare in experimental rodent stroke SOP.

References

1. Endres M, Engelhardt B, Koistinaho J, Lindvall O, Meairs S, Mohr JP, Planas A, Rothwell N, Schwaninger M, Schwab ME, Vivien D, Wieloch T, Dirnagl U (2008) Improving outcome after stroke: overcoming the translational roadblock. Cerebrovasc Dis 25:268–278
2. Dirnagl U, Endres M (2014) Found in translation - preclinical stroke research predicts human pathophysiology, clinical phenotypes, and therapeutic outcomes. Stroke 45:1510–1518
3. Dirnagl U, Macleod MR (2009) Stroke research at a road block: the streets from adversity should be paved with meta-analysis and good laboratory practice. Br J Pharmacol 157:1154–1156
4. Bath PMW, Gray LJ, Bath AJG, Buchan A, Miyata T, Green AR, on behalf of the NXY-059 Efficacy Meta-analysis in individual Animals with Stroke (NEMAS) investigators (2009) Effects of NXY-059 in experimental stroke: an individual animal meta-analysis. Br J Pharmacol 157:1157–1715
5. Crossley NA, Sena E, Goehler J, Horn J, van der Worp B, Bath PM, Macleod M, Dirnagl U (2008) Empirical evidence of bias in the design of experimental stroke studies: a meta-epidemiological approach. Stroke 39(3):929–934
6. Macleod MR, van der Worp HB, Sena ES, Howells DW, Dirnagl U, Donnan GA (2008) Evidence for the efficacy of NXY-059 in experimental focal cerebral ischaemia is confounded by study quality. Stroke 39:2824–2829
7. Begley CG, Ioannidis JP (2015) Reproducibility in science: improving the standard for basic and preclinical research. Circ Res 116:116–126
8. Macleod MR, Lawson McLean A, Kyriakopoulou A, Serghiou S, de Wilde A, Sherratt N, Hirst T, Hemblade R, Bahor Z, Nunes-Fonseca C, Potluru A, Thomson A, Baginskitae J, Egan K, Vesterinen H, Currie GL, Churilov L, Howells DW, Sena ES (2015) Risk of bias in reports of in vivo research: a focus for improvement. PLoS Biol 13:e1002273
9. Macleod MR, Fisher M, O'Collins V, Sena ES, Dirnagl U, Bath PM, Buchan A, van der Worp H.B, Traystman R, Minematsu K, Donnan GA, Howells DW (2009) Good laboratory practice: preventing introduction of bias at the bench. Stroke 40:e50–e52, published as reprint in J Cereb Blood Flow Metab 29:221–223
10. Stroke therapy academic industry roundtable (Fisher, M., Chair) (1999) Recommendations for standards regarding preclinical neuroprotective and restorative drug development. Stroke 30:2752–2758
11. Fisher M, Feuerstein G, Howells DG, Hurn PD, Kent TA, Savitz SI, Lo E (2009) Update of the stroke therapy academic industry roundtable (STAIR) preclinical recommendations. Stroke 40:2244–2250
12. Dirnagl U (2006) Bench to bedside: the quest for quality in experimental stroke research. J Cereb Blood Flow Metab 26:1465–1478
13. NC3R. The ARRIVE guidelines. https://www.nc3rs.org.uk/arrive-guidelines. 29 Dec 2015

Chapter 19

Statistics in Experimental Stroke Research: From Sample Size Calculation to Data Description and Significance Testing

Ulrich Dirnagl

Abstract

Experimental stroke researchers take samples from populations (e.g., certain mouse strains) and make inferences about unknown parameters (e.g., infarct sizes, outcomes). They use statistics to describe their data, and they seek formal ways to decide whether their hypotheses are true ("Compound X is a neuroprotectant"). Unfortunately, experimental stroke research at present lacks statistical rigor in designing and analyzing its results, and this may have negative consequences for its predictiveness. This chapter aims at giving a general introduction into the do's and don'ts of statistical analysis in experimental stroke research. In particular, we will discuss how to design an experimental series and calculate necessary sample sizes, how to describe data with graphics and numbers, and how to apply and interpret formal tests for statistical significance. A surprising conclusion may be that there are no formal ways of deciding whether a hypothesis is correct or not and that we should focus instead on biological (or clinical) significance as measured in the size of an effect and on the implications of this effect for the biological system or organism. "Good evidence" that a hypothesized effect is real comes from replication across multiple studies; it cannot be inferred from the result of a single statistical test!

Key words Box plot, Categorical data, Confidence interval, Descriptive statistics, Null hypothesis, Power, *p*-Value, Sample size, Scatter plot, Statistical significance, Type I/II error, Wilcoxon-Mann-Whitney test

1 Introduction

Experimental stroke researchers produce data: infarct volumes, cell counts, functional outcomes, and such. Collecting data means sampling from a population. Since the population (e.g., all SV 129 mice) is too numerous to be sampled, we collect a sample to represent the population, and we use our sample (e.g., 20 SV 129 mice) to make inferences about unknown parameters of the population: infarct sizes, the effect of treatment with "Compound X," etc. Descriptive statistics help us to do just this. But very often stroke researchers also want an "objective method" to decide whether an observation from

Ulrich Dirnagl (ed.), *Rodent Models of Stroke*, Neuromethods, vol. 120,
DOI 10.1007/978-1-4939-5620-3_19,

a sample justifies accepting a hypothesis about the population. In other words, scientists want to test hypotheses and make decisions! In statistical terms, asking whether Compound X reduces infarct sizes is equivalent to asking whether the two samples (control vs. Compound X) come from the same population. Unfortunately, there is a certain likelihood that our decision might be wrong, as our test statistic could result in a false positive or a false negative. To get a handle on these errors, we calculate *p*-values for levels of significance and power. *P*-values, in particular, $p = 0.05$, have become the graven image of modern biomedicine. Most stroke researchers believe that the *p*-value of a significance test is the probability that the research results are due to chance (i.e., they confuse it with the positive predictive value, PPV) and are completely unaware of the concept of statistical power. It is the overall aim of this chapter to guide the preclinical stroke researcher in the proper experimental planning and statistical evaluation of data. Before presenting an example of a mock study, from hypothesis to significance testing, a few concepts need to be clarified. The following section should serve as a primer in "statistics for the experimental stroke researcher."

2 Concepts

2.1 Descriptive Statistics

Types of Data in Stroke Research

Data might be numerical, such as infarct volume data, or categorical, such as functional score data.

1. Numerical variables tell us "how much and how many?" and can be either continuous (e.g., infarct volumes) or discrete (e.g., hemorrhagic transformation count). Numerical variables can be treated with mathematical operations. Numerical summaries of quantitative data can be used to describe the location (e.g., mean) and the spread (e.g., variance) of the data, and statistical analysis may use parametric tests (e.g., *t*-test, ANOVA), provided the data is normally distributed.
2. Categorical variables tell us "what type?" and can be nominal (unordered, e.g., male, female) or ordinal (ordered, e.g., Bederson outcome score: 0, 1, 2, 3). A categorical variable places an individual into one of several categories. Mathematical operations make no sense with them. They can be numerically summarized with a count or with relative frequencies. Categorical variables can be visualized with dot plots or bar charts; frequency tables such as the chi-square test are used for group comparisons if they are unordered, or the nonparametric Wilcoxon-Mann-Whitney test—also known as Mann-Whitney *U* test—is used if they are unpaired and ordered.

A very common error in preclinical stroke research is the use of parametric statistics (mean, standard deviation (SD), *t*-test, etc.) on categorical data, for example, the use of the Bederson score [1] to assess global neurological function or a score to grade histological damage in the hippocampus [2]. As a consequence, many articles on experimental cerebral ischemia contain faulty statistics and may have reached unfounded conclusions.

Measures of Variance

These describe the variability of observations and serve as a useful basis for describing data in terms of probability: standard deviation (SD), standard error of the mean (SEM), confidence intervals (CI), etc use SDs to describe the spread of your data.

An extremely useful but regrettably underused measure of variance in the experimental stroke literature is the confidence interval (CI, e.g., 95 %: mean ± 2 × standard error of the mean (SEM) if $n > 30$). Its virtue lies in its straightforward interpretation: if we were to repeat the experiment a great many times calculating an interval each time, 95 % of those intervals would contain the mean. Confidence intervals reflect different degrees of precision in the measurement (Fig. 1b, d).

The SEM is an estimate of the SD that would be obtained from the means of a large number of samples drawn from that population. In other words, a SEM is a measure of the precision of an estimate of a population parameter, but it should not be used to describe the variability of the data. SEMs have become popular as a means of data description since they lead to "small" whiskers around the mean and are enticingly suggestive of a low variability of the data. It is for good reason, however, that most journals in their instructions to authors ban the use of SEM data description. Unfortunately, statistical consultants flooded with papers ignoring

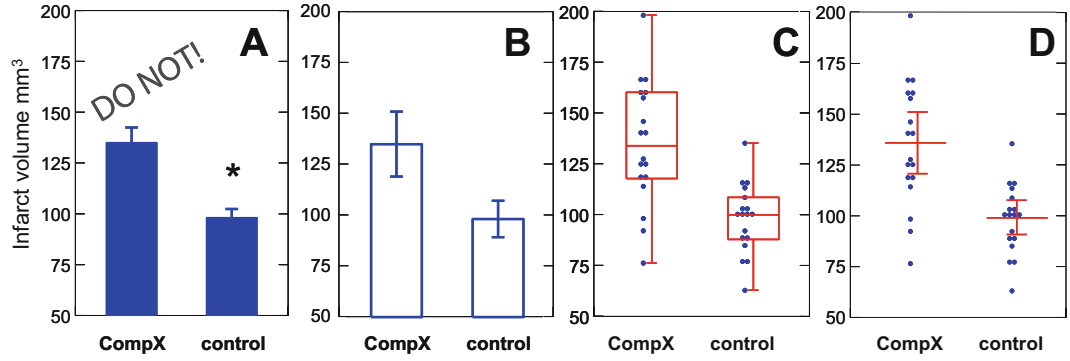

Fig. 1 Examples of noninformative (**a**), acceptable (**b**), and optimal (**c**, **d**) graphical displays of numerical infarct volume data in stroke research. (**a**) Typical but uninformative display as bar graphs of means + SEM. (**b**) Same data, ±95 % confidence interval. (**c**) Same data, displayed as dot plot of the raw data, overlaid by box-and-whisker plot (median, first and third percentile, range). (**d**) Same data, displayed as dot plot of the raw data, overlaid by mean ± 95 % confidence interval. Note that the bar graph in A obscures the dispersion of the data, while C and D allow the viewer a complete assessment

this rule seem to have given up maintaining it. Nevertheless, *don't* uses SEMs to quantify the variance of your stroke data!

Graphing Stroke Data

At the heart of most experimental stroke papers are graphs which summarize outcome in various groups (Fig. 1a). Although time honored, this practice is actually not recommended. For one, SEMs should not be used for data presentation (see above). Secondly, displaying only the mean is the least informative option available. Rather, whenever possible a graph should include each data point as a scatter plot (see Fig. 1c, d). This is the most informative way of displaying data. The scatter plot should be accompanied by a graph displaying summary statistics and valid measures of variance. One very useful graph is the box-and-whisker plot, which is very helpful in interpreting the distribution of data (see Fig. 1b). A box-and-whisker plot provides a graphical summary of a set of data based on the quartiles of that data set: quartiles are used to split the data into four groups, each containing 25% of the measurements. Unfortunately, Microsoft Excel does not have a built-in box-and-whisker plot, but practically all scientific graphing or statistics packages do. Various web pages show how to make box-and-whisker plots in Excel, e.g., [3]. Alternatively, a mean ± 95% confidence interval can be plotted in or next to the scatter plot (Fig. 1d).

Completely unacceptable is the use of bar graphs displaying means ± SDs or SEMs for categorical data (see above) (Fig. 2a). To display categorical data, use scatter plots or stacked bar graphs instead (see Fig. 2). Why is it incorrect to represent categorical variables by mean ± a measure of variance? Categorical variables may be ordered, but the intervals between values are not equally spaced, confounding mathematical operations. As a consequence, interim values between categories normally do not have a meaning. For example, in the modified Bederson score [1], category 1 is given for weakness of the contralateral forepaw, and category 2 for circling. What would be the meaning of the score of 1.6 ± 0.4, as often seen in papers of the experimental stroke literature?

2.2 Test Statistics

Hypothesis-driven experimental stroke research, like most areas of basic biomedicine, is trying to formalize the acceptance or rejection of its hypotheses with "frequentist" statistical tests, so-called null hypothesis statistical testing (NHST). The foundations for statistical testing were laid at the beginning of the twentieth century by William Sealy Gosset, working under the pseudonym "Student" (hence the Student's *t*-test). NHST was further developed and popularized more than 80 years ago by the statistician, geneticist, and eugenicist R. A. Fisher as a conveniently mechanical procedure for statistical data analysis. While the indiscriminate use of NHST has been criticized for many decades [4–6] and while several alternatives have been

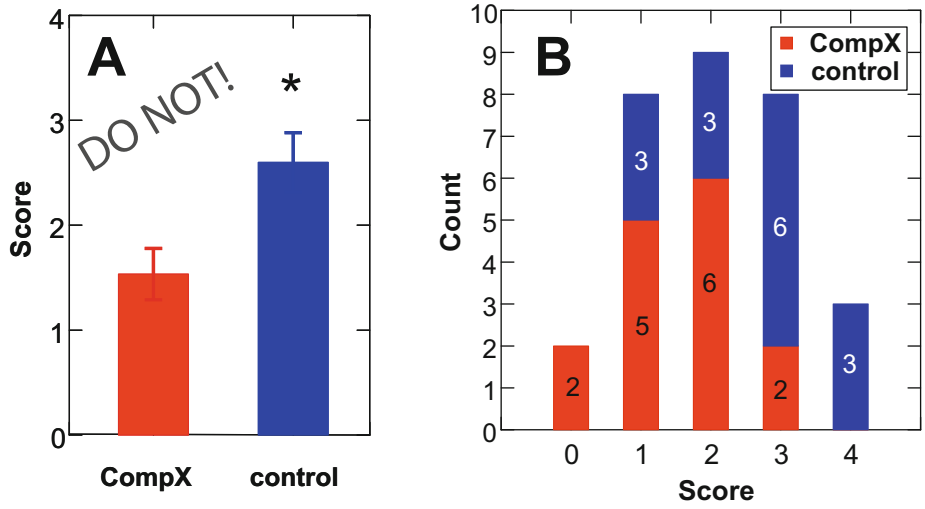

Fig. 2 Examples of erroneous (**a**) and correct (**b**) analysis and graphical display of categorical functional outcome data in stroke research. (**a**) It is not correct to analyze categorical data with parametric statistics. Shown here: bar graphs of mean outcome score (+ SEM). (**a**) *t*-test results in an erroneous statistically significant difference (* = $p = 0.006$). (**b**) Correct display of the same categorical data presented as frequencies (counts) with stacked bars. The Wilcoxon-Mann-Whitney test results in a $p = 0.01$. Note the substantially different *p*-values and the implication that the wrong analysis might reveal significant differences, whereas the correct one does not (or vice versa)

proposed, e.g., Bayesian approaches [5], its convenience and seemingly easy (but in most cases false) interpretation have made it a de facto standard—some say a "cult" [7]—for any statistical testing in experimental preclinical medicine, including in stroke research. Statisticians know that there is no objective ritual for finding out whether a hypothesis is true or false. However, since without NHST it is very unlikely that an experimental stroke paper will get published, we need to understand it and use it carefully and correctly.

Null Hypothesis and Errors

At the heart of NHST lies the insight that if we test hypotheses by sampling from large populations, we may err in concluding whether our hypotheses are true or false. In this process we can make two types of errors: one is to accept our hypothesis when in fact it is false; the other is to reject it when it is actually correct. To get a good mathematical grip on these errors, we can project our reasoning onto a "null hypothesis." If a stroke researcher holds the hypothesis that Compound X reduces infarct sizes, his/her hypothesis is supported by rejecting another hypothesis that Compound X has no effect! More formally expressed, the null hypothesis (H0) states that there is no difference between the two groups, while the alternative hypothesis (H1) states that there is a difference, which is what we usually state in our biological hypothesis. Now two errors may occur:

We may reject H0, but H0 was true (i.e., a "false positive"), which we call a type I error. Type I errors are quantified by α (very often set to 0.05; see below).

We might accept H0, but H1 was true (i.e., a "false negative"), which we call a type II error. Type II errors are quantified by ß (very often ignored, sometimes set to 0.2; see below).

The key criticism of NHST is that it is a trivial exercise because H0, which basically states that two treatments or samples are *identical*, is always false, and rejecting it is merely a matter of carrying out enough experiments (i.e., having enough power, see below) [8].

Alpha and the *p*-Value

The appeal of this approach is that it seems to offer a formal way of deciding whether our hypothesis is correct or not. Conveniently, we might accept an error level α (e.g., 0.05), which is presently interpreted by most (stroke) researchers to represent an index of the importance or size of a difference or relation. In other words, statistical significance appears to imply theoretical or practical significance. This seemingly straightforward interpretation of α, and the ease with which it is calculated through spreadsheets and statistics packages even without understanding its true meaning, underpins the popularity of NHST testing and *p*-values in biomedical research and may have often clouded a more (neuro)biologically driven interpretation of the data.

But what is the true meaning of $P < 0.05$? If we were to repeat the analysis many times using new data each time and *if the null hypothesis were really true*, then on only 5% of those occasions would we (falsely) reject it. To understand the consequences of this statement, we have to first understand the concept of the type II error (see below).

Does α need to be 0.05? R. A. Fisher, at a time when far fewer hypotheses were tested and papers published, suggested the magical 0.05 level for α, which seems to be universally accepted by now and is regarded by most students to be almost a natural constant. There is no theoretical justification for a particular value of α, which some journals even state in their guidelines for authors. An example from the American Physiological Society illustrates this: "If you plan a study in the hopes of finding an effect that could lead to a promising scientific discovery, then $\alpha = 0.10$ is appropriate. Why? When you define α to be 0.10, you increase the probability that you find the effect if it exists! In contrast, if you want to be especially confident of a possible scientific discovery, then $\alpha = 0.01$ is appropriate." [9].

Beta and Statistical Power

As stated above, β quantifies the type II error, i.e., of falsely accepting H0 (false negative). Power is simply derived as $1-\beta$. Power is

the conditional probability of accepting H1 when it is true. It is analogous to the concept of resolving power in evaluating optical instruments. It tells us how likely it is that we can find an effect if it equals or exceeds a prespecified size. Power increases with effect size (e.g., reduction in infarct size): the larger the difference between the parameters tested, the greater the power to detect it. Increasing sample size decreases the standard error, thereby increasing power. Conversely, a large variance (i.e., SD) will decrease power. There is an inverse relation between α and β: increasing alpha increases power (=decreases β) but also increases the risk of rejecting H0 when it is actually true.

Many papers in experimental stroke research report normalized effect sizes of about 1 (normalized effect size = effect/SD); for example, a reduction of infarct size by 30 mm^3 results in a normalized effect size of 1 if the SD was also 30 mm^3. A plot of total sample size (i.e., number of animals) vs. power demonstrates that 54 animals are needed to achieve a power of 0.95 (equivalent to $\beta = 0.05$) at an α level of 0.05. Targeting the same levels for α and β means that we are as afraid of false positives as of false negatives. The plot reveals that at 20 animals (10 per group, a conservative estimate of group sizes prevalent in preclinical stroke research), power is 0.55 (Fig. 3). The power of throwing coins is 0.5! In other words, with respect to statistical power a large fraction of the experimental stroke literature is no more predictive than a game of chance [11].

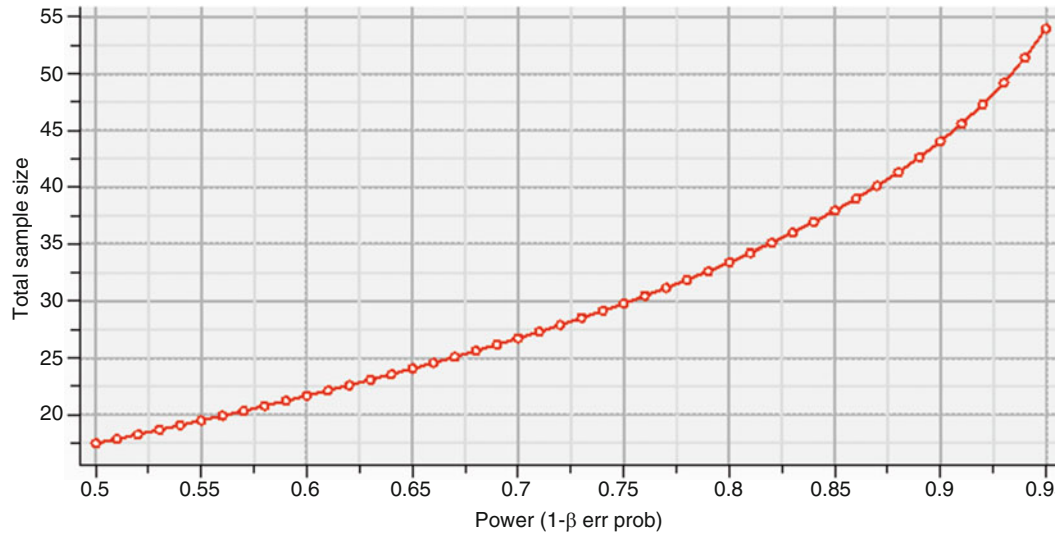

Fig. 3 Graphical display of sample size calculation for two-sided independent *t*-test using the freeware program G-Power [10]. α set at 0.05, effect size (mean difference between groups/SD) set at 1. Total sample size vs. power. Note that to detect an effect size as large as 1, SD at $\alpha = 0.05$, and $\beta = 0.95$, a total sample size of 54 (i.e., group sizes of 27) is required

Most experimental stroke researchers have a misconception of statistical power. They may even argue that if they have obtained a statistically significant p-value (e.g., $p<0.05$), there is no need to waste time worrying about type II errors, as they have not accepted, but rather rejected H0! For various reasons this is a fallacy with potentially calamitous impact. When H0 is in fact false (the drug really works, the knockout mouse has a phenotype, etc.), the overall error rate is not the α level, but the type II error rate β [12]. It is impossible to falsely conclude that H0 is false when in fact it is false! This apparently trivial insight may have important consequences for the interpretation of experimental data in stroke research and ultimately for its translation to the patient: if β is high (i.e., statistical power is low), the probability of being able to reproduce data decreases more and more. For example, at a power of 0.5, which is not uncommon in experimental stroke research (see above), the probability of being able to replicate the findings of a study stands at 50% [13]!

Excellent treatments of the concepts of power, sample size calculation, and positive predictive value can be found in [14–16].

Are Most Published Research Findings False?

This is what was famously claimed in a provocative paper by Ioannidis [17]. What appears silly and outrageous at first sight contains an unpleasant truth.

It was stated above that α measures the likelihood of falsely rejecting H0 *when it is really true*, while β measures the likelihood of falsely accepting H0 *when H1 is really true*. To be able to interpret α and β as likelihoods for our hypothesis being false or correct, we would need to know whether H0 or H1 is correct in the first place, which of course would render statistics superfluous! What we can learn from this is that the interpretation of α and β depends on the prior probability of our hypothesis (e.g., Compound X reduces infarct sizes in a stroke model). Because of the grave implications of this seemingly innocent proposition, I will illustrate it with three examples adapted from the literature.

Example 1 (Adapted from [5])

An experiment is conducted to see whether thoughts can be transmitted from one subject to another. Subject A is presented with a shuffled deck of 50 cards and tries to communicate to subject B whether each card is red or black by thought alone. In the experiment, subject B correctly gives the color of 33 cards. The null hypothesis is that no thought transference takes place and subject B is randomly guessing. The observation of 33 correct is significant, with a (one-sided) p-value of 0.035. Would you now believe that subject A can transmit thoughts to subject B? Probably not, as you correctly recognize that much stronger evidence would be required

to reject a highly plausible H0. This makes clear that the *p*-value cannot mean the same in all situations. But why would you not hesitate to accept a neuroprotective effect of Compound X at $p = 0.035$?

Example 2 (Adapted from [5])
You take a diagnostic test for a grave disease. The test is very accurate; it has a 0.1% false positive rate (very good sensitivity) and a 0.1% false negative rate (very good specificity). The test result comes out positive! What is the probability that you have the disease? Most students (and faculty) will answer 99.9%. But the information that was missing to answer the question is the incidence of the disease in the population. If it is, for example, 1:50,000, a test which is false positive at a rate of 1:1000 will result in a probability of having the disease of only 2% (=1:50). H0 ("you do have the disease") started with a very low probability! In this instructive example, sensitivity is equivalent to type I error, and specificity is equivalent to type II error, while the incidence of disease can be interpreted to be the rate of true hypotheses. It is wrong to interpret a *p*-value as the probability of H0, because this fails to take account of the prior probability of H0.

Example 3 (Adapted from [6, 18])
Let us assume that 10% of all H0 in biomedicine are in fact false, that is, 90% of all hypotheses are incorrect (assumption 1). Although a wild guess, it is backed by evidence from several fields [17]. Let us also assume an α of 0.05 and a power of 0.5 (assumption 2), which is a reasonable estimate for the current experimental stroke literature (see above). If we now test 1000 hypotheses, assumption 1 results in 100 studies in which H0 is truly false. When power is 0.5 (assumption 2), we reject H0 in 50% of those studies. In the 900 studies in which treatment does not work (because our hypothesis was wrong, i.e., H0 was true), we rejected H0 in 45, since α was 0.05 (assumption 2). In 45 of the 95 studies with a "significant result," H0 was true; in other words, the studies were false positives! The likelihood that a significant result is "true" in this example was 52%. This example is a warning to those who argue that once they have obtained a significant result ($p < 0.05$), they need not worry about power, let alone the prior probability of the hypothesis they were testing (Table 1).

Statistical Significance Testing: A "Sizeless Science"
Before moving on to a practical example, let us briefly contemplate the main criticism of the concept of "statistical significance." We need to be aware of the fact that even if we apply significance testing properly (i.e., recognizing α and β), it contains an intrinsic weakness. Statistical significance testing substitutes exploring the existence of a phenomenon or the precision by which we measure

Table 1
Number of times we accept and reject null hypothesis, under plausible assumptions regarding the conduct of medical research (adapted from [6])

Result of exp.	Hypothesis wrong (=H0 true) "treatment does not work"	Hypothesis correct (=H0 false) "treatment works"	Total
"Nonsignificant (i.e., negative) result" (=accept H0)	855	50	905
"Significant (i.e., positive) result" (=reject H0)	45	50	95
Total	900	100	1000

it, for its magnitude. We should ask "What difference does the effect make?" and "Who cares?", but instead are concerned with formal proof of existence and precision of measurement. Increasing sample size is a tedious but nevertheless unconditionally successful exercise to demonstrate statistically significant difference. As Ziliak and McCloskey [7] have put it: through statistical testing, "science has become sizeless." Gosset was already aware of its shortcomings at the beginning of the twentieth century and warned against its "unintelligent use." As it stands, exercising radical criticism of statistical significance and shunning significance testing will not help get scientific papers published. But, thus compelled to use it, we need to use it "intelligently," cognizant of its limitations. Beyond statistical significance testing, we should:

- Focus on biological (or clinical) significance, which is measured in the size of an effect, and the implications the effect has for the biological system or organism
- Be aware that "good evidence" that a hypothesized effect is real comes from replication across multiple studies and cannot be inferred from the result of a single statistical test!

Exploratory Versus Confirmatory Preclinical Stroke Studies
Regarding study design and statistical analysis, an important distinction between two different modes of investigation should be made [19]. Most preclinical stroke researchers are confronted with two overarching agendas: selecting interventions or possible mechanisms amid a vast field of potential candidates and producing rigorous evidence of clinical promise for a small number of interventions developed further in human trials. Hence, two different, complementary modes of investigation can be discriminated: in the first (exploratory investigation), stroke researchers should aim at generating robust pathophysiological theories of disease. In the second (confirmatory investigation), researchers should aim at

demonstrating strong and reproducible treatment effects in animal models relevant to human stroke. Each mode entails different study designs, confronts different validity threats, and supports different kinds of inferences. Many preclinical stroke studies appear to operate in both modes simultaneously, aiming to report novel pathophysiological mechanisms while at the same time presenting evidence for novel treatment. This is highly problematic, as an exploratory study sets out to find what might work in an almost limitless space of mechanisms, molecules, dosages, etc., while a confirmatory study needs to weed out false positives to further develop only robust strategies in the human. Exploratory studies may therefore put a premium on sensitivity, that is, be forgiving with respect to type I errors. On the other hand, confirmatory studies need high specificity, but may be forgiving with respect to type II errors. Table 2 lists how relevant design and analysis features compare in exploratory and confirmatory preclinical studies.

Preclinical Randomized Controlled Trials (pRCTs)

In this context a novel type of preclinical study has to be mentioned, which could be considered the most extreme variant of a confirmatory animal study: pRCTs, many features of which are adapted from clinical randomized controlled trials, may help to

Table 2
Comparison of design and analysis features in exploratory and confirmatory studies

	Exploratory "discovery"	Confirmatory
Hypothesis	+	+++
Establish pathophysiology	+++	+
Sequence and details of experiments established at onset	+	+++
Primary endpoint	–	++
Sample size calculation	+	+++
Blinding	+++	+++
Randomization	+++	+++
External validity (aging, comorbidities, etc.)	–	++
In-/exclusion criteria	++	+++
Test statistics	+	+++
Preregistration	–	++
High sensitivity (high type I error rate, low type II error rate): Find what might work	+++	+
High specificity (low type I error rate, high type II error rate): Weed out false positives	+	+++

overcome the problem of single laboratories to conduct experiments of sufficient power and robustness to justify the expensive and potentially hazardous transition from animal to human studies. A pRCT includes several hundred animals, harmonizes protocols, and features a prospective, blinded, and randomized study design, central monitoring of data quality, as well as centralized analysis and data deposition [20].

Further Reading
Excellent general treatments of the statistical analysis of preclinical studies can be found in [21–24]. For further in depth discussion on many of the issues treated above, readers are directed to my science blog [25], which covers topics such as reproducibility, replication, statistics, power, bias, and bench to bedside translation, among others.

Let us now look at a practical example of an experimental stroke study.

3 A "How To" Example

Before we start conducting stroke experiments, we need to:

- Formulate the underlying biological hypothesis.
- Lay down the experimental design with which we aim to prove or disprove the hypothesis.

1. Hypothesis: In our example, the simple hypothesis, based on prior evidence (e.g., in cell culture) and knowledge of the mechanism(s) of action, is that Compound X is a neuroprotectant, decreases infarct sizes, and improves outcome in experimental stroke.

2. We now design the experiment according to SOPs: We decided to test Compound X in a mouse model of stroke. Infarct sizes will be measured volumetrically (Chap. 15) 72 h after 45 min of middle cerebral artery occlusion (MCAO; Chap. 4). Compound X or saline will be applied intraperitoneally 2 h after MCAO. Inclusion and exclusion criteria, details of randomization, blinding, etc., are defined a priori; in other words, we are following our standard operating procedures (see Chap. 17).

3. We now need to predefine the statistical tests we are going to apply. This needs to be done apriori. The infarct volume data will be numerical, but it is unclear whether it will be distributed normally. Assuming normality (and testing for it after data acquisition), we might compare the two independent group means with a two-tailed *t*-test (or for more

than two groups, with an ANOVA and appropriate post hoc contrast). To be on the safe side with respect to normal distribution, we opt for the nonparametric Mann-Whitney *U* test (or if there are more than two variables, the equivalent Kruskal-Wallis one-way analysis of variance). As stated above, we will accept a type I error level α of 0.05. As outcome test we have opted for a modification of the simple Bederson score [1, 26, 27], which produces the following categories: 0 = no deficit, 1 = weakness of the contralateral forepaw, 2 = circling, 3 = loss of righting reflex, and 4 = no motor activity. Since our score is a categorical variable, we will test for statistical significance between both groups with a Wilcoxon-Mann-Whitney test [28].

4. The next step is to calculate the necessary group (sample) sizes. From previous experiments we know that in the model we are using, SDs are around 25% of the mean infarct volume. If you have not had previous experience, you need either to conduct a pilot series (recommended) or use data from similar experiments in the literature. If we want to detect a change in infarct volume greater than 25% by Compound X, this corresponds to an effect size of 1 (effect size d = (mean infarct volume$_{control}$–mean infarct volume$_{treatement}$)/pooled SD [29]). If we set power at 0.8 and α at 0.05 (see above), the required sample size (two tailed) calculated a priori will be 17 animals per group. All major statistical packages will allow you to calculate sample sizes and power. One very convenient and intuitive freeware program is G*Power [10], which I highly recommend.

   To calculate sample sizes for nonparametric tests such as the ones we perform to analyze behavioral testing after stroke (see above), we can either use expensive, specialized software such as nQuery or PASS, or we can use G*Power (or any other program that can do power calculations). To do this, we find an approximate size by estimating the sample size for a *t*-test and then adjusting this size based on the asymptotic relative efficiency (ARE) of the nonparametric test [30]. So, for example, to estimate sample size for a Wilcoxon-Mann-Whitney test (see above), we compute the sample size needed for a two-sample *t*-test and then adjust the sample size based on the ARE of the Wilcoxon-Mann-Whitney test relative to the *t*-test. To avoid complicated assumptions about the underlying distribution, one could examine a worst case scenario, since the ARE for the Wilcoxon-Mann-Whitney test is never less than 0.864. Thus, in this conservative and simple approach, estimate the sample size for a *t*-test (see above) and divide by 0.864. For example, to detect a change in the Bederson score of

the magnitude given in the example of Fig. 2b, at a power of 0.8 and α of 0.05, a total sample size of approximately 35 (=30/0.864) would be required.

5. After the series of experiments has been conducted and the data evaluated by investigators blinded to treatment allocation, we first produce graphical displays of the data in the form of scatter plots (see Fig. 1c, d) and describe the data by calculating means and SDs (or even better, confidence intervals) for numerical data (infarct volumes) and contingency tables for the categorical data (outcome score), which is graphically represented by stacked bar graphs (Fig. 2b).

6. We then perform the prespecified statistical tests. At this stage no other statistical tests should be used, except for hypothesis generation for future experiments. It is a common practice but a misuse of statistics to "play" with various tests or post hoc contrasts until the "desired" *p*-value is produced by the statistics package ("p-hacking" [31]). Similarly, we are not allowed to "add" animals to a series of predefined group sizes to target a certain *p*-value. This may be tempting, particularly when the resulting *p*-values only narrowly miss the significance level.

7. After all these calculations for significance and plotting of asterisks ($p < 0.05$), we should try to forget them for a moment and answer the relevant question: what is the biological significance of the difference observed?

8. Finally, a word of caution and a recap of what was said above, if the results of our example proved to be "statistically significant" (p slightly below 5%), at a power of 80%, and an a priori probability of the hypothesis of 10%, the false discovery rate (the chance to have obtained a false positive result) would be close to 40% [32], not 5%.

References

1. Bederson JB, Pitts LH, Tsuji M, Nishimura MC, Davis RL, Bartkowski H (1986) Rat middle cerebral artery occlusion: evaluation of the model and development of a neurologic examination. Stroke 17:472–476
2. Buchan A, Pulsinelli WA (1990) Hypothermia but not the N-methyl-D-aspartate antagonist, MK-801, attenuates neuronal damage in gerbils subjected to transient global ischemia. J Neurosci 10:311–316
3. Hunt H. Boxplots in Excel. http://staff.unak.is/not/andy/StatisticsTFV0708/Resources/BoxplotsInExcel.pdf. 29 Dec 2015
4. Harlow LL, Mulaik SA, Steiger JH (eds) (1997) What if there were no significance tests? Lawrence Erlbaum Associates, London
5. O'Hagan A, Luce R (2003) A primer on Bayesian statistics in health economics and outcomes research. https://www.shef.ac.uk/polopoly_fs/1.80635!/file/primer.pdf. 29 Dec 2015
6. Sterne JAC, Smith GD (2001) Sifting the evidence – what's wrong with significance tests? Br Med J 322:226–231
7. Ziliak ST, McCloskey DN (2008) The Cult of Statistical Significance: How the Standard Error Costs Us Jobs, Justice, and Lives. Univ of Michigan Press, Ann Arbor

8. Kirk RE (1996) Practical significance: a concept whose time has come. Edu Psychol Meas 56:746–759
9. Curran-Everett D, Benos DJ (2004) Guidelines for reporting statistics in journals published by the American Physiological Society. Am J Physiol 28(3):85–87
10. G*Power 3. http://www.gpower.hhu.de/. 29 Dec 2015
11. Dirnagl U (2006) Bench to bedside: the quest for quality in experimental stroke research. J Cereb Blood Flow Metab 26:1465–1478
12. Schmidt FL, Hunter JE (1997) Eight common but false objections to the discontinuation of significance testing in the analysis of research data. In: Harlow L, Mulaik SA, Steiger JH (eds) What if there were no significance tests? Lawrence Erlbaum Associates, London, pp 37–64
13. Mulaik SA, Raju NS, Harshman RA (1997) There is a time and a place for significance testing. In: Harlow L, Mulaik SA, Steiger JH (eds) What if there were no significance tests? Lawrence Erlbaum Associates, London, pp 66–115
14. Button KS, Ioannidis JP, Mokrysz C, Nosek BA, Flint J, Robinson ES, Munafò MR (2013) Power failure: why small sample size undermines the reliability of neuroscience. Nat Rev Neurosci 14:365–376
15. Krzywinski M, Altman N (2013) Points of significance: power and sample size. Nat Methods 10:1139–1140
16. Simonsohn U (2015) Small telescopes: detectability and the evaluation of replication results. Psychol Sci 26:559–569
17. Ioannidis JP (2005) Why most published research findings are false. PLoS Med 2(8):e124
18. Oakes M (1986) Statistical inference. Chichester: Wiley
19. Kimmelman J, Mogil JS, Dirnagl U (2014) Distinguishing between exploratory and confirmatory preclinical research will improve translation. PLoS Biol 12:e1001863
20. Llovera G, Hofmann K, Roth S, Salas-Pérdomo A, Ferrer-Ferrer M, Perego C, Zanier ER, Mamrak U, Rex A, Party H, Agin V, Fauchon C, Orset C, Haelewyn B, De Simoni MG, Dirnagl U, Grittner U, Planas AM, Plesnila N, Vivien D, Liesz A (2015) Results of a preclinical randomized controlled multicenter trial (pRCT): Anti-CD49d treatment for acute brain ischemia. Sci Transl Med 7:299ra121
21. Motulsky HJ (2015) Common misconceptions about data analysis and statistics. J Pharmacol Exp Ther 351:200–205
22. Festing MF, Nevalainen T (2014) The design and statistical analysis of animal experiments: introduction to this issue. ILAR J 55:379–382
23. Nuzzo R (2014) Scientific method: statistical errors. Nature 506(7487):150–152
24. Aban IB, George B (2015) Statistical considerations for preclinical studies. Exp Neurol 270:82–87
25. Dirnagl U. To infinity and beyond. http://dirnagl.com. 29 Dec 2015
26. Li X, Blizzard KK, Zeng Z, DeVries AC, Hurn PD, McCullough LD (2004) Chronic behavioral testing after focal ischemia in the mouse: functional recovery and the effects of gender. Exp Neurol 187:94–104
27. Plesnila N, Zinkel S, Le DA, Amin-Hanjani S, Wu Y, Qiu J, Chiarugi A, Thomas SS, Kohane DS, Korsmeyer SJ, Moskowitz MA (2001) BID mediates neuronal cell death after oxygen/glucose deprivation and focal cerebral ischemia. Proc Natl Acad Sci U S A 98:15318–15323
28. Emerson JD, Moses LE (1985) A note on the Wilcoxon-Mann-Whitney test for 2 x k ordered tables. Biometrics 41:303–309
29. Cohen J (1988) Statistical power analysis for the behavioral sciences, 2nd edn. Lawrence Erlbaum Associates, Mahwah, NJ
30. Simon S. Sample size for the Mann-Whitney U test. http://www.pmean.com/00/mann.html. 29 Dec 2015
31. Head ML, Holman L, Lanfear R, Kahn AT, Jennions MD (2015) The extent and consequences of p-hacking in science. PLoS Biol 13:e1002106
32. Colquhoun D (2014) An investigation of the false discovery rate and the misinterpretation of p-values. R Soc Open Sci 1:140216

Chapter 20

Complexities, Confounders, and Challenges in Experimental Stroke Research: A Checklist for Researchers and Reviewers

Ulrich Dirnagl

Abstract

The quest for internal and external validity in experimental stroke research is fraught with pitfalls and confounders. This article, written as a checklist from the perspective of an editor and reviewer of articles on rodent stroke models and an active bench side stroke researcher, presents a compilation of the common pitfalls and quality issues in experimental stroke research. These include selecting controls for genetically modified animals, effects of stroke on systemic parameters (immunodepression, infection, cachexia, etc.), cerebral blood flow measurement, brain edema correction, study design, statistics, and interpretation.

Key words Bias, Body weight, Body temperature, Brain edema correction, Cachexia, Cerebral blood flow measurement, Flanking gene, Gene knockout, Genetically modified animals, Infarct maturation, Internal validity, Laser Doppler flowmetry, Statistics, Triphenyltetrazolium hydrochloride, Wasting

1 Introduction

Modeling disease in animals is highly complex. Many confounders challenge the internal and external validity of this type of research [1, 2]. Modeling stroke is particularly challenging with respect to bias and confounders: It involves damage to the most complex organ in the known universe and produces a plethora of secondary changes in peripheral metabolism as well as in the endocrine, cardiovascular, and immune systems which occur after stroke-induced failures in the brain's homeostatic control function. As a journal editor and reviewer of articles in the cardiovascular field as well as a stroke researcher, I am constantly faced with these complexities and with the various strategies (and sometimes failures) for overcoming them and maintaining quality. In this chapter, I have compiled in the form of a checklist the most common and relevant pitfalls and quality issues in experimental stroke research. It is

Ulrich Dirnagl (ed.), *Rodent Models of Stroke*, Neuromethods, vol. 120,
DOI 10.1007/978-1-4939-5620-3_20,

meant to guide the experimentalist in planning stroke experiments and the reviewer of experimental stroke research in assessing such research. Many of the issues introduced here are covered in greater detail in the preceding chapters.

2 The Checklist

Proper controls for experiments with genetically modified animals?	✓

The potential for manipulating gene expression in vivo by deleting (knockout) or inserting genes (knock in, transgenics) has revolutionized biological research and provided highly relevant insights into mechanisms of disease. Genetically manipulated animals are among the mainstays of modern cerebral ischemia research. However, their use brings with it several highly relevant confounders which need to be taken into account when planning an experimental stroke study. In particular, we need to be aware of genetic background, flanking genes, and insertion-site effects.

The flanking gene problem [3] is of particular relevance when embryonic stem (ES) cells for the generation of the knockout mouse have been derived from substrains of 129 inbred mice, whose germ lines will transmit not only the induced null mutation but also the 129 genetic background. Mating these mice with another inbred strain, very often the C57BL/6, results in an F2 generation that segregates not only for the induced null mutation and its wild-type allele but also for any other alleles at loci where the parental strains differ [4]. The C57BL/6 and 129 mouse strains are highly popular, not only in the genetic engineering of mice but also in experimental stroke research. Solutions to the flanking gene problem include backcrossing and outcrossing strategies that produce congenic or coisogenic lines [3]. Due to gross differences in the vascularization of the brain [5–7] and intrinsic factors of which we understand very little [7], C57BL/6 and 129 mouse strains differ greatly in their susceptibility to cerebral ischemia. Therefore, the flanking gene problem is highly relevant in experimental stroke research.

The Banbury conference on genetic background in mice [8] clearly states that it is "a faulty strategy to maintain separate mutant and control lines by continuous inbreeding of homozygous individuals starting from the original F2 generation, as this will entail genetic drift and, with it, phenotypic line differences unrelated to the targeted mutation." In spite of this warning, many mouse studies in the field of experimental ischemia continue to use homozygous knockout mice (obtained from collaborators or commercial sources) and choose as a control group the mouse strain which has

been used as the background strain, very often even a strain obtained from a different source than the knockout strain. The proper way of doing such experiments is to use littermate controls.

Transgenic animals may be confounded by the random insertion of the transgene into the genome, which might affect the function of an endogenous gene and create a phenotype that is not related to the transgene. The solution to this problem is to create and use various founders [9]. If they are similar with respect to their phenotype after focal cerebral ischemia, it is highly likely that an effect is related to the transcription of the transgene.

Proper observation interval after induction of focal cerebral ischemia? ✓

Maturation of damage after vascular occlusion is a highly dynamic process which evolves over a period of time. Depending on the model and severity of focal cerebral ischemia, infarcts (i.e., tissue pannecrosis) reach their maximum extent within 24 to 72 h. Many models of experimental stroke demonstrate a delay in infarct growth of around 20–30 % between days 1 and 3 post-middle cerebral artery occlusion (MCAO) [10]. This is congruent with observations in human stroke [11]. After around 1 week, infarcts may appear to shrink again [12]. This should not be confused with repair; it is rather the result of resorption of necrotic tissue, glial scarring, and resulting changes in the 3D geometry of the brain. In milder forms of ischemia (transient MCAO ≤30 min), where no outright infarction occurs but neurons die selectively, maturation of neuronal damage (mostly by forms of programmed cell death) is even further delayed and reaches a maximum around day 3 [13]. In most focal cerebral ischemia models, a few days after the demise of tissue within the territory of the occluded artery, remote tissue damage may occur as a result of deafferentation. In MCAO models, this prominently involves the thalamus [14, 15]. An important consequence of all this is that outcome assessment after induction of experimental focal cerebral ischemia has to be appropriately timed. For example, in most instances, it is not acceptable to study outcome only 24 h after MCAO. Even if a neuroprotective effect of an experimental therapeutic strategy has been found at the 24-h time point, it is not guaranteed that this effect will be stable. The treatment may only have delayed damage [16]. As a rule of thumb, the observation period required to determine infarct volumes in acute neuroprotectants is 3–7 days.

At this point, the narrow time window for the use of the metabolic stain 2,3,5-triphenyltetrazolium hydrochloride (TTC) for infarct volume determination should be mentioned. TTC staining is based on the functioning of mitochondrial enzymes. Strictly speaking, it is related to the number of intact mitochondria, but it cannot directly demonstrate pannecrosis (infarcts). This is why

TTC staining works even many hours after the death of the animal [17]. The low density of mitochondria in white matter structures yields only pale staining, rendering it impossible to discriminate between normal white matter structures and ischemic brain tissue, particularly during the first hours after onset of ischemia [18]. Even more serious is the problem that at later time points, inflammatory cells invade the region of the infarct and metabolize TTC. For this reason, TTC should not be used for time points beyond 24 h [19–21].

Did the experimental design allow the establishment of a causal relationship between experimental manipulation and phenotype?

One frequent problem (and cause for rejection of manuscripts) in experimental stroke research relates to the trivial fact that smaller infarcts (e.g., by a certain treatment) lead to a reduction in practically all mechanisms related to primary and secondary ischemic damage. Secondary damage scales with primary injury! For example, the finding that a compound which reduces infarct sizes leads to a reduction in inflammatory markers (cytokines, influx of leukocytes, etc.) in the treatment group does not prove that the effect of the compound is due to anti-inflammatory mechanisms. To illustrate this point, reducing infarct sizes by blocking the *N*-methyl-d-aspartate (NMDA) receptor (which is not found on cells of the immune system) via a reduction of tissue damage also leads to a reduction in secondary release of inflammatory cytokines or an influx of leukocytes into the affected hemisphere.

Unfortunately, this problem is very difficult to overcome, but in principle, there are two possibilities: One is to simply abstain from conclusions or statements that imply the demonstration of a clear-cut causal relationship such as "compound X is an anti-inflammatory neuroprotectant, as it significantly reduced leukocyte influx in the treatment group." Another option, although also not perfect, is to titrate infarct sizes by using longer MCAO intervals in the protected treatment group so that both control and verum group have similar infarct sizes despite neuroprotective treatment [22]. If markers of the targeted putative mechanism (such as inflammation) are still significantly less regulated than in the verum group, this would give indirect evidence that the action of the compound on this mechanism is relevant for protection. Alternatively, one could perform control experiments with a compound that reduces infarct volumes to a similar degree but by other mechanisms (such as the NMDA-receptor antagonist MK801 as opposed to an anti-inflammatory compound).

Proper use and interpretation of cerebral blood flow measurement? ✓

Laser Doppler flowmetry (LDF) is a useful and commonly applied technique in cerebral ischemia research. LDF [23] allows the instantaneous, continuous, and noninvasive measurement of microcirculatory blood flow in small tissue samples. Infrared light from a laser diode (usual wavelength, 780 nm) is delivered to and detected in a tissue area of approximately 1 mm^3 by a flexible fiber optic. Scattering by a moving red blood cell results in a Doppler frequency shift, while light scattered by stationary tissue remains unshifted. Analysis of the backscattered light yields the frequency of the Doppler shift, which is proportional to the red cell velocity. The fraction of the backscattered light that is Doppler shifted is proportional to the total volume of moving blood cells in the tissue sample. An index of red cell flow is then derived from the multiplication of the mean Doppler shift by the fraction of light that is Doppler shifted. This principle dictates that LDF cannot provide accurate measurement of absolute regional cerebral blood flow (rCBF) values, but it does allow the accurate measurement of changes in rCBF due, for example, to induction of focal cerebral ischemia [24]. In experimental stroke research, LDF is often used to verify occlusion of middle cerebral artery with an intraluminal thread, an extraluminal occluder, or reperfusion after removal of these devices. In an individual animal, reduction to 10% of preocclusion values clearly indicates successful induction of focal cerebral ischemia. However, LDF is also often used to compare intra-ischemic CBF values between groups, for example, to demonstrate that a "protected" phenotype of a knockout strain is not due to different vascular supply and consequently higher CBF. This information, however, cannot be provided by LDF and in fact constitutes its misuse: Even if intra-ischemic reductions of CBF are similar, the protected strain may, because of different vascularization, have started with higher initial CBF values. LDF can quantitatively measure percent changes, but a reduction to 20% from an absolute value of 150 mL/100 g/min is not the same as a percent reduction from a baseline of 120 mL/100 g/min. An additional problem of LDF in this context is its small sample volume of approximately 1 mm^3: While LDF may be able to demonstrate that relative changes in CBF are similar in one small spot within the lesion, it cannot enlighten us about the spatial extent of the flow reduction, which may be very different between different strains of animals due to differences in collateral vascular supply. Attempts have been made to overcome this problem by combining LDF with ex vivo evaluation of anastomoses between arteries of the circle of Willis at the dorsal surface of the brain after carbon black injection [25]. While this technique can reveal gross differences in vascular patterns (e.g., missing posterior communicating arteries [26]) between mouse and rat strains, it is clearly not sensitive enough to

exclude the possibility of a different vascular supply and collateralization, in particular at the microcirculatory level. Unfortunately, the only convincing approach to exclude differences in pre-ischemic and/or intra-ischemic CBF between strains is the application of quantitative CBF techniques such as ^{14}C-iodoantipyrine autoradiography [27]. Recently, quantitative magnetic resonance imaging techniques for rat [28] and mouse [29] have been presented and validated. However, due to the very short transit times and high CBF values in rodents, these techniques, while allowing multiple in vivo measurements, have relatively low spatial resolution and high variance and hence have yet to demonstrate their suitability for experimental stroke research in small animals.

Edema correction?	✓

In particular, during the first days after middle cerebral artery occlusion, morphometric determination of infarct sizes in rodents is complicated by ischemic tissue swelling (ischemic brain edema). The space-occupying effect of brain edema leads to an overestimation of the affected tissue volume by a range of 20–30% [30]. If brain edema is not taken into account when calculating infarct sizes, a (hypothetical) compound which acts on brain edema but not on tissue damage might erroneously be understood to reduce infarct sizes by 30%. In most focal cerebral ischemia models in rodents, edema volume is maximal at around 24–48 h after middle cerebral artery occlusion, greatly reduced by 3 days and no longer detectable at day 7. However, the temporal and spatial dynamics of edema formation in these models is highly dynamic and variable and depends on the duration of ischemia, site of vascular occlusion, etc. The literature abounds with articles which do not account for this confounder, but edema correction is now routinely performed on postmortem analysis by calculating the indirect infarct volume as the volume of the contralateral hemisphere minus the non-infarcted volume of the ipsilateral hemisphere [31]. This technique is based on the assumption that edema develops almost exclusively in the infarcted areas. While this may be true as a first approximation, even visual inspection of postmortem sections of MCAO brains at the peak of brain edema development reveals swelling of tissue of the affected hemisphere adjacent to the infarcted area (Fig. 1). It must be therefore kept in mind that infarct volume correction by the direct-indirect volume method may still be confounded by edema. This is also true for MR-based techniques for edema correction because they rely on the same assumptions [30]. In cases in which edema is prominent—and peri-infarct tissue potentially contributes substantially to infarct volumes—infarct volume should be determined after edema has subsided (e.g., after 7 days). In addition, a true quantitation of the edema by the wet-dry method should be considered: Immediately after being removed, the brain is rapidly cut into two halves; the

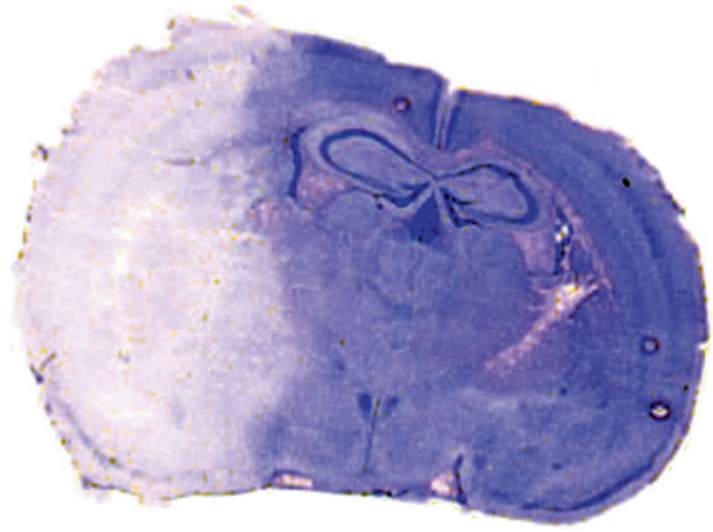

Fig. 1 Prominent edema of the left hemisphere 24 h after 60 min of middle cerebral artery occlusion in the BL6 mouse strain (cresyl violet staining). Note that not only the infarcted area but also the tissue adjacent to the infarct appears swollen

hemispheres are weighed, dried for 24 h at 110 °C, and weighed again. Hemispheric water content is then calculated using the following equation: % water=(wet weight − dry weight)/wet weight × 100 % [32].

Did ischemia-induced or pharmacologically induced systemic alterations confound the results? ✓

Focal cerebral ischemia primarily affects brain tissue. However, via humoral and nervous signaling, it also has remote effects on systemic parameters such as the cardiovascular system, the immune system, or the general metabolism. These effects are further accentuated by the fact that practically all models of rodent stroke involve some degree of anesthesia and surgery, which have systemic effects of their own.

Depending on species, model, and MCAO occlusion interval, rodent stroke models may have *mortality rates* of up to 50% (Fig. 2a) [33, 34]. Besides perioperative mortality, which is strongly influenced by the skills of the surgeon, the major cause of death in rodent stroke models, as in patients [35], is *infection*. As a general rule, occlusion of the MCA proximal to the lenticulostriate arteries leads to a higher risk of infection than do occlusions distal to it. Rate of infection is clearly correlated to the duration of ischemia: While a 30 min occlusion of the MCA is rarely followed by clinically apparent infection, permanent occlusions of the proximal MCA lead to a very high susceptibility to infection-related and sepsis-related death. Following stroke-induced immunodepression mediated to a large degree by sympathetic overactivation [36, 37],

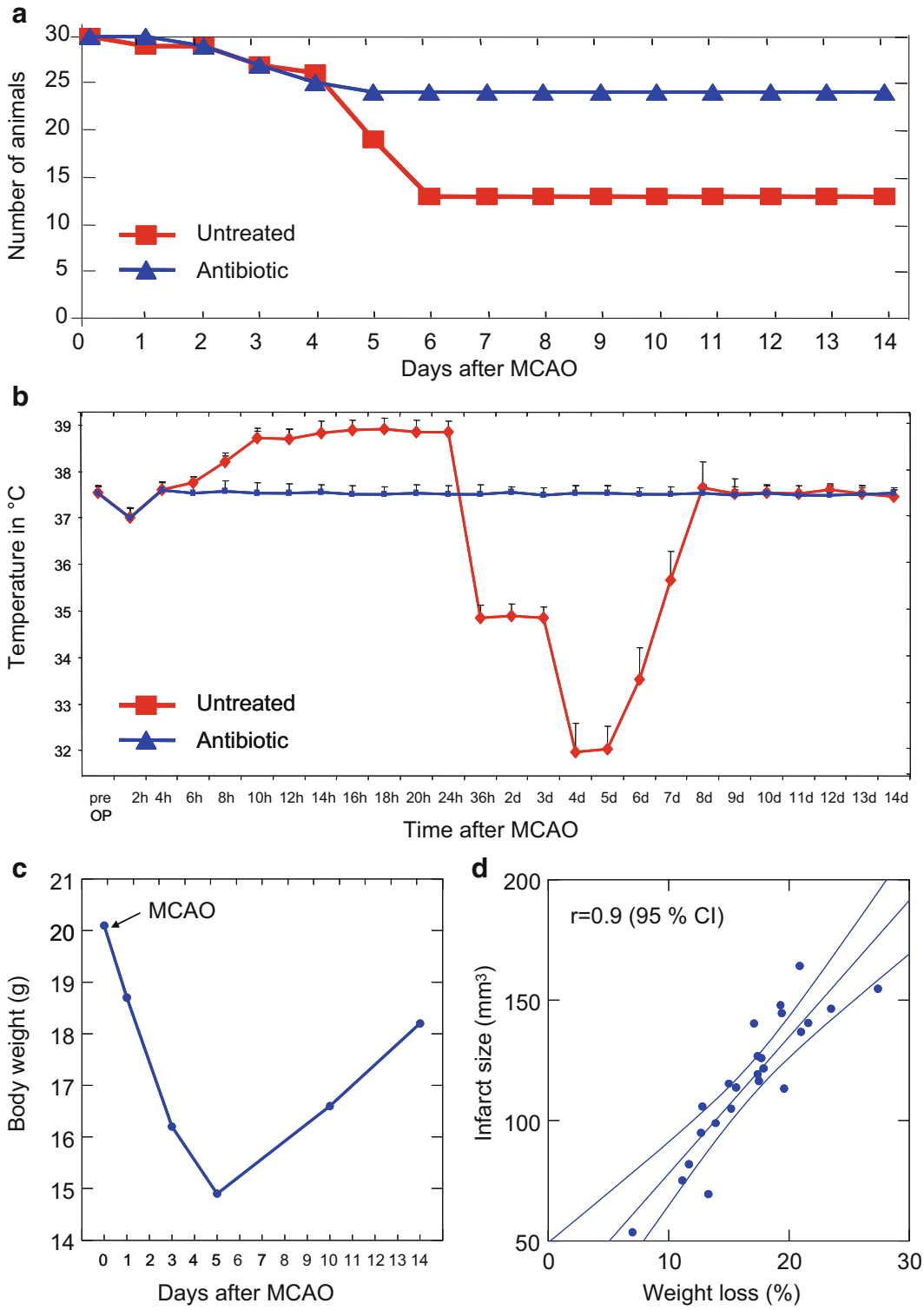

Fig. 2 (**a**) Mortality after 60 min of middle cerebral artery occlusion (MCAO) in the BL6 mouse strain. Note that mortality increases dramatically after 3 days. The mortality is due to bacterial infection, as it is completely blocked by treating the animals with the fluochinolone antibiotic moxifloxacin between 0 and 12 h after MCAO. (**b**) Rectal body temperature after 60 min of MCAO in the BL6 mouse strain. The temperature changes are due to bacterial infection in this model, as they are completely blocked by treating the animals with the fluochinolone antibiotic moxifloxacin between 0 and 12 h after MCAO. Data from **a**, **b** published in [33].

rodents develop pneumonia and sepsis from day 2 on. Infectious mortality starts at day 3 and peaks at day 5. Animals surviving day 7 will normally survive extended time periods. Treatment with antibiotics can completely stop this mortality, demonstrating that in this model, it is mainly caused by infection (Fig. 2a). Infected animals may initially develop fever, but once they have become septic, they will invariably become hypothermic (Fig. 2b). It is of utmost importance for the experimental stroke researcher to be aware of these changes. Not only will infectious mortality introduce a strong selection bias to the surviving animals, infection is also a major modulator of infarct development. These effects may be mediated by the innate or adaptive immune system [34, 38, 39] or physically by hyper- or hypothermia. It is therefore mandatory that stroke researchers closely monitor body temperature over extended time periods, control body temperature in heated cages, and determine the cause of death if mortality rates are higher than a few percent (e.g., by bacterial cultures of the blood and lung, histology of lung tissue).

Temperature dysregulation in animals subjected to cerebral ischemia may not only be related to infection. Another reason for postischemic hypothermia in rodents is the decreased activity after experimental stroke. Furthermore, the parietal cortex, which is affected in most MCAO models, contains neurons which project toward vegetative control regions such as the hypothalamus, which affects not only sympathetic outflow but also body temperature. In addition, those MCAO models which introduce filaments through the internal carotid artery function by blocking blood flow at points where the circle of Willis branches. This intravascular approach may affect hypothalamic arterial perforators originating off the internal carotid artery, as well as hippocampal blood supply [40]. Depending on the model and the surgeon's skill, this may affect vascular supply of the circle of Willis [41], potentially leading to vegetative dysregulation, including temperature dysregulation. Buchan and Pulsinelli demonstrated in 1990 [42] that the neuroprotective effect of the *N*-methyl-d-aspartate receptor antagonist MK-801 can be explained entirely by the hypothermia it produces in animals after global cerebral ischemia but not in controls.

Hypothermia is an important confounder of stroke injury in rodent focal cerebral ischemia models. Experimental stroke researchers need to measure body temperature frequently by deep rectal probe (ideally also temperature in the M. temporalis with a

Fig. 2 (continued) (**c**) Mean body weight after 60 min of MCAO in the BL6 mouse strain ($n=10$). Note the dramatic drop and slow recovery. Also note that non-manipulated control mice gain 1–2 g per week. (**d**) Correlation of infarct size with loss in body weight 72 h after 60 min of middle cerebral artery occlusion in the BL6 mouse strain. Note the very tight correlation between infarct size and loss in body weight. Ninety-five percent confidence intervals for the population mean (regression). For details of **c** and **d**, see [46, 47]

needle probe [43], which correlates better, but not perfectly, with brain temperature than body temperature [44]). Body temperature must also be controlled not only in the acute postoperative phase. Researchers also need to be aware of interaction of putative neuroprotectants with temperature regulation, in particular if any brain circuitry involved in temperature regulation has been damaged.

Another important confounder of stroke-induced systemic changes is the acute and dramatic loss of *body weight* after MCAO (Fig. 2c, d). Again, it appears as if MCAO in rodents faithfully models the human condition, as stroke patients lose weight even while in intensive care [45]. Weight loss other than that attributable to atrophy of a paralyzed limb is often observed after stroke, indicating tissue wasting and loss of muscle tissue. This contributes to the impairment of functional capacity and reduces quality of life [46]. We found that catabolic pathways of muscle tissue are activated after experimental stroke. Impaired feeding, sympathetic overactivation, or infection cannot fully explain this catabolic activation. Wasting of the target muscle of the disrupted innervation correlated to severity of brain injury [47]. Similar findings were obtained in a rat trauma model [48]. While reduced fluid and caloric intake after stroke may play some role in changes of weight and body composition after stroke, it is likely that the main reasons are complex and include hypermetabolism, malabsorption, and catabolism triggered by stroke- and stress-induced neurohormonal and immune pathways. The relationship between lesion size and body weight loss is very close (Fig. 2d), so close, in fact, that 3 days after MCAO body weight could robustly substitute infarct volumetry for outcome assessment! In most MCAO models, rodents lose 10–20% of their body weight within 3 days and slowly regain it over the next few weeks (Fig. 2c). It should be noted that stroke-induced wasting is actually even more dramatic than it appears to be from the weight charts, as healthy adolescent animals gain approximately 10% body weight per week. A body weight "normalization" by return to pre-MCAO levels therefore actually represents a reduction in body weight of around 20%.

Very little is known about the mechanisms and the consequences of stroke-induced cachexia in animals. However, due to the massiveness of these changes, it is very likely that they confound outcome studies in experimental stroke research. Preclinical stroke researchers in rodents need to be aware of these drastic changes, monitor them carefully in their experiments, and use appropriate controls.

Proper statistics?	✓

As discussed in detail in Chap. 19, numerous misconceptions about statistics and outright errors in study planning and statistical testing confound experimental stroke research and may even negatively impact bench-to-bedside translation in this field. The

following important items need to be checked when planning, analyzing, and reporting a rodent stroke study. Further details and "how to" advice are found in Chap. 19:

- Sample sizes with sufficient statistical power should be calculated before the first animal is operated (a priori). Most experimental stroke studies are grossly underpowered. As a rule of thumb, with standard deviations (SD) around 30% of the mean, which is typical for rodent stroke studies, group sizes of close to 20 are needed to detect an effect size on the order of the SD at a power of 0.8 and an α of 0.05. Statements such as "compound X does not reduce infarct sizes" should be made only in the context of type II error considerations.
- Predefined hypotheses need to be clearly stated.
- Categorical data should not be evaluated with parametric statistics.
- Standard error of the mean should not be used to report the variance of the data. SD is acceptable; confidence intervals are preferred.
- Data presentation in graphs should be maximally informative, for example, by providing all the data points as dots in a plot, together with summary information presented, for example, with boxes and whiskers.
- Do not perform multiple comparisons without correction.
- Don't "p-hack"(i.e., do not try out various post hoc analysis methods until one returns $p<0.05$ or, even worse, add animals until $p<0.05$).
- Do not confuse the p-value with the positive predictive value. Even at $p<0.05$ and power of 80%, it is very likely that the false-positive rate is above 30%!
- In case of doubt, seek the advice of a professional biometrician.
- Read Chap. 19 (Statistics in Experimental Stroke Research).

Internal validity?	✓

The failure of bench-to-bedside progression may be due to problems in the way the experiments are performed, or it may result from the use of unsuitable or intrinsically flawed models; in other words, the problem may lie either in the internal or the external validity of the experiments. Bias is a key problem in internal validity, and four major types have been described: selection bias (creating groups with different confounders, solved by randomization), performance bias and detection bias (investigators, respectively, treating or assessing those subjects on the treatment

arm more positively, controlled by blinding interventions and outcome assessments), and attrition bias (dropouts of subjects with a negative outcome not included in the final result, solved by an intention-to-treat analysis or by reporting dropouts) [49]. So the key checkpoints regarding internal validity are:

- Was a hypothesis formulated and an outcome predefined? To prevent "harking" (hypothesizing after the results are known), consider publication of the study protocol. Hopefully, this will become a requirement in the near future, at least for confirmatory studies [50].
- Were *inclusion and exclusion criteria* preset? For example, was it prespecified to exclude animals below or above a certain infarct size (because it would not normally occur in that particular model) or animals in which blood pressure dropped below a certain threshold during anesthesia, etc.?
- Were *excluded animals* reported? A suspicious sign is unequal group sizes (e.g., $N=8$ in control, and $N=6$ in the verum group). Practically, every experimental stroke study has to exclude animals from analysis, for example, due to mortality before an endpoint was reached or because preset criteria were met. Report the number of all animals used in all groups in the Methods section, to allow tracing of the flow of animals through the study (as required by the ARRIVE Guidelines). The number of animals excluded needs to be reported together with the reasons for exclusion. Even the exclusion of one animal can have a major impact on the outcome of the study [51].
- *Randomization*. "The manuscript should describe the method by which animals were allocated to experimental groups. If this allocation was by randomization, the method of randomization (coin toss, computer-generated randomization schedules) should be stated. Picking animals 'at random' from a cage is unlikely to provide adequate randomization. For comparisons between groups of genetically modified animals (transgenic, knockout), the method of allocation to for instance sham operation or focal ischemia should be described" [49].
- *Allocation concealment*. "Allocation is concealed if the investigator responsible for the induction, maintenance and reversal of ischemia and for decisions regarding the care of (including the early sacrifice of) experimental animals, has no knowledge of the experimental group to which an animal belongs. Allocation concealment might be achieved by having the experimental intervention administered by an independent investigator, or by having an independent investigator prepare drug individually and label it for each animal according to the randomization s schedule as outlined above. These considerations also apply to comparisons

between groups of genetically modified animals, and if phenotypic differences (e.g. coat coloring) prevent allocation concealment this should be stated" [49].

- *Blinded assessment of outcome.* "The assessment of outcome is blinded if the investigator responsible for measuring infarct volume, for scoring neurobehavioral outcome or for determining any other outcome measures has no knowledge of the experimental group to which an animal belongs. The method of blinding the assessment of outcome should be described. Where phenotypic differences prevent the blinded assessment of for instance neurobehavioral outcome, this should be stated" [49, 52, 53].
- *Reporting of conflicts of interest and sources of funding.* "Any relationship which could be perceived to introduce a potential conflict of interest, or the absence of such a relationship, should be disclosed in an acknowledgments section, along with information on study funding and for instance supply of drugs or of equipment" [49].
- *Does the reporting comply with the ARRIVE guidelines* ARRIVE (Animal Research: Reporting of In Vivo Experiments) guidelines are intended to improve the reporting of research using animals—maximizing information published and minimizing unnecessary studies [54].

References

1. Howells DW, Sena ES, Macleod MR (2014) Bringing rigour to translational medicine. Nat Rev Neurol 10:37–43
2. Steward O, Balice-Gordon R (2014) Rigor or mortis: best practices for preclinical research in neuroscience. Neuron 84:572–581
3. Wolfer DP, Crusio WE, Lipp HP (2002) Knockout mice: simple solutions to the problems of genetic background and flanking genes. Trends Neurosci 25:336–340
4. Gerlai R (1996) Gene-targeting studies of mammalian behavior: is it the mutation or the background genotype? Trends Neurosci 19:177–181
5. Barone FC, Knudsen DJ, Nelson AH, Feuerstein GZ, Willette RN (1993) Mouse strain differences in susceptibility to cerebral ischemia are related to cerebral vascular anatomy. J Cereb Blood Flow Metab 13:683–692
6. Beckmann N (2000) High resolution magnetic resonance angiography non-invasively reveals mouse strain differences in the cerebrovascular anatomy in vivo. Magn Reson Med 44:252–258
7. Fujii M, Hara H, Meng W, Vonsattel JP, Huang Z, Moskowitz MA (1997) Strain-related differences in susceptibility to transient forebrain ischemia in SV-129 and C57black/6 mice. Stroke 28:1805–1810
8. Conference B (1997) Mutant mice and neuroscience: recommendations concerning genetic background. Neuron 19:755–759
9. Conner DA (2005) Transgenic mouse colony management. Curr Protoc Mol Biol Chapter 23, Unit 23 10
10. Matsui T, Mori T, Tateishi N, Kagamiishi Y, Satoh S, Katsube N, Morikawa E, Morimoto T, Ikuta F, Asano T (2002) Astrocytic activation and delayed infarct expansion after permanent focal ischemia in rats. Part I: enhanced astrocytic synthesis of s-100beta in the periinfarct area precedes delayed infarct expansion. J Cereb Blood Flow Metab 22:711–722
11. Pantano P, Caramia F, Bozzao L, Dieler C, von Kummer R (1999) Delayed increase in infarct volume after cerebral ischemia: correlations with thrombolytic treatment and clinical outcome. Stroke 30:502–507
12. Henrich-Noack P, Baldauf K, Reiser G, Reymann KG (2008) Pattern of time-dependent reduction of histologically determined infarct volume after focal ischaemia in mice. Neurosci Lett 432:141–145

13. Katchanov J, Waeber C, Gertz K, Gietz A, Winter B, Bruck W, Dirnagl U, Veh RW, Endres M (2003) Selective neuronal vulnerability following mild focal brain ischemia in the mouse. Brain Pathol 13:452–464
14. Fujie W, Kirino T, Tomukai N, Iwasawa T, Tamura A (1990) Progressive shrinkage of the thalamus following middle cerebral artery occlusion in rats. Stroke 21:1485–1488
15. Dihne M, Grommes C, Lutzenburg M, Witte OW, Block F (2002) Different mechanisms of secondary neuronal damage in thalamic nuclei after focal cerebral ischemia in rats. Stroke 33:3006–3011
16. Coimbra C, Drake M, Boris-Moller F, Wieloch T (1996) Long-lasting neuroprotective effect of postischemic hypothermia and treatment with an anti-inflammatory/antipyretic drug. Stroke 27:1578–1585
17. Li F, Irie K, Anwer MS, Fisher M (1997) Delayed triphenyltetrazolium chloride staining remains useful for evaluating cerebral infarct volume in a rat stroke model. J Cereb Blood Flow Metab 17:1132–1135
18. Vogel J, Mobius C, Kuschinsky W (1999) Early delineation of ischemic tissue in rat brain cryosections by high-contrast staining. Stroke 30:1134–1141
19. Liszczak TM, Hedley-Whyte ET, Adams JF, Han DH, Kolluri VS, Vacanti FX, Heros RC, Zervas NT (1984) Limitations of tetrazolium salts in delineating infarcted brain. Acta Neuropathol 65:150–157
20. Hatfield RH, Mendelow AD, Perry RH, Alvarez LM, Modha P (1991) Triphenyltetrazolium chloride (TTC) as a marker for ischaemic changes in rat brain following permanent middle cerebral artery occlusion. Neuropathol Appl Neurobiol 17:61–67
21. Bednar MM, Fanburg JC, Anderson ML, Raymond SJ, Dooley RH, Gross CE (1994) Comparison of triphenyltetrazolium dye with light microscopic evaluation in a rabbit model of acute cerebral ischaemia. Neurol Res 16:129–132
22. Klohs J, Grafe M, Graf K, Steinbrink J, Dietrich T, Stibenz D, Bahmani P, Kronenberg G, Harms C, Endres M, Lindauer U, Greger K, Stelzer EH, Dirnagl U, Wunder A (2008) In vivo imaging of the inflammatory receptor CD40 after cerebral ischemia using a fluorescent antibody. Stroke 39:2845–2852
23. Stern MD, Lappe DL, Bowen PD, Chimosky JE, Holloway GA Jr, Keiser HR, Bowman RL (1977) Continuous measurement of tissue blood flow by laser-Doppler spectroscopy. Am J Physiol 232:H441–H448
24. Dirnagl U, Kaplan B, Jacewicz M, Pulsinelli W (1989) Continuous measurement of cerebral cortical blood flow by laser-Doppler flowmetry in a rat stroke model. J Cereb Blood Flow Metab 9:589–596
25. Endres M, Biniszkiewicz D, Sobol RW, Harms C, Ahmadi M, Lipski A, Katchanov J, Mergenthaler P, Dirnagl U, Wilson SH, Meisel A, Jaenisch R (2004) Increased postischemic brain injury in mice deficient in uracil-DNA glycosylase. J Clin Invest 113:1711–1721
26. Kitagawa K, Matsumoto M, Yang G, Mabuchi T, Yagita Y, Hori M, Yanagihara T (1998) Cerebral ischemia after bilateral carotid artery occlusion and intraluminal suture occlusion in mice: evaluation of the patency of the posterior communicating artery. J Cereb Blood Flow Metab 18:570–579
27. Endres M, Laufs U, Huang Z, Nakamura T, Huang P, Moskowitz MA, Liao JK (1998) Stroke protection by 3-hydroxy-3-methylglutaryl (HMG)-CoA reductase inhibitors mediated by endothelial nitric oxide synthase. Proc Natl Acad Sci U S A 95:8880–8885
28. Hoehn M, Kruger K, Busch E, Franke C (1999) ISMRM 7th Annual Meeting, Philadelphia, pp 1843
29. Leithner C, Gertz K, Schrock H, Priller J, Prass K, Steinbrink J, Villringer A, Endres M, Lindauer U, Dirnagl U, Royl G (2008) A flow sensitive alternating inversion recovery (FAIR)-MRI protocol to measure hemispheric cerebral blood flow in a mouse stroke model. Exp Neurol 210:118–127
30. Gerriets T, Stolz E, Walberer M, Muller C, Kluge A, Bachmann A, Fisher M, Kaps M, Bachmann G (2004) Noninvasive quantification of brain edema and the space-occupying effect in rat stroke models using magnetic resonance imaging. Stroke 35:566–571
31. Swanson RA, Morton MT, Tsao-Wu G, Savalos RA, Davidson C, Sharp FR (1990) A semiautomated method for measuring brain infarct volume. J Cereb Blood Flow Metab 10:290–293
32. Elliott KA, Jasper H (1949) Measurement of experimentally induced brain swelling and shrinkage. Am J Physiol 157:122–129
33. Meisel C, Prass K, Braun J, Victorov I, Wolf T, Megow D, Halle E, Volk HD, Dirnagl U, Meisel A (2004) Preventive antibacterial treatment improves the general medical and neurological outcome in a mouse model of stroke. Stroke 35:2–6
34. Liesz A, Suri-Payer E, Veltkamp C, Doerr H, Sommer C, Rivest S, Giese T, Veltkamp R (2009) Regulatory T cells are key cerebroprotective immunomodulators in acute experimental stroke. Nat Med 15:192–199

35. Harms H, Prass K, Meisel C, Klehmet J, Rogge W, Drenckhahn C, Gohler J, Bereswill S, Gobel U, Wernecke KD, Wolf T, Arnold G, Halle E, Volk HD, Dirnagl U, Meisel A (2008) Preventive antibacterial therapy in acute ischemic stroke: a randomized controlled trial. PLoS One 3:e2158
36. Klehmet J, Harms H, Richter M, Prass K, Volk HD, Dirnagl U, Meisel A, Meisel C (2009) Stroke-induced immunodepression and post-stroke infections: Lessons from the preventive antibacterial therapy in stroke trial. Neuroscience 158:1184–1193
37. Prass K, Meisel C, Hoflich C, Braun J, Halle E, Wolf T, Ruscher K, Victorov IV, Priller J, Dirnagl U, Volk HD, Meisel A (2003) Stroke-induced immunodeficiency promotes spontaneous bacterial infections and is mediated by sympathetic activation reversal by poststroke T helper cell type 1-like immunostimulation. J Exp Med 198:725–736
38. Meisel C, Schwab JM, Prass K, Meisel A, Dirnagl U (2005) Central nervous system injury-induced immune deficiency syndrome. Nat Rev Neurosci 6:775–786
39. McColl BW, Allan SM, Rothwell NJ (2009) Systemic infection, inflammation and acute ischemic stroke. Neuroscience 158:1049–1061
40. Ozdemir YG, Bolay H, Erdem E, Dalkara T (1999) Occlusion of the MCA by an intraluminal filament may cause disturbances in the hippocampal blood flow due to anomalies of circle of Willis and filament thickness. Brain Res 822:260–264
41. Furuya K, Kawahara N, Kawai K, Toyoda T, Maeda K, Kirino T (2004) Proximal occlusion of the middle cerebral artery in C57Black6 mice: relationship of patency of the posterior communicating artery, infarct evolution, and animal survival. J Neurosurg 100:97–105
42. Buchan A, Pulsinelli WA (1990) Hypothermia but not the N-methyl-D-aspartate antagonist, MK-801, attenuates neuronal damage in gerbils subjected to transient global ischemia. J Neurosci 10:311–316
43. Busto R, Dietrich WD, Globus MY, Valdes I, Scheinberg P, Ginsberg MD (1987) Small differences in intraischemic brain temperature critically determine the extent of ischemic neuronal injury. J Cereb Blood Flow Metab 7:729–738
44. Miyazawa T, Hossmann KA (1992) Methodological requirements for accurate measurements of brain and body temperature during global forebrain ischemia of rat. J Cereb Blood Flow Metab 12:817–822
45. Jonsson AC, Lindgren I, Norrving B, Lindgren A (2008) Weight loss after stroke: a population-based study from the Lund Stroke Register. Stroke 39:918–923
46. Scherbakov N, Dirnagl U, Doehner W (2011) Body weight after stroke: lessons from the obesity paradox. Stroke 42:3646–3650
47. Springer J, Schust S, Peske K, Tschirner A, Rex A, Engel O, Scherbakov N, Meisel A, von Haehling S, Boschmann M, Anker SD, Dirnagl U, Doehner W (2014) Catabolic signaling and muscle wasting after acute ischemic stroke in mice: indication for a stroke-specific sarcopenia. Stroke 45:3675–3683
48. Roe SY, Rothwell NJ (1997) Whole body metabolic responses to brain trauma in the rat. J Neurotrauma 14:399–408
49. Macleod MR, Fisher M, O'Collins V, Sena ES, Dirnagl U, Bath PM, Buchan A, van der Worp HB, Traystman RJ, Minematsu K, Donnan GA, Howells DW (2009) Reprint: Good laboratory practice: preventing introduction of bias at the bench. J Cereb Blood Flow Metab 29:221–223
50. Kimmelman J, Mogil JS, Dirnagl U (2014) Distinguishing between exploratory and confirmatory preclinical research will improve translation. PLoS Biol 12:e1001863
51. Holman C, Piper SK, Grittner U, Diamantaras AA, Kmmelman J, Siegerink B, Dirnagl U (2016) Where have all the rodents gone? The effects of attrition in experimental research on cancer and stroke. PLoS Biol. 14:e1002331
52. Bello S, Krogsbøll LT, Gruber J, Zhao ZJ, Fischer D, Hróbjartsson A (2014) Lack of blinding of outcome assessors in animal model experiments implies risk of observer bias. J Clin Epidemiol 67:973–983
53. Holman L, Head ML, Lanfear R, Jennions MD (2015) Evidence of experimental bias in the life sciences: why we need blind data recording. PLoS Biol 13:e1002190
54. NC3R. The ARRIVE guidelines. https://www.nc3rs.org.uk/arrive-guidelines. 29 Dec 2015

Index

A

Acclimatization 282
Adhesion molecules 105
Advantage 31, 33, 39, 58, 60, 64, 84, 202, 205, 210, 214, 245, 247, 254, 256, 257, 262, 264, 266
Age 2, 4, 85, 133
Aging 103–104
Allocation concealment 13–14, 16, 326
Alternative hypothesis 303
Alzheimer's 91, 248
Analgesia 280–281
Anesthesia 34, 36–39, 47–48, 61, 121–133, 186, 188, 189, 194
Anesthetic 33, 47, 122–124, 126, 128–133, 188, 194
  neuroprotection 122–124, 132
  preconditioning 123, 124, 131
Anhedonia 200, 216, 217
Animal experiments 1, 3–5, 15–17, 243, 245, 247–249, 251–253, 255, 257, 268
Animal model 1–5, 11, 15, 16, 58, 65, 123, 124, 130, 132, 190–193, 198, 206, 217, 241, 247, 250, 268
Animal selection 22
ANOVA 300
Anxiety 198, 200, 214–216, 254
Apparent diffusion coefficient (ADC) map 150
Apolipoprotein E (apoE) 101
Apoptosis 3, 106, 126, 128, 130, 131
Apoptotic cell death 25, 30
Animal Research: Reporting of In Vivo Experiments (ARRIVE) 14
Arterial spin labeling (ASL) 169
Ascertainment bias 8, 9
Ataxia 202
Atherosclerosis 2, 4, 101–102
Attrition bias 8, 9
Autofluorescence 186, 187, 194
Automated home-cage technology 243, 258
Autoradiographic technique 159

B

Barbiturates 123–126, 130
Bar graphs 302
Basal ganglia 31, 95, 269
Battery of tests 200
Bayesian approaches 302
Beam walking test 227–228
Behavior 8, 9, 84, 85, 88, 198–205, 208, 213–218, 242, 244–247, 249, 251, 252, 254–256
Behavioral phenotyping 241–243, 256–258
Behavioral testing 10, 86, 197–218, 241, 243, 256
Benzodiazepine receptor 127
Beta 304
Bias 8–11, 16, 17, 199, 202, 214, 256
Bio breeding (BB) rat 95
Bioluminescence 186, 188
Bipolar diathermy 45
Bleeding 54, 58, 87
Blinded assessment of outcome 16
Blink reflex 47
Blood–brain barrier (BBB) 24, 191, 194
Blood gas analyzer 45, 148
Blood pressure transducer 45
Body mass index 96
Body temperature 34, 47, 59, 186, 189, 194, 250, 256
Body weight 37, 246, 256
Bradykinesia 205, 207
Brain edema correction 269
Brain injury 86, 122, 129, 131, 267
Brain ischemia 58, 65, 88, 125, 207, 218, 265, 268
Brain tissue preparation 265, 266

C

^{11}C 159
C57 208
Cachexia 87, 256
Cardiopulmonary bypass 131, 132
Carotid endarterectomy 122, 123, 132
Carotid ligation 123
Categorical data 300
Cats 95, 125, 198
CD40-receptor 190
Cell genesis 84
Cerebral blood flow (CBF) 3, 9, 38, 39, 43, 60, 61, 122, 123, 126–129, 132, 266
Cerebral glucose utilization 159
Cerebral ischemia 4, 14, 15, 29–39, 58, 121–133, 190, 191, 263
Cerebral metabolic rate for oxygen 127, 160
Cerebral metabolism (CMRO2) 20, 123, 124, 127, 128, 160
Cerebral neuroprotection 129

Ulrich Dirnagl (ed.), *Rodent Models of Stroke*, Neuromethods, vol. 120,
DOI 10.1007/978-1-4939-5620-3, © Springer Science+Business Media New York 2016

Cerebral oxygen consumption 127
Cerebral perfusion pressure 127
^{11}C-flumazenil 161
Charge-coupled device (CCD) 186, 188
Chemokine receptors 106
Cholesterol 2
[^{14}C] iodoantipyrine autoradiography 52
Circle of Willis 3, 38, 39, 319
Circling 52, 201, 202, 204
Clinical practice 1, 2, 4–5
Clot 25, 30, 58–62
Clot embolism 25–26
Coated filaments 31
Cognitive deficits 129, 198, 218
Collaborative Approach to Meta-Analysis and Review of Animal Data in Experimental Studies (CAMARADES) 10, 14, 16
Common carotid artery (CCA) 30, 33, 34, 36, 37, 39
Comorbidities 1, 8, 11, 16, 92, 107
Compensatory behaviors 224, 258
Confidence interval (CI) 301
Conflicts of interest 327
Confounding factors 92, 211
Contrast-enhanced staining 263
Core 31, 33, 127, 151, 216, 250, 256, 262, 263, 265, 267
Corner test 208–209
Corpulent (*cp/cp*) rats 98
Corticospinal tract 224
Craniectomy 24–25, 33
Cresyl violet 266
Cryoprotected 264
Cryostat 262–265, 267, 268, 271, 272
Cylinder test 201, 225–226
Cytokines 105

D

Dahl salt sensitive rat 94
Dark-light box 214
Dehydration 52
Dental drill 45
Deoxyhemoglobin 170
Depression 83, 128, 198, 200, 201, 216, 217, 252
Depression-like behavior 216
Descriptive statistics 8
Desflurane 131
Developing brain 74
Dextrose 95
Diabetes 2–4, 58, 133
Diabetic (NOD) mouse 95
Diet 3, 5, 193
Diffusion map 149
Diffusion tensor imaging 150
Diffusion-perfusion mismatch 153–154
Diffusion-weighted imaging 149
Disability 19
Disadvantages 262
Dogs 95, 125, 130, 198
Drink 53
Dura 51, 60
DWI/PWI mismatch 154

E

Edema 65, 84, 124, 263, 264, 269
Edema correction 269
Effect size 14, 199, 289
Efficacy 8, 10, 11, 14–16, 123, 125, 126, 128, 132
Egger regression 16
Electrocoagulation 57, 64
Elevated plus maze 214–215, 243
Embryonic stem cells 316
Endothelial damage 33
Endothelin-1 ....24, 85
Endothelium 31
Endovascular approach 24, 57
End points 197, 281
Enriched environment 83–89
Enrichment 85, 87, 88, 242, 245
Enzyme histochemistry 263
Eosinophilic 265
Errors 303
Ethical considerations 87
Ethological 214, 242, 245, 246, 251, 252, 254
Etomidate 128, 130
Evoked potentials 123
Excitatory amino acids 122
Exclusion criteria 13, 86–87, 326
Exercise 3, 5, 83, 252
Experimental animal model 13, 242, 245, 248, 249, 251, 253, 257
Experimental design 12, 125, 245, 254, 256
External validity 7, 16

F

False negative 304
False positive 303
Federation of European Laboratory Animal Science Association (FELASA) 282
Feeding 52, 230, 243, 246, 253, 254
Fentanyl 123, 130
^{18}F-fluorodeoxyglucose (^{18}F-FDG) 159
Fiber optic 35, 38, 60, 186, 319
Fibrin 25, 58, 190
Fibrin rich thrombi 67
Filament 24, 29–31, 33, 34, 37–39
Filament model 64, 85
Fixation 262–265, 270, 273
FK506 ....12, 154

Flumazenil....161
Fluorescence imaging....187
Fluorescence reflectance imaging....187
Fluorescent protein....188
Focal ischemia....10, 20, 121, 126, 130, 200, 206, 208, 212, 214–216, 218, 262, 263, 268, 273
Food....37, 85, 87, 88, 246, 248, 249, 253, 256
Foot faults....227
Forelimb....202, 204, 225
  Forelimb asymmetry....226
  Forelimb inhibition test....228–229
  Forelimb use....228
Fractional anisotropy....170
Free radical scavenger....122
Frontoparietal cortex....25
Functional MRI....153
Functional recovery....83–89, 151
Funnel plotting....16

G

Gadolinium....171
Gait....202, 203, 209–211
Gamma-aminobutyric acid (GABA)....122, 126–128, 131
Gd-DTPA....155
Geller-Seifter conflict test....214
Gender....3, 133, 199
General anesthesia....122, 131
Genetic predisposition....2
Genetic variety....3
Gerbil....93
Glial scar....84
Global ischemia....20, 125
Glucose....35, 37, 95, 125, 130, 242, 261
Glucose utilization....159–160
Glyconanoparticles....156
Good clinical practice (GCP)....290
Good laboratory practice (GLP)....11, 14, 278, 290
Goto-Kakizaki rat....95
Graphing....302
Grasping....207
Grids....85, 86, 204, 211, 254, 255
Grip strength....207

H

H0 (null hypothesis)....303
H1 (alternative hypothesis)....303
Habituation....199, 207, 211, 213, 216, 249
Halothane....123, 130, 131
Handling....9, 87–88, 188, 198, 199, 242, 243, 245, 273, 280
HDL....102
Healthy animals....1, 3, 4, 87, 91, 133
Heating blanket....44
Hematoxylin eosin (H&E) staining....264–266, 270–271
Hemiparesis....52
Hemorrhagic transformation....156, 191
High-throughput....243–245, 254
Histology....263
Hole board....211, 213
Housing condition....84
Hunching....52
Husbandry....282
Hypercapnia....148
Hyperintensity....149
Hypertension....2–4, 58, 133
Hyperthermia....122
Hypointensity....150
Hypotension....50
Hypothalamus....25, 32
Hypothermia....12, 32, 87, 122, 125, 130, 191, 256
Hypothesis....8, 12, 125, 242

I

ICAM-1....105
IL-1β....105
IL-6....105
Immunodepression....88
Immunohistochemistry....263, 264, 266–268, 272–273
Inclusion criteria....13, 15, 326
Infarct....21, 58, 62, 64, 65, 201, 256, 262, 263, 265–269, 273
  Infarct size....15, 25, 86, 88, 127, 262
  Infarct volume....8, 31, 128, 261–269
  Infarct volume calculations....263, 269–270
Infection....38, 49, 87, 88
Inference....198
Inferior cerebral vein....50
Inflammation....128, 156, 190–193
Inhalational anesthetics....130, 131
Internal carotid artery (ICA)....34, 36, 37, 39
Internal validity....7, 10, 16
Intracranial pressure....65, 124, 127
Introduction....1–2, 19–26, 261–263
Intubation....34, 46–48
Ischemic tolerance....124
ISO 9000....291

J

Jaw....53

K

KATP channel....124
Ketamine....123, 127, 130

Knockout mouse....316

L

Lacunar infarcts....2
Laser Doppler flowmetry....13, 51
LDLR-like protein (LRP)....103
Learning....9, 39, 84, 201, 202, 205, 211–213, 233–236, 247, 248
Lenticulostriate arteries....26
Leptin....95
Lethargy....52
Likelihood....306
Limb preference....229
Limb Use Asymmetry Test....225–226
Lipopolysaccharide (LPS)....109
Liquid nitrogen....264, 265
Locomotion....209–211, 215, 247
Long Evans rats....98
Longitudinal relaxation time....168
Low-density lipoprotein receptor (LDLR)....101
L-selectin....105
Luciferase....188, 189, 191, 193, 194

M

Macrophages....105, 269
Magnetic resonance angiography (MRA)....62, 63, 153, 171
Magnetic resonance imaging (MRI)....62, 63, 65, 94, 185, 187, 193, 267
Magnets....146
Manganese....155
Mann-Whitney *U* test....300
Matrix metalloproteinase (MMP)....106, 191, 192
MCP-1....105
Mean....300
Mean transit time....169
Membrane potential....154
Memory....2, 84, 198, 200, 201, 205, 211–213, 247
Meta-analysis....10, 15, 16
Metabolic syndrome....99
Microaneurysm clips....44
Microglia....162, 191, 193, 269
Micromanipulator....45, 58, 61
Microtubule-associated protein 2 (MAP2)....266–268
Midazolam....127–128, 130
Middle cerebral artery (MCA)....15, 23, 29–31, 33, 34, 36–39, 57, 58, 60–62, 85, 209
Middle cerebral artery occlusion (MCAO)....11, 15, 25, 30–35, 37, 38, 61–64, 85, 87, 88, 123, 190–193, 201, 206–208, 210, 218, 262, 267
Mitochondria....268, 269, 318
Mitochondrial....124, 128
MK-801....94
MMP-2....105, 191
MMP-9....105, 191
Monitoring....32, 37, 38, 202, 245, 256
Monkeys....95, 125, 130, 251
Monocytes....105, 156
Monofilament....33–35, 37
Mortality....19, 25, 31, 58, 64, 88, 216
Mortality rate....64, 321
Mouse....4, 29–39, 58, 59, 61, 62, 65, 85, 132, 186, 190, 191, 193, 203–206, 208, 209, 212, 218, 245, 254, 266, 273
Myeloperoxidase....157

N

Nanoparticles....156, 188
Nd/YAG....75
Near-infrared fluorescence (NIRF) imaging....186–194
Neck incision....33, 37
Neocortex....26
NeuN....268
Neural progenitor cells....193
Neuroprotection....39, 122–133, 218
Neuroprotective strategies....22
Neuropsychological symptoms....2
Neuroscore....86, 87
Neutrophils....157
Nitric oxide (NO)....25, 30, 124, 128
N-methyl-d- aspartate (NMDA)....122, 126, 127, 129–131, 318
No reflow....25
NOD-like receptors....108
Nonvolatile anesthetics....124–129
Nitrous oxide (N_2O)....33, 47
Null hypothesis statistical testing (NHST)....302

O

Obesity....2
Obesity models....97
Observation interval....317
^{15}O-O_2....160
Open field....202, 213–216, 252–254, 257
Operating microscope....44
Optical Imaging....185, 186, 188–194
Oral intubation....48
Overview....201, 205–207, 209, 210, 212, 213, 215–217
Oxygen extraction fraction (OEF)....160
Oxygen metabolism....160–161
Oxyhemoglobin....170

P

PaCO2....132, 148
Pain....34, 83
Pannecrosis....21, 31, 262
PaO2....132, 148

Paraffin embedding 262, 263, 265, 266, 269
Paraformaldehyde (PFA) 262, 264, 270, 271, 273
Paralytic agents 280
Paramagnetic 156
Parkinson's disease 205
Passive avoidance 211–212, 254, 257
Paw 204, 206, 207, 210, 212
Pellet reaching task 231–232
Penumbra 21, 31, 85, 153–154, 262, 263, 265, 266
Performance bias 8, 9
Perfusion fixation 264
Periinfarct depolarization 21
Peripheral benzodiazepine receptor 162
Permanent ischemia 25, 31, 33, 273
pH 37, 132, 148, 261, 270
Pharmacological MRI 170
Physical therapy 84
Piglet 131
Piloerection 52, 203
Pilot studies 12, 14, 256
PK11195 162
Plasticity 84
Plus maze 243
Pole test 86, 205–207
Poly-l-lysine 30, 31, 34–37, 271, 272
Population 8, 12, 86, 188, 191, 198
Positron 159
Positron emission tomography 22
Power 10–12, 14, 185, 198, 204
Prevention 1, 2, 128
Primate 3, 5, 43, 84, 126
Prior probability 10–11, 307
Probability 8, 300
Propofol 126, 128, 130
Proton DENSITY-weighted 169
Protons 146
Proximal MCAO 31, 43, 51, 52
P-selectin 105
Publication bias 10, 16
PubMed searches 15

Q

Quartiles 302

R

Rabbits 95
Randomization 13, 16, 199, 326
Randomized clinical trial (RCT) 125, 290
Rat 3–5, 9, 29–39, 59, 85, 132, 188, 191, 198, 200–202, 205, 208, 209, 211, 213–215, 218, 242, 244–249, 252, 267, 268, 273
Recombinant tissue plasminogen activator (rtPA) 26
Rectal temperature recording 44
Reduction 31, 38, 61, 62, 124, 125, 128, 130, 131, 191, 197, 213, 257, 267, 268
Refinement 11, 214, 254, 257
Rehabilitation 84, 88
Remodeling 84, 190–194
Repair 3, 190, 191, 263, 317
Reperfusion 25, 29–31, 34, 38, 58, 61, 62, 64, 65, 123, 132, 154, 269
Reperfusion injury 25, 30
Replacement 11, 257
Replication 12
Report 267, 268
Reporting 10, 11, 14, 15, 246
Reproducibility 29, 31, 39, 64, 243, 245, 256, 289
Retractors 48
Reward system 217
Risk factor 2, 4, 58
Rodent 3, 5, 8–11, 37, 38, 43, 84, 85, 87, 88, 121, 123, 126, 185, 186, 188–191, 193–194, 197–218, 243–245, 247–252, 254, 256, 257, 261–273
Rodent ventilator 45
RotaRod 202–205, 247, 257
Rotating pole test 86
Rung walking task 232–233

S

S100B 126
Salt diet 93
Sample size 12–14, 16
Sample size calculation 12–14, 16
Sedation 214, 280–281
Selection bias 8
Selective citation bias 10, 11
Sensitivity 191, 200, 243, 245, 250, 256, 257, 306
Sensorimotor asymmetry 224–225
Sensorimotor cortex 224
Sensorimotor stimulation 87
Sensory motor testing 200, 201
Sepsis 323
Sevoflurane 131
Shrinkage 263, 269
Silicon 33–34
Silver impregnation solution 272
Silver staining 266–267, 272
Skilled movements 229–233
Skull 38, 50, 60
Slicing 263–266
Small animal imaging 3, 190–193
Snap-freezing 264, 265
Sodium azide 264
Somatosensory 32, 123
Species 3, 5, 121–123, 132, 133, 191, 198, 242
Specific activity 159

Specificity 65, 307
Spin-echo 168
SPIO (small particles of iron oxide) 156
Spontaneously hypertensive (SHR) rat 44, 246
Sprague Dawley rats 36, 38, 85
Staining 262–274
Standard error of the mean (SEM) 301
Standardization 199, 257
Statistics 16, 247, 257
Stereotactic injection 24
Stereotaxic frame 45
Sterilizing 44
Strain differences 38–39, 200, 208
Streptozotocin 44
Striatum 25, 31, 32, 191, 201
Stroke Treatment Academic Industry Roundtable (STAIR) 290
Study quality 16
Subarachnoid hemorrhage 29–31
Subcutaneous fluids 52
Subtemporal approach 43
Sucrose consumption 216–218
Suffering 281–282
Surgical instruments 47
Suture 29–39, 60, 61
Swimming 226
Swimming test 228–229
Sympathetic nervous system 127
Systematic review 10, 12, 14, 38

T

T1 168
T2 ..... 168, 267
Tail vein catheterization 60, 61
Temperature 32, 33, 35–37, 59, 123, 125, 132, 189, 194, 243, 247, 250, 256, 268, 270, 271
dysregulation 32, 323
Tesla 146
T helper cell 108
Thionine 266
Thiopental 125, 130
Thrombin 58, 59, 61, 62, 65
Thromboembolic models 25
Thromboembolic stroke 5, 26, 62, 65, 190
Thrombolysis 25, 31, 58, 62, 64
Time-of-flight MRA 171
Time-to-peak 169
Time to remove that dot 225
Time window 5, 11, 215, 243, 268
Tissue at risk 149, 263
Tissue-type plasminogen activator (tPA) 61–64
TNFα 105
Toll-like receptors (TLRs) 108
Training 39, 83–85, 87, 199, 202, 205–208, 210, 211, 217, 248, 249
Transcardial perfusion 264
Translational road block 7–17, 197, 289
Translocator protein-18 (TSPO) 162
Transversal relaxation time 168
Tray reaching task 229–230
2,3,5-Triphenyltetrazolium hydrochloride (TTC) 266–269, 273–274
t-test 300
Type I error 10, 303
Type II error 10, 304

U

Urinary tract infections 107
USPIO (Ultra-small superparamagnetic particles of iron oxide) 156

V

Validity 8, 10, 12, 15, 199, 242
Variance 12, 14, 199, 205, 301
Vascular clip 25
Vascular risk factors 2, 4
Vascular smooth cells 109
Vascular territory 2, 31, 38
Vasospasm 44
VEGFR 164
Viability thresholds 20
Vibratome 262, 264, 265, 267, 268, 271
Vogel conflict test 214
Volatile anesthetics 33, 123, 129, 130
Volumetry 266–268, 273

W

Water maze 211, 233–235, 243
Western diet 102
Whisker stimulation 170
White matter 2, 3, 266–269
Wire hanging 207–208
Wistar rat 246
Wound healing 52

X

Xenon 130

Z

Zucker diabetic fatty rat 95